Skull Anatomy and Evolution in Scolecophidian Snakes (Squamata: Ophidia), with an Emphasis on the Role of Heterochrony

by

Catherine Rose Christina Strong

A thesis submitted in partial fulfillment of the requirements for the degree of

Master of Science

in

Systematics and Evolution

Department of Biological Sciences
University of Alberta

ABSTRACT

Scolecophidians ('blindsnakes') form an assemblage of miniaturized and fossorial snakes, comprising three main lineages: Anomalepididae, Leptotyphlopidae, and Typhlopoidea. Scolecophidians have long been viewed as diverging basally among snakes, constituting the modern vestige of an ancestrally miniaturized, burrowing, vision-degenerate, and 'microstomatan' (small-mouthed) snake condition. However, despite their pivotal role in hypotheses of the anatomical, ecological, and phylogenetic origins of snakes, several aspects of scolecophidian anatomy and evolution remain poorly understood. In light of this uncertainty, my thesis re-examines the aforementioned paradigmatic view of this group. I focus particularly on the potential role of heterochrony (i.e., evolutionary changes in the rate and/or timing of developmental events)—and particularly paedomorphosis (i.e., juvenilization of morphology)—in influencing scolecophidian evolution.

I first use the genus *Atractaspis* to assess the traditional hypothesis of a fundamental dichotomy between scolecophidians and alethinophidians (i.e., all other extant snakes). As a fossorial but non-miniaturized colubroid, deeply nested among snakes, *Atractaspis* presents an interesting basis for comparison to the miniaturized, fossorial, and assumedly 'basal' scolecophidians. This investigation of atractaspidid anatomy reveals a clear morphological continuum between scolecophidians and various fossorial alethinophidians, with miniaturization—and, concomitantly, extensive paedomorphosis—providing a reasonable mechanism linking these groups.

I next examine the evolution of jaw mechanisms in squamates (i.e., lizards, including snakes). Snakes have traditionally been divided into two major groups based on feeding mechanics: 'macrostomy', the ability to ingest proportionally large prey items; and

‘microstomy’, the lack of this ability. ‘Microstomy’ is in turn generally viewed as a morphologically uniform condition shared by scolecophidians, early-diverging alethinophidians, and non-snake lizards. To investigate this paradigm, I formalize a new framework for conceptualizing and testing the homology of overall character complexes, or ‘morphotypes’. I analyze the morphology of the jaws and suspensorium across purported ‘microstomatan’ squamates, revealing that key components of the jaw complex are not homologous at the level of primary character state identity across these taxa. Therefore, rather than treating ‘microstomy’ as a uniform symplesiomorphy, I instead propose that non-snake lizards, early-diverging alethinophidians, anomalepidids, leptotyphlopids, and typhlopoids each exhibit a unique and non-homologous jaw morphotype: ‘minimal-kinesis microstomy’, ‘snout-shifting’, ‘axle-brace maxillary raking’, ‘mandibular raking’, and ‘single-axle maxillary raking’, respectively. I complement this qualitative approach with a quantitative assessment of squamate skull modularity. Anatomical network analysis of a broad range of squamates reveals that the jaw elements exhibit distinctive patterns of connectivity within each major ‘microstomatan’ group. These contrasting network structures in turn support the aforementioned hypothesis of a complex evolutionary history of ‘microstomy’. Morphospace-based analyses indicate convergence associated with both fossoriality and miniaturization, with their combined influence imposing further evolutionary constraint on skull architecture.

Finally, I provide a preliminary phylogenetic re-assessment of snakes. I first revise the morphological dataset most commonly used in snake phylogenies, thus ameliorating the logical and operational inconsistencies affecting previous studies, as well as introducing several characters relevant to scolecophidian systematics. Maximum parsimony and Bayesian analyses of this revised dataset (which currently includes only extant taxa) recover the traditional

topology of Scolecophidia and Alethinophidia as sister clades. However, a subsequent assessment of the phylogenetic impact of fossil snakes reveals that the position of Scolecophidia can change dramatically when extinct taxa are included. Similarly, an examination of the synapomorphies and symplesiomorphies of Scolecophidia as optimized on the revised-dataset cladogram reveals very few—if any—of them to be reliable, with several being highly susceptible to paedomorphosis- and/or fossoriality-related homoplasy. These results indicate that the inclusion of fossil snakes, alongside mitigation of the aforementioned sources of homoplasy, will be essential in reliably reconstructing the phylogeny of snakes.

Ultimately, this thesis strongly rejects the traditional paradigm of scolecophidians as fundamentally 'basal' to other snakes. The miniaturization-related anatomical spectrum described above instead supports the controversial hypothesis of scolecophidians as 'regressed alethinophidians', reflecting paedomorphosis-driven derivation of the scolecophidian skull from a fossorial alethinophidian condition. Furthermore, the lack of synapomorphy among scolecophidian jaw mechanisms is inconsistent with the notion that they represent a homogenous and ancestral snake morphology; combined with the novel evidence of convergence presented herein, these results instead suggest the independent evolution of fossoriality, miniaturization, and 'microstomy' in each scolecophidian lineage. Altogether, I therefore advocate a hypothesis of scolecophidians as a highly convergent assemblage, marked by extensive paedomorphic 'regression' from a more typical snake-like bauplan.

PREFACE

This thesis includes collaborative research that has been published in peer-reviewed scientific journals. For all relevant chapters, I was the major contributor and was responsible for study design, data collection and analysis, and preparation of the manuscript and figures, with M. W. Caldwell being the supervisory author. Specific author contributions are indicated below.

Chapter Two of this thesis has been published as: Strong, C. R. C., Palci, A., and M. W. Caldwell. 2021. Insights into skull evolution in fossorial snakes, as revealed by the cranial morphology of *Atractaspis irregularis* (Serpentes: Colubroidea). *Journal of Anatomy*, **238**, 146–172. doi:10.1111/joa.13295. In addition to the responsibilities listed above, I conducted the micro-CT scanning of MCZ specimens, performed the digital segmentations, and wrote the anatomical descriptions. A.P. contributed to drafting and critically revising the manuscript. M.W.C. conceived of and supervised the project, and contributed to critical revision of the manuscript. All authors contributed to developing the project.

Chapter Three of this thesis has been published as: Strong, C. R. C., Scherz, M. D., and M. W. Caldwell. 2021. Deconstructing the Gestalt: new concepts and tests of homology, as exemplified by a re-conceptualization of "microstomy" in squamates. *The Anatomical Record*, **2021**, 1–49. doi:10.1002/ar.24630. In addition to the responsibilities listed above, I conducted the micro-CT scanning of MCZ specimens, performed the digital segmentations, wrote the anatomical descriptions, and developed the philosophical framework of the paper. M. D. S. contributed to study conceptualization and critical revision of the manuscript and homological framework. M. W. C. contributed to study conceptualization, discussions of homology, and critical revision of the manuscript and homological framework.

Chapter Four has not been submitted for publication, but was designed in collaboration with M. D. Scherz and M. W. Caldwell. Both collaborators contributed to study design, with M. W. C. also contributing to critical revision of the manuscript. In addition to the responsibilities listed above, I conducted the micro-CT scanning of MCZ specimens, performed the digital segmentations, and coded and conducted all analyses in this chapter.

Chapter Five was carried out in collaboration with M. W. Caldwell, who contributed to study conceptualization and critical revision of the dataset and manuscript.

Chapters One and Six are entirely my own work.

ACKNOWLEDGMENTS

First and foremost, I would like to thank my supervisor, Dr Michael W. Caldwell. Dr Caldwell first welcomed me into his lab four years ago to carry out an undergraduate research project; at the time I knew essentially nothing about snakes and even less about scientific research, and it's largely thanks to his expertise, guidance, and camaraderie that, four years later, my knowledge of those areas has greatly improved (or so I like to think). I wouldn't be the student or researcher I am today without his guidance and support, and for that I am sincerely grateful.

I would also like to thank my supervisory committee—Drs Randall Nydam and Corwin Sullivan—for their advice and insight, which helped guide this thesis, and my arm's-length examiner, John Acorn, for agreeing to read this behemoth. For always being willing to write reference letters for me, without which many of my academic and funding-related achievements would not have been possible, I thank Drs Caldwell, Aaron LeBlanc, and Alison Murray. Finally, I would especially like to thank Dr Tiago Simões for his mentorship over the past several years, starting with my BIOL 399 project and continuing to this day.

For their collaboration on certain chapters of this thesis, and for the associated scientific discussions and debates, I thank Drs Alessandro Palci and Mark D. Scherz. For numerous discussions—scientific and otherwise—throughout the course of my MSc, I would also like to thank the current and former members of the Caldwell lab, as well as my fellow vert-paleo graduate students.

I also thank the researchers, technical staff, and fellow seasonal lab technicians at the Royal Tyrrell Museum of Palaeontology, whom I was fortunate enough to learn from and work alongside during my summers in the Preparation Lab. My time at the RTMP was incredibly influential for me as a young palaeontologist, and as such I thank all of my colleagues there, especially Dr Lorna O'Brien for her mentorship over the years.

Although I was only able to arrange one museum visit before the COVID lockdown, the resulting data have been invaluable in enabling essentially all of the research presented herein. I therefore greatly thank José Rosado and Dr James Hanken of the Museum of Comparative Zoology at Harvard University for their assistance during my visit, Dr Stephanie Pierce for hosting me in her lab, and Dr Tiago Simões for his assistance at the MCZ and CNS.

I also thank the sources of funding that supported this research: the Natural Sciences and Engineering Research Council of Canada, via an Alexander Graham Bell Canada Graduate Scholarship – Master's (NSERC CGS-M); the Government of Alberta, via an Alberta Graduate Excellence Scholarship; the Departments of Biological Sciences and Earth & Atmospheric Sciences, via Graduate Teaching Assistantships; and my supervisor, Michael W. Caldwell, via his NSERC Discovery Grant.

Finally, and most importantly, to my family, whose love and support has meant more than I can put into words: thank you for everything.

TABLE OF CONTENTS

LIST OF TABLES

LIST OF FIGURES

LIST OF ABBREVIATIONS

Institutional Abbreviations

AMNH: American Museum of Natural History, New York, USA

AMS: Australian Museum, Sydney, Australia

CAS: California Academy of Sciences, San Francisco, USA

FMNH: Field Museum of Natural History, Chicago, USA

FRIM: Forest Research Institute Malaysia, Kuala Lumpur, Malaysia

KUH: University of Kansas Biodiversity Institute and Natural History Museum, Lawrence, USA

MCZ: Museum of Comparative Zoology, Harvard University, Cambridge, USA

QM: Queensland Museum, South Brisbane, Australia

SAMA: South Australian Museum, Adelaide, Australia

TCWC: Biodiversity Research and Teaching Collections, Texas A&M University, College Station, USA

TMM: Texas Memorial Museum of Science and History, University of Texas at Austin, Austin, USA

TNHC: Texas Natural History Collections, Texas Memorial Museum of Science and History, University of Texas at Austin, Austin, USA

UAMZ: University of Alberta Museum of Zoology, Edmonton, Canada

UF: Florida Museum of Natural History, University of Florida, Gainesville, USA

UMMZ: University of Michigan Museum of Zoology, Ann Arbor, USA

USNM: Smithsonian National Museum of Natural History, Washington DC, USA

UTA: University of Texas at Arlington, Arlington, USA

YPM: Yale Peabody Museum, New Haven, USA

ZSM: Zoologische Staatssammlung München, Munich, Germany

Anatomical Abbreviations

The reader is referred to the figure captions for anatomical abbreviations relevant to each figure.

CHAPTER ONE: GENERAL INTRODUCTION

Scolecophidians ('blindsnakes') form an assemblage of miniaturized and fossorial snakes, comprising three main lineages (Vidal *et al.* 2010): Typhlopoidea (Fig. 1.1; itself comprising the subclades Gerrhopilidae, Typhlopidae, and Xenotyphlopidae), Leptotyphlopidae (Fig. 1.2), and Anomalepididae (Fig. 1.3). Currently containing around 400 species (Vidal *et al.* 2010; Hedges *et al.* 2014), scolecophidians are known for exhibiting a "vexing mixture of primitive and derived characters" (Kley 2006:510), a phenomenon that has rendered enigmatic the evolution and anatomy of this group. A greater understanding of this assemblage is essential, however, as scolecophidians play a central role in historical perspectives on snake evolution (§1.1), in analyses of snake phylogeny (§1.2), and in hypotheses of the origin of snakes (§1.3). The many aspects of scolecophidian anatomy and evolution that remain understudied and poorly understood thus provide a strong impetus for the re-examination of this group.

1.1. Historical Context

Scolecophidians have long been considered the 'basal-most' group of snakes, even before the advent of formal phylogenetic analysis. In reading early studies of snake anatomy and evolution, the reasoning underlying this perspective becomes clear: These studies and their authors were functioning within a mindset shaped entirely by the modern biota, a scientific zeitgeist exacerbated by the fact that fossil snakes were not yet well-known (see also Caldwell 2007a, 2019). Thus, the extreme jaw elongation and mobility that occurs in the vast majority of extant snakes (i.e., macrostomy, or large-gaped feeding) was taken to be one of the defining features of Ophidia, characterizing 'typical' snakes (see e.g., Brock 1932; Brock 1941; Schmidt 1950; Bellairs & Underwood 1951; List 1966).

Scolecophidians—which, as 'microstomatans' (i.e., small-gaped squamates), do not conform to this jaw configuration—were therefore automatically assumed to be 'primitive' among snakes (see e.g., Brock 1932; Brock 1941; Bellairs & Underwood 1951; see also historical overviews in Rieppel 1988; Lee & Scanlon 2002; Caldwell 2007a, 2019). This assumption indeed harkens back to Müller's (1831) pre-evolutionary division of snakes into the 'Ophidia microstomata' (containing scolecophidians, anilioids, and the decidedly non-snake amphisbaenians) and 'Ophidia macrostomata' (reviewed in Rieppel 1988; Lee & Scanlon 2002; Caldwell 2019). Interestingly, some authors (e.g., McDowell & Bogert 1954) did not even consider scolecophidians to be snakes at all, but rather believed some or all of the scolecophidian

lineages to instead have undergone parallel evolution of a superficially snake-like bauplan (though see rebuttals by Underwood 1957; List 1966).

In light of this accepted 'primitive' status, many aberrant features of scolecophidians (e.g., the paired parietals: Fig. 1.3; Brock 1932; Mahendra 1936; List 1966; or the absence of the medial frontal pillars: Rieppel 1979a; Cundall & Irish 2008) were in turn also assumed to be plesiomorphic. Similarly, although several authors have recognized the many autapomorphies of the scolecophidian skull (and especially the jaws; e.g., Bellairs & Underwood 1951; Evans 1955; Underwood 1957; List 1966; Haas 1968; Rieppel 1979a, 1988; Rieppel & Head 2004; Cundall & Irish 2008; Rieppel *et al.* 2009; Rieppel 2012), these authors somewhat confusingly never contested the underlying presence of 'microstomy' across scolecophidians as plesiomorphic. Instead, the core assumption at the base of this paradigm persists: because scolecophidians are not macrostomatan, therefore they must be fundamentally 'primitive'; in other words, snake evolution reflects a fundamental and essentially linear progression toward macrostomy (see e.g., Rieppel 1984a, 1988; Cundall & Irish 2008; Wilson *et al.* 2010; Rieppel 2012; Ebel *et al.* 2020; see also discussions in Lee & Scanlon 2002; Vidal & Hedges 2002; Harrington & Reeder 2017; Caldwell 2019). The fact that scolecophidians are also fossorial has further reinforced this paradigm of their 'basal' nature (see §1.3; Rieppel 1978a; Haas 1979, 1980; Heise *et al.* 1995; Scanlon & Lee 2000; Caldwell 2007a, 2019), with fossorial snakes and non-snake lizards being considered an "intermediate series which completely bridge the gap" (Brock 1941:87) between 'typical'—i.e., non-fossorial—non-snake lizards and 'typical'—i.e., macrostomatan—snakes (see e.g., Brock 1941; Bellairs & Underwood 1951; Evans 1955; Conrad 2008).

Once established, this paradigm only became stronger over subsequent years, reinforced by the numerous phylogenetic analyses which recovered scolecophidians as the earliest-diverging group of snakes (see §1.2). Such a perspective continues to this day, with recent authors continuing to portray scolecophidians as morphologically homogenous and uniformly plesiomorphic (Wiens *et al.* 2012; Miralles *et al.* 2018), representing the closest extant representatives of the ancestral snake condition (Wiens *et al.* 2006; Wiens *et al.* 2012; Da Silva *et al.* 2018; Miralles *et al.* 2018).

Contradictions of this paradigm have historically been met with strong resistance (see overview of phylogenetic debate below; see also e.g., Rieppel & Zaher 2001a; Rieppel *et al.* 2003; Rieppel & Maisano 2007; Rieppel 2012); however, such heterodox oppositions

nonetheless persist. For example, Schmidt (1950) strongly rejected the notion of scolecophidians as 'primitive', instead considering them to be highly specialized and morphologically 'regressed' from a booid-pythonoid-like ancestor. This dissenting hypothesis is particularly notable in essentially foreshadowing more recent suggestions of scolecophidians as 'regressed macrostomatans', secondarily derived from an ancestrally macrostomate anatomy (e.g., Rage & Escuillié 2000; Lee & Scanlon 2002; Vidal & Hedges 2002; Kley 2006; Scanlon 2006; Palci & Caldwell 2010; Scanferla 2016; Caldwell 2019); however, this revival would not come until much later (see below). Similarly, Schmidt's (1950) proposal of scolecophidian convergence has also been rekindled, with recent authors increasingly advocating a perspective in which miniaturization, fossoriality, and 'microstomy' may have evolved independently among the major blindsnake lineages (e.g., Harrington & Reeder 2017; Caldwell 2019; Chretien *et al.* 2019; Fachini *et al.* 2020). Such a hypothesis—long suggested (e.g., Schmidt 1950), but only recently argued in notable depth—represents an intriguing avenue for further inquiry.

1.2. Phylogenetic Context

A core component of the controversy surrounding scolecophidians is their phylogenetic status (Fig. 1.4).

The first in-group phylogenetic hypothesis of snakes placed scolecophidians at the base of the snake tree (Mahendra 1938), a perspective echoed by many contemporaneous researchers (e.g., Walls 1940; Brock 1941; Walls 1942; Bellairs & Underwood 1951). Indeed, even authors who noted the highly aberrant morphology of scolecophidians (e.g., Bellairs & Underwood 1951; Evans 1955; Underwood 1957; List 1966; Haas 1968; Rieppel 1979a, 1988; Rieppel *et al.* 2003; Rieppel & Head 2004; Cundall & Irish 2008; Rieppel *et al.* 2009; Rieppel 2012) did not contest—and in fact actively advocated—this phylogenetically basal position (Fig. 1.4a,c; see e.g., Bellairs & Underwood 1951; Evans 1955; List 1966; Haas 1979; Rieppel 1979a; Haas 1980; Rieppel 1988; Cundall *et al.* 1993; Rieppel *et al.* 2003; Rieppel 2012). These authors reasoned that, although scolecophidians are in many ways quite autapomorphic, they still exhibit many plesiomorphic features, such as an undivided trigeminal foramen, no medial frontal pillars, an immobile mandibular symphysis, a coronoid, paired parietals, and rudimentary pelvic elements (Figs 1.1–1.3; McDowell & Bogert 1954; Evans 1955; List 1966; Rieppel 1979a; though see Caldwell 2019 for a rebuttal of many of these proposed symplesiomorphies).

Furthermore, because they are cladistically uninformative, these autapomorphies were sometimes disregarded entirely in discussions of snake phylogeny and origins (e.g., Rieppel & Zaher 2001a), thus returning the focus to the aforementioned 'primitive' nature of scolecophidians. Altogether, from this perspective, scolecophidians may be quite aberrant but ultimately remain fundamentally basal among snakes (Fig. 1.4a).

Although this view has never been universal (e.g., Schmidt 1950), for many decades it has prevailed as a near-consensus portraying scolecophidians as an early-diverging lineage fundamentally separate from all other snakes. Again, this dichotomy between scolecophidians and other snakes was first advanced prior to formal phylogenetic analysis (e.g., Brock 1932; Mahendra 1938; Brock 1941; McDowell & Bogert 1954; Rieppel 1979a; see also historical overviews in Rieppel 1988; Lee & Scanlon 2002), but in the ensuing years nearly every phylogeny has recovered this arrangement (Fig. 1.4a,c,d; e.g., Rieppel 1988; Cundall *et al.* 1993; Heise *et al.* 1995; Zaher 1998; Caldwell 1999; Zaher & Rieppel 1999a; Tchernov *et al.* 2000; Rieppel *et al.* 2002; Slowinski & Lawson 2002; Vidal & Hedges 2002; Zaher & Rieppel 2002; Townsend *et al.* 2004; Vidal & Hedges 2004; Conrad 2008; Wiens *et al.* 2008; Vidal *et al.* 2009; Wiens *et al.* 2010; Wiens *et al.* 2012; Pyron *et al.* 2013; Reeder *et al.* 2015; Figueroa *et al.* 2016; Streicher & Wiens 2016; Zheng & Wiens 2016; Miralles *et al.* 2018; Burbrink *et al.* 2020; Singhal *et al.* 2021).

It was not until the discovery and phylogenetic analysis of several key fossil snakes that this dichotomy began to be widely questioned. Particularly, the placement of *Pachyrhachis*, *Eupodophis*, *Haasiophis*, *Wonambi*, and *Yurlunggur* (i.e., extinct macrostomate snakes; Rage & Escuillié 2000; Tchernov *et al.* 2000; Lee & Scanlon 2002; Scanlon 2006; Caldwell 2007a) in positions diverging basally to scolecophidians (Fig. 1.4b; e.g., Caldwell & Lee 1997; Lee & Caldwell 1998; Caldwell 2000; Rage & Escuillié 2000; Scanlon & Lee 2000; Lee & Scanlon 2002; Lee 2005; Scanlon 2006; Palci & Caldwell 2010; Palci *et al.* 2013a; Palci *et al.* 2013b; Caldwell *et al.* 2015; Simões *et al.* 2018; Garberoglio *et al.* 2019a; Garberoglio *et al.* 2019b) provided the first indication since Schmidt (1950) that scolecophidians may reflect a secondarily derived assemblage, not a 'primitive' one (see also discussions in Scanlon & Lee 2000; Lee & Scanlon 2002; Caldwell 2007a; Palci & Caldwell 2010; Caldwell 2019). As mentioned above, these phylogenetic hypotheses were immediately met with strong disagreement, leading to a lengthy debate as to the 'true' position of fossil snakes (and, in turn, scolecophidians).

This debate involved two major camps (reviewed extensively in Rieppel *et al.* 2003; Caldwell 2007a, 2019). On one side, Caldwell, Lee, and others (see references above) advocated an early-diverging position of various fossil taxa, reflecting a non-scolecophidian (i.e., non-fossorial, non-microstomatan) ancestry of snakes (Fig. 1.4b; see also §1.3). On the other side, Rieppel, Zaher, and colleagues (e.g., Zaher 1998; Zaher & Rieppel 1999a; Tchernov *et al.* 2000; Rieppel & Zaher 2001a; Rieppel *et al.* 2002; Zaher & Rieppel 2002; Rieppel *et al.* 2003; Rieppel & Head 2004) argued for a position of *Pachyrhachis*, *Eupodophis*, *Haasiophis*, and *Yurlunggur* alongside extant macrostomatans, thus preserving the perspective of scolecophidians as fundamentally basal to all other snakes and the paradigm of a fossorial, miniaturized, and 'microstomatan' origin of snakes (Fig. 1.4c; see also §1.3).

Molecular phylogenies have further complicated the debate, particularly in their typical (though not quite universal; see Slowinski & Lawson 2002; Vidal & Hedges 2002, 2004) recovery of scolecophidians as paraphyletic (Fig. 1.4d; e.g., Heise *et al.* 1995; Wiens *et al.* 2008; Vidal *et al.* 2009; Vidal *et al.* 2010; Wiens *et al.* 2010; Wiens *et al.* 2012; Pyron *et al.* 2013; Hsiang *et al.* 2015; Figueroa *et al.* 2016; Streicher & Wiens 2016; Zheng & Wiens 2016; Miralles *et al.* 2018; Burbrink *et al.* 2020; Singhal *et al.* 2021). In contrast, morphological phylogenies typically recover scolecophidians as monophyletic (Fig. 1.4a–c,e; e.g., Cundall *et al.* 1993; Scanlon & Lee 2000; Tchernov *et al.* 2000; Lee & Scanlon 2002; Scanlon 2006; Gauthier *et al.* 2012; Palci *et al.* 2013a; Palci *et al.* 2013b; Caldwell *et al.* 2015:fig. 4a; Hsiang *et al.* 2015; Garberoglio *et al.* 2019a:fig. 3), in many cases indeed necessitating this result *a priori* by incorporating Scolecophidia as a single terminal taxon (e.g., Caldwell & Lee 1997; Lee 1997; Lee & Caldwell 1998; Zaher 1998; Caldwell 1999; Zaher & Rieppel 1999a; Caldwell 2000; Rieppel *et al.* 2002; Zaher & Rieppel 2002; Apesteguía & Zaher 2006; Palci & Caldwell 2010; Wilson *et al.* 2010; Zaher & Scanferla 2012; Scanferla *et al.* 2013; Caldwell *et al.* 2015:fig. 4b; Garberoglio *et al.* 2019b). Combined-data approaches variously support either scolecophidian monophyly (e.g., Lee 2005; Hsiang *et al.* 2015) or paraphyly (e.g., Wiens *et al.* 2010; Reeder *et al.* 2015; Garberoglio *et al.* 2019a:fig. 4).

Finally, the most recently published morphology-based snake phylogeny presents an even greater challenge to the traditional view of scolecophidian phylogeny (Fig. 1.4e). Although some of the analyses of Garberoglio *et al.* (2019a) recovered scolecophidians as diverging earliest among extant snakes (Garberoglio *et al.* 2019a:figs 4 and S4–5), a number of their phylogenies

nested scolecophidians among anilioids (Fig. 1.4e; Garberoglio *et al.* 2019a:figs 3 and S6) or even as the sister group to the 'macrostomatan' *Python* (Garberoglio *et al.* 2019a:figs S2–3). Caldwell (2000) and Palci & Caldwell (2010) had earlier obtained similar results, with Macrostomata diverging rootward of scolecophidians and anilioids among extant snakes. Such results thus reinforce that the phylogenetic position of scolecophidians among snakes is yet to be resolved.

1.3. Hypotheses of the Origins of Snakes

The ancestral ecology of snakes has long been debated, with various authors advocating aquatic, fossorial, or surface-terrestrial origins (see also reviews in Rieppel 1988; Caldwell 2007a, 2019). Scolecophidians play an integral role in this debate, as their anatomy and phylogenetic position have often been used to defend a burrowing ancestry of snakes, the most widely-held hypothesis of snake origins (see also Rieppel 1978a, 1988; Simões *et al.* 2015; Caldwell 2019).

1.3.1. Aquatic origins

The aquatic origins hypothesis derives mainly from overinterpretations of proposed similarities between snakes and mosasauroids. These similarities were first noted by Cope (1869; reviewed in Caldwell 2007, 2019), who considered mosasauroids (the Pythonomorpha of Cope 1869) to be the closest relatives of snakes, a hypothesis supported by many later phylogenies (e.g., Caldwell & Lee 1997; Lee 1997; Lee & Caldwell 1998; Caldwell 1999; Lee 2005; Palci & Caldwell 2010; Reeder *et al.* 2015). However, it is essential to note that Cope (1869) never argued that snakes evolved directly from mosasaurs; despite later characterizations of Cope's argument (e.g., Bellairs & Underwood 1951; Rieppel 2012), all Cope ever proposed was that mosasauroids constitute the sister-group of snakes (McDowell & Bogert 1954; Rieppel 1988; Caldwell 2007a, 2019). Such a relationship does not mean that snakes evolved from mosasaurs, nor that the ancestor of this group was necessarily mosasaur-like or even aquatic; all this relationship means is that snakes share a most recent common ancestor with an aquatic lineage (Rieppel 1988; Caldwell 2019). As argued by Caldwell (2019), the characterization of Cope's (1869) hypothesis—and of subsequent phylogenies that recovered snakes as the sister group of mosasauroids (see references above)—as strictly advocating an aquatic origin of snakes is a fundamental misrepresentation.

Rather than this problematic interpretation, more valid evidence for an aquatic origin of snakes may be derived from the proposed aquatic habits of several extinct snakes (e.g., *Haasiophis*, *Pachyrhachis*; Caldwell & Lee 1997; Lee & Caldwell 1998; Caldwell 2000; Tchernov *et al.* 2000; Lee & Scanlon 2002). Analyses recovering snakes as nested within mosasauroids (e.g., Lee 2005, 2009; Palci & Caldwell 2010)—rather than simply as their sister group—also support an aquatic ancestry of snakes.

1.3.2. Burrowing origins

The burrowing origins scenario originated with the placement of scolecophidians as the earliest-diverging group in the first snake phylogeny (Mahendra 1938; reviewed in Rieppel 1988; Caldwell 2019), and was reinforced by the recognition that the assumedly-primitive scolecophidians (see §1.1) shared many features with fossorial non-snake lizards, such as skinks and amphisbaenians (Brock 1941; Bellairs & Underwood 1951). However, this hypothesis truly gained prominence based on observations of the snake eye. Walls (1940, 1942) documented distinct differences in the ocular structure of snakes relative to non-snake lizards, interpreting this as evidence of extensive regeneration of the eye following a highly degenerate, vision-reduced, burrowing phase marking the origin of snakes. The platytrabic condition of the snake skull (see Cundall & Irish 2008:360–363) has also been interpreted in this light, with the modified structure of the snake orbit relative to non-snake lizards—and particularly the absence of several orbital cartilages—being viewed as evidence of loss or heavy reduction of the orbit ancestrally in snakes, followed by re-appearance of this structure (Cundall & Irish 2008:362–363); this interpretation clearly implies the fossorial origins scenario advocated by these authors (see e.g., Cundall & Irish 2008:353). The lateral enclosure of the braincase via the frontals and parietals has also been interpreted as an adaptation for protecting the brain during head-first burrowing (Brock 1941; Bellairs & Underwood 1951; Irish 1989; Cundall & Irish 2008).

From a phylogenetic perspective, the widely-accepted position of scolecophidians and anilioids—i.e., fossorial and semi-fossorial taxa—at the base of Ophidia (Fig. 1.4a,c,d) plays a major role in supporting a burrowing origins scenario (see e.g., Rieppel 1978a; Haas 1979, 1980; Cundall *et al.* 1993; Heise *et al.* 1995; Wiens *et al.* 2006; Reeder *et al.* 2015; Miralles *et al.* 2018; Ebel *et al.* 2020). Despite the differences among scolecophidians (e.g., divergent jaw anatomies; Haas 1964, 1968; Rieppel 1979a, 1988; Cundall & Irish 2008), the fact that fossoriality, microstomy, and miniaturization are all present in some form or another across

scolecophidians and anilioids has been taken to reflect a fossorial, microstomatan, and miniaturized origin of snakes (Bellairs & Underwood 1951; Evans 1955; Haas 1979, 1980; Rieppel 1988; Cundall *et al.* 1993; Cundall & Irish 2008; Rieppel 2012; Yi & Norell 2015; Miralles *et al.* 2018; Ebel *et al.* 2020). In particular, the molecular- and combined-data-based recovery of scolecophidians as a paraphyletic assemblage at the base of Ophidia (Fig. 1.4d) strongly supports, at least superficially, a scolecophidian-like ancestral snake condition (Wiens *et al.* 2012; Simões *et al.* 2015; Miralles *et al.* 2018; Ebel *et al.* 2020; Singhal *et al.* 2021). These phylogenetic interpretations, alongside the aforementioned anatomical observations, have resulted in the burrowing origins scenario becoming "an almost orthodox view" (Rieppel 1988:96) of snake evolution (see also discussions in Rieppel 1978a, 1988; Scanlon & Lee 2000; Simões *et al.* 2015; Caldwell 2019).

However, these lines of evidence are not as definitive as they appear. Recent re-examination of the snake eye has suggested that ancestrally this structure was not as degenerate as traditionally thought, and especially not as reduced as the condition in scolecophidians (Simões *et al.* 2015). Importantly, of the five visual opsin genes examined by Simões *et al.* (2015), non-snake lizards—including fossorial non-snake lizards—typically possess all five (*rh1*, *rh2*, *sws2*, *sws1*, and *lws*), most snakes possess three (*rh1*, *sws1*, and *lws*), and some snakes (scolecophidians and *Anilius*) only have one (*rh1*); thus, if the ancestral snake were scolecophidian-like, the opsins *sws1* and *lws* would have had to evolve completely *de novo* in alethinophidians, a highly unlikely scenario (Simões *et al.* 2015). Simões *et al.* (2015) further interpreted *sws1* and *lws* as being lost convergently in scolecophidians and *Anilius*, in turn arguing for the absence of these genes—and the occurrence of fossoriality—as a secondarily derived condition relative to the ancestral snake. Optic reduction in snakes relative to other squamates has also been associated with nocturnality, rather than strictly fossoriality (Rieppel 1978b, 1988; see also Hsiang *et al.* 2015). Ultimately, this contrasting perspective posits that scolecophidians are in fact an extremely specialized and non-ancestral assemblage, and that neither an extremely degenerate eye structure nor extreme fossoriality characterized the ancestral snake (Schmidt 1950; Simões *et al.* 2015; see also Caldwell 1999; Harrington & Reeder 2017).

Furthermore, the same authors who interpreted the platytrabic skull structure in snakes as suggesting ancestral orbital reduction (Cundall & Irish 2008:362–363) also noted that this condition is consistent with paedomorphosis, reflecting developmental truncation of the

chondrocranium and orbital cartilages (Irish 1989; Cundall & Irish 2008:362; see also Brock 1941; Rieppel 1984b, 1988). Heterochrony (i.e., evolutionary changes in developmental timing and/or rate; Gould 1977; McNamara 1986) has been suggested, especially recently, as a major factor shaping the origins and evolution of snakes (see §1.4.2; e.g., Irish 1989; Palci *et al.* 2013b; Werneburg & Sánchez-Villagra 2015; Da Silva *et al.* 2018; Caldwell 2019). In the context of the orbital structure, this pervasive heterochronic modification thus suggests that fossoriality need not be invoked to explain the origins of the snake bauplan.

Finally, rather than an adaptation for protection during burrowing, the lateral enclosure of the braincase has alternatively been interpreted as protecting the brain during the consumption of large-bodied and/or actively struggling prey items (Bellairs & Underwood 1951; Rieppel 1978b; Cundall & Irish 2008; Palci & Caldwell 2010), or as a consolidation important in suspending the mobile jaws and snout (Rieppel 1978b, 1996). The notable reduction in braincase ossification that occurs in some scolecophidians (e.g., *Myriopholis macrorhyncha*, *M. tanae*, C.S. pers. obs.; see also Mahendra 1936; Haas 1964; List 1966:8–9 and plate 7, fig. 3; Cundall & Irish 2008:374–375, 381, and fig. 2.12), alongside the incomplete enclosure of the braincase in highly fossorial non-snake lizards such as *Dibamus* (Rieppel 1984b), further supports the notion that a fully enclosed braincase is not directly or necessarily tied to fossoriality (see also Cundall & Irish 2008).

The anatomical evidence for a fossorial origin of snakes is thus equivocal; however, equally important evidence lies in the phylogeny of snakes. Notably, although scolecophidians have long been recovered or hypothesized as diverging earliest among snakes (Fig. 1.4a,c,d; see above), this phylogenetic perspective on snake origins has also been questioned. As noted above, scolecophidians are increasingly being recovered as diverging later than their typical basal position among Ophidia, particularly when fossil taxa are incorporated (Fig. 1.4b,e; e.g., Caldwell & Lee 1997; Lee & Caldwell 1998; Caldwell 2000; Scanlon & Lee 2000; Lee & Scanlon 2002; Lee 2005; Apesteguía & Zaher 2006; Scanlon 2006; Palci & Caldwell 2010; Gauthier *et al.* 2012; Zaher & Scanferla 2012; Palci *et al.* 2013a; Scanferla *et al.* 2013; Caldwell *et al.* 2015; Simões *et al.* 2018; Garberoglio *et al.* 2019a; Garberoglio *et al.* 2019b), an outcome that invalidates scolecophidians as directly reflecting the origin of snakes. The similarities between snakes and fossorial non-snake lizards have also widely been considered convergent (e.g., Rieppel 1984b; Estes *et al.* 1988; Rieppel 1988; Lee 1998; Rieppel *et al.* 2003; Townsend

et al. 2004; Wiens *et al.* 2006; Wiens *et al.* 2010; Müller *et al.* 2011; Reeder *et al.* 2015; Da Silva *et al.* 2018; Ebel *et al.* 2020), thus invalidating the notion of a sister-group relationship between snakes and dibamids and/or amphisbaenians (though see a defense of this hypothesis by Conrad 2008). Several authors have further cautioned against interpreting scolecophidian paraphyly as evidence of a scolecophidian-like origin of snakes, emphasizing that the unique nature of these snakes relative both to each other and to other squamates precludes this simple extrapolation of scolecophidian morphologies as ancestral (Simões *et al.* 2015; Harrington & Reeder 2017; Palci *et al.* 2017; Caldwell 2019; Chretien *et al.* 2019).

These contradictory phylogenetic and anatomical interpretations thus present several causes for questioning the burrowing origins hypothesis, particularly in terms of the role scolecophidians play in it.

1.3.3. Surface-terrestrial origins

The final proposed scenario for the origin of snakes involves a surface-terrestrial paleoecology. This hypothesis can be traced back to the early twentieth century, particularly the works of Janensch (1906) and Camp (1923), who proposed a surface-dwelling or perhaps 'grass-swimming' ecology (reviewed in Rieppel 1988; Caldwell 2007a, 2019). However, because much of the debate over the origins of snakes has centred on the aforementioned burrowing *versus* aquatic scenarios, this terrestrial hypothesis has been comparatively neglected until recently (see also Caldwell 2007a, 2019).

Nevertheless, this hypothesis has recently started to become more widespread. For example, Hsiang *et al.* (2015) reconstructed the ancestral ecology of snakes as terrestrial, favouring a surface-terrestrial interpretation (although they were ultimately unable to rule out fossoriality or semi-fossoriality). Similarly, based on morphometric analyses of skull shape and size, Da Silva *et al.* (2018) reconstructed a surface-terrestrial ecomorphology for the ancestor of snakes and their sister group, followed by a transition to fossoriality at the origin of crown snakes.

Finally, the fossil snake *Najash* has largely been recovered as diverging earliest, or nearly earliest, among snakes, often accompanied by *Dinilysia* (Fig. 1.4e; Apesteguía & Zaher 2006; Gauthier *et al.* 2012; Zaher & Scanferla 2012; Scanferla *et al.* 2013; Hsiang *et al.* 2015; Simões *et al.* 2018; Garberoglio *et al.* 2019a). The early-diverging position of these taxa—both discovered in terrestrial deposits (Apesteguía & Zaher 2006; Garberoglio *et al.* 2019a;

Garberoglio *et al.* 2019b), and neither likely to be fossorial due to their large size, among other features (Palci *et al.* 2013a)—in turn suggests a surface-terrestrial origin of snakes (Zaher & Scanferla 2012; Caldwell 2019). Even if these taxa did exhibit some degree of fossoriality, as has been suggested by previous authors (e.g., Rieppel 1978b; Apesteguía & Zaher 2006; though see rebuttal by Palci *et al.* 2013a), this would likely have been similar to the semi-fossorial habits exhibited by many anilioids (e.g., *Cylindrophis*, as discussed by Rieppel 1978b; or *Anilius*, a comparative taxon emphasized by Garberoglio *et al.* 2019b). In anilioids, this semi-fossoriality involves fairly generalized movement through loose soil or leaf litter (Rieppel 1978b), quite distinct from the extensive fossoriality exhibited by scolecophidians and thus still more consistent with a broadly surface-dwelling—rather than purely fossorial—ecology (see also Palci *et al.* 2017).

1.4. Research Approach and Objectives

In light of the preceding overview, it is evident that scolecophidians are central to our understanding of the origins and evolution of snakes, yet simultaneously understudied and subject to competing perspectives and interpretations. Although this thesis does not aim to resolve the origin of snakes (an undertaking far beyond the capacity of any single researcher or thesis), it does aim to examine the status of scolecophidians in relation to this evolutionary transition. Below I describe the methodological and conceptual framework shaping this thesis, as well as the major research questions I aim to address.

1.4.1. Methodological framework

Methodologically, the ensuing research is based primarily on the examination of micro-computed tomography (micro-CT) scans of a broad sampling of squamates, focussing on scolecophidians (see relevant tables in each chapter for specimens; see Appendix 1.1 for sources of scan data). This approach is borne partly out of necessity, due to the pandemic-related logistical constraints under which most of this research was conducted. However, more importantly, this approach is also important in addressing shortcomings affecting much of the existing scolecophidian-related literature.

Primarily, when studying the evolution of the snake skull, form is inextricably linked to function (Cundall & Irish 2008; Rhoda *et al.* 2021); indeed, many of the controversies outlined above concern the interaction of functional morphology and anatomical evolution. However,

studies of both form and function in snakes have historically been hampered by the very anatomy in question (see also Cundall & Irish 2008). Many snakes exhibit loosely connected and highly kinetic skulls, meaning that anatomical relationships among skull elements often become distorted in dried skeletal remains (Cundall & Irish 2008); furthermore, for small organisms, skeletal specimens can also be quite fragile and many sutures quite difficult to observe (List 1966; Cundall & Irish 2008).

Previous authors have addressed these issues by using serially sectioned or cleared-and-stained specimens (Cundall & Irish 2008; e.g., Brock 1932; Mahendra 1936; Evans 1955; Haas 1964; List 1966; Haas 1968). However, these approaches carry their own limitations, such as inaccuracies in staining (e.g., cartilaginous structures that stain in the same manner as bone, as noted by Evans 1955) or extensive distortion in the resulting anatomical reconstructions (see e.g., the rather absurdly wavy anomalepidid skulls figured by Haas 1964; 1968 based on serial sections). These disparate visualization methods can also produce quite different reconstructions and interpretations of the same anatomy (compare e.g., Cundall & Irish 2008:fig. 2.13A to Cundall & Irish 2008:fig. 2.13B).

Relative to these traditional techniques, digital technologies such as micro-CT scanning provide an essential alternative. Micro-CT scans reveal both internal and external morphology, are much less distorted than dried or serially sectioned remains, and are particularly well-suited for the study of very small organisms. My extensive use of these scans throughout this thesis thus represents an important approach to understanding scolecophidian anatomy, especially because much of our current understanding of these snakes stems from classical descriptions based on the aforementioned techniques (e.g., Evans 1955; Haas 1964; List 1966; Haas 1968). These advantages are particularly evident when assessing anatomy in relation to functional morphology (see Chapters 3 and 4), and in enabling the detailed observations necessary for the phylogenetic analysis of miniaturized taxa such as scolecophidians (see Chapter 5).

1.4.2. Conceptual framework

Conceptually, a core theme uniting this research is that of evolutionary development, particularly in terms of examining the potential role of evolutionary developmental processes in shaping snake—and especially scolecophidian—evolution. Popularized by S. J. Gould in his seminal work *Ontogeny and Phylogeny* (Gould 1977), the field of evolutionary developmental biology (colloquially, evo-devo) explores the interface between ontogeny, morphology, and

macroevolution, using a diverse range of research programmes to examine how developmental pathways evolve and themselves influence evolution (Hanken 1984; McNamara 1986; Müller 2007; Hanken 2015). These research programmes include developmental genetics, epigenetics, theoretical ontogeny, and—of particular relevance to the current thesis—the study of heterochrony (Müller 2007).

Heterochrony refers to evolutionary changes in the rate and/or timing of developmental events (Gould 1977; Alberch *et al.* 1979; McNamara 1986; Müller 2007). Using a comparative anatomical and ontogenetic framework, this subset of evo-devo involves the study of developmental pathways in both extant and extinct organisms, viewing changes in these pathways as one of the key mechanisms underlying morphological diversity (Gould 1977; McNamara 1986; Reilly *et al.* 1997; Müller 2007).

Heterochronic change can occur via two basic modes: paedomorphosis and peramorphosis (Gould 1977; Alberch *et al.* 1979; McNamara 1986; Reilly *et al.* 1997). Paedomorphosis describes developmental events that are decelerated, delayed, or truncated relative to an ancestral ontogenetic trajectory; these shifts occur via the processes of neoteny (deceleration *sensu* Reilly *et al.* 1997), post-displacement, and progenesis (hypomorphosis *sensu* Reilly *et al.* 1997), respectively, and cause adults of a descendant taxon to exhibit features typical of earlier ontogenetic stages of ancestral taxa (Gould 1977; Alberch *et al.* 1979; Hanken 1984; McNamara 1986; Wake 1986; Irish 1989; Hanken & Wake 1993; Reilly *et al.* 1997). In contrast, peramorphosis (recapitulation *sensu* Gould 1977) describes development that occurs at a faster rate (via acceleration), begins earlier (via pre-displacement), or lasts longer (via hypermorphosis) than the plesiomorphic ontogenetic trajectory, causing adults of a descendant taxon to be 'over-developed' relative to adults of ancestral taxa (Gould 1977; Alberch *et al.* 1979; McNamara 1986; Irish 1989; Reilly *et al.* 1997). As indicated by these definitions, the study of heterochrony inherently requires both ontogenetic and phylogenetic context, as evolutionary changes in development can only be identified if the plesiomorphic developmental sequence is known (Gould 1977; McNamara 1986; Irish 1989; Hanken & Wake 1993; Rieppel 1996; Reilly *et al.* 1997).

Heterochrony has increasingly been considered a key factor in squamate macroevolution, having been hypothesized as one of the major mechanisms influencing not only the evolution of snakes relative to other squamates (Irish 1989; Palci *et al.* 2013b; Werneburg & Sánchez-

Villagra 2015; Da Silva *et al.* 2018), but also the diversification of snakes relative to each other (Da Silva *et al.* 2018). Of the different types of heterochrony, paedomorphosis is particularly relevant to scolecophidians, especially in the context of the aforementioned hypothesis of a 'regressive' evolution of this group (Schmidt 1950; Kley 2006; Scanferla 2016; Caldwell 2019). For example, many of the distinguishing features of scolecophidians—such as the edentulous and morphologically simple pterygoid and palatine, as well as the anteriorly oriented quadrate—have been interpreted as retentions of the embryonic conditions of these elements in other squamates (Kley 2006; Caldwell 2019). Thus, the hypothesis of scolecophidians as 'regressed macrostomatans' is essentially a hypothesis of scolecophidians as highly paedomorphic macrostomatans, in which the retention of ancestrally embryonic or juvenile features has led to a derived—or 'regressed'—loss of macrostomy. This potential manifestation of evo-devo in scolecophidian evolution is certainly intriguing; however, except for Kley's (2006) revival of Schmidt's (1950) 'regressive evolution' hypothesis, subsequent rebuttals by Rieppel & Maisano (2007) and Rieppel (2012), and recent heterochrony-related contributions by Palci *et al.* (2016), Scanferla (2016), Da Silva *et al.* (2018), Strong *et al.* (2019), and especially Caldwell (2019), this hypothesis ultimately remains under-explored.

Finally, paedomorphosis is also relevant herein in terms of its connection to miniaturization, a phenomenon affecting scolecophidians quite extensively (Caldwell 2019; Chretien *et al.* 2019). Defined as a phylogenetic decrease in body size (Hanken 1984; Rieppel 1984a, 1988), typically extensive enough to cause distinct morphological and physiological modification (Hanken & Wake 1993; Rieppel 1996; Fröbisch & Schoch 2009), miniaturization is often considered to be caused by—or at least strongly correlated with—paedomorphosis, specifically via the process of progenesis (Gould 1977; Hanken 1984; Wake 1986; Hanken & Wake 1993; Rieppel 1996). Hanken (1984) formalized this connection via his proposed 'null hypothesis of miniaturization', according to which morphological reduction, variability, and novelty together reflect paedomorphosis-driven size decrease (see also Hanken & Wake 1993).

Often co-occurring with fossoriality (Rieppel 1984a; Wake 1986; Rieppel 1996; Maddin *et al.* 2011; Olori & Bell 2012), miniaturization has been hypothesized alongside burrowing to explain the origin of snakes, including key features such as limb reduction and enclosure of the braincase (Rieppel 1984a, 1988, 1996). This hypothesis of an ancestrally miniaturized and fossorial snake bauplan is of course compatible with the traditional position of scolecophidians—

which are themselves highly miniaturized fossors—as basally diverging among snakes, although this interpretation has been contested (e.g., Caldwell 2019; Chretien *et al.* 2019; Fachini *et al.* 2020). Miniaturization and paedomorphosis are also important to consider from a phylogenetic perspective, as both phenomena are strongly associated with homoplasy (Rieppel 1988; Hanken & Wake 1993; Rieppel 1996; Rieppel & Zaher 2000; Olori & Bell 2012; Chretien *et al.* 2019), and indeed may play a major role in confounding phylogenetic analysis (Gauthier *et al.* 1988a; Hanken & Wake 1993; Wiens *et al.* 2005; Struck 2007; though see Fröbisch & Schoch 2009). The degree of miniaturization among scolecophidians, combined with the proposed evolutionary developmental basis of this phenomenon, thus presents another example of how evo-devo might provide novel insight into the anatomy and evolution of these enigmatic snakes.

1.4.3. Research questions

Via this research framework, I ultimately use three major questions to guide this thesis:

First, are scolecophidians indeed fundamentally distinct from—and 'basal' to—alethinophidians (see e.g., Rieppel 1988 and other references in §1.2), or is it instead reasonable to hypothesize the derivation of scolecophidians from an alethinophidian-like bauplan (e.g., Kley 2006; Palci & Caldwell 2010; Scanferla 2016; Caldwell 2019; Garberoglio *et al.* 2019a)?

Second, is microstomy truly structurally and functionally consistent across non-snake lizards, scolecophidians, and anilioids, thus reflecting a fundamentally plesiomorphic condition characterizing the ancestor of snakes (e.g., Bellairs & Underwood 1951; Rieppel 1984a, 1988; Cundall & Irish 2008; Rieppel 2012; Miralles *et al.* 2018); or does jaw evolution instead follow a more complex evolutionary path among squamates (e.g., Rage & Escuillié 2000; Lee & Scanlon 2002; Vidal *et al.* 2009; Palci & Caldwell 2010; Scanferla 2016; Harrington & Reeder 2017; Caldwell 2019; Chretien *et al.* 2019; Burbrink *et al.* 2020)?

Finally, what is the phylogenetic status of scolecophidians among snakes? Do they diverge basally (Fig. 1.4a,c,d; e.g., Rieppel 1988; Cundall *et al.* 1993; Zaher 1998; Zaher & Rieppel 1999a; Tchernov *et al.* 2000; Rieppel *et al.* 2002; Conrad 2008; and all molecular phylogenies) or occupy a more deeply nested position (Fig. 1.4b,e; e.g., Caldwell & Lee 1997; Caldwell 2000; Scanlon & Lee 2000; Apesteguía & Zaher 2006; Palci & Caldwell 2010; Zaher & Scanferla 2012; Garberoglio *et al.* 2019a)? Are they monophyletic (as in morphological and some combined-data phylogenies; see §1.2 and Fig. 1.4a–c,e), paraphyletic (as in molecular and

some combined-data phylogenies; see §1.2 and Fig. 1.4d), or even polyphyletic (suggested by Caldwell 2019)?

By examining these questions, I aim to provide insight into scolecophidian anatomy and evolution, with inherent implications for our understanding of the origins and evolution of snakes more broadly.

1.5. Organization of Chapters

In Chapter Two, I assess the traditional hypothesis of a fundamental dichotomy between scolecophidians and alethinophidians. Focussing on the genus *Atractaspis* (a fossorial colubroid), I examine the possibility that scolecophidians may be 'regressed alethinophidians'. As a fossorial but non-miniaturized colubroid, deeply nested among snakes, *Atractaspis* presents an interesting comparison to the miniaturized, fossorial, and assumedly 'basal' scolecophidians, particularly in terms of evaluating the role of miniaturization-related heterochrony in the evolution of the scolecophidian body plan.

In Chapters Three and Four, I examine the evolution of 'microstomy' across squamates from different but complementary perspectives, thus testing the traditional hypothesis that microstomy is fundamentally consistent across squamates and plesiomorphic for snakes.

Chapter Three implements a homology-based approach to evaluate the evolution of the mandibular, suspensorial, and palatomaxillary anatomy across purported 'microstomatans' (i.e., non-snake lizards, anilioids, and typhlopoid, anomalepidid, and leptotyphlopid scolecophidians). I assess the primary homology of key features across these groups, develop a framework for conceptualizing and testing the homology of overall morphofunctional complexes (i.e., 'morphotypes'), and compare the impacts of different hypotheses of homology on higher-level ancestral state reconstructions. I also discuss the implications of these findings for the overall evolution of scolecophidians.

Chapter Four examines squamate skull anatomy via anatomical network analysis, a recently-developed method for quantifying modularity (Rasskin-Gutman & Esteve-Altava 2014). I use specific patterns of connectivity among skull elements to assess 'microstomy' from a quantitative perspective, thus testing my conclusions from Chapter Three. I also use various morphospace-based comparisons to explore the role of fossoriality- and miniaturization-based convergence in squamate—and particularly scolecophidian—evolution.

In Chapter Five, I examine several aspects of scolecophidian phylogeny. First, I present a revised dataset for use in future phylogenetic analyses. Modified heavily from the most recently published snake phylogeny (Garberoglio *et al.* 2019a), this dataset serves both to remediate the logical and methodological inconsistencies affecting previous analyses, and to introduce several characters relevant to scolecophidian anatomy and systematics. I next present preliminary maximum parsimony and Bayesian analyses of this dataset, using a matrix scored almost entirely from scratch and covering a broad taxonomic range of snakes, including a dense sampling of scolecophidians. Due to pandemic-related limitations on specimen access, it was not possible to incorporate extinct taxa into this analysis; as such, I also examine the impact of inclusion *versus* exclusion of fossil taxa based on the dataset of Garberoglio *et al.* (2019a), in order to assess the reliability of the novel phylogenies produced in this chapter. Finally, I critically examine proposed scolecophidian synapomorphies and symplesiomorphies, with a discussion of implications for the phylogeny of scolecophidians and snakes more broadly.

Chapter Six presents my overall conclusions regarding scolecophidian anatomy and evolution, with a focus on the overarching questions and hypotheses presented in Chapter One. I discuss implications for the role of scolecophidians in informing the origin of snakes, and end with suggestions for future research directions.

Figures: Chapter One

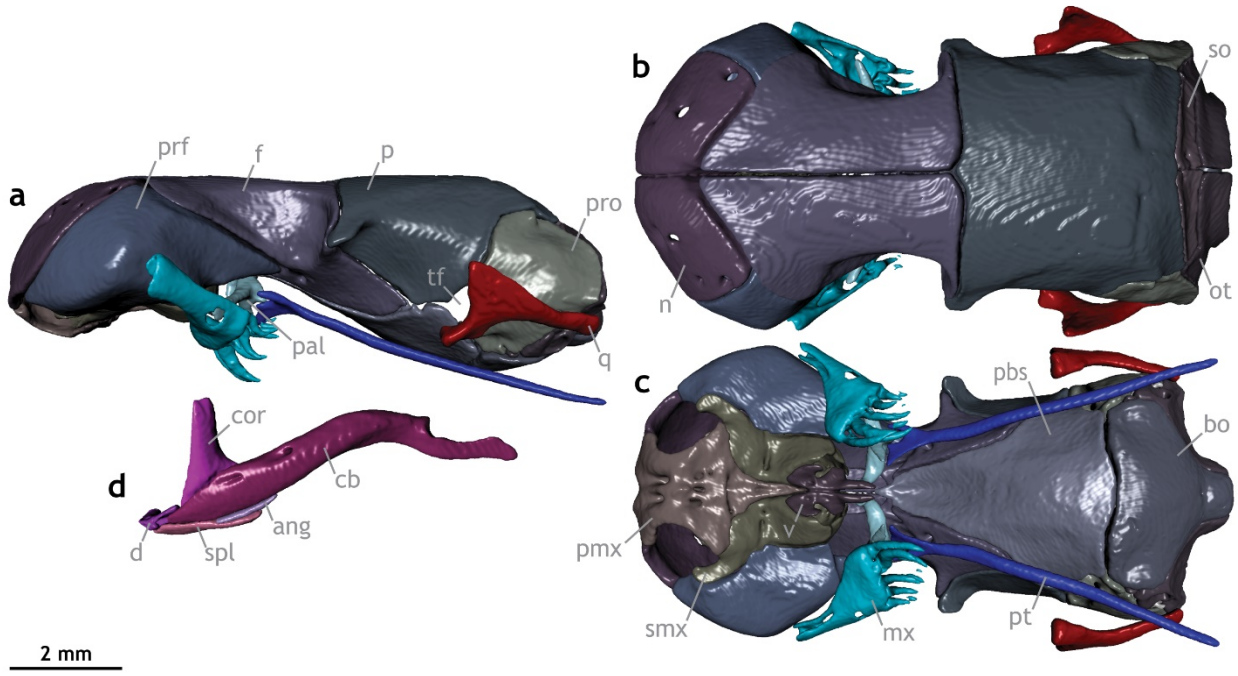

FIGURE 1.1. Overview of typhlopoid skull anatomy. Skull of *Afrotyphlops angolensis* (MCZ R-170385) in (**a**) lateral, (**b**) dorsal, and (**c**) ventral views with mandibles removed, with (**d**) mandible in lateral view. Colouration is consistent throughout all panels. Abbreviations: ang, angular; bo, basioccipital; cb, compound bone; cor, coronoid; d, dentary; f, frontal; mx, maxilla; n, nasal; ot, otoccipital; p, parietal; pal, palatine; pbs, parabasisphenoid; pmx, premaxilla; prf, prefrontal; pro, prootic; pt, pterygoid; q, quadrate; smx, septomaxilla; so, supraoccipital; spl, splenial; tf, trigeminal foramen; v, vomer. MCZ scan data used by permission of the Museum of Comparative Zoology, Harvard University.

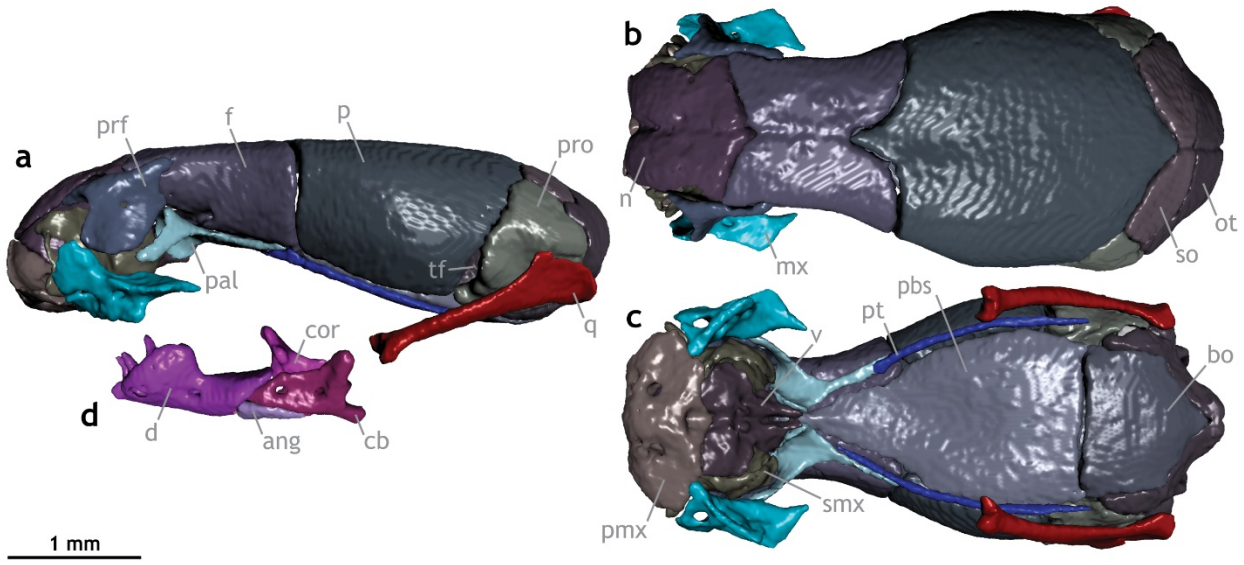

FIGURE 1.2. Overview of leptotyphlopid skull anatomy. Skull of *Epictia albifrons* (MCZ R-2885) in (**a**) lateral, (**b**) dorsal, and (**c**) ventral views with mandibles removed, with (**d**) mandible in lateral view. Colouration is consistent throughout all panels. Abbreviations: ang, angular; bo, basioccipital; cb, compound bone; cor, coronoid; d, dentary; f, frontal; mx, maxilla; n, nasal; ot, otoccipital; p, parietal; pal, palatine; pbs, parabasisphenoid; pmx, premaxilla; prf, prefrontal; pro, prootic; pt, pterygoid; q, quadrate; smx, septomaxilla; so, supraoccipital; tf, trigeminal foramen; v, vomer. MCZ scan data used by permission of the Museum of Comparative Zoology, Harvard University.

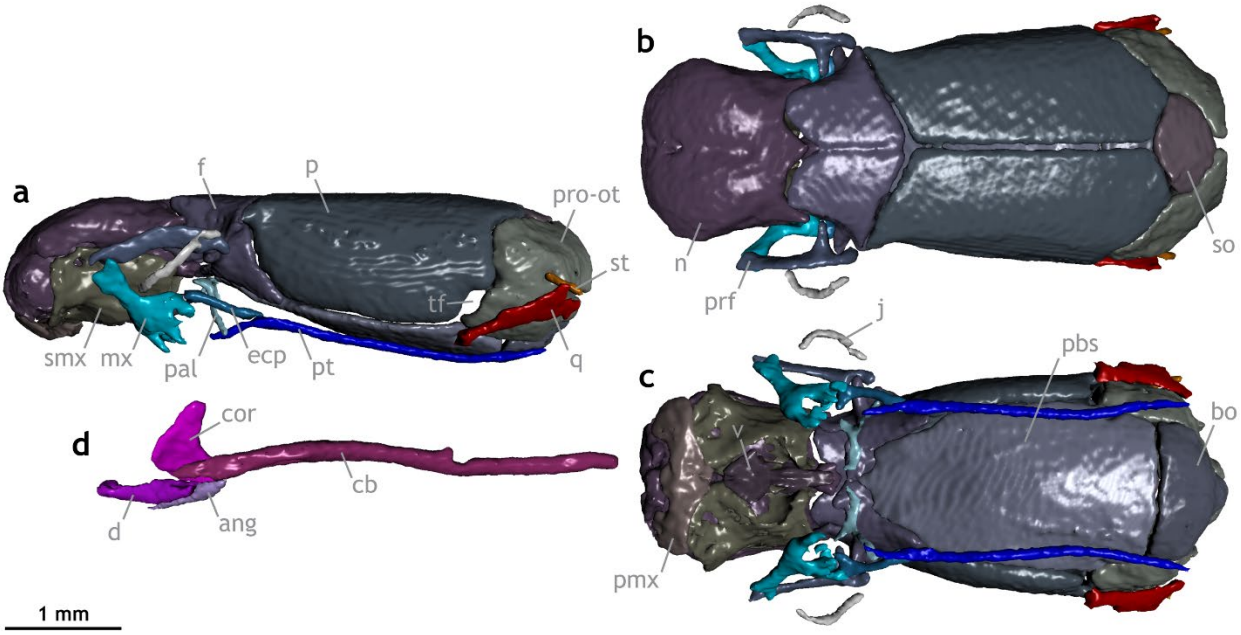

FIGURE 1.3. Overview of anomalepidid skull anatomy. Skull of *Liotyphlops argaleus* (MCZ R-67933) in (**a**) lateral, (**b**) dorsal, and (**c**) ventral views with mandibles removed, with (**d**) mandible in lateral view. Colouration is consistent throughout all panels. Abbreviations: ang, angular; bo, basioccipital; cb, compound bone; cor, coronoid; d, dentary; ecp, ectopterygoid; f, frontal; j, jugal; mx, maxilla; n, nasal; p, parietal; pal, palatine; pbs, parabasisphenoid; pmx, premaxilla; prf, prefrontal; pro-ot, prootic-otoccipital; pt, pterygoid; q, quadrate; smx, septomaxilla; so, supraoccipital; st, supratemporal; tf, trigeminal foramen; v, vomer. MCZ scan data used by permission of the Museum of Comparative Zoology, Harvard University.

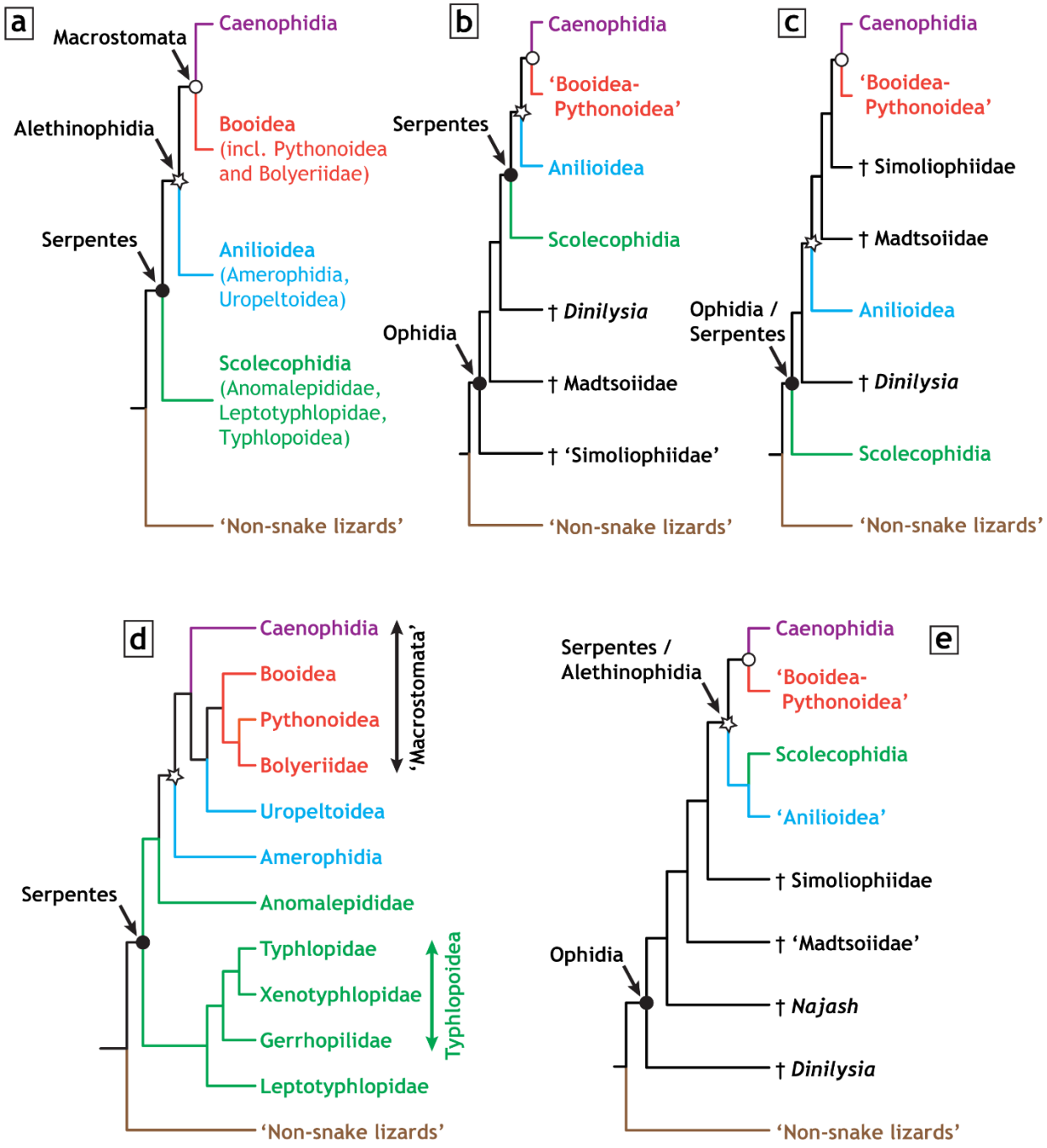
a
Macrostomata
Caenophidia
Alethinophidia
Booidea
(incl. Pythonoidea
and Bolyeriidae)
Serpentes
Anilioidea
(Amerophidia,
Uropeltoidea)
Scolecophidia
(Anomalepididae,
Leptotyphlopidae,
Typhlopoidea)
'Non-snake lizards'
b
Caenophidia
'Booidea-
Pythonoidea'
Serpentes
Anilioidea
Scolecophidia
† Dinilysia
Ophidia
† Madtsoiidae
† 'Simoliophiidae'
'Non-snake lizards'
c
Caenophidia
'Booidea-
Pythonoidea'
† Simoliophiidae
† Madtsoiidae
Ophidia /
Serpentes
Anilioidea
† Dinilysia
Scolecophidia
'Non-snake lizards'
d
Caenophidia
Booidea
Pythonoidea
Bolyeriidae
'Macrostomata'
Uropeltoidea
Amerophidia
Serpentes
Anomalepididae
Typhlopidae
Xenotyphlopidae
Gerrhopilidae
Typhlopoidea
Leptotyphlopidae
'Non-snake lizards'
e
Serpentes /
Alethinophidia
Caenophidia
'Booidea-
Pythonoidea'
Scolecophidia
'Anilioidea'
† Simoliophiidae
† 'Madtsoiidae'
Ophidia
† Najash
† Dinilysia
'Non-snake lizards'

FIGURE 1.4. Competing hypotheses of snake phylogeny. (**a**) Traditional perspective of the phylogeny of extant snakes, based on Rieppel (1988). (**b**) Caldwell, Lee, and colleagues' perspective of fossil snakes as diverging basally to scolecophidians, based on Lee & Scanlon (2002). (**c**) Rieppel, Zaher, and colleagues' perspective of scolecophidians as diverging basally to all other snakes, including extinct taxa, based on Zaher & Rieppel (2002) with placement of Madtsoiidae from Zaher & Scanferla (2012). (**d**) Typical molecular topology recovering scolecophidians as paraphyletic, based on Burbrink *et al.* (2020). (**e**) Recent phylogeny recovering scolecophidians among 'anilioids', within Alethinophidia, based on Garberoglio *et al.* (2019a). Quotation marks indicate non-monophyletic groups. † indicates extinct taxa. Following Caldwell & Lee (1997), Serpentes refers to crown-clade snakes and Ophidia refers to all snakes (both extant and extinct). Key simoliophiid taxa include *Pachyrhachis*, *Haasiophis*, and *Eupodophis*. Key madtsoiid taxa include *Wonambi* and *Yurlunggur*.

References: Chapter One

Alberch, P., Gould, S. J., Oster, G. F. & Wake, D. B. 1979. Size and shape in ontogeny and phylogeny. *Paleobiology*, **5**(3), 296–317.

Apesteguía, S. & Zaher, H. 2006. A Cretaceous terrestrial snake with robust hindlimbs and a sacrum. *Nature*, **440**, 1037–1040. doi:10.1038/nature04413

Bellairs, A. D. & Underwood, G. 1951. The origin of snakes. *Biological Reviews*, **26**, 193–237.

Brock, G. T. 1932. The skull of *Leptotyphlops* (*Glauconia nigricans*). *Anatomischer Anzieger*, **73**, 199–204.

Brock, G. T. 1941. The skull of *Acontias meleagris*, with a study of the affinities between lizards and snakes. *Zoological Journal of the Linnean Society*, **41**, 71–88.

Burbrink, F. T., Grazziotin, F. G., Pyron, R. A., Cundall, D., Donnellan, S., Irish, F., Keogh, J. S., Kraus, F., Murphy, R. W., Noonan, B., Raxworthy, C. J., Ruane, S., Lemmon, A. R., Lemmon, E. M. & Zaher, H. 2020. Interrogating genomic-scale data for Squamata (lizards, snakes, and amphisbaenians) shows no support for key traditional morphological relationships. *Systematic Biology*, **69**(3), 502–520. doi:10.1093/sysbio/syz062

Caldwell, M. W. & Lee, M. S. Y. 1997. A snake with legs from the marine Cretaceous of the Middle East. *Nature*, **386**, 705–709.

Caldwell, M. W. 1999. Squamate phylogeny and the relationships of snakes and mosasauroids. *Zoological Journal of the Linnean Society*, **125**, 115–147. doi:10.1111/j.1096-3642.1999.tb00587.x

Caldwell, M. W. 2000. On the phylogenetic relationships of *Pachyrhachis* within snakes: a response to Zaher (1998). *Journal of Vertebrate Paleontology*, **20**(1), 187–190.

Caldwell, M. W. 2007a. The role, impact, and importance of fossils: snake phylogeny, origins, and evolution (1869–2006). Pp. 253–302 in J. Anderson and H.-D. Sues (eds) *Major Transitions in Vertebrate Evolution*. Indiana University Press, Bloomington, Indiana.

Caldwell, M. W., Nydam, R. L., Palci, A. & Apesteguía, S. 2015. The oldest known snakes from the Middle Jurassic-Lower Cretaceous provide insights on snake evolution. *Nature Communications*, **6**, 5996. doi:10.1038/ncomms6996

Caldwell, M. W. 2019. *The Origin of Snakes: Morphology and the Fossil Record*. Taylor & Francis, Boca Raton.

Camp, C. L. 1923. Classification of the lizards. *Bulletin of the American Museum of Natural History, New York*, **48**, 289–481.

Chretien, J., Wang-Claypool, C. Y., Glaw, F. & Scherz, M. D. 2019. The bizarre skull of *Xenotyphlops* sheds light on synapomorphies of Typhlopoidea. *Journal of Anatomy*, **234**, 637–655. doi:10.1111/joa.12952

Conrad, J. L. 2008. Phylogeny and systematics of Squamata (Reptilia) based on morphology. *Bulletin of the American Museum of Natural History, New York*, **310**, 1–182. doi:10.1206/310.1

Cope, E. D. 1869. On the reptilian orders, Pythonomorpha and Streptosauria. *Boston Society of Natural History Proceedings*, **12**, 250–266.

Cundall, D., Wallach, V. & Rossman, D. A. 1993. The systematic relationships of the snake genus *Anomochilus*. *Zoological Journal of the Linnean Society*, **109**, 275–299.

Cundall, D. & Irish, F. 2008. The snake skull. Pp. 349–692 in C. Gans, A.S. Gaunt and K. Adler (eds) *Biology of the Reptilia: Morphology H, The Skull of Lepidosauria*. Society for the Study of Amphibian and Reptiles, Ithaca, New York.

Da Silva, F. O., Fabre, A.-C., Savriama, Y., Ollonen, J., Mahlow, K., Herrel, A., Müller, J. & Di-Poï, N. 2018. The ecological origins of snakes as revealed by skull evolution. *Nature Communications*, **9**, 376. doi:10.1038/s41467-017-02788-3

Ebel, R., Müller, J., Ramm, T., Hipsley, C. & Amson, E. 2020. First evidence of convergent lifestyle signal in reptile skull roof microanatomy. *BMC Biology*, **18**, 185. doi:10.1186/s12915-020-00908-y

Estes, R., de Queiroz, K. & Gauthier, J. A. 1988. Phylogenetic relationships within Squamata. Pp. 119–281 in R. Estes and G.K. Pregill (eds) *Phylogenetic Relationships of the Lizard Families*. Stanford University Press, Stanford.

Evans, H. E. 1955. The osteology of a worm snake, *Typhlops jamaicensis* (Shaw). *The Anatomical Record*, **122**, 381–396.

Fachini, T. S., Onary, S., Palci, A., Lee, M. S. Y., Bronzati, M. & Hsiou, A. S. 2020. Cretaceous blind snake from Brazil fills major gap in snake evolution. *iScience*, **23**, 101834. doi:10.1016/j.isci. 2020.101834

Figueroa, A., McKelvy, A. D., Grismer, L. L., Bell, C. D. & Lailvaux, S. P. 2016. A species-level phylogeny of extant snakes with description of a new colubrid subfamily and genus. *PLoS ONE*, **11**(9), e0161070. doi:10.1371/journal.pone.0161070

Fröbisch, N. B. & Schoch, R. R. 2009. Testing the impact of miniaturization on phylogeny: Paleozoic dissorophoid amphibians. *Systematic Biology*, **58**(3), 312–327. doi:10.1093/sysbio/syp029

Garberoglio, F. F., Apesteguía, S., Simões, T. R., Palci, A., Gómez, R. O., Nydam, R. L., Larsson, H. C. E., Lee, M. S. Y. & Caldwell, M. W. 2019a. New skulls and skeletons of the Cretaceous legged snake *Najash*, and the evolution of the modern snake body plan. *Science Advances*, **5**(11), eaax5833. doi:10.1126/sciadv.aax5833

Garberoglio, F. F., Gómez, R. O., Apesteguía, S., Caldwell, M. W., Sánchez, M. L. & Veiga, G. 2019b. A new specimen with skull and vertebrae of *Najash rionegrina* (Lepidosauria: Ophidia) from the early Late Cretaceous of Patagonia. *Journal of Systematic Palaeontology*, **17**(18), 1533–1550. doi:10.1080/14772019.2018.1534288

Gauthier, J., Kluge, A. G. & Rowe, T. 1988a. Amniote phylogeny and the importance of fossils. *Cladistics*, **4**, 105–209.

Gauthier, J. A., Kearney, M., Maisano, J. A., Rieppel, O. & Behlke, A. D. B. 2012. Assembling the squamate tree of life: perspectives from the phenotype and the fossil record. *Bulletin of the Peabody Museum of Natural History*, **53**, 3–308. doi:10.3374/014.053.0101

Gould, S. J. 1977. *Ontogeny and Phylogeny*. Harvard University Press, Cambridge.

Haas, G. 1964. Anatomical observations on the head of *Liotyphlops albirostris* (Typhlopidae, Ophidia). *Acta Zoologica*, **1964**, 1–62.

Haas, G. 1968. Anatomical observations on the head of *Anomalepis aspinosus* (Typhlopidae, Ophidia). *Acta Zoologica*, **48**, 63–139.

Haas, G. 1979. On a new snakelike reptile from the Lower Cenomanian of Ein Jabrud, near Jerusalem. *Bulletin du Museum National d'Histoire Naturelle. Section C*, **1**, 51–64.

Haas, G. 1980. *Pachyrhachis problematicus* Haas, snakelike reptile from the lower Cenomanian: ventral view of the skull. *Bulletin du Museum National d'Histoire Naturelle. Section C*, **2**, 87–104.

Hanken, J. 1984. Miniaturization and its effects on cranial morphology in plethodontid salamanders, genus *Thorius* (Amphibia: Plethodontidae). I. Osteological variation. *Biological Journal of the Linnean Society*, **23**, 55–75.

Hanken, J. & Wake, D. B. 1993. Miniaturization of body size: organismal consequences and evolutionary significance. *Annual Review of Ecology and Systematics*, **24**, 501–519.

Hanken, J. 2015. Is heterochrony still an effective paradigm for contemporary studies of evo-devo? Pp. 97–110 in A. Love (ed) *Conceptual Change in Biology*. Springer, Dordrecht.

Harrington, S. M. & Reeder, T. W. 2017. Phylogenetic inference and divergence dating of snakes using molecules, morphology and fossils: new insights into convergent evolution of feeding morphology and limb reduction. *Biological Journal of the Linnean Society*, **121**, 379–394.

Hedges, S. B., Marion, A. B., Lipp, K. M., Marin, J. & Vidal, N. 2014. A taxonomic framework for typhlopid snakes from the Caribbean and other regions (Reptilia, Squamata). *Caribbean Herpetology*, **49**, 1–61. doi:10.31611/ch.49

Heise, P. J., Maxson, L. R., Dowling, H. G. & Hedges, S. B. 1995. Higher-level snake phylogeny inferred from mitochondrial DNA sequences of 12S rRNA and 16S rRNA genes. *Molecular Biology and Evolution*, **12**(2), 259–265.

Hsiang, A. Y., Field, D. J., Webster, T. H., Behlke, A. D. B., Davis, M. B., Racicot, R. A. & Gauthier, J. A. 2015. The origin of snakes: revealing the ecology, behavior, and evolutionary history of early snakes using genomics, phenomics, and the fossil record. *BMC Evolutionary Biology*, **15**, 87. doi:10.1186/s12862-015-0358-5

Irish, F. J. 1989. The role of heterochrony in the origin of a novel bauplan: evolution of the ophidian skull. *Geobios*, **22**, 227–233.

Janensch, W. 1906. Uber Archaeophis proavus Mass., eine schlange aus dem Eocan des Monte Bolca. *Beitrage zur Palaontologie und Geologie Oestreich-Ungarns und des Orients*, **16**, 1–33.

Kley, N. J. 2006. Morphology of the lower jaw and suspensorium in the Texas blindsnake, *Leptotyphlops dulcis* (Scolecophidia: Leptotyphlopidae). *Journal of Morphology*, **267**, 494–515. doi:10.1002/jmor.10414

Lee, M. S. Y. 1997. The phylogeny of varanoid lizards and the affinities of snakes. *Philosophical Transactions of the Royal Society of London, Series B: Biological Sciences*, **352**, 53–91.

Lee, M. S. Y. 1998. Convergent evolution and character correlation in burrowing reptiles: towards a resolution of squamate relationships. *Biological Journal of the Linnean Society*, **65**, 369–453.

Lee, M. S. Y. & Caldwell, M. W. 1998. Anatomy and relationships of *Pachyrhachis problematicus*, a primitive snake with hindlimbs. *Philosophical Transactions of the Royal Society of London, Series B: Biological Sciences*, **353**(1375), 1521–1552.

Lee, M. S. Y. & Scanlon, J. D. 2002. Snake phylogeny based on osteology, soft anatomy and ecology. *Biological Reviews*, **77**, 333–401.

Lee, M. S. Y. 2005. Molecular evidence and marine snake origins. *Biology Letters*, **1**, 227–230. doi:10.1098/rsbl.2004.0282

Lee, M. S. Y. 2009. Hidden support from unpromising data sets strongly unites snakes with anguimorph 'lizards'. *Journal of Evolutionary Biology*, **22**, 1308–1316. doi:10.1111/j.1420-9101.2009.01751.x

List, J. C. 1966. Comparative osteology of the snake families Typhlopidae and Leptotyphlopidae. *Illinois Biological Monographs*, **36**, 1–112.

Maddin, H. C., Olori, J. C. & Anderson, J. S. 2011. A redescription of *Carrolla craddocki* (Lepospondyli: Brachystelechidae) based on high-resolution CT, and the impacts of miniaturization and fossoriality on morphology. *Journal of Morphology*, **272**, 722–743. doi:10.1002/jmor.10946

Mahendra, B. C. 1936. Contributions to the osteology of the Ophidia. I. The endoskeleton of the so-called 'blind-snake', *Typhlops braminus* Daud. *Proceedings of the Indian Academy of Sciences*, **3**, 128–142.

Mahendra, B. C. 1938. Some remarks on the phylogeny of the Ophidia. *Anatomischer Anzieger*, **86**, 347–356.

McDowell, S. B. & Bogert, C. M. 1954. The systematic position of *Lanthanotus* and the affinities of the anguimorphan lizards. *Bulletin of the American Museum of Natural History, New York*, **105**, 1–142.

McNamara, K. J. 1986. A guide to the nomenclature of heterochrony. *Journal of Paleontology*, **60**(1), 4–13.

Miralles, A., Marin, J., Markus, D., Herrel, A., Hedges, S. B. & Vidal, N. 2018. Molecular evidence for the paraphyly of Scolecophidia and its evolutionary implications. *Journal of Evolutionary Biology*, **31**, 1782–1793. doi:10.1111/jeb.13373

Müller, G. B. 2007. Evo–devo: extending the evolutionary synthesis. *Nature Reviews: Genetics*, **8**, 943–949. doi:10.1038/nrg2219

Müller, J. 1831. Beiträge zur Anatomie und Naturgeschichte der Amphibien. *Zeitschrift für Physiologie*, **4**, 90–275.

Müller, J., Hipsley, C. A., Head, J. J., Kardjilov, N., Hilger, A., Wuttke, M. & Reisz, R. R. 2011. Eocene lizard from Germany reveals amphisbaenian origins. *Nature*, **473**, 364–367. doi:10.1038/nature09919

Olori, J. C. & Bell, C. J. 2012. Comparative skull morphology of uropeltid snakes (Alethinophidia: Uropeltidae) with special reference to disarticulated elements and variation. *PLoS ONE*, **7**(3), e32450. doi:10.1371/journal.pone.0032450

Palci, A. & Caldwell, M. W. 2010. Redescription of *Acteosaurus tommasinii* von Meyer, 1860, and a discussion of evolutionary trends within the clade Ophidiomorpha. *Journal of Vertebrate Paleontology*, **30**(1), 94–108. doi:10.1080/02724630903409139

Palci, A., Caldwell, M. W. & Albino, A. M. 2013a. Emended diagnosis and phylogenetic relationships of the Upper Cretaceous fossil snake *Najash rionegrina* Apesteguía and Zaher, 2006. *Journal of Vertebrate Paleontology*, **33**(1), 131–140. doi:10.1080/02724634.2012.713415

Palci, A., Caldwell, M. W. & Nydam, R. L. 2013b. Reevaluation of the anatomy of the Cenomanian (Upper Cretaceous) hind-limbed marine fossil snakes *Pachyrhachis*, *Haasiophis*, and *Eupodophis*. *Journal of Vertebrate Paleontology*, **33**(6), 1328–1342. doi:10.1080/02724634.2013.779880

Palci, A., Lee, M. S. Y. & Hutchinson, M. N. 2016. Patterns of postnatal ontogeny of the skull and lower jaw of snakes as revealed by micro-CT scan data and three-dimensional geometric morphometrics. *Journal of Anatomy*, **229**(6), 723–754. doi:10.1111/joa.12509

Palci, A., Hutchinson, M. N., Caldwell, M. W. & Lee, M. S. Y. 2017. The morphology of the inner ear of squamate reptiles and its bearing on the origin of snakes. *Royal Society Open Science*, **4**, 170685. doi:10.1098/rsos.170685

Pyron, R. A., Burbrink, F. T. & Wiens, J. J. 2013. A phylogeny and revised classification of Squamata, including 4161 species of lizards and snakes. *BMC Evolutionary Biology*, **13**, 93. doi:10.1186/1471-2148-13-93

Rage, J.-C. & Escuillié, F. 2000. Un nouveau serpent bipède du Cénomanien (Crétacé). Implications phylétiques. *Comptes Rendus de l'Académie des Sciences - Series IIA - Sciences de la Terre et des planètes/Earth and Planetary Science*, **330**, 513–520.

Rasskin-Gutman, D. & Esteve-Altava, B. 2014. Connecting the dots: anatomical network analysis in morphological EvoDevo. *Biological Theory*, **9**, 178–193. doi:10.1007/s13752-014-0175-x

Reeder, T. W., Townsend, T. M., Mulcahy, D. G., Noonan, B. P., Wood, P. L., Sites, J. W. & Wiens, J. J. 2015. Integrated analyses resolve conflicts over squamate reptile phylogeny and reveal unexpected placements for fossil taxa. *PLoS ONE*, **10**(3), e0118199. doi:10.1371/journal.pone.0118199

Reilly, S. M., Wiley, E. O. & Meinhardt, D. J. 1997. An integrative approach to heterochrony: the distinction between interspecific and intraspecific phenomena. *Biological Journal of the Linnean Society*, **60**, 119–143.

Rhoda, D., Polly, P. D., Raxworthy, C. & Segall, M. 2021. Morphological integration and modularity in the hyperkinetic feeding system of aquatic-foraging snakes. *Evolution*, **75**(1), 56–72. doi:10.1111/evo.14130

Rieppel, O. 1978a. A functional and phylogenetic interpretation of the skull of the Erycinae (Reptilia, Serpentes). *Journal of Zoology*, **186**, 185–208.

Rieppel, O. 1978b. The evolution of the naso-frontal joint in snakes and its bearing on snake origins. *Journal of Zoological Systematics and Evolutionary Research*, **16**, 14–27. doi:10.1111/j.1439-0469.1978.tb00917.x

Rieppel, O. 1979a. A cladistic classification of primitive snakes based on skull structure. *Journal of Zoological Systematics and Evolutionary Research*, **17**(2), 140–150. doi:10.1111/j.1439-0469.1979.tb00696.x

Rieppel, O. 1984a. Miniaturization of the lizard skull: its functional and evolutionary implications. *Symposia of the Zoological Society of London*, **52**, 503–520.

Rieppel, O. 1984b. The cranial morphology of the fossorial lizard genus *Dibamus* with a consideration of its phylogenetic relationships. *Journal of Zoology*, **204**, 289–327.

Rieppel, O. 1988. A review of the origin of snakes. Pp. 37–130 in M.K. Hecht, B. Wallace and G.T. Prance (eds) *Evolutionary Biology*. Springer, Boston, MA.

Rieppel, O. 1996. Miniaturization in tetrapods: consequences for skull morphology. Pp. 47–61 in P.J. Miller (ed) *Miniature Vertebrates: The Implications of Small Body Size, Vol. 69. Symposia of the Zoological Society of London*. Claredon Press, Oxford.

Rieppel, O. & Zaher, H. 2000. The intramandibular joint in squamates, and the phylogenetic relationships of the fossil snake *Pachyrhachis problematicus* Haas. *Fieldiana Geology*, **43**, 1–69.

Rieppel, O. & Zaher, H. 2001a. Re-building the bridge between mosasaurs and snakes. *Neues Jahrbuch für Geologie und Paläontologie, Abhandlungen*, **221**(1), 111–132.

Rieppel, O., Kluge, A. G. & Zaher, H. 2002. Testing the phylogenetic relationships of the Pleistocene snake *Wonambi naracoortensis* Smith. *Journal of Vertebrate Paleontology*, **22**(4), 812–829. doi:10.1671/0272-4634(2002)022[0812:TTPROT]2.0.CO;2

Rieppel, O., Zaher, H., Tchernov, E. & Polcyn, M. J. 2003. The anatomy and relationships of *Haasiophis terrasanctus*, a fossil snake with well-developed hind limbs from the mid-Cretaceous of the Middle East. *Journal of Paleontology*, **77**(3), 536–558.

Rieppel, O. & Head, J. J. 2004. New specimens of the fossil snake genus *Eupodophis* Rage & Escuillié, from Cenomanian (Late Cretaceous) of Lebanon. *Memorie della Societá Italiana di Scienze Naturali e del Museo Civico di Storia Naturale di Milano*, **32**, 1–26.

Rieppel, O. & Maisano, J. A. 2007. The skull of the rare Malaysian snake *Anomochilus leonardi* Smith, based on high-resolution X-ray computed tomography. *Zoological Journal of the Linnean Society*, **149**, 671–685.

Rieppel, O., Kley, N. J. & Maisano, J. A. 2009. Morphology of the skull of the white-nosed blindsnake, *Liotyphlops albirostris* (Scolecophidia: Anomalepididae). *Journal of Morphology*, **270**, 536–557. doi:10.1002/jmor.10703

Rieppel, O. 2012. “Regressed” macrostomatan snakes. *Fieldiana Life and Earth Sciences*, **2012**(5), 99–103. doi:10.3158/2158-5520-5.1.99

Scanferla, A., Zaher, H., Novas, F. E., de Muizon, C. & Céspedes, R. 2013. A new snake skull from the Paleocene of Bolivia sheds light on the evolution of macrostomatans. *PLoS ONE*, **8**(3), e57583. doi:10.1371/journal.pone.0057583

Scanferla, A. 2016. Postnatal ontogeny and the evolution of macrostomy in snakes. *Royal Society Open Science*, **3**, 160612. doi:10.1098/rsos.160612

Scanlon, J. D. & Lee, M. S. Y. 2000. The Pleistocene serpent *Wonambi* and the early evolution of snakes. *Nature*, **403**, 416–420. doi:10.1038/35000188

Scanlon, J. D. 2006. Skull of the large non-macrostomatan snake *Yurlunggur* from the Australian Oligo-Miocene. *Nature*, **439**, 839–842. doi:10.1038/nature04137

Schmidt, K. P. 1950. Modes of evolution discernible in the taxonomy of snakes. *Evolution*, **4**(1), 79–86.

Simões, B. F., Sampaio, F. L., Jared, C., Antoniazzi, M. M., Loew, E. R., Bowmaker, J. K., Rodriguez, A., Hart, N. S., Hunt, D. M., Partridge, J. C. & Gower, D. J. 2015. Visual system evolution and the nature of the ancestral snake. *Journal of Evolutionary Biology*, **28**, 1309–1320. doi:10.1111/jeb.12663

Simões, T. R., Caldwell, M. W., Tałanda, M., Bernardi, M., Palci, A., Vernygora, O., Bernardini, F., Mancini, L. & Nydam, R. L. 2018. The origin of squamates revealed by a Middle Triassic lizard from the Italian Alps. *Nature*, **557**, 706–709. doi:10.1038/s41586-018-0093-3

Singhal, S., Colston, T. J., Grundler, M. R., Smith, S. A., Costa, G. C., Colli, G. R., Moritz, C., Pyron, R. A. & Rabosky, D. L. 2021. Congruence and conflict in the higher-level phylogenetics of squamate reptiles: an expanded phylogenomic perspective. *Systematic Biology*, **70**(3), 542–557. doi:10.1093/sysbio/syaa054

Slowinski, J. B. & Lawson, R. 2002. Snake phylogeny: evidence from nuclear and mitochondrial genes. *Molecular Phylogenetics and Evolution*, **24**, 194–202.

Streicher, J. W. & Wiens, J. J. 2016. Phylogenomic analyses reveal novel relationships among snake families. *Molecular Phylogenetics and Evolution*, **100**, 160–169. doi:10.1016/j.ympev.2016.04.015

Strong, C. R. C., Simões, T. R., Caldwell, M. W. & Doschak, M. R. 2019. Cranial ontogeny of *Thamnophis radix* (Serpentes: Colubroidea) with a re-evaluation of current paradigms

of snake skull evolution. *Royal Society Open Science*, **6**, 182228. doi:10.1098/rsos.182228

Struck, T. H. 2007. Data congruence, paedomorphosis and salamanders. *Frontiers in Zoology*, **4**, 22. doi:10.1186/1742-9994-4-22

Tchernov, E., Rieppel, O., Zaher, H., Polcyn, M. J. & Jacobs, L. L. 2000. A fossil snake with limbs. *Science*, **287**(5460), 2010–2012. doi:10.1126/science.287.5460.2010

Townsend, T. M., Larson, A., Louis, E. & Macey, J. R. 2004. Molecular phylogenetics of Squamata: the position of snakes, amphisbaenians, and dibamids, and the root of the squamate tree. *Systematic Biology*, **53**(5), 735–757. doi:10.1080/10635150490522340

Underwood, G. 1957. *Lanthanotus* and the anguinomorphan lizards: a critical review. *Copeia*, **1957**(1), 20–30.

Vidal, N. & Hedges, S. B. 2002. Higher-level relationships of snakes inferred from four nuclear and mitochondrial genes. *Comptes Rendus Biologies*, **325**, 977–985.

Vidal, N. & Hedges, S. B. 2004. Molecular evidence for a terrestrial origin of snakes. *Proceedings of the Royal Society of London, Series B: Biological Sciences*, **271**, S226–229. doi:10.1098/rsbl.2003.0151

Vidal, N., Rage, J. C., Couloux, A. & Hedges, S. B. 2009. Snakes (Serpentes). Pp. 390–397 in S. Hedges and S. Kumar (eds) *The TimeTree of Life*. Oxford University Press, New York.

Vidal, N., Marin, J., Morini, M., Donnellan, S., Branch, W. R., Thomas, R., Vences, M., Wynn, A., Cruaud, C. & Hedges, S. B. 2010. Blindsnake evolutionary tree reveals long history on Gondwana. *Biology Letters*, **6**, 558–561 doi:10.1098/rsbl.2010.0220

Wake, M. H. 1986. The morphology of *ldiocranium russeli* (Amphibia: Gymnophiona), with comments on miniaturization through heterochrony. *Journal of Morphology*, **189**, 1–16.

Walls, G. L. 1940. Ophthalmological implications for the early history of the snakes. *Copeia*, **1940**(1), 1–8.

Walls, G. L. 1942. The vertebrate eye and its adaptive radiation. *Bulletin of the Cranbrook Institute of Science*, **19**, 1–785.

Werneburg, I. & Sánchez-Villagra, M. R. 2015. Skeletal heterochrony is associated with the anatomical specializations of snakes among squamate reptiles. *Evolution*, **69**(1), 254–263. doi:10.1111/evo.12559

Wiens, J. J., Bonett, R. M. & Chippindale, P. T. 2005. Ontogeny discombobulates phylogeny: paedomorphosis and higher-level salamander relationships. *Systematic Biology*, **54**(1), 91–110. doi:10.1080/10635150590906037

Wiens, J. J., Brandley, M. C. & Reeder, T. W. 2006. Why does a trait evolve multiple times within a clade? Repeated evolution of snakelike body form in squamate reptiles. *Evolution*, **60**(1), 123–141. doi:10.1111/j.0014-3820.2006.tb01088.x

Wiens, J. J., Kuczynski, C. A., Smith, S. A., Mulcahy, D. G., Sites, J. W. J., Townsend, T. M. & Reeder, T. W. 2008. Branch lengths, support, and congruence: testing the phylogenomic approach with 20 nuclear loci in snakes. *Systematic Biology*, **57**(3), 420–431. doi:10.1080/10635150802166053

Wiens, J. J., Kuczynski, C. A., Townsend, T. M., Reeder, T. W., Mulcahy, D. G. & Sites, J. W. J. 2010. Combining phylogenomics and fossils in higher-level squamate reptile phylogeny: molecular data change the placement of fossil taxa. *Systematic Biology*, **59**(6), 674–688. doi:10.1093/sysbio/syq048

Wiens, J. J., Hutter, C. R., Mulcahy, D. G., Noonan, B. P., Townsend, T. M., Sites, J. W. J. & Reeder, T. W. 2012. Resolving the phylogeny of lizards and snakes (Squamata) with extensive sampling of genes and species. *Biology Letters*, **8**, 1043–1046. doi:10.1098/rsbl.2012.0703

Wilson, J. A., Mohabey, D. M., Peters, S. E. & Head, J. J. 2010. Predation upon hatchling dinosaurs by a new snake from the Late Cretaceous of India. *PLoS Biology*, **8**(3), e1000322. doi:10.1371/journal.pbio.1000322

Yi, H. & Norell, M. A. 2015. The burrowing origin of modern snakes. *Science Advances*, **1**(10), e1500743. doi:10.1126/sciadv.1500743

Zaher, H. 1998. The phylogenetic position of *Pachyrhachis* within snakes (Squamata, Lepidosauria). *Journal of Vertebrate Paleontology*, **18**(1), 1–3. doi:10.1080/02724634.1998.10011029

Zaher, H. & Rieppel, O. 1999a. The phylogenetic relationships of *Pachyrhachis problematicus*, and the evolution of limblessness in snakes (Lepidosauria, Squamata). *Comptes Rendus de l'Académie des Sciences - Series IIA - Sciences de la Terre et des planètes/Earth and Planetary Science*, **329**, 831–837.

Zaher, H. & Rieppel, O. 2002. On the phylogenetic relationships of the Cretaceous snakes with legs, with special reference to *Pachyrhachis problematicus* (Squamata, Serpentes). *Journal of Vertebrate Paleontology*, **22**(1), 104–109.

Zaher, H. & Scanferla, C. A. 2012. The skull of the Upper Cretaceous snake *Dinilysia patagonica* Smith-Woodward, 1901, and its phylogenetic position revisited. *Zoological Journal of the Linnean Society*, **164**, 194–238. doi:10.1111/j.1096-3642.2011.00755.x

Zheng, Y. & Wiens, J. J. 2016. Combining phylogenomic and supermatrix approaches, and a time-calibrated phylogeny for squamate reptiles (lizards and snakes) based on 52 genes and 4162 species. *Molecular Phylogenetics and Evolution*, **94**, 537–547. doi:10.1016/j.ympev.2015.10.009

CHAPTER TWO: INSIGHTS INTO SKULL EVOLUTION IN FOSSORIAL SNAKES, AS REVEALED BY THE CRANIAL MORPHOLOGY OF *ATRACTASPIS IRREGULARIS* (SERPENTES: COLUBROIDEA)

[This chapter has been published as: Strong, C. R. C., Palci, A., and M. W. Caldwell. 2021. Insights into skull evolution in fossorial snakes, as revealed by the cranial morphology of *Atractaspis irregularis* (Serpentes: Colubroidea). *Journal of Anatomy*, **238**, 146–172. doi:10.1111/joa.13295.]

2.1. Introduction

Snakes are a major vertebrate group, comprising well over 3000 species, yet many aspects of their biology and evolution remain unknown (Hsiang *et al.* 2015; Harrington & Reeder 2017). Adaptations in various lineages to functionally constrained environments and habits, such as fossoriality, further complicate interpretations of anatomy and phylogenetic relationships. The genus *Atractaspis*, known commonly as the burrowing asp, is a fossorial lineage within Colubroidea, the most deeply nested clade of extant snakes. This genus has been noted for its distinctive skull morphology and unique feeding methods, primarily the modified palatomaxillary biomechanics which allow it to envenomate prey by protruding the fang posterolaterally while the mouth is closed (Deufel & Cundall 2003). This unique morphology has long confounded snake systematists, resulting in varied placements of *Atractaspis* as an elapid or as a viperid in early analyses (see Underwood & Kochva 1993 for a detailed taxonomic review). More recently, *Atractaspis* has been classified as a member of either its own family, the Atractaspididae (Kochva 1987; Underwood & Kochva 1993; Kochva 2002; Shine *et al.* 2006; Jackson 2007; Zaher *et al.* 2009; Moyer & Jackson 2011; Zaher *et al.* 2019; Burbrink *et al.* 2020), or of the subfamily Atractaspidinae within the Lamprophiidae (Vidal *et al.* 2008; Portillo *et al.* 2019).

Despite this morphological novelty, osteological descriptions of *Atractaspis* and its larger group, the Atractaspididae or Atractaspidinae, are limited; most of the literature related to *Atractaspis* has focussed on the evolution of its fangs and venom apparatus (e.g., Kochva 1987, 2002; Jackson 2007) or on its functional morphology and feeding biomechanics (e.g., Deufel & Cundall 2003), resulting in descriptions and illustrations in turn focussed heavily on the teeth and on skull elements related to feeding. Only one study (Underwood & Kochva 1993) has reviewed the overall anatomy of the Atractaspididae, though this description mainly discussed the general condition of various skull elements within this family, rather than providing a detailed description of any single genus, and was further limited almost exclusively to the select cranial features included in the study's character list. The only recent morphology-based phylogeny focussing on the Atractaspididae used external morphology, rather than osteology (Moyer & Jackson 2011), and other recent phylogenies have exclusively employed molecular data (e.g., Vidal *et al.* 2008; Zaher *et al.* 2009; Portillo *et al.* 2019; Zaher *et al.* 2019). Descriptions of

recently established species of *Atractaspis* have similarly focussed on external morphology, with descriptions of osteology limited almost entirely to skull measurements (e.g., Rödel *et al.* 2019).

An understanding of cranial osteology is especially important in the case of *Atractaspis*, as the fossorial habits of this genus impart strong functional constraints which are key to explaining the derivation of its unique skull morphology. As a colubroid, *Atractaspis* belongs to one of the major groups of macrostomate snakes, i.e., large-gaped snakes capable of ingesting disproportionately large prey items, comprising the Colubroidea, Booidea, and Pythonoidea (Scanferla 2016). This genus therefore provides valuable insight into how fossoriality affects a complex and highly derived morpho-functional system such as macrostomy.

The status of *Atractaspis* as a fossorial colubroid also provides an interesting basis for comparison to other fossorial snakes, most prominently scolecophidians. These miniaturized snakes are traditionally considered to be the most primitive or basally-diverging snake lineage, forming the sister group to all other extant snakes, i.e., alethinophidians (e.g., List 1966; Rieppel 2012; Miralles *et al.* 2018). However, adaptations related to miniaturization and to fossoriality render scolecophidians highly autapomorphic and complicate interpretations of morphology and evolution.

Recognizing this importance of visualizing and understanding the skull of *Atractaspis*, the present study aims to use this taxon to: examine the effect of fossoriality on the colubroid skull, particularly features such as the naso-frontal joint, jaws, and suspensorium; assess the possible presence and extent of heterochronic modification; and compare *Atractaspis* to other fossorial snakes, so as to gain broader insights into the evolution of groups such as scolecophidians. To accomplish this, I present herein the first thorough osteological description and illustration of any species within the Atractaspididae, based on fully segmented micro-computed tomography (micro-CT) imagery of the skull of *Atractaspis irregularis* (Reinhardt 1843) (Figs 2.1–2.9 and S2.1–S2.23). This study thus contributes to a recently growing body of anatomical research using micro-CT data to examine un- or under-described snake taxa (e.g., Rieppel & Maisano 2007; Rieppel *et al.* 2009; Olori & Bell 2012; Palci *et al.* 2016; Chretien *et al.* 2019; Strong *et al.* 2019; Racca *et al.* 2020). This research approach provides an essential foundation for constructing higher-order hypotheses of organismal evolution and phylogenetic relationships, and is particularly important for understanding complicated but evolutionarily significant structures such as the skull. This analysis is especially timely given recent

phylogenies recovering scolecophidians as nested within Alethinophidia (Palci & Caldwell 2010; Garberoglio *et al.* 2019a), thus providing an impetus for re-evaluating assumptions surrounding scolecophidian anatomy and evolution.

2.2. Methods

2.2.1. Imaging

The main specimen featured in this study is *Atractaspis irregularis* (FMNH 62204), originally scanned at the High-Resolution X-ray CT (HRXCT) Facility at the University of Texas at Austin as part of the Squamate Tree of Life / Deep Scaly Project. The specimen was collected in Torit, Torit District, Sudan in 1949. Scanning parameters, as provided by J. Maisano and DigiMorph.org, are: 1600 views taken for each slice, with 2 samples per view; tube voltage / current, 180 kV / 0.133 mA; no X-ray prefilter; empty container wedge; image resolution, 1024 pixels; slice thickness, 2 lines, 0.0359 mm; source-to-object distance, 52 mm; interslice spacing, 0.0359 mm; field of reconstruction, 15 mm (maximum field of view, 17.02393 mm); reconstruction offset, 6900; reconstruction scale, 1400. Reconstruction of the raw HRXCT image projections involved drift- and ring-removal processing. Further information regarding the scan parameters is available in the Supplementary Information (Appendix 2.1).

ImageJ was used to improve the contrast and brightness of the reconstructed slices. The dataset was then loaded in Dragonfly 4.0 (Object Research Systems Inc 2019a) for visualization. The Threshold tool was used to digitally remove remaining soft tissues from the scan, leaving only the skull. The Manual Segmentation tool was used to isolate the individual elements, with these segmentations exported as surface mesh (STL) files. These surface meshes are available as 3D PDFs in the Supplementary Information (Figs S2.1–S2.23). The final segmentations were described qualitatively in comparison to various other specimens from a range of taxa (see §2.2.2 and Table 2.1). Although only the bones were observed directly in FMNH 62204, soft-tissue-related features (e.g., nerve and blood vessel pathways, muscle attachments) were inferred from studies of other taxa and specimens (see below).

FMNH 62204 was used as the primary reference specimen for this study because it is openly available for visualization on DigiMorph.org. Although this specimen does exhibit minor skeletal pathologies, as described in the Supplementary Information (Appendix 2.2), the in-text figures display the non-pathological counterpart of the affected elements whenever possible.

Other *A. irregularis* individuals (see §2.2.2 and Table 2.1) were also examined to ensure that the osteological descriptions herein represent the true conditions of each skull element.

2.2.2. Comparative specimens and literature

Institutional abbreviations are provided in the preliminary pages of this thesis document. Micro-CT scans and 3D surface renderings thereof of various specimens were observed for comparative purposes over the course of this study (Table 2.1). Identification and comparisons of soft-tissue-related structures (e.g., foramina for passage of nerves) were made by reference to the figures and descriptions in several papers, namely Maisano & Rieppel (2007), Rieppel (1979b), Rieppel & Maisano (2007), Rieppel *et al.* (2009), and Underwood & Kochva (1993). Anatomical terminology in my descriptions follows these papers, as well as Strong *et al.* (2019). In the figures, abbreviations of elements are from Strong *et al.* (2019), in turn modified from Rieppel *et al.* (2009) and Rieppel & Maisano (2007); abbreviations of features are original, though follow the format of Chretien *et al.* (2019).

2.3. Results

I herein provide a description of each element of the skull of *Atractaspis irregularis* (Figs 2.1 and S2.1–S2.23), grouped according to skull region (Figs 2.2–2.9). Note that the jugal (following the primary homology arguments of Palci & Caldwell 2013) is absent in *Atractaspis irregularis*, as is typical of this genus (Underwood & Kochva 1993; Deufel & Cundall 2003).

Because *Atractaspis* is a fossorial colubroid, comparisons to non-fossorial (i.e., more 'typical') colubroids are essential in understanding its unique morphology and adaptations. As such, comparisons to other snake taxa are made throughout, based on direct observations of several specimens as well as figures and descriptions provided in several papers (§2.2.2 and Table 2.1). *Thamnophis radix* (Colubroidea: Natricidae) was used as the exemplar for a 'typical' colubroid due to the availability of fully segmented micro-CT scans for this species (see Strong *et al.* 2019 and associated data).

2.3.1. Snout

2.3.1.1. Premaxilla

The premaxilla is a triaxial structure consisting of the nasal process dorsally, the paired vomerine processes posteriorly, and the transverse processes laterally (Fig. 2.2a–h). The nasal

process is stout and globular, rising posterodorsally from the anterior midline of the premaxilla to articulate with the anteroventral extent of the nasal (Figs 2.1a and 2.2a–e). The transverse processes form broad wings extending posterolaterally from the base of the nasal process (Fig. 2.2g). The anterior surface of the premaxilla bears two lateral premaxillary foramina, each of which extends at a slight posterolateral angle to exit from the posterior surface of the premaxilla (Fig. 2.2e–h). Another pair of premaxillary foramina is present on the ventral surface of the premaxilla, at the junction between the vomerine and transverse processes. The vomerine processes project off a broad shelf extending posteriorly from the premaxilla (Fig. 2.2g). They underlie the anterior processes of the septomaxillae and extend posteriorly toward—but do not contact—the premaxillary processes of the vomers (Figs 2.1a,c–d and 2.2a–b). Altogether, the premaxilla is more tightly integrated into the snout complex than is typical of colubroids (e.g., *Thamnophis*, *Afronatrix*, *Agkistrodon*, *Coluber*, *Diadophis*), due largely to its increased contact with the nasals.

2.3.1.2. Nasal

The nasals of *Atractaspis irregularis* are elongated and broadened relative to non-fossorial colubroids (e.g., *Thamnophis*, *Afronatrix*, *Coluber*, *Diadophis*, *Homalopsis*, *Agkistrodon*, *Bothrops*), resulting in much stronger articulation with the frontal posteriorly, the septomaxilla ventrally, and the premaxilla anteriorly (Figs 2.1a–b and 2.2a–d). This elaboration and increased integration of the snout complex occurs in several other fossorial snakes (C.S., pers. obs., e.g., anilioids, scolecophidians; see also Cundall & Rossman 1993; Rieppel *et al.* 2009). The nasals are roughly rectangular in dorsal view, with the anterior margins of the dorsal laminae diverging anterolaterally to create a V-shaped notch that accommodates the nasal process of the premaxilla (Figs 2.1a and 2.2a–d,s). A small flange projects posterolaterally just anterior to the posterolateral corner of each dorsal lamina (Fig. 2.2s–u). The medial nasal flanges, or vertical laminae of the nasals, articulate ventrally with the septomaxillae along nearly their entire length and articulate posteriorly with the medial frontal flanges (Figs 2.1a–b and 2.2b,t–u); in contrast, the nasals of non-fossorial colubroids (e.g., *Thamnophis*, *Afronatrix*, *Coluber*, *Diadophis*, *Agkistrodon*) typically exhibit minimal contact with the septomaxillae and minimal to no contact with the frontal (see also Rieppel 2007). Most of the ventral border of each medial nasal flange is thickened in association with the extensive articulation of the nasals with the septomaxillae (Fig. 2.2t–u).

2.3.1.3. Septomaxilla

Each septomaxilla bears a medial ascending lamina, forming a thin, dorsomedially-angled ridge along its medial margin (Fig. 2.2a–b,i,k). This lamina extends anteromedially as a thin anterior process overlying the corresponding vomerine process of the premaxilla (Figs 2.1c–d and 2.2a–b). The medial ascending lamina also projects as a long, thin posterior process which overlies the dorsomedial surface of the corresponding vomer (Figs 2.1c–d and 2.2b,i–l). The posterior terminus of this process curves laterally (Fig. 2.2k–l) and underlies the anteroventral corner of the corresponding medial frontal flange, where the medial frontal pillar meets the subolfactory process of the frontal (Fig. 2.3g), thus participating in the naso-frontal joint as is typical of colubroids (Rieppel 2007). The septomaxilla articulates along most of its dorsal border with the ventral margin of the corresponding medial nasal flange via the medial ascending lamina (Fig. 2.2b), a contact which is typically much less extensive in other colubroids (e.g., *Thamnophis*, *Afronatrix*, *Coluber*, *Diadophis*, *Agkistrodon*). The lateral ascending lamina of each septomaxilla forms a broad but thin hook which curves around the lateral midpoint of the nasal cavity (Fig. 2.2a–d,i–l). The posterior surface of the septomaxilla articulates with the vomer and bears a broad, dorsomedially angled cavity surrounding the anterior extent of the vomeronasal cupola (Fig. 2.2b,j–k).

2.3.1.4. Vomer

The vomer is a globular element that articulates anteriorly and dorsomedially with the septomaxilla (Fig. 2.2b). The vomer is largely hollow, with a rounded internal cavity that forms the majority of the vomeronasal cupola housing the vomeronasal organ (Fig. 2.2q), the anteriormost extent of which is surrounded by the septomaxilla (Rieppel 2007; Rieppel & Maisano 2007; Rieppel *et al.* 2009). Anteromedially, the premaxillary processes of the vomer occur as triangular projections articulating with the posteromedial surface of the corresponding septomaxilla, ventral to the anterior extent of the vomeronasal cupola as delimited by the septomaxilla (Figs 2.1c–d and 2.2m–p). However, these processes are shorter than in other colubroids (e.g., compared to *Thamnophis*, *Afronatrix*) and do not extend far enough anteriorly to contact the vomerine processes of the premaxilla (Fig. 2.1c–d). The fenestra vomeronasalis occurs along the anterior border of the ventral surface of the vomer, separating the premaxillary process of the vomer medially and the lateral wall of the vomer and vomeronasal cupola laterally (Fig. 2.2p). The palatal processes extend posteriorly as a thin, flat projection from each

ventromedial corner of each vomer (Figs 2.1c–d and 2.2m–r). These processes approach, but do not contact, the choanal processes of the palatines (Fig. 2.1c–d).

2.3.2. Skull roof

2.3.2.1. Frontal

Whereas the frontal typically bears a distinct supraorbital ridge along the dorsal border of the orbit in colubroids (e.g., *Thamnophis*), in *Atractaspis irregularis* this ridge is absent. In non-fossorial colubroids (e.g., *Thamnophis*, *Agkistrodon*, *Naja*, *Diadophis*, *Coluber*, *Afronatrix*), the optic foramen is a large opening bordered anteromedially by the frontal, posterolaterally by the parietal, and ventrally by the parasphenoid rostrum of the parabasisphenoid (e.g., see Strong *et al.* 2019:fig. 1). In contrast, expansion of the descending flange of the frontal and the parasphenoid rostrum in *A. irregularis* relative to non-fossorial colubroids results in pronounced reduction of the orbit and optic foramen (Figs 2.1a and 2.3e,h), as occurs commonly in fossorial snakes (e.g., scolecophidians, *Anomochilus*, *Uropeltis*). The optic foramen is bordered mainly by the frontal, forming a narrow canal running posteromedially along the juncture of the posteroventral processes of the frontal with the rest of the frontal (Fig. 2.3e,h). These posteroventral processes represent an expansion of the descending flange of the frontal and articulate with the expanded parasphenoid rostrum of the parabasisphenoid (Figs 2.1a and 2.3e–f), thus excluding the parabasisphenoid entirely from the optic foramen. The descending flanges of the frontal also bear broad articulatory surfaces ventrally where they contact the parasphenoid rostrum (Fig. 2.3f,h). The parietal contributes slightly to the posterolateral enclosure of the optic foramen (Fig. 2.1a).

Anterolaterally, the frontal bears deep facets for its articulation with the prefrontal (Fig. 2.3e). This suture is more extensive than in non-fossorial colubroids (e.g., *Afronatrix*, *Coluber*, *Diadophis*, *Homalopsis*, *Agkistrodon*, *Naja*), due mainly to elaboration and thickening of the prefrontal.

The medial frontal pillars separate the olfactory tracts and are each fused to the corresponding subolfactory process of the frontal, forming the medial frontal flanges as is typical of caenophidians (Fig. 2.3g; Rieppel 2007). These flanges are well-developed and tightly integrated with the medial nasal flanges (Figs 2.1b and 2.3a). The frontal also articulates anteroventrally with the posterior processes of the septomaxillae. This structure of the naso-frontal joint contrasts that of most other, non-fossorial colubroids, in which the main articulation

between the snout and the rest of the skull typically occurs via the septomaxilla-frontal suture, with no contact between the frontal and the nasal (Rieppel 2007).

2.3.2.2. Parietal

The parietal exhibits a tight sutural contact with all of the surrounding elements, except for openings where it forms the posterior border of the optic foramen (just dorsal to the anteroventral corner of the parietal) and the dorsal border of the primary anterior opening of the Vidian canal (just posterior to its anteroventral corner, along the suture with the parabasisphenoid) (Fig. 2.1a). The anterior border of the parietal flares laterally so as to broadly overlap the posterior border of the frontal (Fig. 2.3a–d). The dorsal surface of the parietal is smooth in FMNH 62204, with neither a sagittal sulcus nor a sagittal crest (Fig. 2.3a), though other observed *A. irregularis* individuals (MCZ R-48555, MCZ R-49237) do show a slight sagittal sulcus. The dorsal surface of the parietal bears a small foramen, likely for a pair of blood vessels (see Palci *et al.* 2019). This foramen is variably present in the species; for example, it can be observed in a specimen of *A. irregularis parkeri* (MCZ R-49237), but is absent in *A. irregularis irregularis* (MCZ R-48555). The internal surface of the parietal roof bears two shallow, lobate depressions, separated medially by a slight ridge that extends from the anterior border of the parietal roof and diverges near the posterior border of the parietal (Fig. 2.3c). The parietal roof thickens posteromedially, resulting in a dorsoventrally deep sutural surface with the supraoccipital and the dorsal extent of the prootic.

2.3.3. Palatomaxillary complex

2.3.3.1. Pterygoid

Typically, in ‘macrostomatans’ (booid-pythonoids and caenophidians), the pterygoid extends posteriorly beyond the level of the occipital condyle (C. S., pers obs.; Scanferla 2016). This occurs in some *Atractaspis* individuals (FMNH 62204; Fig. 2.4a), but in others the pterygoid terminates at the level of the occipital condyle (MCZ R-49237, MCZ R-48555). This intraspecific variation may be related to the posterior expansion of the pterygoid that occurs throughout ontogeny in other macrostomatans (Palci *et al.* 2016; Scanferla 2016; Strong *et al.* 2019). In comparison, non-‘macrostomatan’ snakes, including fossorial taxa, typically possess pterygoids which terminate at or anterior to the occipital condyle (e.g., anilioids, scolecophidians). Unlike typical ‘macrostomatans’, the pterygoid of *A. irregularis* lacks teeth and is much less robust overall (Figs 2.4 and 2.5a–d). This thin, elongate, edentulous

morphology occurs in several other fossorial snakes (C.S., pers. obs., e.g., scolecophidians, *Anomochilus*; to a lesser extent, *Uropeltis*; see also Cundall & Rossman 1993), though some fossorial taxa (e.g., *Cylindrophis*, *Anilius*) do exhibit a more robust, toothed morphology comparable to that of more derived alethinophidians.

The dorsal surface of the pterygoid is smooth, with a slight facet anteriorly where it is overlain by the posterior terminus of the ectopterygoid (Fig. 2.5c). A thin ledge projects laterally along the midpoint of the dorsal margin of the pterygoid in FMNH 62204 (Fig. 2.5a). This may represent a highly reduced remnant of the lateral flange of the quadrate process, a feature present and well-developed in *Aparallactus*; however, as this ledge is absent in all other *Atractaspis* specimens examined, this more likely represents minor individual variation in this element. The right pterygoid of FMNH 62204 shows a pathology (healed fracture) at its posterior terminus (Fig. 2.4a), but its left counterpart is intact and shows the typical tapering to a gently rounded extremity that is typical of the genus (Fig. 2.4b,c). The pterygoid is broadly separated from the palatine anteriorly, articulating only with the ectopterygoid (Figs 2.1c–d and 2.4).

2.3.3.2. Ectopterygoid

The ectopterygoid of *Atractaspis irregularis* consists of an elongate, rod-like pterygoid process posteriorly and a medially expanded maxillary process anteriorly (Fig. 2.5e–f), as in other alethinophidians (e.g., *Thamnophis*, *Coluber*, *Diadophis*, *Homalopsis*, *Boaedon*, *Lampropeltis*, *Afronatrix*, *Natrix*). This morphology of the ectopterygoid contrasts the condition in some other fossorial taxa (e.g., scolecophidians, most anilioids, *Calabaria*), in which the ectopterygoid is greatly reduced or absent. However, this latter reduction of the ectopterygoid is not limited to fossorial taxa, as non-burrowing taxa such as *Chilabothrus* and *Exiliboa* exhibit a similar modified form. The ectopterygoids of viperids such as *Agkistrodon* and *Bothrops* are similar in form to those of *A. irregularis*, except that they are more robust.

2.3.3.3. Palatine

The palatine of *Atractaspis irregularis* is highly reduced compared to other colubroids (e.g., *Thamnophis*, *Natrix*, *Lampropeltis*, *Boaedon*, *Diadophis*, *Coluber*, *Afronatrix*, *Homalopsis*), most notably in that it is dramatically shortened anteroposteriorly and bears a maximum of only four teeth (Figs 2.4 and 2.5g–k; Berkovitz & Shellis 2017). In comparison to other fossorial snakes, the palatine of *A. irregularis* most closely resembles the condition in typhlopoids and anomalepidids and, to a lesser extent, leptotyphlopids, *Anomochilus*, and

Calabaria. In contrast, other fossorial snakes (e.g., *Anilius*, *Cylindrophis*) typically possess a more robust palatine, though in some taxa it is edentulous (e.g., *Uropeltis*). The main body of the palatine is slightly medially concave and is roughly triangular, with its apex pointing posteriorly (Fig. 2.5h). Laterally, the maxillary process occurs as a short hook projecting anterolaterally from the dorsal apex of the palatine (Fig. 2.5g,i–k). The choanal process of the palatine is much more elongate, forming a spindly hook that curves broadly anteromedially before looping posteroventrally (Fig. 2.5g–k). Uniquely, even among fossorial snakes, the palatine is broadly separated from the pterygoid (Figs 2.1c–d and 2.4); this has been recognized as an autapomorphy of atractaspids, including aparallactines (Deufel & Cundall 2003).

2.3.3.4. Prefrontal

The prefrontal is typically subdivided into three major components in snakes: the orbital wall, the outer wall, and the dorsal lappet (Maisano & Rieppel 2007). However, this morphology is quite modified in *Atractaspis irregularis* due to greater integration of the prefrontal with the surrounding elements (Figs 2.1a–b, 2.4, and 2.5l–q). Medially, the prefrontal-frontal articulation is elaborated (Fig. 2.5o). The dorsal lappet of the prefrontal is robust and extends anteromedially (Fig. 2.5m–n,p–q). At the junction between the dorsal lappet and orbital wall, prominent forked processes extend posteromedially (Fig. 2.5l,n–o,q). Altogether these processes create a tight interlocking articulation between the prefrontal and anterolateral corner of the frontal (Figs 2.1a–b and 2.4a). The orbital wall is highly modified compared to other colubroids, as is to be expected given the reduction and extensive modification of the orbit itself; this component of the prefrontal is essentially replaced by the aforementioned forked processes (Fig. 2.5o). The ventral surface of the prefrontal is also modified so as to interlock with complementary processes on the dorsal surface of the maxilla (Figs 2.4 and 2.5l,r–s). The lacrimal duct extends through the ventromedial corner of the prefrontal (Fig. 2.5o).

2.3.3.5. Maxilla

The maxilla is highly modified compared to other snakes. In a more ‘typical’ colubroid skull (e.g., *Thamnophis*, *Natrix*, *Lampropeltis*, *Boaedon*, *Diadophis*, *Coluber*, *Afronatrix*), the maxilla is roughly equal in length to the dentary and bears teeth along its entire length. In contrast, the maxilla of *Atractaspis* is greatly shortened anteroposteriorly, such that it is equal in anteroposterior depth to the prefrontal (Figs 2.1a–b, 2.4, and 2.5r–u). The maxillary teeth are also highly modified: each maxilla bears only two fang sockets, with only one fang—the functional

tooth—being ankylosed to the maxilla (Fig. 2.5r–u; Underwood & Kochva 1993; Deufel & Cundall 2003; Jackson 2007). Several smaller replacement teeth are present posterior to each maxilla and posterolingual to the functional teeth (four associated with the left maxilla and six with the right) (Figs 2.1, 2.4, and 2.5r–u). The structure of the replacement teeth is consistent with developmental observations that formation of the fangs begins at the distal tip and proceeds toward the tooth base (Fig. 2.5r–u; Jackson 2007). The teeth—including the replacement teeth—are hollow, i.e., are 'tubular fangs' *sensu* Jackson (2007), meaning that the venom groove is completely enclosed to form a channel within the tooth. A grooved opening ventrally on the tooth base marks the entrance of the venom duct into the enclosed venom channel of the tooth (Fig. 2.5r,u).

The anterodorsal surface of the maxilla of *Atractaspis irregularis* bears three processes which interlock with the notched ventral surface of the prefrontal (Fig. 2.5r–s); these may represent a highly modified nasal or facial process. The maxilla abuts posteriorly against the anterolateral corner of the ectopterygoid (Fig. 2.4a–b). The superior alveolar canal pierces the maxilla mediolaterally through its anterior surface (Fig. 2.5r–s), marking the lateral and medial openings for the anteriorly extending V2 maxillary branch of the trigeminal nerve, as well as associated blood vessels (Evans 2008).

2.3.4. Braincase

2.3.4.1. Parabasisphenoid

The parabasisphenoid is roughly triangular in dorsal view and consists of a rounded main body posteriorly and an anterodorsally directed rostrum anteriorly (Fig. 2.6b,d–f). These represent the basisphenoid and parasphenoid components of this bone, respectively. The ventral surface bears the basipterygoid processes on either side of the midline, extending from the centre of the main body to the junction between the basisphenoid and parasphenoid rostrum (Fig. 2.6e). The lateral borders of the parabasisphenoid are linear, lacking protrusions such as the clinoid processes (Fig. 2.6d–f; see Strong *et al.* 2019:fig. 6 for comparison to condition in *Thamnophis*). The dorsal surface of the main body is generally smooth, with slight depressions anterior and posterior to the midpoint (Fig. 2.6d). The posterior of these represents a very weakly defined sella turcica (Fig. 2.6d). However, a distinct ossified dorsum sellae overhanging the sella turcica is absent (Fig. 2.6d). This condition occurs in all observed specimens of *A. irregularis* (though

see Sheverdyukova & Kovtun 2020 for comments on the highly variable development and morphology of this region in other snakes).

The posterior opening of the Vidian canal is present just anterior to the point where the basioccipital, parabasisphenoid, and prootic meet (Fig. 2.6c). This canal transmits several blood vessels and nerves, including the internal carotid artery and palatine branch of the facial nerve (Evans 2008). The left posterior opening of the Vidian canal is much larger than the right opening, likely due to asymmetry in the size of the arteries passing through these openings (Underwood & Kochva 1993). The Vidian canal communicates with the inside of the braincase via the internal carotid foramina at the posterior corners of the parabasisphenoid (Fig. 2.6f). The primary anterior opening of the Vidian canal is present as a small foramen near the anterior extent of the parietal-parabasisphenoid suture (Fig. 2.6a,c–f), with the secondary anterior opening of the Vidian canal occurring as an even smaller foramen near the posterior extent of the frontal-parabasisphenoid suture, ventral to the optic foramen (Fig. 2.6a,c–f). Each of these anterior openings is preceded by a narrow groove on the dorsal surface of the parabasisphenoid (Fig. 2.6d,f).

The most notable feature of the parabasisphenoid is the laterally expanded parasphenoid rostrum (Fig. 2.6d–f). Typically, in colubroids (e.g., *Diadophis*, *Thamnophis*), the parasphenoid rostrum forms a thin process projecting anterodorsally from the basisphenoid portion of the parabasisphenoid (though see *Afronatrix*, which also bears a broadened parasphenoid rostrum). In contrast, the parasphenoid rostrum in *Atractaspis irregularis* forms a broad shelf underlying the similarly expanded descending flanges of the frontal, with a longitudinal ridge on its dorsal surface that slots between the paired descending frontal flanges (Figs 2.3h and 2.6d,f). The rostrum thus articulates extensively along its entire length with the frontal, resulting in greater integration of these elements relative to non-fossorial colubroids. Elaboration of the descending flanges of the frontal causes the parasphenoid rostrum to be excluded from the border of the optic foramen (Figs 2.1a and 2.6a).

2.3.4.2. Basioccipital

The basioccipital articulates along broad sutures with the prootic anterodorsally, the otoccipital posterodorsally, and the parabasisphenoid anteriorly (Fig. 2.6a–c). The internal surface of the basioccipital forms a smooth, oval-shaped basin (Fig. 2.6g), whereas the ventral surface of the basioccipital is convex and roughly hexagonal (Fig. 2.6h). The occipital condyle is

broad and forms a rounded lip protruding slightly ventrally from the posterior margin of the basioccipital (Fig. 2.6b–c,g–h). The basioccipital tubercles extend posterolaterally as small, wing-like processes from each lateral apex of the basioccipital (Fig. 2.6g–h).

2.3.4.3. Prootic

The prootic articulates with the supratemporal laterally, with a slight indent centrally on the dorsolateral surface of the prootic to accommodate this articulation (Figs 2.1a, 2.6a, and 2.7a). Ventral to this facet, the prootic bears four large foramina on its lateral surface (Figs 2.6a and 2.7a).

The two dorsal-most foramina represent a subdivision of the trigeminal foramen into separate anterior and posterior openings for the maxillary (V2) and mandibular (V3) branches of the trigeminal nerve (CN V), respectively (Fig. 2.7a; Maisano & Rieppel 2007; Caldwell 2019). This lateral separation of the trigemino-facialis chamber (*sensu* Rieppel 1979b; Maisano & Rieppel 2007) into separate exits is accomplished by the laterosphenoid, a broad ossification separating the smaller anterior V2 foramen from the larger posterior V3 foramen (Figs 2.6c and 2.7a). The anterior trigeminal foramen (V2) is completely surrounded by the prootic, with no contribution from the parietal to its anterior border (Figs 2.6a and 2.7a). A small foramen—likely transmitting the hyomandibular branch of the facial nerve (CN VII)—is present within the V3 trigeminal foramen (Rieppel 1979b), extending dorsomedially into the otic capsule from the internal dorsal surface of the V3 foramen (Fig. 2.7a).

Two smaller foramina are present ventral to the trigeminal openings (Figs 2.6a and 2.7a). The posteriormost of these smaller foramina is just dorsal to the posterior opening of the Vidian canal, connected to this latter opening by a recess along the ventral border of the prootic (Figs 2.6a,c and 2.7a). This foramen leads dorsally into the trigemino-facialis chamber and transmits the palatine branch of the facial nerve (Fig. 2.7a,c; Rieppel 1979b). Underwood & Kochva (1993) note this foramen as also transmitting the protractor pterygoidei and quadrati nerves. The final foramen on the lateral surface of the prootic is at the base of the laterosphenoid ossification (Figs 2.6a,c and 2.7a). This represents the laterosphenoid foramen (Fig. 2.7a), which transmits branches of the cid (constrictor internus dorsalis)-nerve to innervate the cid-musculature complex, including the levator pterygoidei nerve (Rieppel 1979b; Underwood & Kochva 1993; Rieppel & Maisano 2007). It is internally forked, leading anteroventrally to a small foramen located midway along the internal prootic-parabasisphenoid suture and leading posterodorsally

into the trigemino-facialis chamber.

The trigemino-facialis chamber opens internally via a large foramen at the base of the medial surface of the prootic (Fig. 2.7b). Posterodorsally to this medial opening, two other foramina are present on the medial surface of the prootic (Fig. 2.7b). The larger and posteriormost of these is the foramen for the acoustic nerve (CN VIII) (Rieppel & Maisano 2007), anterior to which lies a smaller foramen allowing passage of the facial nerve (CN VII) into the otic capsule (Fig. 2.7b).

The posterior surface of the prootic contains an elaborate cavity housing the anterior portions of the otic capsule and semicircular canals (horizontal and anterior), which lie posterodorsal to the trigemino-facialis chamber (Fig. 2.7d). The anterior part of the stapedial footplate rests within the lateral portion of this cavity, covering the fenestra ovalis (Fig. 2.7d; fenestra vestibuli *sensu* some authors, e.g., Rieppel & Zaher 2001b; Maisano & Rieppel 2007). The fenestra ovalis itself is visible within the prootic as a slight dorsoventral constriction of the otic capsule in posterior view (Fig. 2.7d). The gap between the fenestra ovalis and stapedial footplate medially and the wall of the braincase laterally forms the juxtastapedial recess (Fig. 2.7d). Interestingly, whereas the prootic typically forms the anterior border of the circumstapedial opening in snakes bearing a 'crista prootica' (the anterior component of the crista circumfenestralis; CCF), in FMNH 62204 the prootic is excluded from this border by an anterior bony bridge of the otoccipital (Figs 2.6a,c and 2.7h,l); a 'crista prootica' as typically seen in the CCF of snakes is therefore absent.

2.3.4.4. Supraoccipital

The supraoccipital is a median element composed of a flat roof with a complex descending process on each lateral margin (Fig. 2.7e–g). The dorsal surface of the supraoccipital bears a slight sagittal crest toward its anterior extent, with slight depressions on either side of the midline (Figs 2.1b and 2.7e). The aforementioned descending processes are ventrolaterally excavated so as to surround the dorsal portion of the otic capsules (Fig. 2.7g). Each descending process bears three foramina: one anterior and one posterior for the passage of the anterior and posterior semicircular canals, and one medially representing the endolymphatic foramen (Fig. 2.7g). The two semicircular canals meet at the common crus within the supraoccipital.

2.3.4.5. Otoccipital

The otoccipital results from a fusion of the opisthotic and exoccipital bones. Each

otoccipital bears a posterior projection from its posteroventral corner which forms the lateral component of the occipital condyle (Figs 2.6a–c and 2.7h–i,k–l). On the external surface of the otoccipital, a groove separates the occipital condyle from the rest of the otoccipital (Fig. 2.7l), confluent with the groove externally surrounding the basioccipital portion of the occipital condyle (Fig. 2.6h).

The anterior surface of the otoccipital bears a deep cavity housing the posterior portions of the otic capsule and semicircular canals (horizontal and posterior) (Fig. 2.7i,j). In anterior view, the otic capsule is delimited laterally by the stapedial footplate, which sits in the fenestra ovalis surrounded laterally by the juxtastapedial recess (Fig. 2.7j).

The lateral surface of the otoccipital bears five openings visible in lateral view (Fig. 2.7h). The anteriormost of these is the circumstapedial opening (i.e., the lateral opening of the juxtastapedial recess) (Fig. 2.7h,l). The juxtastapedial recess is the gap between the stapedial footplate and the lateral wall of the braincase, surrounded by an elaboration of three crests—the cristae prootica, interfenestralis, and tuberalis—which form the crista circumfenestralis (CCF) (Palci & Caldwell 2014). In its fully developed form (Type 4 *sensu* Palci & Caldwell 2014), the CCF in turn obscures the stapedial footplate and lateral aperture of the recessus scalae tympani (LARST, also called the fenestra rotunda by some authors) in lateral view (Palci & Caldwell 2014). In *Atractaspis irregularis*, the 'crista prootica' as traditionally conceived is absent; whereas the crista prootica typically forms the anterior border of the circumstapedial opening (Palci & Caldwell 2014), in *A. irregularis* the otoccipital instead bears a bridge of bone delimiting this anterior border, thus contributing to the anterior enclosure of the juxtastapedial recess and excluding the prootic (Figs 2.6a,c and 2.7h,l). Within the juxtastapedial recess and obscured in lateral view, the LARST occurs just posteroventral to the fenestra ovalis and stapedial footplate. The crista interfenestralis separates the LARST from the fenestra ovalis, though is also hidden in lateral view. This is typical of the CCF in its most extreme form, i.e., Type 4 (Palci & Caldwell 2014). The crista tuberalis is the final component of the CCF, separating the LARST anteriorly from the jugular foramen posteriorly (Fig. 2.7h,l). In *A. irregularis*, this crest forms the posterior rim of the juxtastapedial recess, surrounding the posterior portion of the stapedial footplate and partially hiding the jugular foramen in lateral view (Figs 2.6a,c and 2.7h,l).

The second opening on the lateral wall of the otoccipital is the jugular foramen, located

just posterior to the crista tuberalis and internally subdivided into two smaller foramina (Fig. 2.7h,l). The glossopharyngeal (CN IX) and vagus (CN X) nerves presumably pass through this foramen (Rieppel 1979b; Young 1987; Rieppel & Zaher 2001b).

Three more foramina on the lateral surface of the otoccipital, posterior to the jugular foramen, represent exits for branches of the hypoglossal nerve (CN XII) (Fig. 2.7h).

The internal surface of the otoccipital bears a cluster of four large foramina close to the suture with the basioccipital (Fig. 2.7i). The foramen located most anterodorsally in the cluster corresponds to the medial counterpart of the jugular foramen (Fig. 2.7i). The foramen located near the anteroventral corner of the otoccipital represents the medial aperture of the recessus scalae tympani (Fig. 2.7i). The two foramina located posteroventral to the jugular foramen represent openings for branches of the hypoglossal nerve (Fig. 2.7i). A small foramen piercing the lateral border of the foramen magnum represents the posteriormost branch of the hypoglossal nerve (Fig. 2.7i).

2.3.4.6. Stapes

The stapes is a very thin element composed of the stapedial shaft attached to an expanded footplate (Fig. 2.7m–o). In *Atractaspis irregularis*, the stapedial footplate is anteriorly expanded so as to broadly underlie the prootic within the juxtastapedial recess. The stapedial shaft projects posterolaterally from midheight on the stapedial footplate through the circumstapedial opening of the juxtastapedial recess (Figs 2.6a,c and 2.7n). In FMNH 62204, the stapedial shaft is very short and does not extend external to the juxtastapedial recess (Fig. 2.6a,c). This condition occurs among most of the *Atractaspis* individuals examined (*A. aterrima*; *A. dahomeyensis*; all *A. irregularis* specimens; *A. microlepidota* – MCZ R-53556 and SAMA R36770); however, in specimens of *A. bibronii* (MCZ R-190390) and *A. microlepidota* (FMNH 58397), the stapedial shaft extends toward the midpoint of the quadrate shaft (C.S. and A.P., pers. obs.). This reduction of the stapedial shaft in most specimens likely reflects the presence of intervening cartilage connecting the ossified stapes to the quadrate. Interestingly, in colubroids, the cartilaginous component of the quadrate-stapes articulation is typically limited to cartilaginous caps on the stapedial shaft and quadrate articulatory process (see Caldwell 2019:fig. 3.15). The presence of an elongate stapedial shaft in specimens of *A. bibronii* and *A. microlepidota* is consistent with this colubroid condition. Although the stapedial shaft may be easily broken off in specimens from dry skeletal collections, the short shaft is certainly genuine in the micro-CT

scanned specimens of *Atractaspis* examined (*A. aterrima*; *A. dahomeyensis*; *A. irregularis*; *A. microlepidota*).

2.3.5. Suspensorium and mandible

2.3.5.1. Supratemporal

The supratemporal is a thin, anteriorly downcurved element articulating medially with the prootic and otoccipital and laterally with the quadrate (Figs 2.8a and 2.9k–l). The supratemporal of *Atractaspis irregularis* is quite reduced compared to other derived alethinophidians, as it does not extend posteriorly beyond the occiput as in booid-pythonoids and some caenophidians (e.g., *Thamnophis* and *Homalopsis*) and does not extend anteriorly onto the parietal as in other caenophidians (e.g., *Afronatrix*, *Coluber*, *Thamnophis*), instead articulating only with the prootic and otoccipital (Fig. 2.1b). Reduction of the supratemporal occurs in several other fossorial snakes, with scolecophidians exemplifying the most extreme modification of the supratemporal to either a vestigial splint of bone (in most anomalepidids) or more commonly to being entirely absent (in leptotyphlopids, typhlopoids, and *Anomalepis*). The supratemporal is also absent in the genus *Uropeltis* (see also Olori & Bell 2012) and in *Anomochilus leonardi* (though is present in *A. weberi*) (though it is present in *A. weberi*; see also Rieppel & Maisano 2007).

2.3.5.2. Quadrate

The quadrate in *Atractaspis irregularis* is a curved rod articulating dorsally with the supratemporal and ventrally with the compound bone (Fig. 2.8a). As is typical of caenophidians (see also Palci *et al.* 2020a), the quadrate is angled distinctly posteroventrally, such that the quadrato-mandibular joint is well posterior to the occipital condyle (Figs 2.1a–b and 2.8a). This elongate and posteriorly angled form of the quadrate is quite distinct compared to other fossorial snakes, in which the quadrate is either short and vertical (e.g., *Anilius*, *Cylindrophis*, *Loxocemus*, *Xenopeltis*, *Casarea*), short and vertical but displaced anteriorly with a large and posteriorly extending suprastapedial process (e.g., *Anomochilus*, *Uropeltis*), or elongate but angled anteriorly (as in scolecophidians). The cephalic condyle is confluent with the quadrate shaft and tapers to a rounded anterodorsal terminus (Figs 2.8a and 2.9a–b), whereas in other colubroids it is a distinctly expanded process (e.g., *Afronatrix*, *Thamnophis*, *Coluber*, *Diadophis*, *Naja*). Ventrally, the mandibular condyle of the quadrate forms a saddle-shaped joint which articulates with the mandibular condyle of the compound bone (Figs 2.8a and 2.9a–b). The lateral surface of the quadrate is smooth (Fig. 2.9a), whereas the medial surface bears a slight overhanging crest

delimiting the posterodorsal extent of its articulation with the supratemporal (Fig. 2.9b). A small articulatory process is present medially at about midheight for articulation with the stapes or its cartilaginous extension (Fig. 2.9b).

2.3.5.3. Compound bone

As is typical of alethinophidians, the compound bone is a long, slightly bowed, edentulous rod that comprises the majority of the mandible (Figs 2.8 and 2.9e–j). Posteriorly, the compound bone bears a saddle-shaped mandibular condyle that articulates with the mandibular condyle of the quadrate (Figs 2.8 and 2.9e–f,i–j). A foramen for the chorda tympani nerve (CNVII) is present on the dorsomedial surface of the compound bone, just anterior to the articular joint with the quadrate (Fig. 2.9j). The retroarticular process is essentially absent, similar to the condition in other burrowing snakes such as *Cylindrophis*, *Anilius*, and *Calabaria*, but in contrast to the pronounced retroarticular process typical of scolecophidians. The mandibular or adductor fossa occurs about midway along the dorsal margin of the compound bone, leading anterolaterally into a foramen and anteriorly into the Meckelian canal (Fig. 2.9e,g–h,j). The Meckelian canal is completely surrounded by the compound bone posteriorly, whereas anteriorly it is delimited by the compound bone laterally and by the angular medially (Figs 2.8b and 2.9f,i). The compound bone tapers anteriorly to articulate with the deeply notched posterior terminus of the dentary (Figs 2.8 and 2.9g,j).

2.3.5.4. Dentary

The dentary of *Atractaspis* is quite unique compared to other, non-fossorial colubroids. As is common in fossorial snakes (e.g., *Uropeltis*, scolecophidians; but not *Cylindrophis*, *Anilius*, *Anomochilus*, or *Calabaria*), the mandible is underslung relative to the rest of the skull, causing the snout complex to project prominently anterior to the mandible (Figs 2.1a and 2.8a). The dentary is markedly slim and rod-like (Figs 2.8 and 2.9c–d), similar to the compound bone and in contrast to the more robust mandible of other colubroids (C.S., pers. obs.; see also Palci *et al.* 2016; Scanferla 2016; Strong *et al.* 2019; Racca *et al.* 2020). The dentition is also highly reduced, with the dentary of *Atractaspis* typically bearing only two small teeth (Deufel & Cundall 2003), with a maximum of four (Berkovitz & Shellis 2017); the dentary is edentulous in the specimen of *A. irregularis* illustrated here, though this is likely the result of postmortem tooth loss as two tooth sockets are present. The dentary tapers anteriorly to a thin, medially curved apex (Fig. 2.9c–d). The posterior terminus of the dentary bears three prongs: two

dorsally, which form a fork overlying the dorsal margin of the compound bone (Figs 2.8 and 2.9c), and one ventrally, which articulates with the compound bone dorsolaterally and the splenial dorsomedially (Figs 2.8 and 2.9d). The dentary completely encloses the Meckelian canal anteriorly, whereas posteriorly the splenial forms the medial wall of the Meckelian canal (Figs 2.8b and 2.9d). A mental foramen is not evident, representing a state unique to *Atractaspis* relative to all other snakes except some scolecophidians (anomalepidids and some typhlopids; Caldwell 2019).

2.3.5.5. Angular

The angular is a roughly triangular bone overlying the Meckelian canal on the medial surface of the compound bone (Fig. 2.8b). The angular is smooth medially (Fig. 2.9n) but grooved laterally in order to accommodate the Meckelian canal (Fig. 2.9m). It is pierced midway along its length by the posterior mylohyoid foramen (Fig. 2.9m–n). Along its dorsal margin, the angular bears a broad emargination such that the Meckelian canal is slightly exposed at this position along the compound bone (Figs 2.8b and 2.9m–n). The angular tapers posteriorly to a thin apex (Fig. 2.9m–n). Anteriorly, the dorsal margin of the angular extends further than the ventral margin, corresponding to and articulating with the posteroventral tapering of the posterior terminus of the splenial (Fig. 2.8b).

2.3.5.6. Splenial

The splenial is a thin, triangular bone that overlies the Meckelian canal along the dentary and anteriormost extent of the compound bone (Fig. 2.8b). Its medial surface is smooth (Fig. 2.9p), whereas its lateral surface bears a V-shaped groove—beginning near the midpoint of the splenial and continuing posteriorly onto the lateral surface of the angular—that surrounds the medial surface of the Meckelian canal (Fig. 2.9o). The anterior mylohyoid foramen creates an oblong opening leading into the Meckelian canal near the posterior terminus of the splenial (Figs 2.8b and 2.9o–p). The splenial tapers anteriorly to articulate with a medial groove on the dentary, whereas posteriorly it articulates with the angular, tapering such that its ventral margin extends farther posteriorly than its dorsal margin (Figs 2.8b and 2.9o–p).

2.4. Discussion

2.4.1. Adaptations for fossoriality

The overall morphology of the skull of *Atractaspis irregularis* is markedly different from that of other colubroids. This unique structure is due in part to heterochrony (see §2.4.2 and §2.4.3), but is also due largely to several adaptations for fossoriality. Principal among these are reduction of the orbits (§2.3.2.1), modification of the jaws (§2.3.3 and §2.3.5), and increased integration of the snout complex (§2.3.1).

The mandible is underslung relative to the rest of the skull, a condition that occurs in many other fossorial snakes (Figs 2.1a and 2.8a; §2.3.5.4). This reduction aids in limiting resistance and preventing the jaws from being forced open while burrowing or moving in constricted areas (Wake 1993). This reduction of the mandible likely also explains the absence of the mental foramen, as similar absence in scolecophidians has been linked to decreased importance of the labial glands (Caldwell 2019).

The maxilla is also unique in its anatomy and biomechanics of fang rotation. Although the maxilla and dentition are superficially similar to the condition in viperids (e.g., *Agkistrodon*, *Bothrops*), key differences such as the structure of the maxilla-prefrontal articulation strongly suggest these similarities to be convergent (Kochva 1987). In the aforementioned viperids, the articulating surfaces of these elements are smooth, with several ligaments and muscles for control and stabilization of the maxilla (Kochva 1987). In contrast, the anterodorsal surface of the maxilla of *Atractaspis irregularis* is complexly integrated with the prefrontal (Figs 2.1, 2.4, and 2.5).

This difference in morphology in turn implies a difference in function. Rather than relying on ligamentous stabilization of the maxilla as in viperids, the complex ball-and-socket-like articulation of the maxilla-prefrontal in *Atractaspis* provides structural support and limits rotation of the maxilla and fangs to a ventrolateral-dorsomedial axis (Kochva 1987; Deufel & Cundall 2003; see the latter for a detailed examination of functional morphology and feeding mechanisms in *Atractaspis*). Ultimately, rather than the jaws fully opening and the fang swinging ventrally, *Atractaspis* is characterized by a unique ‘side-stabbing’ movement in which the fang protrudes ventrolaterally from the side of the closed mouth (Kochva 1987; Underwood & Kochva 1993; Deufel & Cundall 2003). This phenomenon is facilitated by the underslung or countersunk mandible and is used to envenomate prey via posteroventral movement of the head (Kochva 1987; Underwood & Kochva 1993; Deufel & Cundall 2003), which aids prey envenomation in restricted spaces such as burrows (Deufel & Cundall 2003; Shine *et al.* 2006).

Alongside the reduction of the mandible, this modification to the palatomaxillary arch demonstrates the role of fossoriality in driving adaptations involving complex morphofunctional systems such as macrostomy.

Another important adaptation for fossoriality involves the naso-frontal joint. In *Atractaspis irregularis*, this joint involves the tightly integrated snout complex—composed of the nasals, premaxilla, septomaxillae, and vomers—itself in extensive articulation with the medial frontal flanges (i.e., the fused medial frontal pillars and subolfactory processes of the frontal) (Figs 2.1, 2.2, and 2.3g). This contact contrasts typical, non-fossorial macrostomatans as described by Rieppel (2007), in which the nasal contacts either the medial frontal pillars or the frontal subolfactory processes but not both. In particular, in typical colubroids the nasals tend to contact the frontals ventrally at the subolfactory processes, with the septomaxillae forming the main connection between the snout complex and frontals; in some cases the nasals are completely excluded from contact with the frontals, and the connection between the latter and the snout complex occurs exclusively via the septomaxilla (Rieppel 2007).

The naso-frontal configuration in *Atractaspis* exemplifies the 'central rod design' of the naso-frontal joint in fossorial snakes, in which forces associated with burrowing are transmitted from the snout to the frontals via the articulation of the premaxilla, nasals, and medial frontal flanges (Fig. 2.10a; Cundall & Rossman 1993; Rieppel 2007). As initially described by Cundall & Rossman (1993), this 'central rod design' is one of two main configurations associated with transmission of force from the snout complex in burrowing snakes. The other configuration—termed the 'outer shell design'—involves the transmission of force along the outer margins of the skull, via extensive contact along the dorsal and lateral margins of the premaxilla, nasals, prefrontals, and frontals (Fig. 2.10e; Cundall & Rossman 1993; Rieppel *et al.* 2009). Although these configurations were originally described as characterizing uropeltines and scolecophidians, respectively (Cundall & Rossman 1993), the 'central rod design' has since been expanded to encompass all burrowing alethinophidians based on its reliance on the medial frontal pillars, which are absent in scolecophidians (Rieppel 2007; Rieppel & Maisano 2007; Rieppel *et al.* 2009).

Rieppel & Maisano (2007) used this absence of the medial frontal pillars as evidence refuting scolecophidians as 'regressed macrostomatans'. Coined by Rieppel (2012), this hypothesis of 'regressed macrostomy' places scolecophidians as nested within Alethinophidia,

having secondarily lost the anatomical requirements for macrostomy (Kley 2006; Harrington & Reeder 2017; Caldwell 2019), in contrast to their traditional placement as a plesiomorphic group diverging basally among extant snakes (e.g., Walls 1942; Bellairs & Underwood 1951; List 1966; Rieppel 1988, 2012; Miralles *et al.* 2018). This 'regressive' evolution is typically attributed to paedomorphosis (Kley 2006; Scanferla 2016; Caldwell 2019), a developmental phenomenon in which embryonic or juvenile morphologies of an ancestral taxon are retained in the adult morphology of a descendant taxon (Gould 1977; McNamara 1986; Hanken & Wake 1993). Arguing against this hypothesis, Rieppel & Maisano (2007) concluded that paedomorphic modification of a macrostomatan skull could result in a skull similar to that of *Anomochilus* for example, in which the medial frontal pillars are still essential to the naso-frontal joint (Fig. 2.10c), but could not reasonably result in a scolecophidian skull, in which the medial frontal pillars are absent and force is transmitted entirely along the outer margins of the snout elements and frontal (Fig. 2.10d,e). However, this conclusion warrants re-examination, especially in light of *Atractaspis* and the closely related taxon *Aparallactus* (see below).

Essentially, the concept that the 'central rod' and 'outer shell' designs are fundamentally incompatible does not recognize the numerous examples of gradation between these morphologies in various taxa (Fig. 2.10). For example, *Anomochilus* (Fig. 2.10c)—used by Rieppel & Maisano (2007) as an exemplar of the 'central rod design'—in fact incorporates elements of both naso-frontal morphologies: as recognized by Cundall & Rossman (1993) in their initial description of these designs, the medial frontal pillars are present in *Anomochilus* to transmit force via the medial nasal flanges, but the dorsal laminae of the nasals are also expanded and articulate with the prefrontals to transmit force dorsally and laterally to the frontals (Fig. 2.10c; see also Cundall & Rossman 1993:fig. 25C).

Furthermore, Rieppel *et al.* (2009) describe the scolecophidians *Liotyphlops* and *Leptotyphlops* as incorporating features of a 'central rod design'. In *Liotyphlops*, this partial 'central rod design' consists of a contact between the nasal and the frontal not only dorsally (as in typhlopids) but also ventrally, below the olfactory tracts. In *Leptotyphlops*, it is the expanded posterior processes of the septomaxillae that abut ventrally against the subolfactory processes of the frontals (Fig. 2.10d), a contact described by Rieppel (2007) as generally typical of colubroids. Rieppel *et al.* (2009) further describe the mixture of 'outer shell' and 'central rod' components in *Leptotyphlops* as a potentially plesiomorphic condition for scolecophidians, with

typhlopids subsequently specializing into the idealized ‘outer shell design’ (Fig. 2.10e) and anomalepidids (e.g., *Liotyphlops*) developing a unique hybrid version of a ‘central rod design’.

Finally—and perhaps most relevant here given its frequent recovery as a close relative of *Atractaspis* (Underwood & Kochva 1993; Vidal *et al.* 2008; Zaher *et al.* 2009; Gauthier *et al.* 2012; Portillo *et al.* 2018; Portillo *et al.* 2019)—*Aparallactus* has been noted as exhibiting a more ‘outer shell’-like than ‘central rod’-like morphology (Rieppel 2007). For example, the medial frontal pillars are quite narrow anteroposteriorly, more closely approaching the condition in *Anomochilus* than in *Atractaspis* (C.S., pers. obs.). The nasals are also broader than in *Atractaspis* or *Uropeltis* and articulate laterally with the prefrontals, unlike in *Atractaspis* (Fig. 2.10b).

From these observations and discussions of the naso-frontal joint and its evolutionary implications, it is clear that the ‘outer shell’ and ‘central rod’ designs are not fundamentally incompatible. Rather, there is extensive gradation between these morphologies, with certain scolecophidians (e.g., *Leptotyphlops* and *Liotyphlops*) exhibiting ‘central rod’-like morphologies and certain alethinophidians (e.g., *Anomochilus* and *Aparallactus*) exhibiting ‘outer shell’-like morphologies (Fig. 2.10).

To co-opt the transformational scenario of Rieppel *et al.* (2009)—in which *Leptotyphlops* is hypothesized as ancestral to the typhlopid and anomalepidid conditions—the aforementioned taxa (i.e. *Atractaspis*, *Anomochilus*, and *Aparallactus*) provide insight into earlier stages of this proposed evolutionary scenario. Altogether, these taxa illustrate a possible transition from a typical alethinophidian ‘central rod design’ (as in *Atractaspis*; Fig. 2.10a), to a scolecophidian-like alethinophidian condition (as in *Aparallactus* or *Anomochilus*; Fig. 2.10b,c), to an alethinophidian-like scolecophidian condition (as in *Leptotyphlops*; Fig. 2.10d), and finally to a typical scolecophidian ‘outer shell design’ (as in typhlopids; Fig. 2.10e). Note that this is not a proposal of explicit ancestor-descendant relationships among these taxa, but rather a discussion of how these broader conditions grade into one another and therefore represent a morphological spectrum between two endpoint morphologies, i.e., the ‘outer shell’ and ‘central rod’ designs.

As presented by Rieppel & Maisano (2007), a major obstacle precluding an alethinophidian origin of scolecophidians is the absence of the medial frontal pillars in scolecophidians. This absence has been hypothesized as plesiomorphic in scolecophidians based on similar absence in non-snake lizards and *Dinilysia* (Rieppel 1978b, 1979a). However, this

putative fundamental difference becomes much less restrictive in light of the extensively paedomorphic and autapomorphic condition of the scolecophidian skull in general. That is, given the high degree of paedomorphosis suggested in the scolecophidian skull (see §2.4.2 and §2.4.3), combined with the functional constraints and pressures associated with fossoriality (Wake 1986; Maddin *et al.* 2011), the potential loss of the medial frontal pillars is in fact a relatively minor evolutionary transformation. Scolecophidians have lost entire bones relative to other squamates, such as the supratemporal (see §2.3.5.1), yet this does not preclude their derivation from a supratemporal-bearing squamate ancestor; similarly, the absence of the medial frontal pillars should not automatically preclude derivation from a pillar-bearing (i.e., alethinophidian) ancestor.

In fact, Rieppel & Maisano (2007) were the first to notice that the lack of medial frontal pillars and a laterosphenoid in scolecophidians could easily reflect paedomorphosis. Developmental studies have shown that the frontals of snakes begin as paired ossifications on the sides of the skull that only later in development merge along the midline (e.g., Boughner *et al.* 2007; Polachowski & Werneburg 2013); this implies that the medial flanges are the last feature to ossify and could easily fail to form due to truncations in development (i.e., paedomorphosis). The lack of a laterosphenoid may similarly result from a delay in skull ossification, as the subdivision of the trigeminal foramen into anterior and posterior compartments occurs very late in development (Khannoon & Evans 2015; Khannoon *et al.* 2020).

Despite their initial argument about paedomorphosis, though, Rieppel & Maisano (2007) further discuss the highly modified and expanded snout complex of scolecophidians as refuting the idea of this group being derived from an alethinophidian ancestor. However, this autapomorphic condition represents a morphological novelty that, following the 'null hypothesis' of miniaturization presented by Hanken (1984), clearly relates to the specialized miniaturized and fossorial nature of this group (Hanken 1984; Wake 1986; Hanken & Wake 1993). This is especially true in light of the morphological gradation of the naso-frontal joint in fossorial snakes as presented above (Fig. 2.10). As Hanken & Wake (1993) and Rieppel (1996) discuss, this novelty is often superimposed overtop paedomorphic features in miniaturized taxa, resulting in a complex mixture of autapomorphies related to heterochrony, miniaturization, and fossoriality in these organisms. This certainly seems to be the case in *Anomochilus* and *Aparallactus*, both

burrowing and miniaturized, and both showing an expanded snout complex similar to that of scolecophidians, with extensive contact between broadened nasals and prefrontals (Fig. 2.10).

Certain autapomorphic features of the scolecophidian snout—including the absence of the medial frontal pillars—are further consistent with the loss of the prokinetic joint in these snakes. Modification of the prokinetic joint—including increased articulation and reduced mobility of this joint—has similarly been noted as an adaptation for greater structural integrity in the skull of other burrowing snakes, such as uropeltids, erycines, and colubroids (Rieppel 1978a, b; Savitzky 1983). Altogether, these observations indicate that an 'outer shell design' of the naso-frontal joint as is characteristic of scolecophidians can reasonably be derived from an alethinophidian ancestor, contrary to previous arguments.

2.4.2. Heterochronic modification of the jaws, palate, suspensorium, and braincase

The jaws and palate of *Atractaspis* are distinctly reduced compared to non-fossorial colubroids (Fig. 2.11a). The pterygoid in particular has an elongate, rod-like shape which also occurs in many other fossorial taxa, especially scolecophidians (Figs 2.5a–d and 2.11; §2.3.3.1); however, unlike scolecophidians, the pterygoid of *A. irregularis* projects well posterior to the occiput (Figs 2.1 and 2.11a), as is typical of 'macrostomatan' (i.e., large-gaped) snakes (see e.g., Palci *et al.* 2016; Scanferla 2016; Strong *et al.* 2019). The number of teeth on all typical tooth-bearing elements is highly reduced, so as to be completely absent on the pterygoid and with only a few teeth on the palatine, dentary, and maxilla (Figs 2.1 and 2.11). The compound bone also exhibits a simple, rod-like form, lacking features such as a surangular crest or well-developed retroarticular process (Figs 2.1, 2.8, 2.9e–j, and 2.11).

This widespread reduction is consistent with paedomorphosis. In other words, the reduced forms of the mandibular and palatal elements in *Atractaspis* adults reflect retention of the simple, poorly-developed conditions of these elements in earlier ontogenetic stages of related taxa. In this case, we can infer the plesiomorphic developmental pathways of these elements using the ontogenetic trajectories of closely related species. In embryos of the viperid *Bothropoides jararaca*, the pterygoid maintains a simple, rod-like form until SES stage 4 (i.e., mid-stage embryonic development), at which point it elaborates in form before teeth begin developing from SES stages 6 to 7 (i.e., late-stage embryonic development) (Polachowski & Werneburg 2013). Similar developmental timing characterizes the dentary and palatine in this species (Polachowski & Werneburg 2013). Khannoon & Evans (2015) describe similar timing

for these elements in the elapid *Naja haje haje*. Finally, in late-stage embryos of the natricid *Thamnophis radix*, the mandibular and palatal elements already bear teeth and are much more elaborate in form than in adults of *A. irregularis* (Strong *et al.* 2019). *A. irregularis* is therefore clearly paedomorphic relative to other colubroids regarding the morphology of the mandible and palate, as adults of this species exhibit the conditions present in mid-stage and earlier embryos of surrounding colubroid taxa. This paedomorphosis heavily contributes to the specialized morphology of *Atractaspis* within this larger clade.

This mechanism of heterochrony has been proposed for comparable adaptations in other snakes. These include reduction of the palatal bones and dentition in *Anomochilus* and uropeltine snakes, and reduction of the retroarticular process of the compound bone in *Anomochilus* (Rieppel & Maisano 2007). Most prominently, scolecophidians—blind, miniaturized, fossorial snakes—have been noted as paedomorphic with respect to the mandible, palatomaxillary complex, and suspensorium (Kley 2006; Caldwell 2019).

In fact, the paedomorphosis exhibited by scolecophidians is in many ways comparable to that of *Atractaspis*—e.g., the reduced mandible and highly reduced and often absent dentition (Kley 2006; Caldwell 2019)—though in other aspects it is far more extensive than that noted herein for *Atractaspis* (Fig. 2.11). For example, the proximal epiphysis of the quadrate remains unfused (Kley 2006), the ectopterygoid and supratemporal are typically completely absent or at least extremely reduced (Rieppel *et al.* 2009; Caldwell 2019; Chretien *et al.* 2019), and the quadrate is oriented anteriorly, representing an extreme retention of the embryonic squamate condition (Kamal 1966; Rieppel & Zaher 2000; Kley 2006; Hernández-Jaimes *et al.* 2012; Scanferla 2016; Caldwell 2019). Similar reduction and anterior displacement of the suspensorium occurs in other miniaturized snakes, such as *Anomochilus* and *Uropeltis* (§2.3.5.1 and §2.3.5.2; see also Olori & Bell 2012). These taxa altogether reflect a trend toward extensive paedomorphic modification of the suspensorium and jaws in miniaturized vertebrates (Hanken & Wake 1993; Olori & Bell 2012).

Evidence of paedomorphosis can also be found in the overall shape of the braincase of snakes such as *Atractaspis*, *Anomochilus*, and scolecophidians, in which the external surface of the braincase appears smooth and rounded, devoid of any sharp crests or ridges, a condition resembling that of neonate or juvenile snakes (Palci *et al.* 2016; Strong *et al.* 2019). The braincase is also relatively large in *Atractaspis* compared to adults of other colubroids (e.g.,

Thamnophis), a feature again resembling the condition among juvenile snakes (Palci *et al.* 2016; Strong *et al.* 2019). The lack of a well-developed dorsum sellae overhanging the sella turcica in *Atractaspis*, *Anomochilus*, and scolecophidians may represent another paedomorphic feature, related to the lack of crests and ridges on the external surface of the braincase.

However, not all heterochronic changes to the skull of *Atractaspis* involve paedomorphosis. Certain features—such as the quadrate, the snout complex, and the parasphenoid rostrum of the parabasisphenoid—in fact exhibit peramorphosis (i.e., extended development; McNamara 1986) relative to other colubroids such as *Thamnophis radix* (Fig. 2.11a). In the case of the parasphenoid rostrum (Figs 2.6a–f and 2.11a) and the snout (Figs 2.2 and 2.11a), this peramorphosis contributes to fossoriality, as these components are expanded and tightly integrated with surrounding elements, thus strengthening the skull (see also §2.4.1). The peramorphic extension of the quadrate in *Atractaspis* relative to other colubroids is likely related to reduction of the supratemporal: because the supratemporal of *Atractaspis* is much smaller and terminates farther anteriorly than in typical colubroids (Figs 2.1b, 2.8a, 2.9k–l, and 2.11a; §2.3.5.1), the quadrate must therefore extend anteriorly in order to maintain a functional articulation with this element. For all of these skull components, peramorphosis essentially addresses functional constraints to the skull, related either to burrowing (as for the parasphenoid rostrum and snout complex) or to maintaining functionality of the suspensorium (as for the quadrate). A similar combination of paedomorphosis and peramorphosis, with this latter phenomenon compensating for functional requirements, has been noted throughout paedomorphic tetrapods (Wake 1986; Rieppel 1996).

Finally, the supratemporal of *Atractaspis irregularis* also provides insight into heterochrony in other colubroids. The supratemporal of *A. irregularis* does not extend anteriorly beyond the prootic or posteriorly beyond the occiput (Figs 2.1b and 2.11a), thus reflecting developmental reduction of this element relative to typical caenophidians and booids, respectively (Palci *et al.* 2016; Strong *et al.* 2019). Interestingly, this configuration of the supratemporal in *Atractaspis irregularis* matches that in embryos of the caenophidian *Thamnophis* (Strong *et al.* 2019). In contrast, the supratemporal in *Thamnophis* adults extends both anteriorly onto the parietal and posteriorly well beyond the occiput (Fig. 2.11a; Strong *et al.* 2019). This posterior projection is typically restricted to booids among ‘macrostomatan’ snakes, thus contrasting the typical condition proposed for caenophidians, in which the supratemporal

does not extend distinctly posterior to the occiput (Palci *et al.* 2016; Strong *et al.* 2019). In other words, the posterior elongation of this element throughout ontogeny in *Thamnophis* surpasses the condition typically present in adult caenophidians. Therefore, whereas *Atractaspis* exhibits paedomorphic modification of the supratemporal relative to other caenophidians, the supratemporal of *Thamnophis* exhibits peramorphosis relative to this clade.

Heterochrony therefore plays a major role in the evolution and development of the jaws, suspensorium, and overall skull shape in snakes.

2.4.3. The role of heterochrony in the evolution of fossorial snakes

Heterochrony has been proposed as one of the major forces driving the evolution of the snake skull from that of non-snake lizards (Irish 1989; Hanken & Wake 1993; Werneburg & Sánchez-Villagra 2015; Da Silva *et al.* 2018). Studies of snake skull ontogeny are still relatively rare, tending to focus on embryonic development (e.g., Pringle 1954; Zehr 1962; Jackson 2002; Boughner *et al.* 2007; Boback *et al.* 2012; Polachowski & Werneburg 2013; Khannoon & Evans 2015; Khannoon & Zahradnicek 2017; Sheverdyukova 2017, 2019; Al-Mohammadi *et al.* 2020; Khannoon *et al.* 2020), with only a few studies examining postnatal ontogeny (Young 1989; Scanferla & Bhullar 2014; Palci *et al.* 2016; Scanferla 2016; Sherratt *et al.* 2019; Strong *et al.* 2019). However, our growing understanding of evolutionary development in snakes suggests that heterochrony is an important driver of the evolution not only of snakes relative to other squamates, but of snakes relative to each other (see also Da Silva *et al.* 2018). This importance is clearly supported by the extensive, heterochronic patterns of skull paedomorphosis and peramorphosis in several snake species, as discussed above.

Understanding the role of heterochronic processes in snake skull evolution is in turn essential for understanding snake phylogeny. Although scolecophidians are traditionally considered the most basal group of extant snakes, retaining many plesiomorphic non-snake lizard features (e.g., Walls 1942; Bellairs & Underwood 1951; List 1966; Rieppel 2012; Miralles *et al.* 2018), recent phylogenies have recovered scolecophidians as nested within Alethinophidia (Fig. 2.12; Palci & Caldwell 2010; Garberoglio *et al.* 2019a). This placement of scolecophidians as highly modified alethinophidians is reminiscent of the aforementioned hypothesis of scolecophidians as ‘regressed macrostomatans’ (Kley 2006; Harrington & Reeder 2017; Caldwell 2019). Because this latter perspective proposes heterochrony as a cause of this ‘regressive’ evolution (Kley 2006; Scanferla 2016; Caldwell 2019), the observations above

regarding paedomorphosis in the jaws and suspensorium thus provide novel insight into this hypothesis of 'regressed macrostomy'.

As discussed above, *Atractaspis* and scolecophidians both exhibit paedomorphosis of various cranial elements, with this heterochrony being more extensive in the miniaturized scolecophidians than the fossorial but non-miniaturized *Atractaspis* (Fig. 2.11). For example, certain paedomorphic features (e.g., reduction of the mandible and dentition) occur in both groups, whereas other features (e.g., anterior orientation of the quadrate and marked reduction or loss of the supratemporal and ectopterygoid) occur only in scolecophidians (Fig. 2.11). These observations are consistent with the hypothesis that paedomorphosis causes—or at least strongly correlates with—miniaturization (Gould 1977; Hanken 1984; Wake 1986; Fröbisch & Schoch 2009; Sherratt *et al.* 2019). When considered in the context of these developmental phenomena, the morphologies of these fossorial taxa essentially fall along a continuum, with more 'extreme' paedomorphosis resulting in more 'extreme' anatomies.

This morphological and developmental gradation refutes the traditional concept of scolecophidians as fundamentally different from alethinophidians (Fig. 2.12a). Instead, miniaturization and paedomorphosis together represent a possible mechanism by which a scolecophidian-like morphology may be derived from a fossorially-adapted alethinophidian morphology, such as that of *Atractaspis* (Fig. 2.11a) or *Anomochilus* (Fig. 2.11b). Essentially, the observed morphological continuum suggests a scenario in which miniaturization and associated extensive paedomorphosis have superimposed many unique scolecophidian morphologies overtop the paedomorphic features already present in an ancestral fossorial alethinophidian bauplan (Fig. 2.11); thus, this continuum ultimately supports recent hypotheses of an alethinophidian ancestry of scolecophidians (Fig. 2.12b; Palci & Caldwell 2010; Caldwell 2019; Garberoglio *et al.* 2019a).

This perspective of scolecophidians as paedomorphically 'regressed' alethinophidians is also consistent with Scanferla's (2016) discussion of the skeletal ontogeny of macrostomy. In his developmental analysis of snakes, Scanferla (2016) identified at least ten distinct lineages of fossorial 'macrostomatans' that exhibit truncated development of the jaws and suspensorium relative to closely-related but non-fossorial taxa, thus failing to develop key skeletal requirements for macrostomy such as elongation of the supratemporal and rotation of the quadrate (see Scanferla 2016:fig. S5). Paedomorphic 'regression' of macrostomy—i.e., reversion

to a small-gaped condition—is therefore in fact quite common among fossorial alethinophidians (Scanferla 2016). This connection between fossoriality and derived loss of macrostomy, coupled with the morphological continuum between scolecophidians and fossorial alethinophidians as described above, thus supports the hypothesis of a 'regressive' evolution of scolecophidians (see also Vidal & Hedges 2002; Harrington & Reeder 2017).

Of course, as is typical of miniaturized tetrapods (Hanken & Wake 1993; Rieppel 1996), paedomorphosis alone does not account for all of the unique features of scolecophidians. As noted above, other scolecophidian autapomorphies such as the greatly expanded snout instead represent adaptations related to fossoriality (List 1966; Rieppel 1996; Rieppel *et al.* 2009), exemplifying how ecological constraints can combine with miniaturization and paedomorphosis to create strikingly unique skull morphologies (Hanken & Wake 1993; Rieppel 1996). A similar combination of highly paedomorphic and highly autapomorphic features has been noted in other miniaturized, fossorial taxa, such as the caecilian *Idiocranium russeli* (Wake 1986). As discussed for the naso-frontal joint (§2.4.1), Hanken's (1984) 'null hypothesis' of miniaturization establishes such occurrences of morphological novelty as being consistent with a hypothesis of paedomorphosis-driven miniaturization. I therefore propose that this combination of paedomorphic miniaturization and adaptational autapomorphy may underlie the evolution of the scolecophidian skull from an alethinophidian ancestor (Figs 2.11 and 2.12).

As above (§2.4.1), it is important to emphasize that this is not an argument that scolecophidians are derived specifically from *Atractaspis*, nor that any of the anatomical similarities noted herein are synapomorphic. Indeed, given the well-documented homoplasy involved in adaptations related to fossoriality (Savitzky 1983; Maddin *et al.* 2011) and paedomorphosis (Wiens *et al.* 2005; Fröbisch & Schoch 2009), any similarity in the morphology of these taxa is quite conceivably convergent. Rather than a hypothesis of synapomorphy or of explicit phylogenetic relationships, this is instead a discussion and comparison of broad morphological conditions, as exemplified by *Atractaspis* and scolecophidians. Thus, the core question presented herein is: if an *Atractaspis*-like condition can be derived from an alethinophidian ancestor, is it possible for a scolecophidian-like condition to also be derived from this lineage? In my view, burrowing adaptations in combination with heterochrony—specifically paedomorphosis, and in this case specifically related to the jaws and suspensorium—

can reasonably be hypothesized as enabling derivation of the miniaturized and highly modified scolecophidian skull from an ancestral alethinophidian morphotype (Fig. 2.11).

For example, aside from *Atractaspis*, numerous similarities also exist between scolecophidians and the early-diverging alethinophidian *Anomochilus*, such as the short, rod-like and toothless pterygoids, the laterally expanded nasals in contact with the prefrontals, a lateral contact between the nasal flanges and septomaxillae, the absence of a well-developed dorsum sellae overhanging the sella turcica, a rounded braincase, and an anteroventral tilt of the main axis of the quadrate (Figs 2.10 and 2.11b). Unlike more derived alethinophidians, *Anomochilus* also shares with scolecophidians a reduced ectopterygoid (strongly reduced in Anomalepididae, absent in Leptotyphlopidae and Typhlopoidea; List 1966; Rieppel *et al.* 2009) and the retention of the coronoid bone and vestigial pelvic girdle (Rieppel & Maisano 2007; Palci *et al.* 2020b). Thus, beyond *Atractaspis*, *Anomochilus* clearly provides another 'precedent' for a scolecophidian-like morphology arising within Alethinophidia.

Of course, this hypothesis of scolecophidians as 'regressed alethinophidians' requires rigorous testing. Primarily, any hypothesis of heterochrony requires a robust phylogenetic framework (Wiens *et al.* 2005; Rieppel & Maisano 2007; Fröbisch & Schoch 2009). However, the phylogeny of scolecophidians is uncertain, due in large part to disagreement between morphological and molecular data. Based on morphological evidence alone, scolecophidians would represent a monophyletic assemblage (Gauthier *et al.* 2012; Hsiang *et al.* 2015; Garberoglio *et al.* 2019a). Molecular data, on the other hand, unequivocally support a paraphyletic 'Scolecophidia', with Leptotyphlopidae and Typhlopoidea as sister taxa and Anomalepididae in either a more basal or more derived position (e.g., Figueroa *et al.* 2016; Zheng & Wiens 2016; Miralles *et al.* 2018). The conflicting placement of Anomalepididae relative to the other two scolecophidian lineages in molecular phylogenetic analyses is possibly affected by the early divergence of the group. The limitations of molecular phylogenetics in resolving the placement of early-diverging lineages (deep branches) have been highlighted in a recent study by Mongiardino Koch & Gauthier (2018).

The recovery of a robust scolecophidian phylogeny is also complicated by the fact that paedomorphosis itself may act as a confounding factor in phylogenetic analyses, both morphological and molecular (Gauthier *et al.* 1988a; Hanken & Wake 1993; Wiens *et al.* 2005; Struck 2007). From a molecular perspective, paedomorphosis has been linked to extensive gene

loss, as reported in a recent study on fish (Malmstrøm *et al.* 2018). This implies that the molecular signal from scolecophidian genomes may be significantly altered, and the absence of some putative alethinophidian autapomorphies (e.g., the duplicate control region in the mitochondrial genome; Dong & Kumazawa 2005; Yan *et al.* 2008) could simply represent secondary losses rather than plesiomorphic conditions. It is also entirely possible that scolecophidian synapomorphies linking typhlopoids, leptotyphlopids, and anomalepidids have been lost for the same reason, a potential loss of phylogenetic signal that may contribute to the ambiguous placement of anomalepidids (e.g., Figueroa *et al.* 2016; *versus* Zheng & Wiens 2016). If the scolecophidian genome is the result of simplification via gene loss, then this would have a profound effect on our ability to resolve their phylogenetic relationships based on molecular data alone.

In light of the potential importance of paedomorphosis, an examination of scolecophidian skeletal ontogeny is essential. The most accurate method of identifying paedomorphosis in scolecophidians would be via a comparative ontogenetic analysis incorporating scolecophidians, alethinophidians, and non-snake lizards. To my knowledge, only two such studies (Palci *et al.* 2016; Da Silva *et al.* 2018), both based in geometric morphometrics, have been conducted; in both cases, the results suggested scolecophidians as paedomorphic relative to other squamates. These studies indicate that this largely unexplored evolutionary scenario warrants further analysis, with large-scale sampling—both of taxa and of ontogenetic stages—key to robustly investigating this hypothesis.

Although a robust phylogenetic context is still lacking for snakes (Chretien *et al.* 2019), recently revised and large-scale datasets such as that of Simões *et al.* (2018) and Garberoglio *et al.* (2019a) provide a sound basis for future large-scale studies of snake evolution. Interestingly, a recent morphological phylogeny (Garberoglio *et al.* 2019a) focussing on extinct snakes recovered scolecophidians as nested within Alethinophidia (Fig. 2.12b), in stark contrast to the more orthodox placement of this group as basally divergent among Serpentes (Fig. 2.12a). These results strongly highlight the importance of continued morphological and phylogenetic analyses of this group, including a renewed examination of potential alethinophidian affinities of scolecophidians.

2.5. Conclusions

I herein present the first thorough description of the cranial osteology of *Atractaspis*, using fully segmented micro-CT scans of *A. irregularis* (Figs 2.1–2.9). This analysis reveals the jaws and suspensorium of *Atractaspis* to be paedomorphic relative to other colubroids. This observation in turn provides insight into the evolution of scolecophidian snakes, given the even more pronounced paedomorphosis hypothesized for this latter group (Fig. 2.11; Kley 2006; Palci *et al.* 2016; Da Silva *et al.* 2018; Caldwell 2019). Combined with my discussion of the naso-frontal joint in *Atractaspis* and other fossorial snakes (Fig. 2.10), these results contest the traditional view of scolecophidians as representing a 'primitive' or ancestral morphology among snakes, instead lending support to the hypothesis of scolecophidians as 'regressed macrostomatans' (see Rieppel 2012), or perhaps more precisely put, 'regressed alethinophidians' (Figs 2.11 and 2.12). I propose that this 'regression' is the result of: paedomorphosis, to an extent beyond that present in *Atractaspis* (Fig. 2.11); miniaturization, which is tied to paedomorphosis and typically correlated with morphological novelty (Fig. 2.11; Hanken 1984; Hanken & Wake 1993); and adaptations for fossoriality, such as the structure of the naso-frontal joint, which combine with miniaturization to produce a highly autapomorphic skull morphology (Figs 2.10 and 2.11; Hanken & Wake 1993; Rieppel 1996). Altogether, I hypothesize that these factors have driven the derivation of the scolecophidian skull from an alethinophidian ancestor.

Ultimately, this kind of transformational hypothesis is just that: a hypothesis, requiring robust evidence in order to be supported or refuted, and ultimately refined. This evidence can come in the form of anatomical observations and interpretations such as those I have presented in this study. A key line of evidence also lies in the phylogenetic analysis of the taxa in question. Such an undertaking warrants a treatment of its own and as such is outside the scope of this study; however, the present descriptions, comparisons, micro-CT reconstructions, and preliminary examination of evolutionary scenarios provide an essential basis for future phylogenetic analyses. This is not a circular research program, but rather reflects the nature of scientific inquiry where each new answer generates numerous new questions further probing method, data, hypotheses, and theory. In particular, my observations and interpretations of the jaw, suspensorium, and naso-frontal joint in fossorial snakes raise intriguing possibilities regarding the phylogenetic placement of scolecophidians, thus contributing to recent discussions on the evolution of this group (e.g., Miralles *et al.* 2018; Caldwell 2019; Chretien *et al.* 2019). These interpretations are especially relevant in light of recent phylogenies recovering

scolecophidians as nested among alethinophidians (Palci & Caldwell 2010; Garberoglio *et al.* 2019a), in contrast to their traditional placement as the basal-most living snakes (e.g., Longrich *et al.* 2012; Hsiang *et al.* 2015; Reeder *et al.* 2015).

Figures: Chapter Two

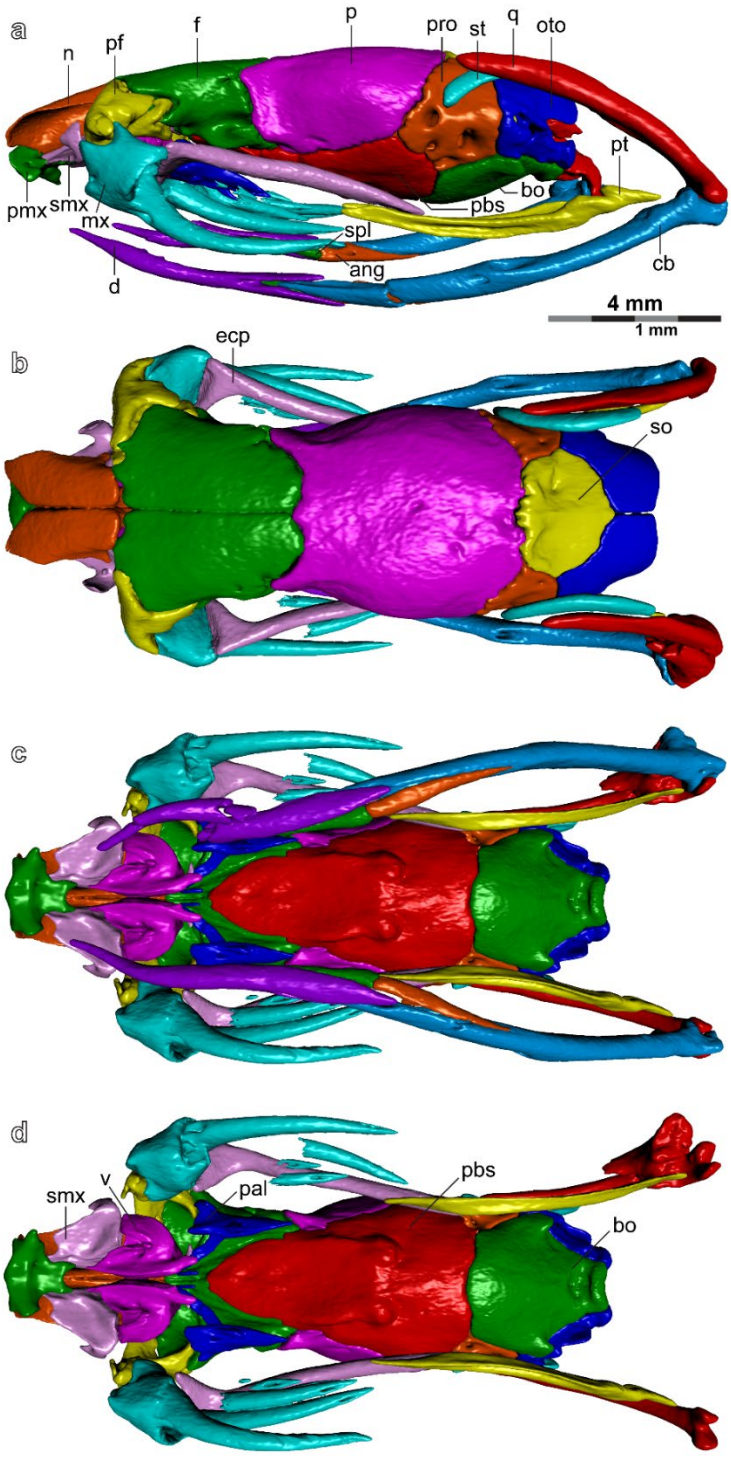

FIGURE 2.1. Overview of skull of *Atractaspis irregularis* (FMNH 62204). (**a**–**d**) Skull in (**a**) lateral view (right lateral, reflected), (**b**) dorsal view, (**c**) ventral view with mandibles, and (**d**) ventral view with mandibles removed. Colouration is consistent throughout all panels. Surface mesh files of each element are available as 3D PDFs in the Supporting Information (Figs S2.1–S2.23). Abbreviations: ang, angular; bo, basioccipital; cb, compound bone; d, dentary; ecp, ectopterygoid; f, frontal; mx, maxilla; n, nasal; oto, otoccipital; p, parietal; pal, palatine; pbs, parabasisphenoid; pf, prefrontal; pmx, premaxilla; pro, prootic; pt, pterygoid; q, quadrate; smx, septomaxilla; so, supraoccipital; spl, splenial; st, supratemporal; v, vomer.

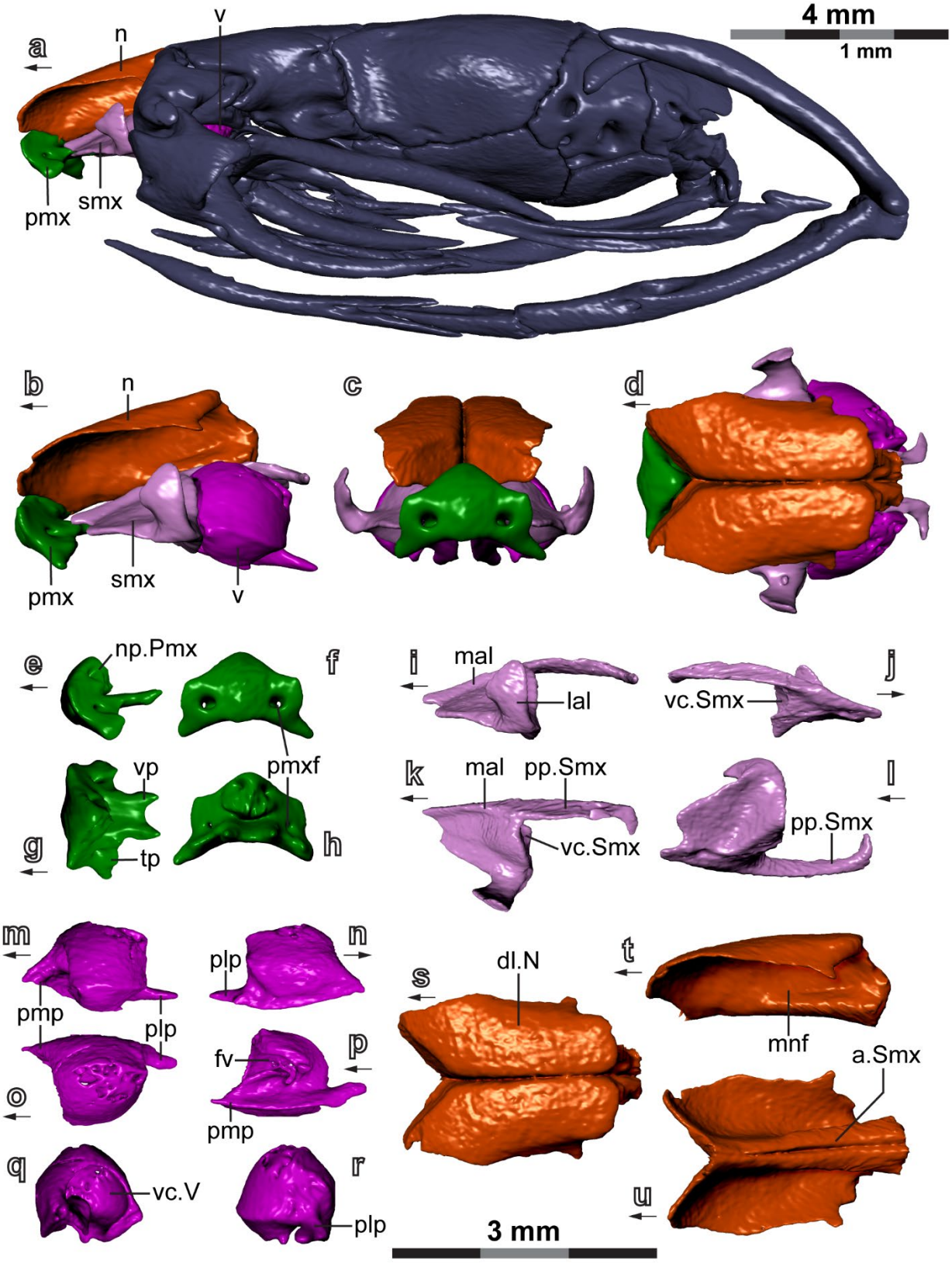
a
n
v
4 mm
1 mm
pmx
smx
b
n
pmx
smx
v
c
d
e
np.Pmx
f
pmxf
vp
g
tp
h
i
mal
lal
j
vc.Smx
k
mal
pp.Smx
vc.Smx
l
pp.Smx
m
pmp
plp
n
plp
o
p
fv
pmp
q
vc.V
r
plp
s
dl.N
t
mnf
a.Smx
u
3 mm

FIGURE 2.2. Snout unit and elements of *Atractaspis irregularis* (FMNH 62204). (**a**) Snout in articulation with the skull (right lateral view, reflected). (**b**–**d**) Articulated snout elements in (**b**) lateral, (**c**) anterior, and (**d**) dorsal views. (**e**–**h**) Premaxilla in (**e**) lateral, (**f**) anterior, (**g**) dorsal, and (**h**) posterior views. (**i**–**l**) Left septomaxilla in (**i)** lateral, (**j**) medial, (**k**) dorsal, and (**l**) ventral views. (**m**–**r**) Left vomer in (**m**) lateral, (**n**) medial, (**o**) dorsal, (**p**) ventral, (**q**) anterior, and (**r**) posterior views. (**s**–**u**) Nasals in (**s**) dorsal, (**t**) lateral, and (**u**) ventral views. Upper scale bar applies to (**a**); lower scale bar applies to (**b**–**u**). Colouration is consistent throughout all panels. Arrows beneath panel labels point anteriorly. Surface mesh files of each element are available as 3D PDFs in the Supporting Information (Figs S2.1–S2.23). Abbreviations: a.Smx, articulatory surface for the septomaxilla; dl.N, dorsal lamina of the nasal; fv, fenestra vomeronasalis; lal, lateral ascending lamina; mal, medial ascending lamina; mnf, medial nasal flange; n, nasal; np.Pmx, nasal process of the premaxilla; pmx, premaxilla; plp, palatal process; pmp, premaxillary process; pmxf, premaxillary foramen; pp.Smx, posterior process of the septomaxilla; smx, septomaxilla; tp, transverse process; v, vomer; vc.Smx, vomeronasal cupola of the septomaxilla; vc.V, vomeronasal cupola of the vomer; vp, vomerine process.

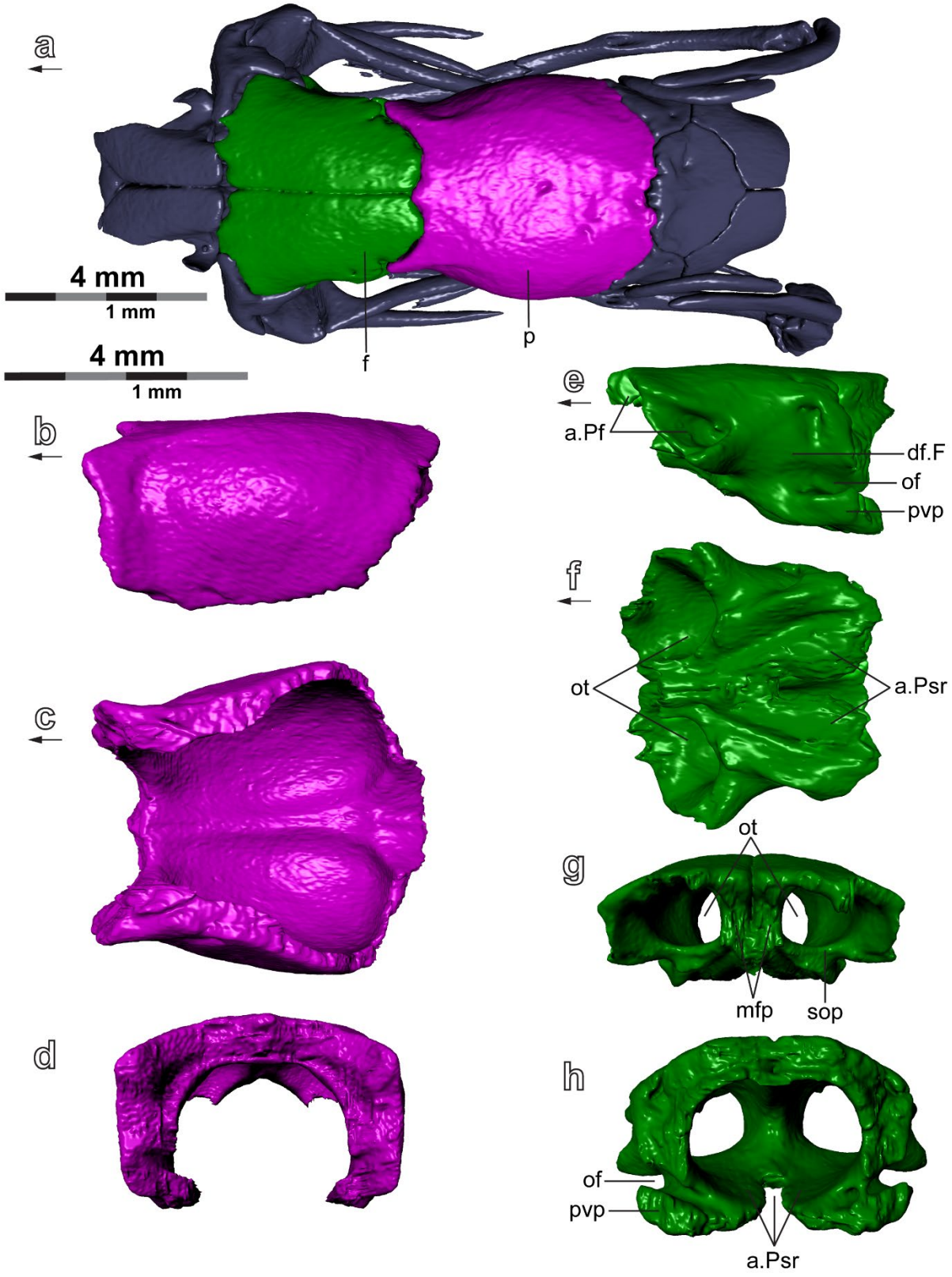
a
4 mm
1 mm
4 mm
1 mm
f
p
b
c
d
e
a.Pf
df.F
of
pvp
f
ot
a.Psr
ot
g
mfp
sop
h
of
pvp
a.Psr

FIGURE 2.3. Skull roof of *Atractaspis irregularis* (FMNH 62204). (**a**) Skull roof in articulation with the skull (dorsal view). (**b**–**d**) Parietal in (**b**) lateral, (**c**) ventral, and (**d**) anterior views. (**e**–**h**) Frontal in (**e**) lateral, (**f**) ventral, (**g**) anterior, and (**h**) posterior views. Upper scale bar applies to (**a**); lower scale bar applies to (**b**–**h**). Colouration is consistent throughout all panels. Arrows beneath panel labels point anteriorly. Surface mesh files of each element are available as 3D PDFs in the Supporting Information (Figs S2.1–S2.23). Abbreviations: a.Pf, articulatory surface for the prefrontal; a.Psr, articulatory surface for the parasphenoid rostrum; df.F, descending flange of the frontal; f, frontal; mfp, medial frontal pillar; of, optic foramen; ot, olfactory tract; p, parietal; pvp, posteroventral process; sop, subolfactory process.

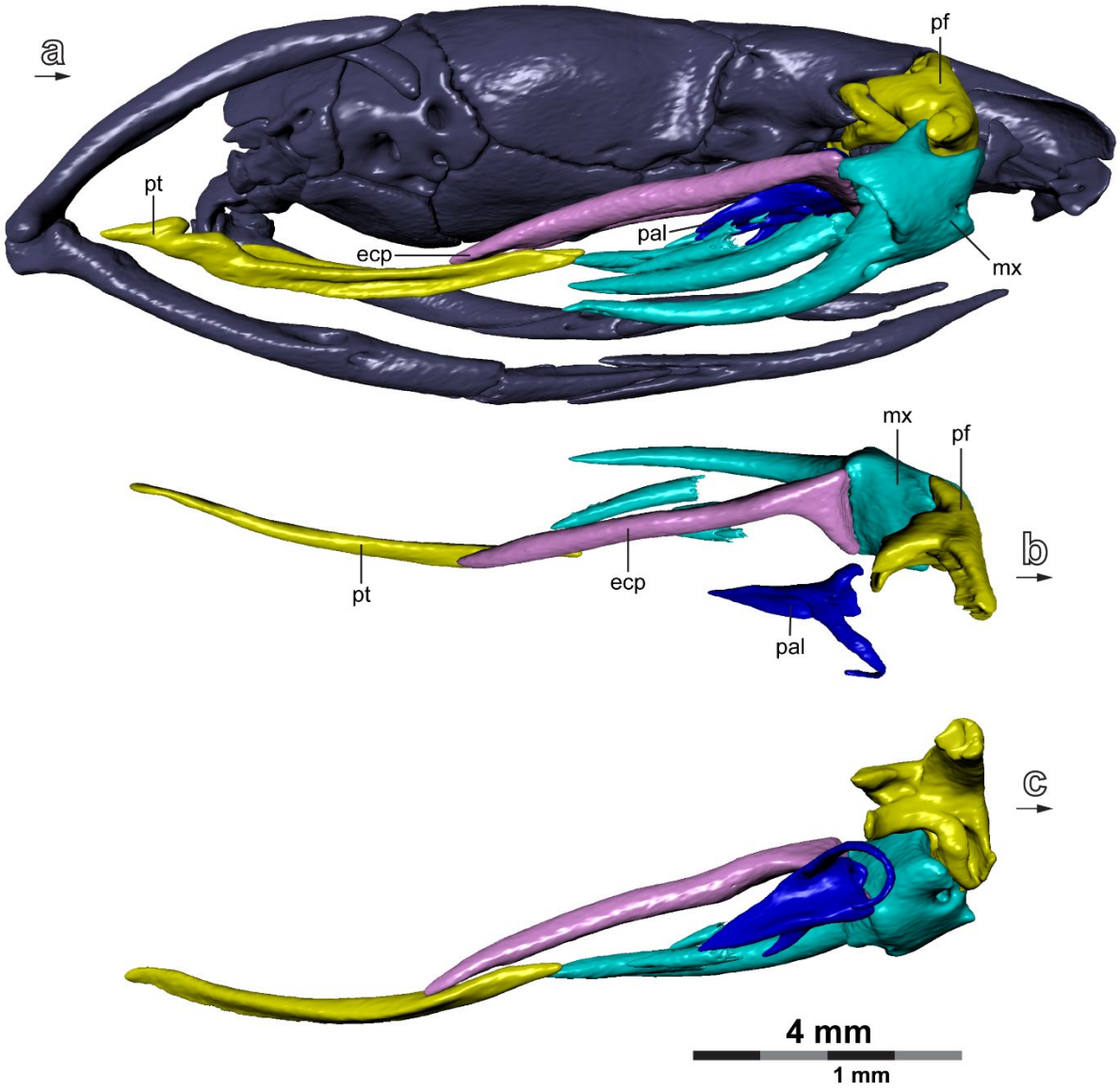

FIGURE 2.4. Overview of palatomaxillary complex of *Atractaspis irregularis* (FMNH 62204). (**a**) Palatomaxillary complex in articulation with the skull (right lateral view). (**b**–**c**) Articulated left palatomaxillary elements in (**b**) dorsal and (**c**) medial views. Colouration is consistent throughout all panels. Arrows beneath panel labels point anteriorly. Surface mesh files of each element are available as 3D PDFs in the Supporting Information (Figs S2.1–S2.23). Abbreviations: ecp, ectopterygoid; mx, maxilla; pal, palatine; pf, prefrontal; pt, pterygoid.

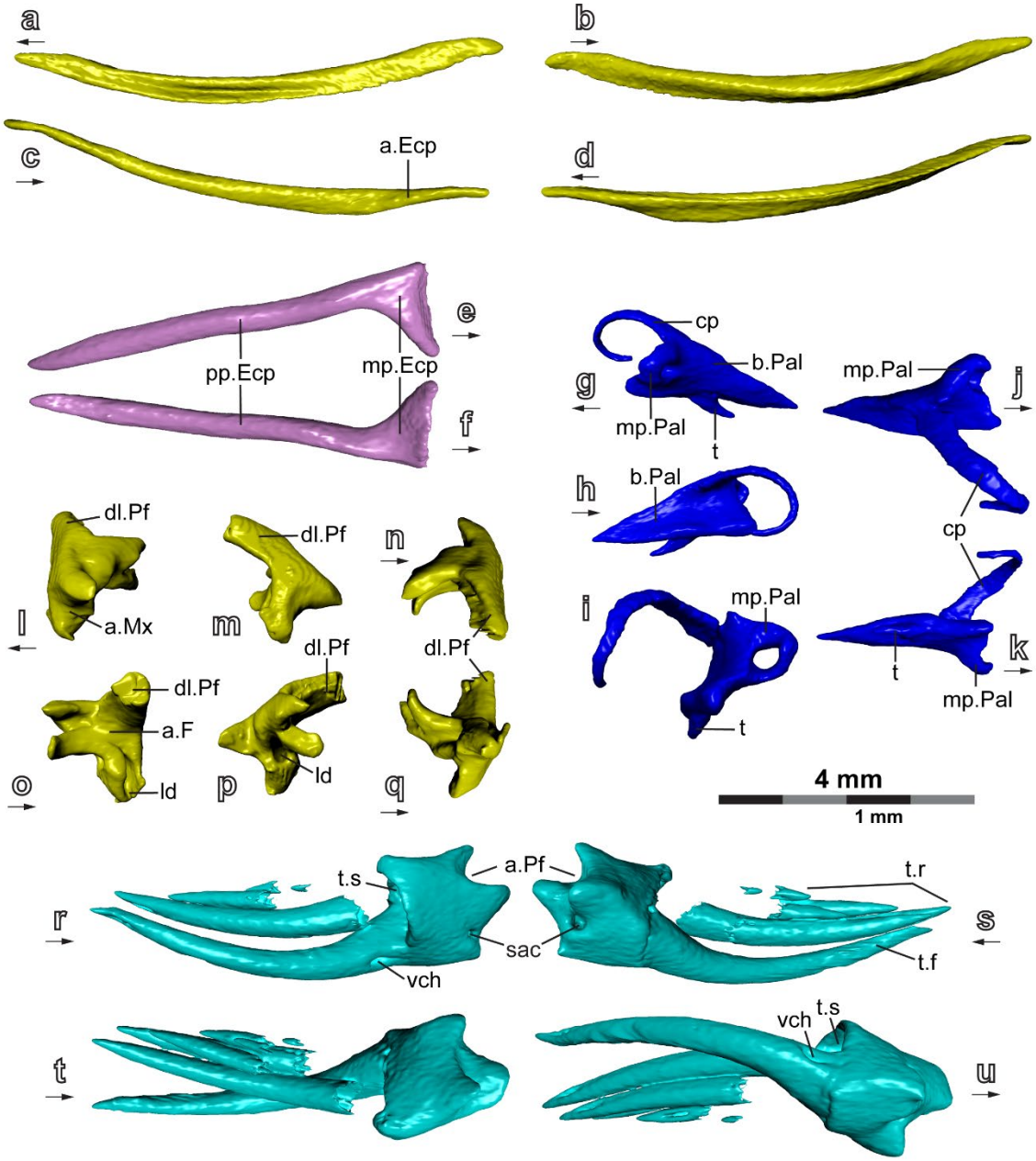
a
b
c
a.Ecp
d
e
pp.Ecp
mp.Ecp
f
cp
g
b.Pal
mp.Pal
t
mp.Pal
j
h
b.Pal
cp
dl.Pf
dl.Pf
n
l
a.Mx
m
dl.Pf
dl.Pf
i
mp.Pal
k
t
mp.Pal
dl.Pf
a.F
o
ld
p
ld
q
t
4 mm
1 mm
a.Pf
t.s
t.r
r
sac
s
vch
t.f
vch
t.s
t
u

FIGURE 2.5. Palatomaxillary elements of *Atractaspis irregularis* (FMNH 62204). (**a**–**d**) Left pterygoid in (**a**) lateral, (**b**) medial, (**c**) dorsal, and (**d**) ventral views. (**e**–**f**) Left ectopterygoid in (**e**) dorsal and (**f**) ventral views. (**g**–**k**) Left palatine in (**g**) lateral, (**h**) medial, (**i**) anterior, (**j**) dorsal, and (**k**) ventral views. (**l**–**q**) Left prefrontal in (**l**) lateral, (**m**) anterior, (**n**) dorsal, (**o**) medial, (**p**) posterior, and (**q**) ventral views. (**r**–**u**) Right maxilla in (**r**) lateral, (**s**) medial, (**t**) dorsal, and (**u**) ventral views. Colouration is consistent with other figures in this chapter. Arrows beneath panel labels point anteriorly. Surface mesh files of each element are available as 3D PDFs in the Supporting Information (Figs S2.1–S2.23). Abbreviations: a.Ecp, articulatory surface for the ectopterygoid; a.F, articulatory surface for the frontal; a.Mx, articulatory surface for the maxilla; a.Pf, articulatory surface for the prefrontal; b.Pal, main body of the palatine; cp, choanal process; dl.Pf, dorsal lappet of the prefrontal; ld, lacrimal duct; mp.Ecp, maxillary process of the ectopterygoid; mp.Pal, maxillary process of the palatine; pp.Ecp, pterygoid process of the ectopterygoid; sac, superior alveolar canal; t, tooth; t,f, functional tooth; t.r, replacement tooth; t.s, tooth socket; vch, venom channel.

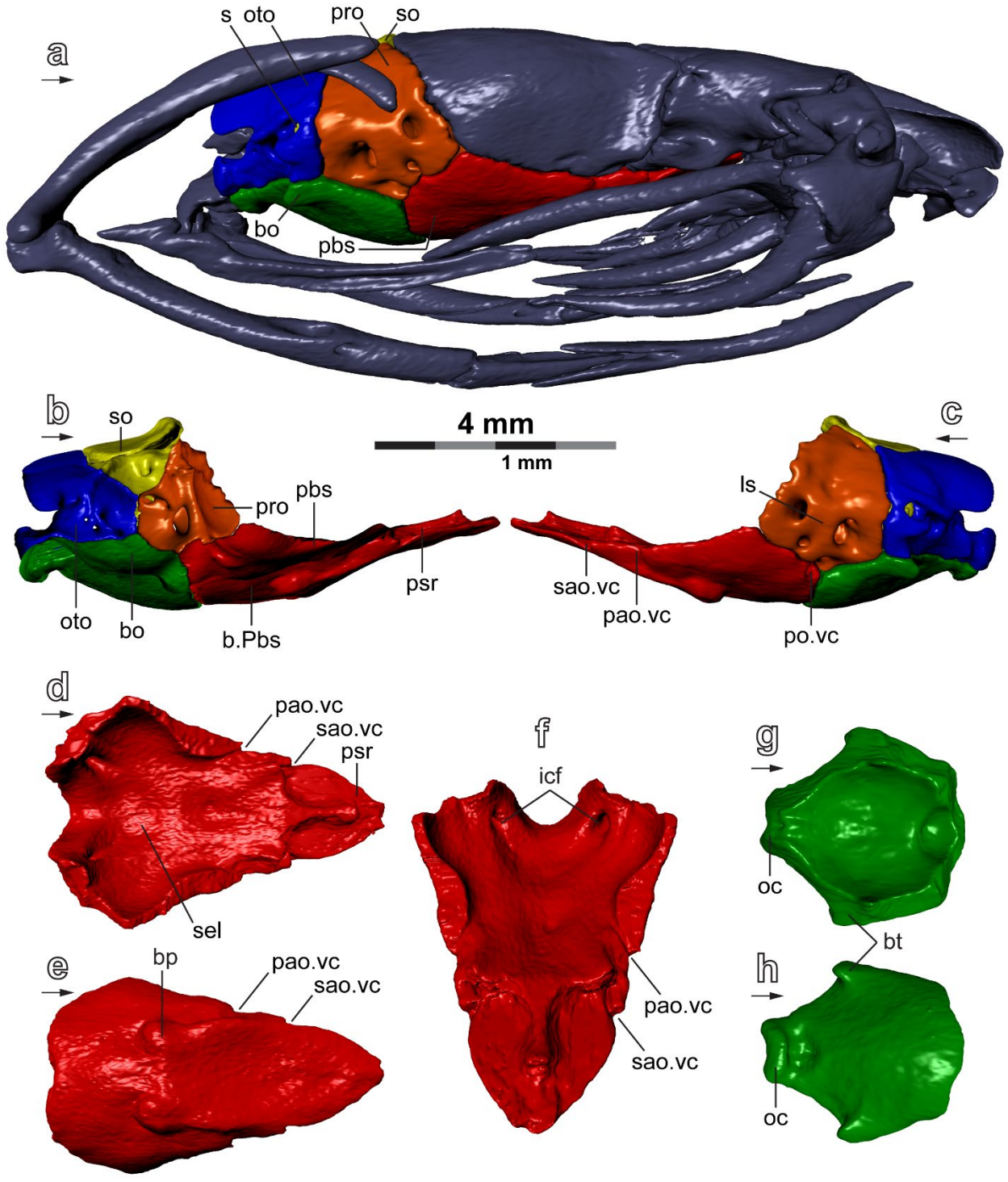
a
s
oto
pro
so
bo
pbs
b
so
pro
pbs
psr
oto
bo
b.Pbs
4 mm
1 mm
c
ls
sao.vc
pao.vc
po.vc
d
pao.vc
sao.vc
psr
sel
e
bp
pao.vc
sao.vc
f
icf
pao.vc
sao.vc
g
oc
bt
h
oc

FIGURE 2.6. Braincase and constituent elements of *Atractaspis irregularis* (FMNH 62204). (**a**) Braincase in articulation with the skull (right lateral view). (**b**–**c**) Articulated braincase elements in (**b**) medial and (**c**) lateral views. (**d**–**f**) Parabasisphenoid in (**d**) dorsal, (**e**) ventral, and (f) anterodorsal views. (**g**–**h**) Basioccipital in (**g**) dorsal and (**h**) ventral views. Panels (**b**) and (**c**) not to scale. Colouration is consistent throughout all panels. Arrows beneath panel labels point anteriorly. Surface mesh files of each element are available as 3D PDFs in the Supporting Information (Figs S2.1–S2.23). Abbreviations: bp, basipterygoid process; b.Pbs, main body of the parabasisphenoid; bo, basioccipital; bt, basioccipital tubercle; icf, internal carotid foramen; ls, laterosphenoid ossification; oc, occipital condyle; oto, otoccipital; pao.vc, primary anterior opening of the Vidian canal; po.vc, posterior opening of the Vidian canal; pbs, parabasisphenoid; pro, prootic; psr, parasphenoid rostrum; s, stapes; sao.vc, secondary anterior opening of the Vidian canal; sel, sella turcica; so, supraoccipital.

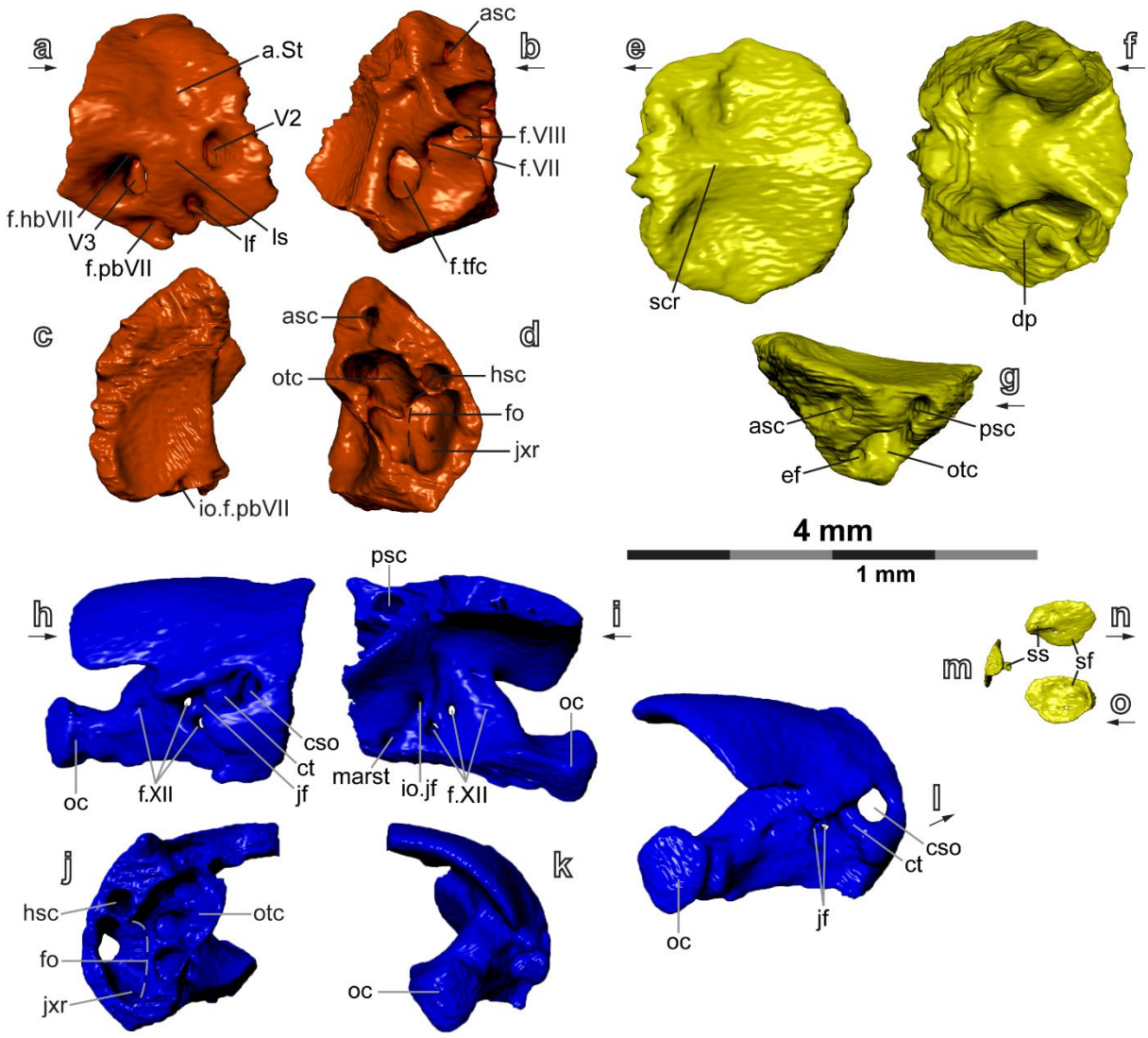
a
a.St
V2
f.hbVII
V3
f.pbVII
lf
ls
b
asc
f.VIII
f.VII
f.tfc
c
io.f.pbVII
d
asc
otc
hsc
fo
jxr
e
scr
f
dp
g
asc
psc
ef
otc
4 mm
1 mm
h
oc
f.XII
cso
ct
jf
i
psc
marst
io.jf
f.XII
oc
m
ss
sf
n
o
l
cso
ct
jf
oc
j
hsc
otc
fo
jxr
k
oc

FIGURE 2.7. Braincase elements of *Atractaspis irregularis* (FMNH 62204). (**a**–**d**) Right prootic in (**a**) lateral, (**b**) medial, (**c**) anterior, and (**d**) posterior views. (**e**–**g**) Supraoccipital in (**e**) dorsal, (**f**) ventral, and (**g**) left lateral views. (**h**–**l**) Right otoccipital in (**h**) lateral, (**i**) medial, (**j**) anterior, (**k**) posterior, and (**l**) right posterolateral views. (**m**–**o**) Right stapes in (**m**) posterior, (**n**) lateral, and (**o**) medial views. Colouration is consistent with other figures in this chapter. Arrows beneath panel labels point anteriorly. Surface mesh files of each element are available as 3D PDFs in the Supporting Information (Figs S2.1–S2.23). Abbreviations: asc, anterior semicircular canal; a.St, articulatory surface for the supratemporal; cso, circumstapedial openings; ct, crista tuberalis; dp, descending process; ef, endolymphatic foramen; f.hbVII, foramen for the hyomandibular branch of the facial nerve (CN VII); fo, fenestra ovalis; f.pbVII, foramen for the palatine branch of the facial nerve (CN VII); f.tfc, foramen for the trigemino-facialis chamber; f.VII, foramen for the facial nerve (CN VII); f.VIII, foramen for the acoustic nerve (CN VIII); f.XII, foramen for the hypoglossal nerve (CN XII); hsc, horizontal semicircular canal; io.f.pbVII, internal opening of the foramen for the palatine branch of the facial nerve (CN VII); io.jf, internal opening of the jugular foramen; jf, jugular foramen; jxr, juxtastapedial recess; lf, laterosphenoid foramen; ls, laterosphenoid ossification; marst, medial aperture of the recessus scalae tympani, oc, occipital condyle; otc, otic capsule; psc, posterior semicircular canal; scr, sagittal crest; sf, stapedial footplate; ss, stapedial shaft; V2, foramen for the maxillary (V2) branch of the trigeminal nerve (CN V); V3, foramen for the mandibular (V3) branch of the trigeminal nerve (CN V).

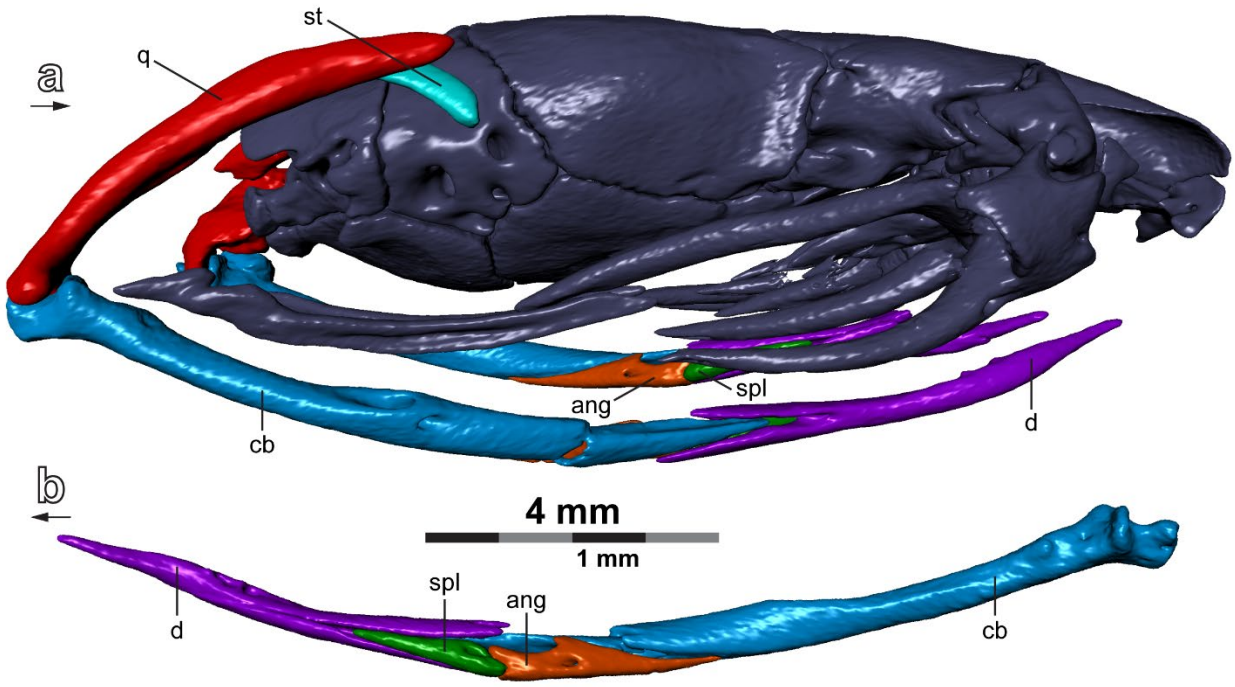

FIGURE 2.8. Overview of suspensorium and mandible of *Atractaspis irregularis* (FMNH 62204). (**a**) Suspensorium and mandible in articulation with the skull (right lateral view). (**b**) Articulated right mandible in medial view. Colouration is consistent throughout all panels. Arrows beneath panel labels point anteriorly. Surface mesh files of each element are available as 3D PDFs in the Supporting Information (Figs S2.1–S2.23). Abbreviations: ang, angular; cb, compound bone; d, dentary; q, quadrate; spl, splenial; st, supratemporal.

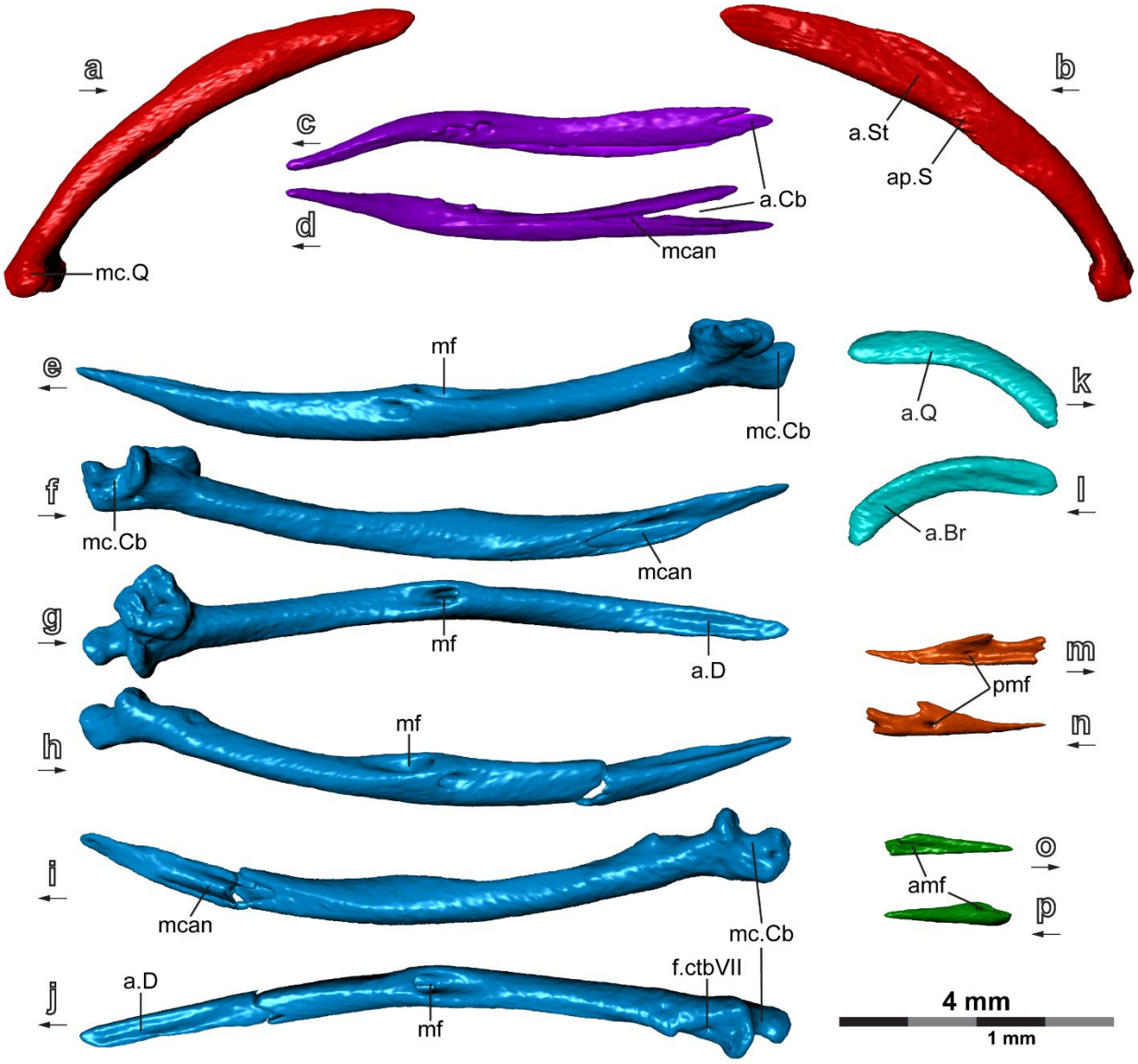
a
b
c
d
a.St
ap.S
a.Cb
mcan
mc.Q
e
f
g
h
i
j
mf
mc.Cb
mcan
mf
a.D
mf
mcan
mc.Cb
a.D
mf
f.ctbVII
k
l
m
n
o
p
a.Q
a.Br
pmf
amf
4 mm
1 mm

FIGURE 2.9. Suspensorial and mandibular elements of *Atractaspis irregularis* (FMNH 62204). (**a**–**b**) Right quadrate in (**a**) lateral and (**b**) medial views. (**c**–**d**) Right dentary in (**c**) dorsal and (**d**) medial views. (**e**–**g**) Left compound bone in (**e**) lateral, (**f**) medial, and (**g**) dorsal views. (**h**–**j**) Right compound bone in (**h**) lateral, (**i**) medial, and (**j**) dorsal views. (**k**–**l**) Right supratemporal in (**k**) lateral and (**l**) medial views. (**m**–**n**) Right angular in (**m**) lateral and (**n**) medial views. (**o**–**p**) Right splenial in (**o**) lateral and (**p**) medial views. Both left and right compound bones are depicted due to likely pathologic alteration posteriorly on the left counterpart and breakage anteriorly on the right counterpart. Colouration is consistent with other figures in this chapter. Arrows beneath panel labels point anteriorly. Surface mesh files of each element are available as 3D PDFs in the Supporting Information (Figs S2.1–S2.23). Abbreviations: a.Br, articulatory surface for the braincase; a.Cb, articulatory surface for the compound bone; a.D, articulatory surface for the dentary; amf, anterior mylohyoid foramen; ap.S, articulatory process for the stapes; a.Q, articulatory surface for the quadrate; a.St, articulatory surface for the supratemporal; f.ctbVII, foramen for the chorda tympani branch of the facial nerve (CN VII); mcan, Meckelian canal; mc.Cb, mandibular condyle of the compound bone; mc.Q, mandibular condyle of the quadrate; mf, mandibular fossa; pmf, posterior mylohyoid foramen.

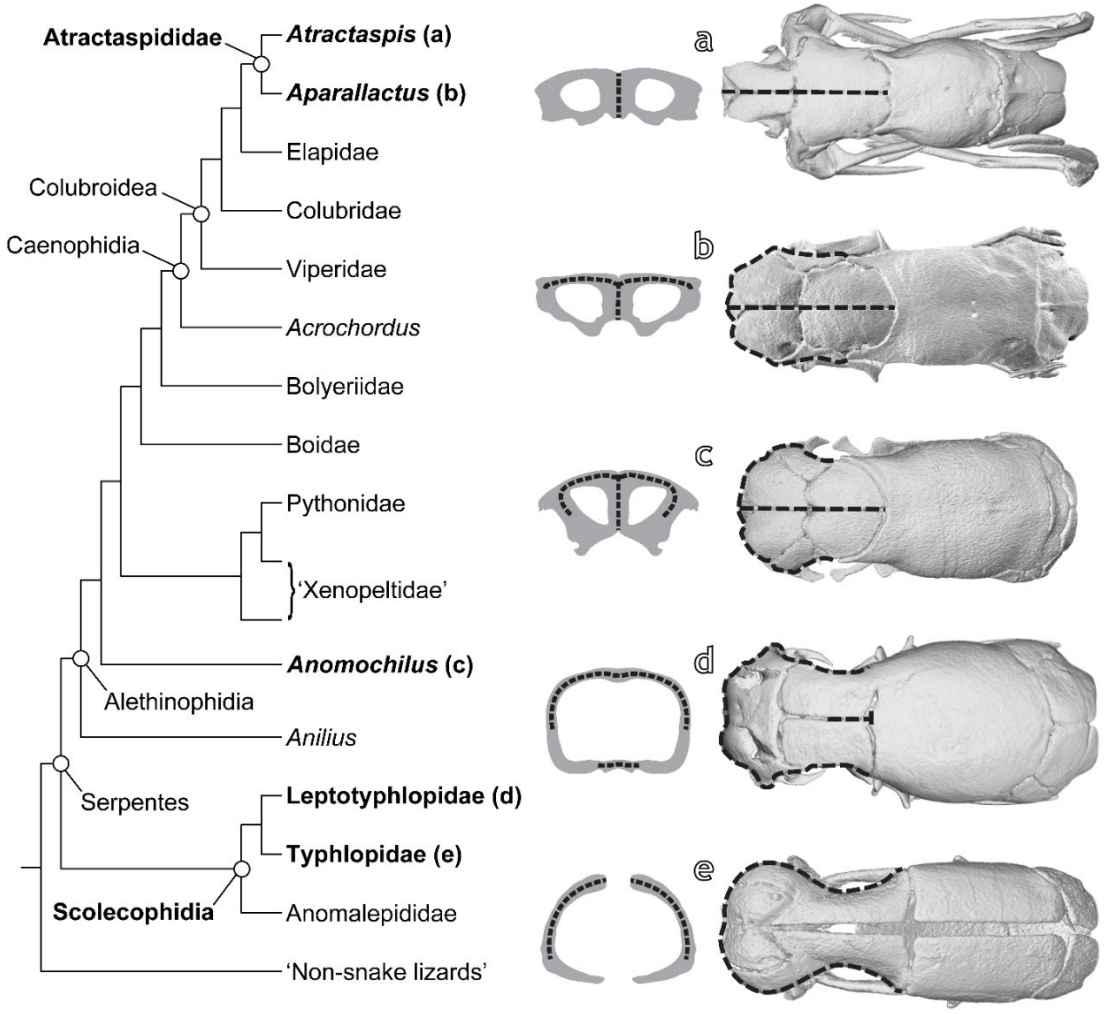

FIGURE 2.10. Morphology of the naso-frontal joint in select fossorial snakes. Each panel shows a cross-section of the frontal and a dorsal view of the skull. Dashed lines represent transmission of force while burrowing, as described by Cundall & Rossman (1993) and Rieppel *et al.* (2009). Key taxa are indicated in bold. (**a**) *Atractaspis irregularis* (FMNH 62204), exemplifying the 'central rod design' of the skull in fossorial snakes. (**b**) *Aparallactus werneri* (FMNH 250439), representing a mixture of the 'central rod' and 'outer shell' designs in an atractaspidid snake. (**c**) *Anomochilus leonardi* (FRIM 0026), representing a mixture of the 'central rod' and 'outer shell' designs in an alethinophidian snake. (**d**) *Rena dulcis* (UAMZ R335), representing a mixture of the 'central rod' and 'outer shell' designs in a scolecophidian snake. (**e**) *Indotyphlops braminus* (UAMZ R363), exemplifying the 'outer shell design' of the skull. Phylogeny from the combined-data analysis of Hsiang *et al.* (2015). Specimens not to scale.

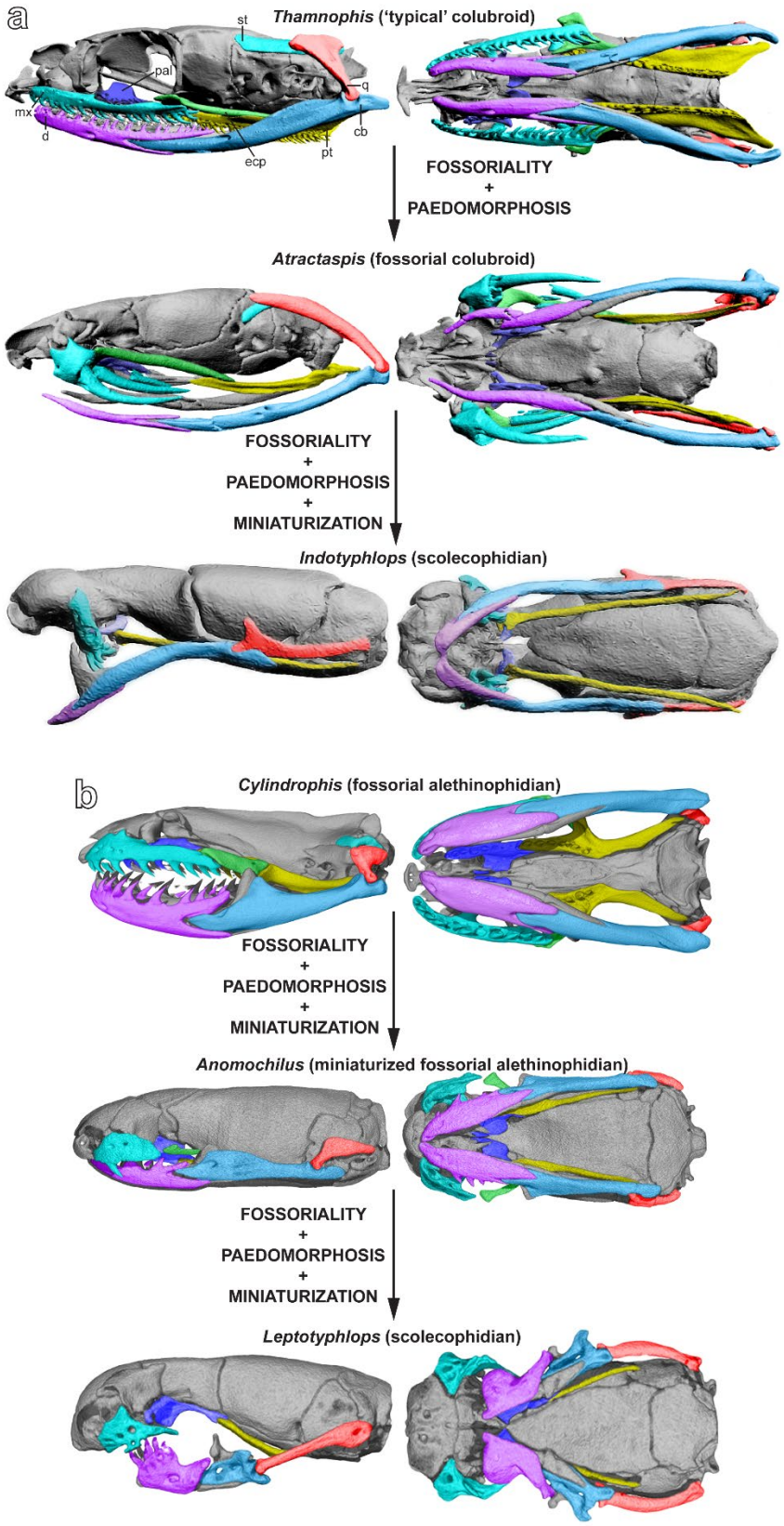
a
Thamnophis ('typical' colubroid)
st
pal
q
mx
d
cb
ecp
pt
FOSSORIALITY
+
PAEDOMORPHOSIS
Atractaspis (fossorial colubroid)
FOSSORIALITY
+
PAEDOMORPHOSIS
+
MINIATURIZATION
Indotyphlops (scolecophidian)
b
Cylindrophis (fossorial alethinophidian)
FOSSORIALITY
+
PAEDOMORPHOSIS
+
MINIATURIZATION
Anomochilus (miniaturized fossorial alethinophidian)
FOSSORIALITY
+
PAEDOMORPHOSIS
+
MINIATURIZATION
Leptotyphlops (scolecophidian)

FIGURE 2.11. ‘Regressed alethinophidian’ hypothesis of scolecophidian evolution. (**a**) Example of how ‘regression’ from a ‘typical’ or non-fossorial alethinophidian skull (represented by the colubroid *Thamnophis radix*, UAMZ R636), to a fossorial alethinophidian (represented by *Atractaspis irregularis*, FMNH 62204), to a typhlopoid skull morphology (*Indotyphlops braminus*, UAMZ R363) could easily occur due to fossorial adaptations, paedomorphosis, and miniaturization. (**b**) Example of how the leptotyphlopid skull (*Rena dulcis*, TNHC 60638) could easily be derived from that of an early-diverging alethinophidian (*Cylindrophis ruffus*, FMNH 60958) through accumulation of fossorial adaptations, paedomorphosis, and miniaturization. In this scenario, *Anomochilus leonardi* (FRIM 0026) would represent an ideal morphological intermediate between the two extremes skull types. I propose that miniaturization in scolecophidians further superimposes unique features overtop an ancestral fossorial alethinophidian morphotype. Note that these are only examples of morphological grades and do not imply phylogenetic relationships, only that the scolecophidian skull typology could be derived from an ancestral alethinophidian condition. Elements of the jaws and suspensorium affected by paedomorphosis are highlighted. Colouration is consistent throughout all panels. Specimens not to scale. Abbreviations: cb, compound bone; d, dentary; ecp, ectopterygoid; mx, maxilla; pal, palatine; pt, pterygoid; q, quadrate; st, supratemporal.

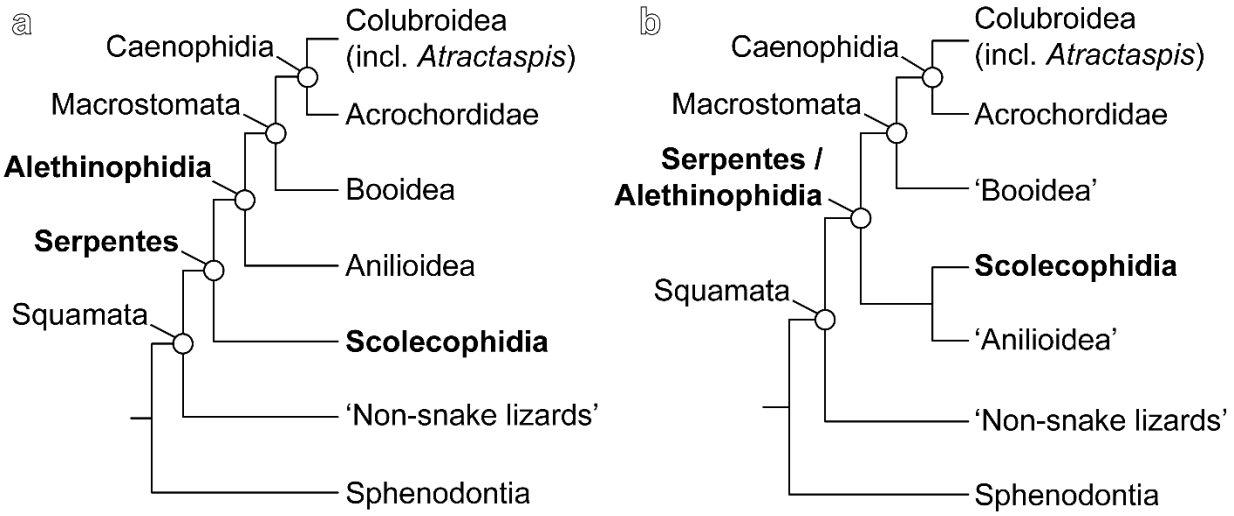

FIGURE 2.12. Competing hypotheses of scolecophidian evolution. (**a**) Traditional phylogeny of extant snakes (Serpentes), in which scolecophidians are the earliest-diverging lineage. (**b**) Recent phylogeny recovering scolecophidians as 'regressed alethinophidians', i.e., descended from an alethinophidian ancestor. Key groups are indicated in bold. Quotation marks indicate paraphyletic groups. Topologies in (**a**) and (**b**) are adapted from Rieppel (1988) and Garberoglio *et al.* (2019a), respectively.

Tables: Chapter Two

TABLE 2.1. List of specimens observed for Chapter Two. See preliminary pages of thesis document for institutional abbreviations. See Appendix 1.1. for sources of scan data.

HIGHER TAXON			SPECIES	SPECIMEN NUMBER
Alethinophidia	**'Anilioidea'**	**Amerophidia**	*Anilius scytale*	USNM 204078
		Uropeltoidea	*Anomochilus leonardi*	FRIM 0026
			Cylindrophis ruffus	FMNH 60958
			Uropeltis melanogaster	FMNH 167048
			Uropeltis woodmasoni	TMM M-10006
	Bolyeriidae		*Casarea dussumieri*	UMMZ 190285
	Booidea	**Boidae**	*Chilabothrus striatus*	USNM 59918
			Exiliboa placata	FMNH 207669
		Calabariidae	*Calabaria reinhardtii*	FMNH 117833
	Colubroidea	**Atractaspididae**	*Aparallactus guentheri*	MCZ R-23363
			Aparallactus modestus	MCZ R-182625
			Aparallactus werneri	FMNH 250439
			Atractaspis aterrima	AMNH R-12352
			Atractaspis bibronii	MCZ R-190390
			Atractaspis dahomeyensis	MCZ R-53644
			Atractaspis irregularis	FMNH 62204 MCZ R-48555 MCZ R-49237

			Atractaspis microlepidota	FMNH 58397 MCZ R-53556 SAMA R36770
		Colubridae	*Coluber constrictor*	FMNH 135284
			Diadophis punctatus	FMNH 244371
			Lampropeltis getula	FMNH 95184
		Elapidae	*Naja naja*	FMNH 22468
		Homalopsidae	*Homalopsis buccata*	FMNH 259340
		Lamprophiidae	*Boaedon fuliginosus*	FMNH 62248
		Natricidae	*Afronatrix anoscopus*	FMNH 179335
			Natrix natrix	FMNH 30522
			Thamnophis radix	UAMZ R636
		Viperidae	*Agkistrodon contortrix*	FMNH 166644
			Bothrops asper	FMNH 31162
	Pythonoidea	**Loxocemidae**	*Loxocemus bicolor*	FMNH 104800
		Xenopeltidae	*Xenopeltis unicolor*	FMNH 148900
'Scolecophidia'	**Anomalepididae**		*Anomalepis aspinosus*	MCZ R-14782
			Anomalepis mexicanus	MCZ R-191201
			Liotyphlops albirostris	FMNH 216257
			Typhlophis squamosus	MCZ R-145403 USNM 289090
	Leptotyphlopidae		*Rena dulcis*	TNHC 60638 UAMZ R335
	Typhlopoidea	**Typhlopidae**	*Indotyphlops braminus*	UAMZ R363
			Typhlops jamaicensis	USNM 12378

References: Chapter Two

Al-Mohammadi, A. G. A., Khannoon, E. R. & Evans, S. E. 2020. The development of the osteocranium in the snake *Psammophis sibilans* (Serpentes: Lamprophiidae). *Journal of Anatomy*, **236**, 117–131. doi:10.1111/joa.13081

Bellairs, A. D. & Underwood, G. 1951. The origin of snakes. *Biological Reviews*, **26**, 193–237.

Berkovitz, B. & Shellis, P. 2017. *The Teeth of Non-Mammalian Vertebrates*. Academic Press, London.

Boback, S. M., Dichter, E. K. & Mistry, H. L. 2012. A developmental staging series for the African house snake, *Boaedon* (*Lamprophis*) *fuliginosus*. *Zoology*, **115**, 38–46. doi:10.1016/j.zool.2011.09.001

Boughner, J. C., Buchtová, M., Fu, K., Diewert, V., Hallgrímsson, B. & Richman, J. M. 2007. Embryonic development of *Python sebae* – I: staging criteria and macroscopic skeletal morphogenesis of the head and limbs. *Zoology*, **110**, 212–230. doi:10.1016/j.zool.2007.01.005

Burbrink, F. T., Grazziotin, F. G., Pyron, R. A., Cundall, D., Donnellan, S., Irish, F., Keogh, J. S., Kraus, F., Murphy, R. W., Noonan, B., Raxworthy, C. J., Ruane, S., Lemmon, A. R., Lemmon, E. M. & Zaher, H. 2020. Interrogating genomic-scale data for Squamata (lizards, snakes, and amphisbaenians) shows no support for key traditional morphological relationships. *Systematic Biology*, **69**(3), 502–520. doi:10.1093/sysbio/syz062

Caldwell, M. W. 2019. *The Origin of Snakes: Morphology and the Fossil Record*. Taylor & Francis, Boca Raton.

Chretien, J., Wang-Claypool, C. Y., Glaw, F. & Scherz, M. D. 2019. The bizarre skull of *Xenotyphlops* sheds light on synapomorphies of Typhlopoidea. *Journal of Anatomy*, **234**, 637–655. doi:10.1111/joa.12952

Cundall, D. & Rossman, D. A. 1993. Cephalic anatomy of the rare Indonesian snake *Anomochilus weberi*. *Zoological Journal of the Linnean Society*, **109**, 235–273.

Da Silva, F. O., Fabre, A.-C., Savriama, Y., Ollonen, J., Mahlow, K., Herrel, A., Müller, J. & Di-Poï, N. 2018. The ecological origins of snakes as revealed by skull evolution. *Nature Communications*, **9**, 376. doi:10.1038/s41467-017-02788-3

Deufel, A. & Cundall, D. 2003. Feeding in *Atractaspis* (Serpentes: Atractaspididae): a study in conflicting functional constraints. *Zoology*, **106**, 43–61.

Dong, S. & Kumazawa, Y. 2005. Complete mitochondrial DNA sequences of six snakes: phylogenetic relationships and molecular evolution of genomic features. *Journal of Molecular Evolution*, **61**, 12–22. doi:10.1007/s00239-004-0190-9

Evans, S. E. 2008. The Skull of Lizards and Tuatara. Pp. 1–347 in C. Gans, A.S. Gaunt and K. Adler (eds) *Biology of the Reptilia, Vol. 20: The Skull of Lepidosauria*. Society for the Study of Amphibians and Reptiles, Ithaca.

Figueroa, A., McKelvy, A. D., Grismer, L. L., Bell, C. D. & Lailvaux, S. P. 2016. A species-level phylogeny of extant snakes with description of a new colubrid subfamily and genus. *PLoS ONE*, **11**(9), e0161070. doi:10.1371/journal.pone.0161070

Fröbisch, N. B. & Schoch, R. R. 2009. Testing the impact of miniaturization on phylogeny: Paleozoic dissorophoid amphibians. *Systematic Biology*, **58**(3), 312–327. doi:10.1093/sysbio/syp029

Garberoglio, F. F., Apesteguía, S., Simões, T. R., Palci, A., Gómez, R. O., Nydam, R. L., Larsson, H. C. E., Lee, M. S. Y. & Caldwell, M. W. 2019a. New skulls and skeletons of the Cretaceous legged snake *Najash*, and the evolution of the modern snake body plan. *Science Advances*, **5**(11), eaax5833. doi:10.1126/sciadv.aax5833

Gauthier, J., Kluge, A. G. & Rowe, T. 1988a. Amniote phylogeny and the importance of fossils. *Cladistics*, **4**, 105–209.

Gauthier, J. A., Kearney, M., Maisano, J. A., Rieppel, O. & Behlke, A. D. B. 2012. Assembling the squamate tree of life: perspectives from the phenotype and the fossil record. *Bulletin of the Peabody Museum of Natural History*, **53**, 3–308. doi:10.3374/014.053.0101

Gould, S. J. 1977. *Ontogeny and Phylogeny*. Harvard University Press, Cambridge.

Hanken, J. 1984. Miniaturization and its effects on cranial morphology in plethodontid salamanders, genus *Thorius* (Amphibia: Plethodontidae). I. Osteological variation. *Biological Journal of the Linnean Society*, **23**, 55–75.

Hanken, J. & Wake, D. B. 1993. Miniaturization of body size: organismal consequences and evolutionary significance. *Annual Review of Ecology and Systematics*, **24**, 501–519.

Harrington, S. M. & Reeder, T. W. 2017. Phylogenetic inference and divergence dating of snakes using molecules, morphology and fossils: new insights into convergent evolution of feeding morphology and limb reduction. *Biological Journal of the Linnean Society*, **121**, 379–394.

Hernández-Jaimes, C., Jerez, A. & Ramírez-Pinilla, M. P. 2012. Embryonic development of the skull of the Andean lizard *Ptychoglossus bicolor* (Squamata, Gymnophthalmidae). *Journal of Anatomy*, **221**, 285–302. doi:10.1111/j.1469-7580.2012.01549.x

Hsiang, A. Y., Field, D. J., Webster, T. H., Behlke, A. D. B., Davis, M. B., Racicot, R. A. & Gauthier, J. A. 2015. The origin of snakes: revealing the ecology, behavior, and evolutionary history of early snakes using genomics, phenomics, and the fossil record. *BMC Evolutionary Biology*, **15**, 87. doi:10.1186/s12862-015-0358-5

Irish, F. J. 1989. The role of heterochrony in the origin of a novel bauplan: evolution of the ophidian skull. *Geobios*, **22**, 227–233.

Jackson, K. 2002. Post-ovipositional development of the monocled cobra, *Naja kaouthia* (Serpentes: Elapidae). *Zoology*, **105**, 203–214.

Jackson, K. 2007. The evolution of venom-conducting fangs: insights from developmental biology. *Toxicon*, **49**, 975–981. doi:10.1016/j.toxicon.2007.01.007

Kamal, A. M. 1966. On the process of rotation of the quadrate cartilage in Ophidia. *Anatomischer Anzieger*, **118**, 87–90.

Khannoon, E. R. & Evans, S. E. 2015. The development of the skull of the Egyptian cobra *Naja h. haje* (Squamata: Serpentes: Elapidae). *PLoS ONE*, **10**, e0122185. doi:10.1371/journal.pone.0122185

Khannoon, E. R. & Zahradnicek, O. 2017. Postovipositional development ofthe sand snake *Psammophis sibilans* (Serpentes:Lamprophiidae) in comparison with other snake species. *Acta Zoologica (Stockholm)*, **98**, 144–153. doi:10.1111/azo.12157

Khannoon, E. R., Ollonen, J. & Di-Poï, N. 2020. Embryonic development of skull bones in the Sahara horned viper (*Cerastes cerastes*), with new insights into structures related to the basicranium and braincase roof. *Journal of Anatomy*, **00**, 1–19. doi:10.1111/joa.13182

Kley, N. J. 2006. Morphology of the lower jaw and suspensorium in the Texas blindsnake, *Leptotyphlops dulcis* (Scolecophidia: Leptotyphlopidae). *Journal of Morphology*, **267**, 494–515. doi:10.1002/jmor.10414

Kochva, E. 1987. The origin of snakes and evolution of the venom apparatus. *Toxicon*, **25**(1), 65–106.

Kochva, E. 2002. *Atractaspis* (Serpentes, Atractaspididae) the burrowing asp; a multidisciplinary minireview. *Bulletin of the Natural History Museum Zoology*, **68**(2), 91–99. doi:10.1017/S0968047002000109

List, J. C. 1966. Comparative osteology of the snake families Typhlopidae and Leptotyphlopidae. *Illinois Biological Monographs*, **36**, 1–112.

Longrich, N. R., Bhullar, B.-A. S. & Gauthier, J. A. 2012. A transitional snake from the Late Cretaceous period of North America. *Nature*, **488**, 205–208. doi:10.1038/nature11227

Maddin, H. C., Olori, J. C. & Anderson, J. S. 2011. A redescription of *Carrolla craddocki* (Lepospondyli: Brachystelechidae) based on high-resolution CT, and the impacts of miniaturization and fossoriality on morphology. *Journal of Morphology*, **272**, 722–743. doi:10.1002/jmor.10946

Maisano, J. A. & Rieppel, O. 2007. The skull of the round island boa, *Casarea dussumieri* Schlegel, based on high-resolution X-ray computed tomography. *Journal of Morphology*, **268**, 371–384. doi:10.1002/jmor.10519

Malmstrøm, M., Britz, R., Matschiner, M., Tørresen, O. K., Kurnia Hadiaty, R., Yaakob, N., Hui Tan, H., Sigurd Jakobsen, K., Salzburger, W. & Rüber, L. 2018. The most developmentally truncated fishes show extensive *Hox* gene loss and miniaturized genomes. *Genome Biology and Evolution*, **10**(4), 1088–1103. doi:10.1093/gbe/evy058

McNamara, K. J. 1986. A guide to the nomenclature of heterochrony. *Journal of Paleontology*, **60**(1), 4–13.

Miralles, A., Marin, J., Markus, D., Herrel, A., Hedges, S. B. & Vidal, N. 2018. Molecular evidence for the paraphyly of Scolecophidia and its evolutionary implications. *Journal of Evolutionary Biology*, **31**, 1782–1793. doi:10.1111/jeb.13373

Mongiardino Koch, N. & Gauthier, J. A. 2018. Noise and biases in genomic data may underlie radically different hypotheses for the position of Iguania within Squamata. *PLoS ONE*, **13**(8), e0202729. doi:10.1371/journal. pone.0202729

Moyer, K. & Jackson, K. 2011. Phylogenetic relationships among the Stiletto Snakes (genus Atractaspis) based on external morphology. *African Journal of Herpetology*, **60**(1), 30–46. doi:10.1080/21564574.2010.520034

Object Research Systems Inc. 2019a. Dragonfly 4.0. Object Research Systems (ORS) Inc., Montreal, Canada. http://www.theobjects.com/dragonfly

Olori, J. C. & Bell, C. J. 2012. Comparative skull morphology of uropeltid snakes (Alethinophidia: Uropeltidae) with special reference to disarticulated elements and variation. *PLoS ONE*, **7**(3), e32450. doi:10.1371/journal.pone.0032450

Palci, A. & Caldwell, M. W. 2010. Redescription of *Acteosaurus tommasinii* von Meyer, 1860, and a discussion of evolutionary trends within the clade Ophidiomorpha. *Journal of Vertebrate Paleontology*, **30**(1), 94–108. doi:10.1080/02724630903409139

Palci, A. & Caldwell, M. W. 2013. Primary homologies of the circumorbital bones of snakes. *Journal of Morphology*, **274**, 973–986. doi:10.1002/jmor.20153

Palci, A. & Caldwell, M. W. 2014. The Upper Cretaceous snake *Dinilysia patagonica* Smith-Woodward, 1901, and the crista circumfenestralis of snakes. *Journal of Morphology*, **275**, 1187–1200. doi:10.1002/jmor.20297

Palci, A., Lee, M. S. Y. & Hutchinson, M. N. 2016. Patterns of postnatal ontogeny of the skull and lower jaw of snakes as revealed by micro-CT scan data and three-dimensional geometric morphometrics. *Journal of Anatomy*, **229**(6), 723–754. doi:10.1111/joa.12509

Palci, A., Seymour, R. S., Van Nguyen, C., Hutchinson, M. N., Lee, M. S. Y. & Sanders, K. L. 2019. Novel vascular plexus in the head of a sea snake (Elapidae, Hydrophiinae) revealed by high-resolution computed tomography and histology. *Royal Society Open Science*, **6**, 191099. doi:10.1098/rsos.191099

Palci, A., Caldwell, M. W., Hutchinson, M. N., Konishi, T. & Lee, M. S. Y. 2020a. The morphological diversity of the quadrate bone in squamate reptiles as revealed by high-resolution computed tomography and geometric morphometrics. *Journal of Anatomy*, **236**, 210–227. doi:10.1111/joa.13102

Palci, A., Hutchinson, M. N., Caldwell, M. W., Smith, K. T. & Lee, M. S. Y. 2020b. The homologies and evolutionary reduction of the pelvis and hindlimbs in snakes, with the first report of ossified pelvic vestiges in an anomalepidid (*Liotyphlops beui*). *Zoological Journal of the Linnean Society*, **188**, 630–652. doi:10.1093/zoolinnean/zlz098

Polachowski, K. M. & Werneburg, I. 2013. Late embryos and bony skull development in *Bothropoides jararaca* (Serpentes, Viperidae). *Zoology*, **116**, 36–63. doi:10.1016/j.zool.2012.07.003

Portillo, F., Branch, W. R., Conradie, W., Rödel, M.-O., Penner, J., Barej, M. F., Kusamba, C., Muninga, W. M., Aristote, M. M., Bauer, A. M., Trape, J.-F., Nagy, Z. T., Carlino, P., Pauwels, O. S. G., Menegon, M., Burger, M., Mazuch, T., Jackson, K., Hughes, D. F., Behangana, M., Zassi-Boulou, A.-G. & Greenbaum, E. 2018. Phylogeny and biogeography of the African burrowing snake subfamily Aparallactinae (Squamata: Lamprophiidae). *Molecular Phylogenetics and Evolution*, **127**, 288–303. doi:10.1016/j.ympev.2018.03.019

Portillo, F., Stanley, E. L., Branch, W. R., Conradie, W., Rödel, M.-O., Penner, J., Barej, M. F., Kusamba, C., Muninga, W. M., Aristote, M. M., Bauer, A. M., Trape, J.-F., Nagy, Z. T., Carlino, P., Pauwels, O. S. G., Menegon, M., Ineich, I., Burger, M., Zassi-Boulou, A.-G., Mazuch, T., Jackson, K., Hughes, D. F., Behangana, M. & Greenbaum, E. 2019. Evolutionary history of burrowing asps (Lamprophiidae: Atractaspidinae) with emphasis on fang evolution and prey selection. *PLoS ONE*, **14**(4), e0214889. doi:10.1371/journal. pone.0214889

Pringle, J. A. 1954. The cranial development of certain South African snakes and the relationship of these groups. *Proceedings of the Zoological Society of London*, **123**, 813–865.

Racca, L., Villa, A., Wencker, L. C. M., Camaiti, M., Blain, H.-A. & Delfino, M. 2020. Skull osteology and osteological phylogeny of the Western whip snake *Hierophis viridiflavus* (Squamata, Colubridae). *Journal of Morphology*, **281**, 808–833. doi:10.1002/jmor.21148

Reeder, T. W., Townsend, T. M., Mulcahy, D. G., Noonan, B. P., Wood, P. L., Sites, J. W. & Wiens, J. J. 2015. Integrated analyses resolve conflicts over squamate reptile phylogeny and reveal unexpected placements for fossil taxa. *PLoS ONE*, **10**(3), e0118199. doi:10.1371/journal.pone.0118199

Reinhardt, J. T. 1843. Beskrivelse af nogle nye Slangearter. *Kongelige Danske Videnskabernes Selskabs, Afhandlinger*, **10**, 233–279.

Rieppel, O. 1978a. A functional and phylogenetic interpretation of the skull of the Erycinae (Reptilia, Serpentes). *Journal of Zoology*, **186**, 185–208.

Rieppel, O. 1978b. The evolution of the naso-frontal joint in snakes and its bearing on snake origins. *Journal of Zoological Systematics and Evolutionary Research*, **16**, 14–27. doi:10.1111/j.1439-0469.1978.tb00917.x

Rieppel, O. 1979a. A cladistic classification of primitive snakes based on skull structure. *Journal of Zoological Systematics and Evolutionary Research*, **17**(2), 140–150. doi:10.1111/j.1439-0469.1979.tb00696.x

Rieppel, O. 1979b. The evolution of the basicranium in the Henophidia (Reptilia: Serpentes). *Zoological Journal of the Linnean Society*, **66**, 411–431.

Rieppel, O. 1988. A review of the origin of snakes. Pp. 37–130 in M.K. Hecht, B. Wallace and G.T. Prance (eds) *Evolutionary Biology*. Springer, Boston, MA.

Rieppel, O. 1996. Miniaturization in tetrapods: consequences for skull morphology. Pp. 47–61 in P.J. Miller (ed) *Miniature Vertebrates: The Implications of Small Body Size, Vol. 69. Symposia of the Zoological Society of London*. Claredon Press, Oxford.

Rieppel, O. & Zaher, H. 2000. The intramandibular joint in squamates, and the phylogenetic relationships of the fossil snake *Pachyrhachis problematicus* Haas. *Fieldiana Geology*, **43**, 1–69.

Rieppel, O. & Zaher, H. 2001b. The development of the skull in *Acrochordus granulatus* (Schneider) (Reptilia: Serpentes), with special consideration of the otico-occipital complex. *Journal of Morphology*, **249**, 252–266.

Rieppel, O. 2007. The naso-frontal joint in snakes as revealed by high-resolution X-ray computed tomography of intact and complete skulls. *Zoologischer Anzeiger*, **246**, 177–191. doi:10.1016/j.jcz.2007.04.001

Rieppel, O. & Maisano, J. A. 2007. The skull of the rare Malaysian snake *Anomochilus leonardi* Smith, based on high-resolution X-ray computed tomography. *Zoological Journal of the Linnean Society*, **149**, 671–685.

Rieppel, O., Kley, N. J. & Maisano, J. A. 2009. Morphology of the skull of the white-nosed blindsnake, *Liotyphlops albirostris* (Scolecophidia: Anomalepididae). *Journal of Morphology*, **270**, 536–557. doi:10.1002/jmor.10703

Rieppel, O. 2012. "Regressed" macrostomatan snakes. *Fieldiana Life and Earth Sciences*, **2012**(5), 99–103. doi:10.3158/2158-5520-5.1.99

Rödel, M.-O., Kucharzewski, C., Mahlow, K., Chirio, L., Pauwels, O. S. G., Carlino, P., Sambolah, G. & Glos, J. 2019. A new stiletto snake (Lamprophiidae, Atractaspidinae, Atractaspis) from Liberia and Guinea, West Africa. *Zoosystematics and Evolution*, **95**(1), 107–123. doi:10.3897/zse.95.31488

Savitzky, A. H. 1983. Coadapted character complexes among snakes: fossoriality, piscivory, and durophagy. *American Zoologist*, **23**, 397–409.

Scanferla, A. & Bhullar, B.-A. S. 2014. Postnatal development of the skull of *Dinilysia patagonica* (Squamata-Stem Serpentes). *The Anatomical Record*, **297**, 560–573. doi:10.1002/ar.22862

Scanferla, A. 2016. Postnatal ontogeny and the evolution of macrostomy in snakes. *Royal Society Open Science*, **3**, 160612. doi:10.1098/rsos.160612

Sherratt, E., Sanders, K. L., Watson, A., Hutchinson, M. N., Lee, M. S. Y. & Palci, A. 2019. Heterochronic shifts mediate ecomorphological convergence in skull shape of microcephalic sea snakes. *Integrative and Comparative Biology*, **59**(3), 616–624. doi:10.1093/icb/icz033

Sheverdyukova, H. V. 2017. Development of the osteocranium in *Natrix natrix* (Serpentes, Colubridae) embryogenesis I: development of cranial base and cranial vault. *Zoomorphology*, **136**, 131–143. doi:10.1007/s00435-016-0333-8

Sheverdyukova, H. V. 2019. Development of the osteocranium in *Natrix natrix* (Serpentes, Colubridae) embryogenesis II: development of the jaws, palatal complex and associated bones. *Acta Zoologica*, **100**, 282–291. doi:10.1111/azo.12253

Sheverdyukova, H. V. & Kovtun, M. F. 2020. Variation in the formation of crista sellaris and basisphenoid in the skull of the grass snake *Natrix natrix* embryos (Serpentes, Colubridae). *Journal of Morphology*, **281**, 338–347. doi:10.1002/jmor.21102

Shine, R., Branch, W. R., Harlow, P. S., Webb, J. K. & Shine, T. 2006. Biology of burrowing asps (Atractaspididae) from Southern Africa. *Copeia*, **1**, 103–115.

Simões, T. R., Caldwell, M. W., Tałanda, M., Bernardi, M., Palci, A., Vernygora, O., Bernardini, F., Mancini, L. & Nydam, R. L. 2018. The origin of squamates revealed by a Middle Triassic lizard from the Italian Alps. *Nature*, **557**, 706–709. doi:10.1038/s41586-018-0093-3

Strong, C. R. C., Simões, T. R., Caldwell, M. W. & Doschak, M. R. 2019. Cranial ontogeny of *Thamnophis radix* (Serpentes: Colubroidea) with a re-evaluation of current paradigms of snake skull evolution. *Royal Society Open Science*, **6**, 182228. doi:10.1098/rsos.182228

Struck, T. H. 2007. Data congruence, paedomorphosis and salamanders. *Frontiers in Zoology*, **4**, 22. doi:10.1186/1742-9994-4-22

Underwood, G. & Kochva, E. 1993. On the affinities of the burrowing asps *Atractaspis* (Serpentes: Atractaspididae). *Zoological Journal of the Linnean Society*, **107**, 3–64.

Vidal, N. & Hedges, S. B. 2002. Higher-level relationships of snakes inferred from four nuclear and mitochondrial genes. *Comptes Rendus Biologies*, **325**, 977–985.

Vidal, N., Branch, W. R., Pauwels, O. S. G., Hedges, S. B., Broadley, D. G., Wink, M., Cruaud, C., Joger, U. & Nagy, Z. T. 2008. Dissecting the major African snake radiation: a molecular phylogeny of the Lamprophiidae Fitzinger (Serpentes, Caenophidia). *Zootaxa*, **1945**, 51–66. doi:10.11646/zootaxa.1945.1.3

Wake, M. H. 1986. The morphology of *ldiocranium russeli* (Amphibia: Gymnophiona), with comments on miniaturization through heterochrony. *Journal of Morphology*, **189**, 1–16.

Wake, M. H. 1993. The Skull as a Locomotor Organ. P. 216 in J. Hanken and B.K. Hall (eds) *The Skull: Functional and Evolutionary Mechanisms*. University of Chicago Press, Chicago.

Walls, G. L. 1942. The vertebrate eye and its adaptive radiation. *Bulletin of the Cranbrook Institute of Science*, **19**, 1–785.

Werneburg, I. & Sánchez-Villagra, M. R. 2015. Skeletal heterochrony is associated with the anatomical specializations of snakes among squamate reptiles. *Evolution*, **69**(1), 254–263. doi:10.1111/evo.12559

Wiens, J. J., Bonett, R. M. & Chippindale, P. T. 2005. Ontogeny discombobulates phylogeny: paedomorphosis and higher-level salamander relationships. *Systematic Biology*, **54**(1), 91–110. doi:10.1080/10635150590906037

Yan, J., Li, H. & Zhou, K. 2008. Evolution of the mitochondrial genome in snakes: gene rearrangements and phylogenetic relationships. *BMC Genomics*, **9**, 569. doi:10.1186/1471-2164-9-569

Young, B. A. 1987. The cranial nerves of three species of sea snakes. *Canadian Journal of Zoology/Revue Canadienne de Zoologie*, **65**, 2236–2240.

Young, B. A. 1989. Ontogenetic changes in the feeding system of the red-sided garter snake, *Thamnophis sirtalis parietalis*. I. Allometric analysis. *Journal of Zoology*, **218**, 365–381.

Zaher, H., Grazziotin, F. G., Cadle, J. E., Murphy, R. W., Moura-Leite, J. C. d. & Bonatto, S. L. 2009. Molecular phylogeny of advanced snakes (Serpentes, Caenophidia) with an emphasis on South American Xenodontines: a revised classification and descriptions of new taxa. *Papeis avulsos de zoologia*, **49**(11), 115–153.

Zaher, H., Murphy, R. W., Arredondo, J. C., Graboski, R., Machado-Filho, P. R., Mahlow, K., Montingelli, G. G., Quadros, A. B., Orlov, N. L., Wilkinson, M., Zhang, Y.-P. & Grazziotin, F. G. 2019. Large-scale molecular phylogeny, morphology, divergence-time estimation, and the fossil record of advanced caenophidian snakes (Squamata: Serpentes). *PLoS ONE*, **14**(5), e0216148. doi:10.1371/journal. pone.0216148

Zehr, D. R. 1962. Stages in the normal development of the Common Garter Snake, *Thamnophis sirtalis sirtalis*. *Copeia*, **1962**(2), 322–329.

Zheng, Y. & Wiens, J. J. 2016. Combining phylogenomic and supermatrix approaches, and a time-calibrated phylogeny for squamate reptiles (lizards and snakes) based on 52 genes and 4162 species. *Molecular Phylogenetics and Evolution*, **94**, 537–547. doi:10.1016/j.ympev.2015.10.009

CHAPTER THREE: DECONSTRUCTING THE GESTALT: NEW CONCEPTS AND TESTS OF HOMOLOGY, AS EXEMPLIFIED BY A RE-CONCEPTUALIZATION OF 'MICROSTOMY' IN SQUAMATES

[This chapter has been published as: Strong, C. R. C., Scherz, M. D., and M. W. Caldwell. 2021. Deconstructing the Gestalt: new concepts and tests of homology, as exemplified by a re-conceptualization of "microstomy" in squamates. *The Anatomical Record*, **2021**, 1–49. doi:10.1002/ar.24630.]

3.1. Introduction

Scolecophidians ('blindsnakes') are a distinctive group of snakes, comprised of three major lineages: Anomalepididae, Leptotyphlopidae, and Typhlopoidea, the latter of which is further subdivided into three families, Typhlopidae, Gerrhopilidae, and Xenotyphlopidae (Figs 3.1 and 3.2). However, due in part to their small size and reclusive life habits, many aspects of scolecophidian anatomy and evolution remain understudied (Kley & Brainerd 1999; Kley 2006). As scolecophidians have traditionally played a key role in our understanding of the origin of snakes (e.g., Bellairs & Underwood 1951; Rieppel 2012; Miralles *et al.* 2018), it is of critical importance that these knowledge gaps continue to shrink; central among these, and the focus of this study, is the role of scolecophidians in informing our understanding of the evolution of feeding mechanisms in squamates.

Most extant snakes—including booids, pythonoids, and caenophidians (Figs 3.1 and 3.2)—exhibit macrostomy, the ability to consume prey items with a disproportionately large cross-sectional area (Rieppel 1988, 2012; Scanferla 2016). Other squamates—including non-snake lizards, as well as 'anilioid' (uropeltoid and amerophidian) and scolecophidian snakes—lack this ability, and have thus been termed 'microstomatan' (Rieppel 1988; Miralles *et al.* 2018). The presence of microstomy in non-snake lizards and several phylogenetically basal snake lineages has traditionally led to the conclusion that the microstomatan condition in 'anilioids' and scolecophidians is a plesiomorphic retention of the ancestral snake condition (e.g., Bellairs & Underwood 1951; Rieppel 2012). This hypothesis ties into a broader perspective in which scolecophidians are considered a largely 'primitive' lineage, retaining several features not just of the ancestor of snakes, but of non-snake lizards more broadly (e.g., List 1966).

However, several authors have cautioned that, because the scolecophidian skull is highly autapomorphic, it is therefore largely uninformative regarding the ancestral snake anatomy (e.g., Kley & Brainerd 1999; Kley 2001; Hsiang *et al.* 2015; Caldwell 2019; Chretien *et al.* 2019). In particular, the combined influences of fossoriality, miniaturization, and heterochrony (evolutionary changes in the rate and/or timing of developmental events; Gould 1977; McNamara 1986) have greatly affected the evolution of the scolecophidian skull (Kley 2006; Palci *et al.* 2016; Harrington & Reeder 2017; Caldwell 2019; Chretien *et al.* 2019; Strong *et al.* 2021a).

Despite these cautions, though, recent analyses have continued to treat scolecophidian microstomy as a plesiomorphic retention of the non-snake lizard condition, particularly via ancestral state reconstructions which codify 'microstomy' as a single, morphologically homogenous condition (e.g., Harrington & Reeder 2017; Miralles *et al.* 2018). This perspective on scolecophidian anatomy has therefore been central in formulating higher-order hypotheses of snake phylogeny and origins, including reconstructions of the ancestral morphology and ecology of snakes (e.g., Harrington & Reeder 2017; Miralles *et al.* 2018). In order to fully evaluate such hypotheses, a close analysis of the validity of this characterization of scolecophidian jaw anatomy is essential.

A re-assessment of this anatomy is also important in evaluating the phylogenetic relationships among scolecophidians. Although morphology-based phylogenies generally recover scolecophidians as monophyletic (e.g., Gauthier *et al.* 2012; Hsiang *et al.* 2015; Garberoglio *et al.* 2019a), molecular-based phylogenies tend to recover this group as paraphyletic (e.g., Pyron *et al.* 2013; Figueroa *et al.* 2016; Zheng & Wiens 2016; Miralles *et al.* 2018; Burbrink *et al.* 2020). Recent authors have further suggested that, based on the highly autapomorphic nature of scolecophidians relative not only to other squamates but also relative to each other, scolecophidians may even represent completely convergent lineages (Harrington & Reeder 2017; Caldwell 2019; Chretien *et al.* 2019), rendering this group potentially polyphyletic (Caldwell 2019). This phylogenetic hypothesis derives largely from the unique jaw structure exhibited by each major scolecophidian clade, as well as a recognition of the role of fossoriality and miniaturization in giving rise to convergent morphotypes (Harrington & Reeder 2017; Caldwell 2019; Chretien *et al.* 2019). Although this hypothesis has only recently been advocated, it presents an intriguing possibility warranting further analysis.

In light of these questions surrounding scolecophidian evolution—primarily regarding whether the scolecophidian jaw anatomy is plesiomorphic and whether 'microstomy' is morphologically homogenous among 'microstomatan' taxa—I herein present an assessment of the jaws and suspensorium of scolecophidians in comparison to other snakes and to non-snake lizards (Fig. 3.1). I address three major questions related to the scolecophidian jaw complex: First, can this morphofunctional system be considered homologous among the three main scolecophidian clades? Second, is this jaw structure homologous to the condition in non-snake

lizards? And ultimately, how do the answers to these questions affect higher-level evolutionary hypotheses, such as phylogenetic analyses or ancestral state reconstructions?

To examine these questions, I begin with comparative descriptions reviewing the jaw structures of various squamates. I then discuss the homology of these conditions and implications for the phylogeny of scolecophidians. Finally, I use ancestral state reconstructions to illustrate the impact that different homology concepts can have on hypotheses of squamate evolution.

On a taxonomic note, all references to scolecophidians throughout this study employ the classical definition of this group—i.e., comprising all major lineages, as outlined above (Fig. 3.2)—rather than the restricted, clade-based definition of 'Scolecophidia *sensu stricto*' as employed by some other authors (e.g., Miralles *et al.* 2018). References to 'anilioids' similarly evoke the classical definition of this group as an informal grade of basally-diverging alethinophidians, with the recognition that this group is likely polyphyletic (e.g., Burbrink *et al.* 2020) and composed of at least two distinct lineages: Amerophidia (Aniliidae and Tropidophiidae) and Uropeltoidea (Cylindrophiidae, Uropeltidae, and Anomochilidae) (Figs 3.1 and 3.2; taxonomy from Burbrink *et al.* 2020).

3.2. Methods

3.2.1. Institutional abbreviations

Institutional abbreviations of specimens examined in this study are provided in the preliminary pages of the thesis document.

3.2.2. Comparative specimens

Various micro-computed tomography (micro-CT) scans of squamate skulls were observed for this study, as listed in Table 3.1. For consistency, nomenclature follows the Reptile Database (http://reptile-database.reptarium.cz/) as of October 2020. Among non-snake lizards, my sampling strategy focussed on phylogenetic breadth rather than completeness, with an emphasis on taxa typically recovered or hypothesized as closely related to snakes. Among snakes, my sampling strategy focussed on 'microstomatan' taxa, including several representatives of each major 'microstomatan' group.

I conducted the micro-CT scanning of the MCZ specimens examined herein (see §3.2.3); these will be made available on MorphoSource.org. Information regarding *Xenotyphlops*

grandidieri, *Gerrhopilus persephone*, and *Cenaspis aenigma* was derived from the figures and supplementary materials of Chretien *et al.* (2019), Kraus (2017), and Campbell *et al.* (2018), respectively. Information regarding the sources of the other scans is provided in Appendix 1.1.

3.2.3. Scanning protocols and visualization

All MCZ specimens observed herein were scanned using a Nikon Metrology X-Tek HMXST225 micro-CT scanner at the Harvard University Center for Nanoscale Systems. Exact scanning parameters varied among specimens, though generally employed the following settings: detector dimensions, 2000 x 2000 pixels; projections, 3142; maximum voltage, 65–80 kV; maximum current output, 116–130 µA. A 0.5 mm aluminum filter was used for MCZ R-33505, R-2885, R-14782, R-92993, R-68571, and R-40099. Exact settings for all specimens are available upon request. Slices were reconstructed using the bundled vendor software CT Pro 3D and exported as VGL files, which were loaded in VG Studio Max and exported as TIFF files.

Brightness and contrast for all scans were adjusted in ImageJ. All scans were visualized in Dragonfly 4.1 (Object Research Systems Inc 2019b), with the Threshold tool used to digitally remove soft tissues and the Manual Segmentation tool used to digitally isolate each skull element for key taxa (Figs 3.3–3.11).

3.2.4. Phylogeny construction

The phylogeny used for the ancestral state reconstructions (ASRs) was constructed using a 'super-tree' approach, i.e., compiling dated finer-scale phylogenies into a higher-level phylogenetic framework (see Appendix 3.1). Other ASRs have used a similar approach in assessing a variety of other animal groups (e.g., Finarelli & Flynn 2006; Asplen *et al.* 2009).

Relationships among families and higher clades are based on Burbrink *et al.* (2020), with the placement of Rhineuridae and Lanthanotidae derived from Pyron *et al.* (2013). Species-level phylogenetic relationships are derived from Burbrink *et al.* (2020) for Amphisbaenia and Iguania, from Pyron *et al.* (2013) for Dibamidae and Leptotyphlopidae, and from Nagy *et al.* (2015) for Typhlopoidea. *Dibamus leucurus* was placed based on Greer (1985) and Pyron *et al.* (2013), *Agamodon anguliceps* was placed based on Kearney & Stuart (2004), *Amphisbaena alba* and *Typhlops titanops* were placed based on Pyron *et al.* (2013), *Trilepida dimidiata* and *Rena myopica* were placed based on the location of congeneric taxa in Pyron *et al.* (2013), and *Amerotyphlops*, *Cubatyphlops*, and *Gerrhopilus* were placed based on the location of congeneric

taxa in Nagy *et al.* (2015). Certain taxa (*Acutotyphlops infralabialis*, *A. solomonis*, *Anomalepis aspinosus*, *A. mexicanus*, *Helminthophis praeocularis*, *Liotyphlops argaleus*, *Myriopholis tanae*, and *M. macrorhyncha*) have not been included in any prior phylogenies based on actual character data to my knowledge, so were placed in the most exclusive clade possible based on taxonomy.

Branch lengths, representing time, are derived mainly from Burbrink *et al.* (2020). Key nodes within Typhlopoidea were also dated using Miralles *et al.* (2018), and nodes involving *Lanthanotus* and *Rhineura* were dated using Simões *et al.* (2018). For some branches, dated phylogenies incorporating the relevant taxa were not available (often because genetic data are not available for those taxa), so dates for these branches were derived by evenly subdividing the distance between the closest dated nodes.

3.2.5. Ancestral state reconstruction

Ancestral state reconstructions of squamate feeding mechanisms were performed in Mesquite v. 3.61 (Maddison & Maddison 2019) using both maximum parsimony (MP) and maximum likelihood (ML) algorithms (see Appendix 3.1 for phylogeny and ASR matrix). For the ML reconstructions, traits were mapped using the Markov k-state 1-parameter (Mk1) model, which assumes that forward and reverse changes occur at the same rate (Lewis 2001; Maddison & Maddison 2006). Feeding mechanisms were examined via three scoring schemes: 'basic', 'detailed microstomy', and 'detailed microstomy and macrostomy'. The more detailed scoring methods aim to reflect morphological variability more accurately within these broad categories, as described herein or as recognized by recent authors (e.g., Palci *et al.* 2016; Harrington & Reeder 2017; Chretien *et al.* 2019). Feeding mechanisms were scored based on personal observations of the specimens in Table 3.1. Nodes were considered 'definitively reconstructed' when a single state was most parsimonious or when the likelihood of any state was greater than 90%. Nodes were considered 'equivocal' when multiple states were equally parsimonious or when none of the states had a likelihood greater than 50%.

The 'basic' character scheme scores taxa simply as 'macrostomatan' or 'microstomatan', reflecting a common though arguably over-simplified approach in the literature (e.g., Harrington & Reeder 2017; Miralles *et al.* 2018). The 'detailed microstomy' scheme divides microstomy into five morphotypes ('minimal-kinesis', 'snout-shifting', 'single-axle maxillary raking', 'axle-brace maxillary raking', and 'mandibular raking') as described below (see §3.3 and 3.4);

however, macrostomy remains a single state following the traditional perspective that macrostomy is a synapomorphy uniting derived alethinophidians (e.g., Rieppel 1988; Miralles *et al.* 2018). The 'detailed microstomy and macrostomy' scheme divides microstomy into these same five morphotypes and also divides macrostomy into two morphotypes ('booid-' and 'caenophidian-type'). Because the current study is focussed on microstomy, and because macrostomy is an equally complex and poorly understood condition, I do not analyze the homology of macrostomatan jaw mechanisms herein; indeed, the homology of these latter mechanisms is a topic more than expansive enough in scope to warrant a detailed treatment of its own. Instead, this latter subdivision is based on recent suggestions from ontogenetic, phylogenetic, and anatomical perspectives that 'macrostomy' may have evolved independently in booid-pythonoids and caenophidians (Palci *et al.* 2016; Burbrink *et al.* 2020).

3.3. Results

I provide below a brief description of the jaw structures of select squamate taxa (Figs 3.1 and 3.3–3.11). Thorough descriptions of the overall cranial anatomy of these taxa have been provided by several previous authors, and so I refer the reader throughout to the relevant literature rather than repeating those detailed efforts here. Instead, my descriptions focus on features relevant in comparing the jaw conditions among 'microstomatan' squamates. These descriptions are grouped according to functional morphology, reflecting the distinct biomechanical arrangements of the jaws and suspensorium that occur in non-snake lizards, uropeltoids and amerophidians, typhlopoids, anomalepidids, and leptotyphlopids. These distinct versions of microstomy are best reflected by the anatomy and functional morphology of the palatomaxillary arch and suspensorium, though the mandible also exhibits key differences among groups. These biomechanics-based categories are discussed from an evolutionary or homology-based perspective in the Discussion.

3.3.1. Non-snake lizards

As discussed by several authors (e.g., Frazzetta 1962; Cundall 1995), some degree of cranial kinesis occurs throughout all major lizard clades. However, this kinesis is much less pronounced in non-snake lizards than the extensive mobility—especially regarding the jaws and suspensorium—present in snakes (Cundall 1995). References herein to the non-snake lizard skull as 'minimally kinetic' thus reflect this comparison to the snake condition.

3.3.1.1. Mandible

The non-snake lizard mandible is long and robust, typically equal in length to the skull (Figs 3.3 and 3.4), except in some burrowing forms (e.g., dibamids and amphisbaenians; Figs 3.5 and 3.6) in which the mandible is 60–70% of the total skull length. The dentaries are similarly long and robust, bearing multiple teeth and articulating closely with all, or almost all, other mandibular elements (Figs 3.3e,f, 3.4e,f, 3.5e,f, and 3.6e,f). Notably, the dentaries approach each other very closely at the mental symphysis, with roughened symphyseal or articular facets for the attachment of connective tissue and cartilage (Kley 2006). A posteroventral process is typically present on the dentary (Figs 3.3e, 3.5e, and 3.6e), though it is reduced or absent in some taxa (e.g., *Lanthanotus*, some iguanians; Fig. 3.4e).

The splenial varies in size and shape among taxa, from large and plate-like in *Varanus* (Fig. 3.3e,f), to much smaller in iguanians (Fig. 3.4e,f), to absent in amphisbaenians (Fig. 3.6e,f) and absent or fused to the articular complex in dibamids (Fig. 3.5e,f; Evans 2008). However, despite these differences in morphology, its overall role in the mandible is similar: integrating tightly with all or almost all other mandibular elements to bridge the intramandibular joint.

The coronoid varies in shape among taxa, though it plays a consistent functional role in the overall mandible. In *Varanus* (Fig. 3.3e,f), iguanians (Fig. 3.4e,f), and amphisbaenians (Fig. 3.6e,f), the coronoid sits dorsally or dorsomedially on the mandible, extending well anteriorly and posteriorly to strongly bridge the intramandibular joint. In dibamids, the anteromedial and posteroventromedial processes of the coronoid are highly reduced or absent, although the elongate posterodorsomedial process articulates extensively with the articular complex and the coronoid process articulates closely with the dentary anterolaterally (Fig. 3.5e,f). Therefore, despite differences in morphology among these taxa, the coronoid plays an equivalent functional role in all of them: bracing the anterior and posterior mandibular elements and bridging the intramandibular joint.

The angular is long and thin, running along the ventral or ventromedial mandible (except in dibamids and amphisbaenians; see §3.3.1.4). The angular exhibits extensive mediolateral overlap with the splenial in *Varanus* (Fig. 3.3e,f) and extensive dorsoventral articulation with this element in iguanians (Fig. 3.4e,f). It also articulates with the dentary in all non-snake lizards observed herein, and with the other elements of the posterior mandible (Figs 3.3–3.6). Via these articulations, the angular thus effectively bridges the intramandibular joint.

In most non-snake lizards, the articular and prearticular are fused—referred to herein as simply the articular, following the convention of other authors such as Evans (2008) and Werneburg *et al.* (2015)—but the surangular remains separate. Additional fusion of the posterior mandibular elements occurs in dibamids (Fig. 3.5e,f), amphisbaenians (Fig. 3.6e,f), and some iguanians, and so these taxa are described separately in §3.3.1.4. The surangular articulates tightly with all or most other mandibular elements, including strong articulation with the coronoid dorsally, the angular ventrally or ventrolaterally, and the articular ventrally (Figs 3.3e,f and 3.4e,f). Of particular note, it extends anteriorly across the intramandibular joint to articulate anterolaterally with the dentary (Figs 3.3f and 3.4f), as well as medially with the splenial in some taxa (e.g., *Varanus*; Fig. 3.3f). The articular also articulates tightly with all other mandibular elements (though see §3.3.1.4 for an exception in *Lanthanotus*), except for the dentary in varanoids and some iguanians. The lower jaw bears a moderate retroarticular process, comprising approximately 25–30% of the total length of the articular (Figs 3.3e,f and 3.4e,f). This process is shorter in dibamids (comprising about 10–15% of articular complex length; Fig. 3.5e,f), amphisbaenians (either essentially absent or barely extending beyond the mandibular condyle; Fig. 3.6e,f), and *Lanthanotus* (comprising about 15–20% of articular length; see e.g., Evans 2008:fig. 1.91).

Altogether, the intramandibular joint is typically quite tightly integrated and well braced by the mandibular elements. Almost all mandibular elements articulate closely across this joint in most non-snake lizards observed herein (Figs 3.3–3.6). Although some mandibular kinesis is possible (Frazzetta 1962; Cundall 1995), this is to a lesser extent and via a different configuration than in snakes, including ‘anilioids’ (Cundall 1995; see also §3.3.2). This mandibular structure also represents a very different configuration than in scolecophidians (Figs 3.9–3.11; §3.3.4–3.3.6).

3.3.1.2. Suspensorium

The non-snake lizard quadrate is stout and robust (Figs 3.3–3.6). It is typically oriented roughly vertically (Figs 3.3 and 3.4), though dibamids and amphisbaenians are exceptions to this (Figs 3.5 and 3.6; §3.3.1.4). The quadrate mainly articulates with the articular ventrally and the supratemporal and squamosal dorsally (Figs 3.3 and 3.4), with the paroccipital process of the otoccipital occasionally also contributing to this dorsal articulation (e.g., *Lanthanotus*).

The supratemporal forms a flattened rod, articulating with the squamosal laterally, the quadrate ventrally, and the postparietal process of the parietal—and paroccipital process of the otoccipital, in some taxa (e.g., *Lanthanotus*, *Sauromalus*)—medially (Figs 3.3 and 3.4). It is absent in dibamids and most amphisbaenians (Figs 3.5 and 3.6; §3.3.1.4).

The squamosal varies in shape among taxa, though typically consistently contributes to the jaw suspension via a ventral articulation with the quadrate (Figs 3.3 and 3.4). Its anterior terminus articulates dorsomedially with the elements bordering the posterior margin of the orbit (e.g., postorbitofrontal in *Varanus*, Fig. 3.3; postorbital, and sometimes jugal, in iguanians, Fig. 3.4) to form the upper temporal bar and enclose the supratemporal fenestra. The posterior terminus of the squamosal articulates medially with the supratemporal (Figs 3.3 and 3.4). The supratemporal and squamosal are somewhat reduced in *Sauromalus* and *Lanthanotus*, and absent in dibamids and most amphisbaenians (Figs 3.5 and 3.6; §3.3.1.4).

3.3.1.3. Palatomaxillary arch

The key features of the palatomaxillary arch in non-snake lizards are its degree of robustness and extensive articulation among elements, resulting in minimal palatomaxillary mobility.

The non-snake lizard maxilla is generally large, robust, and toothed (Figs 3.3–3.6). The maxilla typically bears a distinct facial process, which is posteriorly angled in dibamids (Fig. 3.5b) and amphisbaenians (Fig. 3.6b). The facial process is generally tall (Figs 3.3–3.5), though it is shorter in a few taxa (e.g., *Amphisbaena* and *Anelytropsis*; Fig. 3.6), particularly *Lanthanotus*, in which the facial process is low and broad (see e.g., Evans 2008:fig. 1.91), similar to the condition in 'anilioid' snakes (Figs 3.7 and 3.8). The maxilla articulates very closely with all or almost all surrounding elements, including the snout (premaxilla, septomaxilla, vomer, and nasal, the latter contact absent in varanoids), palatine, ectopterygoid, jugal, lacrimal, frontal (in dibamids and amphisbaenians), and prefrontal, when these elements are present (Figs 3.3–3.6).

The pterygoid is large, robust, and often edentulous (Figs 3.3–3.6), though it does bear teeth in some taxa (e.g., *Lanthanotus*). It is gracile in dibamids (Fig. 3.5), but still well-developed, like other non-snake lizards (Figs 3.3, 3.4, and 3.6) and unlike scolecophidians (Figs 3.9–3.11; §3.3.4–3.6). The pterygoid articulates extensively with the palatine and ectopterygoid,

and is further braced by the basipterygoid processes of the parabasisphenoid medially and by the quadrate posterolaterally (Figs 3.3–3.6).

The palatine is robust and edentulous, with well-developed pterygoid, maxillary, and vomerine processes (Figs 3.3b,d, 3.4b,d, 3.5b,d, and 3.6b,d). These processes articulate tightly with: the pterygoid posteriorly; the maxilla, ectopterygoid, and often the lacrimal and/or jugal laterally; and the vomer anteriorly, respectively. An additional process is present in dibamids, arching over the ventral or main shelf of the palatine in a manner analogous to the choanal process of snakes (Fig. 3.5d).

The ectopterygoid is short and robust (Figs 3.3–3.6). Although its specific form and articulations vary slightly across taxa, it plays a consistent functional role in tightly bracing the palatopterygoid bar medially against the maxilla and certain orbital elements (e.g., jugal, prefrontal) laterally, thus supporting and helping to immobilize the tightly integrated palatomaxillary arch.

The prefrontal is closely integrated with the skull (Figs 3.3–3.6), though in a manner quite different to typhlopoids and leptotyphlopids (Figs 3.1, 3.9, and 3.11; §3.3.4 and 3.3.6). The prefrontal typically exhibits minimal to no contact with the snout, instead mainly articulating with the frontal medially and the maxilla laterally (Figs 3.3a,c, 3.4a,c, 3.5a,c, and 3.6a,c). In some taxa (e.g., many iguanians; Fig. 3.4a), contact with the nasal can be fairly extensive, though this is of a very different nature than in any scolecophidian (Figs 3.9–3.11). The prefrontal may also articulate with other surrounding elements (e.g., the lacrimal laterally in varanoids and iguanians, the palpebral dorsolaterally in *Varanus*, and the palatine ventrally in iguanians; Figs 3.3 and 3.4).

The premaxilla is tightly integrated with the other snout elements and the maxilla, thus playing an important role in ‘locking together’ the left and right palatomaxillary arches (Figs 3.3a–c, 3.4a–c, 3.5a–c, and 3.6a–c). The palatomaxillary arch is often additionally braced by: the lacrimal anteriorly, at the junction between the maxilla, prefrontal, and palatine (Figs 3.3c and 3.4c); the jugal laterally, between the maxilla, ectopterygoid, and sometimes palatine (Figs 3.3c and 3.4c); the vomer anteriorly (Figs 3.3b, 3.4b, 3.5b, and 3.6b); the basipterygoid processes of the parabasisphenoid posteromedially (Figs 3.3b, 3.4b, 3.5b, and 3.6b); and the quadrate posterolaterally (Figs 3.3–3.6). In many taxa, the prefrontal also either braces the palatine

dorsally (e.g., many iguanians; Fig. 3.4) or very closely approaches this element (e.g., amphisbaenians, *Lanthanotus*, some iguanians).

Overall, the tight integration of the upper jaw elements in non-snake lizards therefore reflects an essentially akinetic palatomaxillary arch. This occurs via a completely different anatomical configuration than in leptotyphlopids (Figs 3.1 and 3.11; §3.3.6).

3.3.1.4. Exceptions and variations

Given the phylogenetic, ecological, and functional diversity of non-snake lizards, it is inevitable that certain taxa present variations to the general condition described above. However, despite this variation, all taxa exhibit key features justifying their grouping with other non-snake lizards.

A particularly notable exception among non-snake lizards is *Lanthanotus* (e.g., see Evans 2008:fig. 1.91). In this genus, the integration between the anterior and posterior mandibular elements is reduced such that a distinct and flexible intramandibular joint occurs (Evans 2008). This condition involves: reduced integration of the splenial with the posterior mandible (Evans 2008); less extensive articulation of the angular with the anterior mandible and the articular with the splenial; and reduction of the anterior terminus of the coronoid and thus less distinct bracing of the intramandibular joint, including the presence of a facet anteriorly to accommodate the dentary, somewhat similar to the condition in *Cylindrophis* (Fig. 3.7; §3.3.2). Furthermore, the palatine-pterygoid articulation in *Lanthanotus* is looser than is typical of non-snake lizards (e.g., compare Evans 2008:fig. 1.91a to Figs 3.4–3.6 herein). Regarding these features, *Lanthanotus* could therefore be considered morphologically intermediate between typical non-snake lizards (Figs 3.3–3.6) and early-diverging alethinophidians (Figs 3.7 and 3.8).

Importantly, though, despite this looser palatine-pterygoid articulation, the overall structure of the jaws and suspensorium—especially the suspensorium and palatomaxillary arch—is otherwise consistent with the typical non-snake lizard condition. For example, the palatomaxillary arch of *Lanthanotus* lacks key ‘anilioid’ features such as a loosened maxilla-premaxilla articulation, ‘ball-and-socket’-like maxilla-palatine articulation, simplified ectopterygoid articulations, and the ability for unilateral movement, and the mandible lacks features such as an abutting splenial-angular contact (see Fig. 3.7 and §3.3.2). In light of the absence of these features, and due to the otherwise similar condition of *Lanthanotus* compared to

other non-snake lizards, it is therefore most reasonable to consider *Lanthanotus* as a variation of the general non-snake lizard condition.

Dibamids and amphisbaenians represent another apparent exception among non-snake lizards. As mentioned above, the lower jaw differs in these taxa compared to other non-snake lizards due to additional fusion of the posterior mandibular elements (Figs 3.5e,f and 3.6e,f). In dibamids, bipedids, and trogonophiids, this involves fusion of the articular, angular, surangular, and possibly splenial (in dibamids) to form a single articular complex (Fig. 3.5e,f; Evans 2008; Gans & Montero 2008). A similar condition occurs in amphisbaenids and rhineurids, although the angular remains separate, resulting in a compound bone comparable to that of snakes (Fig. 3.6e,f). Some iguanians also exhibit fusion of the angular and/or articular and/or surangular, again forming a 'compound bone' or articular complex (Evans 2008). These fused complexes articulate closely with the other mandibular elements, suturing dorsally or dorsomedially with the coronoid and articulating ventrally and laterally with the dentary (Figs 3.5e,f and 3.6e,f). In dibamids, this latter articulation involves a long prearticular process (*sensu* Evans 2008) extending anteriorly along the medial surface of the dentary, thus bridging the intramandibular joint and bracing the dentary (Fig. 3.5e,f).

Dibamids and amphisbaenians also differ quite distinctly from the typical condition of the non-snake lizard suspensorium. The supratemporal is highly reduced in *Trogonophis* and completely absent in *Dibamus* and most amphisbaenians (Figs 3.5 and 3.6; Evans 2008; Gans & Montero 2008). The squamosal is similarly absent in *Dibamus* and most amphisbaenians, though it is present but quite reduced in *Bipes* (Figs 3.5 and 3.6; Gans & Montero 2008). *Anelytropsis* bears a small temporal element representing either a highly reduced squamosal or supratemporal (Evans 2008). Due to this extreme reduction, the dorsal articulation of the quadrate with the skull is therefore quite different than in other non-snake lizards (e.g., Figs 3.3 and 3.4). Ventrally, the quadrate articulates with the articular complex or compound bone (Figs 3.5 and 3.6). In amphisbaenids and rhineurids, the quadrate also articulates extensively with the pterygoid medially via a broad articulatory facet on the medial surface of the quadrate shaft (Fig. 3.6). Finally, the quadrate itself is notable in being anteriorly displaced and angled distinctly anteroventrally (Figs 3.5c and 3.6c).

The structure of the prefrontal in dibamids further differs from other non-snake lizards. In dibamids, the prefrontal is greatly simplified and essentially plate-like (Fig. 3.5a,c), similar to the

form in leptotyphlopids (Fig. 3.11a,c; §3.3.6). The ectopterygoid also exhibits a simpler structure and simpler articulations with the maxilla and pterygoid than in other non-snake lizards, similar to the condition in *Cylindrophis* (Fig. 3.7; §3.3.2.3).

Finally, the lacrimal and jugal are absent in dibamids and most amphisbaenians (Figs 3.5 and 3.6), with the jugal being present but highly reduced in *Rhineura* (Gans & Montero 2008). The lacrimal is also reduced in *Lanthanotus* and *Uranoscodon*. The palatomaxillary arch in these taxa therefore lacks these additional bracing structures as present in other non-snake lizards.

However, despite these differences, the functionality of the complexes in question remains consistent with other non-snake lizards. For example, the fused mandibular structures articulate closely with the other mandibular elements, therefore playing the same functional role as their constituent components in other non-snake lizards, i.e., bracing the intramandibular joint (Figs 3.5e,f and 3.6e,f). Similarly, although the lacrimal and jugal are often absent, the palatomaxillary arch still articulates quite strongly among its constituent elements and is still braced by the vomers, premaxilla, and basipterygoid processes (Figs 3.5a–d and 3.6a–d), a configuration consistent with the general non-snake lizard condition (Figs 3.3 and 3.4). Finally, although the dibamid prefrontal is similar in form to that of leptotyphlopids, major differences include a lack of contact with the snout elements and much greater contact with the maxilla (Figs 3.5 and 3.11; see also §3.3.6 for comparison), as well as the completely different configuration of the upper jaw complex compared to any scolecophidian (Fig. 3.1). Therefore, because the skulls of these taxa—particularly the structure and biomechanics of the palatomaxillary arch (e.g., robust, tightly interlocking, and immobile)—are otherwise consistent with the condition in other non-snake lizards, I find it reasonable to consider dibamids and amphisbaenians as variations of this general non-snake lizard condition, and the similarities between their anatomical arrangements and those of the blindsnakes as having arisen convergently (see also §3.4.4).

3.3.2. ‘Anilioids’ – Uropeltoidea

The description of this morphotype is based on *Cylindrophis* (Fig. 3.7). Minor variations in other uropeltoid taxa are noted where relevant, with major variations being described at the end of this section. This description of uropeltoids is largely applicable to Amerophidia (Fig. 3.8)—the other major lineage of ‘anilioid’ snakes—but, because Amerophidia forms a distinct phylogenetic lineage, rendering ‘anilioids’ polyphyletic (Figs 3.1 and 3.2; Burbrink *et al.* 2020), this latter clade is presented separately in the next section. Previous treatments of the uropeltoid

skull supplement the descriptions provided herein; primary among these are Cundall (1995), Cundall & Irish (2008), Cundall & Rossman (1993), Olori & Bell (2012), Rieppel (1977), and Rieppel & Maisano (2007).

3.3.2.1. Mandible

The uropeltoid mandible is robust and approximately equal in length to the skull (Fig. 3.7). The dentary is large and robust (Fig. 3.7e,f), similar to the form in non-snake lizards (Figs 3.1 and 3.3–3.6) and quite distinct from the reduced form in scolecophidians (Figs 3.1 and 3.9–3.11). The dentary tooth row is oriented anteroposteriorly (Fig. 3.7e,f). The mandibles approach each other medially, much more so than in 'macrostomatans', but slightly less so than in scolecophidians and especially non-snake lizards. A fibrocartilaginous interramal pad and collagenous intergular pad (*sensu* Cundall 1995) occur at the mandibular symphysis in *Cylindrophis*, preventing lateral separation of the dentary tips (Cundall 1995). The dentary distinctly articulates with surrounding elements, but its articulations with the compound bone and coronoid are typically quite loose compared to the tight junctions in non-snake lizards (Figs 3.3–3.6), resulting in a greater capacity for kinesis at the intramandibular joint (Fig. 3.7e,f; Cundall 1995). The posteroventral process of the dentary is present (Fig. 3.7e,f).

The splenial and angular are typically well-developed (Fig. 3.7f). These elements form low, anteriorly- and posteriorly-tapering triangles, respectively, as is typical of snakes (Fig. 3.7f). Laterally, they articulate closely with the dentary and compound bone, respectively (Fig. 3.7f). The splenial and angular articulate with each other via a simple abutting contact, with their articulating surfaces exhibiting slight concavo-convexity, thus enabling intramandibular kinesis (Fig. 3.7f; Cundall 1995).

The coronoid is robust in *Cylindrophis* (Fig. 3.7e,f). It bears a tall coronoid process (Fig. 3.7f), though proportionally this is not quite as tall as in scolecophidians (Figs 3.1 and 3.9–3.11; §3.3.4–3.3.6). The coronoid articulates closely with the compound bone laterally and ventrally (Fig. 3.7e,f). The anteromedial process of the coronoid is long and extends under the posterior extent of the dentary tooth row (Fig. 3.7f). The coronoid-dentary articulation is relatively loose, with the coronoid being dorsoventrally flattened anteriorly with a distinct dorsal facet to accommodate the dentary, which permits intramandibular kinesis (Fig. 3.7e,f; Cundall 1995).

The compound bone is typically elongate and robust, comprising about 60–70% of the total skull length (Fig. 3.7). The retroarticular process is very short, typically barely extending

beyond the mandibular condyle (Fig. 3.7e,f), though is slightly longer in *Anomochilus* (see Rieppel & Maisano 2007).

Overall, the intramandibular joint is relatively mobile in *Cylindrophis*, particularly via lateral flexion near the angular-splenial, dentary-compound bone, and dentary-coronoid joints (Fig. 3.7e,f; Cundall 1995). This is presumably also the case for *Anomochilus* and *Uropeltis*, both of which exhibit similar angular-splenial and dentary-compound bone articulations. This mobility is much more extensive than the limited mandibular kinesis present in scleroglossans (Cundall 1995).

3.3.2.2. Suspensorium

The quadrate is stout and robust (Fig. 3.7). It is oriented roughly vertically (though is tilted slightly anteriorly in *Anomochilus*), with a large suprastapedial process posterodorsally (Fig. 3.7c). This process is particularly elongate in *Anomochilus* and especially *Uropeltis*, to an extent unique among snakes (Olori & Bell 2012). Dorsally, the quadrate typically articulates mainly with the prootic and supratemporal and minimally with the otoccipital (Fig. 3.7a,c). The supratemporal is present and well-developed (Fig. 3.7a,c). As in all snakes, the squamosal is absent.

3.3.2.3. Palatomaxillary arch

The maxilla is large and robust (Fig. 3.7a–d), similar to the robust condition in non-snake lizards (Figs 3.1 and 3.3–3.6), though it differs from that of non-snake lizards in the nature of its articulations with surrounding elements. The maxilla articulates posteriorly with the ectopterygoid, medially with the palatine via a ‘ball-and-socket’-like joint enabling rotation and minor anteroposterior movement of the maxilla (Fig. 3.7b,d; Cundall 1995), and dorsally with the prefrontal via a low facial process (Fig. 3.7a–d). The maxilla approaches the septomaxilla and premaxilla medially and is attached to these elements via septomaxillo-maxillary and premaxillo-maxillary ligaments, respectively (Cundall 1995), but does not directly contact them (Fig. 3.7b). As such, although the maxilla articulates closely with surrounding elements, this articulation is not as tight as in non-snake lizards (Figs 3.3–3.6), resulting in less restricted palatomaxillary mobility. The maxillary tooth row is oriented anteroposteriorly (Fig. 3.7).

The pterygoid is large, robust, and well-developed (Fig. 3.7a–d). In this manner it is similar to non-snake lizards (Figs 3.3–3.6), but differs in bearing a more pronounced tooth row anteriorly. The pterygoid interlocks with the palatine anteriorly (Fig. 3.7b,d), though in a slightly

more flexible manner than in non-snake lizards (Figs 3.3–3.6; except e.g., *Lanthanotus*: see §3.3.1.4). As in non-snake lizards, the pterygoids are braced medially by the basipterygoid processes of the parabasisphenoid (Figs 3.3b, 3.4b, 3.5b, 3.6b, and 3.7b), a junction further strengthened by the basipterygoid ligaments (Cundall 1995). The pterygoids are also braced by the ectopterygoid laterally (Fig. 3.7a–d), though via a less complex and less extensive articulation than is typical of non-snake lizards (Figs 3.3–3.6).

The palatine is similarly large and robust (Fig. 3.7b,d). It differs from the non-snake lizard palatine primarily in bearing teeth along the length of its main body and in bearing a distinct choanal process (Fig. 3.7b,d). As noted above, its posterior articulation with the pterygoid is not as tight as in most non-snake lizards. The choanal processes very closely approach the palatine processes of the vomers, with these elements being linked by the vomero-palatine ligaments, such that movements of the palatine are transferred to the corresponding vomer (Cundall 1995). Although this is superficially similar to the close palatine-vomer articulation in non-snake lizards, it lacks the extensive direct osseous contact between these elements that occurs in non-snake lizards (Figs 3.3–3.7). The palatine articulates with the maxilla via a 'ball-and-socket'-like joint (Fig. 3.7b,d).

The ectopterygoid is short and robust, articulating with the ectopterygoid process of the pterygoid posteriorly and the posterior terminus of the maxilla anteriorly (Fig. 3.7a–d). Both articulations are less extensive and/or less complexly integrated than in non-snake lizards (e.g., compared to the broadly abutting contacts in *Physignathus* or the complexly interlocking articulations in *Varanus*; Figs 3.3–3.6).

The uropeltoid prefrontal is very similar to non-snake lizards (except *Dibamus*; see Fig. 3.5 and §3.3.1.4) in its articulations with other skull elements. For example, as in non-snake lizards (Figs 3.3–3.6), the prefrontal exhibits minimal contact with the snout, instead articulating mainly with the frontal medially and the maxilla laterally (Fig. 3.7a,c). It also articulates ventrally with the palatine, and is further connected to the maxilla via the lateral prefronto-maxillary ligament and to the palatine via the prefronto-palatine ligament (Cundall 1995). According to Cundall (1995), though, the integration with the maxilla and palatine is looser in alethinophidians—including 'anilioids'—than in non-snake lizards. Of note, typhlopoids and leptotyphlopids also exhibit tight integration of the prefrontal with the skull roof (Figs 3.9 and

3.11; §3.3.4 and 3.3.6), though this condition differs quite distinctly from that in non-snake lizards (Figs 3.3–3.6) or 'anilioids' (Figs 3.7 and 3.8).

The premaxilla is integrated into the snout more loosely than in non-snake lizards (Figs 3.3–3.6) and scolecophidians (Figs 3.9–3.11), though more tightly than in more derived alethinophidians. The premaxilla is connected to the maxilla via the premaxillo-maxillary ligament (Cundall 1995), though, unlike non-snake lizards, it lacks direct osseous contact with the maxilla (Fig. 3.7a,b). This configuration enables slightly more unilateral movement of the left and right palatomaxillary arches, compared to the tightly braced condition in non-snake lizards.

Overall, the palatomaxillary arch is generally similar to the condition in non-snake lizards (e.g., large, robust, interlocking elements; Figs 3.3–3.6), though its components are less tightly articulated with each other and with surrounding elements than in non-snake lizards (Fig. 3.7a–d). The palatomaxillary arch therefore has somewhat greater kinesis than in non-snake lizards, including the ability for unilateral movement of the left and right palatomaxillary arches, albeit limited compared to more 'derived' alethinophidians (Cundall 1995). This movement is largely enabled by minor decoupling of the ventral (vomer and septomaxilla) and dorsal (nasal and premaxilla) snout elements, and the ventral snout elements from their contralaterals (Cundall 1995). This decoupling enables slight unilateral movement within the ventral snout, which extends to the rest of the palatomaxillary arch due largely to the integration of the palatine-vomer and maxilla-septomaxilla (Fig. 3.7; Cundall 1995). The 'ball-and-socket'-like joint between the maxilla and palatine is also essential in enabling this kinesis.

3.3.2.4. Exceptions and variations

As noted above for non-snake lizards, the phylogenetic diversity among uropeltoids inevitably causes variation within this group. Much of this variation arises from miniaturization, paedomorphosis, and adaptations related to fossoriality, as explained further in the Discussion.

Representing key exceptions to the general uropeltoid condition as described above, both *Anomochilus* and *Uropeltis* (and indeed other members of the Uropeltidae such as *Plectrurus* and *Melanophidium*; Cundall & Irish 2008) exhibit reduction of certain elements compared to *Cylindrophis*. For example: the mandible is shorter (about 70–80% of total skull length); the splenial and angular are smaller or lost altogether (*Plectrurus*; Cundall & Irish 2008); the dentary and maxilla are robust but anteroposteriorly shorter in *Anomochilus*, and of typical length but

more gracile in uropeltids; the posteroventral process of the dentary is absent in uropeltids; the coronoid is highly reduced and articulates only with the compound bone; and the compound bone is shorter in *Uropeltis* (comprising about 40–50% of the total skull length), and somewhat less robust in both taxa (see also Rieppel & Maisano 2007; Olori & Bell 2012). The compound bone's length varies dramatically within the Uropeltidae (Cundall & Irish 2008). Presumably as a consequence of the drastic reduction of its posterior extent, the maxillary tooth row is angled somewhat anteromedially in *Anomochilus* (see also Rieppel & Maisano 2007). The jaw suspension is anteriorly displaced in both *Anomochilus* and uropeltids compared to *Cylindrophis* and *Anilius*, more closely resembling the placement in scolecophidians, and the supratemporal is absent in uropeltids and *Anomochilus leonardi*, causing the quadrate to articulate dorsally with the prootic and otoccipital in *Anomochilus* and with the fused braincase in *Uropeltis* (see also Rieppel & Maisano 2007; Olori & Bell 2012). The pterygoid and palatine are both edentulous in these taxa, and the ectopterygoid is also reduced, to the extent that it is entirely suspended within the pterygomaxillary ligament in *Anomochilus* (see also Cundall & Rossman 1993; Rieppel & Maisano 2007).

Other differences involve increased robustness of the skull, such as the lateral expansion of the nasals, causing tighter integration of the prefrontal with the snout (see also Rieppel & Maisano 2007). The premaxilla is also more tightly integrated with surrounding elements, limiting the capacity for unilateral movement of the palatomaxillary arches (see also Rieppel & Maisano 2007; Olori & Bell 2012). Finally, the maxilla more closely approaches the septomaxilla and premaxilla in *Anomochilus* and makes extensive contact with these elements, especially the premaxilla, in *Uropeltis*.

Despite these differences, however, *Anomochilus* and *Uropeltis* still exhibit many similarities to *Cylindrophis*. For instance, although the prefrontal is more tightly integrated into the skull, it is otherwise consistent in form with the typical uropeltoid condition as described above (see also Rieppel & Maisano 2007; Olori & Bell 2012). Similarly, although the palatine is edentulous, the rest of its anatomy is quite similar to other uropeltoids (see also Rieppel & Maisano 2007; Olori & Bell 2012). Most importantly, both *Anomochilus* and *Uropeltis* appear capable of moving the ventral snout elements independently of the dorsal snout elements (Cundall & Rossman 1993; Cundall 1995), a key component of the functional morphology of *Cylindrophis*. Taking these similarities into account—and also recognizing that *Anomochilus* and

Uropeltis lack the hallmark features of any of the scolecophidian morphotypes, especially regarding the palatomaxillary suspension and biomechanics (see Figs 3.9–3.11 and §3.3.4–3.3.6)—I ultimately consider it reasonable to classify these taxa as miniaturized variants of the general uropeltoid condition, rather than creating a different morphotype or referring them to any of the scolecophidian conditions (see also §3.4.4 for further discussion).

3.3.3. 'Anilioids' – Amerophidia

The clade Amerophidia is herein represented by *Anilius* (Figs 3.1, 3.2, and 3.8). The cranial morphology of this clade is largely consistent with that of Uropeltoidea (Fig. 3.7), as described above, especially regarding the suspensorium and palatomaxillary arch. However, amerophidians form a lineage that is phylogenetically separate from uropeltoids, creating a polyphyletic 'anilioid' assemblage (Figs 3.1 and 3.2; Burbrink *et al.* 2020), and also exhibit a mandibular structure different from that of uropeltoids. For these reasons, these clades of early-diverging alethinophidians are treated separately. To avoid repetition, however, I here describe only the mandible of Amerophidia in detail, and refer readers to §3.3.2.2 and §3.3.2.3 for a general impression of the suspensorium and palatomaxillary arch, respectively.

3.3.3.1. Mandible

Anilius is notable in that the structure of its mandible differs somewhat compared to *Cylindrophis* (Figs 3.7 and 3.8). In *Anilius*, the splenial and angular are absent or extremely reduced (Fig. 3.8; Rieppel 1977; Cundall & Irish 2008). The anterior terminus of the compound bone articulates rather extensively with the medial surface of the dentary (Fig. 3.8f), in contrast to the interlocking configuration in *Cylindrophis* (Fig. 3.7e,f), and the coronoid overlaps this articulation dorsally (Fig. 3.8e,f). Altogether, this suggests a potentially lower degree of intramandibular kinesis in *Anilius* compared to *Cylindrophis*.

However, the dentary-compound bone articulation appears to still enable some degree of lateral flexion at the intramandibular joint, as the coronoid is reduced and so does not act as a medial 'buttress' preventing this flexion (Fig. 3.8e,f). This is unlike the typhlopoid mandible, for instance, in which the coronoid would prevent this movement (see Fig. 3.9 and §3.3.4.1). Furthermore, although the intramandibular joint of *Anilius* does differ somewhat from *Cylindrophis*, the articulations and apparent mobility of this condition are much more functionally and anatomically similar to *Cylindrophis* (Fig. 3.7) than to the tightly and

pervasively interlocking condition of the non-snake lizard mandible (Figs 3.3–3.6). Combined with the consistent nature of the palatomaxillary arch in these taxa, including the suggestion that *Anilius* is also capable of unilateral movement of the palatomaxillary arches (Cundall 1995), it is therefore reasonable to include *Anilius* under the same biomechanical category as *Cylindrophis*.

3.3.4. Typhlopoidea

The clade Typhlopoidea contains three families: Gerrhopilidae, Typhlopidae, and Xenotyphlopidae (Figs 3.1 and 3.2). My micro-CT scans of gerrhopilids were not of sufficient resolution to digitally segment or figure these specimens in the same detail as the other scolecophidian families, but did allow the assessment of key aspects of their anatomy. Iordansky (1997), Kley (2001), and Chretien *et al.* (2019) present detailed descriptions of typhlopoid jaw anatomy, with Iordansky (1997) and Kley (2001) also discussing the functional morphology of the typhlopid jaw complex. Classical studies such as Haas (1930), Mahendra (1936), Evans (1955), and List (1966) also provide descriptions of the typhlopid skull; much of the historical literature was summarized by Cundall & Irish (2008).

3.3.4.1. Mandible

The typhlopoid mandible is long and slender, measuring approximately 60–75% of the total skull length (Fig. 3.9). The dentaries are highly reduced, each typically forming a flat crescent or slightly rod-like form curved medially toward the mandibular symphysis (Fig. 3.9e,f), though the dentary is more straight and rod-like in some taxa (e.g., *Acutotyphlops kunuaensis*, *A. subocularis*). The dentaries closely approach each other medially, linked by a cartilaginous nodule as in leptotyphlopids (Kley 2001). The dentary exhibits broad contact ventrally with the splenial, also overlapping the coronoid and compound bone posteroventrally (Fig. 3.9e,f). The interramal surface is smooth, lacking articulatory or symphyseal facets, unlike the condition in non-snake lizards (see also Kley 2006). The posteroventral process of the dentary is absent (Fig. 3.9e,f); Rieppel *et al.* (2009) described this absence as uniting all scolecophidians, though see §3.3.5.1 for my interpretation in anomalepidids. The dentary is edentulous (Fig. 3.9e,f), a condition unique to typhlopoids among snakes (Kley 2001), if not squamates overall.

The typhlopoid splenial is proportionally quite large compared to other squamates, ranging from approximately equal in length to the dentary (e.g., *Acutotyphlops infralabialis*, among others) to approximately twice the length of the dentary (e.g., *Afrotyphlops*,

Amerotyphlops, *Anilios*, among others; Fig. 3.9e,f). The gerrhopilid splenial is somewhat more gracile, being slightly shorter and thinner than the dentary in *Gerrhopilus persephone*, of typical length but thin and rod-like in *G. beddomii*, and of typical length but not extending as far anteriorly in *G. ater*. The splenial typically extends anteriorly almost to the anterior terminus of the mandible in most typhlopoids (Fig. 3.9e,f), though it terminates farther posteriorly in a few taxa (*Acutotyphlops infralabialis*, *A. kunuaensis*, *Gerrhopilus persephone*, *G. ater*). The splenial articulates extensively with all other mandibular elements, fully spanning the intramandibular joint (Fig. 3.9e,f).

The angular is quite reduced, forming a thin splint lying between the dorsal margin of the splenial and the ventral margins of the compound bone and coronoid (Fig. 3.9e,f). The angular directly contacts the coronoid in some taxa (e.g., *Acutotyphlops*, *Afrotyphlops*, *Typhlops*; Fig. 3.9f) and closely approaches but does not directly contact it in others (e.g., *Antillotyphlops*, *Xenotyphlops*). The angular is absent in some typhlopoids (e.g., *Anilios*, *Indotyphlops*, *Ramphotyphlops*, *Xerotyphlops*, and potentially *Gerrhopilus*).

The coronoid is large, flat, and triangular, with a tall coronoid process (dorsal process *sensu* Kley 2006; Fig. 3.9e,f). The base of the coronoid extends well anteriorly and posteriorly, articulating closely with the dentary, splenial, and compound bone in all typhlopoids (Fig. 3.9e,f), though it does not extend as far anteriorly in *Gerrhopilus ater* and *G. persephone* as in other typhlopoids. Contact with the angular varies among taxa (see above).

The typhlopoid compound bone is long, measuring approximately 50–65% of the total skull length, and is distinctly anteriorly downcurved (Fig. 3.9). This curvature is especially pronounced in xenotyphlopids, in conjunction with the distinctive ventral inflection of the anterior skull (see Chretien *et al.* 2019). The compound bone bears a moderate retroarticular process, typically comprising about 20–25% of the total length of the compound bone (Fig. 3.9e,f), though this process is shorter in some taxa (about 7–10% in *Acutotyphlops*, and 16–18% in *Antillotyphlops*, *Cubatyphlops*, and *Gerrhopilus*). The retroarticular process terminates well anterior to the level of the occipital condyle (Fig. 3.9). The compound bone articulates with all other mandibular elements (Fig. 3.9e,f).

Altogether, the intramandibular hinge is essentially immobile, with the mandibular elements articulating tightly with each other, especially the broadly overlapping splenial, coronoid, and compound bone (see also Kley 2001). However, some longitudinally rotational

intermandibular mobility is possible, as indicated by the configuration of the jugomandibular ligament and the muscular attachments of the compound bone and suspensorium, which permit a deeper intermandibular oral trough than would be possible were the mandibles medially linked by more tightly interlocking articulatory or symphyseal facets (Iordansky 1997).

3.3.4.2. Suspensorium

As is typical of scolecophidians, the quadrate is elongate and strongly anteroventrally angled (Fig. 3.9c). However, it is not as elongate as in leptotyphlopids, with the long axis of the quadrate equivalent to approximately 25–30% of the total skull length in typhlopoids (Fig. 3.9; though it is longer in some taxa, e.g., 37–40% in *Indotyphlops*, *Typhlops*, and *Xerotyphlops*), compared to approximately 40–45% in leptotyphlopids (Fig. 3.11). In typhlopids and gerrhopilids, the quadrate bears a pronounced anterior process (*sensu* Palci *et al.* 2020a) slightly posterior to the mandibular condyle (Fig. 3.9c). This process is somewhat smaller and more posteriorly positioned in *Xenotyphlops* (see Chretien *et al.* 2019). The quadrate articulates dorsally with the prootic and otoccipital in most typhlopoids (Fig. 3.9; e.g., *Afrotyphlops*, *Amerotyphlops*, *Anilios*, *Antillotyphlops*, *Cubatyphlops*, *Typhlops*, *Xerotyphlops*), though these elements are fused in xenotyphlopids, gerrhopilids, and some typhlopids (e.g., *Acutotyphlops*, *Indotyphlops*, *Ramphotyphlops*, and *Madatyphlops*; see also Hawlitschek *et al.* 2021). The supratemporal is absent in all typhlopoids. As is typical of snakes, the squamosal is also absent.

3.3.4.3. Palatomaxillary arch

The typhlopoid maxilla is highly mobile and is unique among squamates in rotating about the maxillary process of the palatine via a large foramen (in most typhlopoids; Fig. 3.9) or deep medial excavation (e.g., *Acutotyphlops infralabialis*, *A. kunuaensis*, *A. solomonis*, *Afrotyphlops schlegelii*). The maxillary tooth row is directed roughly transversely, with the maxilla angled posteroventrally at rest (Fig. 3.9a–d). A pronounced facial process articulates loosely alongside the lateral surface of the prefrontal (Fig. 3.9a–d).

As is typical of scolecophidians, the pterygoid is long, rod-like, and edentulous (Fig. 3.9a–d). Its anterior terminus, or palatine process, is forked to articulate with the palatine (Fig. 3.9b,d). The pterygoid and palatine underlie the skull more broadly than in leptotyphlopids (Fig. 3.11; §3.3.6.3). The parabasisphenoid lacks basipterygoid processes in most typhlopoids (Fig. 3.9b), though rudimentary processes are present in *Xenotyphlops* (Chretien *et al.* 2019). However, these processes are much less prominent than in non-snake lizards and do not

approach the pterygoids as closely, and the pterygoids lack corresponding articulatory facets (see Chretien *et al.* 2019).

The palatine is edentulous and highly reduced, essentially consisting only of its maxillary and choanal processes (Fig. 3.9b,d). The palatine also bears a highly reduced pterygoid process and distinct ventral process (the latter of which may reflect a uniquely forked condition of the former) which articulate with the forked anterior terminus of the pterygoid (Fig. 3.9b,d). The choanal process forms a thin and narrow arch very closely approaching the corresponding vomer (Fig. 3.9b), though—like most snakes (Figs 3.7–3.10) and unlike non-snake lizards (Figs 3.3–3.6) and leptotyphlopids (Fig. 3.11)—there is no direct osseous contact between these elements. Most distinctively, the maxillary process of the palatine is unique among squamates in forming an elongate rod projecting laterally to articulate with a foramen and/or medial depression in the maxilla (Fig. 3.9a–d).

The ectopterygoid is absent in all typhlopoids (see also Chretien *et al.* 2019). The prefrontals are expanded and immobile, being tightly integrated into the snout and skull roof via extensive articulation with the nasals, septomaxillae, and frontals in all typhlopoids (Fig. 3.9a–d), as well as the premaxilla in xenotyphlopids (see also Chretien *et al.* 2019). The premaxilla is tightly integrated with the other snout elements, but does not contact the palatomaxillary arches and therefore does not affect palatomaxillary mobility (Fig. 3.9a–c).

Altogether, the palatomaxillary arch is highly mobile, with its functionality reliant upon a unique maxilla-palatine articulation (see also Iordansky 1997; Kley 2001; Chretien *et al.* 2019). Drastic reduction of the ligamentous connection between the pterygoid and quadrate further reflects decoupling of the upper (palatomaxillary arch) and lower (mandible and suspensorium) jaws, as in leptotyphlopids (Kley 2001).

3.3.5. Anomalepididae

Like typhlopoids, anomalepidid jaw biomechanics rely heavily on movements of the palatomaxillary arches; however, this occurs via a totally different anatomical configuration than in typhlopoids (Figs 3.9 and 3.10; Chretien *et al.* 2019). Unfortunately, although typhlopoid jaw anatomy has been described in detail from a functional morphological perspective (Iordansky 1997; Kley 2001), this system has yet to be examined in similar morphofunctional detail in anomalepidids. Rieppel *et al.* (2009) recently provided a detailed description of the anomalepidid skull, focussing on *Liotyphlops* and *Typhlophis*, with Santos & Reis (2019) providing detailed

imaging of *Anomalepis*. Classical work was summarized by Cundall & Irish (2008). Important among historical works are those by Haas (1964, 1968) describing anomalepidid skull anatomy, although it is worth noting that these studies were based on serial sectioning and suffered greatly from the small size of these animals, leading to almost comically wavy bone shapes in Haas' illustrations. This issue has been completely overcome by micro-CT approaches.

3.3.5.1. Mandible

The anomalepidid mandible is extremely long and slender, measuring approximately 85–90% of the total skull length in most anomalepidids and 100% of the total skull length in *Typhlophis* (Fig. 3.10). The dentary is highly reduced (Fig. 3.10e,f), with a rod-like form—rather than the more crescentic form of typhlopoids (Fig. 3.9e,f)—and a flattened and expanded anterior terminus. The dentary is typically toothed, like leptotyphlopids (Fig. 3.11e,f) and unlike typhlopoids (Fig. 3.9e,f). However, the anomalepidid dentary bears only a few tooth positions at its anterior terminus (List 1966; Haas 1968; Rieppel *et al.* 2009), and so is not as extensively or robustly toothed as in leptotyphlopids (see Fig. 3.11e,f and §3.3.6.1). Furthermore, several specimens do indeed have edentulous mandibles (a condition which Chretien *et al.* 2019 mistakenly generalized to all anomalepidids); among the examined specimens, teeth are only distinctly visible on specimens of *Anomalepis mexicanus*, *Liotyphlops beui*, and *Typhlophis*, although this may be an artifact of scan resolution. List (1966) and Haas (1964) found teeth on the dentary of *Liotyphlops albirostris*, Haas (1968) in *Anomalepis aspinosus*, and McDowell & Bogert (1954) in *Helminthophis flavoterminatus* and *Typhlophis squamosus*. As in other snakes, the interramal surface lacks articulatory or symphyseal facets (see also Kley 2006). Finally, although Rieppel *et al.* (2009) described the posteroventral process of the dentary as being absent in all scolecophidians, I consider it present in anomalepidids: in other squamates (Figs 3.3 and 3.5–3.8), this process constitutes an extension of the dentary ventral to the surangular or compound bone, which is also the condition in anomalepidids (Fig. 3.10e). In contrast, the dentary in other scolecophidians (Figs 3.9 and 3.11) extends posterodorsal to the compound bone, reflecting an absence of the posteroventral process and presence of the posterodorsal process of other squamates (Figs 3.3–3.8).

The angular is present in anomalepidids, although the splenial is absent (Fig. 3.10e,f; see Rieppel *et al.* 2009 regarding the homology of this element). The angular is elongate and rod-like, extending ventrally across the intramandibular joint (Fig. 3.10e,f), though it does not bridge

this joint as extensively as the splenial does in typhlopoids (see Fig. 3.9e,f and §3.3.4.1). It is similar in overall shape and position to the typhlopoid angular (Fig. 3.9e,f), though is typically larger and longer, extending anteriorly to around the midpoint of the dentary in most anomalepidids (Fig. 3.10e,f; *Liotyphlops albirostris*, *L. argaleus*, *Typhlophis*, and, to a lesser extent, *Anomalepis mexicanus* and *Helminthophis*).

The coronoid is flat and boomerang-shaped, with a tall coronoid process as in typhlopoids (Figs 3.9e,f and 3.10e,f). Because the base of the anomalepidid coronoid (Fig. 3.10e,f) typically does not project anteriorly as in typhlopoids (Fig. 3.9e,f), this element does not bridge the intramandibular joint as extensively as in typhlopoids. However, *Anomalepis* is an exception to this, as the anteroposterior extent of the coronoid in this genus is similar to the typhlopoid condition. The anomalepidid coronoid articulates with the dentary and compound bone, but does not articulate to an appreciable extent with the angular (Fig. 3.10e,f).

The compound bone is elongate, measuring about 70–75% of the total skull length in most anomalepidids (Fig. 3.10e,f) and about 80% in *Typhlophis*, and as such is longer than in typhlopoids (Fig. 3.9e,f) and especially leptotyphlopids (Fig. 3.11e,f). The compound bone shows shallow sinusoidal curvature in anomalepidids (Fig. 3.10e,f), rather than the distinct downward curvature of the typhlopoid compound bone (Fig. 3.9e,f). The retroarticular process is typically extremely long, comprising approximately 35–40% of the total length of the compound bone (Fig. 3.10e,f), though it is slightly shorter in *Anomalepis mexicanus*. It extends posteriorly to—or just beyond, in the case of *A. aspinosus* and *Typhlophis*—the level of the occiput (Fig. 3.10). Near the anterior terminus of the compound bone, the prearticular and surangular laminae briefly separate medially and laterally, respectively, before re-fusing at the anterior terminus (Fig. 3.10f; Rieppel *et al.* 2009). Rieppel *et al.* (2009) also note this separation in anomalepidids, describing it as uniquely shared with leptotyphlopids among snakes; however, leptotyphlopids differ in that these laminae remain completely separate, rather than re-fusing anteriorly as occurs in anomalepidids (see Fig. 3.11e,f and §3.3.6.1).

Although functional studies of the anomalepidid mandible are lacking, the structure and articulations of the mandibular elements suggest that the intramandibular joint is relatively immobile, with the angular and coronoid both bridging this gap via their articulations with the dentary and compound bone (Fig. 3.10e,f). This condition is therefore more similar to the akinetic typhlopoid mandible (Fig. 3.9e,f; §3.3.4.1) than to the highly mobile intramandibular

joint of leptotyphlopids (Fig. 3.11e,f; §3.3.6.1). However, the integration between the anterior (dentary and splenial) and posterior (compound bone and angular) mandibular subunits is less extensive than in typhlopoids (Fig. 3.9e,f), suggesting a less rigid condition in anomalepidids (Fig. 3.10e,f).

3.3.5.2. Suspensorium

The quadrate is elongate and anteroventrally oriented so as to be nearly horizontal (Fig. 3.10), as is typical of scolecophidians (Figs 3.9–3.11). The quadrate is similar in length to typhlopoids (i.e., long axis equivalent to approximately 20–30% of the total skull length; Figs 3.9c and 3.10c) and shorter than in leptotyphlopids (in which the long axis of the quadrate is equivalent to approximately 40–45% of the total skull length; Fig. 3.11c). The anterior process of the quadrate typically occurs near the same location as in typhlopids and gerrhopilids (Figs 3.9c and 3.10c)—i.e., between the mandibular condyle and the midpoint of the quadrate shaft—but is similar to or smaller than the size in xenotyphlopids (see §3.3.4.2). The dorsal terminus of the quadrate is broadly forked in most anomalepidids—except *Anomalepis*—where it meets the supratemporal (Fig. 3.10a,c). The quadrate articulates dorsally with the fused prootic-otoccipital and the extremely reduced supratemporal in *Helminthophis*, *Liotyphlops*, and *Typhlophis* (Fig. 3.10a,c); in *Anomalepis*, it articulates only with the fused prootic-otoccipital as the supratemporal is absent (see also Haas 1968; Rieppel *et al.* 2009). The former taxa are unique among scolecophidians in retaining a supratemporal, albeit as a highly reduced splint of bone (see also Haas 1968; Rieppel *et al.* 2009). As is typical of snakes, the squamosal is absent.

The overall mandibular and suspensorial structure of anomalepidids is therefore somewhat similar to that of typhlopoids (e.g., elongate mandible, immobile intramandibular joint, and similar length of the quadrate), but with several key differences (e.g., intramandibular structure and articulation, compound bone structure, presence of the supratemporal, absence of the splenial, specific structure of the quadrate, and general presence of teeth on the dentary).

3.3.5.3. Palatomaxillary arch

The anomalepidid maxilla is similar to that of typhlopoids (Fig. 3.9a–d) in being toothed and highly mobile, bearing a pronounced facial process and transversely-to-anteromedially directed tooth row, and being angled posteroventrally at rest (Fig. 3.10a–d). However, the suspension of the maxilla is fundamentally different from typhlopoids: in anomalepidids, the maxilla articulates posteriorly with the ectopterygoid and anterodorsally with the highly reduced

prefrontal (Fig. 3.10a–d), rather than pivoting around the palatine as in typhlopoids (Fig. 3.9a–d). This configuration is unique to anomalepidids among squamates.

The pterygoid is elongate and edentulous (Fig. 3.10a–d), as is typical of scolecophidians (Figs 3.9–3.11). Unlike typhlopoids (Fig. 3.9), the anterior terminus of the pterygoid is not forked, instead tapering to a simple point as in leptotyphlopids (Fig. 3.11), ventromedial to the pterygoid process of the palatine (Fig. 3.10). The pterygoid does not articulate with the ventral surface of the skull (Fig. 3.10a–d), as in typhlopoids (Fig. 3.9a–d) and unlike leptotyphlopids (Fig. 3.11a–d; §3.3.6.3).

As in typhlopoids (Fig. 3.9b,d), the palatine is highly reduced, with the choanal process forming a spindly arch closely approaching the corresponding vomer (Fig. 3.10b,d). However, unlike typhlopoids, the maxillary process in anomalepidids is quite stubby, extending toward but still quite broadly distant from the maxilla (Fig. 3.10a–d; see also Rieppel *et al.* 2009). The palatine instead bears an elongate pterygoid process deflected posterolaterally toward the space between the pterygoid and ectopterygoid (Fig. 3.10b–d). The palatine is therefore not in distinct contact with any other element; this differs greatly from the typhlopoid condition, in which the palatine is an integral component of the palatomaxillary biomechanics (Fig. 3.9a–d; §3.3.4.3). A variation of this condition occurs in *Anomalepis*, in which the maxillary process is absent.

The ectopterygoid is present in anomalepidids (Fig. 3.10b–d), a condition unique among scolecophidians (as also noted by e.g., Rieppel *et al.* 2009; Chretien *et al.* 2019). The ectopterygoid articulates with the pterygoid posteriorly and braces the maxilla anteriorly (Fig. 3.10b–d). It has the same general shape as in most alethinophidians—i.e., comprising a forked maxillary process anteriorly and rod-like pterygoid process posteriorly (Fig. 3.10b–d)—but is markedly reduced compared to other squamates (Fig. 3.1).

The anomalepidid prefrontal is quite distinct from other squamates, including other scolecophidians. It is heavily reduced, forming a thin arch connecting the frontal posteriorly to the maxilla anteroventrally (Fig. 3.10a–c). Its posterior terminus is forked to articulate loosely with the frontal (Fig. 3.10a,b). The prefrontal is thus highly mobile, playing a key role in upper jaw mobility; this is notably distinct from the condition in other scolecophidians, in which the prefrontal is firmly integrated into the lateral snout and skull roof (Figs 3.9 and 3.11). The premaxilla is tightly integrated with the rest of the snout, but does not contact the palatomaxillary arches and therefore does not affect palatomaxillary mobility (Fig. 3.10a–c).

Altogether, the palatomaxillary arch is distinctly mobile, as in typhlopoids (Fig. 3.9a–d). However, the configuration and connectivity of the palatomaxillary arch is quite different than in typhlopoids, particularly regarding the presence of the ectopterygoid, the suspension of the maxilla, and the structure, role, and articulation of the prefrontal (Figs 3.9 and 3.10). Therefore, although both groups rely on upper jaw mobility and maxillary rotation, the unique palatomaxillary configuration of anomalepidids justifies the classification of this system as a biomechanically distinct version of microstomy.

3.3.6. Leptotyphlopidae

A thorough description of the leptotyphlopid mandible is provided by Kley (2006), who describes in detail many of the unique features noted in this section. Detailed analyses of the functional morphology of the leptotyphlopid jaws are provided by Kley & Brainerd (1999) and Kley (2001). Earlier studies such as Brock (1932) and List (1966) also describe leptotyphlopid skull anatomy (work summarized in Cundall & Irish 2008), with micro-CT imagery of various leptotyphlopids available in Rieppel *et al.* (2009), Pinto *et al.* (2015), and Martins *et al.* (2019).

3.3.6.1. Mandible

The leptotyphlopid mandible is short and robust, typically measuring approximately 45% of the total skull length (Fig. 3.11), although it measures approximately 35% in *Myriopholis tanae* and 40% in *M. macrorhyncha* and *Namibiana*. The dentary is large and robust relative to other scolecophidians (Fig. 3.11e,f), with the tooth row angled roughly transversely and the teeth sitting on an expanded dental concha (*sensu* Kley 2006). Each dentary also bears a prominent symphyseal process (*sensu* Kley 2006) anteromedially, extending toward the mental symphysis (Fig. 3.11e,f). As in other snakes, the interramal surface lacks symphyseal facets (see also Kley 2006). As in typhlopoids—but not anomalepidids, *contra* Rieppel *et al.* (2009)—the dentary does not bear a posteroventral process (Fig. 3.11e,f).

The splenial and angular are both quite reduced, but are similar in shape to those of other snakes, forming low, anteriorly- and posteriorly-tapering triangles, respectively (Fig. 3.11e,f). The angular and splenial abut against each other; the angular is slightly concave and the splenial slightly convex in the specimens observed herein (Fig. 3.11f), though Kley (2001, 2006) notes the splenial-angular articulation in *Leptotyphlops* (= *Rena*) as being strongly concavoconvex.

The coronoid is smaller than in typhlopoids and anomalepidids (Figs 3.9–3.11). Primarily, it is anteroposteriorly shorter, such that it closely approaches the dentary anteroventrally but only directly contacts the compound bone (Fig. 3.11e,f), thus lacking the more extensive articulation with other mandibular elements as present in other scolecophidians (Figs 3.9e,f and 3.10e,f). However, it is also much more robust and complex in structure than in other scolecophidians, bearing distinct coronoid, surangular (= posterodorsomedial), and prearticular (= posteroventromedial; present in *Rena*) processes (Fig. 3.11e,f; Kley 2006).

Similarly, the compound bone is greatly shortened relative to other scolecophidians, measuring only 20–25% of the total skull length in most leptotyphlopids and only approximately 15% in *Myriopholis tanae*, though it is quite robust and complex (Fig. 3.11e,f). The compound bone articulates posteriorly with the quadrate, dorsally with the coronoid, ventrolaterally with the angular, and anteriorly with the dentary via a loosely overlapping intramandibular hinge (Fig. 3.11e,f). The retroarticular process barely extends beyond the mandibular condyle (Fig. 3.11e,f). Uniquely among snakes, the prearticular and surangular laminae are separate anteriorly (Fig. 3.11f); this condition was noted by Rieppel *et al.* (2009) as being uniquely shared with anomalepidids among snakes, though see §3.3.5.1 for a comparison of these conditions. Kley (2006) also notes the leptotyphlopid compound bone as being unique among snakes in the presence of a supracotylar process and a horizontal shelf extending along the surangular lamina from this process toward the anterior surangular foramen (Fig. 3.11e,f).

Overall, the intramandibular joint is loosely articulated and quite flexible (Kley & Brainerd 1999; Kley 2001, 2006): the splenial abuts against the angular, the dentary and compound bone overlap loosely, and the coronoid approaches but does not directly contact the dentary anteriorly (Fig. 3.11e,f). In contrast, the mandibles of typhlopoids (Fig. 3.9e,f) and anomalepidids (Fig. 3.10e,f) show more extensive integration between the anterior and posterior mandibular elements. This looser articulation in leptotyphlopids is essential in enabling retraction and flexion of the mandible during feeding (Kley & Brainerd 1999; Kley 2001, 2006).

3.3.6.2. Suspensorium

The leptotyphlopid quadrate is oriented at the same anteroventral angle as other scolecophidians, but is comparatively much longer, with its long axis typically equivalent to about 40–45% of the total skull length (Fig. 3.11c), compared to 20–30% in typhlopoids (Fig. 3.9c) and anomalepidids (Fig. 3.10c). Dorsally, the quadrate typically bears a broad, paddle-like

cephalic condyle, which is confluent with the quadrate shaft and pierced by a large foramen (Fig. 3.11c; see also Palci *et al.* 2020a), although in some leptotyphlopids the cephalic condyle is somewhat simpler and not as expanded (e.g., *Myriopholis tanae*, *Namibiana*, *Rena*, *Tricheilostoma*). The supratemporal and squamosal are both absent, so the quadrate articulates directly with either the prootic and otoccipital in most taxa (Fig. 3.11b,c), or with the fused braincase elements in some taxa (e.g., *Tricheilostoma*).

Altogether, leptotyphlopids therefore exhibit an overall mandibular and suspensorial structure that is quite distinct from other scolecophidians (Figs 3.9 and 3.10), consisting of short, robust, and complex mandibular elements (especially the dentary and compound bone), bearing a flexible intramandibular joint, and being suspended from the skull via an extremely elongate quadrate (Fig. 3.11).

3.3.6.3. Palatomaxillary arch

Most distinctively, the palatomaxillary arch is completely edentulous in leptotyphlopids, a condition unique to leptotyphlopids among snakes (see also Kley 2001), if not all squamates. The maxilla is immobile, articulating broadly with the premaxilla, septomaxilla, and prefrontal and closely approaching the palatine (Fig. 3.11a–d), with contact occurring with the latter in some taxa (e.g., *Trilepida*). Extensive ligamentous connections between the maxilla and snout further impede movement of the maxilla, and thus the palatomaxillary arch (Kley 2001).

The pterygoid is elongate, rod-like, and edentulous (Fig. 3.11b–d), like other scolecophidians (Figs 3.9 and 3.10), but underlies the skull much more closely than in other scolecophidians. Uniquely among squamates, the frontal bears a shallow ventral facet posteriorly to accommodate the palatine and the anterior terminus of the pterygoid (Fig. 3.11b). This palatine process of the pterygoid lies alongside the pterygoid process of the palatine in a structurally quite simple articulation (Fig. 3.11b–d).

The palatine is rather robust relative to other scolecophidians (Figs 3.9 and 3.10; §3.3.4.3 and 3.3.5.3), though it is still quite reduced compared to other squamates (Figs 3.3–3.7). Similar to the pterygoid, the palatine is more integrated into the skull than in other scolecophidians (Figs 3.9 and 3.10), articulating extensively with the frontal dorsally—which bears a corresponding ventral facet—and vomer ventromedially, and very closely approaching the prefrontal, septomaxilla, and maxilla anteriorly (Fig. 3.11b,c). The choanal process is particularly well-developed, articulating broadly with the vomer and frontal (Fig. 3.11b–d).

The ectopterygoid is absent in all leptotyphlopids (see also Chretien *et al.* 2019). The prefrontal is broad and plate-like (Fig. 3.11a,c), superficially similar in structure to that of dibamids (Fig. 3.5a,c), though see §3.3.1.4 for a comparison to the dibamid condition. The prefrontal is closely integrated with several elements—including the nasal, septomaxilla, maxilla, frontal, and palatine (Fig. 3.11a–c)—although this integration is not as extensive and the prefrontal not as expanded as in typhlopoids (Fig. 3.10a–c). The premaxilla is tightly integrated with the rest of the snout (Fig. 3.11b,c). It briefly contacts the maxilla, but to a much lesser extent and in a different configuration than in non-snake lizards (Figs 3.3–3.6). Therefore, whereas the non-snake lizard premaxilla plays a direct role in bracing the palatomaxillary arches and preventing unilateral movement (see §3.3.1.3), this condition is quite different in leptotyphlopids.

Altogether, the palatomaxillary arches are essentially immobile in leptotyphlopids, with feeding being performed entirely by the mandibles (Kley & Brainerd 1999; Kley 2001, 2006). Decoupling of the upper and lower jaws is also evident from the extensive reduction of the ligamentous connection between the pterygoid and quadrate, as in typhlopoids (Kley 2001). However, in typhlopoids, the palatomaxillary arch is highly mobile and the mandible is relatively rigid (Fig. 3.9; §3.3.4), whereas the opposite is true of leptotyphlopids (Fig. 3.11).

3.3.7. Ancestral state reconstruction

The ‘basic’, ‘detailed microstomy’, and ‘detailed microstomy and macrostomy’ scoring methods each produced different ancestral state reconstructions, especially at key nodes representing the origins of major clades.

Under the ‘basic’ scoring method (Fig. 3.12), microstomy is the most parsimonious state for the origin of snakes and of alethinophidians; however, the evolution of macrostomy was reconstructed equivocally, with microstomy and macrostomy being equally parsimonious in the nodes separating booid-pythonoids and caenophidians (Fig. 3.12a). In contrast, under the ‘detailed microstomy’ scoring method (Fig. 3.13), all states are equally parsimonious for the origins of snakes and of alethinophidians, as well as the origins of Scolecophidia *sensu stricto* (i.e., Typhlopoidea and Leptotyphlopidae; *sensu* Miralles *et al.* 2018) and of all other snakes (i.e., Anomalepididae and Alethinophidia). As in the ‘basic’ scoring method, the reconstruction of macrostomy is equivocal (Fig. 3.13a). Finally, under the ‘detailed microstomy and macrostomy’ scoring method (Fig. 3.14), all versions of microstomy are again equally

parsimonious for the origin of snakes, the origin of Scolecophidia *sensu stricto*, and the origin of all other snakes. However, in contrast to previous scoring methods, the reconstruction of macrostomy is definitive: booid-type and caenophidian-type macrostomy are reconstructed as evolving independently, with 'snout-shifting' being most parsimonious for the intervening nodes (Fig. 3.14a).

A similar trend of increasing complexity and decreasing certainty occurs in the ML reconstructions (Figs 3.12b, 3.13b, and 3.14b). Under the 'basic' scoring method (Fig. 3.12), microstomy is definitively reconstructed at the origin of snakes (99.996%) and is also the most likely state for the origin of alethinophidians (77.459%), consistent with the MP reconstruction. Unlike the MP reconstruction, however, macrostomy is definitively reconstructed (90.059–90.121%) for the nodes connecting booid-pythonoids and caenophidians (Fig. 3.12b). Microstomy is thus reconstructed as having evolved independently in Uropeltoidea compared to Amerophidia (Fig. 3.12b). Under the 'detailed microstomy' scoring method (Fig. 3.13), reconstructions at the origin of snakes, of Scolecophidia *sensu stricto*, and of the ancestor of Anomalepididae and Alethinophidia become equivocal (Fig. 3.13b), as in the MP reconstruction (Fig. 3.13a). In contrast to the MP analysis, though, macrostomy is reconstructed as by far the most likely ancestral alethinophidian state (88.466%; Fig. 3.13b), again reflecting an independent evolution of microstomy (specifically, 'snout-shifting') in Uropeltoidea and Amerophidia as in the 'basic' ML scoring method (Fig. 3.12b). Finally, under the 'detailed microstomy and macrostomy' scoring method (Fig. 3.14), the ancestral nodes for snakes, for Scolecophidia *sensu stricto*, and for all other snakes (Anomalepididae + Alethinophidia) are again equivocal (Fig. 3.14b). 'Snout-shifting' is reconstructed as the most likely ancestral state for alethinophidians (58.225%) and at the nodes connecting booid-pythonoids and caenophidians (just over 57% at both nodes). Thus, as in the MP reconstruction for this scoring method (Fig. 3.14a), booid- and caenophidian-type macrostomy are reconstructed as evolving independently from an ancestral 'snout-shifting' condition (Fig. 3.14b).

3.4. Discussion

3.4.1. Homology

As the ensuing discussion centres around homology, a complex topic accompanied by a vast literature, it is important to first define my approach to homology and homology assessment.

Homology can be divided into two sequential concepts: primary homology followed by secondary homology (de Pinna 1991; Brower & Schawaroch 1996; Hawkins *et al.* 1997). Primary homology is essentially a conjecture of homology, in which an anatomical or molecular feature in a taxon is proposed—based on various criteria but prior to any test of phylogenetic congruence—to be homologous to a similar feature in different taxa (de Pinna 1991; Brower & Schawaroch 1996; Rieppel & Kearney 2002; Simões *et al.* 2017). Principal among these criteria is 'topological equivalence', i.e., articulations with the same surrounding elements, which allow morphological structures in different taxa to be recognized as evolutionarily equivalent (Rieppel & Kearney 2002; Simões *et al.* 2017). Ancillary to topological correspondence are the criteria of 'special similarity or quality' of structures and 'intermediate forms' (Rieppel & Kearney 2002). The former refers to specific anatomical similarities among the structures in question, whereas the latter encapsulates ontogeny, fossils, and morphoclines as evidence for 'intermediacy' and thus anatomical correspondence of a structure across taxa (Rieppel & Kearney 2002). These criteria together constitute the 'test of similarity' by which a hypothesis of primary homology is either refuted or supported (Patterson 1982; Rieppel & Kearney 2002).

Secondary homology is the corroboration of this hypothesis via recovery of the feature in question as synapomorphic across the relevant taxa (Patterson 1982; de Pinna 1991; Rieppel 1994; Rieppel & Kearney 2002). Just as the 'test of similarity' forms the basis for primary homology, this 'test of congruence' constitutes the test of secondary homology, and it is only by passing these tests of similarity and congruence that features can be considered homologous or synapomorphic (Patterson 1982; de Pinna 1991; Rieppel 1994; Rieppel & Kearney 2002). Because a feature must pass this test of secondary homology to be homologous, and because it can only reach this stage by first being accepted as a primary homolog, it is therefore clear that a hypothesis of primary homology is the most fundamental step in the recognition of homology among taxa and their traits (de Pinna 1991; Rieppel & Kearney 2002; Simões *et al.* 2017).

Beyond the 'test of congruence', a final test of homology in extant taxa can also be performed in the form of genetic and/or developmental confirmation, i.e., determining whether secondary homologs are consistent at an underlying genetic or developmental level. However, this, too, requires primary homology to even be considered, and then requires substantial resources, not least of which are financial. Furthermore, ontogeny has been debated as a sufficient indicator of homology (e.g., Rieppel 1988, 1994; Simões *et al.* 2017; Mabee *et al.*

2020), and this approach would also require far greater knowledge of the connection between genotype and phenotype than generally currently exists. Thus, for now, such assessment of 'absolute' homology is of tertiary relevance from the perspective of researchers interested in trait evolution; assessments of primary and secondary homology remain paramount.

However, an important distinction must be drawn between the homology of characters and the homology of character states. Although Patterson (1982, 1988) considered characters and character states to both be 'characters', just at more or less inclusive levels, I agree with several other authors (e.g., Brower & Schawaroch 1996; Hawkins *et al.* 1997; Sereno 2007; Simões *et al.* 2017) that this distinction is not trivial. Characters and character states are indeed similar in that they are both a type of homolog, but differ in that characters are comparable categories which must first be established and tested before character states can be assessed (Brower & Schawaroch 1996; Hawkins *et al.* 1997). For example, a modern bird and an extinct non-avian theropod may both bear feathers on the forelimb. However, before attempting to create states reflecting the conditions of these feathers, we must first determine whether the feathers themselves are homologous across these taxa. Only once we have established the homology of these feathers—i.e., the existence of the 'feather' as a character—can we parse this anatomical structure into meaningful states. In other words, character states are conditioned on the fundamental existence of the character itself, in this example the feather. Thus, just as primary and secondary homology are inherently sequential subdivisions of homology as a whole, character and character state homology are inherently sequential subdivisions of primary homology.

Brower & Schawaroch (1996) addressed this distinction by considering primary homology at two levels: 'topographical identity' (i.e., primary homology of characters) and 'character state identity' (i.e., primary homology of character states). Essentially, topographical identity concerns the homology of structures, whereas character state identity concerns the homology of conditions of those structures. Sereno (2007) presented a similar argument for distinguishing between characters as independent variables and character states as mutually exclusive conditions of that character, though specifically eschewed the subject of homology in his treatment of this logical distinction. Unfortunately, despite the significant attention directed toward the identification and testing of topographical identity or character homology (Patterson 1982, 1988; Rieppel 1994), the concept of character state identity or homology has been

comparatively neglected (Brower & Schawaroch 1996; Hawkins *et al.* 1997). Yet, it is this latter concept which is central to answering the questions at the core of this study, as it is character states which ultimately reflect synapomorphies.

Most importantly, the question of how to test proposed character state homologs has not been explicitly addressed. Previous discussions of the 'test of similarity' have focussed on primary homology at the level of topographical identity, with this test's major criterion—topological correspondence—being particularly well-suited for testing the homology of characters (e.g., whether two bones are homologous). However, as an organism's anatomy becomes more and more atomized—i.e., considered at finer and finer levels of constituent elements, as is necessary to identify homology (Rieppel 1994; Wilkinson 1995)—this criterion eventually becomes inadequate. Consider, for example, the squamate quadrate. The observation that this element consistently connects the mandible ventrally with the skull dorsally allows this element to be considered a primary character homolog across squamates. When considering how to test the homology of its character states (e.g., quadrate orientation), though, this criterion is not useful, as the proposed states often differ in some manner unrelated to topology. Indeed, apart from character states dealing with presence/absence of an element or structure or dealing specifically with how a structure articulates with surrounding components, the criterion of topology is often entirely uninformative. How, then, can character state homology be effectively tested?

Given the uninformative nature of the criterion of connectivity, the subsidiary criteria of 'special similarity or quality' and 'intermediate forms' must be employed (Rieppel & Kearney 2002). Herein lies another important difference between the primary homology of characters and character states: for characters, anatomical topology is the main arbiter of primary homology, with the specific shape and function of structures being largely disregarded (Rieppel 1994; Rieppel & Kearney 2002; Zaher & Rieppel 2002); in contrast, testing the primary homology of character states requires the consideration almost exclusively of 'special quality' of the shape and size of the character in question, with topological relations serving only to identify the structure in question. This approach is often employed operationally, such as Simões *et al.*'s (2017) proposal that states for continuous characters should only be delimited when there are breaks in the distribution of that character, i.e., distinct subdivisions of size and shape that justify consideration of these subdivisions as distinct conditions. Admittedly, 'special similarity' may

seem rather nebulous compared to the more concrete process of testing character homology by assessing topological relations and connectivity. However, by comparing characters using a combination of shape, size, and function, and by employing operational criteria such as that described above, it is possible to establish and test hypotheses of character state homology in a manner that is replicable and logically consistent, as exemplified below and as is necessary to establish a 'meaningful' character statement (Rieppel & Kearney 2002; Simões *et al.* 2017).

Assessing the homology or identity of character states is in turn necessary to assess the homology of overall character complexes, such as microstomy. This concept of 'character complex homology' differs from, and is essentially an expansion upon, the concept of secondary homology. Whereas secondary homology focusses on identifying a single character and its states as synapomorphic, the identification of an integrated set of characters as 'homologous' is an inherently more holistic process, requiring the simultaneous consideration of several characters so as to compare entire morphofunctional systems across taxa. Although such an undertaking may seem quite subjective, this is exactly the implication of hypotheses such as whether scolecophidians retain and share an ancestral 'microstomatan' feeding mechanism (e.g., Bellairs & Underwood 1951; Miralles *et al.* 2018). Such hypotheses of entire morphofunctional systems as homologous are common, yet typically not explicitly assessed or justified. Thus, through this discussion of squamate feeding mechanisms, I aim to explain and enact a more transparent, replicable, and theoretically consistent approach to this broader conceptualization of homology. This more explicit approach is essential in rendering subsequent hypotheses of character evolution replicable, testable, and falsifiable (Rieppel & Kearney 2002), as well as in avoiding the pitfalls of either under- or over-atomizing complex anatomies (e.g., as discussed by Wilkinson 1995 for 'composite' *versus* 'reductive' character construction).

Despite the differences between the homology of individual characters and of overall character complexes, the fundamental question underlying the search for homology remains the same: did these structures (or complexes) evolve once, thus uniting these taxa as a monophyletic group bearing a synapomorphic condition, or did these structures (or complexes) evolve independently? Of course, for character complexes there is no single 'test of congruence' which can instantly characterize the entire complex as synapomorphic. Rather, a different benchmark for considering such conditions as 'homologous' or 'synapomorphic' is necessary.

Most critically, such an approach must be able to recognize shared common ancestry while also allowing for variation among taxa. To this end, I propose a guideline based on Patterson's (1982:35) definition of a morphotype as "a list of the homologies (synapomorphies) of a group". I herein use the term 'morphotype' to refer to homologous character complexes, defined by the possession of key synapomorphies (i.e., secondarily homologous character states). Similar to a taxonomic diagnosis, a character complex can be considered homologous among taxa—i.e., considered to belong to the same morphotype—if it possesses the key synapomorphies of that morphotype and does not possess the features 'diagnosing' other morphotypes. Character complexes can only be considered homologous if their constituent characters and character states pass the tests of primary and secondary homology, as well as the guideline described above; as such, this approach to morphotype homology allows such a hypothesis to be tested and falsified. This rigorous assessment is essential for proper identification of homology (Rieppel & Kearney 2002), which is in turn critical for higher-level evolutionary analyses, such as ancestral state reconstructions (see below) or recent computational advances related to homology (e.g., Mabee *et al.* 2020 and the Phenoscape project).

3.4.2. Is the jaw complex homologous among scolecophidians?

An intriguing hypothesis proposed in recent works suggests that the jaw structures in anomalepidids, leptotyphlopids, and typhlopoids may have evolved independently (Harrington & Reeder 2017; Caldwell 2019; Chretien *et al.* 2019). This is of course in distinct contrast to characterizations of the scolecophidian condition as more-or-less homogenous and as reflecting the ancestral snake condition (e.g., Miralles *et al.* 2018). Even in previous acknowledgments of the autapomorphic nature of the scolecophidian skull (e.g., Rieppel 1988; Kley & Brainerd 1999; Hsiang *et al.* 2015), the uniqueness of this morphology is typically emphasized for scolecophidians as a whole in comparison to other squamates, rather than scolecophidians in comparison to each other (though see Bellairs & Underwood 1951; Haas 1964; List 1966; Haas 1968; Kley 2001; Cundall & Irish 2008 for preliminary discussions of this hypothesis).

The results of this study provide strong support for the independent evolution of microstomy in each major scolecophidian clade. I propose that each clade exhibits a unique morphotype of microstomy (Fig. 3.1)—'single-axle maxillary raking' in typhlopoids, 'axle-brace maxillary raking' in anomalepidids, and 'mandibular raking' (*sensu* Kley & Brainerd 1999) in leptotyphlopids—each of which is distinguished by several features that are universal within and

entirely unique to each morphotype (Tables 3.2 and 3.3; see also Kley 2001; Caldwell 2019; Chretien *et al.* 2019).

In the 'single-axle maxillary raking' morphotype (Fig. 3.9; Tables 3.2 and 3.3), prey ingestion and transport occurs exclusively via asynchronous unilateral movements of the maxillae, which rotate about the elongate maxillary process of the palatine (Kley 2001; Chretien *et al.* 2019). The palatines and pterygoids are highly reduced; these elements contribute to rotation of the maxillae, but only the maxillae bear teeth and thus only the maxillae are directly responsible for prey transport (Fig. 3.9a–d; Kley 2001; Caldwell 2019; Chretien *et al.* 2019). The mandibles are highly reduced and rigidly integrated, so as to also not contribute to prey transport (Fig. 3.9e–f; Kley 2001; Caldwell 2019).

In the 'axle-brace maxillary raking' morphotype (Fig. 3.10; Tables 3.2 and 3.3), the maxilla is suspended from the reduced and mobile prefrontal and braced posteriorly by the ectopterygoid (Chretien *et al.* 2019). The pterygoids and palatines are highly reduced, similar to 'single-axle maxillary raking', and the mandibles are reduced and immobile, though to a lesser extent than in the 'single-axle' morphotype (Figs 3.9 and 3.10). The highly reduced teeth on the mandible at most help to hold the prey in the mouth during maxillary raking.

In the 'mandibular raking' morphotype (Fig. 3.11; Tables 3.2 and 3.3), the palatomaxillary arch is immobile and edentulous, thus not contributing at all to prey transport (Kley & Brainerd 1999; Kley 2001, 2006; Chretien *et al.* 2019). Rather, it is the highly mobile mandible—including a flexible intramandibular joint—that drives feeding, bearing a quite robust and complex structure in comparison to the conditions in 'single-axle' and 'axle-brace' microstomy (Figs 3.1 and 3.9–3.11; List 1966; Kley & Brainerd 1999; Kley 2001, 2006; Caldwell 2019; Chretien *et al.* 2019). The mandibles move in a bilaterally synchronous manner, being joined at the symphysis via a cartilaginous nodule (Kley 2006) which enables rotation between the left and right mandibles, but prevents lateral and anteroposterior separation of the mandibular tips (Kley 2001, 2006).

These morphotypes are distinct and non-homologous because they each comprise key features that are not homologous with the corresponding conditions in other taxa (Figs 3.9–3.11; Tables 3.2 and 3.3). Consider, for example, the maxillary process of the palatine as a character, and its degree of elongation as the character states in question. At the level of topographical identity, the maxillary process passes the 'test of similarity' among squamates, as it occurs in a

consistent topographic location and so can be considered a primary homolog. However, when considering its character states, the elongate condition of the maxillary process is consistent among typhlopoids (Fig. 3.9), but is both anatomically and functionally unique compared to the condition of this process in any other squamate (Figs 3.3–3.8, 3.10, and 3.11). Thus, this character state passes the 'test of similarity' among typhlopoids but fails this test in comparison to other squamates, and so cannot be considered synapomorphic between typhlopoids and other squamates.

This same process of rejecting homology at the level of character state identity also applies to other key typhlopoid features, such as the medially excavated maxilla, the downcurved compound bone, and the enlarged splenial, among many other features (Fig. 3.9; Tables 3.2 and 3.3; §3.3.4). These unique primary homologs, alongside a unique combination of other distinct features, ultimately result in a feeding mechanism that is fundamentally different from the condition in any other squamate, including other scolecophidians; this mechanism therefore represents a morphotype functionally and evolutionarily unique to typhlopoids: 'single-axle maxillary raking'.

This process can also be applied to the key features of anomalepidids (Fig. 3.10; Tables 3.2 and 3.3; §3.3.5), such as the structure of the prefrontal and ectopterygoid, and those of leptotyphlopids (Fig. 3.11; Tables 3.2 and 3.3; §3.3.6), such as the edentulous maxilla, fixed palatine and pterygoid, uniquely structured dentary, and extremely elongate quadrate. Again, because the character states in question are anatomically consistent within each clade but distinct from the condition in any other taxon, each state passes the 'test of similarity' within each clade but fails across clades. Thus, 'axle-brace maxillary raking' and 'mandibular raking' each comprise their own set of unique character states that cannot be synapomorphic with any other squamate, just as in 'single-axle maxillary raking', and so are also distinct morphotypes not representative of an ancestral snake condition (see also Kley & Brainerd 1999; Kley 2001, 2006).

Of course, there are certain features of the jaws and suspensorium that are consistent across scolecophidians, such as the anteriorly oriented quadrate, absent or heavily reduced supratemporal and ectopterygoid, tall coronoid, and, at least in typhlopoids and leptotyphlopids, the cartilaginous interramal nodule (Figs 3.9–3.11; Kley 2001, 2006; Rieppel *et al.* 2009). The presence of these shared conditions would appear to undermine a hypothesis of the independent evolution of microstomy: each of these conditions passes the 'test of similarity' across

scolecophidians and, according to morphology-based phylogenies in which scolecophidians are monophyletic (e.g., Gauthier *et al.* 2012; Hsiang *et al.* 2015; Garberoglio *et al.* 2019a), also passes the 'test of congruence'. Thus, based on these criteria, these character states can be accepted as synapomorphic for scolecophidians.

However, an important counterpoint to this 'undermining' is the extensive paedomorphosis exhibited by scolecophidians relative to other squamates (Kley 2006; Palci *et al.* 2016; Da Silva *et al.* 2018; Caldwell 2019; Strong *et al.* 2021a). Paedomorphosis is the retention of features typical of embryonic or juvenile individuals of an ancestral taxon into adults of a descendant taxon (Gould 1977; McNamara 1986). In scolecophidians, as noted by other authors (e.g., Kley 2006; Caldwell 2019; Strong *et al.* 2021a), this paedomorphosis occurs throughout the skull, but is particularly prevalent in the mandible, palatomaxillary arch, and suspensorium.

This includes the anteroventral orientation of the quadrate (Figs 3.9–3.11), a condition typical of embryonic squamates (Kamal 1966; Rieppel & Zaher 2000; Kley 2006; Scanferla 2016; Caldwell 2019). The cartilaginous interramal nodule is likely also paedomorphic: although Kley (2006) interpreted this feature as a fibrocartilaginous elaboration of the midline raphe in *Leptotyphlops* (= *Rena*), he also noted that the midline raphe is universally absent in other scolecophidians, causing this identification to seem unlikely. I instead agree with other interpretations of this nodule as an extension of the Meckelian cartilages anterior to the dentary tips (e.g., Bellairs & Kamal 1981; Kley 2001; Caldwell 2019), a phenomenon that is known to occur throughout the embryonic development of the mandible in snakes (e.g., Al-Mohammadi *et al.* 2020) and that therefore renders the scolecophidian interramal nodule paedomorphic. Features related to the reduction and simplification of elements (e.g., pterygoid, palatine, supratemporal; Figs 3.9–3.11) are also tied to paedomorphosis, with the reduction or absence of these structures reflecting early developmental stages in other squamates (e.g., see Polachowski & Werneburg 2013; Werneburg *et al.* 2015; Ollonen *et al.* 2018). Finally, a disproportionately tall coronoid (Figs 3.9e,f, 3.10e,f, and 3.11e,f) aids in increasing mechanical advantage of the lower jaw musculature (Rieppel 1984a, b, 1996), an adaptation important in compensating for the re-organization of the lower jaw that occurs in miniaturized and paedomorphic vertebrates (Hanken & Wake 1993; Olori & Bell 2012).

Given that scolecophidians are highly miniaturized, that miniaturization often co-occurs with fossoriality (Olori & Bell 2012), and that miniaturization has been hypothesized as being

caused by—or at least strongly correlated with—paedomorphosis (Gould 1977; Hanken 1984; Wake 1986; Fröbisch & Schoch 2009), these shared features thus all relate to miniaturization. Importantly, miniaturization, fossoriality, and paedomorphosis are all strongly associated with homoplasy (Hanken & Wake 1993; Wiens *et al.* 2005; Fröbisch & Schoch 2009; Maddin *et al.* 2011; Olori & Bell 2012). In other words, the only major features of the scolecophidian jaw complexes which fully pass the test of primary homology—and which potentially unite scolecophidians to the exclusion of other snakes—are highly homoplastic. It is therefore quite possible that the aforementioned conditions apparently shared among scolecophidians in fact arose independently, as the result of the independent evolution of fossoriality and miniaturization in each scolecophidian clade (see also Caldwell 2019; Chretien *et al.* 2019).

Indeed, such a hypothesis is consistent with the separate morphotypes of 'microstomy' present in scolecophidians. This proposed scenario of independent excursions into fossoriality and miniaturization presents a logical explanation for why the jaws and suspensorium reflect so many entirely unique and non-homologous conditions across the scolecophidian clades (see also Caldwell 2019; Chretien *et al.* 2019). This degree of variation is consistent with the morphological novelty typical of miniaturized vertebrates (Hanken 1984; Hanken & Wake 1993). Occurring simultaneously along these independent paths of miniaturization and fossoriality, I in turn propose that other elements—such as the supratemporal, pterygoid, and quadrate—converged upon conditions that are known to have frequently evolved independently throughout Squamata (e.g., dibamids: see Fig. 3.5 and Rieppel 1984b; amphisbaenians: see Fig. 3.6 and Gans & Montero 2008; uropeltids: see Olori & Bell 2012; colubroids: see Strong *et al.* 2021a).

Although such a hypothesis clearly contradicts the morphology-based phylogenetic placement of scolecophidians as a single clade (e.g., Gauthier *et al.* 2012; Hsiang *et al.* 2015; Garberoglio *et al.* 2019a), it is important to recognize the potential role of homoplasy in biasing phylogenies, especially as associated with paedomorphosis and/or fossoriality (Hanken & Wake 1993; Wiens *et al.* 2005; Struck 2007; Pinto *et al.* 2015). As examined previously for paedomorphic salamanders, morphology-based phylogenies can be misled by the shared presence of paedomorphic traits, causing the affected taxa to be artificially grouped together (Wiens *et al.* 2005). The distinct incongruence between molecular and morphological phylogenies of scolecophidians (e.g., Gauthier *et al.* 2012; Hsiang *et al.* 2015; *versus* Figueroa *et*

al. 2016; Zheng & Wiens 2016) further supports the possibility that confounding factors may be at play. It is thus clear that, in order to resolve longstanding questions regarding scolecophidian phylogeny and further assess the evolutionary hypotheses presented herein, a robust morphological and molecular framework for scolecophidians is crucial. Although such an undertaking is beyond the scope of this study, morphological analyses similar to the present study represent a key component in laying the foundation for such a framework.

Ultimately, we can definitively reject the contention that scolecophidians are "morphologically and ecologically consistent" (Miralles *et al.* 2018:1785). From a biomechanical perspective, the jaws of each scolecophidian clade function in a completely different manner, as outlined in the Results. This lack of consistency also occurs from an evolutionary perspective, on the basis of primary homology, as argued above. Beyond superficially similar reduction of the jaw complex in each scolecophidian clade, almost every element of the upper and lower jaws shows fundamental anatomical and functional differences (Figs 3.9–3.11; Tables 3.2 and 3.3), and those elements that do remain consistent (e.g., pterygoid, suspensorium) are highly susceptible to homoplasy.

Importantly, because microstomy occurs via a distinct, non-homologous, and thus independently evolving morphotype in each scolecophidian clade, we can therefore logically reject the hypothesis that scolecophidians as a whole represent a morphologically homogenous remnant of the ancestral snake condition, as per Caldwell (2019), Chretien *et al.* (2019), and Strong *et al.* (2021a), and *contra*, for example, Rieppel (2012) and Miralles *et al.* (2018). Indeed, scolecophidians are so strongly influenced by the constraints of ecology and heterochrony (see also §3.4.4)—and thus so highly modified relative to other squamates and to each other—that for this group to have given rise to the morphology of all other snakes is in my view highly unlikely (see also Caldwell 2019; Chretien *et al.* 2019; Strong *et al.* 2021a). Rather than a plesiomorphic condition, the various scolecophidian lineages instead reflect convergence upon a miniaturized, fossorial, and myrmecophagous ecomorph, superficially similar to each other but in reality highly autapomorphic (Harrington & Reeder 2017; Caldwell 2019; Chretien *et al.* 2019). The combination of strongly homoplastic and strikingly divergent features across scolecophidians highlights the complicated interplay between determinism and contingency in organismal evolution, especially in the context of phenomena such as fossoriality, myrmecophagy, miniaturization, and paedomorphosis.

3.4.3. Is the scolecophidian jaw complex homologous to the condition in non-snake lizards?

The hypothesis that scolecophidians are retaining the same version of microstomy as in non-snake lizards—i.e., that these conditions are homologous—is an implicit though inherent assumption of how these taxa are scored in ancestral state reconstructions of this feature (e.g., Harrington & Reeder 2017; Miralles *et al.* 2018). This assumption of homology is more broadly reflected in the traditional division of squamates into 'Macrostomata' and non-macrostomatans (reviewed in Rieppel 1988), with the corresponding assumption that, because scolecophidians, early-diverging alethinophidians, and non-snake lizards all lack macrostomy, this lack of macrostomy—as characterized in this simplistic manner (on the complexities of macrostomy, see Palci *et al.* 2016; Caldwell 2019)—is a fundamentally plesiomorphic retention from non-snake lizards (e.g., Bellairs & Underwood 1951; Rieppel 2012). However, I argue that these groups exhibit distinct morphotypes of microstomy (Tables 3.2 and 3.3), rendering the evolution of this feeding mechanism much more complex than the aforementioned perspective.

From one line of reasoning, if we accept the hypothesis that microstomy is not homologous across scolecophidians and instead evolved independently in each clade (as argued above), then logically we must reject the hypothesis that 'microstomy' as present in scolecophidians is 'primitive' or homologous to that of non-snake lizards. Recent discussions arguing that the scolecophidian skull could quite reasonably be derived from an alethinophidian or even 'macrostomatan' ancestor (Vidal & Hedges 2002; Kley 2006; Scanferla 2016; Harrington & Reeder 2017; Caldwell 2019; Strong *et al.* 2021a) further indicate that the presence of a scolecophidian morphotype—including the presence of microstomy—does not in and of itself indicate a 'microstomatan' ancestral condition of snakes. Even if we accept the proposition from several authors—problematic as these hypotheses may be (Kley 2006; Caldwell 2019)—that scolecophidians retain certain plesiomorphic features of non-snake lizards (e.g., multipennate jaw adductor musculature, tall coronoid; Kley 2006; Rieppel 2012), the presence of many non-homologous features indicates that microstomy cannot be considered a homogenous or consistent condition across these taxa.

A particularly important feature is the mandibular symphysis, which in non-snake lizards bears distinct symphyseal facets but which in snakes—including scolecophidians—is smooth and more widely separated (see also Kley 2006). As discussed by Kley (2006), this observation suggests that scolecophidians in fact evolved from a more 'snake-like' ancestor, in which the

mandibles were already capable of independent movement and possibly macrostomy. This of course contradicts the hypothesis of scolecophidians retaining a non-snake lizard-like version of this component of 'microstomy'. Similarly, although the tightly-linked interramal symphysis in scolecophidians may superficially evoke the condition in non-snake lizards, the robust cartilaginous nodule in scolecophidians is entirely different from other squamates (Kley 2006) and, as noted above, is most likely a distinctly paedomorphic—not plesiomorphic—condition. Finally, Kley (2006) also notes the *M. retractor pterygoidei* and *M. protractor pterygoidei* in leptotyphlopids as suggesting derivation from an ancestral condition in which the palatomaxillary arch was quite mobile. This in turn implicates a possibly 'macrostomatan' ancestral condition and contradicts Rieppel's (2012) conclusion that the scolecophidian jaw adductor musculature reflects a plesiomorphic non-snake lizard anatomy (see also Caldwell 2019).

Several other key conditions of the jaws and suspensorium are also not homologous among scolecophidians, 'anilioids', and non-snake lizards. The maxillary process of the palatine was discussed above in the context of 'single-axle maxillary raking', though it is also important when considering 'anilioids' and non-snake lizards (Tables 3.2 and 3.3). In non-snake lizards, this process is quite broad, articulating extensively with the maxilla (Figs 3.3b,d, 3.4b,d, 3.5b,d, and 3.6b,d); in uropeltoids and amerophidians, however, this process is reduced and the maxilla-palatine articulation is instead a 'ball-and-socket'-like joint formed mainly by the palatine process of the maxilla (Figs 3.7b,d and 3.8b,d). Thus, although the maxillary process of the palatine passes the 'test of similarity' at the level of topographical identity (i.e., primary character homology), it fails at the level of character state identity, as it exhibits anatomically and functionally distinct forms across these taxa. The condition of this character in uropeltoids and amerophidians is further notable in that, although these lineages are not closely related (Figs 3.1 and 3.2), they exhibit primary homology or character state identity of the 'ball-and-socket'-like joint. This is a key innovation of the feeding mechanism in these taxa, distinct from any other 'microstomatan' squamate. The shared presence of this feature in these distinct lineages suggests it to better reflect the ancestral snake condition than any state exhibited by scolecophidians for this character.

The vomerine process of the palatine also differs among these taxa (Table 3.3), with non-snake lizards bearing a broad vomerine process in extensive osseous contact with the vomer

(Figs 3.3b,d, 3.4b,d, 3.5b,d, and 3.6b,d), uropeltoids and amerophidians bearing a broad choanal process lacking this sutural contact (Figs 3.7b,d and 3.8b,d), and scolecophidians bearing a highly reduced and likely paedomorphic choanal process (Figs 3.9b,d, 3.10b,d, and 3.11b,d). Other characters with states that differ across non-snake lizards, 'anilioids', and scolecophidians include: the basipterygoid processes and their size and extent of articulation with the pterygoids; the presence and extent of the premaxilla-maxilla articulation; the integration and extent of mobility between the ventral and dorsal snout elements; and the suspension of the quadrate (Figs 3.1 and 3.3–3.11; Tables 3.2 and 3.3).

All of these characters exhibit character states which differ distinctly and consistently among the taxa in question (Tables 3.2 and 3.3; as described in the Results), which bear distinct functional consequences, and which altogether reflect a lack of primary and thus secondary homology across these taxa. As a result, because so many of these key features are non-homologous, the overall jaw complex cannot be considered consistent across these taxa. Rather, non-snake lizards, 'anilioids', and the scolecophidian clades each exhibit distinct morphotypes of microstomy, characterized by their own unique sets of character states (Figs 3.1 and 3.3–3.11; Tables 3.2 and 3.3).

The morphotype exhibited by non-snake lizards (Figs 3.3–3.6; Tables 3.2 and 3.3) is characterized by robust and tightly integrated jaw elements compared to the condition in snakes, particularly at the intramandibular joint and mandibular symphysis. I herein term this morphotype 'minimal-kinesis microstomy', in recognition of the numerous robustness-related character states of this morphotype, as well as previous discussions of the minimally kinetic nature of the non-snake lizard skull relative to that of snakes (e.g., Cundall 1995).

The uropeltoid and amerophidian morphotype (Figs 3.7 and 3.8; Tables 3.2 and 3.3) is similar to non-snake lizards in terms of general robustness, though it differs in certain key aspects (see also Cundall 1995). These aspects include greater kinesis of the intramandibular joint and, perhaps most importantly, the capacity for unilateral movement of the palatomaxillary arches (§3.3.2; Cundall 1995). Because decoupling of the snout elements is integral to the jaw biomechanics of *Cylindrophis* (see §3.3.2.3; analyzed in greater detail by Cundall 1995), and has further been proposed to occur throughout Uropeltoidea and Amerophidia (Cundall 1995), I retain Cundall's (1995) use of the term 'snout-shifting' to describe this biomechanical morphotype (Tables 3.2 and 3.3).

Despite its capacity for unilateral palatomaxillary movement, though, the 'snout-shifting' jaw complex is still more closely integrated than the condition in 'macrostomatan' snakes, indicating a much more limited degree of kinesis in uropeltoids and amerophidians relative to these more derived alethinophidians (Cundall 1995). The 'snout-shifting' morphotype is therefore intermediate between the 'minimally-kinetic microstomatan' and 'macrostomatan' conditions in terms of both anatomy and function (Cundall & Rossman 1993; Cundall 1995; Kley 2001). Due to this intermediacy, it is tempting to hypothesize the 'anilioid' skull as representing the ancestral snake condition. Indeed, the presence of a highly consistent jaw morphotype in uropeltoids and amerophidians—two basally-diverging but phylogenetically distinct alethinophidian lineages (Figs 3.1 and 3.2)—provides compelling evidence for this morphotype as ancestral for alethinophidians, if not all snakes.

However, attempts to reconstruct the ancestral condition for snakes should not rest solely on extant taxa (see also Caldwell 2019). Given that millions of years have elapsed since the origin of snakes (e.g., 166.76 Ma; Garberoglio *et al.* 2019a), a more logical approach would be to give precedence to the fossil record, using morphological information from taxa temporally—and thus likely morphologically—much closer to the origins event in question (Gauthier *et al.* 1988a; Caldwell 2019; Mongiardino Koch & Parry 2020). This is especially true as extinct taxa can provide character state information not present in modern taxa, thus providing a necessary supplement to the neontological record (Finarelli & Flynn 2006; Finarelli & Goswami 2013; Betancur-R *et al.* 2015; Hsiang *et al.* 2015; Puttick 2016; Caldwell 2019; Mongiardino Koch & Parry 2020).

This is not to say that extant taxa are altogether uninformative in hypothesizing the ancestral snake morphology. Indeed, recently discovered and exceptionally preserved specimens of the extinct *Najash* (Garberoglio *et al.* 2019a; Garberoglio *et al.* 2019b) reveal a morphology similar to 'anilioids', suggesting uropeltoids and amerophidians to be the extant taxa most representative of this ancestral condition (Caldwell 2019; Garberoglio *et al.* 2019b). However, an important logical distinction must be emphasized: uropeltoids and amerophidians are not representative of this ancestral morphology because they are the most 'lizard-like' groups of snakes; rather, they are representative of this ancestral condition because they are the extant groups most morphologically similar to early-evolving fossil snakes (Garberoglio *et al.* 2019b). The primacy of the fossil record in hypothesizing ancestral conditions is paramount (Caldwell

2019), as reflected by the key role of fossils in fuelling phylogenetic debates regarding the origin of snakes (e.g., Lee & Caldwell 1998; Zaher 1998; Zaher & Rieppel 1999a; Caldwell 2000; Zaher & Rieppel 2002; Apesteguía & Zaher 2006; Caldwell 2007a; Harrington & Reeder 2017).

On a similar note, this intermediate status of 'anilioids' may suggest that their jaw complex ought to be considered homologous to the non-snake lizard condition, i.e., grouped under the same morphotype due to the shared presence of robust features. However, as outlined above, a number of key character states do differ between non-snake lizards and 'anilioids', in turn reflecting the distinct functional nature of the uropeltoid and amerophidian jaw complex (e.g., the ability for 'snout-shifting') compared to that of non-snake lizards (Figs 3.3–3.8; Tables 3.2 and 3.3). Because of these consistent homological and functional differences between the non-snake lizard and early-diverging alethinophidian jaw mechanisms, these conditions therefore cannot be considered directly homologous; although hypotheses of the 'anilioid' condition as representing an evolutionarily intermediate stage between non-snake lizards and 'macrostomatan' snakes are possible, any such hypothesis must recognize the distinct nature of the 'anilioid' skull. Other studies have similarly cautioned against drawing direct parallels between 'anilioids' and non-snake lizards (e.g., Harrington & Reeder 2017).

Finally, an important clarification to this discussion of homology is that synapomorphies can only be fully corroborated by the 'test of congruence' *sensu* Patterson (1982, 1988), a test requiring rigorous phylogenetic analysis and thus falling beyond the scope of the current study. Although I do not perform this test herein, the rejection of homology at the level of character state identity for several key features means that we *can* definitively deem these conditions—and, by extension, their morphotypes of 'microstomy'—as non-homologous and non-synapomorphic. Essentially, my perspective that the jaw complexes in non-snake lizards, early-diverging alethinophidians, and the scolecophidian lineages are not primary homologs by definition precludes them from being secondary homologs, i.e., synapomorphic.

A related caveat applies to 'snout-shifting' snakes. Amerophidians and uropeltoids both possess the character states comprising this morphotype, thus satisfying the test of primary homology. However, under the current phylogenetic framework (Figs 3.1 and 3.2), two evolutionary scenarios for this morphotype are equally plausible: either each constituent character state—and thus the overall 'snout-shifting' morphotype—arose once at the base of Alethinophidia and was subsequently lost in caenophidians and booid-pythonoids, meaning that

'snout-shifting' is indeed a synapomorphy of uropeltoids and amerophidians and the plesiomorphic state for Alethinophidia (e.g., Fig. 3.14a); or 'snout-shifting' arose independently in Amerophidia and Uropeltoidea, and is in fact convergent (e.g., Fig. 3.13b). It is therefore currently ambiguous as to whether this morphotype would pass the test of congruence. However, the fossil evidence presented above, combined with the presence of numerous consistent character states in such distantly-related lineages—not least of which is an unusual morphological innovation, the 'ball-and-socket'-like maxilla-palatine joint—in my view favours the interpretation of this morphotype as indeed homologous across these early-diverging alethinophidian clades, reflecting a strong candidate for the ancestral morphology of Alethinophidia, if not Ophidia as a whole.

3.4.4. Variation within morphotypes

As a final note when considering the homology of 'microstomy' across squamates, the anatomical variants discussed in §3.3.1.4 and §3.3.2.4 raise the question of whether it is appropriate to include the taxa in question (dibamids and amphisbaenians, and *Anomochilus* and *Uropeltis*) under the same morphotype as other non-snake lizards and other early-diverging alethinophidians, respectively. As mentioned in §3.4.1, when considering the homology of entire morphofunctional complexes, it is inevitable that some variation will arise due to the taxonomic breadth of each morphotype and thus must be allowed and accounted for. For the taxa mentioned above, although certain features may vary relative to their respective morphotypes, ultimately these taxa do remain consistent with these overall morphotypes.

For all of these taxa, many of the differences they exhibit compared to other non-snake lizards or 'anilioids' are paedomorphic. In this case, these paedomorphic features mainly include the absence or drastic reduction of elements (e.g., supratemporal, squamosal, ectopterygoid; Figs 3.5 and 3.6), which can be recognized as paedomorphic by comparison to the typical, well-developed condition of these elements in other squamates (e.g., see Polachowski & Werneburg 2013; Werneburg *et al.* 2015; Ollonen *et al.* 2018). Anterior displacement of the jaw suspension and anteroventral orientation of the quadrate (Figs 3.5 and 3.6) are also paedomorphic traits, common among miniaturized vertebrates (Olori & Bell 2012; Strong *et al.* 2021a) and reflecting retention of the embryonic condition of the suspensorium in squamates (Kamal 1966; Rieppel & Zaher 2000; Kley 2006; Scanferla 2016). This paedomorphosis is likely tied to miniaturization (Rieppel 1984b; Rieppel & Maisano 2007; Maddin *et al.* 2011; Olori & Bell 2012), as dibamids,

Anomochilus, and uropeltids have all been recognized as miniaturized (e.g., Rieppel 1984b; Olori & Bell 2012), and developmental truncation has been hypothesized as one of the main processes by which such drastic size reduction occurs (Gould 1977; Hanken 1984; Wake 1986; Hanken & Wake 1993).

Other features, such as the structure of the suspensorium (Figs 3.5 and 3.6), are also common among miniaturized and fossorial taxa (see also Rieppel 1984b; Evans 2008; Maddin *et al.* 2011). Similarly, features such as the more tightly integrated premaxilla and prefrontal in *Anomochilus* and *Uropeltis*, as well as the laterally enclosed braincase in dibamids and amphisbaenians, are logical consequences of fossoriality in these taxa (Cundall & Rossman 1993). Miniaturization may also play a role, as elements must be more compactly arranged in a smaller skull, resulting in tighter integration relative to non-miniaturized taxa.

In light of these phenomena, it is reasonable to hypothesize the derivation of the dibamid or amphisbaenian skull from a more 'typical' non-snake lizard morphotype via miniaturization- and/or fossoriality-related modification, or the derivation of the skull of *Anomochilus* or *Uropeltis* from a more 'typical' uropeltoid condition in a similar manner. As in scolecophidians, features susceptible to homoplasy—such as those related to fossoriality, miniaturization, and paedomorphosis—must be taken into account and recognized as superimposing potentially misleading features upon the morphology in question. For scolecophidians, this means recognizing these potentially homoplastic features as quite weak evidence for synapomorphy or homology (see §3.4.2); for dibamids, amphisbaenians, and paedomorphic uropeltoids, this means recognizing this homoplasy as a likely independent superimposition overtop the core morphotype in question. After accounting for such phenomena as miniaturization and fossoriality, the dibamid and amphisbaenian skulls otherwise share several conditions with other non-snake lizards, and the same is true for *Anomochilus* and *Uropeltis* in comparison to other 'anilioids' (see §3.3.1.4 and §3.3.2.4). In contrast, after taking these phenomena into account for scolecophidians, the jaw complexes are still fundamentally different, justifying separate morphotypes. Accounting for these phenomena is therefore essential in recognizing and accounting for homoplasy when evaluating the homology of character complexes.

Of these taxa, *Anomochilus* most prominently displays a unique skull structure that is not easily referable to any of the main morphotypes. As described by Cundall & Rossman (1993), the skull of *Anomochilus* is unique among snakes, having been proposed as an intermediate

between scolecophidians and alethinophidians. One of the most unique features of *Anomochilus* is its palatomaxillary structure: the maxilla is reduced compared to other 'anilioids', especially in anteroposterior length, and does not contact the reduced ectopterygoid (Cundall & Rossman 1993; Rieppel & Maisano 2007). This would suggest different palatomaxillary biomechanics, as movement of the maxilla would presumably be driven only by the palatine, with which it articulates medially (Cundall & Rossman 1993). This is reminiscent of 'maxillary raking' as occurs in some scolecophidians.

However, the rest of the jaws and suspensorium differ sufficiently from scolecophidians—and molecular evidence places *Anomochilus* firmly within Uropeltoidea, possibly as sister to Cylindrophiidae (Pyron *et al.* 2013)—such that I consider this similarity convergent, driven by paedomorphosis affecting the ectopterygoid and maxilla in *Anomochilus*, rather than modification from a 'maxillary raking' scolecophidian ancestor. Cundall & Rossman (1993) similarly reject the possibility that *Anomochilus* and scolecophidians (in their discussion, specifically typhlopids) share a homologous feeding mechanism. Ultimately, the exact nature and phylogenetic position of *Anomochilus* requires its own detailed treatment, beyond the scope of the current paper. However, following the effects of paedomorphosis and fossoriality as discussed above—and in light of previous morphological analyses supporting the uropeltoid affinities of *Anomochilus* (e.g., Rieppel & Maisano 2007) and genetic evidence affirming this conclusion (e.g., Pyron *et al.* 2013)—I consider it most reasonable to classify *Anomochilus* as a modified 'snout-shifting' taxon.

Finally, many morphological phylogenies often recover dibamids, amphisbaenians, and snakes as part of a clade of fossorial and/or limb-reduced taxa (e.g., the Scincophidia of Conrad 2008). Indeed, certain features are consistent among these taxa; for example, the suspensorium in dibamids and amphisbaenians (Figs 3.5 and 3.6; §3.3.1) is quite similar to the condition in scolecophidians (Figs 3.9–3.11; §3.3.4–3.3.6), particularly regarding the extreme reduction of the supratemporal and anterior tilt of the quadrate. However, as noted above, these features likely result from miniaturization-driven paedomorphosis (Rieppel 1984b; Maddin *et al.* 2011; Olori & Bell 2012). Given that miniaturization, paedomorphosis, and fossoriality are often associated with homoplasy (Rieppel 1984b, 1988; Hanken & Wake 1993; Wiens *et al.* 2005; Fröbisch & Schoch 2009; Maddin *et al.* 2011), and the fact that amphisbaenians, dibamids, and scolecophidians are not considered to be closely related in most recent phylogenies (e.g., Wiens

et al. 2010; Reeder *et al.* 2015; Simões *et al.* 2018; Burbrink *et al.* 2020), these similarities are therefore almost certainly driven by the independent evolution of miniaturization and fossoriality in these groups. This conclusion is consistent with previous arguments that the recovery of a 'fossorial clade' is simply the result of a homoplastic fossorial ecomorph evolving convergently in these taxa (e.g., Rieppel 1988; Lee 1998). The numerous ways in which the amphisbaenian or dibamid skull differs from that of scolecophidians—especially regarding the robustness and degree of integration of the jaw elements (Figs 3.5, 3.6, and 3.9–3.11)—further supports the hypothesis that these similarities are convergent, rather than reflecting that the scolecophidian jaw condition is strictly homologous to, or a retention of, the dibamid or amphisbaenian condition.

3.4.5. Ancestral state reconstruction

The overarching outcome of the various ancestral state reconstructions is that different hypotheses of homology result in very different reconstructions of key nodes (Figs 3.12–3.14). For example, the ancestral snake node is definitively reconstructed as 'microstomy' under the simplest scoring scheme (Fig. 3.12), but is equivocal under both other schemes (Figs 3.13 and 3.14) under both ML and MP algorithms. Similarly, the ancestral alethinophidian node is variably reconstructed as definitively 'microstomy' (Fig. 3.12a) or 'snout-shifting' (Fig. 3.14a), very likely 'macrostomy' (Fig. 3.13b), or ambiguous (Figs 3.12b, 3.13a, and 3.14b).

Although it may seem a foregone conclusion that increasing the number of character states increases the uncertainty of reconstruction, such an outcome is not trivial. Simple approaches to reconstruction tend to produce correspondingly straightforward hypotheses of character evolution, such as 'microstomy' as the definitive ancestral condition for snakes. However, scoring 'microstomy' under a single state reflects an implicit assumption that this condition is directly comparable—i.e., homologous—across the taxa in question. Once homology is explicitly assessed and character scoring adjusted to reflect this homology (or lack thereof), ancestral state reconstructions become more complicated, more ambiguous, and therefore less apparently informative. However, most importantly, these reconstructions also become more accurate, as they more closely reflect the biological reality of the conditions in question and thus provide a more realistic reconstruction of their evolution.

Arguably, to provide the most realistic reconstruction of ancestral nodes, any semblance of morphotypes or overarching character complexes should be eliminated altogether, and each

character should instead be reconstructed separately (e.g., the 'reductive coding' approach of Wilkinson 1995). Indeed, such an approach is essential in reconstructing hypothetical transitional taxa, i.e., nodes bearing novel combinations of character states (Wilkinson 1995). However, this method is not without flaws. For example, how much atomization is enough, or is too much (Wilkinson 1995)? Are these novel trait combinations plausible, or even biologically possible? Focussing on morphotypes—rather than individual characters—avoids these issues, as this concept involves accurately conceptualizing morphofunctional systems without sacrificing their inherent integration and complexity. Ultimately, both approaches to ancestral state reconstruction have merit, with the morphotype concept in particular avoiding both the under-atomization (e.g., treating 'microstomy' as homogenous) and over-atomization (e.g., as may occur in 'reductive coding') of complex morphofunctional systems.

Conversely, one could instead argue that more complex scoring methods essentially 'over-separate' microstomy into so many states as to be uninformative. For example, what if the purpose of the analysis is simply to determine if the ancestral snake was 'some kind of microstomatan' *versus* 'some kind of macrostomatan', regardless of the specific morphology of this condition? In this case, would it not be acceptable to simply score taxa as 'microstomy' *versus* 'macrostomy'? Such an approach, however, is untenable, and would be similar to the problems created, for example, by using the term 'big wing' *versus* 'small wing' in systematizing birds using wing size. In any examination of the evolution of a character and its states, the anatomy in all of its details must take primacy (Wilkinson 1995; Rieppel & Kearney 2002; Simões *et al.* 2017). Hypotheses regarding character evolution must be constructed using a 'bottom-up' approach, i.e., starting with assessments of fundamental homology and building from this starting point. 'Top-down' approaches—i.e., lumping various conditions together from the outset, and only later considering non-homology—represent a theoretically 'backwards' approach to the study of character evolution.

The fallacy of this approach is especially true when it results in hypotheses that taxa such as scolecophidians are plesiomorphically 'retaining' ancestral conditions (e.g., Miralles *et al.* 2018). Of note, Harrington & Reeder (2017) also scored all taxa as simply 'macrostomy' or 'non-macrostomy' in their analysis of snake evolution. However, following their ancestral state reconstruction, they did critically examine the relevant morphologies in a manner similar to that recommended by Griffith *et al.* (2015), ultimately concluding that the scolecophidian

morphotype is not representative of the ancestral snake condition and in fact may have evolved convergently (Harrington & Reeder 2017). This comparative anatomical perspective is commendable, and these authors' conclusions are ultimately consistent with the present study. However, in order to be fully theoretically sound, this assessment of homology should be performed prior to the analysis—i.e., when delimiting character states—rather than afterwards.

Critical examination of primary homology prior to reconstructing ancestral states is indeed crucial: non-homologous conditions cannot be included under the same character or state in a phylogenetic analysis (Rieppel & Kearney 2002; Simões *et al.* 2017), a principle which logically must also apply to ancestral state reconstructions. To do otherwise is to equate conditions which are fundamentally incomparable, creating an artificial category—in this case, of uniform 'microstomy'—without reflecting the morphological nuance associated with this condition. Just as Simões *et al.* (2017:200) caution against 'naïve connectivity' in the employment of the 'test of similarity', I caution against the issue of 'naïve homology' when comparing character complexes across taxa. Admittedly, for certain conditions (e.g., diel activity pattern, biome, aquatic habits, prey preference: Hsiang *et al.* 2015; limb reduction: Harrington & Reeder 2017), primary homology is difficult or impossible to assess; as such, it is often unavoidable to group each of these conditions under the same overarching character state. However, for a condition such as microstomy, for which homology can be thoroughly assessed, conflating non-homologous conditions introduces substantive, not to mention unnecessary, logical error into the analysis. I therefore advocate the importance of a thorough comparative anatomical approach when formulating hypotheses regarding evolution (see also Rieppel & Kearney 2002; Simões *et al.* 2017). This echoes recent discussions that ancestral state reconstructions should not be an analytical endpoint, but rather should be treated as hypotheses to be rigorously assessed in their own right (Griffith *et al.* 2015).

Although the present study focusses on 'microstomy', the concept of 'macrostomy' is equally in need of re-examination. Recent authors have suggested that the versions of 'macrostomy' present in booid-pythonoids and caenophidians may have evolved independently, based on both molecular (Burbrink *et al.* 2020) and ontogenetic (Palci *et al.* 2016) evidence. Even within each of these groups, different variations of macrostomy may have arisen convergently (Caldwell 2019; Strong *et al.* 2019), and 'macrostomy' may have been paedomorphically lost several times (Scanferla 2016). Similarly, although specimens of

tropidophiids were not available for the present study, this family is particularly worthy of attention: recent phylogenies (e.g., Burbrink *et al.* 2020) have recovered these 'macrostomatans' as the sister group to Aniliidae within Amerophidia, an early-diverging placement in turn suggesting that macrostomy may have evolved earlier among snakes than is often recognized, including within my own ancestral state reconstructions (Figs 3.12–3.14). Therefore, much like the conflation of 'microstomy' as a uniform character state is inaccurate, as presented herein, the conflation of 'macrostomy' in a similar manner may also be incorrect. My scoring methods include 'macrostomy' as both single and separate morphotypes in order to recognize this uncertainty; however, a detailed re-examination of macrostomy very much requires its own treatment, so as to better understand the complexity of this feeding mechanism and its evolution.

Finally, this ancestral state reconstruction is not an attempt to definitively determine the ancestral snake morphology. Indeed, certain aspects of this analysis—particularly regarding limited sampling of 'macrostomatans' (given the focus on microstomy) and no sampling of extinct taxa (given the chosen phylogenetic framework)—largely preclude such a definitive determination of such a complex problem. Rather, my aim was to assess the impact that different perspectives on homology and morphology might have in shaping higher-level hypotheses of character and taxon evolution, as examined above.

As for future studies which do aim to definitively reconstruct the 'ancestral snake morphology', the inclusion of extinct taxa is a particularly crucial component. Data from fossils have consistently been shown to improve ancestral state reconstructions by providing critical information not reflected by extant taxa, such as taxonomic diversity, character state distributions, unique character states or state combinations, and impact upon the phylogeny itself on which the ancestral state reconstruction is based (Finarelli & Flynn 2006; Finarelli & Goswami 2013; Betancur-R *et al.* 2015; Hsiang *et al.* 2015; Puttick 2016; Caldwell 2019; Mongiardino Koch & Parry 2020). Exceptionally preserved snake fossils, such as recently described specimens of *Najash* (Garberoglio *et al.* 2019a; Garberoglio *et al.* 2019b), are particularly promising in allowing the detailed anatomical analysis necessary for accurate reconstructions. I therefore encourage the inclusion of extinct taxa alongside thorough comparative anatomical analysis in future attempts at reconstructing the 'ancestral snake morphology'.

Figures: Chapter Three

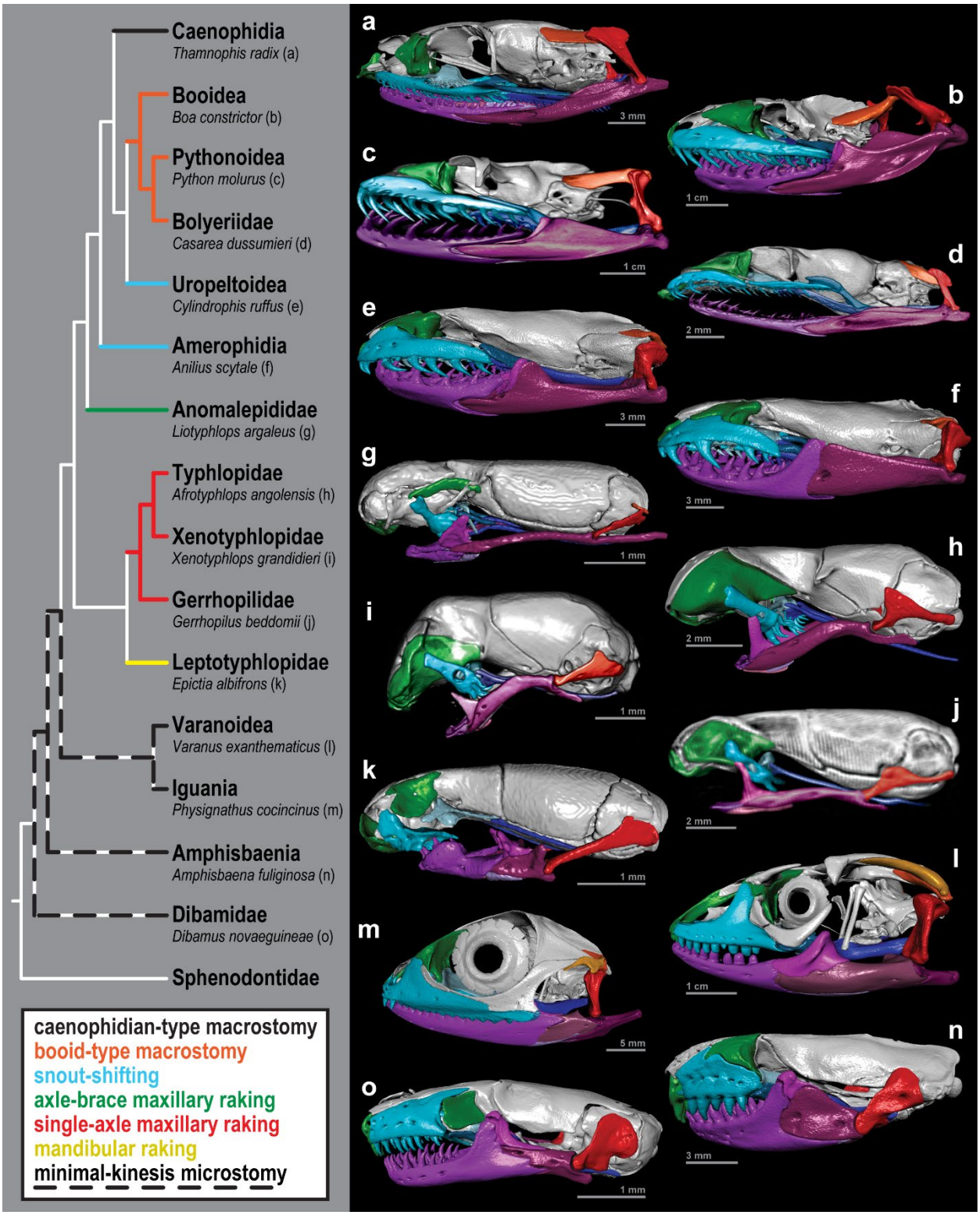

FIGURE 3.1. Overview of hypothesized jaw evolution in squamates. Coloured branches reflect the proposed jaw morphotype for each major squamate clade (see legend, Figures 3.12–3.14, and main text). Relevant skull elements are highlighted in an exemplar specimen from each group (colouration as in Figures 3.3–3.11). See Table 3.1 for specimen numbers. MCZ scan data used by permission of the Museum of Comparative Zoology, Harvard University.

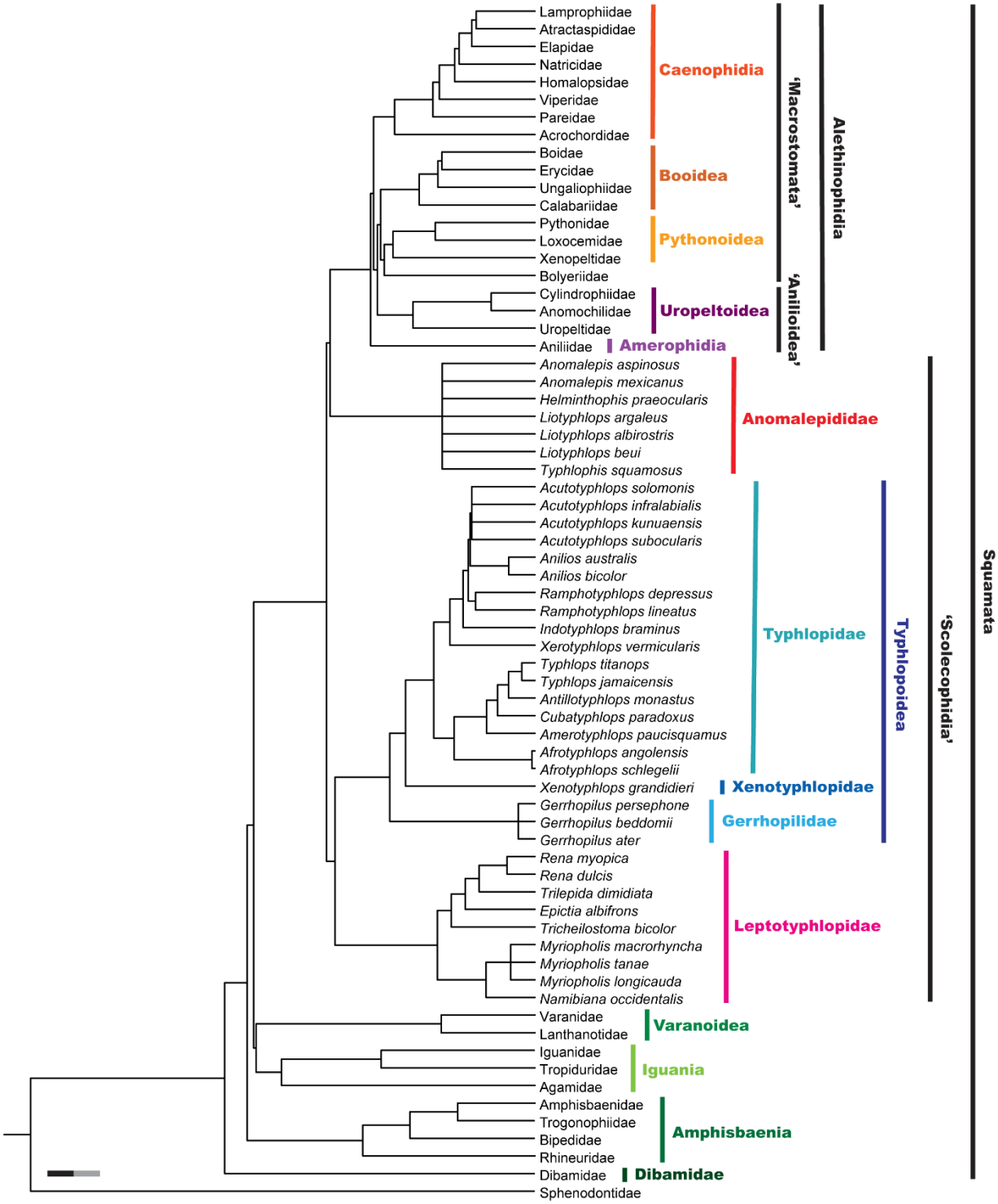
Lamprophiidae
Atractaspididae
Elapidae
Natricidae
Homalopsidae
Viperidae
Pareidae
Acrochordidae
Caenophidia
Boidae
Erycidae
Ungaliophiidae
Calabariidae
Booidea
Pythonidae
Loxocemidae
Xenopeltidae
Pythonoidea
Bolyeriidae
Cylindrophiidae
Anomochilidae
Uropeltidae
Uropeltoidea
'Macrostomata'
Aniliidae
Amerophidia
'Anilioidea'
Alethinophidia
Anomalepis aspinosus
Anomalepis mexicanus
Helminthophis praeocularis
Liotyphlops argaleus
Liotyphlops albirostris
Liotyphlops beui
Typhlophis squamosus
Anomalepididae
Acutotyphlops solomonis
Acutotyphlops infralabialis
Acutotyphlops kunuaensis
Acutotyphlops subocularis
Anilios australis
Anilios bicolor
Ramphotyphlops depressus
Ramphotyphlops lineatus
Indotyphlops braminus
Xerotyphlops vermicularis
Typhlops titanops
Typhlops jamaicensis
Antillotyphlops monastus
Cubatyphlops paradoxus
Amerotyphlops paucisquamus
Afrotyphlops angolensis
Afrotyphlops schlegelii
Typhlopidae
Xenotyphlops grandidieri
Xenotyphlopidae
Gerrhopilus persephone
Gerrhopilus beddomii
Gerrhopilus ater
Gerrhopilidae
Typhlopoidea
Rena myopica
Rena dulcis
Trilepida dimidiata
Epictia albifrons
Tricheilostoma bicolor
Myriopholis macrorhyncha
Myriopholis tanae
Myriopholis longicauda
Namibiana occidentalis
Leptotyphlopidae
'Scolecophidia'
Varanidae
Lanthanotidae
Varanoidea
Iguanidae
Tropiduridae
Agamidae
Iguania
Amphisbaenidae
Trogonophiidae
Bipedidae
Rhineuridae
Amphisbaenia
Dibamidae
Dibamidae
Sphenodontidae
Squamata

FIGURE 3.2. Phylogenetic context of taxa examined in Chapter Three. Relationships are provided at the species level for scolecophidians and at the family level for other taxa. Relevant higher taxa are indicated in colour, with broader groups labelled in black. Branch lengths represent divergence time, with the scale bar measuring 30 million years. See Materials and Methods for phylogeny construction, including relevant literature sources.

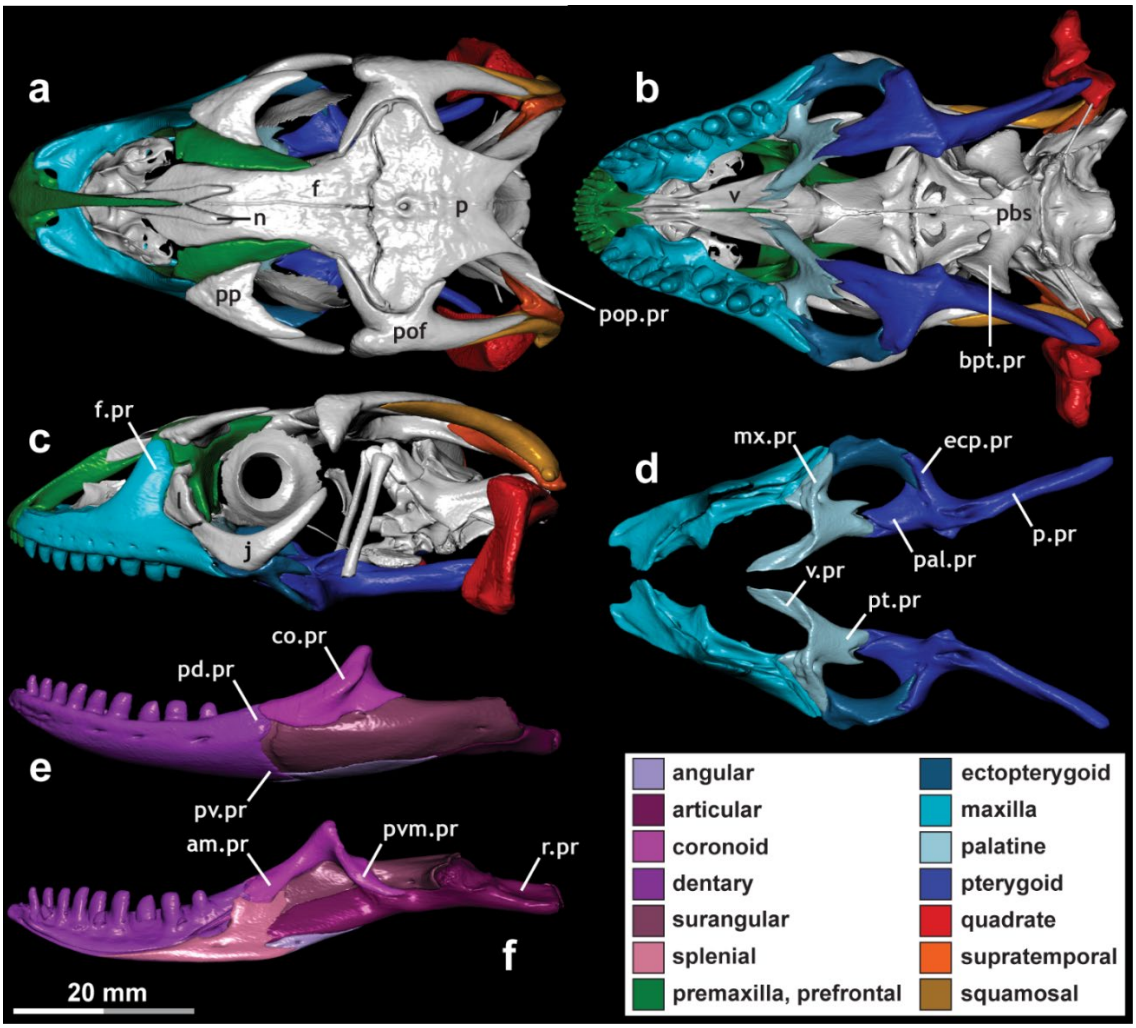

FIGURE 3.3. Skull of *Varanus exanthematicus* (FMNH 58299), exemplifying 'minimal-kinesis microstomy'. Key elements related to feeding are highlighted. In this morphotype, these elements are robust and solidly braced (see text for details). (**a**–**c**) Skull, with mandibles digitally removed, in (**a**) dorsal, (**b**) ventral, and (**c**) lateral view. (**d**) Palatomaxillary arch in dorsal view. (**e**–**f**) Mandible in (**e**) lateral and (**f**) medial view. Abbreviations: am.pr, anteromedial process; bpt.pr, basipterygoid process; co.pr, coronoid process; ecp.pr, ectopterygoid process; f, frontal; f.pr, facial process; j, jugal; l, lacrimal; mx.pr, maxillary process; n, nasal; p, parietal; pal.pr, palatine process; pbs, parabasisphenoid; pd.pr, posterodorsal process; pof, postorbitofrontal; pop.pr, postparietal process; pp, palpebral; p.pr, posterior process; pt.pr, pterygoid process; pvm.pr, posteroventromedial process; pv.pr, posteroventral process; r.pr, retroarticular process; v, vomer; v.pr, vomerine process.

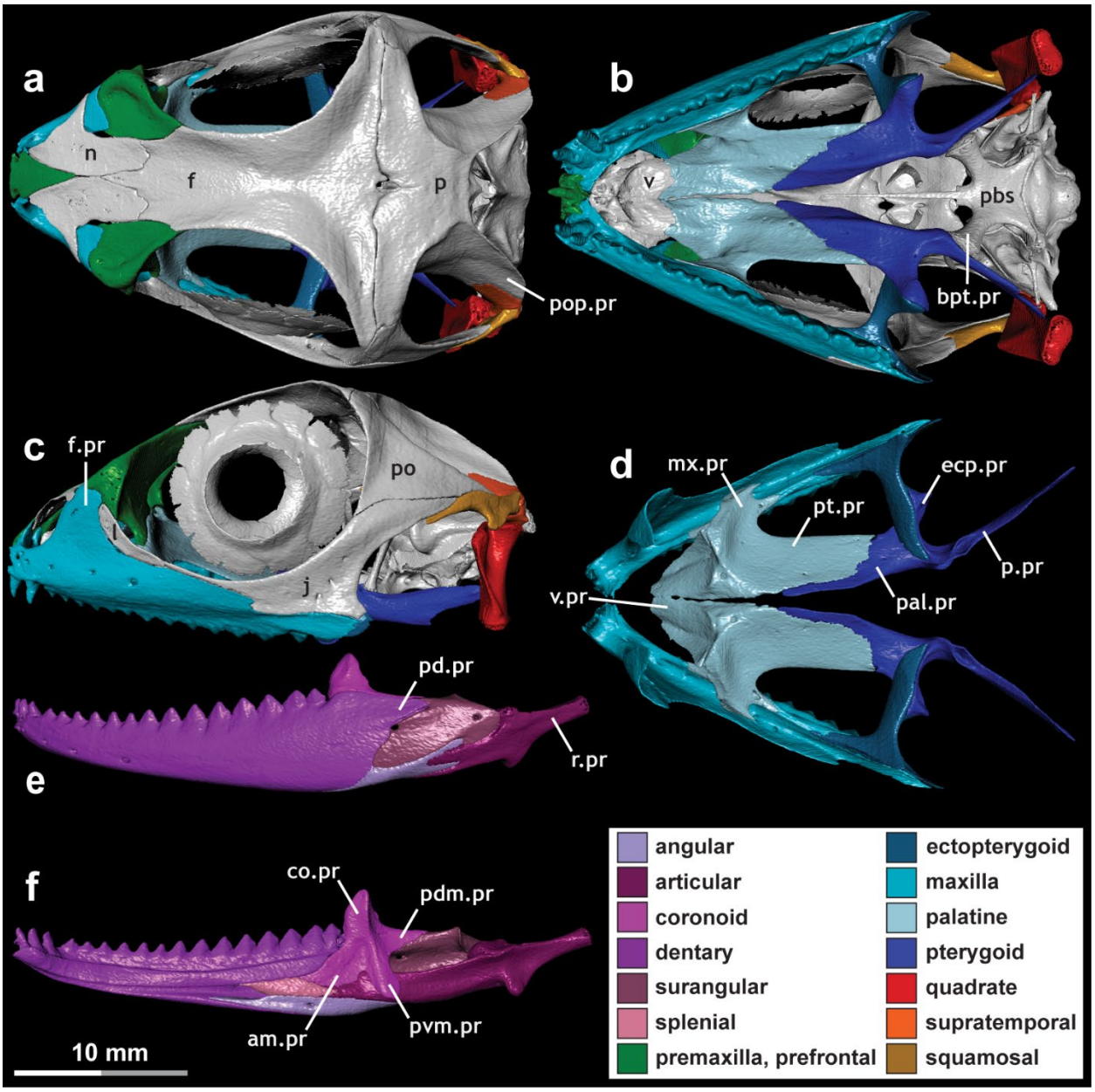
a
n
f
p
pop.pr
b
v
pbs
bpt.pr
c
f.pr
po
l
j
d
mx.pr
ecp.pr
pt.pr
p.pr
v.pr
pal.pr
pd.pr
r.pr
e
f
co.pr
pdm.pr
am.pr
pvm.pr
10 mm
angular
articular
coronoid
dentary
surangular
splenial
premaxilla, prefrontal
ectopterygoid
maxilla
palatine
pterygoid
quadrate
supratemporal
squamosal

FIGURE 3.4. Skull of *Physignathus cocincinus* (YPM 14378), exemplifying 'minimal-kinesis microstomy'. Key elements related to feeding are highlighted. In this morphotype, these elements are robust and solidly braced (see text for details). (**a**–**c**) Skull, with mandibles digitally removed, in (**a**) dorsal, (**b**) ventral, and (**c**) lateral view. (**d**) Palatomaxillary arch in dorsal view. (**e**–**f**) Mandible in (**e**) lateral and (**f**) medial view. Abbreviations: am.pr, anteromedial process; bpt.pr, basipterygoid process; co.pr, coronoid process; ecp.pr, ectopterygoid process; f, frontal; f.pr, facial process; j, jugal; l, lacrimal; mx.pr, maxillary process; n, nasal; p, parietal; pal.pr, palatine process; pbs, parabasisphenoid; pdm.pr, posterodorsomedial process; pd.pr, posterodorsal process; po, postorbital; pop.pr, postparietal process; p.pr, posterior process; pt.pr, pterygoid process; pvm.pr, posteroventromedial process; r.pr, retroarticular process; v, vomer; v.pr, vomerine process.

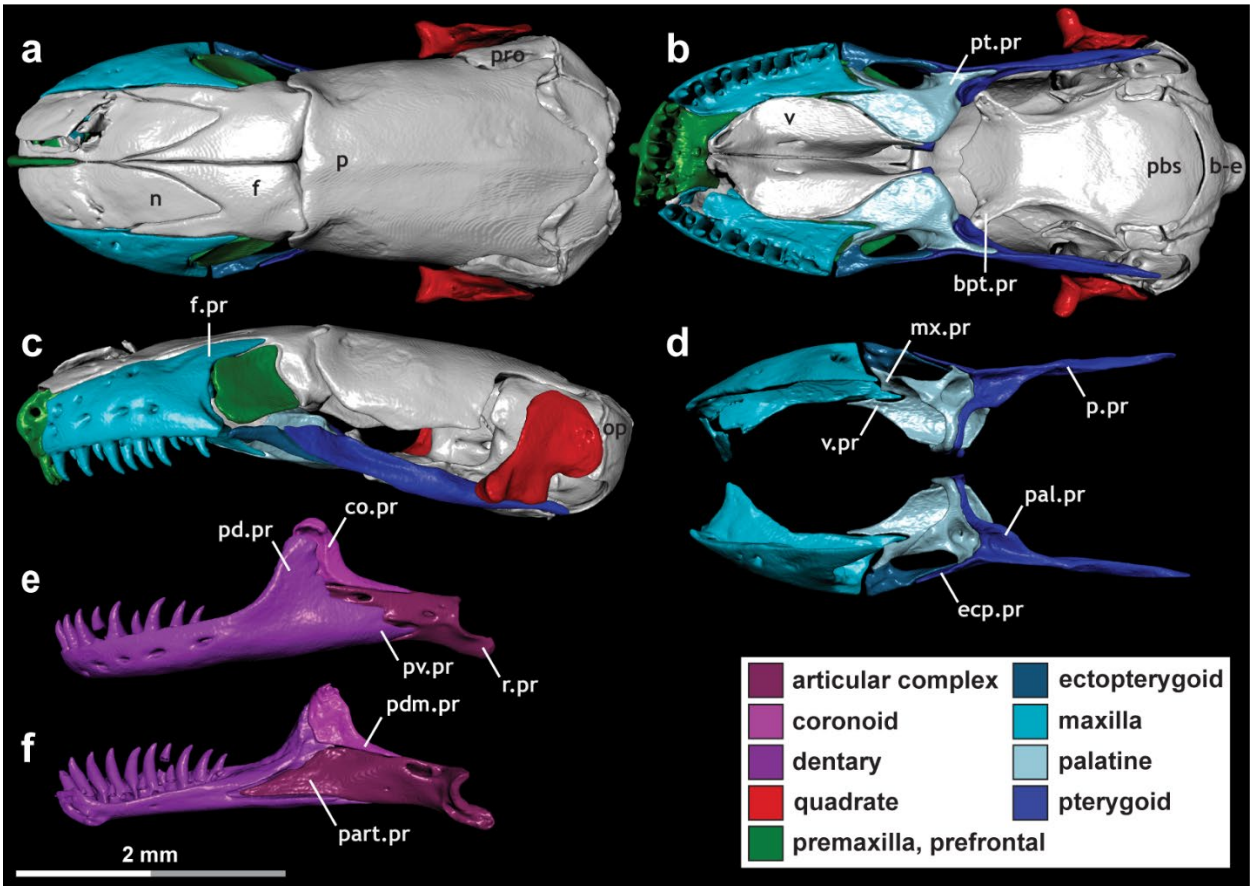

FIGURE 3.5. Skull of *Dibamus novaeguineae* (UF 33488), exemplifying 'minimal-kinesis microstomy' in a miniaturized and fossorial non-snake lizard. Key elements related to feeding are highlighted. In this morphotype, these elements are robust and solidly braced (see text for details). (**a**–**c**) Skull, with mandibles digitally removed, in (**a**) dorsal, (**b**) ventral, and (**c**) lateral view. (**d**) Palatomaxillary arch in dorsal view. (**e**–**f**) Mandible in (**e**) lateral and (**f**) medial view. Abbreviations: b-e, basioccipital-exoccipital; bpt.pr, basipterygoid process; ch.pr, choanal process; co.pr, coronoid process; ecp.pr, ectopterygoid process; f, frontal; f.pr, facial process; mx.pr, maxillary process; n, nasal; op, opisthotic; p, parietal; pal.pr, palatine process; part.pr, prearticular process; pbs, parabasisphenoid; pdm.pr, posterodorsomedial process; pd.pr, posterodorsal process; p.pr, posterior process; pro, prootic; pt.pr, pterygoid process; pv.pr, posteroventral process; r.pr, retroarticular process; v, vomer; v.pr, vomerine process.

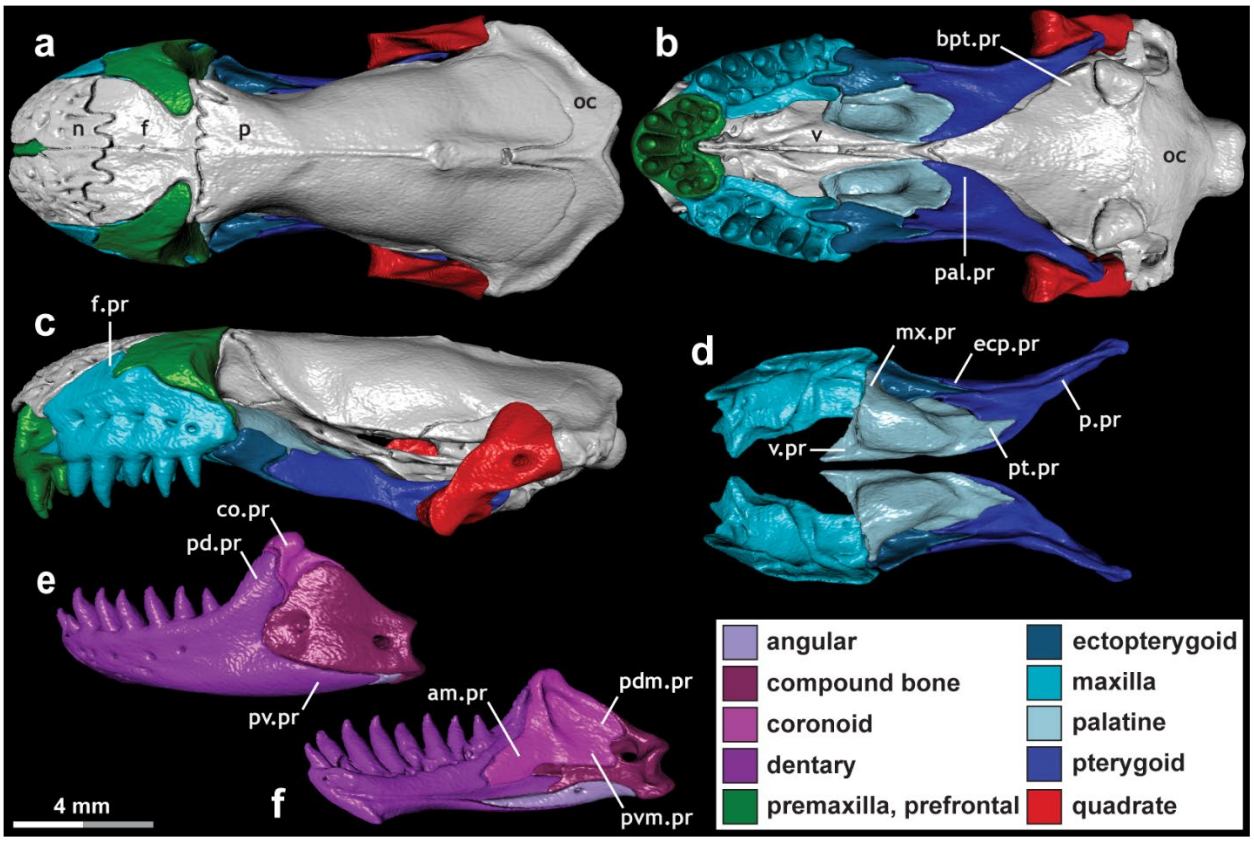

FIGURE 3.6. Skull of *Amphisbaena fuliginosa* (FMNH 22847), exemplifying 'minimal-kinesis microstomy' in a fossorial non-snake lizard. Key elements related to feeding are highlighted. In this morphotype, these elements are robust and solidly braced (see text for details). (**a**–**c**) Skull, with mandibles digitally removed, in (**a**) dorsal, (**b**) ventral, and (**c**) lateral view. (**d**) Palatomaxillary arch in dorsal view. (**e**–**f**) Mandible in (**e**) lateral and (**f**) medial view. Abbreviations: am.pr, anteromedial process; bpt.pr, basipterygoid process; co.pr, coronoid process; ecp.pr, ectopterygoid process; f, frontal; f.pr, facial process; mx.pr, maxillary process; n, nasal; oc, occipital complex; p, parietal; pal.pr, palatine process; pdm.pr, posterodorsomedial process; pd.pr, posterodorsal process; p.pr, posterior process; pt.pr, pterygoid process; pvm.pr, posteroventromedial process; pv.pr, posteroventral process; v, vomer; v.pr, vomerine process.

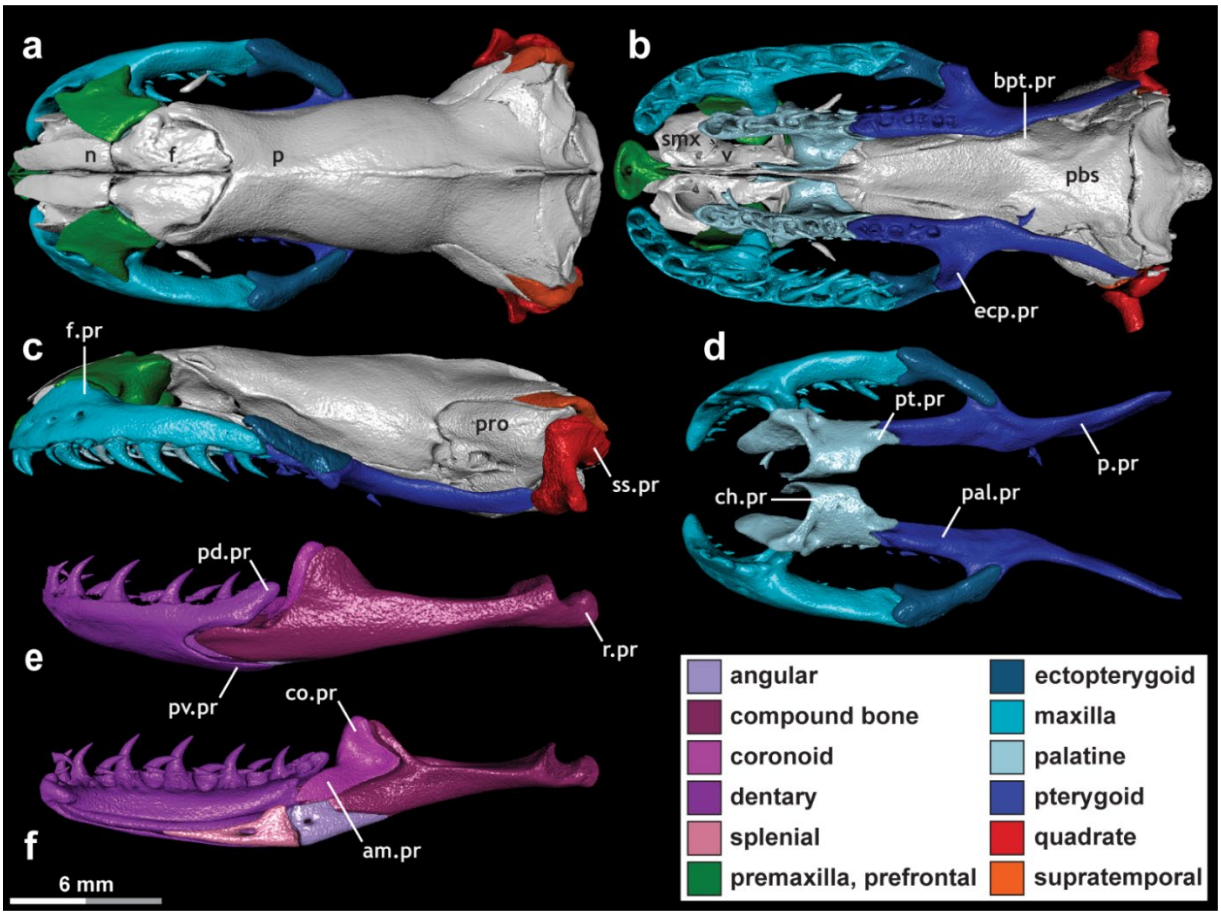

FIGURE 3.7. Skull of *Cylindrophis ruffus* (UMMZ 201901), exemplifying 'snout-shifting' (*sensu* Cundall 1995) in a uropeltoid alethinophidian. Key elements related to feeding are highlighted. In this morphotype, these elements are generally robust and well-braced; however, the maxilla-palatine joint exhibits a distinct 'ball-and-socket'-like form and the vomers and septomaxillae are more loosely connected to the dorsal snout elements and to their contralaterals, thus enabling a slight degree of unilateral movement of the left and right palatomaxillary arches (see text for details). (**a**–**c**) Skull, with mandibles digitally removed, in (**a**) dorsal, (**b**) ventral, and (**c**) lateral view. (**d**) Palatomaxillary arch in dorsal view. (**e**–**f**) Mandible in (**e**) lateral and (**f**) medial view. Abbreviations: am.pr, anteromedial process; bpt.pr, basipterygoid process; ch.pr, choanal process; co.pr, coronoid process; ecp.pr, ectopterygoid process; f, frontal; f.pr, facial process; n, nasal; p, parietal; pal.pr, palatine process; pbs, parabasisphenoid; pd.pr, posterodorsal process; p.pr, posterior process; pro, prootic; pt.pr, pterygoid process; pv.pr, posteroventral process; r.pr, retroarticular process; smx, septomaxilla; ss.pr, suprastapedial process; v, vomer.

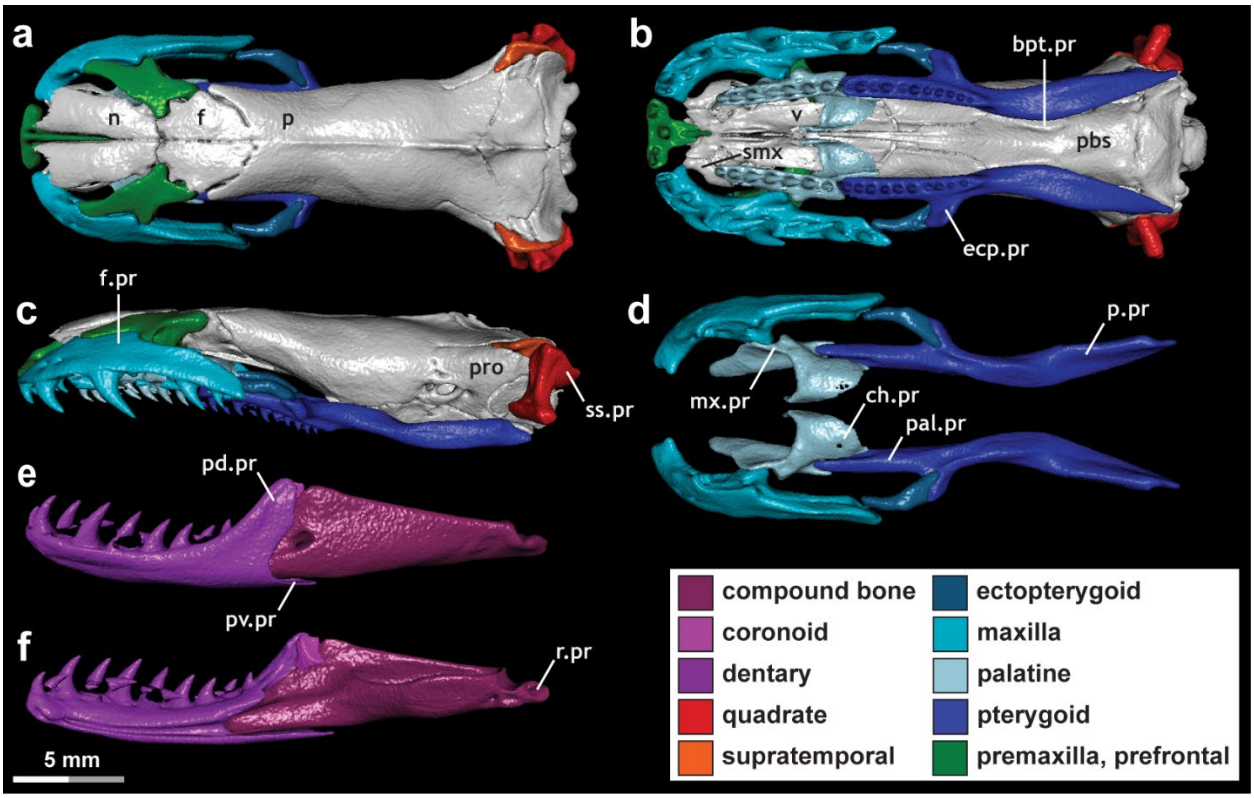

FIGURE 3.8. Skull of *Anilius scytale* (KUH 125976), exemplifying 'snout-shifting' (*sensu* Cundall, 1995) in an amerophidian alethinophidian. Key elements related to feeding are highlighted. This taxon largely resembles *Cylindrophis*, though the mandibular structure differs somewhat (see Figure 3.7 and text for details). (**a**–**c**) Skull, with mandibles digitally removed, in (**a**) dorsal, (**b**) ventral, and (**c**) lateral view. (**d**) Palatomaxillary arch in dorsal view. (**e**–**f**) Mandible in (**e**) lateral and (**f**) medial view. Abbreviations: bpt.pr, basipterygoid process; ch.pr, choanal process; ecp.pr, ectopterygoid process; f, frontal; f.pr, facial process; mx.pr, maxillary process; n, nasal; p, parietal; pal.pr, palatine process; pbs, parabasisphenoid; pd.pr, posterodorsal process; p.pr, posterior process; pro, prootic; pv.pr, posteroventral process; r.pr, retroarticular process; smx, septomaxilla; ss.pr, suprastapedial process; v, vomer.

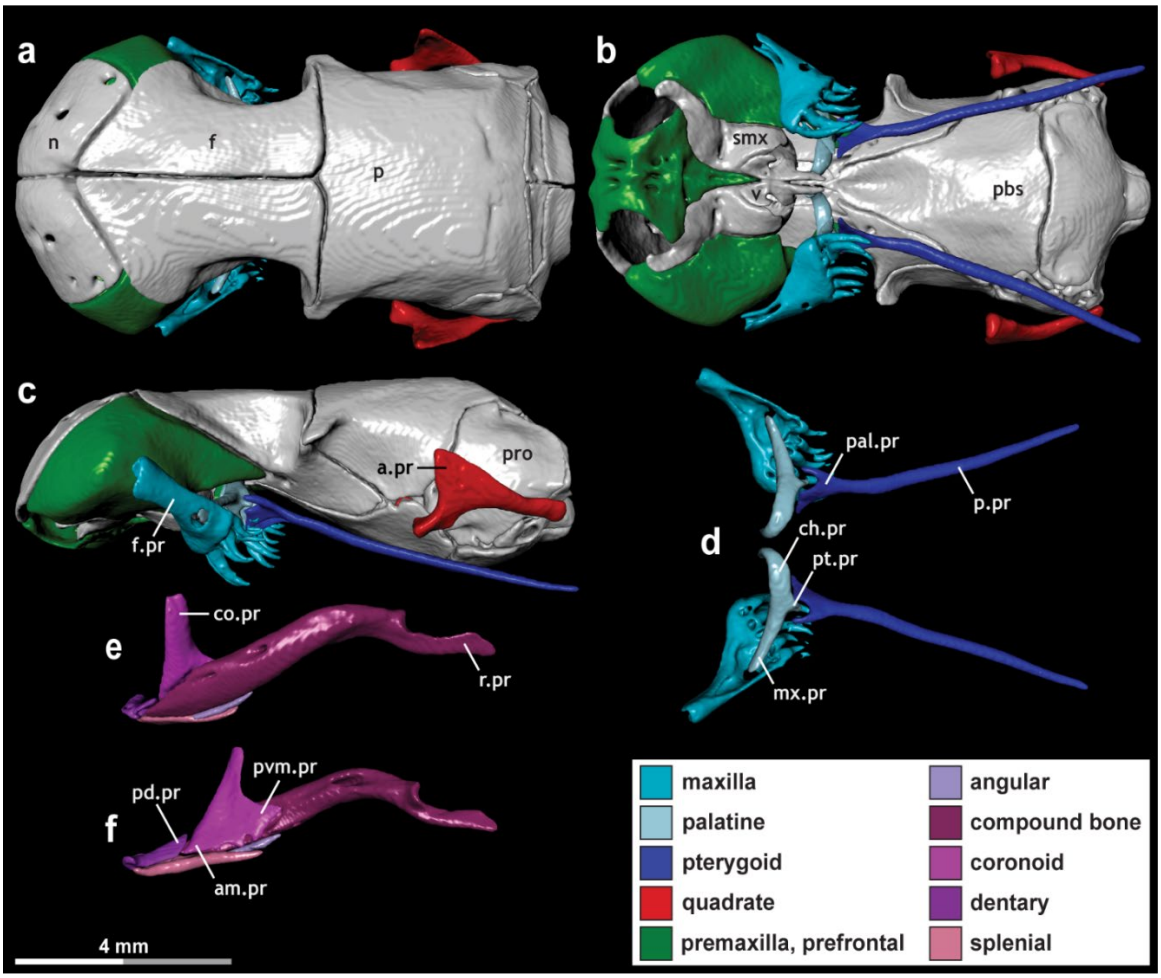

FIGURE 3.9. Skull of *Afrotyphlops angolensis* (MCZ R-170385), exemplifying 'single-axle maxillary raking'. Key elements related to feeding are highlighted. In this morphotype of microstomy, the mandible is reduced and largely akinetic, with feeding being driven by rotation of the maxilla about the elongate maxillary process of the palatine (see text for details). (**a**–**c**) Skull, with mandibles digitally removed, in (**a**) dorsal, (**b**) ventral, and (**c**) lateral view. (**d**) Palatomaxillary arch in dorsal view. (**e**–**f**) Mandible in (**e**) lateral and (**f**) medial view. Abbreviations: am.pr, anteromedial process; a.pr, anterior process; ch.pr, choanal process; co.pr, coronoid process; f, frontal; f.pr, facial process; mx.pr, maxillary process; n, nasal; p, parietal; pal.pr, palatine process; pbs, parabasisphenoid; pd.pr, posterodorsal process; p.pr, posterior process; pro, prootic; pt.pr, pterygoid process; pvm.pr, posteroventromedial process; r.pr, retroarticular process; smx, septomaxilla; v, vomer. MCZ scan data used by permission of the Museum of Comparative Zoology, Harvard University.

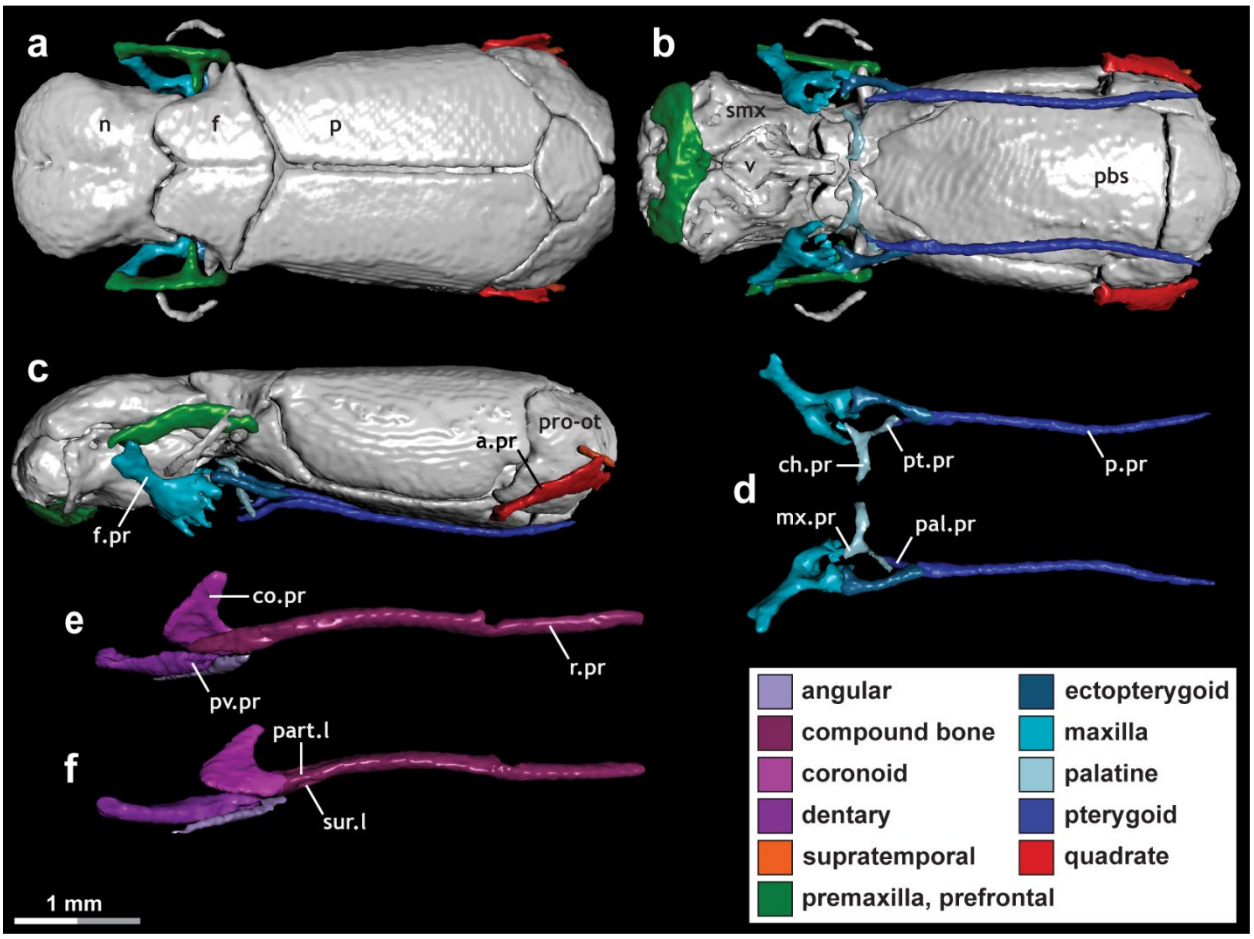

FIGURE 3.10. Skull of *Liotyphlops argaleus* (MCZ R-67933), exemplifying 'axle-brace maxillary raking'. Key elements related to feeding are highlighted. In this morphotype of microstomy, the maxilla is suspended from the mobile and highly reduced prefrontal and is braced posteriorly by the ectopterygoid. As in typhlopoids, the mandible is reduced and does not contribute to feeding (see text for details). (**a**–**c**) Skull, with mandibles digitally removed, in (**a**) dorsal, (**b**) ventral, and (**c**) lateral view. (**d**) Palatomaxillary arch in dorsal view. (**e**–**f**) Mandible in (**e**) lateral and (**f**) medial view. Abbreviations: a.pr, anterior process; ch.pr, choanal process; co.pr, coronoid process; f, frontal; f.pr, facial process; mx.pr, maxillary process; n, nasal; p, parietal; pal.pr, palatine process; part.l, prearticular lamina; pbs, parabasisphenoid; p.pr, posterior process; pro-ot, prootic-otoccipital; pt.pr, pterygoid process; pv.pr, posteroventral process; r.pr, retroarticular process; smx, septomaxilla; sur.l, surangular lamina; v, vomer. MCZ scan data used by permission of the Museum of Comparative Zoology, Harvard University.

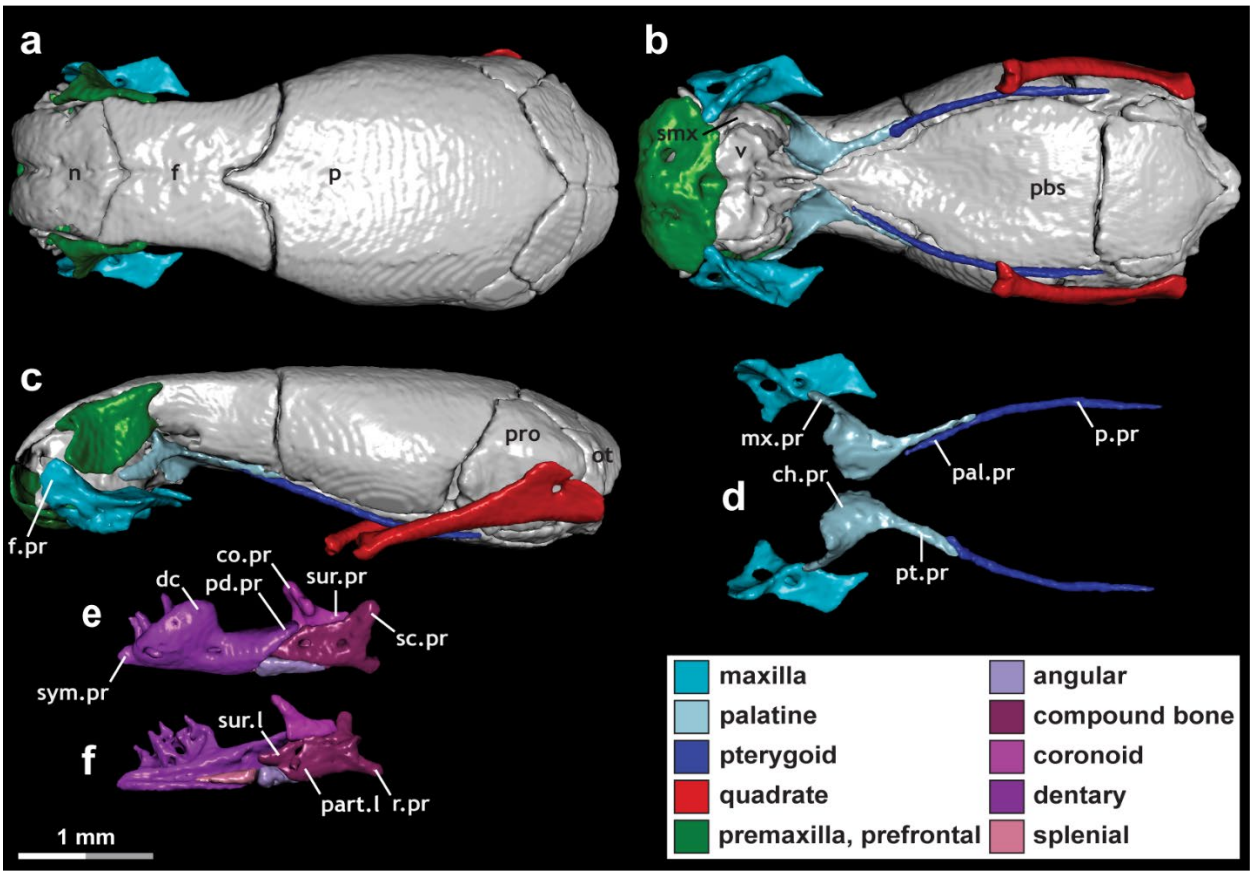

FIGURE 3.11. Skull of *Epictia albifrons* (MCZ R-2885), exemplifying 'mandibular raking' *(sensu* Kley & Brainerd 1999). Key elements related to feeding are highlighted. In this morphotype of microstomy, feeding is driven by rapid retraction of the mandibles, enabled by a flexible intramandibular joint, whereas the palatomaxillary arches are edentulous and do not contribute to feeding (see text for details). (**a**–**c**) Skull, with mandibles digitally removed, in (**a**) dorsal, (**b**) ventral, and (**c**) lateral view. (**d**) Palatomaxillary arch in dorsal view. (**e**–**f**) Mandible in (**e**) lateral and (**f**) medial view. Abbreviations: ch.pr, choanal process; co.pr, coronoid process; dc, dental concha; f, frontal; f.pr, facial process; mx.pr, maxillary process; n, nasal; ot, otoccipital; p, parietal; pal.pr, palatine process; part.l, prearticular lamina; pbs, parabasisphenoid; pd.pr, posterodorsal process; p.pr, posterior process; pro, prootic; pt.pr, pterygoid process; r.pr, retroarticular process; sc.pr, supracotylar process; smx, septomaxilla; sur.l, surangular lamina; sur.pr, surangular process; sym.pr, symphyseal process; v, vomer. MCZ scan data used by permission of the Museum of Comparative Zoology, Harvard University.

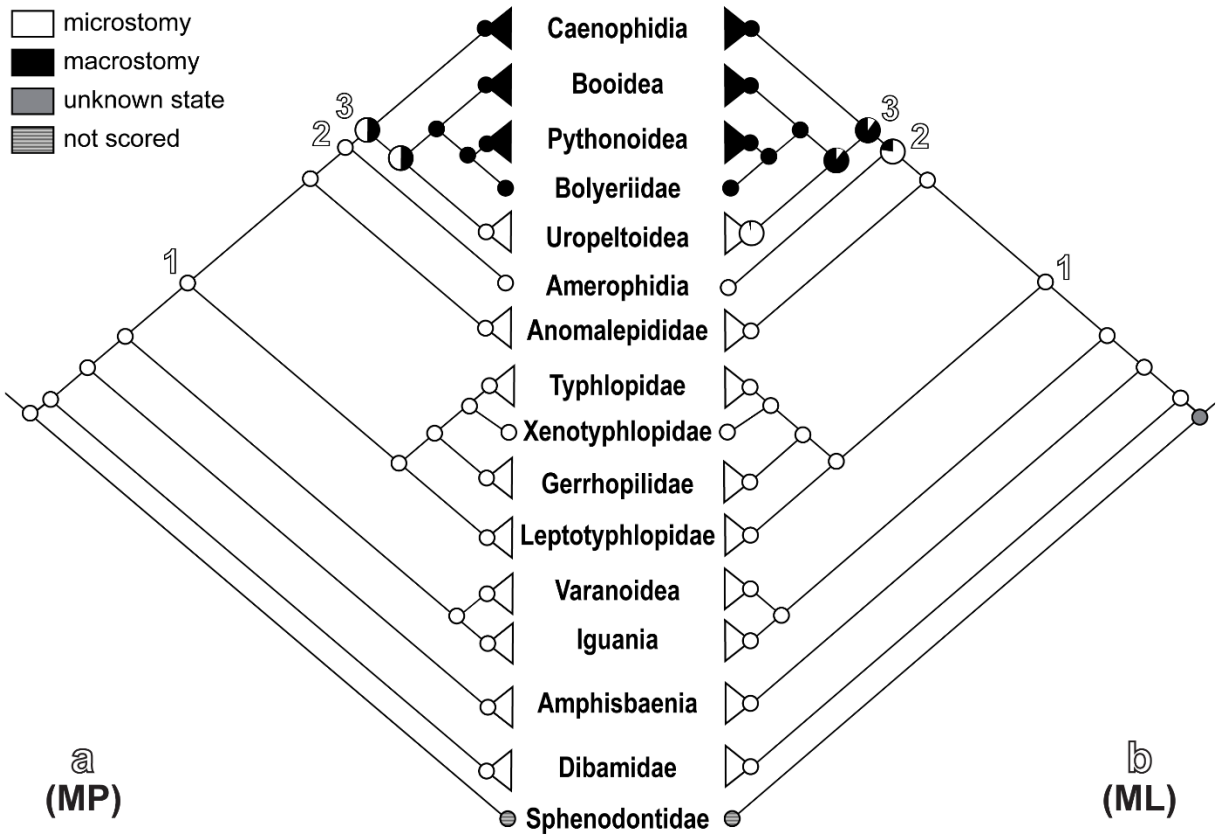

FIGURE 3.12. Ancestral state reconstruction (ASR) of feeding mechanisms in squamates, using a 'basic' character scoring scheme. This scheme involves only two states: microstomy and macrostomy. (**a**) Maximum parsimony (MP)-based ASR; (**b**) maximum likelihood (ML)-based ASR. Key nodes are numbered: **1**, origin of snakes; **2**, origin of Alethinophidia; **3**, origin of 'Macrostomata'. See text for details regarding results, including the impact of different character scoring approaches.

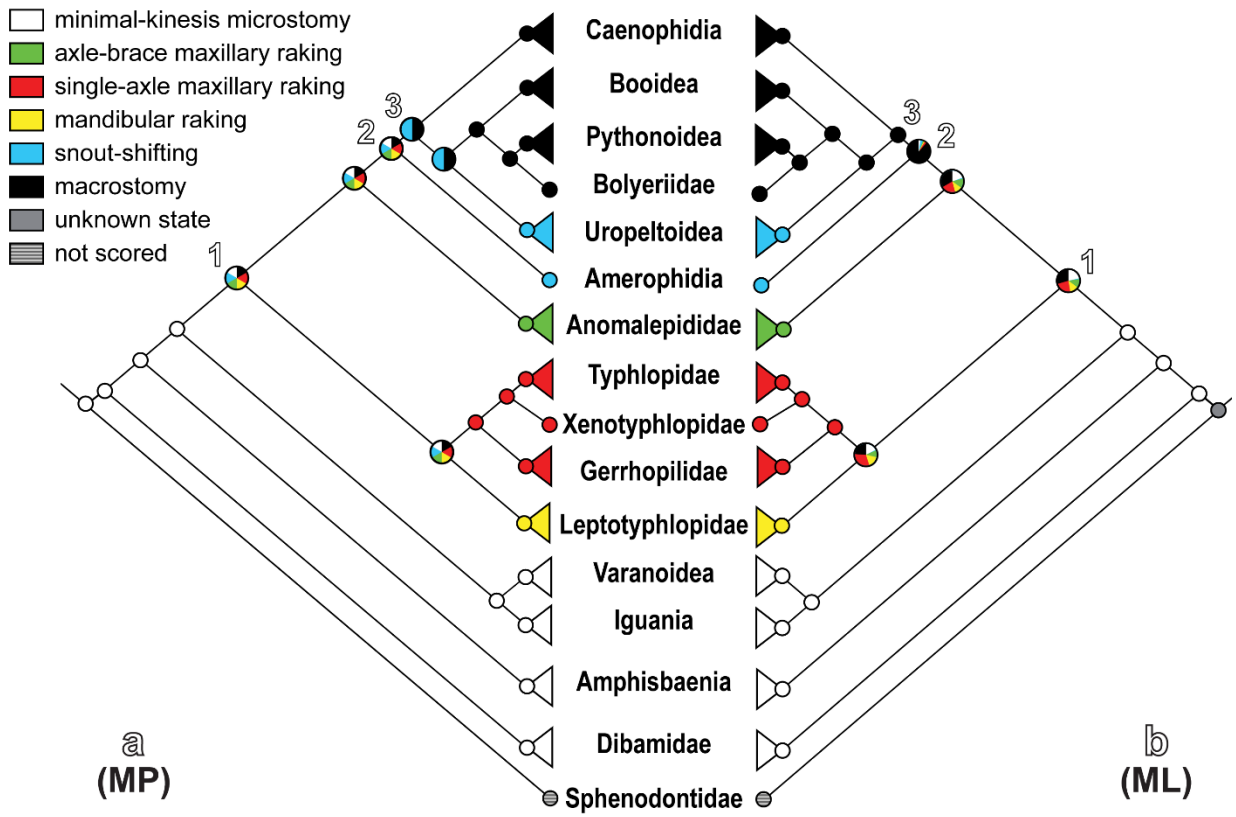

FIGURE 3.13. Ancestral state reconstruction (ASR) of feeding mechanisms in squamates, using a 'detailed microstomy' character scoring scheme. This scheme divides microstomy into the five morphotypes described herein: 'axle-brace maxillary raking', 'mandibular raking', 'minimal-kinesis microstomy', 'single-axle maxillary raking', and 'snout-shifting'. Macrostomy is scored under a single state. (**a**) Maximum parsimony (MP)-based ASR; (**b**) maximum likelihood (ML)-based ASR. Key nodes are numbered: **1**, origin of snakes; **2**, origin of Alethinophidia; **3**, origin of 'Macrostomata'. See text for details regarding results, including anatomical descriptions and the impact of different character scoring approaches.

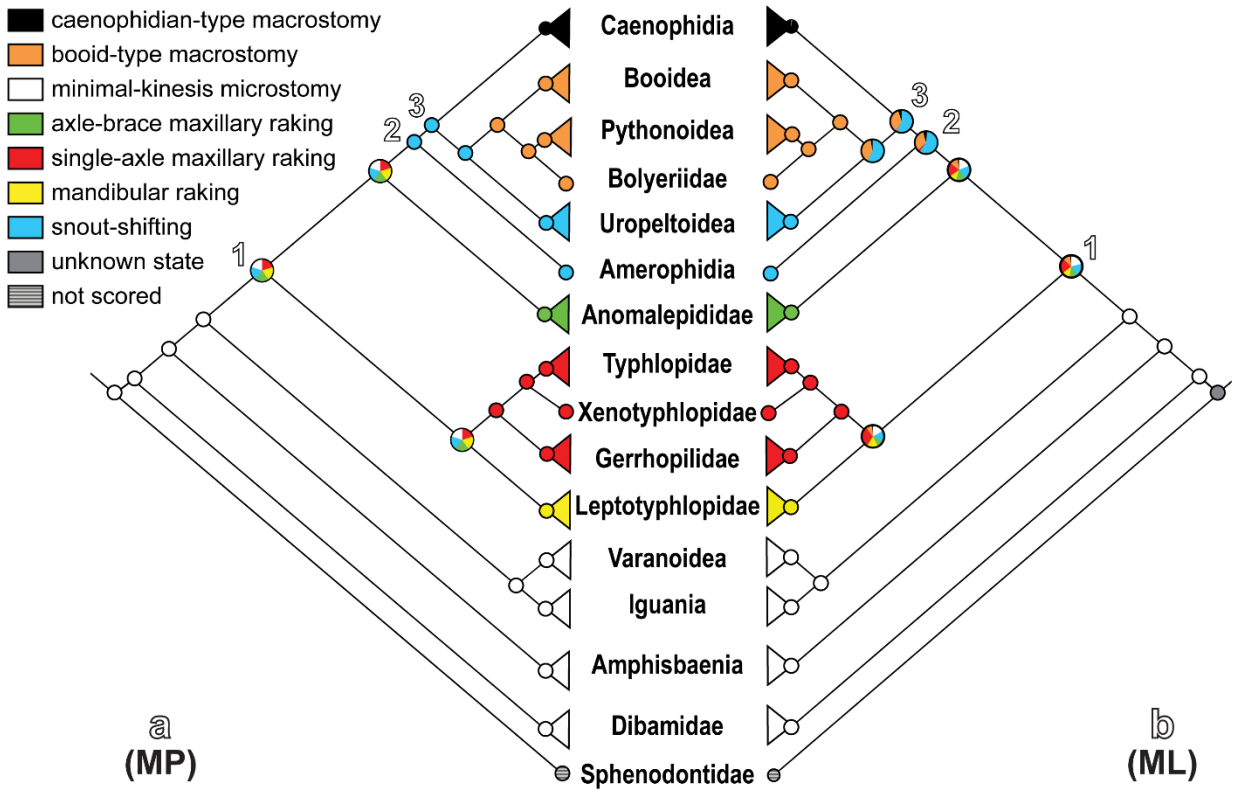

FIGURE 3.14. Ancestral state reconstruction (ASR) of feeding mechanisms in squamates, using a 'detailed microstomy and macrostomy' character scoring scheme. This scheme divides microstomy into the five morphotypes described herein ('axle-brace maxillary raking', 'mandibular raking', 'minimal-kinesis microstomy', 'single-axle maxillary raking', and 'snout-shifting') and divides macrostomy into separate morphotypes ('booid-type' and 'caenophidian-type' macrostomy) as proposed in recent literature (e.g., Palci *et al.* 2016; Strong *et al.* 2019; Burbrink *et al.* 2020). (**a**) Maximum parsimony (MP)-based ASR; (**b**) maximum likelihood (ML)-based ASR. Key nodes are numbered: **1**, origin of snakes; **2**, origin of Alethinophidia; **3**, origin of 'Macrostomata'. See text for details regarding results, including anatomical descriptions and the impact of different character scoring approaches.

Tables: Chapter Three

TABLE 3.1. List of specimens observed for Chapter Three. See preliminary pages of thesis document for institutional abbreviations. See Appendix 1.1 for sources of scan data.

HIGHER TAXON			SPECIES	SPECIMEN NUMBER
Alethinophidia	**'Anilioidea'**	**Amerophidia**	*Anilius scytale*	USNM 204078 KUH 125976
		Uropeltoidea	*Anomochilus leonardi*	FRIM 0026
			Cylindrophis ruffus	UMMZ 201901 FMNH 60958
			Uropeltis melanogaster	FMNH 167048
			Uropeltis woodmasoni	TMM M-10006
	Bolyeriidae		*Casarea dussumieri*	UMMZ 190285
	Booidea	**Boidae**	*Boa constrictor*	FMNH 31182
		Calabariidae	*Calabaria reinhardtii*	FMNH 117833
		Erycidae	*Eryx colubrinus*	FMNH 63117
		Ungaliophiidae	*Ungaliophis continentalis*	UTA 50569
	Caenophidia	**Acrochordidae**	*Acrochordus arafurae*	QM J11033
			Acrochordus granulatus	MCZ R-146128
		Atractaspididae	*Atractaspis irregularis*	FMNH 62204
		Elapidae	*Naja naja*	FMNH 22468
		Homalopsidae	*Homalopsis buccata*	FMNH 259340
		Lamprophiidae	*Boaedon fuliginosus*	FMNH 62248
			Lycophidion capense	FMNH 58322

		Natricidae	*Afronatrix anoscopus*	FMNH 179335
			Natrix natrix	FMNH 30522
			Thamnophis radix	UAMZ R636
		Pareidae	*Pareas hamptoni*	FMNH 128304
		Viperidae	*Bothrops asper*	FMNH 31162
	Pythonoidea	**Loxocemidae**	*Loxocemus bicolor*	FMNH 104800
		Pythonidae	*Python molurus*	TNHC 62769
			Python regius	UAMZ R381
		Xenopeltidae	*Xenopeltis unicolor*	FMNH 148900
'Scolecophidia'	**Anomalepididae**		*Anomalepis aspinosus*	MCZ R-14782
			Anomalepis mexicanus	MCZ R-191201
			Helminthophis praeocularis	MCZ R-17960
			Liotyphlops albirostris	FMNH 216257
			Liotyphlops argaleus	MCZ R-67933
			Liotyphlops beui	SAMA 40142
			Typhlophis squamosus	MCZ R-145403
	Leptotyphlopidae		*Epictia albifrons*	MCZ R-2885
			Myriopholis longicauda	MCZ R-184447
			Myriopholis macrorhyncha	MCZ R-9650
			Myriopholis tanae	MCZ R-40099
			Namibiana occidentalis	MCZ R-193094
			Rena dulcis	TNHC 60638 UAMZ R335
			Rena myopica	MCZ R-45563

			Tricheilostoma bicolor	MCZ R-49718
			Trilepida dimidiata	SAMA 40143
	Typhlopoidea	**Gerrhopilidae**	*Gerrhopilus ater*	MCZ R-33505
			Gerrhopilus beddomii	MCZ R-22372
			Gerrhopilus persephone	UMMZ 242536
		Typhlopidae	*Acutotyphlops infralabialis*	AMS R.77116
			Acutotyphlops kunuaensis	AMS R.12305
			Acutotyphlops solomonis	AMS R.11452
			Acutotyphlops subocularis	SAMA R64770
			Afrotyphlops angolensis	MCZ R-170385
			Afrotyphlops schlegelii	MCZ R-190405
			Amerotyphlops paucisquamus	MCZ R-147336
			Anilios australis	SAMA R26901
			Anilios bicolor	SAMA 60626 SAMA 62252
			Antillotyphlops monastus	MCZ R-81112
			Cubatyphlops paradoxus	MCZ R-92993
			Indotyphlops braminus	UAMZ R363
			Ramphotyphlops depressus	AMS R.129537
			Ramphotyphlops lineatus	MCZ R-37751
			Typhlops jamaicensis	USNM 12378

			Typhlops titanops	MCZ R-68571
			Xerotyphlops vermicularis	MCZ R-56477
		Xenotyphlopidae	*Xenotyphlops grandidieri*	ZSM 2194/2007 ZSM 2213/2007 ZSM 2216/2007
'Non-snake lizards'	**Amphisbaenia**	**Amphisbaenidae**	*Amphisbaena alba*	FMNH 195924
			Amphisbaena fuliginosa	FMNH 22847
		Bipedidae	*Bipes biporus*	CAS 126478
			Bipes canaliculatus	CAS 134753
		Rhineuridae	*Rhineura floridana*	FMNH 31774
		Trogonophiidae	*Agamodon anguliceps*	FMNH 264702
			Trogonophis wiegmanni	FMNH 109462
	Dibamidae		*Anelytropsis papillosus*	TCWC 45501
			Dibamus leucurus	UMMZ 174763
			Dibamus novaeguineae	UF 33488 CAS 26937
	Iguania	**Agamidae**	*Physignathus cocincinus*	YPM 14378
		Iguanidae	*Dipsosaurus dorsalis*	YPM 14376
			Sauromalus ater	TNHC 18483
		Tropiduridae	*Uranoscodon superciliosus*	YPM 12871
	Varanoidea	**Lanthanotidae**	*Lanthanotus borneensis*	FMNH 148589 YPM 6057
		Varanidae	*Varanus exanthematicus*	FMNH 58299

TABLE 3.2. Summary of morphotypes of 'microstomy', including select key synapomorphies of each morphotype. See text for details, including anatomical descriptions and additional synapomorphies. See Table 3.3 for key features summarized in taxon-character matrix format.

MORPHOTYPE AND TAXA	KEY BIOMECHANICS	KEY SYNAPOMORPHIES
Axle-brace maxillary raking (Anomalepididae)	- Suspension of maxilla from prefrontal - Bracing of maxilla by ectopterygoid - No contribution of mandible to feeding	- Reduced, arch-like, and mobile prefrontal - Reduced ectopterygoid - Highly reduced palatine, including stubby maxillary process - Inflexible mandible, with elongate angular and reduced dentition - Elongate and anteroventrally oriented quadrate
Mandibular raking (Leptotyphlopidae)	- Bilaterally synchronous retraction of mandibles - No contribution of palatomaxillary arch to feeding	- Edentulous and fixed palatomaxillary arch - Reduced mandible with flexible intramandibular joint - Robust dentary, including dental concha and symphyseal process - Structurally complex coronoid and compound bone - Extremely elongate and anteroventrally oriented quadrate
Minimal-kinesis microstomy	- No unilateral movement of jaws	- Robust and tightly integrated palatomaxillary arch elements

(Non-snake lizards)	- Minimal kinesis due to tight integration and strong bracing of jaw elements	- Tight bracing at ectopterygoid-maxilla and -pterygoid articulations - Osseous contact between premaxilla and maxilla - Well-developed basipterygoid processes - Robust mandibular elements tightly integrated, including across intramandibular joint - Symphyseal facets on mandibular symphysis - Stout and upright quadrate, with squamosal present
Single-axle maxillary raking (Typhlopoidea)	- Rotation of maxilla about maxillary process of palatine - No contribution of mandible to feeding	- Elongate and rod-like maxillary process of palatine - Deep medial excavation or foramen in maxilla - Edentulous and inflexible mandible, including elongate splenial and reduced angular - Elongate and anteroventrally oriented quadrate
Snout-shifting (Uropeltoidea and Amerophidia)	- Minor unilateral movement of palatomaxillary arches - Flexion of mandibles	- 'Ball-and-socket'-like maxilla-palatine joint - Loose palatine-pterygoid joint - Robust palatine, though lacking osseous contact with vomer - Moderate basipterygoid processes

		- Robust mandible with flexible intramandibular joint, including abutting splenial-angular contact - Stout and upright quadrate, bearing large suprastapedial process

TABLE 3.3. Key features of each morphotype of 'microstomy', presented in taxon-character matrix format. Each morphotype comprises a distinct suite of character states, with many features being entirely unique to and consistent within each morphotype (indicated by ***). Scorings are based on the exemplar taxa in Figures 3.3–3.4 for non-snake lizards, Figure 3.7 for 'anilioids', and Figures 3.9–3.11 for scolecophidians; see main text for variations within these broader groups, as well as for anatomical descriptions and additional synapomorphies.

	Axle-brace maxillary raking (Anomalepididae)	**Mandibular raking** (Leptotyphlopidae)	**Minimal-kinesis microstomy** (Non-snake lizards)	**Single-axle maxillary raking** (Typhlopoidea)	**Snout-shifting** (Uropeltoidea and Amerophidia)
Dentary teeth: present (0); absent (1).	0/1	0	0	1	0
***Dentary, tooth row, orientation**: roughly anteroposterior (0); transverse (1).	0	1	0	–	0
***Maxillary teeth**: present (0); absent (1).	0	1	0	0	0
Maxilla, tooth row, orientation: roughly anteroposterior (0); transverse (1).	1	–	0	1	0
Pterygoid teeth: absent (0); present (1).	0	0	0	0	1
Palatine teeth: absent (0); present (1).	0	0	0	0	1
***Premaxilla, articulation with maxilla, extent of integration**: broad osseous contact (0); loosely articulated (1); broadly separate (2).	2	1	0	2	1
***Frontal, articulation with prefrontal, complexity**: extensive, abutting or overlapping (0); reduced, clasping (1).	1	0	0	0	0
***Frontal, ventral facet accommodating palatine and pterygoid**: absent (0); present (1).	0	1	0	0	0
***Prefrontal, articulation with maxilla, configuration**: abutting or overlapping (0); interlocking along facial process of maxilla in	2	0	0	3	1

'peg-and-socket'-like joint (1); forked/bifurcating (2); broadly swiveling (3).					
***Palatine, articulation with pterygoid, configuration**: broadly abutting or overlapping (0); interlocking, complex but mobile (1); interlocking, simple forking (2); simple flap-overlap (3).	3	3	0/1	2	1
Palatine, medial (= choanal, vomerine) process, osseous contact with vomer: present (0); absent (1).	1	0	0	1	1
***Palatine, medial (= choanal, vomerine) process, form**: flat process extending horizontally (0); broad arch (1); narrow arch (2).	2	1	0	2	1
***Palatine, maxillary process**: present (0); highly reduced or absent (1).	1	0	0	0	0
***Palatine, maxillary process, articulation with maxilla, configuration**: broad osseous contact (0); articulating via 'ball-and-socket'-like joint accommodating palatine process of maxilla (1); articulating with large medial excavation or foramen on maxilla (2); articulation minimal (3).	–	3	0	2	1
Pterygoid, posterior process (= quadrate ramus), form: robust (0); simple, rod-like (1).	1	1	0	1	0
Ectopterygoid: present (0); absent (1).	0	1	0	1	0
***Ectopterygoid, form**: robust (0); distinctly reduced, rod-like (1).	1	–	0	–	0
Quadrate, orientation in lateral view: roughly vertical (0); slanted clearly anteriorly, nearly horizontal (1).	1	1	0	1	0
***Quadrate, shaft, length:** short/stout (0); elongate (1); extremely elongate (2).	1	2	0	1	0
Supratemporal: present (0); highly reduced or absent (1).	1	1	0	1	0
Squamosal: present (0); absent (1).	1	1	0	1	1
Parabasisphenoid, basipterygoid processes: present (0); absent (1).	1	1	0	1	0
***Parabasisphenoid, basipterygoid processes, size:** large, forming distinct projections (0); moderate, forming low ridges (1).	–	–	0	–	1

***Dentary, dental concha**: absent (0); present (1).	0	1	0	0	0
***Dentary, symphysis, articular facet**: present (0); absent (1).	1	1	0	1	1
***Dentary, symphysis, symphyseal process**: absent (0); present (1).	0	1	0	0	0
Dentary, symphysis, cartilaginous inter-ramal nodule: absent (0); present (1).	?	1	0	1	0
Angular, form: robust (0); simple, rod-like (1).	1	0	0	1	0
Splenial: present (0); absent (1).	1	0	0	0	0
Splenial, articulation with angular, configuration: overlapping (0); abutting (1).	–	1	0	0	1
***Splenial, length relative to dentary**: shorter than (0); subequal to or longer than (1).	–	0	0	1	0
Surangular-articular, fusion: unfused (0); fused to form compound bone (1).	1	1	0	1	1
***Compound bone, surangular and prearticular laminae, fusion**: fully fused (0); briefly separate (1); fully separate (2).	1	2	–	0	0
***Compound bone / surangular, anterior terminus, orientation**: not downcurved (0); distinctly downcurved (1); slightly downcurved, resulting in gentle sinusoidal shape (2).	2	0	0	1	0
***Surangular, supracotylar process**: absent (0); present (1).	0	1	0	0	0

References: Chapter Three

Al-Mohammadi, A. G. A., Khannoon, E. R. & Evans, S. E. 2020. The development of the osteocranium in the snake *Psammophis sibilans* (Serpentes: Lamprophiidae). *Journal of Anatomy*, **236**, 117–131. doi:10.1111/joa.13081

Apesteguía, S. & Zaher, H. 2006. A Cretaceous terrestrial snake with robust hindlimbs and a sacrum. *Nature*, **440**, 1037–1040. doi:10.1038/nature04413

Asplen, M. K., Whitfield, J. B., de Boer, J. G. & Heimpel, G. E. 2009. Ancestral state reconstruction analysis of hymenopteran sex determination mechanisms. *Journal of Evolutionary Biology*, **22**, 1762–1769. doi:10.1111/j.1420-9101.2009.01774.x

Bellairs, A. D. & Underwood, G. 1951. The origin of snakes. *Biological Reviews*, **26**, 193–237.

Bellairs, A. D. & Kamal, A. M. 1981. The chondrocranium and the development of the skull in recent reptiles. Pp. 1–263 in C. Gans and T.S. Parsons (eds) *Biology of the Reptilia: Morphology F*. Academic Press, London, New York, Toronto, Sydney, and San Francisco.

Betancur-R, R., Ortí, G. & Pyron, R. A. 2015. Fossil-based comparative analyses reveal ancient marine ancestry erased by extinction in ray-finned fishes. *Ecology Letters*, **18**, 441–450. doi:doi: 10.1111/ele.12423

Brock, G. T. 1932. The skull of *Leptotyphlops* (*Glauconia nigricans*). *Anatomischer Anzieger*, **73**, 199–204.

Brower, A. V. Z. & Schawaroch, V. 1996. Three steps of homology assessment. *Cladistics*, **12**, 265–272.

Burbrink, F. T., Grazziotin, F. G., Pyron, R. A., Cundall, D., Donnellan, S., Irish, F., Keogh, J. S., Kraus, F., Murphy, R. W., Noonan, B., Raxworthy, C. J., Ruane, S., Lemmon, A. R., Lemmon, E. M. & Zaher, H. 2020. Interrogating genomic-scale data for Squamata (lizards, snakes, and amphisbaenians) shows no support for key traditional morphological relationships. *Systematic Biology*, **69**(3), 502–520. doi:10.1093/sysbio/syz062

Caldwell, M. W. 2000. On the phylogenetic relationships of *Pachyrhachis* within snakes: a response to Zaher (1998). *Journal of Vertebrate Paleontology*, **20**(1), 187–190.

Caldwell, M. W. 2007a. The role, impact, and importance of fossils: snake phylogeny, origins, and evolution (1869–2006). Pp. 253–302 in J. Anderson and H.-D. Sues (eds) *Major Transitions in Vertebrate Evolution*. Indiana University Press, Bloomington, Indiana.

Caldwell, M. W. 2019. *The Origin of Snakes: Morphology and the Fossil Record*. Taylor & Francis, Boca Raton.

Campbell, J. A., Smith, E. N. & Hall, A. S. 2018. Caudals and calyces: the curious case of a consumed Chiapan colubroid. *Journal of Herpetology*, **52**(4), 459–472. doi:10.1670/18-042

Chretien, J., Wang-Claypool, C. Y., Glaw, F. & Scherz, M. D. 2019. The bizarre skull of *Xenotyphlops* sheds light on synapomorphies of Typhlopoidea. *Journal of Anatomy*, **234**, 637–655. doi:10.1111/joa.12952

Conrad, J. L. 2008. Phylogeny and systematics of Squamata (Reptilia) based on morphology. *Bulletin of the American Museum of Natural History, New York*, **310**, 1–182. doi:10.1206/310.1

Cundall, D. & Rossman, D. A. 1993. Cephalic anatomy of the rare Indonesian snake *Anomochilus weberi*. *Zoological Journal of the Linnean Society*, **109**, 235–273.

Cundall, D. 1995. Feeding behaviour in *Cylindrophis* and its bearing on the evolution of alethinophidian snakes. *Journal of Zoology*, **237**, 353–376.

Cundall, D. & Irish, F. 2008. The snake skull. Pp. 349–692 in C. Gans, A.S. Gaunt and K. Adler (eds) *Biology of the Reptilia: Morphology H, The Skull of Lepidosauria*. Society for the Study of Amphibian and Reptiles, Ithaca, New York.

Da Silva, F. O., Fabre, A.-C., Savriama, Y., Ollonen, J., Mahlow, K., Herrel, A., Müller, J. & Di-Poï, N. 2018. The ecological origins of snakes as revealed by skull evolution. *Nature Communications*, **9**, 376. doi:10.1038/s41467-017-02788-3

de Pinna, M. G. G. 1991. Concepts and tests of homology in the cladistic paradigm. *Cladistics*, **7**, 367–394.

Evans, H. E. 1955. The osteology of a worm snake, *Typhlops jamaicensis* (Shaw). *The Anatomical Record*, **122**, 381–396.

Evans, S. E. 2008. The Skull of Lizards and Tuatara. Pp. 1–347 in C. Gans, A.S. Gaunt and K. Adler (eds) *Biology of the Reptilia, Vol. 20: The Skull of Lepidosauria*. Society for the Study of Amphibians and Reptiles, Ithaca.

Figueroa, A., McKelvy, A. D., Grismer, L. L., Bell, C. D. & Lailvaux, S. P. 2016. A species-level phylogeny of extant snakes with description of a new colubrid subfamily and genus. *PLoS ONE*, **11**(9), e0161070. doi:10.1371/journal.pone.0161070

Finarelli, J. A. & Flynn, J. J. 2006. Ancestral state reconstruction of body size in the Caniformia (Carnivora, Mammalia): the effects of incorporating data from the fossil record. *Systematic Biology*, **55**(2), 301–313. doi:10.1080/10635150500541698

Finarelli, J. A. & Goswami, A. 2013. Potential pitfalls of reconstructing deep time evolutionary history with only extant data, a case study using the Canidae (Mammalia, Carnivora). *Evolution*, **67**(12), 3678–3685. doi:10.1111/evo.12222

Frazzetta, T. H. 1962. A functional consideration of cranial kinesis in lizards. *Journal of Morphology*, **111**(3), 287–319.

Fröbisch, N. B. & Schoch, R. R. 2009. Testing the impact of miniaturization on phylogeny: Paleozoic dissorophoid amphibians. *Systematic Biology*, **58**(3), 312–327. doi:10.1093/sysbio/syp029

Gans, C. & Montero, R. 2008. An atlas of amphisbaenian skull anatomy. Pp. 621–738 in C. Gans, A.S. Gaunt and K. Adler (eds) *Biology of the Reptilia. Volume 21. Morphology I. The Skull and Appendicular Locomotor Apparatus of Lepidosauria*. Society for the Study of Amphibians and Reptiles, Ithaca, New York.

Garberoglio, F. F., Apesteguía, S., Simões, T. R., Palci, A., Gómez, R. O., Nydam, R. L., Larsson, H. C. E., Lee, M. S. Y. & Caldwell, M. W. 2019a. New skulls and skeletons of the Cretaceous legged snake *Najash*, and the evolution of the modern snake body plan. *Science Advances*, **5**(11), eaax5833. doi:10.1126/sciadv.aax5833

Garberoglio, F. F., Gómez, R. O., Apesteguía, S., Caldwell, M. W., Sánchez, M. L. & Veiga, G. 2019b. A new specimen with skull and vertebrae of *Najash rionegrina* (Lepidosauria: Ophidia) from the early Late Cretaceous of Patagonia. *Journal of Systematic Palaeontology*, **17**(18), 1533–1550. doi:10.1080/14772019.2018.1534288

Gauthier, J., Kluge, A. G. & Rowe, T. 1988a. Amniote phylogeny and the importance of fossils. *Cladistics*, **4**, 105–209.

Gauthier, J. A., Kearney, M., Maisano, J. A., Rieppel, O. & Behlke, A. D. B. 2012. Assembling the squamate tree of life: perspectives from the phenotype and the fossil

record. *Bulletin of the Peabody Museum of Natural History*, **53**, 3–308. doi:10.3374/014.053.0101

Gould, S. J. 1977. *Ontogeny and Phylogeny*. Harvard University Press, Cambridge.

Greer, A. E. 1985. The relationships of the lizard genera *Anelytropsis* and *Dibamus*. *Journal of Herpetology*, **19**(1), 116–156.

Griffith, O. W., Blackburn, D. G., Brandley, M. C., van Dyke, J. U., Whittington, C. M. & Thompson, M. B. 2015. Ancestral state reconstructions require biological evidence to test evolutionary hypotheses: a case study examining the evolution of reproductive mode in squamate reptiles. *Journal of Experimental Zoology, Part B: Molecular and Developmental Evolution*, **324B**, 493–503. doi:10.1002/jez.b.22614

Haas, G. 1930. Über das Kopfskelett und die Kaumuskulatur der Typhlopiden und Glauconiiden. *Zoologische Jahrbücher. Abteilung für Anatomie*, **52**, 1–94.

Haas, G. 1964. Anatomical observations on the head of *Liotyphlops albirostris* (Typhlopidae, Ophidia). *Acta Zoologica*, **1964**, 1–62.

Haas, G. 1968. Anatomical observations on the head of *Anomalepis aspinosus* (Typhlopidae, Ophidia). *Acta Zoologica*, **48**, 63–139.

Hanken, J. 1984. Miniaturization and its effects on cranial morphology in plethodontid salamanders, genus *Thorius* (Amphibia: Plethodontidae). I. Osteological variation. *Biological Journal of the Linnean Society*, **23**, 55–75.

Hanken, J. & Wake, D. B. 1993. Miniaturization of body size: organismal consequences and evolutionary significance. *Annual Review of Ecology and Systematics*, **24**, 501–519.

Harrington, S. M. & Reeder, T. W. 2017. Phylogenetic inference and divergence dating of snakes using molecules, morphology and fossils: new insights into convergent evolution of feeding morphology and limb reduction. *Biological Journal of the Linnean Society*, **121**, 379–394.

Hawkins, J. A., Hughes, C. E. & Scotland, R. W. 1997. Primary homology assessment, characters and character States. *Cladistics*, **13**, 275–283.

Hawlitschek, O., Scherz, M. D., Webster, K. C., Ineich, I. & Glaw, F. 2021. Morphological, osteological, and genetic data support a new species of *Madatyphlops* (Serpentes: Typhlopidae) endemic to Mayotte Island, Comoros Archipelago. *The Anatomical Record*, **2021**, 1–15. doi:10.1002/ar.24589

Hsiang, A. Y., Field, D. J., Webster, T. H., Behlke, A. D. B., Davis, M. B., Racicot, R. A. & Gauthier, J. A. 2015. The origin of snakes: revealing the ecology, behavior, and evolutionary history of early snakes using genomics, phenomics, and the fossil record. *BMC Evolutionary Biology*, **15**, 87. doi:10.1186/s12862-015-0358-5

Iordansky, N. N. 1997. Jaw apparatus and feeding mechanics of *Typhlops* (Ophidia: Typhlopidae): a reconsideration. *Russian Journal of Herpetology*, **4**(2), 120–127.

Kamal, A. M. 1966. On the process of rotation of the quadrate cartilage in Ophidia. *Anatomischer Anzieger*, **118**, 87–90.

Kearney, M. & Stuart, B. L. 2004. Repeated evolution of limblessness and digging heads in worm lizards revealed by DNA from old bones. *Proceedings of the Royal Society of London, Series B: Biological Sciences*, **271**, 1677–1683. doi:10.1098/rspb.2004.2771

Kley, N. J. & Brainerd, E. L. 1999. Feeding by mandibular raking in a snake. *Nature*, **402**, 369–370. doi:10.1038/46460

Kley, N. J. 2001. Prey transport mechanisms in blindsnakes and the evolution of unilateral feeding systems in snakes. *American Zoologist*, **41**, 1321–1337.

Kley, N. J. 2006. Morphology of the lower jaw and suspensorium in the Texas blindsnake, *Leptotyphlops dulcis* (Scolecophidia: Leptotyphlopidae). *Journal of Morphology*, **267**, 494–515. doi:10.1002/jmor.10414

Kraus, F. 2017. New species of blindsnakes (Squamata: Gerrhopilidae) from the offshore islands of Papua New Guinea. *Zootaxa*, **4299**(7), 75–94. doi:10.11646/zootaxa.4299.1.3

Lee, M. S. Y. 1998. Convergent evolution and character correlation in burrowing reptiles: towards a resolution of squamate relationships. *Biological Journal of the Linnean Society*, **65**, 369–453.

Lee, M. S. Y. & Caldwell, M. W. 1998. Anatomy and relationships of *Pachyrhachis problematicus*, a primitive snake with hindlimbs. *Philosophical Transactions of the Royal Society of London, Series B: Biological Sciences*, **353**(1375), 1521–1552.

Lewis, P. O. 2001. A likelihood approach to estimating phylogeny from discrete morphological character data. *Systematic Biology*, **50**(6), 913–925.

List, J. C. 1966. Comparative osteology of the snake families Typhlopidae and Leptotyphlopidae. *Illinois Biological Monographs*, **36**, 1–112.

Mabee, P. M., Balhoff, J. P., Dahdul, W. M., Lapp, H., Mungall, C. J. & Vision, T. J. 2020. A logical model of homology for comparative biology. *Systematic Biology*, **69**(2), 345–362. doi:10.1093/sysbio/syz067

Maddin, H. C., Olori, J. C. & Anderson, J. S. 2011. A redescription of *Carrolla craddocki* (Lepospondyli: Brachystelechidae) based on high-resolution CT, and the impacts of miniaturization and fossoriality on morphology. *Journal of Morphology*, **272**, 722–743. doi:10.1002/jmor.10946

Maddison, W. P. & Maddison, D. R. 2006. StochChar: a package of Mesquite modules for stochastic models of character evolution

Maddison, W. P. & Maddison, D. R. 2019. Mesquite: a modular system for evolutionary analysis. http://mesquiteproject.org

Mahendra, B. C. 1936. Contributions to the osteology of the Ophidia. I. The endoskeleton of the so-called 'blind-snake', *Typhlops braminus* Daud. *Proceedings of the Indian Academy of Sciences*, **3**, 128–142.

Martins, A., Koch, C., Pinto, R., Folly, M., Fouquet, A. & Passos, P. 2019. From the inside out: discovery of a new genus of threadsnakes based on anatomical and molecular data, with discussion of the leptotyphlopid hemipenial morphology. *Journal of Zoological Systematics and Evolutionary Research*, **57**, 840–863. doi:10.1111/jzs.12316

McDowell, S. B. & Bogert, C. M. 1954. The systematic position of *Lanthanotus* and the affinities of the anguimorphan lizards. *Bulletin of the American Museum of Natural History, New York*, **105**, 1–142.

McNamara, K. J. 1986. A guide to the nomenclature of heterochrony. *Journal of Paleontology*, **60**(1), 4–13.

Miralles, A., Marin, J., Markus, D., Herrel, A., Hedges, S. B. & Vidal, N. 2018. Molecular evidence for the paraphyly of Scolecophidia and its evolutionary implications. *Journal of Evolutionary Biology*, **31**, 1782–1793. doi:10.1111/jeb.13373

Mongiardino Koch, N. & Parry, L. A. 2020. Death is on our side: paleontological data drastically modify phylogenetic hypotheses. *Systematic Biology*, **69**(6), 1052–1067. doi:10.1093/sysbio/syaa023

Nagy, Z. T., Marion, A. B., Glaw, F., Miralles, A., Nopper, J., Vences, M. & Hedges, S. B. 2015. Molecular systematics and undescribed diversity of Madagascan scolecophidian snakes (Squamata: Serpentes). *Zootaxa*, **4040**(1), 31–47. doi:10.11646/zootaxa.4040.1.3

Object Research Systems Inc. 2019b. Dragonfly 4.1. Object Research Systems (ORS) Inc., Montreal, Canada. https://theobjects.com/dragonfly/

Ollonen, J., Silva, F. O. D., Mahlow, K. & Di-Poï, N. 2018. Skull development, ossification pattern, and adult shape in the emerging lizard model organism *Pogona vitticeps*: a comparative analysis with other squamates. *Frontiers in Physiology*, **9**, 278. doi:10.3389/fphys.2018.00278

Olori, J. C. & Bell, C. J. 2012. Comparative skull morphology of uropeltid snakes (Alethinophidia: Uropeltidae) with special reference to disarticulated elements and variation. *PLoS ONE*, **7**(3), e32450. doi:10.1371/journal.pone.0032450

Palci, A., Lee, M. S. Y. & Hutchinson, M. N. 2016. Patterns of postnatal ontogeny of the skull and lower jaw of snakes as revealed by micro-CT scan data and three-dimensional geometric morphometrics. *Journal of Anatomy*, **229**(6), 723–754. doi:10.1111/joa.12509

Palci, A., Caldwell, M. W., Hutchinson, M. N., Konishi, T. & Lee, M. S. Y. 2020a. The morphological diversity of the quadrate bone in squamate reptiles as revealed by high-resolution computed tomography and geometric morphometrics. *Journal of Anatomy*, **236**, 210–227. doi:10.1111/joa.13102

Patterson, C. 1982. Morphological characters and homology. Pp. 21–74 in K.A. Joysey and A.E. Friday (eds) *Problems of Phylogenetic Reconstruction*. Academic Press, London and New York.

Patterson, C. 1988. Homology in classical and molecular biology. *Molecular Biology and Evolution*, **5**(6), 603–625.

Pinto, R. R., Martins, A. R., Curcio, F. & Ramos, L. O. 2015. Osteology and cartilaginous elements of *Trilepida salgueiroi* (Amaral, 1954) (Scolecophidia: Leptotyphlopidae). *The Anatomical Record*, **298**, 1722–1747. doi:10.1002/ar.23191

Polachowski, K. M. & Werneburg, I. 2013. Late embryos and bony skull development in *Bothropoides jararaca* (Serpentes, Viperidae). *Zoology*, **116**, 36–63. doi:10.1016/j.zool.2012.07.003

Puttick, M. N. 2016. Partially incorrect fossil data augment analyses of discrete trait evolution in living species. *Biology Letters*, **12**, 20160392. doi:10.1098/rsbl.2016.0392

Pyron, R. A., Burbrink, F. T. & Wiens, J. J. 2013. A phylogeny and revised classification of Squamata, including 4161 species of lizards and snakes. *BMC Evolutionary Biology*, **13**, 93. doi:10.1186/1471-2148-13-93

Reeder, T. W., Townsend, T. M., Mulcahy, D. G., Noonan, B. P., Wood, P. L., Sites, J. W. & Wiens, J. J. 2015. Integrated analyses resolve conflicts over squamate reptile phylogeny and reveal unexpected placements for fossil taxa. *PLoS ONE*, **10**(3), e0118199. doi:10.1371/journal.pone.0118199

Rieppel, O. 1977. Studies on the skull of the Henophidia (Reptilia: Serpentes). *Journal of Zoology*, **181**, 145–173.

Rieppel, O. 1984a. Miniaturization of the lizard skull: its functional and evolutionary implications. *Symposia of the Zoological Society of London*, **52**, 503–520.

Rieppel, O. 1984b. The cranial morphology of the fossorial lizard genus *Dibamus* with a consideration of its phylogenetic relationships. *Journal of Zoology*, **204**, 289–327.

Rieppel, O. 1988. A review of the origin of snakes. Pp. 37–130 in M.K. Hecht, B. Wallace and G.T. Prance (eds) *Evolutionary Biology*. Springer, Boston, MA.

Rieppel, O. 1994. Homology, topology, and typology: the history of modern debates. Pp. 63–100 in B.K. Hall (ed) *Homology: The Hierarchical Basis of Comparative Biology*. Academic Press, San Diego.

Rieppel, O. 1996. Miniaturization in tetrapods: consequences for skull morphology. Pp. 47–61 in P.J. Miller (ed) *Miniature Vertebrates: The Implications of Small Body Size, Vol. 69. Symposia of the Zoological Society of London*. Claredon Press, Oxford.

Rieppel, O. & Zaher, H. 2000. The intramandibular joint in squamates, and the phylogenetic relationships of the fossil snake *Pachyrhachis problematicus* Haas. *Fieldiana Geology*, **43**, 1–69.

Rieppel, O. & Kearney, M. 2002. Similarity. *Biological Journal of the Linnean Society*, **75**, 59–82.

Rieppel, O. & Maisano, J. A. 2007. The skull of the rare Malaysian snake *Anomochilus leonardi* Smith, based on high-resolution X-ray computed tomography. *Zoological Journal of the Linnean Society*, **149**, 671–685.

Rieppel, O., Kley, N. J. & Maisano, J. A. 2009. Morphology of the skull of the white-nosed blindsnake, *Liotyphlops albirostris* (Scolecophidia: Anomalepididae). *Journal of Morphology*, **270**, 536–557. doi:10.1002/jmor.10703

Rieppel, O. 2012. "Regressed" macrostomatan snakes. *Fieldiana Life and Earth Sciences*, **2012**(5), 99–103. doi:10.3158/2158-5520-5.1.99

Santos, F. J. M. & Reis, R. E. 2019. Redescription of the blind snake *Anomalepis colombia* (Serpentes: Anomalepididae) using high-resolution X-ray computed tomography. *Copeia*, **107**(2), 239–243. doi:10.1643/CH-19-181

Scanferla, A. 2016. Postnatal ontogeny and the evolution of macrostomy in snakes. *Royal Society Open Science*, **3**, 160612. doi:10.1098/rsos.160612

Sereno, P. C. 2007. Logical basis for morphological characters in phylogenetics. *Cladistics*, **23**(6), 565–587. doi:10.1111/j.1096-0031.2007.00161.x

Simões, T. R., Caldwell, M. W., Palci, A. & Nydam, R. L. 2017. Giant taxon-character matrices: quality of character constructions remains critical regardless of size. *Cladistics*, **33**, 198–219. doi:10.1111/cla.12163

Simões, T. R., Caldwell, M. W., Tałanda, M., Bernardi, M., Palci, A., Vernygora, O., Bernardini, F., Mancini, L. & Nydam, R. L. 2018. The origin of squamates revealed by a Middle Triassic lizard from the Italian Alps. *Nature*, **557**, 706–709. doi:10.1038/s41586-018-0093-3

Strong, C. R. C., Simões, T. R., Caldwell, M. W. & Doschak, M. R. 2019. Cranial ontogeny of *Thamnophis radix* (Serpentes: Colubroidea) with a re-evaluation of current paradigms of snake skull evolution. *Royal Society Open Science*, **6**, 182228. doi:10.1098/rsos.182228

Strong, C. R. C., Palci, A. & Caldwell, M. W. 2021a. Insights into skull evolution in fossorial snakes, as revealed by the cranial morphology of *Atractaspis irregularis* (Serpentes: Colubroidea). *Journal of Anatomy*, **238**, 146–172. doi:10.1111/joa.13295

Struck, T. H. 2007. Data congruence, paedomorphosis and salamanders. *Frontiers in Zoology*, **4**, 22. doi:10.1186/1742-9994-4-22

Vidal, N. & Hedges, S. B. 2002. Higher-level relationships of snakes inferred from four nuclear and mitochondrial genes. *Comptes Rendus Biologies*, **325**, 977–985.

Wake, M. H. 1986. The morphology of *ldiocranium russeli* (Amphibia: Gymnophiona), with comments on miniaturization through heterochrony. *Journal of Morphology*, **189**, 1–16.

Werneburg, I., Polachowski, K. M. & Hutchinson, M. N. 2015. Bony skull development in the Argus monitor (Squamata, Varanidae, *Varanus panoptes*) with comments on developmental timing and adult anatomy. *Zoology*, **118**, 255–280. doi:10.1016/j.zool.2015.02.004

Wiens, J. J., Bonett, R. M. & Chippindale, P. T. 2005. Ontogeny discombobulates phylogeny: paedomorphosis and higher-level salamander relationships. *Systematic Biology*, **54**(1), 91–110. doi:10.1080/10635150590906037

Wiens, J. J., Kuczynski, C. A., Townsend, T. M., Reeder, T. W., Mulcahy, D. G. & Sites, J. W. J. 2010. Combining phylogenomics and fossils in higher-level squamate reptile phylogeny: molecular data change the placement of fossil taxa. *Systematic Biology*, **59**(6), 674–688. doi:10.1093/sysbio/syq048

Wilkinson, M. 1995. A comparison of two methods of character construction. *Cladistics*, **11**, 297–308.

Zaher, H. 1998. The phylogenetic position of *Pachyrhachis* within snakes (Squamata, Lepidosauria). *Journal of Vertebrate Paleontology*, **18**(1), 1–3. doi:10.1080/02724634.1998.10011029

Zaher, H. & Rieppel, O. 1999a. The phylogenetic relationships of *Pachyrhachis problematicus*, and the evolution of limblessness in snakes (Lepidosauria, Squamata). *Comptes Rendus de l'Académie des Sciences - Series IIA - Sciences de la Terre et des planètes/Earth and Planetary Science*, **329**, 831–837.

Zaher, H. & Rieppel, O. 2002. On the phylogenetic relationships of the Cretaceous snakes with legs, with special reference to *Pachyrhachis problematicus* (Squamata, Serpentes). *Journal of Vertebrate Paleontology*, **22**(1), 104–109.

Zheng, Y. & Wiens, J. J. 2016. Combining phylogenomic and supermatrix approaches, and a time-calibrated phylogeny for squamate reptiles (lizards and snakes) based on 52 genes and 4162 species. *Molecular Phylogenetics and Evolution*, **94**, 537–547. doi:10.1016/j.ympev.2015.10.009

CHAPTER FOUR: CONVERGENCE, DIVERGENCE, AND MACROEVOLUTIONARY CONSTRAINT AS REVEALED BY ANATOMICAL NETWORK ANALYSIS OF THE SQUAMATE SKULL

4.1. Introduction

Squamates (i.e., lizards, including snakes) are one of the major groups of vertebrates and as such exhibit a broad range of ecological, morphological, and taxonomic diversity. Not surprisingly, though, a number of aspects of their anatomy and evolution remain poorly understood and thus highly debated (Watanabe *et al.* 2019). Recent discussions of snake anatomy and evolutionary development (e.g., Palci *et al.* 2016; Da Silva *et al.* 2018; Caldwell 2019; Chretien *et al.* 2019; Garberoglio *et al.* 2019a; Strong *et al.* 2019; Strong *et al.* 2021a; Strong *et al.* 2021b) have undertaken renewed examination of several broader problems concerning the evolution of snakes as a kind of lizard; many of these controversies concern the ecological and phylogenetic origins of snakes, focussing particularly on the enigmatic scolecophidians (Caldwell 2019).

Scolecophidians ('blindsnakes') have traditionally been considered to occupy a fundamentally plesiomorphic status among snakes, with their miniaturized and fossorial ecomorphology viewed as reflecting the ancestral snake condition (e.g., Mahendra 1936, 1938; Bellairs & Underwood 1951; List 1966; Wiens *et al.* 2012; Miralles *et al.* 2018). However, this perspective on scolecophidian anatomy and evolution is not universal. Over the past several decades, many authors have suggested that scolecophidians may instead be a highly autapomorphic group not strictly reflecting an ancestral snake morphology (e.g., Schmidt 1950; Rieppel 1988; Kley & Brainerd 1999; Lee & Scanlon 2002; Palci & Caldwell 2010; Hsiang *et al.* 2015). Only recently, though, has this hypothesis been examined in detail and strongly advocated (e.g., Simões *et al.* 2015; Caldwell 2019; Chretien *et al.* 2019; Strong *et al.* 2021a; Strong *et al.* 2021b).

This dissenting perspective focusses largely on the role of miniaturization, fossoriality, and heterochrony in misleading existing perspectives on snake evolution (see e.g., Caldwell 2019; Chretien *et al.* 2019; Strong *et al.* 2021a; Strong *et al.* 2021b). Indeed, fossoriality and miniaturization are widely recognized as major sources of convergence in vertebrates (e.g., Hanken & Wake 1993; Lee 1998; Maddin *et al.* 2011), and particularly squamates (e.g., Savitzky 1983; Rieppel 1984b, 1988, 1996; Lee 1998; Rieppel & Zaher 2000; Townsend *et al.* 2004; Wiens *et al.* 2006; Wiens *et al.* 2010; Olori & Bell 2012; Reeder *et al.* 2015; Da Silva *et al.* 2018; Watanabe *et al.* 2019; Ebel *et al.* 2020; Strong *et al.* 2021a; Strong *et al.* 2021b), which

has contributed greatly to ongoing conflicts in hypotheses of squamate evolution (see also Lee 1998; Cundall & Irish 2008).

Prominent among the purportedly plesiomorphic conditions exhibited by scolecophidians—and in turn playing a major role in recent re-examinations of snake evolution and hypotheses of convergence (e.g., Chretien *et al.* 2019; Strong *et al.* 2021b)—is the feeding mechanism of 'microstomy'. Snakes have traditionally been divided into two groups based on jaw mechanics: 'macrostomy' and 'microstomy', i.e., large- and small-gaped feeding, respectively (see e.g., Rieppel 1988). Reflecting a condition in which the snake is able to consume prey items larger than its own head (Rieppel 2012; Scanferla 2016; Harrington & Reeder 2017; Caldwell 2019), 'macrostomy' has traditionally been considered a synapomorphic condition uniting 'advanced' snakes (i.e., booid-pythonoids and caenophidians) into the clade Macrostomata (Fig. 4.1a; see Rieppel 1988; Caldwell 2019, and historical overviews therein). In contrast, 'microstomy' is the inability to consume these proportionally large prey items (Rieppel 1988; Caldwell 2019). Traditionally considered present in early-diverging snakes such as scolecophidians and anilioids, as well as in non-snake lizards (Fig. 4.1), the 'microstomatan' feeding mechanisms of these taxa are typically viewed as homologous, with scolecophidians in particular portrayed as retaining the non-snake lizard condition (e.g., Rieppel 2012; Miralles *et al.* 2018).

However, this traditional morphofunctional categorization has been the subject of recent re-examination. 'Macrostomatan' snakes have increasingly been recovered as non-monophyletic in molecular (Fig. 4.1b; e.g., Vidal & Hedges 2002; Wiens *et al.* 2012; Pyron *et al.* 2013; Streicher & Wiens 2016; Burbrink *et al.* 2020) and combined-data (e.g., Reeder *et al.* 2015) analyses, with booid-pythonoids and caenophidians also undergoing different ontogenetic trajectories before reaching their respective endpoint 'macrostomatan' morphologies (Cundall & Irish 2008; Palci *et al.* 2016). Similarly, recent authors (e.g., Harrington & Reeder 2017; Caldwell 2019; Chretien *et al.* 2019; Strong *et al.* 2021b) have strongly argued for the non-homology of 'microstomy' across supposedly 'microstomatan' squamates, based on fundamental anatomical differences across these groups. Most recently, Strong *et al.* (2021b) proposed five non-homologous and morphofunctionally distinct morphotypes of 'microstomy': 'minimal-kinesis microstomy' in non-snake lizards, 'snout-shifting' (*sensu* Cundall 1995) in anilioid snakes, 'single-axle maxillary raking' in typhlopoid scolecophidians, 'axle-brace maxillary

raking' in anomalepidid scolecophidians, and 'mandibular raking' (*sensu* Kley & Brainerd 1999) in leptotyphlopid scolecophidians. These findings altogether indicate that the squamate jaw complex may have a much more complicated evolutionary history—including much more widespread convergence—than the traditional paradigm of derived 'macrostomy' *versus* plesiomorphic 'microstomy' would suggest (Vidal & Hedges 2002; Palci *et al.* 2016; Scanferla 2016; Harrington & Reeder 2017; Caldwell 2019; Chretien *et al.* 2019; Strong *et al.* 2019; Burbrink *et al.* 2020; Strong *et al.* 2021a; Strong *et al.* 2021b).

However, even though these analyses present numerous arguments regarding squamate evolution, they are all mainly qualitative in nature, based primarily on comparative anatomical descriptions and re-assessments. Except for a few ancestral state reconstructions (e.g., Hsiang *et al.* 2015; Harrington & Reeder 2017; Miralles *et al.* 2018; Watanabe *et al.* 2019; Strong *et al.* 2021b) and geometric morphometric analyses (e.g., Monteiro & Abe 1997; Sanger *et al.* 2012; Palci *et al.* 2016; Andjelković *et al.* 2017; Da Silva *et al.* 2018; Urošević *et al.* 2019; Watanabe *et al.* 2019; Rhoda *et al.* 2021), snake skull evolution—including the question of jaw structure—has yet to be thoroughly examined from a quantitative anatomical perspective.

One method capable of addressing this gap is the recently developed technique of anatomical network analysis (AnNA; Rasskin-Gutman & Esteve-Altava 2014). Based on the mathematical discipline of graph theory, AnNA assesses morphological integration by distilling anatomical structures into a network of 'nodes' and 'connections' (Rasskin-Gutman & Buscalioni 2001; Rasskin-Gutman 2003; Esteve-Altava *et al.* 2011; Esteve-Altava & Rasskin-Gutman 2014; Rasskin-Gutman & Esteve-Altava 2014). This technique thus enables the analysis of organizational modularity, i.e., the arrangement of a complex anatomical system into subdivisions comprising parts that interact more closely with each other than with the anatomical parts of other such regions (Esteve-Altava 2017a). This connectivity-based approach is particularly useful when studying morphofunctional arrangements and interactions (Rasskin-Gutman & Esteve-Altava 2014; Esteve-Altava 2017a; Werneburg *et al.* 2019).

Although connectivity has long played an important role in evolutionary morphology (see Rasskin-Gutman & Esteve-Altava 2014 for a historical overview), AnNA was only recently fully formalized into an explicit quantitative framework (Rasskin-Gutman & Esteve-Altava 2014). Since 2014, this method has been used to study morphological integration across vertebrates, from early tetrapods (e.g., Esteve-Altava *et al.* 2018; Esteve-Altava *et al.* 2019) to archosaurs

(e.g., Werneburg *et al.* 2019; Lee *et al.* 2020; Plateau & Foth 2020) to synapsids (e.g., Esteve-Altava *et al.* 2013; Esteve-Altava *et al.* 2015; Navarro-Díaz *et al.* 2019; Ziermann *et al.* 2021). However, non-archosaur reptiles have not yet been examined in depth using this method.

Indeed, squamates have been the focus of only a handful of analyses of skull modularity and integration (e.g., Monteiro & Abe 1997; Sanger *et al.* 2012; Andjelković *et al.* 2017; Urošević *et al.* 2019; Watanabe *et al.* 2019; Rhoda *et al.* 2021), all of which used geometric-morphometric (GM)-based approaches and only two of which (Watanabe *et al.* 2019; Rhoda *et al.* 2021) included a broad taxonomic sampling. Furthermore, because AnNA assesses connectivity rather than form (i.e., shape or size), this method thus provides a complementary but fundamentally distinct perspective on modularity and integration compared to covariation-based analyses of these phenomena (Rasskin-Gutman & Buscalioni 2001; Rasskin-Gutman 2003; Esteve-Altava *et al.* 2013; Rasskin-Gutman & Esteve-Altava 2014; Esteve-Altava 2017a).

AnNA also provides certain advantages over GM-based analysis. For example, the specific identity of the anatomical 'nodes' does not play a role in AnNA, meaning that, in contrast to GM (Monteiro & Abe 1997; Polly 2008; Palci & Lee 2019), this approach to modularity analysis is not affected by assessments of homology (Esteve-Altava *et al.* 2018). This is especially important when incorporating elements whose homology is debated (e.g., the angular in anomalepidids, the circumorbital ossifications among squamates, several skull elements in amphisbaenians; see Gans & Montero 2008; Rieppel *et al.* 2009; Palci & Caldwell 2013). Similarly, because AnNA assesses patterns of connectivity independent of element identity, elements that are absent or highly aberrant in some study taxa do not have to be excluded *a priori* from the overall analysis (Esteve-Altava *et al.* 2019); in contrast, such structures interfere with the landmark correspondence required for GM-based analyses, and thus these non-universal landmarks—or the specimens lacking them—would typically have to be excluded from those analyses (Adams *et al.* 2004; Polly 2008; Palci & Lee 2019).

Anatomical network analysis thus presents a promising avenue for research into the evolutionary morphology of squamates. Based on recent discussions of scolecophidian anatomy and evolution (e.g., Simões *et al.* 2015; Harrington & Reeder 2017; Caldwell 2019; Chretien *et al.* 2019; Strong *et al.* 2021a; Strong *et al.* 2021b)—including re-examinations of 'microstomy' (Harrington & Reeder 2017; Caldwell 2019; Chretien *et al.* 2019; Strong *et al.* 2021b)—and suggestions of convergence among squamates (e.g., Savitzky 1983; Rieppel 1984b, 1988, 1996;

Lee 1998; Rieppel & Zaher 2000; Townsend *et al.* 2004; Wiens *et al.* 2006; Wiens *et al.* 2010; Olori & Bell 2012; Reeder *et al.* 2015; Da Silva *et al.* 2018; Watanabe *et al.* 2019; Ebel *et al.* 2020; Strong *et al.* 2021a; Strong *et al.* 2021b)—including scolecophidians (Caldwell 2019; Chretien *et al.* 2019; Strong *et al.* 2021b)—I therefore present two major hypotheses to be tested herein.

First, following recent arguments of the non-homology of 'microstomy' across squamates (e.g., Harrington & Reeder 2017; Caldwell 2019; Chretien *et al.* 2019; Strong *et al.* 2021b), I hypothesize that the major groups of 'microstomatans' (i.e., non-snake lizards, anilioids, anomalepidids, leptotyphlopids, and typhlopoids; Fig. 4.1) will exhibit different patterns of skull modularity, particularly in relation to the jaw elements. If 'microstomy' occurs via distinct mechanisms across squamates, as recently suggested, then we would expect the jaw elements to form different modules across 'microstomatans'. Conversely, if 'microstomy' is indeed equivalent across squamates, then we would expect the jaw elements to show consistent modularity across all 'microstomatans'. I will test this hypothesis using the network dendrograms produced by AnNA, focussing on the modularity of the upper jaw elements because the mandibles tend to form consistent modules across all vertebrates (compare e.g., Werneburg *et al.* 2019; Plateau & Foth 2020).

Based on hypotheses of convergence among squamates (see references above), I further hypothesize that the fossorial taxa included in this analysis (i.e., scolecophidians, amphisbaenians, dibamids, many anilioids, and some caenophidians) will exhibit convergent network structures, as will the miniaturized taxa (i.e., scolecophidians, dibamids, many amphisbaenians, many anilioids, and some caenophidians). I will test this hypothesis using the patterns of morphospace occupation produced by principal component analysis (PCA) of the underlying network parameters. If these phenomena are not associated with convergence, then we would expect miniaturized taxa to be dispersed across morphospace, and to occupy the same region of morphospace as non-miniaturized taxa; conversely, if miniaturization does drive anatomical convergence, then we would expect miniaturized and non-miniaturized taxa to occupy distinct regions of morphospace. The same prediction applies to the question of convergence associated with habitat.

By applying AnNA to squamates for the first time, this study therefore addresses the dearth of quantitative analyses related to the anatomical modularity and integration of this group.

Focussing on snakes and especially scolecophidians, this network analysis thus provides novel quantitative insight into the anatomy and evolution of the squamate skull.

4.2. Methods

4.2.1. Taxon sampling

Because this study aims in part to compare 'microstomy' across squamates, taxon sampling was in turn focussed on 'microstomatan' groups. This includes representatives of every major typhlopoid subclade, every anomalepidid genus, almost every leptotyphlopid tribe as outlined by Adalsteinsson *et al.* (2009), every anilioid family, and each of the major non-snake lizard groups often hypothesized as the sister-group of snakes (Fig. 4.1; Table 4.1). I also included several 'macrostomatans' (i.e., booid-pythonoids and caenophidians; Fig. 4.1; Table 4.1) in order to encapsulate the variation across squamates, thus providing a comparative framework in relation to 'microstomatans' and more fully establishing the squamate morphospace.

4.2.2. Network modelling

I modelled each anatomical network by coding each skull into an unweighted and undirected adjacency matrix (Appendix 4.1), in which scores of '1' indicate a connection between elements and scores of '0' indicate a lack of connection (see e.g., Rasskin-Gutman & Esteve-Altava 2014; Esteve-Altava 2017a; Werneburg *et al.* 2019). Although other studies typically consider these connections to represent the sutures or direct physical contacts among elements (e.g., Esteve-Altava *et al.* 2019; Plateau & Foth 2020), this is not a requisite definition; depending on the goal of the analysis and the nature of the question being examined, 'connections' could represent any of countless forms of linkage between nodes in the network (Esteve-Altava 2017a). Due to the loose overall articulation of the snake skull, bones were herein considered 'connected' if in osseous contact or if closely integrated though lacking direct physical contact. For example, in snakes, the palatine typically does not directly contact the maxilla, in contrast to the extensive osseous contact typical of non-snake lizards; however, these elements do come into close proximity, with one or both bones often bearing processes mediating this junction. As such, it is reasonable to still consider these elements 'connected'. This more lenient method of scoring the adjacency matrix is important when analyzing a highly

kinetic structure such as the snake skull, particularly in accurately reflecting patterns of connectivity and functional integration without over-estimating modularity or separation among elements.

Each anatomical network was scored based on direct observation of micro-computed tomography (micro-CT) scans of each specimen (Table 4.1), visualized using Dragonfly 4.1 (Object Research Systems Inc 2019b). I performed the scans of MCZ specimens, which are available on MorphoSource.org; other scans were obtained from DigiMorph.org and MorphoSource.org (see Appendix 1.1 for further information). These observations were supplemented with published descriptions of anatomy and functional integration where available; relevant taxa include typhlopids (Mahendra 1936; Evans 1955), gerrhopilids (Kraus 2017), xenotyphlopids (Chretien *et al.* 2019), anomalepidids (Haas 1968; Rieppel *et al.* 2009), leptotyphlopids (Kley 2006; Koch *et al.* 2019), *Atractaspis* (Deufel & Cundall 2003), booid-pythonoids (Frazzetta 1966; Rieppel 1977), *Casarea* (Maisano & Rieppel 2007), anilioids (Rieppel 1977; Cundall & Rossman 1993; Cundall 1995; Rieppel & Maisano 2007; Olori & Bell 2012), amphisbaenians (Gans & Montero 2008), dibamids (Rieppel 1984b; Evans 2008), iguanians (Evans 2008; Bell *et al.* 2009; Gray 2018), and varanids (Evans 2008; Werneburg *et al.* 2015).

4.2.3. Anatomical network analysis

All anatomical network analyses were performed in R v4.0.3 (R Core Team 2020), using the package *igraph* (Csárdi & Nepusz 2006) and the core R package *stats* (R Core Team 2020). The AnNA script (Appendix 4.2) is modified from Werneburg *et al.* (2019) and Plateau & Foth (2020), with the parcellation calculation adapted from Esteve-Altava *et al.* (2018). This network analysis algorithm produces two major outputs, as described below, reflecting the modularity and integration of each skull network.

4.2.3.1. Network dendrograms and modular composition

A key output of AnNA is the generation of dendrograms reflecting the pattern of connectivity among each network's nodes (Figs 4.2–4.8 and S4.1–S4.57). These dendrograms were created using the generalized topological overlap measure (GTOM) introduced by Yip & Horvath (2006) and Yip & Horvath (2007). This method first converts the aforementioned adjacency matrix into a similarity matrix—i.e., a generalized topological overlap matrix—based

on the extent to which each node overlaps with (i.e., connects to the same neighbouring nodes as) each other node (Yip & Horvath 2006). This GTOM matrix is then converted into a dissimilarity or distance matrix, which is in turn analyzed by a hierarchical clustering algorithm—in this case, UPGMA (i.e., unweighted pair group method with arithmetic mean)—to arrange the nodes into a dendrogram. Essentially, nodes with a greater number of shared neighbours have a higher topological overlap than nodes with fewer shared neighbours, are therefore more likely to belong to the same anatomical module, and thus are ultimately recovered closer to each other in the dendrogram than nodes with fewer shared neighbours (Yip & Horvath 2006; Esteve-Altava *et al.* 2013; Rasskin-Gutman & Esteve-Altava 2014; Esteve-Altava 2017a; Werneburg *et al.* 2019; Plateau & Foth 2020).

Once established, each dendrogram must then be partitioned into modules. The main technique used herein for module identification implements the modularity Q-value as introduced by Clauset *et al.* (2004) and Newman & Girvan (2004). This parameter reflects how distinctly the observed modularity varies relative to a randomly-connected network; the Q-value is 0 when the number of connections within modules is no greater than what would be expected under random organization of the overall network, whereas higher Q-values indicate greater connectivity within modules than expected at random, in turn reflecting a more strongly modular network (Newman & Girvan 2004; Rasskin-Gutman & Esteve-Altava 2014; Esteve-Altava 2017a; Werneburg *et al.* 2019; Plateau & Foth 2020). To determine where to cut the dendrogram, the Q-value was calculated for every possible partition, with the cut-off associated with the highest Q-value (i.e., Q_{max}) being considered the preferred partition (Newman & Girvan 2004; Esteve-Altava *et al.* 2013; Rasskin-Gutman & Esteve-Altava 2014; Esteve-Altava 2017a; Werneburg *et al.* 2019). Modules identified in this manner are herein referred to as Q-modules, as in other AnNA studies (e.g., Werneburg *et al.* 2019; Plateau & Foth 2020).

As a supplementary strategy for module detection, each dendrogram was also assessed statistically, using a two-sample Wilcoxon rank-sum or Mann-Whitney U test. This test evaluates whether the number of internal connections significantly exceeds the number of external connections for every cluster within the dendrogram (Esteve-Altava 2017a; Werneburg *et al.* 2019; Plateau & Foth 2020). Statistically significant clusters reflect S-modules *sensu* e.g., Werneburg *et al.* (2019) and Plateau & Foth (2020).

4.2.3.2. Anatomical network parameters

The AnNA algorithm also calculates several parameters describing the anatomical network in question. I briefly outline these parameters below, and refer the reader to Rasskin-Gutman & Esteve-Altava (2014) and Esteve-Altava *et al.* (2018) for further explanation.

The most fundamental components of a network are the nodes (*N*) and the connections linking those nodes (*K*), as represented by the adjacency matrix described above (see §4.2.2 and Appendix 4.1; Rasskin-Gutman & Esteve-Altava 2014). As in most anatomical network analyses (e.g., Esteve-Altava *et al.* 2019; Navarro-Díaz *et al.* 2019; Werneburg *et al.* 2019; Plateau & Foth 2020), *N* herein represents the total number of skull bones in each network. *K* represents the total number of articulations, assessed as described above (see §4.2.2).

The density of connections (*D*) is the ratio of the actual number of connections in the network to the maximum possible number of connections, thus reflecting how fully-integrated the network is (Rasskin-Gutman & Esteve-Altava 2014).

The mean clustering coefficient (*C*) is the ratio of the actual number of interconnections among a node's neighbours to the maximum possible number of inter-neighbour connections for that node, averaged over the entire network (Rasskin-Gutman & Esteve-Altava 2014).

The mean shortest path length (*L*) is the shortest distance between any pair of nodes, averaged over every pair in the network (Rasskin-Gutman & Esteve-Altava 2014). *D*, *C*, and *L* together reflect network complexity or co-dependence, as a more thoroughly interconnected or integrated network will have a higher density, higher mean clustering coefficient, and lower mean shortest path length (Esteve-Altava *et al.* 2013; Rasskin-Gutman & Esteve-Altava 2014; Werneburg *et al.* 2019).

The heterogeneity of connections (*H*) measures the variance in connectivity across the network, reflecting whether all nodes connect to a similar number of neighbours (low H) or whether some nodes have much higher connectivity compared to more isolated nodes (high H) (Rasskin-Gutman & Esteve-Altava 2014; Esteve-Altava *et al.* 2019). This variance in turn reflects anisomerism, i.e., the extent of imbalance in network structure, with greater heterogeneity typically considered to reflect greater anatomical specialization of the affected nodes (Rasskin-Gutman & Esteve-Altava 2014; Werneburg *et al.* 2019).

Finally, network parcellation (*P*) is another measure of modularity, using a community detection algorithm to reflect how extensively and how uniformly the network is modularized (Esteve-Altava *et al.* 2018; Esteve-Altava *et al.* 2019; Plateau & Foth 2020). Of note, previous

analyses have used the *cluster_spinglass* function in *igraph* (Csárdi & Nepusz 2006) to calculate parcellation; however, this function cannot incorporate isolated elements (e.g., the anomalepidid jugal, which has no articulations), so I instead used a leading eigenvector community detection algorithm as described by Newman (2006) and implemented in *igraph* under the *leading.eigenvector.community* function (Csárdi & Nepusz 2006).

4.2.4. Principal component analysis

To analyze the network parameters as calculated by AnNA (see §4.2.3.2), I performed a principal component analysis (PCA; see Appendix 4.3) using the core R package *stats* (R Core Team 2020). In order to examine various aspects of squamate macroevolution, I grouped taxa according to several criteria (see below; Table S4.1). These were visualized using the package *ggplot2* (Wickham 2016) to create plots and generate normal data ellipses, with the package *ggConvexHull* (Martin 2017) being used to generate the convex hulls upon which I based my interpretations (see Results and Discussion). I assessed the statistical significance of each grouping method via permutational analysis of variance (PERMANOVA) with 10 000 permutations and using a Euclidean distance matrix. These PERMANOVA tests were performed using the packages *vegan* (Oksanen *et al.* 2019) and *pairwiseAdonis* (Martinez-Arbizu 2020), the latter of which was used to perform pairwise PERMANOVA for groupings with more than two categories (i.e., higher taxon, jaw morphotype, habitat, and combined size-habitat; see below).

4.2.4.1. Higher taxon and jaw mechanism

I first assessed basic patterns of morphospace occupation by grouping specimens based on higher taxon (i.e., non-snake lizards, anilioids, typhlopoids, anomalepidids, leptotyphlopids, booid-pythonoids, and caenophidians; Tables 4.1 and S4.1). I then grouped specimens based on the jaw morphotypes proposed by Strong *et al.* (2021b) (Table S4.1), so as to quantitatively examine this hypothesis of squamate jaw evolution, particularly in terms of which combinations of network parameters characterize each morphotype.

4.2.4.2. Habitat

Based on previous recognitions of extensive fossoriality-driven convergence across squamates (e.g., Savitzky 1983; Rieppel 1984b, 1988, 1996; Lee 1998; Townsend *et al.* 2004; Wiens *et al.* 2006; Wiens *et al.* 2010; Olori & Bell 2012; Reeder *et al.* 2015; Da Silva *et al.* 2018; Watanabe *et al.* 2019; Ebel *et al.* 2020; Strong *et al.* 2021a; Strong *et al.* 2021b), I divided

specimens based on habitat, with categories for fossoriality, semi-fossoriality, and non-fossoriality (Table S4.1). 'Fossoriality' herein refers to taxa that actively burrow (e.g., amphisbaenians; Gans & Montero 2008) or that have extensively subterranean habits (e.g., the occupation of ant nests by scolecophidians, which are myrmecophagous; Webb & Shine 1992; Pinto & Fernandes 2012; Chretien *et al.* 2019). 'Semi-fossoriality' describes taxa that show an affinity for leaf litter or loose soil, but are not strictly tied to subterranean habitats (e.g., *Cylindrophis*, *Loxocemus*; Rieppel 1978b; Palci *et al.* 2017).

However, as is likely inevitable when assessing a phenomenon as complex as habitat usage, these categories are ultimately arbitrary. As emphasized by Palci *et al.* (2017), many taxa do not in reality strictly conform to idealized ecological categories (e.g., accounts of arboreality in the classically fossorial scolecophidians; Das & Wallach 1998), with this ambiguity further exacerbated by a dearth of rigorous field studies of squamate—and particularly scolecophidian—ecology (Webb & Shine 1992; Webb *et al.* 2000). The definitions above therefore provide a general—but by no means definitive—guideline for demarcating habitat type and its influence on morphological evolution.

Habitat designations for most snake taxa are based on Figueroa (2016:table S3.1). The scolecophidian genera *Antillotyphlops*, *Anomalepis*, *Helminthophis*, and *Tricheilostoma* were not included in Figueroa's (2016) analysis, so were instead assigned to habitat types based on morphology. Designations of non-snake lizard habitat types are based on Gans & Montero (2008) for amphisbaenians, Rieppel (1984b) for dibamids, Norris (1953) for *Dipsosaurus*, Langner (2017) for *Lanthanotus*, Nguyen *et al.* (2018) for *Physignathus*, Johnson (1965) for *Sauromalus*, Howland *et al.* (1990) for *Uranoscodon*, and Bennett (2000) for *Varanus*.

4.2.4.3. Size

Like fossoriality, miniaturization has also been proposed as a major source of convergence in squamates (e.g., Rieppel 1988; Hanken & Wake 1993; Rieppel 1996; Rieppel & Zaher 2000; Olori & Bell 2012; Chretien *et al.* 2019; Strong *et al.* 2021a; Strong *et al.* 2021b) and is thus a phenomenon worth examining herein. However, as is often the case in vertebrates (Hanken & Wake 1993), there is no set guideline or measurement for what constitutes 'miniaturization' in squamates (similar to the issue noted above regarding guidelines for determining fossoriality *versus* semi-fossoriality). For the present study, I assigned taxa to these categories by measuring the snout-occiput length of each specimen (either directly from micro-

CT scans or from the images available on DigiMorph.org), plotting these values, and looking for breaks in the distribution (Table S4.2). For the observed specimens, skull length increased by about 1 mm or less between taxa until a length of 11.74 mm, after which the next value is 14.05 mm. After this point, skull length varies more distinctly among specimens. Based on this distribution, taxa with skull lengths ≤ 11.74 mm were considered 'miniaturized', whereas those with skull lengths ≥ 14.05 mm were considered 'non-miniaturized' (Tables S4.1 and S4.2).

4.2.4.4. Size and habitat

Fossoriality and miniaturization often co-occur in squamates, and their respective influences can be quite complexly intertwined (Rieppel 1984a, b; Wake 1986; Rieppel 1996; Maddin *et al.* 2011; Olori & Bell 2012; Strong *et al.* 2021a). Furthermore, the interaction between these phenomena has been hypothesized to exert a strong influence on squamate evolution and anatomy (Strong *et al.* 2021a). To examine this potential interplay, and to enable comparison of this combined influence to the patterns of morphospace occupation that arise when these phenomena are considered separately (see above), as my final analysis I divided taxa into three categories, based on their categorization under preceding variables: those that are both miniaturized and fossorial, those that are neither miniaturized nor fossorial, and those that are either miniaturized or fossorial but not both (Table S4.1). Focussing on the end-point categories (i.e., miniaturized–fossorial *versus* non-miniaturized–non-fossorial), I compared this plot to those generated by habitat or size alone, so as to assess relative patterns of morphospace occupation.

4.3. Results

4.3.1. Skull modularity

Each major squamate group exhibits a distinctive pattern of skull element connectivity, as described below (Figs 4.2–4.8; see Figs S4.1–S4.57 for all anatomical network dendrograms). These different patterns are particularly evident in the connectivity and modularity of the palatomaxillary elements (ectopterygoid, maxilla, palatine, and pterygoid); as such, I preface each subsection with a brief description of the palatomaxillary anatomy of the group in question. I further refer the reader to Strong *et al.* (2021b) for a more detailed comparative anatomical assessment of squamate jaw anatomy.

4.3.1.1. Typhlopoidea

Typhlopoid scolecophidians exhibit a unique palatomaxillary configuration in which the maxilla rotates about a rod-like maxillary process of the palatine (Iordansky 1997; Kley 2001; Chretien *et al.* 2019; Strong *et al.* 2021b), forming a 'single-axle maxillary raking' mechanism *sensu* Strong *et al.* (2021b) (Fig. 4.2a–d). The maxilla is reduced in size and angled transversely, both the palatine and pterygoid are edentulous and structurally simple, and the ectopterygoid is absent (Fig. 4.2a–d; see also Iordansky 1997; Kley 2001; Chretien *et al.* 2019; Strong *et al.* 2021b).

The typhlopoid skull is typically arranged into six major modules: the braincase, the snout, the left and right mandibles, and the left and right palatomaxillary arches (Figs 4.2 and S4.1–S4.13). In some taxa (*Afrotyphlops*, *Amerotyphlops*, *Antillotyphlops*, and *Typhlops*; Figs S4.3, S4.4, S4.6, and S4.11), Q_{max} occurs just beside this region of the dendrogram, such that the left palatomaxillary elements are included in the snout module; however, the snout elements do still form a distinct S-module ($p < 0.001$) to the exclusion of the palatomaxillary elements. This overall pattern is highly consistent across typhlopoids; the only exceptions are *Gerrhopilus ater* (in which the vomers are included in the palatomaxillary modules; Fig. S4.7) and *G. beddomii* (in which the parietal occurs in the snout module, rather than the braincase as in all other typhlopoids; Fig. S4.8).

4.3.1.2. Anomalepididae

In anomalepidid scolecophidians, the maxilla is suspended from a reduced and rod-like prefrontal and braced posteriorly by the ectopterygoid (Fig. 4.3a–d; Rieppel *et al.* 2009; Chretien *et al.* 2019; Strong *et al.* 2021b). Despite superficial similarities to typhlopoids (Fig. 4.2)—including the reduced and angled maxilla, and the reduced and edentulous palatine and pterygoid—anomalepidids differ dramatically from typhlopoids in the structure of the prefrontal and the presence of the ectopterygoid, which together result in an anatomically and functionally distinct palatomaxillary configuration (Figs 4.2 and 4.3; Strong *et al.* 2021b). Although this clade has yet to be examined from a functional perspective, this arrangement strongly suggests a maxillary raking mechanism (Kley 2001; Chretien *et al.* 2019), termed 'axle-brace maxillary raking' by Strong *et al.* (2021b).

The anomalepidid skull forms eight modules: the braincase, the snout, the left and right mandibles, the left and right jugals, and the left and right ectopterygoid and maxilla (Figs 4.3 and

S4.14–S4.19). The ectopterygoid-maxilla module also contains the pterygoid (in all taxa except *Typhlophis*), prefrontal (in all taxa except *Anomalepis* and *Liotyphlops beui*), and palatine (in all taxa except *Anomalepis* and *Typhlophis*). The composition of this palatomaxillary module is therefore distinct from that of typhlopoids (Figs 4.2 and S4.1–S4.13), particularly regarding the presence of the ectopterygoid and the inclusion of the prefrontal. When not grouped with the ectopterygoid and maxilla, the prefrontal, palatine, and/or pterygoid are recovered alongside the snout elements (Figs S4.14, S4.18, and S4.19). This overall pattern of skull modularity is again quite consistent across anomalepidids, with the only exceptions being the formation of a separate vomer-palatine module in *Anomalepis* (Fig. S4.14), the inclusion of the vomer in the palatomaxillary module in *Helminthophis* (Fig. S4.15), and the presence of separate left and right palatine-pterygoid-vomer modules and subdivision of the braincase into three modules in *Typhlophis* (Fig. S4.19).

4.3.1.3. Leptotyphlopidae

Leptotyphlopid scolecophidians are unique among snakes in that the palatomaxillary arch is completely edentulous (Fig. 4.4a–d; Kley 2001, 2006; Strong *et al.* 2021b). In further contrast to other scolecophidians, which rely on highly mobile upper jaws for prey ingestion, the palatomaxillary elements are essentially immobile in leptotyphlopids: the pterygoid and palatine articulate dorsally with the frontal, the palatine is in broad osseous contact with the vomer, and the maxilla articulates immovably with the snout (Fig. 4.4a–d; Kley 2001, 2006; Chretien *et al.* 2019; Strong *et al.* 2021b). Leptotyphlopids instead exhibit extensive mandibular kinesis—including a flexible intramandibular joint (Kley & Brainerd 1999; Kley 2001, 2006; Caldwell 2019; Chretien *et al.* 2019; Strong *et al.* 2021b)—which reflects a ‘mandibular raking’ mechanism *sensu* Kley & Brainerd (1999). As in typhlopoids (Fig. 4.2a–d), the ectopterygoid is absent (Fig. 4.4a–d).

The leptotyphlopid skull forms five modules: the braincase, the left and right mandibles, and the left and right snout and palatomaxillary elements (Figs 4.4 and S4.20–S4.25). This pattern of modularity clearly contrasts other scolecophidians: whereas typhlopoids (Figs 4.2 and S4.1–S4.13) and anomalepidids (Figs 4.3 and S4.14–S4.19) both exhibit distinct palatomaxillary modules, in leptotyphlopids these elements are always closely integrated with the snout and anterior skull (Figs 4.4 and S4.20–S4.25), reflecting the presence of an exclusively mandible-driven feeding mechanism. These modules are highly consistent across leptotyphlopids, with

only *Tricheilostoma* and *Myriopholis tanae* deviating from this pattern. This deviation is quite minor in *Tricheilostoma* (Fig. S4.24), with the only difference being the assignment of the right vomer to the left—rather than right—snout-palatomaxillary module. *M. tanae* (Fig. S4.22) differs more distinctly from other leptotyphlopids, with the braincase being divided into separate left and right modules and the parietals and parabasisphenoid joining the left snout-palatomaxillary module; however, given the extreme dorsal separation of the skull roof and braincase in this taxon (see Cundall & Irish 2008:fig. 2.12B,C for a comparable condition in another leptotyphlopid), this variation in the braincase modules is not unexpected.

4.3.1.4. Anilioidea (Aniliidae + Uropeltoidea)

Anilioid snakes (Fig. 4.5) exhibit a palatomaxillary configuration enabling slight unilateral movement of the left and right upper jaws (Cundall 1995). This mobility is afforded by a unique 'ball-and-socket'-like maxilla-palatine articulation (Fig. 4.5b), as well as by ligamentous attachment of the palatomaxillary arches to a loosened snout unit (Cundall 1995). However, the tightness of the ligamentous palatomaxillary-skull connections, alongside the bracing of the pterygoids by the basipterygoid processes (Fig. 4.5b), limits the extent of palatomaxillary mobility (Cundall 1995; Strong *et al.* 2021b). The maxilla, palatine, and pterygoid typically bear teeth, with these elements and the ectopterygoid generally being robust (Fig. 4.5a–d; Strong *et al.* 2021b). Although paedomorphic simplification of the palatomaxillary arch occurs in some anilioids (see Strong *et al.* 2021b), the unique maxilla-palatine joint and functional decoupling within the snout are universal within this group (Cundall 1995; Strong *et al.* 2021b). In light of the integral role of the snout elements in the anilioid feeding mechanism, this morphofunctional configuration was termed 'snout-shifting' by Cundall (1995).

The anilioid skull generally forms six modules: the braincase (sometimes separated into posterior and mid-skull modules), the snout, the left and right mandibles, and the left and right palatomaxillary arches (Figs 4.5 and S4.26–S4.30). However, this pattern of modularity is much more variable than in any scolecophidian clade, with this variation manifesting mainly in the palatomaxillary elements, and particularly in the pervasive integration of these elements with the snout and/or braincase. In uropeltids (Figs S4.29 and S4.30), the ectopterygoid, palatine, and pterygoid form distinct left and right modules, but the maxillae are incorporated into the snout module. In *Anilius* (Fig. S4.26), the snout and palatomaxillary elements are even more closely integrated, with the left palatomaxillary arch grouping with the frontals, parabasisphenoid, left

septomaxilla, and left prefrontal, and the right palatomaxillary arch grouping with the premaxilla, nasals, vomers, right septomaxilla, and right prefrontal. *Anomochilus* (Fig. S4.27) shows a similar degree of palatomaxillary-snout integration as in *Anilius*, although the ectopterygoids do not articulate directly with any other element (see Rieppel & Maisano 2007) and thus each form a separate module. Finally, the snout and left and right palatomaxillary arches form generally distinct modules in *Cylindrophis* (Figs 4.5 and S4.28), but with notable overlap into other skull regions: the right prefrontal is integrated with the right palatomaxillary arch; the left septomaxilla and prefrontal are integrated with the left palatine, ectopterygoid, and maxilla; and the left pterygoid is integrated with the mid-skull module (i.e., the frontals, postfrontals, parietal, and parabasisphenoid).

4.3.1.5. Non-snake lizards

The non-snake lizard skull consists of robust and tightly articulated elements (Fig. 4.6a–f). This is especially true of the palatomaxillary elements, which—due to their extensive osseous contact with each other and surrounding bones (Fig. 4.6a–d)—exhibit a much lower degree of mobility than in snakes (Cundall 1995). The presence of elements such as the lacrimal, and degree of development of structures such as the jugal and basipterygoid processes, contribute to this minimal mobility (Fig. 4.6a–d); of note, though, even in taxa lacking some of these additional bracing structures (e.g., dibamids, amphisbaenians), the palatomaxillary arches remain extensively articulated with other skull elements (Strong *et al.* 2021b). Due to this robustness and bracing, this jaw configuration was termed ‘minimal-kinesis microstomy’ by Strong *et al.* (2021b).

The non-snake lizard skull broadly separates into five modules: the braincase, the left and right mandibles, and the left and right anterior skull elements (i.e., the snout, palatomaxillary arches, and circumorbital bones) (Figs 4.6 and S4.31–S4.41). However, this pattern is highly variable, with the distinction between these skull regions generally being quite blurred. For example: one or both of the pterygoids are often integrated with the braincase, rather than with the other palatomaxillary elements (e.g., *Dipsosaurus*, *Physignathus*, *Rhineura*, *Sauromalus*, *Uranoscodon*, *Varanus*; Figs 4.6, S4.35, and S4.37–S4.41); the dorsal skull elements (i.e., frontals, postorbitals / postfrontals / postorbitofrontals, parietal, premaxilla, nasals, or some combination thereof) may form a module separate from the snout or braincase (e.g., *Anelytropsis*, *Lanthanotus*, *Sauromalus*, *Uranoscodon*, *Varanus*; Figs 4.6, S4.32, S4.36, and

S4.39–S4.41); and some (e.g., *Rhineura*; Fig. S4.38) or all (e.g., *Bipes*, *Lanthanotus*; Figs S4.33 and S4.36) of the snout elements may form a distinct module. Overall, the skull modules are thus much less consistent across taxa and the skull regions are much less distinct within each taxon, with the palatomaxillary elements often being separated into different modules alongside the snout, circumorbital elements, and/or braincase.

4.3.1.6. Booidea and Pythonoidea

Booids and pythonoids together form one of the major groups of 'macrostomatan' snakes (Fig. 4.1). In booid-pythonoids, the upper and lower jaw complexes are both highly kinetic, with the palatomaxillary arch bearing particularly strongly recurved teeth (Fig. 4.7a–f). The ability to consume proportionally large prey items is achieved mainly via marked posterior elongation of the supratemporal throughout ontogeny (Cundall & Irish 2008; Palci *et al.* 2016). The quadrate also exhibits positive allometric growth, with its distal terminus being displaced laterally throughout development (Palci *et al.* 2016). Although the basipterygoid processes are typically present (Fig. 4.7b), they are smaller and much more loosely articulated with the pterygoids than in anilioids or non-snake lizards (Figs 4.5b and 4.6b; see also Frazzetta 1966; Cundall 1995; Caldwell 2019).

All booid-pythonoids exhibit distinct modules for the braincase and left and right mandibles (Figs 4.7 and S4.42–S4.48). However, the remaining skull elements show three different patterns of modularity across this clade. In *Casarea* (Fig. S4.44), *Loxocemus* (Fig. S4.46), and *Python* (Fig. S4.47), the snout, left palatomaxillary arch and prefrontal, and right palatomaxillary arch and prefrontal each form separate modules, as in caenophidians (see Fig. 4.8 and below). The braincase is also subdivided into separate posterior and mid-skull modules, resulting in a total of seven skull modules. In *Boa* (Figs 4.7 and S4.42), *Eryx* (Fig. S4.45), and *Xenopeltis* (Fig. S4.48), the snout, palatomaxillary arch, and prefrontal together form left and right modules, resulting in a total of five skull modules. In *Calabaria* (Fig. S4.43), the remaining skull elements form a dorsal skull module (i.e., the frontals, postfrontals, parietal, premaxilla, and nasals), a left anterior skull module (i.e., the left septomaxilla, vomer, palatomaxillary arch, prefrontal, and jugal, and the parabasisphenoid), and a right anterior skull module (i.e., the right septomaxilla, vomer, palatomaxillary arch, prefrontal, and jugal); this results in six total skull modules. In many booid-pythonoids, either one (*Calabaria*, *Loxocemus*, *Python*, *Xenopeltis*; Figs S4.43 and S4.46–S4.48) or both (*Boa*, *Eryx*; Figs 4.7, S4.42, and S4.45) of the quadrates group

into the corresponding mandibular module, rather than with the braincase as is typical of squamates.

Minor variation also occurs within the three aforementioned patterns; for example, both nasals occur in the left snout-palatomaxillary-prefrontal module in *Boa* (Figs 4.7 and S4.42) and *Eryx* (Fig. S4.45), whereas the left and right nasal occur in the corresponding left and right modules in *Xenopeltis* (Fig. S4.48). Overall, despite these different patterns, the palatomaxillary arch and prefrontal consistently group together across booid-pythonoid taxa, often incorporated with some (*Calabaria*; Fig. S4.43) or all (*Boa*, *Eryx*, *Xenopeltis*; Figs 4.7, S4.42, S4.45, and S4.48) of the snout elements. This pattern of modularity contrasts the more consistent palatomaxillary arches recovered in caenophidians—the other major 'macrostomatan' group (see below; Figs 4.1, 4.8, and S4.49–S4.57)—and the more pervasive palatomaxillary-snout and palatomaxillary-braincase integration typical of anilioids (see above; Figs 4.5 and S4.26–S4.30).

4.3.1.7. Caenophidia

Caenophidians constitute one of the two major groups of 'macrostomatan' snakes, alongside booid-pythonoids (see above; Figs 4.1 and 4.8). Notably, though, 'macrostomy' arises via a different ontogenetic pathway in caenophidians than in booid-pythonoids (Palci *et al.* 2016). In caenophidians, elongation and rotation of the quadrate throughout ontogeny causes posterior or posterolateral displacement of the quadrate-mandible articulation, whereas the supratemporal typically does not undergo notable posterior elongation (Cundall & Irish 2008; Palci *et al.* 2016). Some taxa—e.g., *Homalopsis*, *Thamnophis*—form exceptions to this general caenophidian ontogeny, exhibiting posterior elongation of the supratemporal (especially in *Homalopsis*), as is typical of booid-pythonoids, in addition to the distinct posterolateral orientation of the quadrate as is typical of caenophidians (Palci *et al.* 2016; Strong *et al.* 2019). The basipterygoid processes are absent in caenophidians, reflecting an entirely ligamentous or muscular connection between the pterygoid and braincase (see also Cundall 1983; Caldwell 2019 for discussions of the jaw-related musculature in caenophidians).

The caenophidian skull is typically arranged into distinct modules for the braincase, snout, left and right mandibles, and left and right palatomaxillary elements and prefrontal (Figs 4.8 and S4.49–S4.57). The braincase is often further split into separate posterior and mid-skull modules (observed in *Acrochordus*, *Aparallactus*, *Lampropeltis*, and *Naja*; Figs S4.49, S4.50, S4.54, and S4.55), with the posterior braincase elements (i.e., prootic, otoccipital, supraoccipital,

basioccipital, stapes, supratemporal, and quadrate) sometimes forming separate left and right modules (*Crotalus*, *Homalopsis*; Figs S4.52 and S4.53). In a few taxa (*Pareas*, *Thamnophis*; Figs 4.8, S4.56, and S4.57), the left posterior braincase elements form a module with the mid-skull elements, leaving the right posterior braincase as a separate module. Some variation also arises regarding the snout module: in *Aparallactus* (Fig. S4.50), the vomers are excluded from this module; in *Atractaspis* (Fig. S4.51), the palatines form separate left and right modules with the vomers, and the other snout elements group with the mid-skull elements and prefrontals; in *Pareas* (Fig. S4.56), the frontals are incorporated into the snout module; and, in *Homalopsis* (Fig. S4.53), the left and right vomers are incorporated into the corresponding palatomaxillary-prefrontal modules, as are the jugals. Altogether, there is therefore a noticeable degree of variation among caenophidians. However, given the high taxonomic and morphological diversity of Caenophidia—which contains over 2500 species, constituting over 85% of extant snake species (Lawson *et al.* 2005; Pyron *et al.* 2011)—such variation is to be expected and is in fact arguably quite minimal given the scope of this clade.

This comparative consistency in modularity is especially true for the palatomaxillary arches, which consistently form distinct left and right modules alongside the prefrontals (Figs 4.8 and S4.49–S4.57). The only notable deviation to this palatomaxillary modularity is *Atractaspis* (Fig. S4.51)—as described above and as is to be expected given the unique palatine-pterygoid separation in atractaspidids (see Underwood & Kochva 1993; Deufel & Cundall 2003; Strong *et al.* 2021a)—with minimal deviation in *Homalopsis* (see above; Fig. S4.53) and *Naja* (in which the left prefrontal is incorporated into the mid-skull module; Fig. S4.55). Thus, the palatomaxillary arches in particular show more consistent modularity across caenophidians than across booid-pythonoids (see above).

4.3.2. Anatomical network parameters and PCA

Apart from the network dendrograms and patterns of modularity described above, AnNA also calculates several parameters which describe various aspects of each anatomical network (Tables 4.2 and S4.1; see Methods for explanation of parameters). Following PCA on these parameters to further assess skull network diversity across squamates, I grouped taxa under various criteria to assess the influence of macroevolutionary and adaptational factors such as habitat and body size (Fig. 4.9; see Table S4.1 for groupings and Table S4.3 for full statistical results).

4.3.2.1. Overview of morphospace

PC1 accounts for 41.02% of the total variance in the dataset, PC2 accounts for 31.04% of this variance, and PC3 accounts for 14.55%. Because PC1 and PC2 together encapsulate a distinct majority of the total variance, the ensuing Results and Discussion will centre around these principal components.

PC1 is strongly positively influenced by L and strongly negatively influenced by D and C (Fig. 4.9a; Table S4.4). The other parameters contribute less distinctly to this principal component, with H exerting a moderate positive influence, N and P exerting a weak positive influence, and K exerting a weak negative influence (Fig. 4.9a; Table S4.4). Thus, taxa toward the lower bound of this axis exhibit extensively interconnected skull elements (i.e., high C and D, low L), whereas taxa toward the higher bound of this axis exhibit less integrated skull networks (i.e., low C and D, high L).

PC2 is strongly positively influenced by N and K (Fig. 4.9a; Table S4.4). To a lesser extent, it is moderately negatively influenced by H, weakly positively influenced by P and C, and weakly negatively influenced by D and L (Fig. 4.9a; Table S4.4). Thus, a higher position along this axis reflects a greater number of skull elements (i.e., higher N) and greater number of total articulations among elements (i.e., higher K).

4.3.2.2. Distribution of higher taxa and jaw morphotypes

I first separated specimens based on higher taxon (Fig. 4.9b), followed by jaw morphotype as described by Strong *et al.* (2021b) (Fig. 4.9c). These methods of grouping are equivalent for most specimens, as most of the higher taxa examined herein each exhibit a distinct and non-homologous jaw mechanism (Fig. 4.9b,c; Table S4.1; see also Strong *et al.* 2021b). However, booid-pythonoids and caenophidians are an exception, as these taxa occupy distinct regions of morphospace but are both ‘macrostomatan’ (Fig. 4.9b,c; Table S4.1).

Non-snake lizards (i.e., ‘minimal-kinesis microstomatans’) occupy the largest region of morphospace, spanning from the upper bound of PC2 (reflecting taxa with a high number of skull elements and total skull articulations, i.e., ‘typical’ non-snake lizards such as *Varanus* or *Physignathus*) to the lower bound of both PC1 and PC2 (reflecting taxa with fewer, more extensively connected skull elements, i.e., amphisbaenians and *Dibamus*) (Fig. 4.9a–c). However, although this region is large, it does not overlap with any other higher taxa or jaw morphotypes (Fig. 4.9b,c). Anomalepidids (i.e., ‘axle-brace maxillary rakers’) also occupy a

distinct region of morphospace, reflecting a somewhat loosely integrated skull (i.e., moderately high L and moderately low C and D) with relatively few elements (i.e., relatively low N and K) (Fig. 4.9a–c). This region is notably separate from other scolecophidians (Fig. 4.9b). Both typhlopoids (i.e., 'single-axle maxillary rakers') and leptotyphlopids (i.e., 'mandibular rakers') overlap distinctly with each other and with anilioids (i.e., 'snout-shifters') (Fig. 4.9a–c). This region reflects a skull structure again with relatively few elements, as in anomalepidids, but with somewhat greater integration among those elements (i.e., higher C, higher D, and lower L than in anomalepidids) (Fig. 4.9a–c). Finally, as mentioned above, booid-pythonoids and caenophidians occupy almost entirely distinct regions of morphospace (Fig. 4.9b). Specifically, despite both higher taxa exhibiting 'macrostomy' (Fig. 4.9c), caenophidians generally have fewer skull elements (i.e., lower N) and less extensive integration among those elements (i.e., lower K and higher L) than booid-pythonoids (Fig. 4.9b).

4.3.2.3. Distribution of habitat types

Fossorial taxa occupy a large region of morphospace, reflecting a relatively low number of generally well-integrated skull elements (i.e., concentrated toward the lower bound of both PCs, especially PC2) (Fig. 4.9d). In contrast, non-fossorial taxa exhibit skull networks ranging from a high number of moderately integrated skull elements (i.e., midway along PC1, high on PC2; primarily non-fossorial non-snake lizards) to a moderate number of loosely integrated skull elements (i.e., high on PC1, midway along PC2; primarily non-fossorial caenophidians) (Fig. 4.9a,d). These fossorial and non-fossorial regions are significantly different ($F_{1,48} = 19.265$, $p = 0.0003$); however, they do exhibit noticeable overlap, mainly due to the placement of the fossorial colubroids *Atractaspis* and *Aparallactus* (Fig. 4.9a,d). Semi-fossorial taxa occupy an intermediate region of morphospace, significantly distinct from the fossorial region ($F_{1,40} = 12.816$, $p = 0.0008$) but not the non-fossorial region ($F_{1,20} = 0.161$, $p = 0.6872$) and overlapping strongly with both other habitat types (Fig. 4.9d).

4.3.2.4. Distribution based on size

Miniaturized taxa occupy a similar region of morphospace as fossorial taxa, again reflecting skull networks with relatively few and relatively tightly integrated elements (Fig. 4.9e). However, due to the status of *Atractaspis* as fossorial but not miniaturized (i.e., its exclusion from the current category; Table S4.1), this region is slightly smaller than that defined by fossoriality (Fig. 4.9d). Non-miniaturized taxa occupy a large region spanning most of

morphospace, ranging from skull networks with a high number of moderately interconnected elements (i.e., high N and K, moderate C, D, and L; many non-snake lizards) to networks with a moderate number of quite strongly interconnected elements (i.e., moderate N and K, high C and D, low L; *Amphisbaena*) to networks with a moderate number of quite minimally interconnected elements (i.e., moderate N and K, low C and D, high L; most caenophidians) (Fig. 4.9a,e). These miniaturized and non-miniaturized regions are significantly different ($F_{1,55}$ = 19.436, p = 0.0001), but overlap quite extensively (Fig. 4.9e).

4.3.2.5. Combined influence of size and habitat

Taxa that are both miniaturized and fossorial (Fig. 4.9f) occupy a more distinct region of morphospace than when these factors are considered independently (Fig. 4.9d,e). Specifically, miniaturized–fossorial taxa (Fig. 4.9f) occupy a region equivalent to that delimited by miniaturization alone (Fig. 4.9e), but smaller than that delimited by fossoriality alone (Fig. 4.9d). Conversely, non-miniaturized–non-fossorial taxa (Fig. 4.9f) occupy a region equivalent to that defined by non-fossoriality alone (Fig. 4.9d), but smaller than that defined by non-miniaturization alone (Fig. 4.9e). Thus, when considered simultaneously, these patterns of morphospace occupation result in less overlap between contrasting regions (Fig. 4.9f), which again are significantly different ($F_{1,45}$ = 19.768, p = 0.0001). In other words, miniaturization and fossoriality together constrain taxa to a comparatively more distinct region of morphospace than either phenomenon does individually.

4.4. Discussion

4.4.1. The evolution of ‘microstomy’

Although often considered a fundamentally plesiomorphic and homogenous condition among squamates (e.g., Bellairs & Underwood 1951; Miralles *et al.* 2018), recent discussions of ‘microstomy’ have emphasized the highly divergent nature of this condition in many taxa (Kley & Brainerd 1999; Kley 2001, 2006; Caldwell 2019; Chretien *et al.* 2019). Most recently, Strong *et al.* (2021b) proposed, based on primary homology-centred anatomical assessments of ‘microstomatans’, that ‘microstomy’ in fact occurs via five morphofunctionally distinct and non-homologous morphotypes across squamates; this was interpreted as reflecting a complex evolutionary history of ‘microstomy’ (Strong *et al.* 2021b).

The network analyses conducted herein ultimately support this hypothesis. Rather than the palatomaxillary elements showing consistent patterns of modularity across 'microstomatans' (as would be expected if 'microstomy' were indeed morphologically homogenous), these elements instead show distinct patterns of connectivity in each 'microstomatan' group (Figs 4.2–4.6), reflecting the various morphofunctional arrangements unique to each of these groups.

Among scolecophidians, the left and right palatomaxillary arches consistently form separate modules in typhlopoids (Figs 4.2 and S4.1–S4.13), in line with the 'single-axle maxillary raking' morphotype described by Strong *et al.* (2021b). In anomalepidids (Figs 4.3 and S4.14–S4.19), the ectopterygoid and maxilla are universally united into left and right modules—alongside some combination of the palatine, prefrontal, and pterygoid—reflecting an 'axle-brace maxillary raking' morphotype (Strong *et al.* 2021b). In contrast to these clades, the palatomaxillary arches are completely integrated into the snout module in leptotyphlopids (Figs 4.4 and S4.20–S4.25), reflecting the unique absence of palatomaxillary kinesis relative to other snakes and thus total reliance on 'mandibular raking' *sensu* Kley & Brainerd (1999).

Among non-scolecophidian 'microstomatans', the snout, braincase, and left and right palatomaxillary arches form generally separate modules in anilioids, but often with notable overlap between these skull regions (Figs 4.5 and S4.26–S4.30). This pattern thus reflects the greater integration of the upper jaws with the skull as is characteristic of the 'snout-shifting' mechanism introduced by Cundall (1995). Finally, non-snake lizards exhibit highly variable skull modularity relative to other squamates, with extensive overlap between skull regions (Figs 4.6 and S4.31–S4.41). This variation across non-snake lizards is likely at least partially influenced by the taxonomic breadth of this group; however, the pervasive lack of definition or modular consistency of skull regions—even within individual specimens—more strongly suggests a genuine lack of modularity corresponding to distinct skull regions. This is consistent with the 'minimal-kinesis' morphotype proposed by Strong *et al.* (2021b): because the skull elements are all quite well-braced and universally integrated, AnNA recovers distinct overlap between different skull regions rather than the more well-defined modules present in other squamates.

Each of these patterns of modularity is consistent within each higher taxon, distinct from the patterns exhibited by other 'microstomatans', and consistent with the morphofunctional mechanisms proposed by Strong *et al.* (2021b). Although AnNA is not itself a test of homology

(see Patterson 1982; de Pinna 1991; Rieppel & Kearney 2002; Strong *et al.* 2021b), these results complement and ultimately support the hypothesis of 'microstomy' occurring in several evolutionarily distinct forms (as per Harrington & Reeder 2017; Caldwell 2019; Chretien *et al.* 2019; Strong *et al.* 2021b): not only is there a lack of primary homology for key character states across 'microstomatan' taxa (see Strong *et al.* 2021b), the proposed morphotypes are indeed sufficiently distinct to result in quantifiably different patterns of palatomaxillary modularity across these major groups, as shown herein. As such, 'microstomy' should not be considered morphologically homogenous among squamates, nor assumed among snakes to reflect simple retention of an ancestral condition (see also Caldwell 2019; Chretien *et al.* 2019; Strong *et al.* 2021b).

4.4.2. The evolution of 'macrostomy'

Although this study focusses largely on 'microstomy', the inclusion of several 'macrostomatan' taxa as a comparative outgroup provides unexpected insight into the evolution of this equally complex feeding mechanism. Specifically, these results support recent hypotheses (e.g., Cundall & Irish 2008; Palci *et al.* 2016; Caldwell 2019; Burbrink *et al.* 2020) of 'macrostomy' occurring via distinct mechanisms in booid-pythonoids compared to caenophidians.

Based on modular composition, the palatomaxillary elements again show distinct patterns of modularity in each of these groups. In caenophidians, the palatomaxillary arches and prefrontals form distinct left and right modules, with relatively few exceptions given the size of this clade (see §4.3.1.7; Figs 4.8 and S4.49–S4.57). In contrast, booid-pythonoids exhibit much more variability in palatomaxillary modularity, with the upper jaw arches sometimes forming separate modules with the prefrontals as in caenophidians, or, more often, being integrated to some extent with the snout elements (see §4.3.1.6; Figs 4.7 and S4.42–S4.48). Because 'macrostomy' has not been morphologically re-assessed in the same detail as 'microstomy', these conclusions ultimately remain preliminary; however, by reinforcing previous suggestions of the non-homology of this jaw mechanism (Vidal & Hedges 2002; Palci *et al.* 2016; Caldwell 2019; Strong *et al.* 2019; Burbrink *et al.* 2020), these results strongly emphasize a renewed examination of 'macrostomy' as a key avenue for future research.

These results also contrast with those of previous studies examining skull modularity in 'macrostomatans'. Watanabe *et al.* (2019) and Rhoda *et al.* (2021) recently assessed cranial

integration in snakes via analyses of shape covariation, incorporating a broad sampling of squamates (including typhlopoids, anilioids, booids, and colubroids) and of aquatic-foraging caenophidians, respectively. Although the details of their results differ, both studies broadly recovered a much more modular arrangement of the snake skull—and notably the palatomaxillary arch—than the present analysis, with Watanabe *et al.* (2019) also recovering consistent patterns of skull integration across snakes and non-snake lizards (Watanabe *et al.* 2019; Rhoda *et al.* 2021). These contrasting results likely reflect, at least in part, the impact of shape- *versus* connectivity-based analyses of modularity (i.e., analyses of variational *versus* organizational modularity, respectively; Esteve-Altava 2017a), thus highlighting the importance of both approaches in future studies of skull integration and modularity (see also Eble 2005; Esteve-Altava *et al.* 2013; Esteve-Altava 2017a, b).

4.4.3. Convergence among squamates

Analyses of morphospace occupation (Fig. 9) support hypotheses of miniaturization-driven and fossoriality-driven convergence in squamates. These convergences have been discussed by several authors from a comparative anatomical perspective (e.g., Savitzky 1983; Rieppel 1984b, 1988; Hanken & Wake 1993; Rieppel 1996; Lee 1998; Rieppel & Zaher 2000; Olori & Bell 2012; Chretien *et al.* 2019; Strong *et al.* 2021a; Strong *et al.* 2021b), with fossoriality-driven convergence recently supported via GM-based analysis of squamate skull shape (Da Silva *et al.* 2018) and integration (Watanabe *et al.* 2019).

Regarding habitat, fossorial squamates occupy a distinct region of morphospace relative to both semi-fossorial and especially non-fossorial squamates (see §4.3.2.3; Fig. 4.9d), reflecting a significantly different skull network structure than taxa occupying other habitats. Although some previous authors have considered fossorial squamates to form a genuine clade (e.g., the Scincophidia of Conrad 2008), I disagree with this perspective based on the numerous phylogenies that recover dibamids, amphisbaenians, and snakes—including fossorial snakes—as distantly related (e.g., Pyron *et al.* 2013; Simões *et al.* 2018; Burbrink *et al.* 2020). Based on this phylogenetic context, I therefore consider the similar skull network structure of these fossorial squamates to reflect convergence, not phylogenetic affinity. Generally characterized by a lower number of more tightly integrated skull elements (Fig. 4.9a,d), this network architecture is consistent with previous recognitions of the reduction or loss of skull elements, and reinforcement of articulations among the remaining elements, as major sources of convergence

in fossorial taxa (Savitzky 1983; Rieppel 1984b; Lee 1998). These results therefore quantitatively reflect the evolutionary constraints associated with this habitat.

Similarly, miniaturized and non-miniaturized taxa also occupy distinct regions of morphospace (see §4.3.2.4; Fig. 4.9e), reflecting convergence toward a specific skull architecture in miniaturized squamates. This network structure is similar to that in fossorial taxa (Fig. 4.9d), again reflecting a comparatively low number of thoroughly interconnected skull elements. However, the biological factors promoting this structure are somewhat different for miniaturization than for fossoriality. Whereas increased connectivity is important in fossorial taxa for mechanical integrity (Savitzky 1983; Rieppel 1984b; Cundall & Rossman 1993; Lee 1998), in miniaturized taxa this greater integration is more likely a consequence of size constraints forcing elements into close proximity.

Furthermore, miniaturization has been hypothesized to occur via paedomorphosis (Gould 1977; Hanken 1984; Wake 1986; Fröbisch & Schoch 2009; Sherratt *et al.* 2019), an evolutionary developmental phenomenon in which early ontogenetic conditions of an ancestral taxon are retained into the adult stages of a descendant taxon (Gould 1977; McNamara 1986). Paedomorphosis is in turn often associated with skeletal reduction, as certain elements are either totally absent (e.g., the supratemporal in typhlopoids, leptotyphlopids, *Anomalepis*, uropeltids, and *Anomochilus leonardi*; Rieppel *et al.* 2009; Olori & Bell 2012; Strong *et al.* 2021b) or develop in highly reduced form (e.g., the supratemporal in most anomalepidids; Rieppel *et al.* 2009; Strong *et al.* 2021b), reflecting early embryonic conditions along more typical ontogenetic trajectories (see e.g., Polachowski & Werneburg 2013; Khannoon & Evans 2015; Werneburg *et al.* 2015; Ollonen *et al.* 2018). Although paedomorphosis also occurs in fossorial taxa (e.g., *Atractaspis*; Strong *et al.* 2021a), it is much more pervasive in taxa that are also miniaturized (Maddin *et al.* 2011; Strong *et al.* 2021a; see below for further discussion). Thus, paedomorphic skeletal reduction likely explains the lower number of skull elements in miniaturized compared to non-miniaturized squamates.

Analysis of the combined influence of miniaturization and fossoriality (see §4.3.2.5; Fig. 4.9f) provides further insight into the pressures and constraints shaping squamate macroevolution. Importantly, when these phenomena are analyzed together (Fig. 4.9f), the opposing regions exhibit even less overlap than when size (Fig. 4.9e) or habitat (Fig. 4.9d) are treated separately (see §4.3.2.5). In other words, fossoriality and miniaturization are each

associated with a specific set of skull network parameters, constraining fossorial or miniaturized taxa to particular regions of morphospace relative to non-fossorial or non-miniaturized taxa (see above; Fig. 4.9d,e); however, when these phenomena co-occur, the endpoint categories (i.e., miniaturized–fossorial *versus* non-miniaturized–non-fossorial; Fig. 4.9f) exhibit even more distinct separation.

From an evolutionary perspective, this comparatively greater constraint is logical in light of the aforementioned pressures associated with fossoriality and miniaturization. For example, increased connectivity among skull elements is important for structural strength in fossorial taxa, and is also a logical consequence of size reduction in miniaturized taxa (see above). Taxa that are neither miniaturized nor fossorial do not face either of these pressures, whereas taxa that are both miniaturized and fossorial are subject to both of them, thus even further promoting variation in cranial integration between these categories (see also Maddin *et al.* 2011; Strong *et al.* 2021a). Greater network integration is also associated with greater structural inter-dependence among elements, which in turn promotes evolutionary constraint (Esteve-Altava *et al.* 2013; Rasskin-Gutman & Esteve-Altava 2014; Lee *et al.* 2020); thus, trends toward a more interconnected skull architecture in miniaturized or fossorial taxa in turn constrain morphological evolution, essentially generating a feedback cycle that becomes amplified when both of these phenomena are at play.

In the context of scolecophidian evolution, this interplay between habitat and size was recently discussed by Strong *et al.* (2021a) as part of a hypothesis that fossoriality, miniaturization, and paedomorphosis together produce a morphological continuum linking scolecophidians to more 'typical' (i.e., non-miniaturized, non-fossorial) snakes. The present analysis supports this hypothesis: Miniaturized-fossorial squamates are subject to strong morphological and evolutionary constraints, as indicated by their more distinctive occupation of morphospace relative to when these phenomena are considered separately (Fig. 4.9d–f). This in turn implies, as argued by Strong *et al.* (2021a), that the evolution of miniaturization in an already-fossorial lineage would promote further morphological adaptation and derivation, a compounding effect that could reasonably explain the evolution of the miniaturized and fossorial scolecophidian baupläne from a fossorial but non-miniaturized alethinophidian ancestor.

Finally, recent authors have also hypothesized potential convergence among scolecophidians themselves, arguing that miniaturization, fossoriality, and 'microstomy' may

have evolved independently in anomalepidids, leptotyphlopids, and typhlopoids (Harrington & Reeder 2017; Caldwell 2019; Chretien *et al.* 2019; Fachini *et al.* 2020; Strong *et al.* 2021b). As discussed above, the network dendrograms reveal each scolecophidian lineage to exhibit a different pattern of skull connectivity and modularity (Figs 4.2–4.4), supporting the hypothesis of distinct jaw morphotypes, distinct evolutionary trajectories, and clearly non-ancestral conditions in each of these lineages (Harrington & Reeder 2017; Caldwell 2019; Chretien *et al.* 2019; Strong *et al.* 2021b).

Furthermore, although typhlopoids and leptotyphlopids overlap in morphospace (Fig. 4.9b,c), their jaw mechanisms ('single-axle maxillary raking' *versus* 'mandibular raking', respectively) are functionally and anatomically highly divergent (Figs 4.2 and 4.4; Strong *et al.* 2021b). In contrast, anomalepidids are separate from other scolecophidians in morphospace (Fig. 4.9b,c), but like typhlopoids are maxillary rakers (though they exhibit 'axle-brace maxillary raking', rather than the 'single-axle' mechanism in typhlopoids; Figs 4.2 and 4.3; Strong *et al.* 2021b). Essentially, typhlopoids and leptotyphlopids are performing different functions (i.e., maxillary *versus* mandibular raking, non-homologous morphotypes associated with distinct patterns of modular composition; Figs 4.2 and 4.4; Strong *et al.* 2021b) within a similar overall network structure (i.e., overlapping in morphospace; Fig. 4.9b,c); conversely, typhlopoids and anomalepidids are performing superficially similar functions (i.e., maxillary raking) within highly distinct network structures (i.e., exhibiting different patterns of skull modularity, occupying different regions within the miniaturized–fossorial morphospace, and also comprising non-homologous morphotypes; Figs 4.2, 4.3, and 4.9b,c; Strong *et al.* 2021b).

When considered in the context of fossoriality, miniaturization, and the interplay between those phenomena, these patterns of morphospace occupation ultimately support a hypothesis of convergence among scolecophidians. Although scolecophidians do exhibit superficial similarities—such as overlapping occupation of morphospace (typhlopoids and leptotyphlopids) or seemingly similar jaw mechanisms (typhlopoids and anomalepidids)—the anatomical and functional configurations underlying each of the scolecophidian lineages are in reality dramatically different, with each clade exhibiting a non-homologous (see Strong *et al.* 2021b) and uniquely modularized (see above; Figs 4.2–4.4) jaw mechanism. At the same time, because these snakes are fossorial and highly miniaturized, they are therefore restricted to a highly specific region of network morphospace among squamates (Fig. 4.9). In light of this constraint,

these fundamental differences are thus ultimately most consistent with a hypothesis of convergence among the three scolecophidian lineages, driven by the ecological and morphofunctional constraints associated with miniaturization and fossoriality.

4.5. Conclusions

This study represents the first application of anatomical network analysis to non-archosaur reptiles, focussing on the evolution of the 'microstomatan' jaw mechanism and the potential role of fossoriality- and miniaturization-related convergence in shaping squamate evolution. By supporting recent hypotheses of a complex evolutionary history of 'microstomy' (e.g., Harrington & Reeder 2017; Caldwell 2019; Chretien *et al.* 2019; Strong *et al.* 2021b), and by providing novel quantitative support for various causes of convergence in squamates, this study therefore provides important insight into squamate evolution. These findings hold particular relevance regarding the origin of snakes, as they refute the traditional perspective of scolecophidians as a miniaturized and fossorial vestige of the ancestral snake condition (e.g., Miralles *et al.* 2018) and instead support hypotheses of scolecophidians as a convergent and highly morphologically derived assemblage (see also Harrington & Reeder 2017; Caldwell 2019; Chretien *et al.* 2019; Strong *et al.* 2021b).

This study therefore demonstrates the importance of quantitative methods such as AnNA in providing insight into complex macroevolutionary phenomena. For example, assessments of jaw evolution via AnNA represent a novel application of this method to the investigation of homology, thus highlighting the utility of integrating traditional comparative anatomical analysis with recently developed quantitative approaches in order to address major uncertainties in vertebrate evolution. The inclusion of modularity-based analyses—including the analysis of both organizational and variational modules, via, e.g., AnNA and GM, respectively (Esteve-Altava 2017a)—alongside comparative anatomical analysis represents a promising avenue for future research into other complex morphofunctional systems, such as 'macrostomy' in snakes.

Figures: Chapter Four

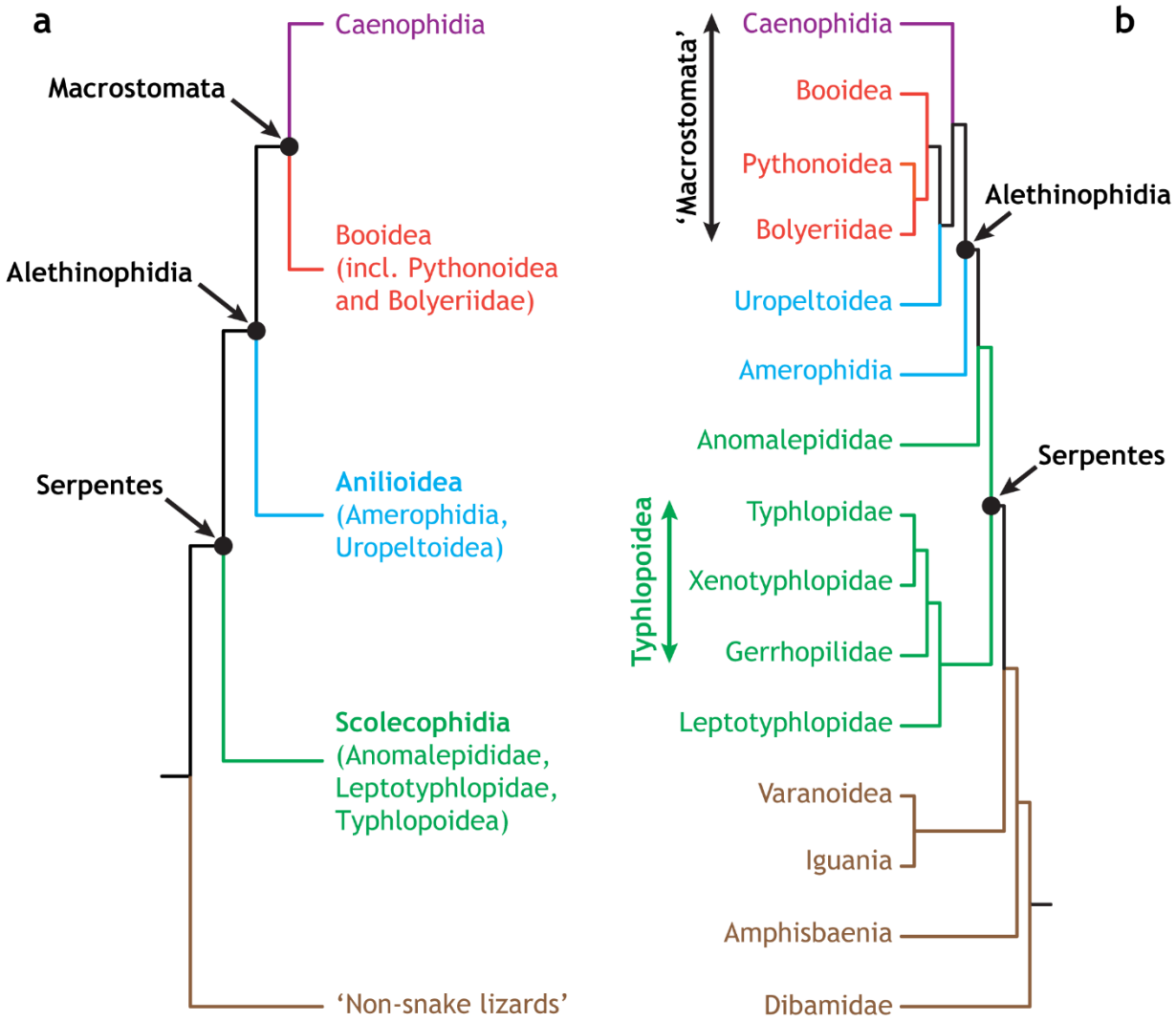

FIGURE 4.1. Overview of phylogenetic context for Chapter Four. (**a**) Traditional and (**b**) recent phylogenies of Squamata, derived from Rieppel (1988) and Burbrink *et al.* (2020), respectively. Major differences include the paraphyly of 'Scolecophidia' and polyphyly of 'Anilioidea' and 'Macrostomata' in molecular phylogenies (**b**), as opposed to their respective monophyly under the traditional view of snake evolution (**a**). The phylogeny in (**b**) also provides phylogenetic context for the specimens examined herein (see also Table 4.1). Colours indicate corresponding higher taxa.

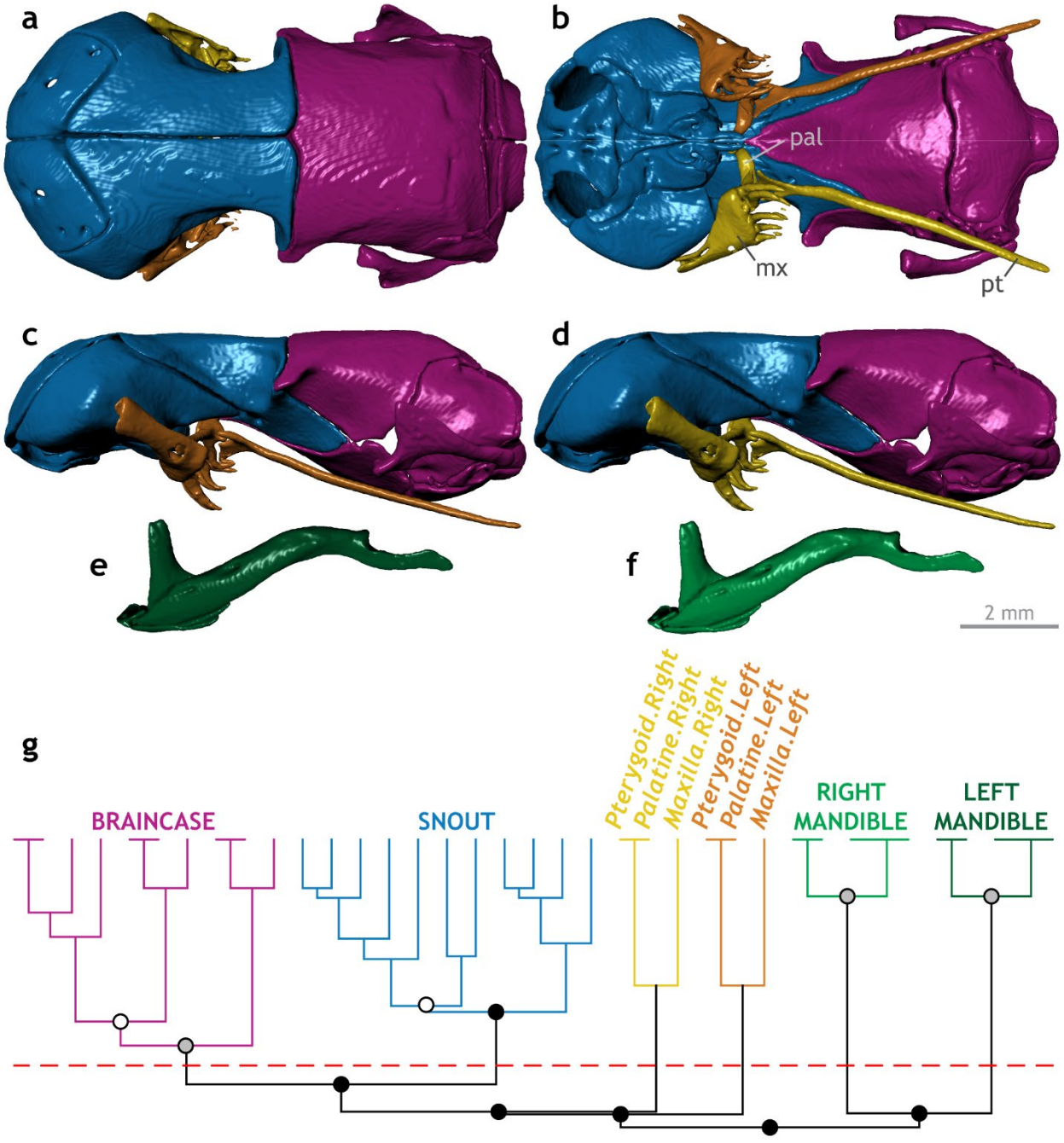
a
b
pal
mx
pt
c
d
e
f
2 mm
g
BRAINCASE
SNOUT
Pterygoid.Right
Palatine.Right
Maxilla.Right
Pterygoid.Left
Palatine.Left
Maxilla.Left
RIGHT MANDIBLE
LEFT MANDIBLE

FIGURE 4.2. Skull modularity of typhlopoid scolecophidians. Typhlopoids exhibit a highly uniform network structure, including consistent formation of left and right palatomaxillary modules (in italicized boldface). (**a–f**) Typical pattern of typhlopoid skull modularity, illustrated using *Afrotyphlops angolensis* (MCZ R-170385) in (**a**) dorsal, (**b**) ventral, (**c**) left lateral, and (**d**) right lateral views of the skull, and (**e**) left lateral and (**f**) right lateral views of the mandible. (**g**) Network dendrogram of *Xenotyphlops*, reflecting this general typhlopoid network structure. Q-modules are indicated by Q_{max} (represented by the red dotted line). S-modules are indicated by black ($p < 0.001$), grey ($0.001 \leq p < 0.01$), or white ($0.01 \leq p < 0.05$) circles. Abbreviations: mx, maxilla; pal, palatine; pt, pterygoid. MCZ scan data used by permission of the Museum of Comparative Zoology, Harvard University.

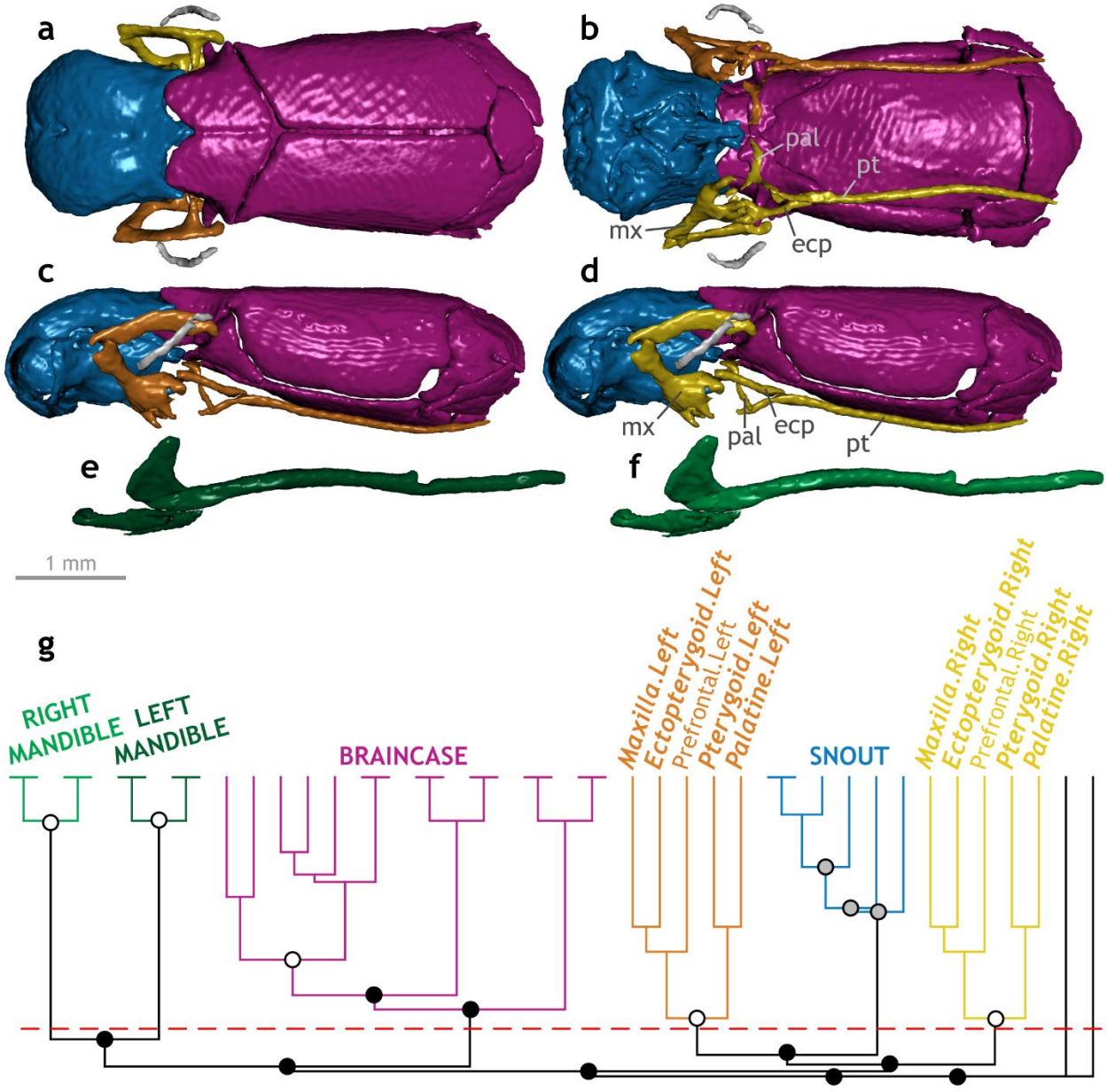
a
b
pal
pt
mx
ecp
c
d
mx
pal
ecp
pt
e
f
1 mm
g
RIGHT MANDIBLE
LEFT MANDIBLE
BRAINCASE
Maxilla.Left
Ectopterygoid.Left
Prefrontal.Left
Pterygoid.Left
Palatine.Left
SNOUT
Maxilla.Right
Ectopterygoid.Right
Prefrontal.Right
Pterygoid.Right
Palatine.Right

FIGURE 4.3. Skull modularity of anomalepidid scolecophidians. In anomalepidids, the ectopterygoids and maxillae always form left and right modules, typically alongside the other palatomaxillary elements (in italicized boldface) and the prefrontals. (**a–f**) Typical pattern of anomalepidid skull modularity, illustrated using *Liotyphlops argaleus* (MCZ R-67933) in (**a**) dorsal, (**b**) ventral, (**c**) left lateral, and (**d**) right lateral views of the skull, and (**e**) left lateral and (**f**) right lateral views of the mandible. (**g**) Network dendrogram of *L. argaleus*, reflecting this general anomalepidid network structure. Q-modules are indicated by Q_{max} (represented by the red dotted line). S-modules are indicated by black ($p < 0.001$), grey ($0.001 \leq p < 0.01$), or white ($0.01 \leq p < 0.05$) circles. Abbreviations: ecp, ectopterygoid; mx, maxilla; pal, palatine; pt, pterygoid. MCZ scan data used by permission of the Museum of Comparative Zoology, Harvard University.

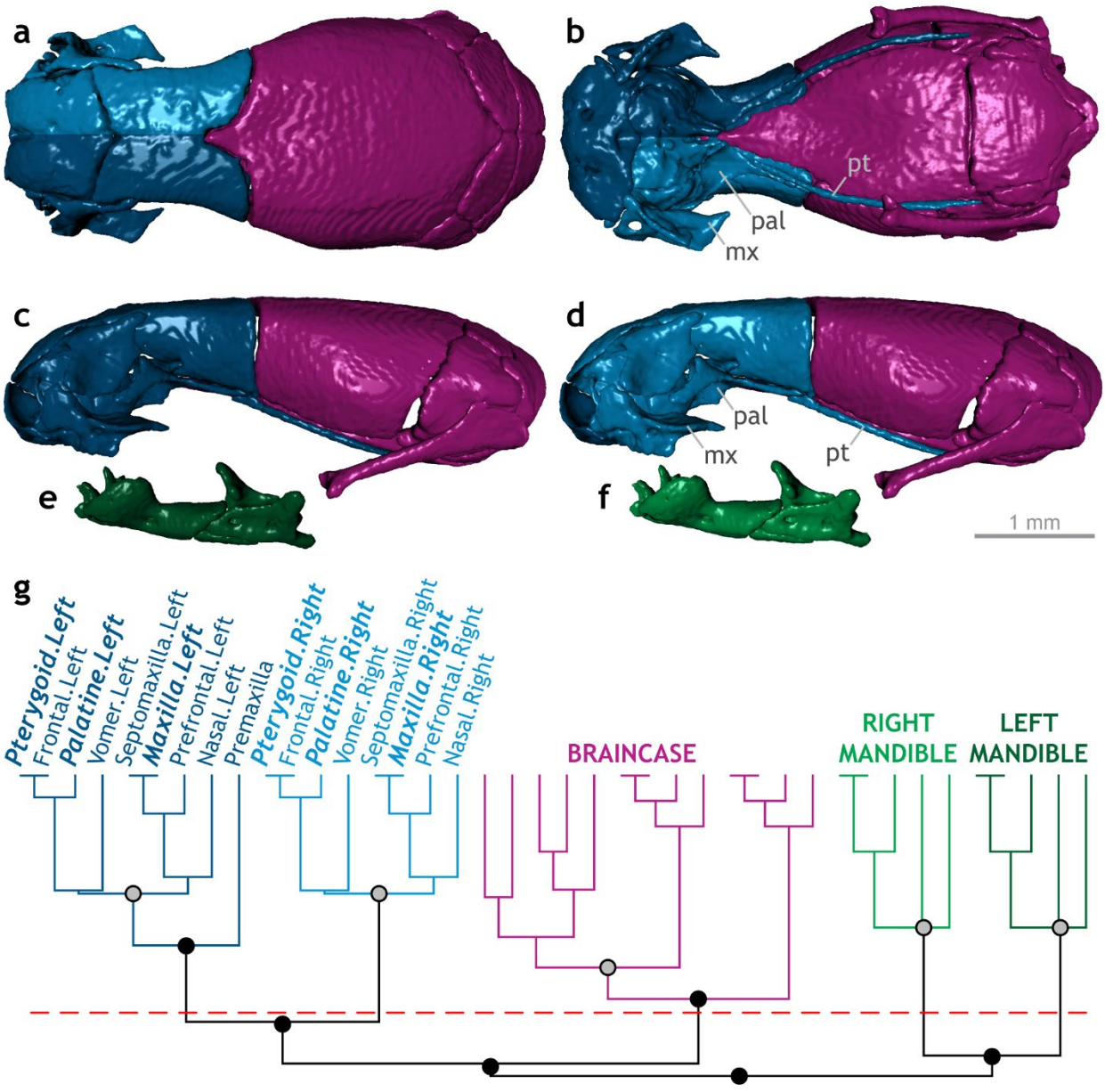
a
b
pt
pal
mx
c
d
pal
mx
pt
e
f
1 mm
g
Pterygoid.Left
Frontal.Left
Palatine.Left
Vomer.Left
Septomaxilla.Left
Maxilla.Left
Prefrontal.Left
Nasal.Left
Premaxilla
Pterygoid.Right
Frontal.Right
Palatine.Right
Vomer.Right
Septomaxilla.Right
Maxilla.Right
Prefrontal.Right
Nasal.Right
BRAINCASE
RIGHT MANDIBLE
LEFT MANDIBLE

FIGURE 4.4. Skull modularity of leptotyphlopid scolecophidians. Leptotyphlopids exhibit a highly consistent pattern of modularity, in which the palatomaxillary elements (in italicized boldface) are completely integrated with the snout. (**a–f**) Typical pattern of leptotyphlopid skull modularity, illustrated using *Epictia albifrons* (MCZ R-2885) in (**a**) dorsal, (**b**) ventral, (**c**) left lateral, and (**d**) right lateral views of the skull, and (**e**) left lateral and (**f**) right lateral views of the mandible. (**g**) Network dendrogram of *Epictia*, reflecting this general leptotyphlopid network structure. Q-modules are indicated by Q_{max} (represented by the red dotted line). S-modules are indicated by black ($p < 0.001$), grey ($0.001 \leq p < 0.01$), or white ($0.01 \leq p < 0.05$) circles. Abbreviations: mx, maxilla; pal, palatine; pt, pterygoid. MCZ scan data used by permission of the Museum of Comparative Zoology, Harvard University.

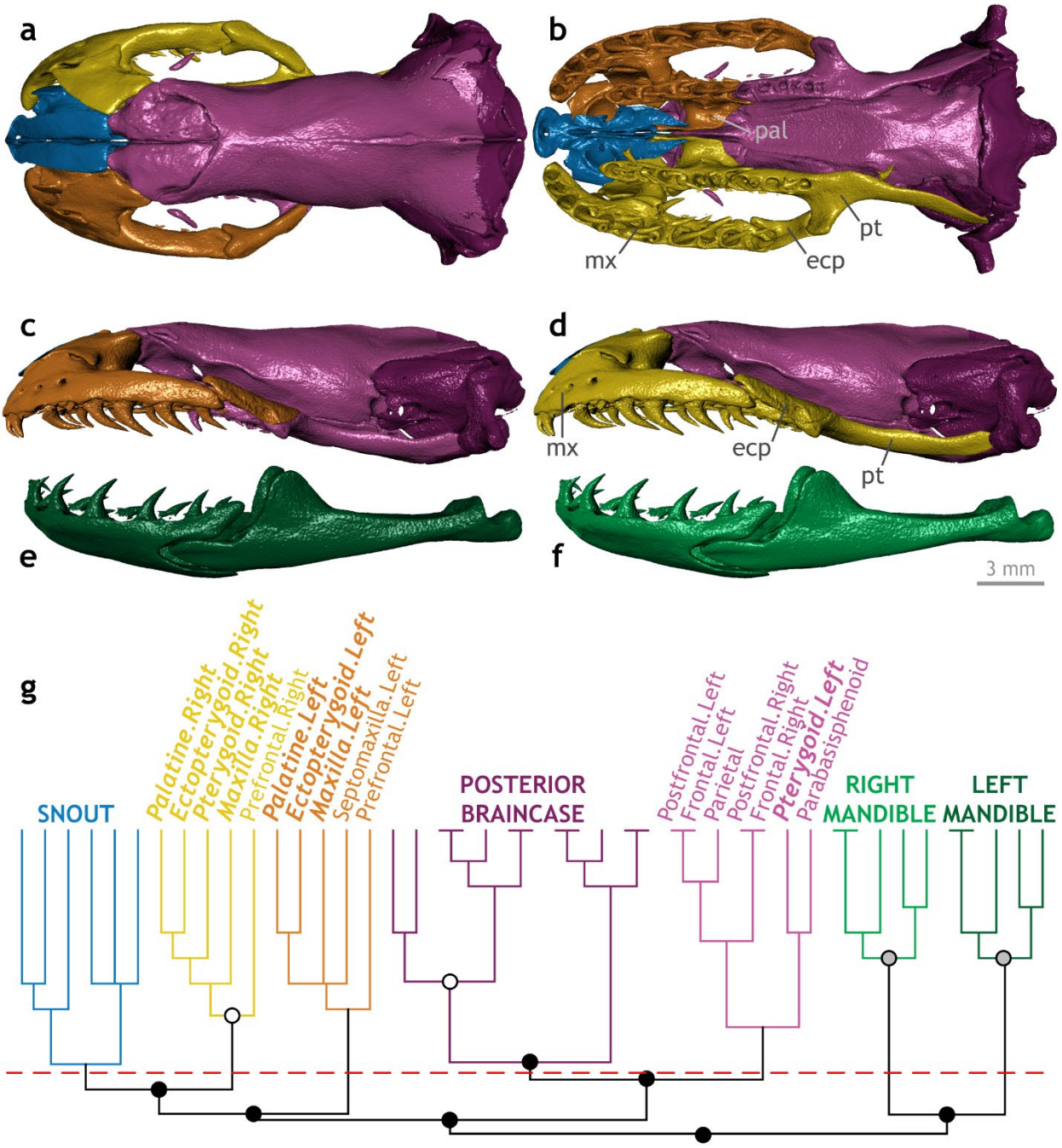
a
b
pal
pt
mx
ecp
c
d
mx
ecp
pt
e
f
3 mm
g
SNOUT
Palatine.Right
Ectopterygoid.Right
Pterygoid.Right
Maxilla.Right
Prefrontal.Right
Palatine.Left
Ectopterygoid.Left
Maxilla.Left
Septomaxilla.Left
Prefrontal.Left
POSTERIOR BRAINCASE
Postfrontal.Left
Frontal.Left
Parietal
Postfrontal.Right
Frontal.Right
Pterygoid.Left
Parabasisphenoid
RIGHT MANDIBLE
LEFT MANDIBLE

FIGURE 4.5. Skull modularity of anilioid snakes. In anilioids, the palatomaxillary elements (in italicized boldface) are integrated to variable extents with the braincase and particularly the snout. (**a–f**) Representative pattern of anilioid skull modularity, illustrated using *Cylindrophis ruffus* (UMMZ 201901) in (**a**) dorsal, (**b**) ventral, (**c**) left lateral, and (**d**) right lateral views of the skull, and (**e**) left lateral and (**f**) right lateral views of the mandible. (**g**) Network dendrogram of *Cylindrophis*, reflecting this network architecture. Q-modules are indicated by Q_{max} (represented by the red dotted line). S-modules are indicated by black ($p < 0.001$), grey ($0.001 \leq p < 0.01$), or white ($0.01 \leq p < 0.05$) circles. Abbreviations: ecp, ectopterygoid; mx, maxilla; pal, palatine; pt, pterygoid.

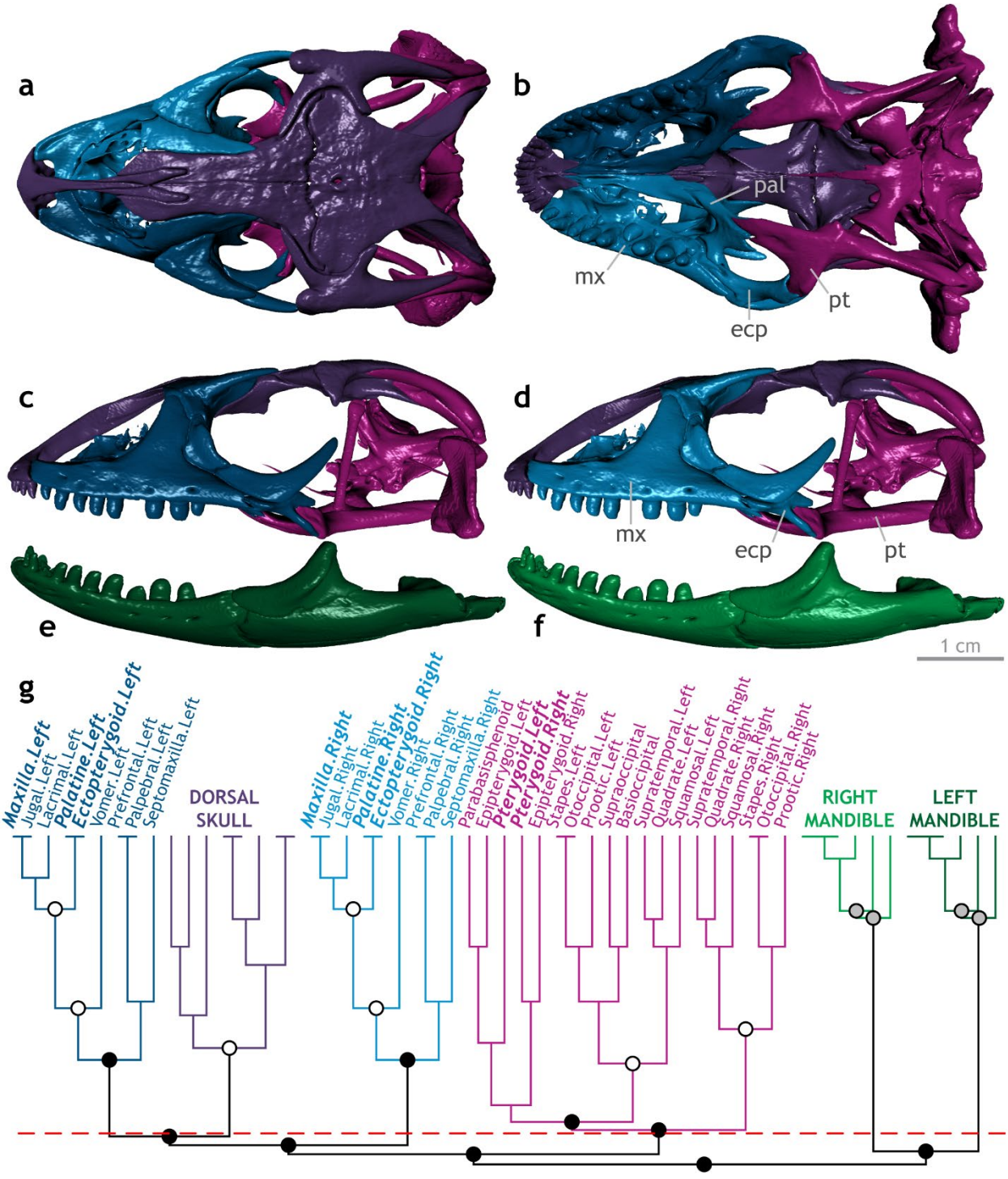
a
b
pal
mx
ecp
pt
c
d
mx
ecp
pt
e
f
1 cm
g
Maxilla.Left
Jugal.Left
Lacrimal.Left
Palatine.Left
Ectopterygoid.Left
Vomer.Left
Prefrontal.Left
Palpebral.Left
Septomaxilla.Left
DORSAL SKULL
Maxilla.Right
Jugal.Right
Lacrimal.Right
Palatine.Right
Ectopterygoid.Right
Vomer.Right
Prefrontal.Right
Palpebral.Right
Septomaxilla.Right
Parabasisphenoid
Epipterygoid.Left
Pterygoid.Left
Epipterygoid.Right
Pterygoid.Right
Stapes.Left
Otoccipital.Left
Prootic.Left
Supraoccipital
Basioccipital
Supratemporal.Left
Quadrate.Left
Squamosal.Left
Supratemporal.Right
Quadrate.Right
Squamosal.Right
Stapes.Right
Otoccipital.Right
Prootic.Right
RIGHT MANDIBLE
LEFT MANDIBLE

FIGURE 4.6. Skull modularity of non-snake lizards. Patterns of skull integration are highly variable among non-snake lizards, with skull regions often being separated into different modules. This is particularly true for the palatomaxillary elements (in italicized boldface), which are typically integrated to some extent with the snout, circumorbital elements, and braincase. (**a–f**) Representative pattern of non-snake lizard skull modularity, illustrated using *Varanus exanthematicus* (FMNH 58299) in (**a**) dorsal, (**b**) ventral, (**c**) left lateral, and (**d**) right lateral views of the skull, and (**e**) left lateral and (**f**) right lateral views of the mandible. (**g**) Network dendrogram of *Varanus*, reflecting this network architecture. Q-modules are indicated by Q_{max} (represented by the red dotted line). S-modules are indicated by black ($p < 0.001$), grey ($0.001 \leq p < 0.01$), or white ($0.01 \leq p < 0.05$) circles. Abbreviations: ecp, ectopterygoid; mx, maxilla; pal, palatine; pt, pterygoid.

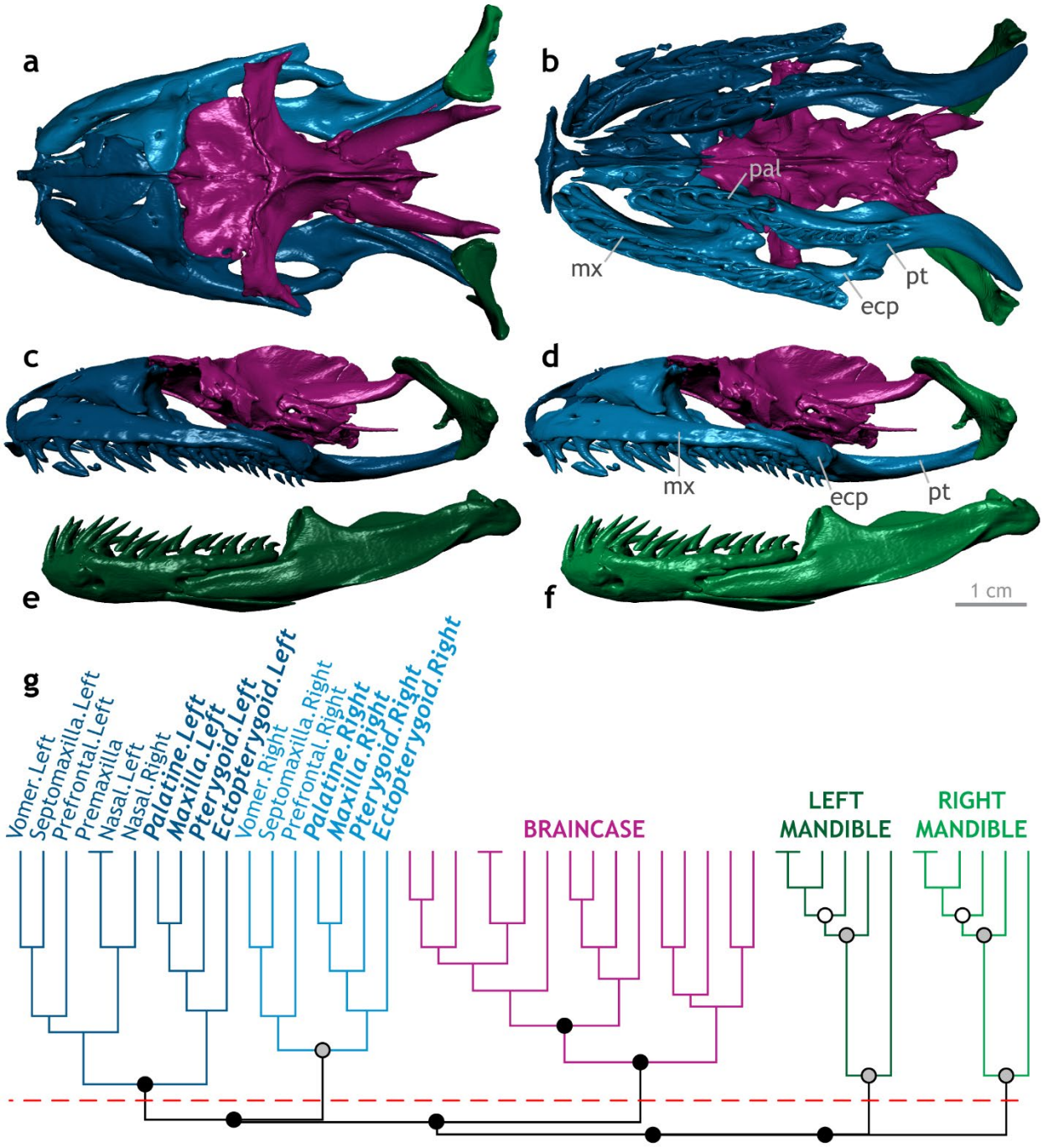
a
b
pal
mx
pt
ecp
c
d
mx
ecp
pt
e
f
1 cm
g
Vomer.Left
Septomaxilla.Left
Prefrontal.Left
Premaxilla
Nasal.Left
Nasal.Right
Palatine.Left
Maxilla.Left
Pterygoid.Left
Ectopterygoid.Left
Vomer.Right
Septomaxilla.Right
Prefrontal.Right
Palatine.Right
Maxilla.Right
Pterygoid.Right
Ectopterygoid.Right
BRAINCASE
LEFT MANDIBLE
RIGHT MANDIBLE

FIGURE 4.7. Skull modularity of booid-pythonoid snakes. In booids and pythonoids, the palatomaxillary elements (in italicized boldface) and prefrontals consistently form left and right modules, often alongside some or all of the snout elements. (**a–f**) Representative pattern of booid-pythonoid skull modularity, illustrated using *Boa constrictor* (FMNH 31182) in (**a**) dorsal, (**b**) ventral, (**c**) left lateral, and (**d**) right lateral views of the skull, and (**e**) left lateral and (**f**) right lateral views of the mandible. (**g**) Network dendrogram of *Boa*, reflecting this network architecture. Q-modules are indicated by Q_{max} (represented by the red dotted line). S-modules are indicated by black ($p < 0.001$), grey ($0.001 \leq p < 0.01$), or white ($0.01 \leq p < 0.05$) circles. Abbreviations: ecp, ectopterygoid; mx, maxilla; pal, palatine; pt, pterygoid.

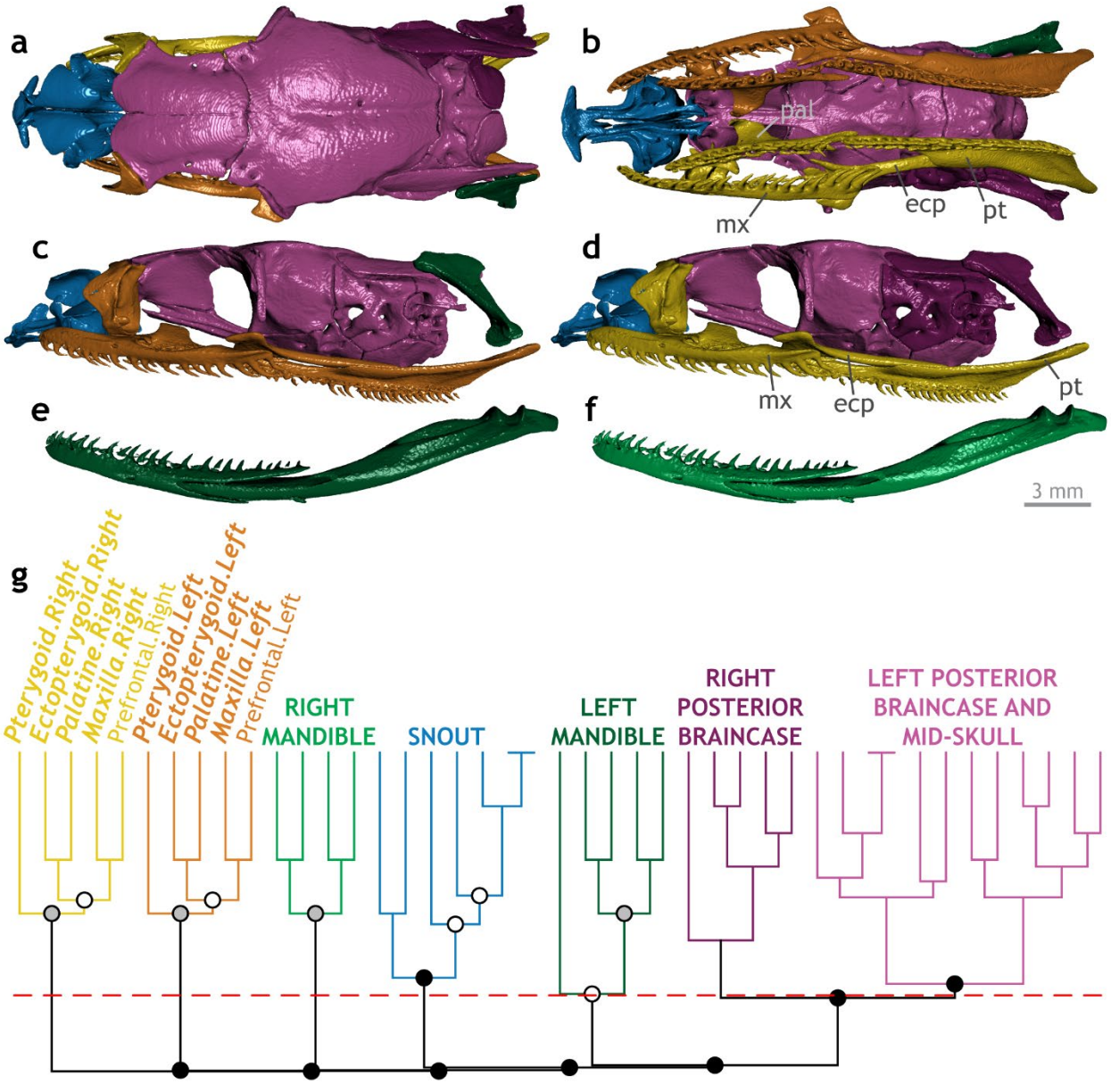
a
b
pal
mx
ecp
pt
c
d
mx
ecp
pt
e
f
3 mm
g
Pterygoid.Right
Ectopterygoid.Right
Palatine.Right
Maxilla.Right
Prefrontal.Right
Pterygoid.Left
Ectopterygoid.Left
Palatine.Left
Maxilla.Left
Prefrontal.Left
RIGHT MANDIBLE
SNOUT
LEFT MANDIBLE
RIGHT POSTERIOR BRAINCASE
LEFT POSTERIOR BRAINCASE AND MID-SKULL

FIGURE 4.8. Skull modularity of caenophidian snakes. In caenophidians, the palatomaxillary arches (in italicized boldface) and prefrontals consistently form left and right modules, almost always distinct from all other skull elements (see text for minor exceptions). (**a–f**) Representative pattern of caenophidian skull modularity, illustrated using *Thamnophis radix* (UAMZ R636) in (**a**) dorsal, (**b**) ventral, (**c**) left lateral, and (**d**) right lateral views of the skull, and (**e**) left lateral and (**f**) right lateral views of the mandible. (**g**) Network dendrogram of *Thamnophis*, reflecting this network structure. Q-modules are indicated by Q_{max} (represented by the red dotted line). S-modules are indicated by black ($p < 0.001$), grey ($0.001 \leq p < 0.01$), or white ($0.01 \leq p < 0.05$) circles. Abbreviations: ecp, ectopterygoid; mx, maxilla; pal, palatine; pt, pterygoid.

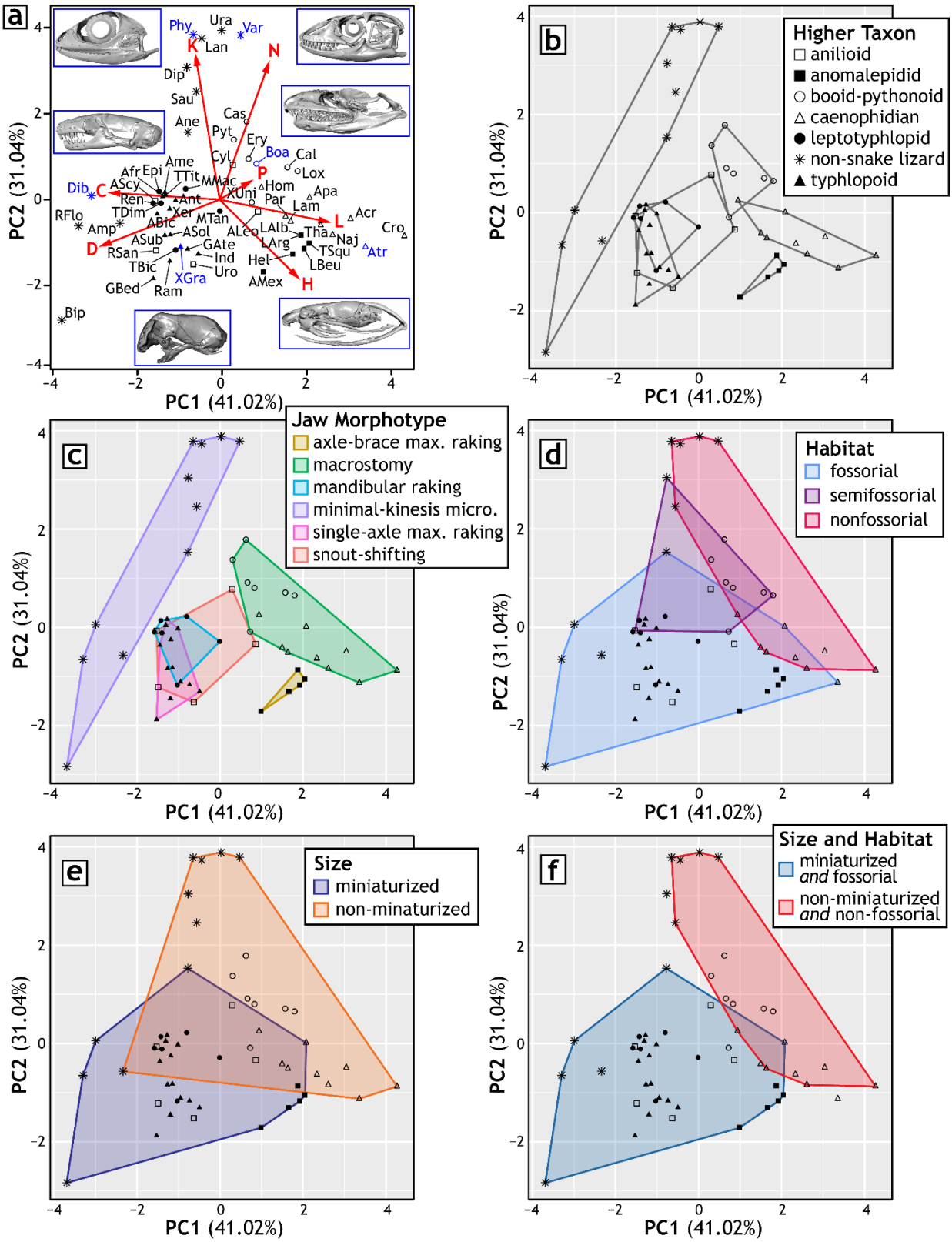
a
b
c
d
e
f
PC1 (41.02%)
PC2 (31.04%)
Higher Taxon
anilioid
anomalepidid
booid-pythonoid
caenophidian
leptotyphlopid
non-snake lizard
typhlopoid
Jaw Morphotype
axle-brace max. raking
macrostomy
mandibular raking
minimal-kinesis micro.
single-axle max. raking
snout-shifting
Habitat
fossorial
semifossorial
nonfossorial
Size
miniaturized
non-minaturized
Size and Habitat
miniaturized and fossorial
non-miniaturized and non-fossorial
Phy
Ura
Var
Lan
Dip
Sau
Ane
Cas
Pyt
Ery
Cyl
Boa
Cal
Lox
Ame
Afr
Epi
TTit
MMac
Hom
Apa
Par
Lam
Acr
Cro
Dib
AScy
Ren
Ant
XUni
RFlo
Amp
TDim
Xer
MTan
ABic
ASol
ALeo
LAlb
Tha
Naj
TSqu
Atr
ASub
RSan
GAte
LArg
Ind
Uro
Hel
LBeu
TBic
XGra
GBed
Ram
AMex
Bip
K
N
P
C
L
D
H

FIGURE 4.9. Principal component analysis (PCA) based on anatomical network parameters (see Tables 4.2 and S4.1). Patterns of morphospace occupation are represented using convex hulls. See legend in (**b**) for symbols used throughout all panels. (**a**) Biplot showing overall morphospace composition. Red arrows indicate the contribution of each network parameter to the first two principal components. Specimens are labelled using the first three letters of their respective genus, or the first letter of the genus and first three letters of the specific epithet (see Table 4.1). Representative specimens spanning morphospace are indicated in blue. (**b**) Distribution of higher taxa across morphospace. Non-snake lizards, anomalepidids, booid-pythonoids, and caenophidians occupy generally distinct regions, whereas typhlopoids, leptotyphlopids, and anilioids overlap extensively. (**c**) Distribution across morphospace of jaw morphotypes proposed by Strong *et al.* (2021b). (**d**) Distribution of habitat types across morphospace. Fossorial and non-fossorial taxa occupy distinct regions, although these regions do overlap somewhat. Semi-fossorial taxa occupy an intermediate region overlapping broadly with both other habitats. (**e**) Distribution of size classes across morphospace. Miniaturized and non-miniaturized taxa both occupy large regions of morphospace; these regions are generally distinct but do exhibit noticeable overlap. (**f**) Distribution of taxa when considering size and habitat simultaneously. Miniaturization and fossoriality together define a more distinct region of morphospace than when either phenomenon is considered individually, reflected by reduced overlap between opposing regions (i.e., miniaturized–fossorial *versus* non-miniaturized–non-fossorial). Abbreviations: N, number of nodes; K, number of connections; D, density of connections; C, mean clustering coefficient; L, mean shortest path length; H, heterogeneity of connections; P, parcellation.

Tables: Chapter Four

TABLE 4.1. List of specimens analyzed in Chapter Four. Taxonomic assignments are based on Burbrink *et al.* (2020). See Methods and Appendix 1.1 for information regarding sources of micro-CT scan data. See preliminary pages of thesis document for institutional abbreviations.

HIGHER TAXON			SPECIES	SPECIMEN NUMBER
Alethinophidia	**'Anilioidea'**	**Amerophidia (Aniliidae)**	*Anilius scytale*	KUH 125976
		Uropeltoidea (Anomochilidae) (Cylindrophiidae) (Uropeltidae x2)	*Anomochilus leonardi*	FRIM 0026
			Cylindrophis ruffus	UMMZ 201901
			Rhinophis sanguineus	UF 78397
			Uropeltis melanogaster	FMNH 167048
	Bolyeriidae		*Casarea dussumieri*	UMMZ 190285
	Booidea	**Boidae**	*Boa constrictor*	FMNH 31182
		Calabariidae	*Calabaria reinhardtii*	FMNH 117833
		Erycidae	*Eryx colubrinus*	FMNH 63117
	Caenophidia	**Acrochordidae**	*Acrochordus granulatus*	MCZ R-146128
		Atractaspididae	*Aparallactus guentheri*	MCZ R-23363
			Atractaspis irregularis	FMNH 62204
		Colubridae	*Lampropeltis getula*	FMNH 95184
		Elapidae	*Naja naja*	FMNH 22468
		Homalopsidae	*Homalopsis buccata*	FMNH 259340
		Natricidae	*Thamnophis radix*	UAMZ R636

		Pareidae	*Pareas hamptoni*	FMNH 128304
		Viperidae	*Crotalus adamanteus*	UF 103268
	Pythonoidea	**Loxocemidae**	*Loxocemus bicolor*	FMNH 104800
		Pythonidae	*Python molurus*	TNHC 62769
		Xenopeltidae	*Xenopeltis unicolor*	FMNH 148900
Scolecophidia	**Anomalepididae**		*Anomalepis mexicanus*	MCZ R-191201
			Helminthophis praeocularis	MCZ R-17960
			Liotyphlops albirostris	FMNH 216257
			Liotyphlops argaleus	MCZ R-67933
			Liotyphlops beui	SAMA 40142
			Typhlophis squamosus	MCZ R-145403
	Leptotyphlopidae		*Epictia albifrons*	MCZ R-2885
			Myriopholis macrorhyncha	MCZ R-9650
			Myriopholis tanae	MCZ R-40099
			Rena dulcis	UAMZ R335
			Tricheilostoma bicolor	MCZ R-49718
			Trilepida dimidiata	SAMA 40143
	Typhlopoidea	**Gerrhopilidae**	*Gerrhopilus ater*	MCZ R-33505
			Gerrhopilus beddomii	MCZ R-22372
		Typhlopidae	*Acutotyphlops solomonis*	AMS R.11452
			Acutotyphlops subocularis	SAMA R64770
			Afrotyphlops angolensis	MCZ R-170385

			Amerotyphlops paucisquamus	MCZ R-147336
			Anilios bicolor	SAMA 60626
			Antillotyphlops monastus	MCZ R-81112
			Indotyphlops braminus	UAMZ R363
			Ramphotyphlops lineatus	MCZ R-37751
			Typhlops titanops	MCZ R-68571
			Xerotyphlops vermicularis	MCZ R-56477
		Xenotyphlopidae	*Xenotyphlops grandidieri*	ZSM 2194/2007
'Non-snake lizards'	**Amphisbaenia**	**Amphisbaenidae**	*Amphisbaena fuliginosa*	FMNH 22847
		Bipedidae	*Bipes biporus*	CAS 126478
		Rhineuridae	*Rhineura floridana*	FMNH 31774
	Dibamidae		*Anelytropsis papillosus*	TCWC 45501
			Dibamus novaeguineae	UF 33488
	Iguania	**Agamidae**	*Physignathus cocincinus*	YPM 14378
		Iguanidae	*Dipsosaurus dorsalis*	YPM 14376
			Sauromalus ater	TNHC 18483
		Tropiduridae	*Uranoscodon superciliosus*	YPM 12871
	Varanoidea	**Lanthanotidae**	*Lanthanotus borneensis*	FMNH 148589
		Varanidae	*Varanus exanthematicus*	FMNH 58299

TABLE 4.2. Parameters calculated for each anatomical network. Abbreviations: N, total number of nodes or elements; K, total number of connections or articulations; D, density of connections; C, mean clustering coefficient; L, mean shortest path length; H, heterogeneity of connections; P, parcellation. See Methods for further explanation.

TAXON	N	K	D	C	L	H	P
Anilius	39	91	0.1228	0.4276	3.1134	0.4406	0.7811
Anomochilus	41	81	0.0988	0.3181	3.5897	0.5060	0.8209
Cylindrophis	45	96	0.0970	0.3664	3.5091	0.4645	0.7714
Rhinophis	35	72	0.1210	0.4642	3.1815	0.4633	0.7853
Uropeltis	35	68	0.1143	0.3500	3.2118	0.4906	0.7478
Casarea	49	107	0.0910	0.4522	4.0765	0.4199	0.7888
Boa	45	94	0.0949	0.3760	3.9263	0.4457	0.8148
Calabaria	47	95	0.0879	0.2770	3.7299	0.5131	0.7614
Eryx	45	95	0.0960	0.3760	3.8758	0.4311	0.8148
Acrochordus	43	77	0.0853	0.2257	4.5969	0.5214	0.8069
Aparallactus	45	83	0.0838	0.2875	4.2677	0.4999	0.7180
Atractaspis	41	67	0.0817	0.1857	4.7512	0.5212	0.7531
Lampropeltis	43	81	0.0897	0.2763	4.1030	0.5208	0.6533
Naja	43	77	0.0853	0.2123	4.3865	0.5525	0.6555
Homalopsis	43	88	0.0975	0.2768	3.8228	0.4486	0.7572
Thamnophis	43	75	0.0831	0.2275	4.2182	0.5210	0.6879
Pareas	43	79	0.0875	0.3412	4.0853	0.5168	0.7074
Crotalus	43	67	0.0742	0.1802	4.8126	0.5611	0.8643
Loxocemus	47	95	0.0879	0.2776	3.9112	0.5157	0.7614
Python	47	105	0.0971	0.4102	3.7761	0.4399	0.7777
Xenopeltis	41	79	0.0963	0.3467	4.1049	0.4085	0.7567
Anomalepis	37	59	0.0886	0.4706	3.8807	0.5621	0.8108
Helminthophis	40	65	0.0833	0.4479	4.0427	0.5861	0.8125
Liotyphlops albirostris	41	68	0.0829	0.4427	4.2186	0.5495	0.8638
Liotyphlops argaleus	41	68	0.0829	0.4427	4.2186	0.5495	0.8638
Liotyphlops beui	41	67	0.0817	0.4227	4.0472	0.5965	0.8150
Typhlophis	40	62	0.0795	0.4211	4.2774	0.5308	0.8638
Epictia	40	97	0.1244	0.4735	3.4397	0.4418	0.7725

Myriopholis macrorhyncha	41	95	0.1159	0.4773	3.5085	0.4647	0.8245
Myriopholis tanae	40	85	0.1090	0.4588	3.8667	0.4758	0.8250
Rena	39	95	0.1282	0.4769	3.4345	0.4447	0.7705
Tricheilostoma	36	78	0.1238	0.4790	3.5746	0.4903	0.7870
Trilepida	39	93	0.1255	0.4634	3.4507	0.4421	0.7771
Gerrhopilus ater	35	66	0.1109	0.4776	3.8958	0.4020	0.7739
Gerrhopilus beddomii	31	58	0.1247	0.5048	3.5548	0.4138	0.8429
Acutotyphlops solomonis	36	72	0.1143	0.5196	4.0127	0.3732	0.7377
Acutotyphlops subocularis	36	74	0.1175	0.5272	3.7841	0.4061	0.7824
Afrotyphlops	40	89	0.1141	0.5116	3.8705	0.3840	0.6825
Amerotyphlops	40	87	0.1115	0.4994	3.9167	0.3513	0.6825
Anilios	38	83	0.1181	0.4940	3.6046	0.4033	0.7355
Antillotyphlops	40	85	0.1090	0.4941	3.9192	0.3796	0.6825
Indotyphlops	35	66	0.1109	0.4554	3.8958	0.4270	0.7739
Ramphotyphlops	33	63	0.1193	0.4968	3.9356	0.3787	0.7787
Typhlops	40	89	0.1141	0.5116	3.8705	0.3840	0.6825
Xerotyphlops	38	81	0.1152	0.4901	3.8094	0.3726	0.7604
Xenotyphlops	37	80	0.1201	0.5171	3.4730	0.5314	0.8006
Amphisbaena	37	83	0.1246	0.5353	3.1351	0.4288	0.7232
Bipes	30	67	0.1540	0.5963	2.8759	0.5380	0.6200
Rhineura	36	94	0.1492	0.5658	2.8540	0.4693	0.7701
Anelytropsis	47	107	0.0990	0.5212	3.3673	0.4435	0.7759
Dibamus	37	90	0.1351	0.5293	3.2583	0.3292	0.7363
Physignathus	54	135	0.0943	0.4717	3.3487	0.3561	0.8203
Dipsosaurus	52	126	0.0950	0.4861	3.3718	0.3798	0.7633
Sauromalus	50	118	0.0963	0.4536	3.4188	0.3924	0.7608
Uranoscodon	56	134	0.0870	0.4492	3.4825	0.3774	0.8182
Lanthanotus	54	135	0.0943	0.4966	3.5618	0.3624	0.8354
Varanus	57	130	0.0815	0.4669	3.9467	0.3636	0.7584

References: Chapter Four

Adalsteinsson, S. A., Branch, W. R., Trape, S., Vitt, L. J. & Hedges, S. B. 2009. Molecular phylogeny, classification, and biogeography of snakes of the Family Leptotyphlopidae (Reptilia, Squamata). *Zootaxa*, **2244**, 1–50.

Adams, D. C., Rohlf, F. J. & Slice, D. E. 2004. Geometric morphometrics: ten years of progress following the 'revolution'. *Italian Journal of Zoology*, **71**(1), 5–16. doi:10.1080/11250000409356545

Andjelković, M., Tomović, L. & Ivanović, A. 2017. Morphological integration of the kinetic skull in *Natrix* snakes. *Journal of Zoology*, **303**, 188–198. doi:10.1111/jzo.12477

Bell, C. J., Mead, J. I. & Swift, S. L. 2009. Cranial osteology of *Moloch horridus* (Reptilia: Squamata: Agamidae). *Records of the Western Australian Museum*, **25**, 201–237. doi:10.18195/issn.0312-3162.25(2).2009.201-237

Bellairs, A. D. & Underwood, G. 1951. The origin of snakes. *Biological Reviews*, **26**, 193–237.

Bennett, D. 2000. Observations on Bosc's monitor lizard (*Varanus exanthematicus*) in the wild. *Bulletin of the Chicago Herpetological Society*, **35**(8), 177–180.

Burbrink, F. T., Grazziotin, F. G., Pyron, R. A., Cundall, D., Donnellan, S., Irish, F., Keogh, J. S., Kraus, F., Murphy, R. W., Noonan, B., Raxworthy, C. J., Ruane, S., Lemmon, A. R., Lemmon, E. M. & Zaher, H. 2020. Interrogating genomic-scale data for Squamata (lizards, snakes, and amphisbaenians) shows no support for key traditional morphological relationships. *Systematic Biology*, **69**(3), 502–520. doi:10.1093/sysbio/syz062

Caldwell, M. W. 2019. *The Origin of Snakes: Morphology and the Fossil Record*. Taylor & Francis, Boca Raton.

Chretien, J., Wang-Claypool, C. Y., Glaw, F. & Scherz, M. D. 2019. The bizarre skull of *Xenotyphlops* sheds light on synapomorphies of Typhlopoidea. *Journal of Anatomy*, **234**, 637–655. doi:10.1111/joa.12952

Clauset, A., Newman, M. E. J. & Moore, C. 2004. Finding community structure in very large networks. *Physical Review E*, **70**, 066111. doi:10.1103/PhysRevE.70.066111

Conrad, J. L. 2008. Phylogeny and systematics of Squamata (Reptilia) based on morphology. *Bulletin of the American Museum of Natural History, New York*, **310**, 1–182. doi:10.1206/310.1

Csárdi, G. & Nepusz, T. 2006. The igraph software package for complex network research. *InterJournal Complex Systems*, **1695**, 1–9.

Cundall, D. 1983. Activity of head muscles during feeding by snakes: a comparative study. *American Zoologist*, **23**, 383–396.

Cundall, D. & Rossman, D. A. 1993. Cephalic anatomy of the rare Indonesian snake *Anomochilus weberi*. *Zoological Journal of the Linnean Society*, **109**, 235–273.

Cundall, D. 1995. Feeding behaviour in *Cylindrophis* and its bearing on the evolution of alethinophidian snakes. *Journal of Zoology*, **237**, 353–376.

Cundall, D. & Irish, F. 2008. The snake skull. Pp. 349–692 in C. Gans, A.S. Gaunt and K. Adler (eds) *Biology of the Reptilia: Morphology H, The Skull of Lepidosauria*. Society for the Study of Amphibian and Reptiles, Ithaca, New York.

Da Silva, F. O., Fabre, A.-C., Savriama, Y., Ollonen, J., Mahlow, K., Herrel, A., Müller, J. & Di-Poï, N. 2018. The ecological origins of snakes as revealed by skull evolution. *Nature Communications*, **9**, 376. doi:10.1038/s41467-017-02788-3

Das, I. & Wallach, V. 1998. Scolecophidian arboreality revisited. *Herpetological Review*, **29**(1), 15–16.

de Pinna, M. G. G. 1991. Concepts and tests of homology in the cladistic paradigm. *Cladistics*, **7**, 367–394.

Deufel, A. & Cundall, D. 2003. Feeding in *Atractaspis* (Serpentes: Atractaspididae): a study in conflicting functional constraints. *Zoology*, **106**, 43–61.

Ebel, R., Müller, J., Ramm, T., Hipsley, C. & Amson, E. 2020. First evidence of convergent lifestyle signal in reptile skull roof microanatomy. *BMC Biology*, **18**, 185. doi:10.1186/s12915-020-00908-y

Eble, G. J. 2005. Morphological modularity and macroevolution: conceptual and empirical aspects. Pp. 221–238 in W. Callebaut and D. Rasskin-Gutman (eds) *Modularity: Understanding the Development and Evolution of Natural Complex Systems*. MIT Press, Cambridge, MA.

Esteve-Altava, B., Marugán-Lobón, J., Botella, H. & Rasskin-Gutman, D. 2011. Network models in anatomical systems. *Journal of Anthropological Sciences*, **89**, 175–184. doi:10.4436/jass.89016

Esteve-Altava, B., Marugán-Lobón, J., Botella, H., Bastir, M. & Rasskin-Gutman, D. 2013. Grist for Riedl's mill: a network model perspective on the integration and modularity of the human skull. *Journal of Experimental Zoology, Part B: Molecular and Developmental Evolution*, **320B**, 489–500. doi:10.1002/jez.b.22524

Esteve-Altava, B. & Rasskin-Gutman, D. 2014. Theoretical morphology of tetrapod skull networks. *Comptes Rendus Palevol*, **13**, 41–50. doi:10.1016/j.crpv.2013.08.003

Esteve-Altava, B., Diogo, R., Smith, C., Boughner, J. C. & Rasskin-Gutman, D. 2015. Anatomical networks reveal the musculoskeletal modularity of the human head. *Scientific Reports*, **5**, 8298. doi:10.1038/srep08298

Esteve-Altava, B. 2017a. Challenges in identifying and interpreting organizational modules in morphology. *Journal of Morphology*, **278**, 960–974. doi:10.1002/jmor.20690

Esteve-Altava, B. 2017b. In search of morphological modules: a systematic review. *Biological Reviews of the Cambridge Philosophical Society*, **92**, 1332–1347. doi:10.1111/brv.12284

Esteve-Altava, B., Molnar, J. L., Johnston, P., Hutchinson, J. R. & Diogo, R. 2018. Anatomical network analysis of the musculoskeletal system reveals integration loss and parcellation boost during the fins-to-limbs transition. *Evolution*, **72**(3), 601–618. doi:10.1111/evo.13430

Esteve-Altava, B., Pierce, S. E., Molnar, J. L., Johnston, P., Diogo, R. & Hutchinson, J. R. 2019. Evolutionary parallelisms of pectoral and pelvic network-anatomy from fins to limbs. *Science Advances*, **5**, eaau7459. doi:10.1126/sciadv.aau7459

Evans, H. E. 1955. The osteology of a worm snake, *Typhlops jamaicensis* (Shaw). *The Anatomical Record*, **122**, 381–396.

Evans, S. E. 2008. The Skull of Lizards and Tuatara. Pp. 1–347 in C. Gans, A.S. Gaunt and K. Adler (eds) *Biology of the Reptilia, Vol. 20: The Skull of Lepidosauria*. Society for the Study of Amphibians and Reptiles, Ithaca.

Fachini, T. S., Onary, S., Palci, A., Lee, M. S. Y., Bronzati, M. & Hsiou, A. S. 2020. Cretaceous blind snake from Brazil fills major gap in snake evolution. *iScience*, **23**, 101834. doi:10.1016/j.isci. 2020.101834

Figueroa, A. 2016. *Phylogenetic Relationships and Evolution of Snakes*. PhD thesis, University of New Orleans, New Orleans, LA.

Frazzetta, T. H. 1966. Studies of the morphology and function of the skull in the Boidae (Serpentes). Part II. Morphology and function of the jaw apparatus in *Python sebae* and *Python molurus*. *Journal of Morphology*, **118**, 217–296.

Fröbisch, N. B. & Schoch, R. R. 2009. Testing the impact of miniaturization on phylogeny: Paleozoic dissorophoid amphibians. *Systematic Biology*, **58**(3), 312–327. doi:10.1093/sysbio/syp029

Gans, C. & Montero, R. 2008. An atlas of amphisbaenian skull anatomy. Pp. 621–738 in C. Gans, A.S. Gaunt and K. Adler (eds) *Biology of the Reptilia. Volume 21. Morphology I. The Skull and Appendicular Locomotor Apparatus of Lepidosauria*. Society for the Study of Amphibians and Reptiles, Ithaca, New York.

Garberoglio, F. F., Apesteguía, S., Simões, T. R., Palci, A., Gómez, R. O., Nydam, R. L., Larsson, H. C. E., Lee, M. S. Y. & Caldwell, M. W. 2019a. New skulls and skeletons of the Cretaceous legged snake *Najash*, and the evolution of the modern snake body plan. *Science Advances*, **5**(11), eaax5833. doi:10.1126/sciadv.aax5833

Gould, S. J. 1977. *Ontogeny and Phylogeny*. Harvard University Press, Cambridge.

Gray, J. A. 2018. *Skull Evolution in the Australian Dragon Lizards*. PhD thesis, University of Adelaide, Adelaide.

Haas, G. 1968. Anatomical observations on the head of *Anomalepis aspinosus* (Typhlopidae, Ophidia). *Acta Zoologica*, **48**, 63–139.

Hanken, J. 1984. Miniaturization and its effects on cranial morphology in plethodontid salamanders, genus *Thorius* (Amphibia: Plethodontidae). I. Osteological variation. *Biological Journal of the Linnean Society*, **23**, 55–75.

Hanken, J. & Wake, D. B. 1993. Miniaturization of body size: organismal consequences and evolutionary significance. *Annual Review of Ecology and Systematics*, **24**, 501–519.

Harrington, S. M. & Reeder, T. W. 2017. Phylogenetic inference and divergence dating of snakes using molecules, morphology and fossils: new insights into convergent evolution of feeding morphology and limb reduction. *Biological Journal of the Linnean Society*, **121**, 379–394.

Howland, J. M., Vitt, L. J. & Lopez, P. T. 1990. Life on the edge: the ecology and life history of the tropidurine iguanid lizard *Uranoscodon superciliosum*. *Canadian Journal of Zoology/Revue Canadienne de Zoologie*, **68**, 1366–1373.

Hsiang, A. Y., Field, D. J., Webster, T. H., Behlke, A. D. B., Davis, M. B., Racicot, R. A. & Gauthier, J. A. 2015. The origin of snakes: revealing the ecology, behavior, and evolutionary history of early snakes using genomics, phenomics, and the fossil record. *BMC Evolutionary Biology*, **15**, 87. doi:10.1186/s12862-015-0358-5

Iordansky, N. N. 1997. Jaw apparatus and feeding mechanics of *Typhlops* (Ophidia: Typhlopidae): a reconsideration. *Russian Journal of Herpetology*, **4**(2), 120–127.

Johnson, S. R. 1965. An ecological study of the chuckwalla, *Sauromalus obesus* Baird, in the western Mojave Desert. *American Midland Naturalist*, **73**(1), 1–29.

Khannoon, E. R. & Evans, S. E. 2015. The development of the skull of the Egyptian cobra *Naja h. haje* (Squamata: Serpentes: Elapidae). *PLoS ONE*, **10**, e0122185. doi:10.1371/journal.pone.0122185

Kley, N. J. & Brainerd, E. L. 1999. Feeding by mandibular raking in a snake. *Nature*, **402**, 369–370. doi:10.1038/46460

Kley, N. J. 2001. Prey transport mechanisms in blindsnakes and the evolution of unilateral feeding systems in snakes. *American Zoologist*, **41**, 1321–1337.

Kley, N. J. 2006. Morphology of the lower jaw and suspensorium in the Texas blindsnake, *Leptotyphlops dulcis* (Scolecophidia: Leptotyphlopidae). *Journal of Morphology*, **267**, 494–515. doi:10.1002/jmor.10414

Koch, C., Martins, A. & Schweiger, S. 2019. A century of waiting: description of a new *Epictia* Gray, 1845 (Serpentes: Leptotyphlopidae) based on specimens housed for more than 100 years in the collection of the Natural History Museum Vienna (NMW). *PeerJ*, **7**, e7411. doi:10.7717/peerj.7411

Kraus, F. 2017. New species of blindsnakes (Squamata: Gerrhopilidae) from the offshore islands of Papua New Guinea. *Zootaxa*, **4299**(7), 75–94. doi:10.11646/zootaxa.4299.1.3

Langner, C. 2017. Hidden in the heart of Borneo – Shedding light on some mysteries of an enigmatic lizard: first records of habitat use, behavior, and food items of *Lanthanotus borneensis* Steindachner, 1878 in its natural habitat. *Russian Journal of Herpetology*, **24**(1), 1–10.

Lawson, R., Slowinski, J. B., Crother, B. I. & Burbrink, F. T. 2005. Phylogeny of the Colubroidea (Serpentes): New evidence from mitochondrial and nuclear genes. *Molecular Phylogenetics and Evolution*, **37**, 581–601. doi:10.1016/j.ympev.2005.07.016

Lee, H. W., Esteve-Altava, B. & Abzhanov, A. 2020. Evolutionary and ontogenetic changes of the anatomical organization and modularity in the skull of archosaurs. *Scientific Reports*, **10**, 16138. doi:10.1038/s41598-020-73083-3

Lee, M. S. Y. 1998. Convergent evolution and character correlation in burrowing reptiles: towards a resolution of squamate relationships. *Biological Journal of the Linnean Society*, **65**, 369–453.

Lee, M. S. Y. & Scanlon, J. D. 2002. Snake phylogeny based on osteology, soft anatomy and ecology. *Biological Reviews*, **77**, 333–401.

List, J. C. 1966. Comparative osteology of the snake families Typhlopidae and Leptotyphlopidae. *Illinois Biological Monographs*, **36**, 1–112.

Maddin, H. C., Olori, J. C. & Anderson, J. S. 2011. A redescription of *Carrolla craddocki* (Lepospondyli: Brachystelechidae) based on high-resolution CT, and the impacts of miniaturization and fossoriality on morphology. *Journal of Morphology*, **272**, 722–743. doi:10.1002/jmor.10946

Mahendra, B. C. 1936. Contributions to the osteology of the Ophidia. I. The endoskeleton of the so-called 'blind-snake', *Typhlops braminus* Daud. *Proceedings of the Indian Academy of Sciences*, **3**, 128–142.

Mahendra, B. C. 1938. Some remarks on the phylogeny of the Ophidia. *Anatomischer Anzieger*, **86**, 347–356.

Maisano, J. A. & Rieppel, O. 2007. The skull of the round island boa, *Casarea dussumieri* Schlegel, based on high-resolution X-ray computed tomography. *Journal of Morphology*, **268**, 371–384. doi:10.1002/jmor.10519

Martin, C. 2017. ggConvexHull. https://github.com/cmartin/ggConvexHull

Martinez-Arbizu, P. 2020. pairwiseAdonis. https://github.com/pmartinezarbizu/pairwiseAdonis

McNamara, K. J. 1986. A guide to the nomenclature of heterochrony. *Journal of Paleontology*, **60**(1), 4–13.

Miralles, A., Marin, J., Markus, D., Herrel, A., Hedges, S. B. & Vidal, N. 2018. Molecular evidence for the paraphyly of Scolecophidia and its evolutionary implications. *Journal of Evolutionary Biology*, **31**, 1782–1793. doi:10.1111/jeb.13373

Monteiro, L. R. & Abe, A. S. 1997. Allometry and morphological integration in the skull of *Tupinambis merianae* (Lacertilia: Teiidae). *Amphibia-Reptilia*, **18**, 397–405.

Navarro-Díaz, A., Esteve-Altava, B. & Rasskin-Gutman, D. 2019. Disconnecting bones within the jaw-otic network modules underlies mammalian middle ear evolution. *Journal of Anatomy*, **235**, 15–33. doi:10.1111/joa.12992

Newman, M. E. J. & Girvan, M. 2004. Finding and evaluating community structure in networks. *Physical Review E*, **69**, 026113. doi:10.1103/PhysRevE.69.026113

Newman, M. E. J. 2006. Finding community structure in networks using the eigenvectors of matrices. *Physical Review E*, **74**, 036104. doi:10.1103/PhysRevE.74.036104

Nguyen, T. Q., Ngo, H. N., Pham, C. T., Van, H. N., Ngo, C. D., Schingen, M. v. & Ziegler, T. 2018. First population assessment of the Asian Water Dragon (*Physignathus cocincinus* Cuvier, 1829) in Thua Thien Hue Province, Vietnam. *Nature Conservation*, **26**, 1–14. doi:10.3897/natureconservation.26.21818

Norris, K. S. 1953. The ecology of the desert iguana *Dipsosaurus dorsalis*. *Ecology*, **34**(2), 265–287.

Object Research Systems Inc. 2019b. Dragonfly 4.1. Object Research Systems (ORS) Inc., Montreal, Canada. https://theobjects.com/dragonfly/

Oksanen, J., Blanchet, F. G., Friendly, M., Kindt, R., Legendre, P., McGlinn, D., Minchin, P. R., O'Hara, R. B., Simpson, G. L., Solymos, P., Stevens, M. H. H., Szoecs, E. & Wagner, H. 2019. vegan: community ecology package. https://CRAN.R-project.org/package=vegan

Ollonen, J., Silva, F. O. D., Mahlow, K. & Di-Poï, N. 2018. Skull development, ossification pattern, and adult shape in the emerging lizard model organism *Pogona vitticeps*: a comparative analysis with other squamates. *Frontiers in Physiology*, **9**, 278. doi:10.3389/fphys.2018.00278

Olori, J. C. & Bell, C. J. 2012. Comparative skull morphology of uropeltid snakes (Alethinophidia: Uropeltidae) with special reference to disarticulated elements and variation. *PLoS ONE*, **7**(3), e32450. doi:10.1371/journal.pone.0032450

Palci, A. & Caldwell, M. W. 2010. Redescription of *Acteosaurus tommasinii* von Meyer, 1860, and a discussion of evolutionary trends within the clade Ophidiomorpha. *Journal of Vertebrate Paleontology*, **30**(1), 94–108. doi:10.1080/02724630903409139

Palci, A. & Caldwell, M. W. 2013. Primary homologies of the circumorbital bones of snakes. *Journal of Morphology*, **274**, 973–986. doi:10.1002/jmor.20153

Palci, A., Lee, M. S. Y. & Hutchinson, M. N. 2016. Patterns of postnatal ontogeny of the skull and lower jaw of snakes as revealed by micro-CT scan data and three-dimensional geometric morphometrics. *Journal of Anatomy*, **229**(6), 723–754. doi:10.1111/joa.12509

Palci, A., Hutchinson, M. N., Caldwell, M. W. & Lee, M. S. Y. 2017. The morphology of the inner ear of squamate reptiles and its bearing on the origin of snakes. *Royal Society Open Science*, **4**, 170685. doi:10.1098/rsos.170685

Palci, A. & Lee, M. S. Y. 2019. Geometric morphometrics, homology and cladistics: review and recommendations. *Cladistics*, **35**, 230–242. doi:10.1111/cla.12340

Patterson, C. 1982. Morphological characters and homology. Pp. 21–74 in K.A. Joysey and A.E. Friday (eds) *Problems of Phylogenetic Reconstruction*. Academic Press, London and New York.

Pinto, R. R. & Fernandes, R. 2012. A new blind snake species of the genus *Tricheilostoma* from Espinhaço Range, Brazil and taxonomic status of *Rena dimidiata* (Jan, 1861) (Serpentes: Epictinae: Leptotyphlopidae). *Copeia*, **2012**(1), 37–48. doi:10.1643/CH-11-040

Plateau, O. & Foth, C. 2020. Birds have peramorphic skulls, too: anatomical network analyses reveal oppositional heterochronies in avian skull evolution. *Communications Biology*, **3**, 195. doi:10.1038/s42003-020-0914-4

Polachowski, K. M. & Werneburg, I. 2013. Late embryos and bony skull development in *Bothropoides jararaca* (Serpentes, Viperidae). *Zoology*, **116**, 36–63. doi:10.1016/j.zool.2012.07.003

Polly, P. D. 2008. Developmental dynamics and G-matrices: can morphometric spaces be used to model phenotypic evolution? *Evolutionary Biology*, **35**, 83–96. doi:10.1007/s11692-008-9020-0

Pyron, R. A., Burbrink, F. T., Colli, G. R., Nieto Montes de Oca, A., Vitt, L. J., Kuczynski, C. A. & Wiens, J. J. 2011. The phylogeny of advanced snakes (Colubroidea), with discovery of a new subfamily and comparison of support methods for likelihood trees. *Molecular Phylogenetics and Evolution*, **58**, 329–342. doi:10.1016/j.ympev.2010.11.006

Pyron, R. A., Burbrink, F. T. & Wiens, J. J. 2013. A phylogeny and revised classification of Squamata, including 4161 species of lizards and snakes. *BMC Evolutionary Biology*, **13**, 93. doi:10.1186/1471-2148-13-93

R Core Team. 2020. R: a language and environment for statistical computing. R Foundation for Statistical Computing, Vienna, Austria. https://www.R-project.org/

Rasskin-Gutman, D. & Buscalioni, A. D. 2001. Theoretical morphology of the Archosaur (Reptilia: Diapsida) pelvic girdle. *Paleobiology*, **27**(1), 59–78. doi:10.1666/0094-8373(2001)027<0059:TMOTAR>2.0.CO;2

Rasskin-Gutman, D. 2003. Boundary constraints for the emergence of form. Pp. 305–322 in G.B. Müller and S.A. Newman (eds) *Origination of Organismal Form: Beyond the Gene in Developmental and Evolutionary Biology*. MIT Press, Cambridge, MA.

Rasskin-Gutman, D. & Esteve-Altava, B. 2014. Connecting the dots: anatomical network analysis in morphological EvoDevo. *Biological Theory*, **9**, 178–193. doi:10.1007/s13752-014-0175-x

Reeder, T. W., Townsend, T. M., Mulcahy, D. G., Noonan, B. P., Wood, P. L., Sites, J. W. & Wiens, J. J. 2015. Integrated analyses resolve conflicts over squamate reptile phylogeny and reveal unexpected placements for fossil taxa. *PLoS ONE*, **10**(3), e0118199. doi:10.1371/journal.pone.0118199

Rhoda, D., Polly, P. D., Raxworthy, C. & Segall, M. 2021. Morphological integration and modularity in the hyperkinetic feeding system of aquatic-foraging snakes. *Evolution*, **75**(1), 56–72. doi:10.1111/evo.14130

Rieppel, O. 1977. Studies on the skull of the Henophidia (Reptilia: Serpentes). *Journal of Zoology*, **181**, 145–173.

Rieppel, O. 1978b. The evolution of the naso-frontal joint in snakes and its bearing on snake origins. *Journal of Zoological Systematics and Evolutionary Research*, **16**, 14–27. doi:10.1111/j.1439-0469.1978.tb00917.x

Rieppel, O. 1984a. Miniaturization of the lizard skull: its functional and evolutionary implications. *Symposia of the Zoological Society of London*, **52**, 503–520.

Rieppel, O. 1984b. The cranial morphology of the fossorial lizard genus *Dibamus* with a consideration of its phylogenetic relationships. *Journal of Zoology*, **204**, 289–327.

Rieppel, O. 1988. A review of the origin of snakes. Pp. 37–130 in M.K. Hecht, B. Wallace and G.T. Prance (eds) *Evolutionary Biology*. Springer, Boston, MA.

Rieppel, O. 1996. Miniaturization in tetrapods: consequences for skull morphology. Pp. 47–61 in P.J. Miller (ed) *Miniature Vertebrates: The Implications of Small Body Size, Vol. 69. Symposia of the Zoological Society of London*. Claredon Press, Oxford.

Rieppel, O. & Zaher, H. 2000. The intramandibular joint in squamates, and the phylogenetic relationships of the fossil snake *Pachyrhachis problematicus* Haas. *Fieldiana Geology*, **43**, 1–69.

Rieppel, O. & Kearney, M. 2002. Similarity. *Biological Journal of the Linnean Society*, **75**, 59–82.

Rieppel, O. & Maisano, J. A. 2007. The skull of the rare Malaysian snake *Anomochilus leonardi* Smith, based on high-resolution X-ray computed tomography. *Zoological Journal of the Linnean Society*, **149**, 671–685.

Rieppel, O., Kley, N. J. & Maisano, J. A. 2009. Morphology of the skull of the white-nosed blindsnake, *Liotyphlops albirostris* (Scolecophidia: Anomalepididae). *Journal of Morphology*, **270**, 536–557. doi:10.1002/jmor.10703

Rieppel, O. 2012. "Regressed" macrostomatan snakes. *Fieldiana Life and Earth Sciences*, **2012**(5), 99–103. doi:10.3158/2158-5520-5.1.99

Sanger, T. J., Mahler, D. L., Abzhanov, A. & Losos, J. B. 2012. Roles for modularity and constraint in the evolution of cranial diversity among *Anolis* lizards. *Evolution*, **66**(5), 1525–1542. doi:10.1111/j.1558-5646.2011.01519.x

Savitzky, A. H. 1983. Coadapted character complexes among snakes: fossoriality, piscivory, and durophagy. *American Zoologist*, **23**, 397–409.

Scanferla, A. 2016. Postnatal ontogeny and the evolution of macrostomy in snakes. *Royal Society Open Science*, **3**, 160612. doi:10.1098/rsos.160612

Schmidt, K. P. 1950. Modes of evolution discernible in the taxonomy of snakes. *Evolution*, **4**(1), 79–86.

Sherratt, E., Sanders, K. L., Watson, A., Hutchinson, M. N., Lee, M. S. Y. & Palci, A. 2019. Heterochronic shifts mediate ecomorphological convergence in skull shape of microcephalic sea snakes. *Integrative and Comparative Biology*, **59**(3), 616–624. doi:10.1093/icb/icz033

Simões, B. F., Sampaio, F. L., Jared, C., Antoniazzi, M. M., Loew, E. R., Bowmaker, J. K., Rodriguez, A., Hart, N. S., Hunt, D. M., Partridge, J. C. & Gower, D. J. 2015. Visual

system evolution and the nature of the ancestral snake. *Journal of Evolutionary Biology*, **28**, 1309–1320. doi:10.1111/jeb.12663

Simões, T. R., Caldwell, M. W., Tałanda, M., Bernardi, M., Palci, A., Vernygora, O., Bernardini, F., Mancini, L. & Nydam, R. L. 2018. The origin of squamates revealed by a Middle Triassic lizard from the Italian Alps. *Nature*, **557**, 706–709. doi:10.1038/s41586-018-0093-3

Streicher, J. W. & Wiens, J. J. 2016. Phylogenomic analyses reveal novel relationships among snake families. *Molecular Phylogenetics and Evolution*, **100**, 160–169. doi:10.1016/j.ympev.2016.04.015

Strong, C. R. C., Simões, T. R., Caldwell, M. W. & Doschak, M. R. 2019. Cranial ontogeny of *Thamnophis radix* (Serpentes: Colubroidea) with a re-evaluation of current paradigms of snake skull evolution. *Royal Society Open Science*, **6**, 182228. doi:10.1098/rsos.182228

Strong, C. R. C., Palci, A. & Caldwell, M. W. 2021a. Insights into skull evolution in fossorial snakes, as revealed by the cranial morphology of *Atractaspis irregularis* (Serpentes: Colubroidea). *Journal of Anatomy*, **238**, 146–172. doi:10.1111/joa.13295

Strong, C. R. C., Scherz, M. D. & Caldwell, M. W. 2021b. Deconstructing the Gestalt: new concepts and tests of homology, as exemplified by a re-conceptualization of "microstomy" in squamates. *The Anatomical Record*, **2021**, 1–49. doi:10.1002/ar.24630

Townsend, T. M., Larson, A., Louis, E. & Macey, J. R. 2004. Molecular phylogenetics of Squamata: the position of snakes, amphisbaenians, and dibamids, and the root of the squamate tree. *Systematic Biology*, **53**(5), 735–757. doi:10.1080/10635150490522340

Underwood, G. & Kochva, E. 1993. On the affinities of the burrowing asps *Atractaspis* (Serpentes: Atractaspididae). *Zoological Journal of the Linnean Society*, **107**, 3–64.

Urošević, A., Ljubisavljević, K. & Ivanović, A. 2019. Multilevel assessment of the Lacertid lizard cranial modularity. *Journal of Zoological Systematics and Evolutionary Research*, **57**, 145–158. doi:10.1111/jzs.12245

Vidal, N. & Hedges, S. B. 2002. Higher-level relationships of snakes inferred from four nuclear and mitochondrial genes. *Comptes Rendus Biologies*, **325**, 977–985.

Wake, M. H. 1986. The morphology of *ldiocranium russeli* (Amphibia: Gymnophiona), with comments on miniaturization through heterochrony. *Journal of Morphology*, **189**, 1–16.

Watanabe, A., Fabre, A.-C., Felice, R. N., Maisano, J. A., Müller, J., Herrel, A. & Goswami, A. 2019. Ecomorphological diversification in squamates from conserved pattern of cranial integration. *Proceedings of the National Academy of Sciences*, **116**(29), 14688–14697. doi:10.1073/pnas.1820967116

Webb, J. K. & Shine, R. 1992. To find an ant: trail-following in Australian blindsnakes (Typhlopidae). *Animal Behaviour*, **43**, 941–948.

Webb, J. K., Shine, R., Branch, W. R. & Harlow, P. S. 2000. Life-history strategies in basal snakes: reproduction and dietary habits of the African thread snake *Leptotyphlops scutifrons* (Serpentes: Leptotyphlopidae). *Journal of Zoology*, **250**, 321–327.

Werneburg, I., Polachowski, K. M. & Hutchinson, M. N. 2015. Bony skull development in the Argus monitor (Squamata, Varanidae, *Varanus panoptes*) with comments on developmental timing and adult anatomy. *Zoology*, **118**, 255–280. doi:10.1016/j.zool.2015.02.004

Werneburg, I., Esteve-Altava, B., Bruno, J., Ladeira, M. T. & Diogo, R. 2019. Unique skull network complexity of *Tyrannosaurus rex* among land vertebrates. *Scientific Reports*, **9**, 1520. doi:10.1038/s41598-018-37976-8

Wickham, H. 2016. ggplot2: elegant graphics for data analysis. Springer-Verlag, New York. https://ggplot2.tidyverse.org

Wiens, J. J., Brandley, M. C. & Reeder, T. W. 2006. Why does a trait evolve multiple times within a clade? Repeated evolution of snakelike body form in squamate reptiles. *Evolution*, **60**(1), 123–141. doi:10.1111/j.0014-3820.2006.tb01088.x

Wiens, J. J., Kuczynski, C. A., Townsend, T. M., Reeder, T. W., Mulcahy, D. G. & Sites, J. W. J. 2010. Combining phylogenomics and fossils in higher-level squamate reptile phylogeny: molecular data change the placement of fossil taxa. *Systematic Biology*, **59**(6), 674–688. doi:10.1093/sysbio/syq048

Wiens, J. J., Hutter, C. R., Mulcahy, D. G., Noonan, B. P., Townsend, T. M., Sites, J. W. J. & Reeder, T. W. 2012. Resolving the phylogeny of lizards and snakes (Squamata) with extensive sampling of genes and species. *Biology Letters*, **8**, 1043–1046. doi:10.1098/rsbl.2012.0703

Yip, A. M. & Horvath, S. 2006. The generalized topological overlap matrix for detecting modules in gene networks. *BIOCOMP*, **00**, 1–19.

Yip, A. M. & Horvath, S. 2007. Gene network interconnectedness and the generalized topological overlap measure. *BMC Bioinformatics*, **8**, 22. doi:10.1186/1471-2105-8-22

Ziermann, J. M., Boughner, J. C., Esteve-Altava, B. & Diogo, R. 2021. Anatomical comparison across heads, fore- and hindlimbs in mammals using network models. *Journal of Anatomy*, **00**, 1–20. doi:10.1111/joa.13409

CHAPTER FIVE: A PRELIMINARY RE-ASSESSMENT OF SNAKE PHYLOGENY, WITH AN EMPHASIS ON SCOLECOPHIDIANS (SQUAMATA: OPHIDIA)

5.1. Introduction

Scolecophidians are an intriguing assemblage, playing a critical role in major debates regarding snake origins and phylogeny (Caldwell 2019). However, their phylogenetic status remains largely underexplored. From the past several decades of phylogenetic research into snakes, three major points of contention arise regarding this enigmatic group (see also detailed overview in Chapter One, §1.2—*Phylogenetic context*):

Position among Ophidia (i.e., all snakes, extinct and extant). Scolecophidians have long been considered the most basally-diverging group of snakes (Fig. 5.1a–c), thus reflecting an ancestrally miniaturized and fossorial snake condition (e.g., Mahendra 1938; Brock 1941; Bellairs & Underwood 1951; Rieppel 1984a; Wiens *et al.* 2006; Wiens *et al.* 2012; Miralles *et al.* 2018). However, this perspective has increasingly been questioned in recent years: several phylogenetic analyses have recovered various fossil snakes as diverging rootward of scolecophidians (Fig. 5.1d,e; e.g., Caldwell & Lee 1997; Lee & Caldwell 1998; Caldwell 2000; Rage & Escuillié 2000; Scanlon & Lee 2000; Lee & Scanlon 2002; Lee 2005; Scanlon 2006; Palci & Caldwell 2010; Palci *et al.* 2013a; Palci *et al.* 2013b; Caldwell *et al.* 2015; Hsiang *et al.* 2015; Simões *et al.* 2018; Garberoglio *et al.* 2019a; Garberoglio *et al.* 2019b), and several authors have further argued from a morphological perspective that scolecophidians are not an appropriate exemplar for the ancestral snake condition (e.g., Schmidt 1950; Caldwell 1999; Hsiang *et al.* 2015; Simões *et al.* 2015; Caldwell 2019; Chretien *et al.* 2019; Strong *et al.* 2021b).

Position among Serpentes (i.e., crown-clade snakes). Tied to the aforementioned uncertainty around Ophidia as a whole, the position of scolecophidians specifically within the extant assemblage (i.e., crown-clade snakes, or Serpentes *sensu* Caldwell & Lee 1997) is also contentious. Scolecophidians have almost universally been considered to be fundamentally separate from Alethinophidia, i.e., all other extant snakes (Fig. 5.1a–d; see e.g., Rieppel 1988; Cundall *et al.* 1993; Heise *et al.* 1995; Lee 1997; Zaher 1998; Caldwell 1999; Zaher & Rieppel 1999a; Tchernov *et al.* 2000; Rieppel *et al.* 2002; Slowinski & Lawson 2002; Vidal & Hedges 2002; Zaher & Rieppel 2002; Townsend *et al.* 2004; Vidal & Hedges 2004; Apesteguía & Zaher 2006; Conrad 2008; Wiens *et al.* 2008; Vidal *et al.* 2009; Vidal *et al.* 2010; Wiens *et al.* 2010; Wilson *et al.* 2010; Gauthier *et al.* 2012; Wiens *et al.* 2012; Zaher & Scanferla 2012; Pyron *et al.* 2013; Scanferla *et al.* 2013; Hsiang *et al.* 2015; Reeder *et al.* 2015; Figueroa *et al.* 2016; Streicher & Wiens 2016; Zheng & Wiens 2016; Miralles *et al.* 2018; Burbrink *et al.* 2020;

Singhal *et al.* 2021). Even phylogenies recovering scolecophidians as crownward of fossil snakes still almost always recover them as separate from alethinophidians (Fig. 5.1d; see e.g., Caldwell & Lee 1997; Lee & Caldwell 1998; Rage & Escuillié 2000; Scanlon & Lee 2000; Lee & Scanlon 2002; Lee 2005; Scanlon 2006; Palci *et al.* 2013a; Palci *et al.* 2013b; Caldwell *et al.* 2015; Simões *et al.* 2018; Garberoglio *et al.* 2019b). However, some authors have questioned this dichotomy (e.g., Schmidt 1950; Kley 2006; Palci & Caldwell 2010; Caldwell 2019; Strong *et al.* 2021a), and recent phylogenies have supported the nesting of scolecophidians within Alethinophidia (Fig. 5.1e; e.g., Caldwell 2000:fig. 1A,C; Palci & Caldwell 2010; Garberoglio *et al.* 2019a).

Monophyly, paraphyly, or polyphyly. Morphological phylogenies almost universally recover scolecophidians as monophyletic (Fig. 5.1a,c–e; e.g., Cundall *et al.* 1993; Scanlon & Lee 2000; Tchernov *et al.* 2000; Lee & Scanlon 2002; Scanlon 2006; Gauthier *et al.* 2012; Palci *et al.* 2013a; Palci *et al.* 2013b; Caldwell *et al.* 2015:fig. 4a; Hsiang *et al.* 2015; Garberoglio *et al.* 2019a), often in association with the traditional perspective of this group as a basally-diverging clade separate from Alethinophidia (see above). In contrast, molecular phylogenies almost universally recover scolecophidians as a paraphyletic assemblage (Fig. 5.1b; e.g., Heise *et al.* 1995; Wiens *et al.* 2008; Vidal *et al.* 2009; Vidal *et al.* 2010; Wiens *et al.* 2010; Wiens *et al.* 2012; Pyron *et al.* 2013; Hsiang *et al.* 2015; Figueroa *et al.* 2016; Streicher & Wiens 2016; Zheng & Wiens 2016; Miralles *et al.* 2018; Burbrink *et al.* 2020; Singhal *et al.* 2021), supporting a possibility raised earlier from a morphological perspective (Rieppel 1988). Combined-data analyses are equivocal, supporting both scolecophidian monophyly (e.g., Lee 2005; Hsiang *et al.* 2015) and paraphyly (e.g., Wiens *et al.* 2010; Reeder *et al.* 2015; Garberoglio *et al.* 2019a). Recent arguments (primarily Caldwell 2019) have even suggested scolecophidian polyphyly, based on the highly divergent morphologies of each lineage and the high degree of homoplasy associated with miniaturization, fossoriality, and myrmecophagy (see Harrington & Reeder 2017; Caldwell 2019; Chretien *et al.* 2019; Strong *et al.* 2021b).

Despite these many uncertainties, however, phylogenetic analyses of scolecophidians remain rather limited in scope. Although molecular phylogenies often sample several scolecophidian species (see molecular analyses referenced above), morphological phylogenies are typically limited to at most one representative of each scolecophidian lineage (e.g., Cundall *et al.* 1993; Scanlon & Lee 2000; Tchernov *et al.* 2000; Lee & Scanlon 2002; Scanlon 2006;

Conrad 2008; Palci *et al.* 2013a; Palci *et al.* 2013b; Garberoglio *et al.* 2019a:fig. 3), and often even fewer than that (e.g., Caldwell & Lee 1997; Lee 1997; Lee & Caldwell 1998; Zaher 1998; Caldwell 1999; Zaher & Rieppel 1999a; Caldwell 2000; Rieppel *et al.* 2002; Zaher & Rieppel 2002; Apesteguía & Zaher 2006; Palci & Caldwell 2010; Wilson *et al.* 2010; Zaher & Scanferla 2012; Scanferla *et al.* 2013; Caldwell *et al.* 2015:fig. 4b; Garberoglio *et al.* 2019b). Consequently, several important features relevant to scolecophidians (e.g., the many unique features of the jaw apparatus; see Strong *et al.* 2021b) have been neglected as character data, as they would be autapomorphic and thus not parsimony-informative under this sampling strategy. The dearth of combined-data analyses of squamates (limited to contributions by Lee 2005, 2009; Wiens *et al.* 2010; Hsiang *et al.* 2015; Reeder *et al.* 2015; Simões *et al.* 2018; Garberoglio *et al.* 2019a:fig. 4) only exacerbates this lack of a robust phylogenetic framework.

Recognizing these issues, in this chapter I aim to provide a foundation for future morphological and combined-data analyses of snake evolution. I first present an extensive revision of the morphological dataset most commonly used in snake phylogenies (Appendix 5.1). I next analyze this modified dataset (hereafter referred to as the Revised Dataset) using both parsimony-based and probabilistic methods. As an important caveat, although fossils have often been recognized as providing important phylogenetic data (e.g., Gauthier *et al.* 1988a; Lee 1997, 1998; Caldwell 1999; Zaher & Rieppel 1999a; Wiens 2004; Lee 2005; Wiens 2005; Caldwell 2007a; Palci & Caldwell 2010; Wiens *et al.* 2010; Gauthier *et al.* 2012; Hsiang *et al.* 2015; Reeder *et al.* 2015; Caldwell 2019; Mongiardino Koch & Parry 2020), this Revised dataset currently only includes extant taxa (Table 5.1) due to pandemic-related constraints on specimen access. To examine the potential effects of this taxon sampling on the phylogenies produced herein, I therefore also explore the phylogenetic impact of extinct snakes. Finally, I discuss the reliability of the synapomorphies and symplesiomorphies of scolecophidians as optimized in the Revised analysis, focussing on the potential impacts of homoplasy, heterochrony (i.e., evolutionary changes in the timing and/or rate of developmental events; Gould 1977; McNamara 1986), and especially paedomorphosis (i.e., the retention of ancestrally embryonic or juvenile conditions into the adult stage of a descendant taxon; Gould 1977; McNamara 1986). Altogether, this chapter thus presents core methodological and conceptual contributions relevant both to our current understanding of scolecophidian evolution and to future analyses of snake phylogeny.

5.2. Methods

5.2.1. Taxon sampling

Taxa were selected to ensure both phylogenetic breadth across snakes and taxonomic density among scolecophidians. Several genera from each major group of snakes (scolecophidians, anilioids, booid-pythonoids, and caenophidians) were sampled (see Table 5.1), representing all scolecophidian families, all anilioid families, 45% (5 / 11) of the booid-pythonoid families, and 33% (6 / 18) of the caenophidian families recognized by Burbrink *et al.* (2020). Among scolecophidians, taxon sampling was much denser than in any previous morphological phylogeny, with several families (Gerrhopilidae, Xenotyphlopidae) and genera (Leptotyphlopidae: *Epictia*, *Myriopholis*, *Trilepida*; Anomalepididae: *Helminthophis*; Typhlopidae: *Acutotyphlops*, *Afrotyphlops*) being assessed for the first time. These taxa represent every anomalepidid genus, almost every leptotyphlopid tribe as outlined by Adalsteinsson *et al.* (2009), every typhlopoid family as established by Vidal *et al.* (2010), and 75% (3 / 4) of the typhlopid subfamilies recognized by Miralles *et al.* (2018).

5.2.2. Dataset construction

The Revised Dataset presented in this chapter (Appendices 5.1 and 5.2) utilizes a character list modified heavily from the most recently published morphology-based snake phylogeny (Garberoglio *et al.* 2019a:dataset 1 therein). The core of this dataset was established by Lee & Scanlon (2002) and Rieppel *et al.* (2002), but it has since been modified and expanded by several authors, most notably Apesteguía & Zaher (2006), Wilson *et al.* (2010), and Zaher & Scanferla (2012). The most recent major contributions have been: Longrich *et al.* (2012), who added several characters in their analysis of *Coniophis*; Caldwell *et al.* (2015), who modified this dataset—including re-scoring several characters—in their analysis of the earliest known snakes; and Garberoglio and colleagues (2019a; 2019b), who added several characters, removed a number of problematic characters, and further modified several of the remaining characters in their studies of *Najash*. Unfortunately, as is likely inevitable given such varied contributions, several characters in this dataset are either poorly constructed, logically redundant, or inconsistently scored. My modifications to this dataset thus aim to address these issues.

Based on the operational and conceptual guidelines discussed by Sereno (2007) and Simões *et al.* (2017), these modifications range from relatively minor (e.g., re-wording

characters to ensure consistent character statement 'syntax') to quite extensive (e.g., fundamentally re-conceptualizing the homolog concepts underlying problematic characters). Several characters were also added, based largely on anatomical observations stemming from Strong *et al.* (2021a) and Strong *et al.* (2021b). Finally, a number of problematic characters were removed altogether. All of these modifications, additions, and removals are presented and explained in Appendix 5.1.

The cranial portion of the Revised Dataset (246 of the 292 total characters; Appendices 5.1. and 5.2) was then scored based entirely on primary observations of all specimens, using micro-computed tomography (micro-CT) scans (Table 5.1) visualized in Dragonfly 4.1 (Object Research Systems Inc 2019b). I performed the micro-CT scanning of all MCZ specimens (available on MorphoSource.org), and obtained the scan data for the remaining specimens from MorphoSource.org and DigiMorph.org (see Appendix 1.1).

Scorings for postcranial characters were derived from Garberoglio *et al.* (2019a). Many taxa in the present analysis have direct representatives in Garberoglio *et al.* (2019a:dataset 1), and so their scorings were transferred directly into the revised matrix (Appendix 5.2). Of course, this approach was not applicable for the numerous scolecophidians newly incorporated into this dataset, as Garberoglio *et al.* (2019a) only sampled *Typhlops*, *Leptotyphlops*, and Anomalepididae. The scorings for those terminal taxa were therefore transferred to the closest representative in the Revised Dataset.

Regarding typhlopoids, Garberoglio *et al.* (2019a) do not state which species within the genus *Typhlops* they used in their phylogeny. These scorings were therefore combined with the cranial characters from *Typhlops jamaicensis* (scored by C.S.), forming the terminal taxon *Typhlops* herein. Garberoglio *et al.* (2019a) similarly do not state which species within the genus *Leptotyphlops* they used in their phylogeny. These scorings have therefore been added to the present terminal taxon *Rena*, as *Rena dulcis* (which was used to score the cranial characters) has previously been considered *Leptotyphlops dulcis* and has traditionally been used as a morphological and phylogenetic exemplar for the genus *Leptotyphlops* (e.g., Kley 2006; Gauthier *et al.* 2012). Finally, although Garberoglio *et al.* (2019a) do not state which species they used to score their terminal taxon 'Anomalepididae', in their supplementary materials they comment on *Anomalepis* and *Liotyphlops*. As such, the postcranial scorings for

‘Anomalepididae’ were combined with the cranial characters from both *Anomalepis mexicanus* and *Liotyphlops argaleus*.

5.2.3. Phylogenetic analysis

5.2.3.1. Analysis of revised dataset

I analyzed the Revised Dataset (Appendix 5.2) using both maximum parsimony and Bayesian inference approaches. In all analyses, *Varanus exanthematicus* was used as the outgroup, following Garberoglio *et al.* (2019a).

Maximum parsimony analysis was performed in TNT v.1.5 (Goloboff *et al.* 2008; Goloboff & Catalano 2016) via a heuristic ‘traditional search’ using the tree bisection and reconnection (TBR) algorithm, with 1000 random-addition-sequence replicates and holding 10 trees per replication. All characters were equally weighted. For analyses producing multiple most-parsimonious trees (MPTs), these were compiled into a 50% majority-rule consensus tree. Synapomorphies were mapped onto all trees in TNT v.1.5 (Goloboff *et al.* 2008; Goloboff & Catalano 2016), and the consistency index (CI) and retention index (RI) were calculated in Mesquite v.3.61 (Maddison & Maddison 2019).

Bayesian analysis was performed in MrBayes v.3.2.7a (Ronquist *et al.* 2012), using XSEDE via the CIPRES Science Gateway (Miller *et al.* 2010). Analytical settings were consistent with those implemented by Garberoglio *et al.* (2019a): the data were analyzed using the Mk model (Lewis 2001) of morphological evolution; rates of evolution were allowed to vary across all characters under a gamma distribution; the analysis was set to run for 20 000 000 generations, involving two runs, each with eight chains set to a temperature of 0.07; trees were sampled every 1000 generations, with diagnostics calculated and results printed at this same rate; and the first 25% of trees were discarded as burn-in, with the remaining trees being compiled into a 50% majority-rule consensus tree. Following the analysis, mixing and convergence were verified using Tracer v.1.7.1 (Rambaut *et al.* 2018) and MrBayes (Ronquist *et al.* 2012), based on the following indicators: average standard deviation of split frequencies ≤ 0.01 (Lakner *et al.* 2008); estimated sample size (ESS) > 200 for all parameters; potential scale reduction factor (PSRF) ≈ 1 (Gelman & Rubin 1992); chain swap acceptance rate between 0.10–0.70 (Ronquist *et al.* 2019); and evidence of stationarity being reached in the trace plot in Tracer.

All trees were visualized in Mesquite v.3.61 (Maddison & Maddison 2019) and/or FigTree v.1.4.4 (Rambaut 2018), and prepared for figures using Adobe Illustrator 2021. Mesquite v.3.61 (Maddison & Maddison 2019) was also used to trace character history, with ancestral states reconstructed using parsimony.

5.2.3.2. Phylogenetic impact of fossils

In order to assess the impact of fossils on analyses of snake phylogeny, I also analyzed two versions of the snake-focussed dataset from Garberoglio *et al.* (2019a; dataset 1 therein, from which the current dataset was revised). The first version was unmodified from Garberoglio *et al.* (2019a:data file S1), and thus includes both extinct and extant taxa; this will be referred to hereafter as the Original Dataset. The second version was modified to remove all fossil taxa (Appendix 5.3), and will be referred to as the Reduced Dataset. Each dataset was analyzed using both maximum parsimony and Bayesian inference, following the methods described above (see §5.2.3.1). The resulting phylogenies were then compared to each other and to the results of the Revised Dataset, so as to determine whether sampling fossils changes the relationships among Serpentes.

5.3. Results

5.3.1. Revised dataset

Maximum parsimony analysis of the Revised Dataset (Appendices 5.1 and 5.2) recovered one MPT with a length of 724 steps (Fig. 5.2a; CI = 0.4661; RI = 0.7225). In this phylogeny, Scolecophidia and Alethinophidia constitute separate clades, with 'anilioids' forming a paraphyletic assemblage basally among alethinophidians (Fig. 5.2a). Within Scolecophidia, each lineage—Anomalepididae, Leptotyphlopidae, and Typhlopoidea—is monophyletic, and Anomalepididae is the sister-group to Typhlopoidea (Fig. 5.2a). Unlike molecular phylogenies, in which Xenotyphlopidae and Typhlopidae are sister taxa with Gerrhopilidae diverging basally among Typhlopoidea (Fig. 5.1b; e.g., Vidal *et al.* 2010; Zheng & Wiens 2016; Miralles *et al.* 2018; Burbrink *et al.* 2020), in the present phylogeny *Xenotyphlops* diverges earliest among typhlopoids and *Gerrhopilus* is nested within Typhlopidae (Fig. 5.2a).

Bayesian analysis of the Revised Dataset recovers a very similar topology (Fig. 5.2b). Among scolecophidians, the only differences involve the relationships among typhlopoids: both

Xenotyphlopidae and Gerrhopilidae are now nested within Typhlopidae alongside *Acutotyphlops*, with *Typhlops* and *Afrotyphlops* diverging earlier (Fig. 5.2b). Among alethinophidians, the only difference is a switch in position of *Naja* and *Crotalus* (Fig. 5.2).

As optimized by TNT v.1.5. (Goloboff *et al.* 2008; Goloboff & Catalano 2016), the following synapomorphies unite Scolecophidia: alveoli and base of teeth wider transversely than anteroposteriorly [character 12, state 1; hereafter formatted as 012:1]; transverse processes of premaxilla positioned anterior to maxillae [017:1]; nasal process of premaxilla transversely expanded, partly roofing external nares [021:0]; transverse horizontal shelf of frontal absent [044:1]; lacrimal foramen indistinct or absent [067:1]; palatine articulating with pterygoid via simple flap-overlap configuration [108:2]; maxillary branch of trigeminal nerve passing dorsally between palatine and prefrontal [120:1]; transverse process of pterygoid absent [123:1]; quadrate slanted clearly anteriorly, nearly horizontal in lateral view [133:0]; suprastapedial process of quadrate indistinct or absent [134:1]; anterior mylohyoid foramen of splenial absent [219:1]; hemapophyses absent [248:1].

As optimized by TNT v.1.5. (Goloboff *et al.* 2008; Goloboff & Catalano 2016), the following synapomorphies unite Alethinophidia: transverse processes of premaxilla oriented transversely [018:1]; lateral vertical flange of septomaxilla bearing posterior dorsal process [029:1]; posterior dorsal lamina of vomer present [038:1]; preorbital ridge of frontal present [046:1]; frontal-prefrontal articulation structurally complex, with prefrontal clasping frontal dorsally and ventrally [049:1]; facial process of maxilla shorter than main body of maxilla [090:1]; palatine process of maxilla present [097:1]; accessory foramen posterior to superior alveolar foramen on maxilla present [101:1]; maxillary process of palatine articulating with ventromedial margin of prefrontal [118:1]; medial finger-like process of ectopterygoid absent [129:0]; crista interfenestralis not occurring as an individualized component around the juxtastapedial space [153:1]; laterosphenoid present [162:1]; crista trabeculares elongate and distinct [192:1]; cultriform process of parabasisphenoid bearing interchoanal process [195:1]; posterior dentigerous process of dentary present [207:1]; angular narrowly exposed in lateral view [223:1]; coronoid process of coronoid subequal to or lower than compound bone at corresponding position [227:1]; dentary process of surangular bearing flattened dorsal surface [241:1]; coronoid eminence of surangular well-developed [244:1].

5.3.2. Inclusion *versus* exclusion of fossils

Maximum parsimony analysis of the Original Dataset (Garberoglio *et al.* 2019a:dataset 1 and data file S1) recovered 272 MPTs with a length of 624 steps (CI = 0.5617; RI = 0.7235). The resulting 50% majority-rule topology (Figs 5.3a and S5.1) is consistent, as expected, with the corresponding analysis in Garberoglio *et al.* (2019a:fig. S5): *Xiaophis* and 'Jurassic snakes' form a basal polytomy; *Dinilysia*, *Najash*, and Madtsoiidae diverge next as a clade; Scolecophidia and Alethinophidia form separate clades; and Simoliophiidae is nested within Alethinophidia crownward of the paraphyletic 'anilioids', as the sister-group to Macrostomata (Fig. 5.3a).

Bayesian analysis of the Original Dataset (Figs 5.3b and S5.2; Garberoglio *et al.* 2019a:dataset 1 and data file S1) differs in several ways (see also Garberoglio *et al.* 2019a:figs 3 and S6): *Najash*, *Dinilysia*, and 'madtsoiids' now form a paraphyletic assemblage; Simoliophiidae is the sister group to Serpentes (crown-clade snakes) and *Xiaophis*, rather than being nested within Alethinophidia; and *Xiaophis* occurs in a polytomy alongside two clades of extant snakes (Figs 5.3b). Most notably, Scolecophidia is now nested within Alethinophidia alongside 'anilioids', with Macrostomata forming a neighbouring clade (Fig. 5.3b).

The Reduced Dataset (Fig. 5.4; Appendix 5.3) does not recover a notably different result than the Original Dataset (Fig. 5.3) when analyzed under maximum parsimony (Figs 5.3a and 5.4a). Producing 46 MPTs with a length of 445 steps (CI = 0.7009; RI = 0.7633), this analysis recovers essentially the same topology of extant taxa (Figs 5.4a and S5.3): Scolecophidia and Alethinophidia again form separate clades, with 'anilioids' forming a paraphyletic assemblage basal to Macrostomata within Alethinophidia. This topology also matches that produced by maximum parsimony and Bayesian analyses of the Revised Dataset (Fig. 5.2).

In contrast, removal of extinct taxa causes dramatic differences when analyzed via Bayesian inference (Figs 5.4b and S5.4). Whereas scolecophidians initially formed a clade nested within Alethinophidia in the Original Bayesian analysis (Fig. 5.3b; Garberoglio *et al.* 2019a:figs 3 and S6), when fossil taxa are removed (Fig. 5.4b) scolecophidians revert to the basally-diverging position among Serpentes recovered by all maximum parsimony analyses herein (Figs 5.2a, 5.3a, and 5.4a). This topology is also largely consistent with that produced by Bayesian analysis of the Revised Dataset (Fig. 5.2b), with the only differences involving relationships within Macrostomata and thus likely resulting simply from underlying differences in taxon sampling of alethinophidians.

5.4. Discussion

Both phylogenies produced from the Revised Dataset (Fig. 5.2) are consistent with traditional perspectives of snake evolution: Scolecophidia and Alethinophidia form separate clades, and anilioids form a paraphyletic assemblage leading to a monophyletic Macrostomata. These trees would therefore seem to strongly support this widespread view of snake phylogeny, as this topology occurs in both parsimony-based and probabilistic analyses, even after extensive logical and methodological revisions to the underlying dataset (see §5.2 and comments in Appendix 5.1).

However, there are several reasons to be skeptical of this outcome, rendering the above interpretation premature. Primary among these are: the dramatic influence that fossils have on snake phylogeny, especially the position of scolecophidians (§5.4.1); and the reliability—or lack thereof—of the synapomorphies underlying this topology (§5.4.2).

5.4.1. Scolecophidian phylogeny: the impact of fossils

Although the exclusion of extinct taxa from Garberoglio *et al.* (2019a:dataset 1) did not affect the topology of Serpentes when analyzed under maximum parsimony (Figs 5.3a and 5.4a), the same cannot be said for the outcome under Bayesian inference (Figs 5.3b and 5.4b). Under this latter method, the exclusion of fossil data (Fig. 5.4b) causes scolecophidians to occupy a distinctly more basally-diverging position among extant snakes than that recovered when fossils are included (Fig. 5.3b). This difference in placement is especially relevant in light of the competing hypotheses of snake evolution outlined in §5.1: scolecophidians occupy their traditional position at the base of Serpentes when only extant taxa are analyzed (Fig. 5.4b), but occupy a distinctly heterodox position nested within Alethinophidia when extinct taxa are also sampled (Fig. 5.3b). Whether fossils are included or not therefore plays a key role in influencing scolecophidian phylogeny.

This finding is in turn important for interpreting the novel phylogenies presented herein (Fig. 5.2). Specifically, the Revised Bayesian topology (Fig. 5.2b; which only sampled extant taxa) is consistent with the Reduced Bayesian topology (Fig. 5.4b); however, as demonstrated above, this Reduced topology—and particularly the basally-diverging position of scolecophidians—is ultimately the result of fossils being excluded from the analysis, with scolecophidians instead occupying a very different position when taxon sampling is more complete (Fig. 5.3b). These comparisons raise the distinct possibility that the basally-diverging

position of scolecophidians in the Revised phylogenies (Fig. 5.2) may simply be an artifact of fossils not being sampled, with the current reliance on extant taxa potentially masking a more deeply-nested position. Although this possibility is ultimately speculative, and it remains possible that scolecophidians will continue to occupy this early-diverging position even after fossils are included, this result nevertheless clearly indicates that the current Revised phylogenies should not simply be taken at face value. Instead, this evidence of the profound impact of fossil data provides a necessary caveat regarding the interpretation of these topologies, in particular suggesting that the placement of scolecophidians may not be reliable.

More broadly, this demonstration of the impact of extinct taxa adds to an extensive body of evidence emphasizing the importance of fossils in both morphological and molecular phylogenetics (e.g., Gauthier *et al.* 1988a; Lee 1997, 1998; Caldwell 1999; Zaher & Rieppel 1999a; Wiens 2004; Lee 2005; Wiens 2005; Caldwell 2007a; Palci & Caldwell 2010; Wiens *et al.* 2010; Gauthier *et al.* 2012; Hsiang *et al.* 2015; Reeder *et al.* 2015; Caldwell 2019; Mongiardino Koch & Parry 2020). From a molecular perspective, not only does the addition of molecular data change the position of fossil taxa relative to morphology-only analyses (Wiens *et al.* 2010; Reeder *et al.* 2015), but the opposite is also true: the addition of morphological data—and particularly fossils—to a molecular phylogenetic analysis can distinctly change the topology among extant taxa (Lee 2005; Wiens *et al.* 2010; Hsiang *et al.* 2015; Mongiardino Koch & Parry 2020).

From a morphological perspective, Gauthier *et al.* (1988a) found phylogenetic relationships among extant amniotes to change dramatically with the addition of fossil taxa, mirroring the results presented herein (Figs 5.3 and 5.4). In another analysis exploring the impact of taxon sampling, Caldwell (1999) recovered snakes as the sister-group of dibamids and amphisbaenians when analyzing only extant taxa (Caldwell 1999:fig. 3); however, the addition of just a single extinct snake, *Dinilysia*, resulted in a dramatically different topology, in which snakes were instead recovered as most closely related to varanoids (Caldwell 1999:fig. 4). This latter study is particularly relevant in showing that the inclusion of fossils is important not only when assessing in-group relationships of snakes, as examined herein (see also Palci & Caldwell 2010; Gauthier *et al.* 2012), but also when reconstructing their overall position within Squamata (see also Lee 1998).

This clear phylogenetic impact of fossils can be explained by several factors. From an operational perspective, extinct taxa are particularly important in helping to break up the 'long branches' characterizing highly modified lineages, thus mitigating the effects of systematic biases such as long-branch attraction (Lee 1997; Zaher & Rieppel 1999a; Wiens 2005; Wiens *et al.* 2010; Mongiardino Koch & Parry 2020). Fossils are further important in influencing character state distributions, combinations, and ultimately polarity (Lee 1997, 2005; Palci & Caldwell 2010; Hsiang *et al.* 2015; Caldwell 2019; Mongiardino Koch & Parry 2020), and can also provide key insight into convergence (Lee 1998). A particularly relevant example is Lee's (1998) recognition that the extinct relatives of snakes (i.e., mosasauroids, *Pachyrhachis*) and of amphisbaenians and dibamids (i.e., *Sineoamphisbaena*) do not exhibit the extreme specializations of these extant groups, indicating that the elongate and limb-reduced ecomorph of snakes and fossorial non-snake lizards has evolved independently (Lee 1998).

Finally, and perhaps most importantly, fossils embody an often-under-appreciated component of evolution, one which the neontological record by definition cannot address: the dimension of time (Gauthier *et al.* 1988a; Caldwell 2007a, 2019). Simply put, extinct taxa have had less time to evolve relative to key ancestral nodes than extant taxa have (Gauthier *et al.* 1988a; Mongiardino Koch & Parry 2020), a phenomenon especially important when considering deep-time events such as the origin of snakes (see also Caldwell 2019). Altogether, these factors underline the core argument presented in this section: extinct taxa are essential to phylogenetic analysis. Any phylogeny based only on extant taxa thus presents inherent reason for skepticism, regardless of the methodological rigour of the underlying character construction and scoring.

5.4.2. Scolecophidian phylogeny: assessment of character reliability

Beyond the aforementioned caveats surrounding taxon sampling and the importance of fossils, it is also essential to examine the characters underlying the Revised phylogenies presented herein. The ensuing discussion therefore assesses the synapomorphies of Scolecophidia and Alethinophidia as reconstructed by maximum parsimony analysis of the Revised Dataset.

5.4.2.1. Synapomorphies of Scolecophidia

Alveoli and base of teeth wider transversely than anteroposteriorly [012:1]. As scored by Lee & Scanlon (2002:character 178), who introduced this character, this state also

occurs in *Haasiophis* and madtsoiids, so is not as definitive a synapomorphy as it may appear. Furthermore, Kley (2006) interpreted the posterolingual excavation of the dentary teeth in leptotyphlopids as an adaptation for grasping prey, an explanation that would also apply to the tooth morphology of other scolecophidians given their similar, myrmecophagous diets (Webb & Shine 1992, 1993; Kley 2001, 2006). Because myrmecophagy is potentially convergent among scolecophidians (Chretien *et al.* 2019; Strong *et al.* 2021b), and because tooth morphology in general is highly homoplastic (Savitzky 1983; Massare 1987; LeBlanc *et al.* 2012; Strong *et al.* 2020), the presence of this condition is therefore not necessarily a reliable synapomorphy.

Transverse processes of premaxilla positioned anterior to maxillae [017:1]. This character state in fact occurs in almost all sampled taxa, except for *Varanus*, most anilioids, and *Python*. Therefore, although this state optimizes as a synapomorphy of Scolecophidia on the current topology, it is not a particularly compelling one.

Nasal process of premaxilla transversely expanded, partly roofing external nares [021:0]. This character state is limited to scolecophidians among the sampled taxa, supporting its reliability as a synapomorphy of this clade. However, it is important to note that this expansion of the premaxilla is likely associated with fossoriality, particularly with the bulbous, tightly-integrated snout condition typical of scolecophidians (see e.g., Rieppel *et al.* 2009). If fossoriality is indeed convergent to some extent among scolecophidians, as has been suggested by some authors (e.g., Harrington & Reeder 2017; Strong *et al.* 2021b), then this would undermine the reliability of this synapomorphy.

Transverse horizontal shelf of frontal absent [044:1]. The transverse horizontal shelf is a component of the naso-frontal joint, contributing to the dorsal articulation between the snout and the braincase (Frazzetta 1966). Its universal absence in scolecophidians supports its reliability as a synapomorphy of this clade. However, this absence also occurs in *Atractaspis*, a fossorial colubroid. It is therefore possible that this condition is again related to fossoriality, with modification of the naso-frontal joint (a common occurrence in fossorial snakes; Savitzky 1983) resulting in a convergent attainment of this character state.

Lacrimal foramen indistinct or absent [067:1]. The absence of the lacrimal foramen is universal among scolecophidians and exclusive to Scolecophidia among the sampled taxa, rendering the distribution of this character state unique and unreversed. Because the lacrimal foramen (when present) is either partially or completely enclosed by the prefrontal, the absence

of this foramen is presumably tied to the extreme modification of the prefrontal in scolecophidians relative to other squamates. Notably, however, the prefrontal exhibits a highly distinct morphology in each scolecophidian lineage, constituting one of the key features defining the unique jaw morphotypes of typhlopoids, anomalepidids, and leptotyphlopids (Strong *et al.* 2021b). Thus, although the lacrimal foramen is indeed absent across scolecophidians, this absence is not as unambiguous as it may initially appear.

Palatine articulating with pterygoid via simple flap-overlap configuration [108:2]. Although this configuration of the palatine-pterygoid articulation optimizes herein as a synapomorphy of Scolecophidia, it is in fact limited to leptotyphlopids and anomalepidids; in contrast, typhlopoids exhibit a forked, interlocking articulation. This character state distribution is notable for a number of reasons. For one, the aforementioned forked condition is a synapomorphy of Typhlopoidea, reflecting the 'single-axle maxillary raking' mechanism unique to this clade (Chretien *et al.* 2019; Strong *et al.* 2021b); this articulation is fundamentally distinct from the condition in other scolecophidians, and indeed other squamates more broadly, thus undermining the validity of this proposed synapomorphy of Scolecophidia. Furthermore, the flap-overlap configuration in leptotyphlopids and anomalepidids is a by-product of the extremely reduced palatine and especially pterygoid in these lineages, which resemble the simple morphologies typical of embryonic squamates (see e.g., Polachowski & Werneburg 2013; Werneburg *et al.* 2015; Ollonen *et al.* 2018). This reduction in turn reflects paedomorphic—and thus potentially homoplastic—truncation of these features (see §5.4.2.3). Finally, although the overlapping articulation of the palatine and pterygoid is morphologically similar in leptotyphlopids and anomalepidids, and thus is a valid primary homolog *sensu* de Pinna (1991), the overall function of the palatomaxillary arches is completely different: anomalepidids rely on extreme maxillary rotation ('axle-brace maxillary raking' *sensu* Strong *et al.* 2021b), whereas leptotyphlopids rely on 'mandibular raking' *sensu* Kley & Brainerd (1999) and thus exhibit essentially complete akinesis of the upper jaws (see also Strong *et al.* 2021b). These unique morphofunctional arrangements support a hypothesis of the independent evolution of each jaw morphotype (Caldwell 2019; Chretien *et al.* 2019; Strong *et al.* 2021b), and in turn support the aforementioned suggestion of potential homoplasy in this feature.

Maxillary branch of trigeminal nerve passing dorsally between palatine and prefrontal [120:1]. In scolecophidians, the passage of the maxillary branch of the trigeminal

nerve dorsal to the palatine—rather than piercing the maxillary process of the palatine as occurs in most other squamates—may be related to the reduction of the maxillary process relative to other squamates. This reduction represents another example of paedomorphosis, and therefore again carries with it a distinct possibility of convergence (see §5.4.2.3). This character state also occurs in some alethinophidians (*Anilius*, *Boa*, *Acrochordus*, and *Crotalus*), supporting this suggestion of homoplasy both because these taxa are not closely related and because they all exhibit some degree of reduction of the maxillary process. However, the impact of paedomorphosis on this character state is not definitive: some taxa (e.g., *Atractaspis*) also exhibit a reduced maxillary process, but it is nonetheless pierced by this nerve branch, suggesting that the passage of the trigeminal maxillary branch may not be related to the degree of development of the maxillary process. Therefore, although the distribution of this character state—including its presence in scolecophidians—may be tied to paedomorphosis, this association is ultimately ambiguous.

Transverse process of pterygoid absent [123:1]. This character state is clearly associated with paedomorphosis, as the absence of this feature in some adult snakes (scolecophidians and *Atractaspis*) reflects a retention of the morphologically simple structure of the pterygoid that typically occurs in early embryonic squamates (see e.g., Polachowski & Werneburg 2013; Werneburg *et al.* 2015; Ollonen *et al.* 2018). Therefore, although this character state is almost exclusive to scolecophidians among the sampled taxa, both its association with developmental truncation and its presence in *Atractaspis* (itself a rather paedomorphic snake; Strong *et al.* 2021a) suggest possible convergence of this condition (see also §5.4.2.3).

Quadrate slanted clearly anteriorly, nearly horizontal in lateral view [133:0]. In squamate embryos, the quadrate originates as a cartilaginous rod oriented horizontally, parallel to the Meckelian cartilage (Kamal 1966; Hernández-Jaimes *et al.* 2012). Throughout embryonic development it rotates posteriorly, ending in a roughly vertical position in anilioids and most non-snake lizards, or in a posterior to posterolateral position in booid-pythonoids and caenophidians (Kamal 1966; Hernández-Jaimes *et al.* 2012; Palci *et al.* 2016; Scanferla 2016). The extreme anteroventral orientation of the quadrate in scolecophidians is therefore clearly paedomorphic, as this condition otherwise occurs only in embryonic squamates and thus reflects a retention of this early embryonic condition (Kley 2006; Caldwell 2019; Strong *et al.* 2021a; Strong *et al.* 2021b).

Suprastapedial process of quadrate indistinct or absent [134:1]. The presence *versus* absence of the suprastapedial process in scolecophidians has been debated (e.g., Zaher 1998; Caldwell 2000), but I interpret it as being absent or at least indistinct. This absence is universal among scolecophidians; however, the suprastapedial process is also absent in simoliophiids, caenophidians, and many booid-pythonoids (Zaher 1998; Caldwell 2000; Garberoglio *et al.* 2019a), meaning that this character state by no means definitively distinguishes scolecophidians from alethinophidians.

Anterior mylohyoid foramen of splenial absent [219:1]. In scolecophidians, the splenial is either quite reduced (typhlopoids and leptotyphlopids) or altogether absent (anomalepidids; see Rieppel *et al.* 2009 for comments on the homology of this element), reflecting a condition otherwise occurring only in embryonic squamates (see e.g., Polachowski & Werneburg 2013; Khannoon & Evans 2015; Werneburg *et al.* 2015; Ollonen *et al.* 2018). The absence of the anterior mylohyoid foramen is presumably tied to this reduction, and is thus itself an example of paedomorphic modification. The anterior mylohyoid foramen is absent in many other snakes, some (*Xenopeltis*, *Naja*)—but not all (*Loxocemus*, *Python*, *Crotalus*)—of which also show some degree of simplification of the splenial. The homoplasy associated with this character state—as demonstrated by its distribution among taxa and implied by its association with paedomorphosis in scolecophidians (see §5.4.2.3)—thus undermines the reliability of this synapomorphy of Scolecophidia.

Hemapophyses absent [248:1]. The absence of various vertebral processes has been interpreted as an adaptation related to fossoriality (Hoffstetter & Gasc 1969). Furthermore, based on observations of alethinophidian (*Bothrops* and *Lichanura*) embryos, Gauthier *et al.* (2012) noted that the hemapophyses arise as distal extensions of the pleurocentral body (see also Garberoglio *et al.* 2019c). If this reflects the typical developmental pathway for squamates, then the absence of the hemapophyses in scolecophidians would in turn reflect truncation of this development. However, given the dearth of studies on postcranial embryology in squamates and especially snakes, this suggestion of paedomorphosis for now remains speculative. Overall, the universal absence of the hemapophyses in scolecophidians, and the uniqueness of this condition among sampled taxa (though see Hoffstetter & Gasc 1969, who report the haemapophyses as also being absent in *Anilius*, *Cylindrophis*, and *Calabaria*; an interpretation *contra* Garberoglio

et al. 2019c), supports the reliability of this condition as a genuine synapomorphy of scolecophidians, with the aforementioned caveat that it is potentially paedomorphic.

5.4.2.2. Synapomorphies of Alethinophidia

Beyond the synapomorphies optimized herein for Alethinophidia (which are discussed below), a few other traditionally-recognized synapomorphies are worth briefly emphasizing.

Presence of prokinetic naso-frontal joint (Rieppel 1979a; Lee 1997) and medial frontal pillars (Rieppel 1988; Lee 1997; Lee & Scanlon 2002; Cundall & Irish 2008). The medial frontal pillars subdivide the olfactory foramen anteriorly in alethinophidians, and are considered an integral component of the mobile naso-frontal joint in this clade (Rieppel 1978a, b, 1979a, 1988, 2007; Cundall & Irish 2008). These pillars are absent in non-snake lizards, extinct snakes (except *Yurlunggur*; Garberoglio *et al.* 2019a), and scolecophidians, a distribution traditionally viewed as reflecting one of the fundamental symplesiomorphies of scolecophidians (e.g., Rieppel 1979a; Lee & Scanlon 2002). Alternatively, however, it is also possible to consider this absence in scolecophidians as a paedomorphic reversal, reflecting miniaturized derivation from an ancestrally alethinophidian-like condition (see extensive discussion in Strong *et al.* 2021a). The absence of these pillars, and indeed of a mobile prokinetic joint more broadly, is also consistent with the fossorial nature of scolecophidians, as modification and stabilization of the naso-frontal joint is a common occurrence in fossorial snakes (Rieppel 1978a, b; Savitzky 1983; see also Strong *et al.* 2021a). Thus, although it is most parsimonious given the current phylogenetic framework to consider the prokinetic joint and medial frontal pillars as synapomorphies setting Alethinophidia apart from the more plesiomorphic Scolecophidia, it is also quite reasonable to hypothesize the absence of these features in scolecophidians as a paedomorphic reversal (see also §5.4.2.3).

Presence of toothed anterior process of palatine (Rieppel 1988; Lee 1997; Zaher 1998; Rieppel *et al.* 2002; Cundall & Irish 2008). Although the palatine of most alethinophidians does indeed bear an anterior dentigerous process (see character 110 herein), this synapomorphy is somewhat misleading. Primarily, scolecophidians do not possess palatal teeth, so their palatines by definition cannot have a toothed anterior process. Even if we re-conceptualize this proposed alethinophidian synapomorphy to more generally concern presence/absence of the palatine teeth, this is still not informative: the palatine is also edentulous in some alethinophidians (e.g., *Anomochilus*, *Uropeltis*), and more broadly the absence of the

palatal teeth is a paedomorphic and highly homoplastic condition (see Olori & Bell 2012; Strong *et al.* 2021a; Strong *et al.* 2021b). Caldwell (2000) presented similar criticisms of this character, which Zaher & Rieppel (2002) rebutted by focussing on the basic presence/absence of an anterior process, regardless of the presence of palatine teeth. However, even this resolution is not particularly satisfactory, both because some alethinophidians (e.g., *Atractaspis*, *Crotalus*) do not bear an anterior process on the palatine and because the absence of this process in scolecophidians could easily be secondarily derived, resulting from the generally paedomorphic nature of their palatine (see Strong *et al.* 2021b). Overall, none of these possibilities provide compelling support for the interpretation of this feature as a defining synapomorphy of alethinophidians.

Transverse processes of premaxilla oriented transversely [018:1]. Although this character state optimizes herein as a synapomorphy of alethinophidians, it is in fact quite variable, occurring in only 60% (9 / 15) of the sampled alethinophidians and also occurring in a few scolecophidians. This condition is therefore not a particularly compelling synapomorphy defining Alethinophidia.

Lateral vertical flange of septomaxilla bearing posterior dorsal process [029:1]. This process is unique to alethinophidians, although not universal within this group. The posterior dorsal process is absent in most colubroids, reflecting a failure of this process to develop (see e.g., Polachowski & Werneburg 2013). As indicated by the presence of the posterior dorsal process in surrounding taxa, its absence in these colubroids therefore constitutes a paedomorphic reversal to the plesiomorphic ‘absent’ condition. In scolecophidians, however, it is more parsimonious to consider the absence of this process as a plesiomorphic retention of the outgroup condition, due to the recovery of scolecophidians as diverging basally among snakes (though see discussion in §5.4.2.3).

Posterior dorsal lamina of vomer present [038:1]. This lamina is universal among alethinophidians (except *Atractaspis*), but also occurs in anomalepidids. This character state therefore does not fully distinguish alethinophidians from scolecophidians.

Preorbital ridge of frontal present [046:1]. Again, this feature is universal among alethinophidians, but also occurs in anomalepidids. In extant snakes, this ridge is involved in the mobile suspension of the frontal from the prefrontal; thus, although it is more parsimonious to consider its absence in typhlopoids and leptotyphlopids as a retention of the ‘absent’ outgroup

condition (implying independent evolution of this ridge in anomalepidids), it is also possible that this ridge was independently lost in typhlopoids and leptotyphlopids due to fossoriality-related modification and stabilization of the prefrontal-frontal articulation.

Frontal-prefrontal articulation structurally complex, with prefrontal clasping frontal dorsally and ventrally [049:1]. This character state has the same distribution as [046:1] (see above), except that it does not occur in *Acrochordus*. Thus, the same reasoning as presented for the preceding synapomorphy also applies here.

Facial process of maxilla shorter than main body of maxilla [090:1]. This character state technically optimizes as a synapomorphy of Alethinophidia; however, it is in fact limited to anilioids among the observed alethinophidians, with the facial process being absent (thus rendering this character inapplicable) in booid-pythonoids and caenophidians. Nevertheless, the short-to-absent condition of the facial process in alethinophidians is ultimately distinct from the tall facial process typical of non-snake lizards and scolecophidians (except *Anomalepis*), supporting the reliability of this synapomorphy.

Palatine process of maxilla present [097:1]. The palatine process occurs exclusively in Alethinophidia, though it is absent in *Xenopeltis*, *Atractaspis*, and *Crotalus*. These latter genera are particularly important, as the extreme reduction of the maxilla in atractaspidines and viperids in many ways resembles the reduction of this element in scolecophidians, especially typhlopoids and anomalepidids (i.e., 'maxillary rakers'; see Kley 2001; Caldwell 2019; Chretien *et al.* 2019; Strong *et al.* 2021b). This is not to say that this reduction is homologous in scolecophidians and viper-like snakes; however, this similarity does emphasize that the condition in Alethinophidia is not fundamentally distinct from that in scolecophidians.

Accessory foramen posterior to superior alveolar foramen on maxilla present [101:1]. Although this character state optimizes as a synapomorphy of Alethinophidia, this accessory foramen is present in less than half (47%; 7 / 15) of the sampled alethinophidians, including only 36% (4 / 11) of the sampled booid-pythonoids and caenophidians. This disparate distribution thus reduces the reliability of this proposed synapomorphy.

Maxillary process of palatine articulating with ventromedial margin of prefrontal [118:1]. This articulation is recovered as a synapomorphy of Alethinophidia, though it also occurs in most leptotyphlopids. Furthermore, the maxillary process of the palatine is reduced-to-absent in *Crotalus*, and does not contact the prefrontal in *Naja* or *Atractaspis*; these character

states also occur in anomalepidids and typhlopoids, respectively. As noted above regarding the palatine process of the maxilla [097:1], this is not an argument that these similarities are homologous in alethinophidians *versus* scolecophidians, but rather an indication that the morphologies of these groups are more similar than the present proposed synapomorphy of Alethinophidia would suggest.

Medial finger-like process of ectopterygoid absent [129:0]. This character state optimizes as a synapomorphy of Alethinophidia, but this absence in fact only occurs in *Anomochilus*, *Uropeltis*, and *Anilius*. The medial finger-like process of the ectopterygoid is indeed present in all other sampled taxa bearing an ectopterygoid (i.e., anomalepidids and the alethinophidians not listed above), thus undermining the reliability of this potential alethinophidian synapomorphy.

Crista interfenestralis not occurring as an individualized component around the juxtastapedial space [153:1]. Similar to the previous synapomorphy [129:0], this character state is in fact limited to anilioids; all other taxa for which this character could be scored exhibit a distinct crista interfenestralis. Because this synapomorphy does not describe most alethinophidians, and because scolecophidians show the same state as most alethinophidians, this proposed synapomorphy is therefore not a compelling feature to separate Alethinophidia from other squamates.

Laterosphenoid present [162:1]. The laterosphenoid ossification separates the anterior (maxillary; V2) and posterior (mandibular; V3) openings of the trigeminal foramen in alethinophidians, and is one of the most commonly invoked (e.g., Rieppel 1979a, 1988; Lee 1997; Lee & Scanlon 2002; Rieppel *et al.* 2002; Cundall & Irish 2008)—and commonly contested (e.g., Caldwell 2019; Garberoglio *et al.* 2019b; Strong *et al.* 2021a)—synapomorphies of Alethinophidia. Of all the synapomorphies optimized herein, this feature is one of only two character states to be fully exclusive to and universal among the sampled alethinophidians (see also [241:1] below). This distribution therefore strongly supports the legitimacy of the laterosphenoid as a genuine alethinophidian synapomorphy. However, there are a few caveats worth discussing. First, some alethinophidians do lack a laterosphenoid (e.g., the colubrid *Heterodon*; Cundall & Irish 2008:364 and fig. 2.7E), meaning that the distribution of this character state is not as clear-cut as the present phylogeny suggests. Furthermore, the laterosphenoid does not appear until quite late in ontogeny (Khannoon & Evans 2015; Palci *et al.*

2016; Khannoon *et al.* 2020). This latter point is particularly important, as the absence of the laterosphenoid has been proposed as a secondarily-derived, paedomorphic condition (Rieppel & Maisano 2007; Garberoglio *et al.* 2019b; Strong *et al.* 2021a). This is clearly the case for alethinophidians in which the laterosphenoid is absent, as this condition reflects developmentally-truncated absence of this feature relative to the typical laterosphenoid-bearing condition of adult alethinophidians. However, this interpretation is equivocal for scolecophidians, depending on their phylogenetic position (see §5.4.2.3). Altogether, even with the observed distribution of this character state, the laterosphenoid therefore should potentially not be taken for granted as a defining feature of alethinophidians.

Crista trabeculares elongate and distinct [192:1]. This character state occurs in most alethinophidians (except for most colubroids), and does not occur in any other observed squamate. Therefore, despite these few exceptions, this character state appears to be a reliable synapomorphy of Alethinophidia.

Cultriform process of parabasisphenoid bearing interchoanal keel [195:1]. Similar to some of the synapomorphies discussed above [090:1, 129:0, 153:1], the presence of the interchoanal keel is in fact limited to anilioids among alethinophidians. Therefore, although the paraphyletic arrangement of anilioids at the base of Alethinophidia causes this condition to optimize as an alethinophidian synapomorphy, in reality this feature does not describe the vast majority of alethinophidians, and does not distinguish non-anilioid alethinophidians from scolecophidians.

Posterior dentigerous process of dentary present [207:1]. The posterior dentigerous process of the dentary occurs only in alethinophidians among the observed squamates, and is nearly universal among this clade (except for *Atractaspis*). This character state distribution therefore supports this feature as a synapomorphy of Alethinophidia. However, the absence of this process in *Atractaspis* is notable in that this condition results from paedomorphic reduction of the dentary—both in structure and in number of teeth—relative to other alethinophidians (see Strong *et al.* 2021a). Simplification of the dentary also occurs in scolecophidians, particularly typhlopoids and anomalepidids, in which the rod-like dentary resembles the simple condition in early embryonic squamates (compare e.g., Polachowski & Werneburg 2013; Werneburg *et al.* 2015; Ollonen *et al.* 2018; to Strong *et al.* 2021b) and is indeed so strongly reduced as to be entirely edentulous (rendering the current character inapplicable). The connection between

paedomorphosis of the dentary and absence of the posterior dentigerous process, as exemplified by *Atractaspis*, in turn suggests that this explanation might also apply to scolecophidians; in other words, scolecophidians may lack this process not because they are retaining a plesiomorphic non-snake lizard condition (the most parsimonious interpretation), but because they are subject to paedomorphic reduction of the dentary (a less parsimonious but still distinctly plausible suggestion; see also discussion in §5.4.2.3).

Angular narrowly exposed in lateral view [223:1]. This character state is universal among alethinophidians (except *Anilius*, which does not bear a separate angular; see Strong *et al.* 2021b) and does not occur in any other observed squamate. Thus, this narrow exposure of the angular would appear to be a reliable synapomorphy of Alethinophidia. However, it is also important to recognize that the broad lateral exposure of the angular in scolecophidians is closely tied to the highly reduced nature of the mandibular elements in these snakes, particularly the dentary and compound bone (compare e.g., Polachowski & Werneburg 2013; Werneburg *et al.* 2015; Ollonen *et al.* 2018; to Strong *et al.* 2021b). The recognition of this reduction again implicates paedomorphosis as a potential factor giving rise to this condition in scolecophidians.

Coronoid process of coronoid subequal to or lower than compound bone at corresponding position [227:1]. The relatively low coronoid process of alethinophidians contrasts distinctly with the much taller process in non-snake lizards and scolecophidians, and is a condition universal within alethinophidians bearing a coronoid. However, although the tall coronoid process in scolecophidians may be interpreted as a retention of the non-snake lizard condition (Kley 2006), it can also be interpreted as a by-product of miniaturization and fossoriality, adapted for increasing mechanical advantage of the jaw musculature (Rieppel 1984a, b, 1996). This latter interpretation would imply that the proportionally tall scolecophidian coronoid may be a specialized, rather than plesiomorphic, condition, and further indicates that the scolecophidian condition could conceivably be derived from an alethinophidian-like state due to the constraints of miniaturization and fossoriality (for elaboration on this line of reasoning, see Strong *et al.* 2021a).

Dentary process of surangular bearing flattened dorsal surface [241:1]. Apart from the presence of the laterosphenoid [162:1], this state is the only synapomorphy optimized herein that is both exclusive to and universal within Alethinophidia. Unlike the laterosphenoid,

however, there are no immediately evident reasons to question this synapomorphy; as such, this character state unequivocally supports the clade Alethinophidia.

Coronoid eminence of surangular well-developed [244:1]. Although this character state optimizes as a synapomorphy of Alethinophidia, it does not occur in *Xenopeltis*, *Casarea*, or any observed caenophidian. Therefore, this synapomorphy does not provide particularly compelling support for the clade Alethinophidia. Furthermore, although non-snake lizards and scolecophidians both lack a coronoid eminence on the surangular or compound bone, this condition is arguably not directly equivalent. In particular, the scolecophidian compound bone is quite reduced compared to other squamates, including non-snake lizards; in typhlopoids and anomalepidids (see Strong *et al.* 2021b) the compound bone largely resembles earlier ontogenetic stages of other squamates (see e.g., Werneburg *et al.* 2015), and, despite the more robust nature of the compound bone in leptotyphlopids, it is still quite reduced relative to other squamates (see Strong *et al.* 2021b). As such, the absence of the coronoid eminence in scolecophidians could well reflect a secondarily-derived, paedomorphic loss, rather than a plesiomorphic retention (see also §5.4.2.3).

5.4.2.3. Implications for scolecophidian evolution

From the preceding discussion, it is evident that, although several synapomorphies arise for both Scolecophidia and Alethinophidia, very few of them—if any—are fully reliable. Cundall & Irish (2008:394) faced a similar conundrum, lamenting that "none of [their proposed synapomorphies of Alethinophidia, i.e., the laterosphenoid, medial frontal pillars, and toothed anterior process of the palatine] is uniformly present in all alethinophidians, and no other skull characters serve as reliable autapomorphies for the taxon."

Of the various caveats described above for these synapomorphies, two major themes recur: paedomorphosis and fossoriality. These phenomena are particularly relevant when assessing the phylogenetic position of scolecophidians, as both phenomena exert profound influences on scolecophidian morphology (Kley 2006; Caldwell 2019; Strong *et al.* 2021a; Strong *et al.* 2021b), and both phenomena are associated with extensive homoplasy (Savitzky 1983; Rieppel 1988; Hanken & Wake 1993; Rieppel 1996; Lee 1998; Rieppel & Zaher 2000; Olori & Bell 2012; Chretien *et al.* 2019; Strong *et al.* 2021a; Strong *et al.* 2021b). Furthermore, both phenomena represent major sources of potential systematic bias in morphology-based

phylogenetics (Gauthier *et al.* 1988a; Hanken & Wake 1993; Lee 1998; Rieppel & Zaher 2000; Wiens *et al.* 2005; Struck 2007).

For example, analyses of salamander phylogeny (Wiens *et al.* 2005; Struck 2007) have found that characters influenced by paedomorphosis can cause unrelated taxa to artificially group together, resulting in an ultimately misleading phylogeny. This phylogenetic artifact may result both from developmentally-truncated taxa failing to develop key synapomorphies that arise later in ontogeny (Wiens *et al.* 2005), and from paedomorphic taxa tending to revert to the same early-developing conditions (Hanken & Wake 1993; Wiens *et al.* 2005). This latter phenomenon, termed 'paedomorphic parallelism' by Hanken & Wake (1993), arises due to independent reversals along similar underlying developmental trajectories. Another confounding effect is that of 'compensatory convergence' *sensu* Hanken & Wake (1993), in which paedomorphic—and specifically miniaturized—taxa independently evolve the same conditions in order to compensate for the structural constraints of miniaturization.

Finally, pervasive developmental truncation is especially problematic because paedomorphosis often causes reversal to a plesiomorphic state (Hanken & Wake 1993). For example, as noted above, the paedomorphic absence of the laterosphenoid in the colubroid *Heterodon* (Cundall and Irish 2008:364 and fig. 2.7E) produces a reversion to the plesiomorphic, laterosphenoid-less condition occurring in non-snake lizards. Thus, as warned by Hanken & Wake (1993:510), "when organismal-wide, or global, paedomorphosis is involved, there may be profound difficulty in determining whether taxa are basal or highly derived". This warning indeed echoes earlier criticisms by Gould (1977) of the common conflation of 'simple' morphologies as 'primitive'; as noted by Gould (1977:281), "since larval morphology is usually quite simple, the adults that retain it are [typically] treated as ancestral groups rather than recent paedomorphic derivatives".

These biases are especially relevant when considering the scolecophidian phylogeny, as these snakes are highly miniaturized (thus susceptible to 'compensatory convergence'), highly paedomorphic (Kley 2006; Caldwell 2019; Strong *et al.* 2021a; Strong *et al.* 2021b; and thus susceptible to 'paedomorphic parallelism'), and extensively fossorially-adapted (thus exacerbating the potential for convergence; see e.g., Savitzky 1983; Rieppel 1984b, 1988, 1996; Lee 1998; Rieppel & Zaher 2000; Townsend *et al.* 2004; Wiens *et al.* 2006; Wiens *et al.* 2010; Olori & Bell 2012; Reeder *et al.* 2015; Da Silva *et al.* 2018; Watanabe *et al.* 2019; Ebel *et al.*

2020; Strong *et al.* 2021a; Strong *et al.* 2021b). In light of this potential bias, recent authors have strongly advocated hypotheses of morphological convergence (Caldwell 2019; Chretien *et al.* 2019; Strong *et al.* 2021b) and even phylogenetic polyphyly (Caldwell 2019) among scolecophidians. This perspective essentially argues that scolecophidians may reflect completely independent excursions into fossoriality and miniaturization, with their supposed similarities instead being highly homoplastic (see Caldwell 2019; Chretien *et al.* 2019; Strong *et al.* 2021b). The potential impacts of paedomorphosis on several of the synapomorphies discussed above reinforce this suggestion: because Scolecophidia is defined largely by paedomorphic character states, and because paedomorphosis is known to elicit extensively homoplastic morphologies (as discussed above), it is therefore quite plausible that some or all of these character states may simply reflect the parallel effects of miniaturization, rather than being genuine synapomorphies.

Such an interpretation ultimately remains to be tested, but is a viable hypothesis warranting further empirical investigation. Thus, beyond sampling fossil taxa (see §5.4.1), another factor essential in reconstructing the phylogeny of snakes will be the thorough investigation, recognition, and mitigation of potential extenuating factors such as fossoriality- and/or paedomorphosis-driven convergence. In order to do so, it is of course essential to first identify which characters may be affected by these phenomena. However, such an undertaking is much easier said than done.

The difficulties in identifying paedomorphic characters in particular become evident when considering the circularity intrinsic to this task: as emphasized by several authors (e.g., Gould 1977; McNamara 1986; Irish 1989; Hanken & Wake 1993; Rieppel 1996; Reilly *et al.* 1997; Wiens *et al.* 2005), any identification of heterochrony is an inherently phylogenetic statement, requiring knowledge of the ancestral ontogeny in order to determine if or how this ontogeny has been altered; however, in the case of paedomorphosis, the very presence of this developmental alteration can profoundly affect the phylogenetic framework itself (Gould 1977; Hanken & Wake 1993; Wiens *et al.* 2005; Struck 2007) and thus bias our understanding of this evolutionary context.

This circularity is especially notable for scolecophidians. For example, a number of the reconstructed synapomorphies of scolecophidians are clearly paedomorphic, regardless of the specific phylogenetic position of scolecophidians among snakes. These features include the anteriorly oriented quadrate [133:0], the edentulous and rod-like pterygoid [108:2, 123:1], the

reduced splenial [219:1], and potentially the passage of the trigeminal nerve's maxillary branch [120:1] and the absence of hemapophyses [248:1]. These features all otherwise occur only in embryonic or juvenile squamates, rendering them paedomorphic in scolecophidians regardless of which taxa are used to bracket or infer the plesiomorphic developmental pathway for this group.

Conversely, however, other features are more ambiguous, as they may be either paedomorphic or plesiomorphic depending on the position of scolecophidians among Ophidia. Consider, for example, the absence of the laterosphenoid. This ossification is present in alethinophidians, and absent in non-snake lizards, fossil snakes (e.g., *Dinilysia*, madtsoiids; unknown in other fossil snakes), and scolecophidians (Rieppel 1979a; Lee & Scanlon 2002). If scolecophidians do indeed diverge basally to Alethinophidia (Figs 5.2, 5.3a, and 5.4), then it would be most parsimonious to interpret this absence as a plesiomorphic retention of the condition in non-snake lizards and early-diverging fossil snakes; in other words, the laterosphenoid is absent in scolecophidians because it never evolved in this lineage to begin with. However, if scolecophidians are instead nested within Alethinophidia—as has been suggested from both comparative anatomical (e.g., Caldwell 2019; Strong *et al.* 2021a) and phylogenetic (Fig. 5.3b; Caldwell 2000:fig. 1A; Palci & Caldwell 2010; Garberoglio *et al.* 2019a) perspectives—then this would be a paedomorphic condition; in other words, the laterosphenoid is absent in scolecophidians because it has been secondarily lost, reflecting truncation of the ontogenetic pathway of surrounding taxa.

This ambiguity also applies to several other features, such as the absence of the medial frontal pillars (see also Strong *et al.* 2021a), the absence of the posterior dorsal process of the septomaxillary lateral vertical flange [029:1], the absence of the palatine process of the maxilla [097:1], the absence of the posterior dentigerous process of the dentary [207:1], the broad exposure of the angular in lateral view [223:1], and the absence of a distinct coronoid eminence on the compound bone [244:1]. In all of these cases, the paedomorphic condition matches the plesiomorphic condition, a confounding phenomenon discussed above and by Hanken & Wake (1993). Thus, whether the relevant conditions are plesiomorphically absent or paedomorphically lost depends entirely on the position of scolecophidians relative to alethinophidians; however, this position may itself be biased toward an inaccurate—and even artificially basal—placement by the very existence of paedomorphosis (Gould 1977; Hanken & Wake 1993; Wiens *et al.* 2005; Struck 2007).

Ultimately, the major question arising from this discussion is how to adequately recognize and account for the effects of homoplasy. Previous authors have suggested removing characters associated with paedomorphosis (e.g., the clearly paedomorphic characters identified above), re-scoring highly paedomorphic taxa as 'unknown' morphologically and relying entirely on molecular data for their placement, or removing paedomorphic taxa altogether (Wiens *et al.* 2005; Struck 2007). This last possibility can immediately be discarded for scolecophidians, but the former two are each potentially viable.

Several authors have held a similar debate regarding fossoriality, drawing very different conclusions. On one side, Lee (1998) advocated drastically down-weighting characters associated with fossoriality in order to remove the bias they exert on snake-dibamid-amphisbaenian relationships; this is essentially equivalent to the first possibility listed above, involving the removal of characters susceptible to paedomorphosis. However, Rieppel & Zaher (2000) criticized this approach, arguing that convergence cannot be assumed *a priori*, no matter how rampant it is suspected to be. They instead suggested including molecular or soft-tissue characters, which they proposed to be less susceptible to fossoriality-related constraints (Rieppel & Zaher 2000); this approach mirrors the suggestion by Wiens *et al.* (2005) to analyze paedomorphic taxa using only molecular data (see also Hanken & Wake 1993). However, based on preliminary observations of extreme genomic reduction in paedomorphic fish (Malmstrøm *et al.* 2018), it is worth noting that molecular data itself may not be immune to the effects of paedomorphosis (see also discussion in Strong *et al.* 2021a).

The way forward for scolecophidian systematics—particularly regarding how to assess possible convergence among these snakes—is therefore quite complex. Ultimately this conundrum can be distilled into two competing hypotheses: either Scolecophidia genuinely forms a clade of miniaturized and fossorial snakes, in which the paedomorphic body plan is indeed synapomorphic (as per the traditional perspective on snake evolution; e.g., Rieppel 1988); or scolecophidians instead form a convergent assemblage, in which fossoriality, miniaturization, and paedomorphosis have caused the independent evolution of several features across typhlopoids, anomalepidids, and leptotyphlopids (as per e.g., Caldwell 2019; Chretien *et al.* 2019; Strong *et al.* 2021b). The presence of vastly different jaw mechanisms in each scolecophidian lineage supports the latter scenario of independent excursions into fossoriality and miniaturization, with the 'synapomorphies' of Scolecophidia in fact being convergent

conditions in evolutionarily distinct lineages (see also Chretien *et al.* 2019; Strong *et al.* 2021b). In contrast, if scolecophidians were still to group together even after paedomorphosis and fossoriality being accounted for, this would tend to support the former, traditional scenario (for a comparable outcome, see the analysis of miniaturized Palaeozoic amphibians by Fröbisch & Schoch 2009). Although the resolution of such a complex debate very much warrants its own treatment, falling beyond the scope of the current study, the present discussion of scolecophidian phylogeny should provide a useful basis for future investigations into the effect of evolutionary developmental processes on snake evolution.

5.5. Conclusions

This chapter presents a preliminary re-assessment of snake, and particularly scolecophidian, evolution, motivated by a recognition of the logical and methodological issues affecting previous snake phylogenies. However, it is important to emphasize that the Revised phylogenies produced herein are not intended as a final hypothesis of the 'true' phylogeny of snakes; indeed, the demonstrated phylogenetic impact of fossil snakes—including profound effects on the position of scolecophidians—indicates that such an interpretation would be quite naïve. Instead, this chapter represents very much the opposite: an initial step in the complex process of more fully understanding snake evolution. As examined above, the potential impact of heterochrony and homoplasy on several key scolecophidian synapomorphies and symplesiomorphies highlights a need for caution in implementing and interpreting these characters. Similarly, the inclusion of fossils is clearly essential in reconstructing ophidian phylogeny, and analyses neglecting a rigorous consideration of these data should be regarded with skepticism, regardless of the logical and operational rigour of the underlying dataset and characters. These core conclusions are highly relevant for both morphological and molecular phylogenetic analysis; alongside the revised dataset presented herein, these findings will hopefully prove important in future attempts to decipher the evolutionary history of scolecophidians and of snakes more broadly.

Figures: Chapter Five

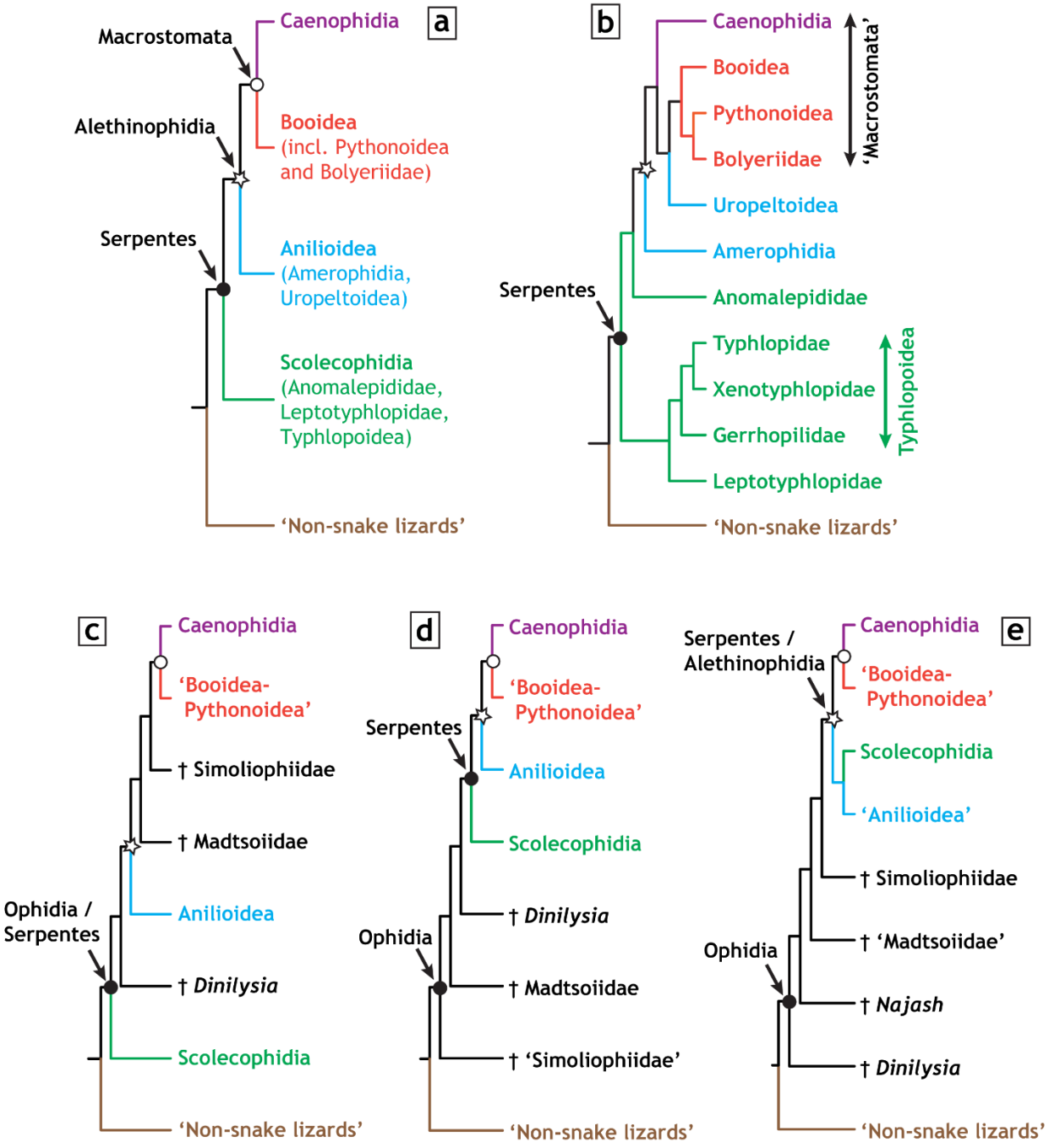

FIGURE 5.1. Overview of previous snake phylogenies. (**a**) Traditional perspective of the phylogeny of extant snakes, based on Rieppel (1988). (**b**) Typical molecular topology recovering scolecophidians as paraphyletic, based on Burbrink *et al.* (2020). (**c**) Rieppel, Zaher, and colleagues' perspective of scolecophidians as diverging basally to all other snakes, including extinct taxa, based on Zaher & Rieppel (2002) with placement of Madtsoiidae from Zaher & Scanferla (2012). (**d**) Caldwell, Lee, and colleagues' perspective of fossil snakes as diverging basally to scolecophidians, based on Lee & Scanlon (2002). (**e**) Recent phylogeny recovering scolecophidians among 'anilioids', within Alethinophidia, based on Garberoglio *et al.* (2019a). Quotation marks indicate non-monophyletic groups. † indicates extinct taxa. Following Caldwell & Lee (1997), Serpentes refers to crown-clade snakes and Ophidia refers to all snakes (both extant and extinct). Key simoliophiid taxa include *Pachyrhachis*, *Haasiophis*, and *Eupodophis*. Key madtsoiid taxa include *Wonambi*, *Yurlunggur*, and *Sanajeh*.

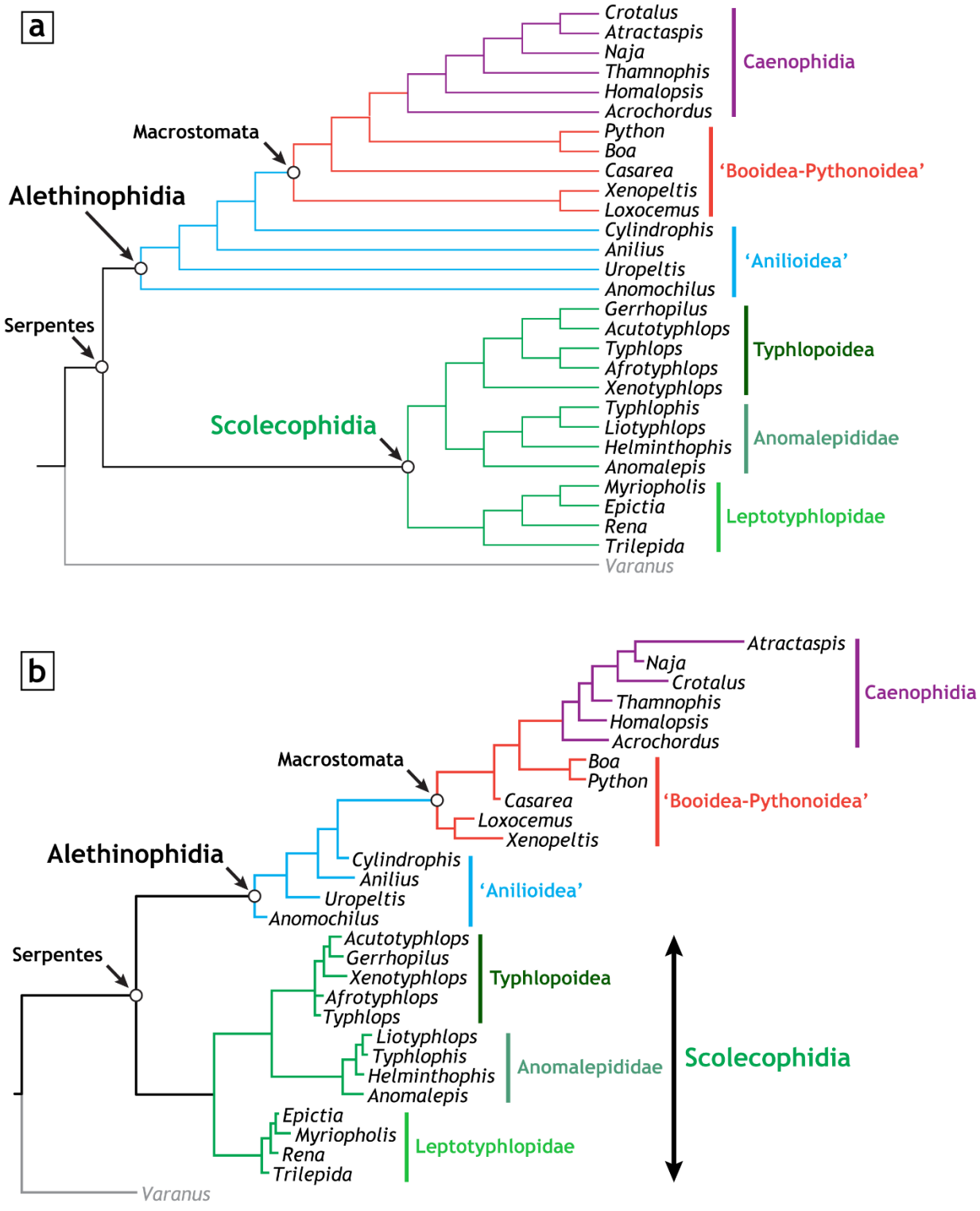
a
Crotalus
Atractaspis
Naja
Thamnophis
Homalopsis
Acrochordus
Caenophidia
Macrostomata
Python
Boa
Casarea
Xenopeltis
Loxocemus
'Booidea-Pythonoidea'
Alethinophidia
Cylindrophis
Anilius
Uropeltis
Anomochilus
'Anilioidea'
Serpentes
Gerrhopilus
Acutotyphlops
Typhlops
Afrotyphlops
Xenotyphlops
Typhlopoidea
Typhlophis
Liotyphlops
Helminthophis
Anomalepis
Scolecophidia
Anomalepididae
Myriopholis
Epictia
Rena
Trilepida
Leptotyphlopidae
Varanus
b
Atractaspis
Naja
Crotalus
Thamnophis
Homalopsis
Acrochordus
Caenophidia
Macrostomata
Boa
Python
Casarea
Loxocemus
Xenopeltis
'Booidea-Pythonoidea'
Alethinophidia
Cylindrophis
Anilius
Uropeltis
Anomochilus
'Anilioidea'
Serpentes
Acutotyphlops
Gerrhopilus
Xenotyphlops
Afrotyphlops
Typhlops
Typhlopoidea
Liotyphlops
Typhlophis
Helminthophis
Anomalepis
Anomalepididae
Scolecophidia
Epictia
Myriopholis
Rena
Trilepida
Leptotyphlopidae
Varanus

FIGURE 5.2. Phylogenies generated from the Revised Dataset presented in this chapter. (**a**) Single most-parsimonious tree (724 steps) generated via maximum parsimony analysis of the Revised Dataset. (**b**) 50% majority-rule consensus tree produced via Bayesian analysis of the Revised Dataset. Both phylogenies recover the traditional hypothesis of a monophyletic Scolecophidia as the sister-group of Alethinophidia. Quotation marks indicate non-monophyletic groups. Following Caldwell & Lee (1997), Serpentes refers to crown-clade snakes.

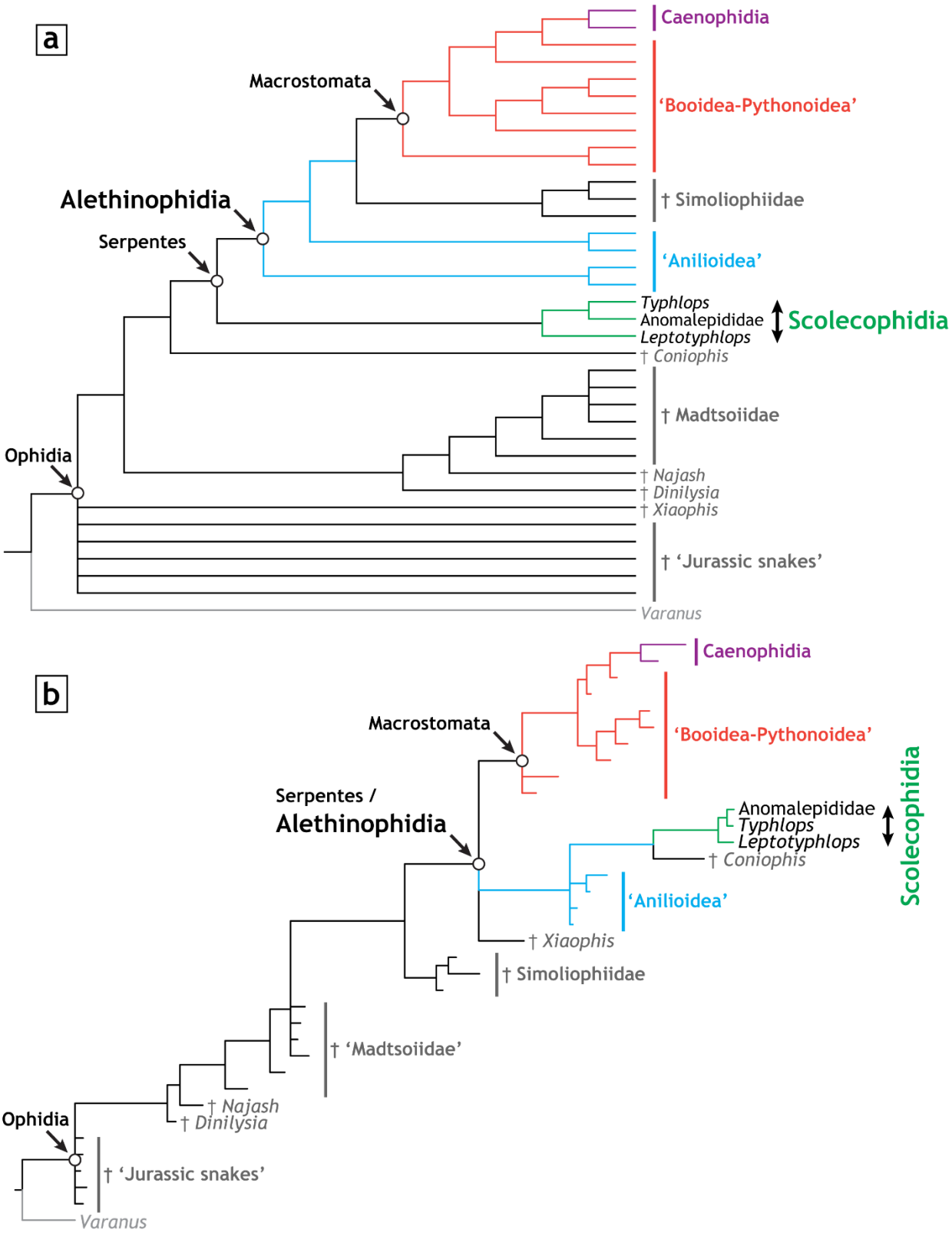
a
Caenophidia
'Booidea-Pythonoidea'
Macrostomata
† Simoliophiidae
Alethinophidia
Serpentes
'Anilioidea'
Typhlops
Anomalepididae
Leptotyphlops
Scolecophidia
† Coniophis
† Madtsoiidae
Ophidia
† Najash
† Dinilysia
† Xiaophis
† 'Jurassic snakes'
Varanus
b
Caenophidia
'Booidea-Pythonoidea'
Macrostomata
Serpentes /
Alethinophidia
Anomalepididae
Typhlops
Leptotyphlops
Scolecophidia
† Coniophis
'Anilioidea'
† Xiaophis
† Simoliophiidae
† 'Madtsoiidae'
Ophidia
† Najash
† Dinilysia
† 'Jurassic snakes'
Varanus

FIGURE 5.3. Phylogenies generated from the Original Dataset (Garberoglio *et al.* 2019a:dataset 1 and data file S1 therein), reflecting the phylogenetic position and impact of fossils. (**a**) 50% majority-rule consensus tree constructed from the 272 most-parsimonious trees (624 steps) generated via maximum parsimony (MP) analysis of the Original Dataset. (**b**) 50% majority-rule consensus tree produced via Bayesian analysis of the Original Dataset. In the MP tree, scolecophidians occupy their standard position at the base of Serpentes; however, in the Bayesian tree, scolecophidians are nested within Alethinophidia. Quotation marks indicate non-monophyletic groups. † indicates extinct taxa. Following Caldwell & Lee (1997), Serpentes refers to crown-clade snakes and Ophidia refers to all snakes (both extant and extinct).

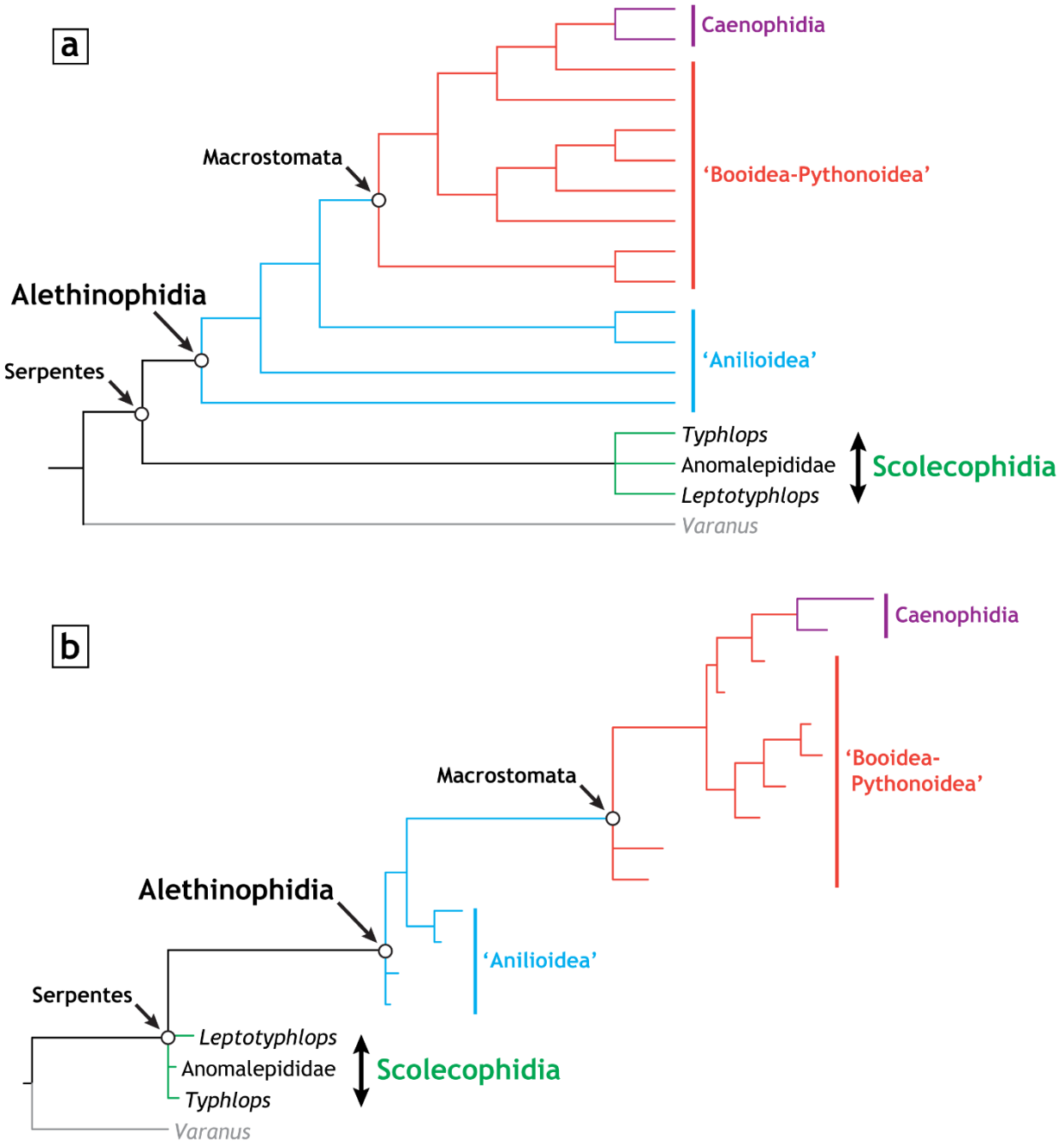
a
Caenophidia
'Booidea-Pythonoidea'
Macrostomata
Alethinophidia
'Anilioidea'
Serpentes
Typhlops
Anomalepididae
Leptotyphlops
Scolecophidia
Varanus
b
Caenophidia
'Booidea-
Pythonoidea'
Macrostomata
Alethinophidia
'Anilioidea'
Serpentes
Leptotyphlops
Anomalepididae
Typhlops
Scolecophidia
Varanus

FIGURE 5.4. Phylogenies generated from the Reduced Dataset, reflecting the impact of excluding fossils from Garberoglio *et al.* (2019a:dataset 1). (**a**) 50% majority-rule consensus tree constructed from the 46 most-parsimonious trees (445 steps) generated via maximum parsimony (MP) analysis of the Reduced Dataset. (**b**) 50% majority-rule consensus tree produced via Bayesian analysis of the Reduced Dataset. The position of scolecophidians is consistent in the Reduced MP analysis compared to the Original MP analysis (Fig. 5.3a); however, in the Reduced Bayesian analysis, scolecophidians revert to a distinctly more basal position than in the Original Bayesian analysis (Fig. 5.3b). Quotation marks indicate non-monophyletic groups. Following Caldwell & Lee (1997), Serpentes refers to crown-clade snakes.

Tables: Chapter Five

TABLE 5.1. List of specimens sampled for phylogenetic analysis. See preliminary pages of thesis document for institutional abbreviations. See Appendix 1.1 for sources of scan data.

HIGHER TAXON			SPECIES	SPECIMEN NUMBER
Alethinophidia	**'Anilioidea'**	**Amerophidia (Aniliidae)**	*Anilius scytale*	KUH 125976
		Uropeltoidea (Anomochilidae) (Cylindrophiidae) (Uropeltidae)	*Anomochilus leonardi*	FRIM 0026
			Cylindrophis ruffus	UMMZ 201901
			Uropeltis melanogaster	FMNH 167048
	Bolyeriidae		*Casarea dussumieri*	UMMZ 190285
	Booidea	**Boidae**	*Boa constrictor*	FMNH 31182
	Caenophidia	**Acrochordidae**	*Acrochordus granulatus*	MCZ R-146128
		Atractaspididae	*Atractaspis irregularis*	FMNH 62204 MCZ R-49237 MCZ R-48555
		Elapidae	*Naja naja*	FMNH 22468
		Homalopsidae	*Homalopsis buccata*	FMNH 259340
		Natricidae	*Thamnophis radix*	UAMZ R636
		Viperidae	*Crotalus adamanteus*	UF 103268
	Pythonoidea	**Loxocemidae**	*Loxocemus bicolor*	FMNH 104800
		Pythonidae	*Python molurus*	TNHC 62769
		Xenopeltidae	*Xenopeltis unicolor*	FMNH 148900
Scolecophidia	**Anomalepididae**		*Anomalepis mexicanus*	MCZ R-191201
			Helminthophis praeocularis	MCZ R-17960

			Liotyphlops argaleus	MCZ R-67933
			Typhlophis squamosus	MCZ R-145403
	Leptotyphlopidae		*Epictia albifrons*	MCZ R-2885
			Myriopholis macrorhyncha	MCZ R-9650
			Rena dulcis	UAMZ R335
			Trilepida dimidiata	SAMA 40143
	Typhlopoidea	**Gerrhopilidae**	*Gerrhopilus beddomii*	MCZ R-22372
		Typhlopidae	*Acutotyphlops subocularis*	SAMA R64770
			Afrotyphlops angolensis	MCZ R-170385
			Typhlops jamaicensis	USNM 12378
		Xenotyphlopidae	*Xenotyphlops grandidieri*	ZSM 2194/2007 ZSM 2213/2007 ZSM 2216/2007
'Non-snake lizards'		**Varanidae**	*Varanus exanthematicus*	FMNH 58299

References: Chapter Five

Adalsteinsson, S. A., Branch, W. R., Trape, S., Vitt, L. J. & Hedges, S. B. 2009. Molecular phylogeny, classification, and biogeography of snakes of the Family Leptotyphlopidae (Reptilia, Squamata). *Zootaxa*, **2244**, 1–50.

Apesteguía, S. & Zaher, H. 2006. A Cretaceous terrestrial snake with robust hindlimbs and a sacrum. *Nature*, **440**, 1037–1040. doi:10.1038/nature04413

Bellairs, A. D. & Underwood, G. 1951. The origin of snakes. *Biological Reviews*, **26**, 193–237.

Brock, G. T. 1941. The skull of *Acontias meleagris*, with a study of the affinities between lizards and snakes. *Zoological Journal of the Linnean Society*, **41**, 71–88.

Burbrink, F. T., Grazziotin, F. G., Pyron, R. A., Cundall, D., Donnellan, S., Irish, F., Keogh, J. S., Kraus, F., Murphy, R. W., Noonan, B., Raxworthy, C. J., Ruane, S., Lemmon, A. R., Lemmon, E. M. & Zaher, H. 2020. Interrogating genomic-scale data for Squamata (lizards, snakes, and amphisbaenians) shows no support for key traditional morphological relationships. *Systematic Biology*, **69**(3), 502–520. doi:10.1093/sysbio/syz062

Caldwell, M. W. & Lee, M. S. Y. 1997. A snake with legs from the marine Cretaceous of the Middle East. *Nature*, **386**, 705–709.

Caldwell, M. W. 1999. Squamate phylogeny and the relationships of snakes and mosasauroids. *Zoological Journal of the Linnean Society*, **125**, 115–147. doi:10.1111/j.1096-3642.1999.tb00587.x

Caldwell, M. W. 2000. On the phylogenetic relationships of *Pachyrhachis* within snakes: a response to Zaher (1998). *Journal of Vertebrate Paleontology*, **20**(1), 187–190.

Caldwell, M. W. 2007a. The role, impact, and importance of fossils: snake phylogeny, origins, and evolution (1869–2006). Pp. 253–302 in J. Anderson and H.-D. Sues (eds) *Major Transitions in Vertebrate Evolution*. Indiana University Press, Bloomington, Indiana.

Caldwell, M. W., Nydam, R. L., Palci, A. & Apesteguía, S. 2015. The oldest known snakes from the Middle Jurassic-Lower Cretaceous provide insights on snake evolution. *Nature Communications*, **6**, 5996. doi:10.1038/ncomms6996

Caldwell, M. W. 2019. *The Origin of Snakes: Morphology and the Fossil Record*. Taylor & Francis, Boca Raton.

Chretien, J., Wang-Claypool, C. Y., Glaw, F. & Scherz, M. D. 2019. The bizarre skull of *Xenotyphlops* sheds light on synapomorphies of Typhlopoidea. *Journal of Anatomy*, **234**, 637–655. doi:10.1111/joa.12952

Conrad, J. L. 2008. Phylogeny and systematics of Squamata (Reptilia) based on morphology. *Bulletin of the American Museum of Natural History, New York*, **310**, 1–182. doi:10.1206/310.1

Cundall, D., Wallach, V. & Rossman, D. A. 1993. The systematic relationships of the snake genus *Anomochilus*. *Zoological Journal of the Linnean Society*, **109**, 275–299.

Cundall, D. & Irish, F. 2008. The snake skull. Pp. 349–692 in C. Gans, A.S. Gaunt and K. Adler (eds) *Biology of the Reptilia: Morphology H, The Skull of Lepidosauria*. Society for the Study of Amphibian and Reptiles, Ithaca, New York.

Da Silva, F. O., Fabre, A.-C., Savriama, Y., Ollonen, J., Mahlow, K., Herrel, A., Müller, J. & Di-Poï, N. 2018. The ecological origins of snakes as revealed by skull evolution. *Nature Communications*, **9**, 376. doi:10.1038/s41467-017-02788-3

de Pinna, M. G. G. 1991. Concepts and tests of homology in the cladistic paradigm. *Cladistics*, **7**, 367–394.

Ebel, R., Müller, J., Ramm, T., Hipsley, C. & Amson, E. 2020. First evidence of convergent lifestyle signal in reptile skull roof microanatomy. *BMC Biology*, **18**, 185. doi:10.1186/s12915-020-00908-y

Figueroa, A., McKelvy, A. D., Grismer, L. L., Bell, C. D. & Lailvaux, S. P. 2016. A species-level phylogeny of extant snakes with description of a new colubrid subfamily and genus. *PLoS ONE*, **11**(9), e0161070. doi:10.1371/journal.pone.0161070

Frazzetta, T. H. 1966. Studies of the morphology and function of the skull in the Boidae (Serpentes). Part II. Morphology and function of the jaw apparatus in *Python sebae* and *Python molurus*. *Journal of Morphology*, **118**, 217–296.

Fröbisch, N. B. & Schoch, R. R. 2009. Testing the impact of miniaturization on phylogeny: Paleozoic dissorophoid amphibians. *Systematic Biology*, **58**(3), 312–327. doi:10.1093/sysbio/syp029

Garberoglio, F. F., Apesteguía, S., Simões, T. R., Palci, A., Gómez, R. O., Nydam, R. L., Larsson, H. C. E., Lee, M. S. Y. & Caldwell, M. W. 2019a. New skulls and skeletons

of the Cretaceous legged snake *Najash*, and the evolution of the modern snake body plan. *Science Advances*, **5**(11), eaax5833. doi:10.1126/sciadv.aax5833

Garberoglio, F. F., Gómez, R. O., Apesteguía, S., Caldwell, M. W., Sánchez, M. L. & Veiga, G. 2019b. A new specimen with skull and vertebrae of *Najash rionegrina* (Lepidosauria: Ophidia) from the early Late Cretaceous of Patagonia. *Journal of Systematic Palaeontology*, **17**(18), 1533–1550. doi:10.1080/14772019.2018.1534288

Garberoglio, F. F., Gómez, R. O., Simões, T. R., Caldwell, M. W. & Apesteguía, S. 2019c. The evolution of the axial skeleton intercentrum system in snakes revealed by new data from the Cretaceous snakes *Dinilysia* and *Najash*. *Scientific Reports*, **9**, 1276. doi:10.1038/s41598-018-36979-9

Gauthier, J., Kluge, A. G. & Rowe, T. 1988a. Amniote phylogeny and the importance of fossils. *Cladistics*, **4**, 105–209.

Gauthier, J. A., Kearney, M., Maisano, J. A., Rieppel, O. & Behlke, A. D. B. 2012. Assembling the squamate tree of life: perspectives from the phenotype and the fossil record. *Bulletin of the Peabody Museum of Natural History*, **53**, 3–308. doi:10.3374/014.053.0101

Gelman, A. & Rubin, D. M. 1992. Inference from iterative simulation using multiple sequences. *Statistical Science*, **7**(4), 457–511.

Goloboff, P. A., Farris, J. S. & Nixon, K. C. 2008. TNT, a free program for phylogenetic analysis. *Cladistics*, **24**, 774–786. doi:10.1111/j.1096-0031.2008.00217.x

Goloboff, P. A. & Catalano, S. A. 2016. TNT version 1.5, including a full implementation of phylogenetic morphometrics. *Cladistics*, **32**, 221–238. doi:10.1111/cla.12160

Gould, S. J. 1977. *Ontogeny and Phylogeny*. Harvard University Press, Cambridge.

Hanken, J. & Wake, D. B. 1993. Miniaturization of body size: organismal consequences and evolutionary significance. *Annual Review of Ecology and Systematics*, **24**, 501–519.

Harrington, S. M. & Reeder, T. W. 2017. Phylogenetic inference and divergence dating of snakes using molecules, morphology and fossils: new insights into convergent evolution of feeding morphology and limb reduction. *Biological Journal of the Linnean Society*, **121**, 379–394.

Heise, P. J., Maxson, L. R., Dowling, H. G. & Hedges, S. B. 1995. Higher-level snake phylogeny inferred from mitochondrial DNA sequences of 12S rRNA and 16S rRNA genes. *Molecular Biology and Evolution*, **12**(2), 259–265.

Hernández-Jaimes, C., Jerez, A. & Ramírez-Pinilla, M. P. 2012. Embryonic development of the skull of the Andean lizard *Ptychoglossus bicolor* (Squamata, Gymnophthalmidae). *Journal of Anatomy*, **221**, 285–302. doi:10.1111/j.1469-7580.2012.01549.x

Hoffstetter, R. & Gasc, J.-P. 1969. Vertebrae and ribs of modern reptiles. Pp. 201–310 in C. Gans, A.D. Bellairs and T.S. Parsons (eds) *Biology of the Reptilia: Morphology A*. Academic Press, London and New York.

Hsiang, A. Y., Field, D. J., Webster, T. H., Behlke, A. D. B., Davis, M. B., Racicot, R. A. & Gauthier, J. A. 2015. The origin of snakes: revealing the ecology, behavior, and evolutionary history of early snakes using genomics, phenomics, and the fossil record. *BMC Evolutionary Biology*, **15**, 87. doi:10.1186/s12862-015-0358-5

Irish, F. J. 1989. The role of heterochrony in the origin of a novel bauplan: evolution of the ophidian skull. *Geobios*, **22**, 227–233.

Kamal, A. M. 1966. On the process of rotation of the quadrate cartilage in Ophidia. *Anatomischer Anzieger*, **118**, 87–90.

Khannoon, E. R. & Evans, S. E. 2015. The development of the skull of the Egyptian cobra *Naja h. haje* (Squamata: Serpentes: Elapidae). *PLoS ONE*, **10**, e0122185. doi:10.1371/journal.pone.0122185

Khannoon, E. R., Ollonen, J. & Di-Poï, N. 2020. Embryonic development of skull bones in the Sahara horned viper (*Cerastes cerastes*), with new insights into structures related to the basicranium and braincase roof. *Journal of Anatomy*, **00**, 1–19. doi:10.1111/joa.13182

Kley, N. J. & Brainerd, E. L. 1999. Feeding by mandibular raking in a snake. *Nature*, **402**, 369–370. doi:10.1038/46460

Kley, N. J. 2001. Prey transport mechanisms in blindsnakes and the evolution of unilateral feeding systems in snakes. *American Zoologist*, **41**, 1321–1337.

Kley, N. J. 2006. Morphology of the lower jaw and suspensorium in the Texas blindsnake, *Leptotyphlops dulcis* (Scolecophidia: Leptotyphlopidae). *Journal of Morphology*, **267**, 494–515. doi:10.1002/jmor.10414

Lakner, C., Mark, P. v. d., Huelsenbeck, J. P., Larget, B. & Ronquist, F. 2008. Efficiency of Markov Chain Monte Carlo tree proposals in Bayesian phylogenetics. *Systematic Biology*, **57**(1), 86–103. doi:10.1080/10635150801886156

LeBlanc, A. R. H., Caldwell, M. W. & Bardet, N. 2012. A new mosasaurine from the Maastrichtian (Upper Cretaceous) phosphates of Morocco and its implications for mosasaurine systematics. *Journal of Vertebrate Paleontology*, **32**(1), 82–104. doi:10.1080/02724634.2012.624145

Lee, M. S. Y. 1997. The phylogeny of varanoid lizards and the affinities of snakes. *Philosophical Transactions of the Royal Society of London, Series B: Biological Sciences*, **352**, 53–91.

Lee, M. S. Y. 1998. Convergent evolution and character correlation in burrowing reptiles: towards a resolution of squamate relationships. *Biological Journal of the Linnean Society*, **65**, 369–453.

Lee, M. S. Y. & Caldwell, M. W. 1998. Anatomy and relationships of *Pachyrhachis problematicus*, a primitive snake with hindlimbs. *Philosophical Transactions of the Royal Society of London, Series B: Biological Sciences*, **353**(1375), 1521–1552.

Lee, M. S. Y. & Scanlon, J. D. 2002. Snake phylogeny based on osteology, soft anatomy and ecology. *Biological Reviews*, **77**, 333–401.

Lee, M. S. Y. 2005. Molecular evidence and marine snake origins. *Biology Letters*, **1**, 227–230. doi:10.1098/rsbl.2004.0282

Lee, M. S. Y. 2009. Hidden support from unpromising data sets strongly unites snakes with anguimorph 'lizards'. *Journal of Evolutionary Biology*, **22**, 1308–1316. doi:10.1111/j.1420-9101.2009.01751.x

Lewis, P. O. 2001. A likelihood approach to estimating phylogeny from discrete morphological character data. *Systematic Biology*, **50**(6), 913–925.

Longrich, N. R., Bhullar, B.-A. S. & Gauthier, J. A. 2012. A transitional snake from the Late Cretaceous period of North America. *Nature*, **488**, 205–208. doi:10.1038/nature11227

Maddison, W. P. & Maddison, D. R. 2019. Mesquite: a modular system for evolutionary analysis. http://mesquiteproject.org

Mahendra, B. C. 1938. Some remarks on the phylogeny of the Ophidia. *Anatomischer Anzieger*, **86**, 347–356.

Malmstrøm, M., Britz, R., Matschiner, M., Tørresen, O. K., Kurnia Hadiaty, R., Yaakob, N., Hui Tan, H., Sigurd Jakobsen, K., Salzburger, W. & Rüber, L. 2018. The most developmentally truncated fishes show extensive *Hox* gene loss and miniaturized genomes. *Genome Biology and Evolution*, **10**(4), 1088–1103. doi:10.1093/gbe/evy058

Massare, J. A. 1987. Tooth morphology and prey preference of Mesozoic marine reptiles. *Journal of Vertebrate Paleontology*, **7**(2), 121–137. doi:10.1080/02724634.1987.10011647

McNamara, K. J. 1986. A guide to the nomenclature of heterochrony. *Journal of Paleontology*, **60**(1), 4–13.

Miller, M. A., Pfeiffer, W. & Schwartz, T. 2010. Creating the CIPRES Science Gateway for inference of large phylogenetic trees. Pp. 1–8. *Proceedings of the Gateway Computing Environments Workshop (GCE)*. New Orleans.

Miralles, A., Marin, J., Markus, D., Herrel, A., Hedges, S. B. & Vidal, N. 2018. Molecular evidence for the paraphyly of Scolecophidia and its evolutionary implications. *Journal of Evolutionary Biology*, **31**, 1782–1793. doi:10.1111/jeb.13373

Mongiardino Koch, N. & Parry, L. A. 2020. Death is on our side: paleontological data drastically modify phylogenetic hypotheses. *Systematic Biology*, **69**(6), 1052–1067. doi:10.1093/sysbio/syaa023

Object Research Systems Inc. 2019b. Dragonfly 4.1. Object Research Systems (ORS) Inc., Montreal, Canada. https://theobjects.com/dragonfly/

Ollonen, J., Silva, F. O. D., Mahlow, K. & Di-Poï, N. 2018. Skull development, ossification pattern, and adult shape in the emerging lizard model organism *Pogona vitticeps*: a comparative analysis with other squamates. *Frontiers in Physiology*, **9**, 278. doi:10.3389/fphys.2018.00278

Olori, J. C. & Bell, C. J. 2012. Comparative skull morphology of uropeltid snakes (Alethinophidia: Uropeltidae) with special reference to disarticulated elements and variation. *PLoS ONE*, **7**(3), e32450. doi:10.1371/journal.pone.0032450

Palci, A. & Caldwell, M. W. 2010. Redescription of *Acteosaurus tommasinii* von Meyer, 1860, and a discussion of evolutionary trends within the clade Ophidiomorpha. *Journal of Vertebrate Paleontology*, **30**(1), 94–108. doi:10.1080/02724630903409139

Palci, A., Caldwell, M. W. & Albino, A. M. 2013a. Emended diagnosis and phylogenetic relationships of the Upper Cretaceous fossil snake *Najash rionegrina* Apesteguía and Zaher, 2006. *Journal of Vertebrate Paleontology*, **33**(1), 131–140. doi:10.1080/02724634.2012.713415

Palci, A., Caldwell, M. W. & Nydam, R. L. 2013b. Reevaluation of the anatomy of the Cenomanian (Upper Cretaceous) hind-limbed marine fossil snakes *Pachyrhachis*, *Haasiophis*, and *Eupodophis*. *Journal of Vertebrate Paleontology*, **33**(6), 1328–1342. doi:10.1080/02724634.2013.779880

Palci, A., Lee, M. S. Y. & Hutchinson, M. N. 2016. Patterns of postnatal ontogeny of the skull and lower jaw of snakes as revealed by micro-CT scan data and three-dimensional geometric morphometrics. *Journal of Anatomy*, **229**(6), 723–754. doi:10.1111/joa.12509

Polachowski, K. M. & Werneburg, I. 2013. Late embryos and bony skull development in *Bothropoides jararaca* (Serpentes, Viperidae). *Zoology*, **116**, 36–63. doi:10.1016/j.zool.2012.07.003

Pyron, R. A., Burbrink, F. T. & Wiens, J. J. 2013. A phylogeny and revised classification of Squamata, including 4161 species of lizards and snakes. *BMC Evolutionary Biology*, **13**, 93. doi:10.1186/1471-2148-13-93

Rage, J.-C. & Escuillié, F. 2000. Un nouveau serpent bipède du Cénomanien (Crétacé). Implications phylétiques. *Comptes Rendus de l'Académie des Sciences - Series IIA - Sciences de la Terre et des planètes/Earth and Planetary Science*, **330**, 513–520.

Rambaut, A. 2018. FigTree: Tree Figure Drawing Tool (v.1.4.4).

Rambaut, A., Drummond, A. J., Xie, D., Baele, G. & Suchard, M. A. 2018. Posterior summarization in Bayesian phylogenetics using Tracer 1.7. *Systematic Biology*, **67**(5), 901–904. doi:10.1093/sysbio/syy032

Reeder, T. W., Townsend, T. M., Mulcahy, D. G., Noonan, B. P., Wood, P. L., Sites, J. W. & Wiens, J. J. 2015. Integrated analyses resolve conflicts over squamate reptile phylogeny and reveal unexpected placements for fossil taxa. *PLoS ONE*, **10**(3), e0118199. doi:10.1371/journal.pone.0118199

Reilly, S. M., Wiley, E. O. & Meinhardt, D. J. 1997. An integrative approach to heterochrony: the distinction between interspecific and intraspecific phenomena. *Biological Journal of the Linnean Society*, **60**, 119–143.

Rieppel, O. 1978a. A functional and phylogenetic interpretation of the skull of the Erycinae (Reptilia, Serpentes). *Journal of Zoology*, **186**, 185–208.

Rieppel, O. 1978b. The evolution of the naso-frontal joint in snakes and its bearing on snake origins. *Journal of Zoological Systematics and Evolutionary Research*, **16**, 14–27. doi:10.1111/j.1439-0469.1978.tb00917.x

Rieppel, O. 1979a. A cladistic classification of primitive snakes based on skull structure. *Journal of Zoological Systematics and Evolutionary Research*, **17**(2), 140–150. doi:10.1111/j.1439-0469.1979.tb00696.x

Rieppel, O. 1984a. Miniaturization of the lizard skull: its functional and evolutionary implications. *Symposia of the Zoological Society of London*, **52**, 503–520.

Rieppel, O. 1984b. The cranial morphology of the fossorial lizard genus *Dibamus* with a consideration of its phylogenetic relationships. *Journal of Zoology*, **204**, 289–327.

Rieppel, O. 1988. A review of the origin of snakes. Pp. 37–130 in M.K. Hecht, B. Wallace and G.T. Prance (eds) *Evolutionary Biology*. Springer, Boston, MA.

Rieppel, O. 1996. Miniaturization in tetrapods: consequences for skull morphology. Pp. 47–61 in P.J. Miller (ed) *Miniature Vertebrates: The Implications of Small Body Size, Vol. 69. Symposia of the Zoological Society of London*. Claredon Press, Oxford.

Rieppel, O. & Zaher, H. 2000. The intramandibular joint in squamates, and the phylogenetic relationships of the fossil snake *Pachyrhachis problematicus* Haas. *Fieldiana Geology*, **43**, 1–69.

Rieppel, O., Kluge, A. G. & Zaher, H. 2002. Testing the phylogenetic relationships of the Pleistocene snake *Wonambi naracoortensis* Smith. *Journal of Vertebrate Paleontology*, **22**(4), 812–829. doi:10.1671/0272-4634(2002)022[0812:TTPROT]2.0.CO;2

Rieppel, O. 2007. The naso-frontal joint in snakes as revealed by high-resolution X-ray computed tomography of intact and complete skulls. *Zoologischer Anzeiger*, **246**, 177–191. doi:10.1016/j.jcz.2007.04.001

Rieppel, O. & Maisano, J. A. 2007. The skull of the rare Malaysian snake *Anomochilus leonardi* Smith, based on high-resolution X-ray computed tomography. *Zoological Journal of the Linnean Society*, **149**, 671–685.

Rieppel, O., Kley, N. J. & Maisano, J. A. 2009. Morphology of the skull of the white-nosed blindsnake, *Liotyphlops albirostris* (Scolecophidia: Anomalepididae). *Journal of Morphology*, **270**, 536–557. doi:10.1002/jmor.10703

Ronquist, F., Teslenko, M., van der Mark, P., Ayres, D. L., Darling, A., Höhna, S., Larget, B., Liu, L., Suchard, M. A. & Huelsenbeck, J. P. 2012. MrBayes 3.2: efficient Bayesian phylogenetic inference and model choice across a large model space. *Systematic Biology*, **61**(3), 539–542. doi:10.1093/sysbio/sys029

Ronquist, F., Huelsenbeck, J. P., Teslenko, M. & Nylander, J. A. A. 2019. MrBayes version 3.2 manual: tutorials and model summaries.

Savitzky, A. H. 1983. Coadapted character complexes among snakes: fossoriality, piscivory, and durophagy. *American Zoologist*, **23**, 397–409.

Scanferla, A., Zaher, H., Novas, F. E., de Muizon, C. & Céspedes, R. 2013. A new snake skull from the Paleocene of Bolivia sheds light on the evolution of macrostomatans. *PLoS ONE*, **8**(3), e57583. doi:10.1371/journal.pone.0057583

Scanferla, A. 2016. Postnatal ontogeny and the evolution of macrostomy in snakes. *Royal Society Open Science*, **3**, 160612. doi:10.1098/rsos.160612

Scanlon, J. D. & Lee, M. S. Y. 2000. The Pleistocene serpent *Wonambi* and the early evolution of snakes. *Nature*, **403**, 416–420. doi:10.1038/35000188

Scanlon, J. D. 2006. Skull of the large non-macrostomatan snake *Yurlunggur* from the Australian Oligo-Miocene. *Nature*, **439**, 839–842. doi:10.1038/nature04137

Schmidt, K. P. 1950. Modes of evolution discernible in the taxonomy of snakes. *Evolution*, **4**(1), 79–86.

Sereno, P. C. 2007. Logical basis for morphological characters in phylogenetics. *Cladistics*, **23**(6), 565–587. doi:10.1111/j.1096-0031.2007.00161.x

Simões, B. F., Sampaio, F. L., Jared, C., Antoniazzi, M. M., Loew, E. R., Bowmaker, J. K., Rodriguez, A., Hart, N. S., Hunt, D. M., Partridge, J. C. & Gower, D. J. 2015. Visual system evolution and the nature of the ancestral snake. *Journal of Evolutionary Biology*, **28**, 1309–1320. doi:10.1111/jeb.12663

Simões, T. R., Caldwell, M. W., Palci, A. & Nydam, R. L. 2017. Giant taxon-character matrices: quality of character constructions remains critical regardless of size. *Cladistics*, **33**, 198–219. doi:10.1111/cla.12163

Simões, T. R., Caldwell, M. W., Tałanda, M., Bernardi, M., Palci, A., Vernygora, O., Bernardini, F., Mancini, L. & Nydam, R. L. 2018. The origin of squamates revealed by a Middle Triassic lizard from the Italian Alps. *Nature*, **557**, 706–709. doi:10.1038/s41586-018-0093-3

Singhal, S., Colston, T. J., Grundler, M. R., Smith, S. A., Costa, G. C., Colli, G. R., Moritz, C., Pyron, R. A. & Rabosky, D. L. 2021. Congruence and conflict in the higher-level phylogenetics of squamate reptiles: an expanded phylogenomic perspective. *Systematic Biology*, **70**(3), 542–557. doi:10.1093/sysbio/syaa054

Slowinski, J. B. & Lawson, R. 2002. Snake phylogeny: evidence from nuclear and mitochondrial genes. *Molecular Phylogenetics and Evolution*, **24**, 194–202.

Streicher, J. W. & Wiens, J. J. 2016. Phylogenomic analyses reveal novel relationships among snake families. *Molecular Phylogenetics and Evolution*, **100**, 160–169. doi:10.1016/j.ympev.2016.04.015

Strong, C. R. C., Caldwell, M. W., Konishi, T. & Palci, A. 2020. A new species of longirostrine plioplatecarpine mosasaur (Squamata: Mosasauridae) from the Late Cretaceous of Morocco, with a re-evaluation of the problematic taxon *'Platecarpus' ptychodon*. *Journal of Systematic Palaeontology*, **18**(21), 1769–1804. doi:10.1080/14772019.2020.1818322

Strong, C. R. C., Palci, A. & Caldwell, M. W. 2021a. Insights into skull evolution in fossorial snakes, as revealed by the cranial morphology of *Atractaspis irregularis* (Serpentes: Colubroidea). *Journal of Anatomy*, **238**, 146–172. doi:10.1111/joa.13295

Strong, C. R. C., Scherz, M. D. & Caldwell, M. W. 2021b. Deconstructing the Gestalt: new concepts and tests of homology, as exemplified by a re-conceptualization of "microstomy" in squamates. *The Anatomical Record*, **2021**, 1–49. doi:10.1002/ar.24630

Struck, T. H. 2007. Data congruence, paedomorphosis and salamanders. *Frontiers in Zoology*, **4**, 22. doi:10.1186/1742-9994-4-22

Tchernov, E., Rieppel, O., Zaher, H., Polcyn, M. J. & Jacobs, L. L. 2000. A fossil snake with limbs. *Science*, **287**(5460), 2010–2012. doi:10.1126/science.287.5460.2010

Townsend, T. M., Larson, A., Louis, E. & Macey, J. R. 2004. Molecular phylogenetics of Squamata: the position of snakes, amphisbaenians, and dibamids, and the root of the squamate tree. *Systematic Biology*, **53**(5), 735–757. doi:10.1080/10635150490522340

Vidal, N. & Hedges, S. B. 2002. Higher-level relationships of snakes inferred from four nuclear and mitochondrial genes. *Comptes Rendus Biologies*, **325**, 977–985.

Vidal, N. & Hedges, S. B. 2004. Molecular evidence for a terrestrial origin of snakes. *Proceedings of the Royal Society of London, Series B: Biological Sciences*, **271**, S226–229. doi:10.1098/rsbl.2003.0151

Vidal, N., Rage, J. C., Couloux, A. & Hedges, S. B. 2009. Snakes (Serpentes). Pp. 390–397 in S. Hedges and S. Kumar (eds) *The TimeTree of Life*. Oxford University Press, New York.

Vidal, N., Marin, J., Morini, M., Donnellan, S., Branch, W. R., Thomas, R., Vences, M., Wynn, A., Cruaud, C. & Hedges, S. B. 2010. Blindsnake evolutionary tree reveals long history on Gondwana. *Biology Letters*, **6**, 558–561 doi:10.1098/rsbl.2010.0220

Watanabe, A., Fabre, A.-C., Felice, R. N., Maisano, J. A., Müller, J., Herrel, A. & Goswami, A. 2019. Ecomorphological diversification in squamates from conserved pattern of cranial integration. *Proceedings of the National Academy of Sciences*, **116**(29), 14688–14697. doi:10.1073/pnas.1820967116

Webb, J. K. & Shine, R. 1992. To find an ant: trail-following in Australian blindsnakes (Typhlopidae). *Animal Behaviour*, **43**, 941–948.

Webb, J. K. & Shine, R. 1993. Prey-size selection, gape limitation and predator vulnerability in Australian blindsnakes (Typhlopidae). *Animal Behaviour*, **45**, 1117–1126.

Werneburg, I., Polachowski, K. M. & Hutchinson, M. N. 2015. Bony skull development in the Argus monitor (Squamata, Varanidae, *Varanus panoptes*) with comments on developmental timing and adult anatomy. *Zoology*, **118**, 255–280. doi:10.1016/j.zool.2015.02.004

Wiens, J. J. 2004. The role of morphological data in phylogeny reconstruction. *Systematic Biology*, **53**(4), 653–661. doi:10.1080/10635150490472959

Wiens, J. J. 2005. Can incomplete taxa rescue phylogenetic analyses from long-branch attraction? *Systematic Biology*, **54**(5), 731–742. doi:10.1080/10635150500234583

Wiens, J. J., Bonett, R. M. & Chippindale, P. T. 2005. Ontogeny discombobulates phylogeny: paedomorphosis and higher-level salamander relationships. *Systematic Biology*, **54**(1), 91–110. doi:10.1080/10635150590906037

Wiens, J. J., Brandley, M. C. & Reeder, T. W. 2006. Why does a trait evolve multiple times within a clade? Repeated evolution of snakelike body form in squamate reptiles. *Evolution*, **60**(1), 123–141. doi:10.1111/j.0014-3820.2006.tb01088.x

Wiens, J. J., Kuczynski, C. A., Smith, S. A., Mulcahy, D. G., Sites, J. W. J., Townsend, T. M. & Reeder, T. W. 2008. Branch lengths, support, and congruence: testing the phylogenomic approach with 20 nuclear loci in snakes. *Systematic Biology*, **57**(3), 420–431. doi:10.1080/10635150802166053

Wiens, J. J., Kuczynski, C. A., Townsend, T. M., Reeder, T. W., Mulcahy, D. G. & Sites, J. W. J. 2010. Combining phylogenomics and fossils in higher-level squamate reptile phylogeny: molecular data change the placement of fossil taxa. *Systematic Biology*, **59**(6), 674–688. doi:10.1093/sysbio/syq048

Wiens, J. J., Hutter, C. R., Mulcahy, D. G., Noonan, B. P., Townsend, T. M., Sites, J. W. J. & Reeder, T. W. 2012. Resolving the phylogeny of lizards and snakes (Squamata) with extensive sampling of genes and species. *Biology Letters*, **8**, 1043–1046. doi:10.1098/rsbl.2012.0703

Wilson, J. A., Mohabey, D. M., Peters, S. E. & Head, J. J. 2010. Predation upon hatchling dinosaurs by a new snake from the Late Cretaceous of India. *PLoS Biology*, **8**(3), e1000322. doi:10.1371/journal.pbio.1000322

Zaher, H. 1998. The phylogenetic position of *Pachyrhachis* within snakes (Squamata, Lepidosauria). *Journal of Vertebrate Paleontology*, **18**(1), 1–3. doi:10.1080/02724634.1998.10011029

Zaher, H. & Rieppel, O. 1999a. The phylogenetic relationships of *Pachyrhachis problematicus*, and the evolution of limblessness in snakes (Lepidosauria, Squamata). *Comptes Rendus de l'Académie des Sciences - Series IIA - Sciences de la Terre et des planètes/Earth and Planetary Science*, **329**, 831–837.

Zaher, H. & Rieppel, O. 2002. On the phylogenetic relationships of the Cretaceous snakes with legs, with special reference to *Pachyrhachis problematicus* (Squamata, Serpentes). *Journal of Vertebrate Paleontology*, **22**(1), 104–109.

Zaher, H. & Scanferla, C. A. 2012. The skull of the Upper Cretaceous snake *Dinilysia patagonica* Smith-Woodward, 1901, and its phylogenetic position revisited. *Zoological Journal of the Linnean Society*, **164**, 194–238. doi:10.1111/j.1096-3642.2011.00755.x

Zheng, Y. & Wiens, J. J. 2016. Combining phylogenomic and supermatrix approaches, and a time-calibrated phylogeny for squamate reptiles (lizards and snakes) based on 52 genes and 4162 species. *Molecular Phylogenetics and Evolution*, **94**, 537–547. doi:10.1016/j.ympev.2015.10.009

CHAPTER SIX: GENERAL CONCLUSIONS

At the end of Chapter One, I presented three guiding questions for this thesis, each addressing one of the major paradigms surrounding scolecophidians: First, are scolecophidians indeed fundamentally different from alethinophidians? Second, is microstomy truly homogenous across squamates and plesiomorphic for snakes? And finally, what is the phylogenetic and macroevolutionary status of scolecophidians? Synthesizing the results, discussions, and conclusions presented individually in each chapter, I address these questions below.

6.1. Scolecophidia *versus* Alethinophidia

The results of this research strongly reject the traditional notion of a fundamental dichotomy between scolecophidians and alethinophidians. As argued in Chapter Two, there is a clear morphological continuum between scolecophidians and various fossorial alethinophidians, with miniaturization—and, concomitantly, extensive paedomorphosis—providing a reasonable mechanism linking these groups. As argued in that chapter, this continuum is especially evident for seemingly 'definitive' scolecophidian features such as the structure of the naso-frontal joint, jaws, and suspensorium, all of which exhibit comparable conditions among Alethinophidia.

The results of the network analyses in Chapter Four further support this dissenting perspective. Both miniaturization and fossoriality were found to be associated with specific regions of morphospace, a phenomenon particularly evident when they co-occur. These results demonstrate the macroevolutionary constraint imparted by these phenomena, thus supporting the proposal in Chapter Two of a heterochrony- and habitat-driven spectrum defining the evolution of scolecophidians relative to other snakes.

Finally, although phylogenetic analysis of the revised dataset in Chapter Five recovered Scolecophidia and Alethinophidia as separate clades, the synapomorphies and symplesiomorphies of Scolecophidia as optimized on this topology provide reason for skepticism. A number of the recovered synapomorphies of Scolecophidia are associated with paedomorphosis (e.g., anterior orientation of the quadrate, simple configuration of the palatine-pterygoid articulation), and a number of the symplesiomorphies of Scolecophidia relative to Alethinophidia could just as reasonably be interpreted as paedomorphic reversals (e.g., absence of the laterosphenoid and medial frontal pillars). Thus, although these phylogenies superficially support the traditional split between Scolecophidia and Alethinophidia, the underlying characters

are in fact also largely consistent with a hypothesis of scolecophidians as extremely morphologically 'regressed' alethinophidians, as argued in Chapter Two.

Therefore, from a morphological perspective, the traditional notion of scolecophidians as fundamentally 'basal' to alethinophidians is simply not tenable. From a phylogenetic perspective, recent phylogenies (Caldwell 2000; Palci & Caldwell 2010; Garberoglio *et al.* 2019a) have indeed recovered Scolecophidia as nested within Alethinophidia; however, the position of scolecophidians among Serpentes is heavily dependent upon the inclusion of fossil taxa, as demonstrated in Chapter Five. Thus, future examinations of scolecophidian phylogeny should not only emphasize rigorous character construction and scoring (as implemented by the dataset revisions in Chapter Five), but must also include extinct taxa in order to reliably reconstruct the position of scolecophidians.

6.2. Microstomy *versus* macrostomy

Altogether, this thesis strongly supports a much more complex scenario of jaw evolution in squamates than the traditional perspective of plesiomorphic 'microstomy' *versus* derived 'macrostomy' would entail. As demonstrated in Chapters Three and Four, each major 'microstomatan' squamate group exhibits a morphofunctionally and evolutionarily distinct morphotype of 'microstomy': 'minimal-kinesis microstomy' (non-snake lizards), 'snout-shifting' (anilioids), 'axle-brace maxillary raking' (anomalepidids), 'mandibular raking' (leptotyphlopids), and 'single-axle maxillary raking' (typhlopoids). These morphotypes are evident both qualitatively (based on assessments of primary homology within a novel homological framework; Chapter Three) and quantitatively (based on different patterns of network connectivity; Chapter Four), thus strongly rejecting the traditional notion of 'microstomy' as morphologically uniform across squamates.

In turn, the remarkable diversity of 'microstomatan' jaw mechanisms contradicts the traditional view that 'microstomy' is inherently plesiomorphic for snakes, simply being retained from non-snake lizards into anilioids and scolecophidians. Ultimately, this traditional perspective is based on simplistic assessments of homology, as made evident via the concept of 'morphotype homology' developed in Chapter Three. As demonstrated by various ancestral state reconstructions, different perspectives on jaw homology in turn produce very different

reconstructions of the ancestral snake condition, thus emphasizing the importance of rigorous homology assessment when formulating higher-level evolutionary hypotheses.

6.3. Scolecophidian phylogeny and the origin of snakes

Overall, this research supports a hypothesis of scolecophidians, not as a plesiomorphic and homogenous lineage, but rather as a highly modified, highly diverse, and ultimately entirely non-ancestral assemblage. Although the debate surrounding the phylogenetic status of scolecophidians ultimately remains unresolved, this thesis represents a major step toward answering this larger question.

From a methodological perspective, the revised dataset presented in Chapter Five addresses many of the inconsistencies in character construction and scoring that have affected previous analyses of snake phylogeny. Therefore, although this dataset does not yet include fossils—and thus in its current form is not extensive enough to confidently reconstruct the phylogeny of snakes—it provides an essential basis for future analyses. The dramatic impact of fossil snakes on the position of scolecophidians is a particularly notable finding, emphasizing the necessity of sampling these taxa and in turn casting doubt on phylogenies that only incorporate extant squamates. Finally, an examination of the character states underlying the traditional topology of Scolecophidia *versus* Alethinophidia revealed very few of them to be reliable synapomorphies, thus undermining the proposed monophyly of these groups.

More broadly, although a formal phylogenetic resolution to this debate remains elusive, this thesis does provide extensive insight into the broader evolutionary status of scolecophidians. As demonstrated throughout this thesis, the traditional perspective of scolecophidians as fundamentally ‘primitive’ is ultimately inaccurate. This paradigm is contradicted primarily by the vastly different jaw mechanisms of each scolecophidian lineage (Chapters Three and Four), which reflect a distinct lack of synapomorphy both among this assemblage and among ‘microstomatans’ more broadly. This lack of synapomorphy in turn indicates that ‘microstomy’ should not simply be assumed to be plesiomorphic for snakes, nor should it even be viewed as homologous among scolecophidians. Furthermore, the features that supposedly unite scolecophidians are either highly paedomorphic or associated with fossoriality, and are thus susceptible to distinct homoplasy (Chapters Two–Five). The systematic bias associated with these phenomena (Hanken & Wake 1993; Lee 1998; Rieppel & Zaher 2000; Wiens *et al.* 2005;

Struck 2007) in turn suggests that the apparently close phylogenetic relationships among the scolecophidian lineages may in fact be artificial, and artificially basal (Gould 1977; Hanken & Wake 1993) at that.

Altogether, these observations are deeply inconsistent with the notion that scolecophidians represent an ancestral snake condition; building on recent re-examinations of scolecophidian evolution (Caldwell 2019; Chretien *et al.* 2019), these findings instead suggest a scenario of scolecophidians as a highly convergent assemblage, marked by extensive paedomorphic 'regression' from a more typical snake-like bauplan and reflecting the independent evolution of fossoriality, miniaturization, and 'microstomy' throughout these lineages.

Of course, although this hypothesis is logically consistent with the major results of this research, such a scenario remains to be supported via formal phylogenetic analysis. Indeed, it remains possible that Scolecophidia truly does form an early diverging clade (or perhaps paraphyletic assemblage) of fossorial, miniaturized, and paedomorphic snakes. However, even this outcome would not necessarily be at odds with many of the overarching hypotheses presented herein; for example, even if scolecophidians do form an early-diverging group, it remains quite plausible for 'microstomy' to have evolved separately in each lineage, and for each lineage to have independently become miniaturized (as per Chretien *et al.* 2019; Fachini *et al.* 2020, respectively). In other words, even if scolecophidians do not end up being formally polyphyletic, this does not mean that miniaturization, fossoriality, and 'microstomy' are inherently synapomorphic for this group; similarly, even if scolecophidians truly do diverge quite early from other snakes, this does not make them inherently 'primitive' or ancestral.

Essentially, regardless of their specific phylogenetic position, each scolecophidian lineage is highly specialized, relative both to each other and to snakes more broadly; this assemblage should therefore not be invoked in hypotheses of the origin of snakes, and especially not as evidence of an ancestrally burrowing ecology, miniaturized anatomy, or microstomatan feeding mechanism among Ophidia.

6.4. Suggestions for future research

6.4.1. Phylogenetics

Several promising lines of inquiry are available to expand upon this thesis. Primary among these is a continued investigation of snake—and especially scolecophidian—phylogeny. As emphasized in Chapter Five, the inclusion of fossils is an essential step in building on the current phylogenetic contribution; similarly, the addition of molecular data is also important.

On an operational note, the differing impact of fossils on maximum parsimony *versus* Bayesian analyses (Chapter Five) not only indicates the importance of incorporating various analytical approaches (see e.g., Simões *et al.* 2018; Garberoglio *et al.* 2019a), but also presents an interesting question: Why do parsimony-based and probabilistic analyses respond so differently to the inclusion *versus* exclusion of fossils? More broadly, which analytical approach is best suited for addressing the homoplasy prevalent throughout squamates? The field of phylogenetic methodology is an undoubtedly vibrant one (e.g., Wright & Hillis 2014; O'Reilly *et al.* 2016; Goloboff *et al.* 2018; O'Reilly *et al.* 2018; Schrago *et al.* 2018; King & Rücklin 2020; Simões *et al.* 2020; Vernygora *et al.* 2020), and the results obtained herein present yet another avenue for investigating the performance of competing phylogenetic algorithms.

From a conceptual perspective, as highlighted throughout this thesis, the effects of paedomorphosis on scolecophidian anatomy are extensive and, troublingly, potentially problematic in biasing phylogenetic analyses. Recently, methods have been proposed to quantify phylogenetic trends related to heterochrony (see Lamsdell 2020), and to mitigate the systematic bias induced by paedomorphosis (see Wiens *et al.* 2005; Struck 2007; Fröbisch & Schoch 2009), as well as that induced by fossoriality (see Lee 1998; Rieppel & Zaher 2000); however, the accuracy and efficacy of these latter methods have been debated (see discussions in preceding references). Furthermore, some authors have also debated the existence of this heterochronic bias. Most notably, in their study of dissorophoid amphibians, Fröbisch & Schoch (2009) found branchiosaurids and amphibamids to still be recovered as closely related, even after accounting for miniaturization. *Contra* Wiens *et al.* (2005) and Struck (2007), who had both identified biasing effects of paedomorphosis in amphibians, Fröbisch & Schoch (2009) interpreted this result as indicating that these dissorophoids are genuinely closely related, and that small body size is synapomorphic—not homoplastic—within this assemblage.

In order to quantitatively investigate the impact of paedomorphosis on scolecophidian phylogeny, future studies should therefore employ the various methods proposed by previous authors (Wiens *et al.* 2005; Struck 2007; Fröbisch & Schoch 2009; Lamsdell 2020) for assessing

morphological data. Another interesting avenue would be to investigate the impact of miniaturization on genetic data, as has recently been recognized in highly miniaturized fish (Malmstrøm *et al.* 2018).

6.4.2. Ontogeny

The identification of heterochrony is a complex process, requiring knowledge of both the phylogenetic and ontogenetic context of the organisms in question. As noted above, a robust phylogenetic framework is still lacking for snakes, although this thesis and other recent advances (e.g., the advent of phylogenomics in squamate research; Burbrink *et al.* 2020) contribute toward this goal. However, even with a more reliable phylogeny, the other prerequisite—that of ontogeny—remains quite poorly known for scolecophidians, and indeed snakes more broadly. In particular, beyond a few limited studies of scolecophidian reproductive anatomy (e.g., Webb *et al.* 2000; Khouri *et al.* 2020; Amaral *et al.* 2021), one study to my knowledge of scolecophidian embryology (Sandoval *et al.* 2020), and a few morphometric studies incorporating embryonic or juvenile scolecophidians (Palci *et al.* 2016; Da Silva *et al.* 2018), the literature related to scolecophidian ontogeny is quite sparse.

As such, identifications of heterochrony in this group rely entirely on comparison of adult scolecophidian morphologies to the relatively few squamates whose ontogenies are well-known (see e.g., Polachowski & Werneburg 2013; Khannoon & Evans 2015; Werneburg *et al.* 2015; Ollonen *et al.* 2018). This can be an effective method—for example, as exercised throughout this thesis in identifying paedomorphosis in scolecophidians—but a greater knowledge of developmental trajectories in this group would be quite useful in facilitating, and essentially 'ground-truthing', such hypotheses regarding the evolutionary modification of these pathways.

6.4.3. Fossoriality

The biomechanical performance of the scolecophidian skull in relation to burrowing is also an intriguing area of research. Several scolecophidians bear paired skull roof elements (see e.g., Brock 1932; Mookerjee & Das 1932; Mahendra 1936; McDowell & Bogert 1954; Evans 1955; Cundall & Irish 2008; Palci *et al.* 2016), with some taxa (e.g., *Myriopholis*, among other members of the *Leptotyphlops longicaudus* species group; C.S., pers. obs. and Broadley & Wallach 2007) even exhibiting a broad dorsal fontanelle reflecting an almost total lack of skull roof ossification (see Broadley & Wallach 2007:plate 4; Cundall & Irish 2008:fig. 2.12B,C). As

noted by previous authors (e.g., Mahendra 1936; Palci *et al.* 2016), this reduced ossification is quite counterintuitive given the broadly-accepted fossorial nature of these snakes. Indeed, this phenomenon raises the distinct possibility that scolecophidians may not in fact be as fossorial as traditionally thought (see also Cundall & Irish 2008). This is certainly an intriguing implication, but the biomechanics of scolecophidian 'burrowing' have yet to be examined in detail (Cundall & Irish 2008; Palci *et al.* 2016; though see a recent preliminary analysis by Herrel *et al.* 2021), and even this strange skull roof morphology has largely been mentioned only in passing.

The paired condition of the skull roof elements is also relevant from a phylogenetic perspective, as this reflects another supposedly 'primitive' feature (see e.g., Mahendra 1936; List 1966) that is in fact almost certainly paedomorphically derived, a possibility indicated by Méhely (1907; as cited by Mahendra 1936 and List 1966) and Palci *et al.* (2016) (see also recognitions of size-related and ontogenetic fusion of the parietals by Evans 1955; List 1966; Rieppel 1996). This interpretation of paedomorphosis is especially applicable in the case of the aforementioned fontanelle. An investigation of the structure, function, and evolution of the skull roof in scolecophidians would therefore be quite interesting.

Finally, scolecophidian 'fossoriality' is further intriguing in that this ecology is explicitly tied to these snakes' specialized predation upon ants and termites (Webb *et al.* 2000; Herrel *et al.* 2021). This ecological interaction has further been hypothesized to have influenced several aspects of scolecophidian evolution, including speciation (e.g., suggested links between macroevolutionary patterns of diversification in ants and scolecophidians: Herrel *et al.* 2021) and morphological adaptations (e.g., the presence of extensive scaly 'armour' in typhlopids as defense against aggressive ants: Webb & Shine 1993; Webb *et al.* 2000; or the evolution of the extremely downcurved snout in xenotyphlopids as a potential shield against ant soldiers during feeding: Chretien *et al.* 2019). However, detailed observations of ecological interactions between scolecophidians and their prey are quite limited, as are detailed observations of scolecophidian behaviour in general (Webb & Shine 1992; Webb *et al.* 2000). In order to better understand the nature of fossoriality in scolecophidians, as well as related phenomena such as miniaturization, it is imperative to understand the potential ecological drivers behind these phenomena; as such, improved field observations will ultimately be crucial in informing broader hypotheses of scolecophidian evolution.

6.5. Final thoughts

Ultimately, the debate around scolecophidian evolution has lasted nearly a century since Mahendra (1938) first placed them as basally-diverging among snakes, and the broader debate around the origin of snakes—initiated by Cope (1869)—even longer. These controversies are sure to persist for many years to come, bolstered by new discoveries, new interpretations, and new hypotheses. Many of these new hypotheses—such as the overarching view of scolecophidian evolution presented in this thesis—will no doubt contradict the current 'accepted wisdom' of snake evolution, provoking further disagreement and scholarly debate. Ultimately the story of snake evolution will likely never be fully revealed or understood; in light of the inevitably incomplete fossil record and the unfathomable complexity of evolution as a whole, perhaps all we can strive for as evolutionary biologists is to produce, defend, and critique hypotheses in as logical a manner as possible, prioritizing data over assumptions and rational skepticism over adherence to paradigms. In light of this epistemic reality, I cannot—and therefore will not—assert that the perspective on snake evolution presented throughout this thesis is 'correct' in an absolute sense; however, what I can assert is that, to the best of my ability, this perspective is logically consistent, explicitly reasoned, and empirically derived. As such, the current collection of research will hopefully constitute a useful methodological, conceptual, and philosophical contribution to the study of snake evolution.

References: Chapter Six

Amaral, J. M. d. S., Araújo, P., Barbosa, V. d. N. & França, F. G. R. 2021. First record of egg development time and hatchling morphology of *Amerotyphlops paucisquamus* (Dixon and Hendricks 1979) (Scolecophidia: Typhlopidae), northeastern Brazil. *Revista de Ciências Ambientais*, **14**(3), 79–83. doi:10.18316/rca.v14i.6598

Broadley, D. G. & Wallach, V. 2007. A revision of the genus *Leptotyphlops* in northeastern Africa and southwestern Arabia (Serpentes: Leptotyphlopidae). *Zootaxa*, **1408**, 1–78.

Brock, G. T. 1932. The skull of *Leptotyphlops* (*Glauconia nigricans*). *Anatomischer Anzieger*, **73**, 199–204.

Burbrink, F. T., Grazziotin, F. G., Pyron, R. A., Cundall, D., Donnellan, S., Irish, F., Keogh, J. S., Kraus, F., Murphy, R. W., Noonan, B., Raxworthy, C. J., Ruane, S., Lemmon, A. R., Lemmon, E. M. & Zaher, H. 2020. Interrogating genomic-scale data for Squamata (lizards, snakes, and amphisbaenians) shows no support for key traditional morphological relationships. *Systematic Biology*, **69**(3), 502–520. doi:10.1093/sysbio/syz062

Caldwell, M. W. 2000. On the phylogenetic relationships of *Pachyrhachis* within snakes: a response to Zaher (1998). *Journal of Vertebrate Paleontology*, **20**(1), 187–190.

Caldwell, M. W. 2019. *The Origin of Snakes: Morphology and the Fossil Record*. Taylor & Francis, Boca Raton.

Chretien, J., Wang-Claypool, C. Y., Glaw, F. & Scherz, M. D. 2019. The bizarre skull of *Xenotyphlops* sheds light on synapomorphies of Typhlopoidea. *Journal of Anatomy*, **234**, 637–655. doi:10.1111/joa.12952

Cope, E. D. 1869. On the reptilian orders, Pythonomorpha and Streptosauria. *Boston Society of Natural History Proceedings*, **12**, 250–266.

Cundall, D. & Irish, F. 2008. The snake skull. Pp. 349–692 in C. Gans, A.S. Gaunt and K. Adler (eds) *Biology of the Reptilia: Morphology H, The Skull of Lepidosauria*. Society for the Study of Amphibian and Reptiles, Ithaca, New York.

Da Silva, F. O., Fabre, A.-C., Savriama, Y., Ollonen, J., Mahlow, K., Herrel, A., Müller, J. & Di-Poï, N. 2018. The ecological origins of snakes as revealed by skull evolution. *Nature Communications*, **9**, 376. doi:10.1038/s41467-017-02788-3

Evans, H. E. 1955. The osteology of a worm snake, *Typhlops jamaicensis* (Shaw). *The Anatomical Record*, **122**, 381–396.

Fachini, T. S., Onary, S., Palci, A., Lee, M. S. Y., Bronzati, M. & Hsiou, A. S. 2020. Cretaceous blind snake from Brazil fills major gap in snake evolution. *iScience*, **23**, 101834. doi:10.1016/j.isci. 2020.101834

Fröbisch, N. B. & Schoch, R. R. 2009. Testing the impact of miniaturization on phylogeny: Paleozoic dissorophoid amphibians. *Systematic Biology*, **58**(3), 312–327. doi:10.1093/sysbio/syp029

Garberoglio, F. F., Apesteguía, S., Simões, T. R., Palci, A., Gómez, R. O., Nydam, R. L., Larsson, H. C. E., Lee, M. S. Y. & Caldwell, M. W. 2019a. New skulls and skeletons of the Cretaceous legged snake *Najash*, and the evolution of the modern snake body plan. *Science Advances*, **5**(11), eaax5833. doi:10.1126/sciadv.aax5833

Goloboff, P. A., Torres, A. & Arias, J. S. 2018. Weighted parsimony outperforms other methods of phylogenetic inference under models appropriate for morphology. *Cladistics*, **34**, 407–437. doi:10.1111/cla.12205

Gould, S. J. 1977. *Ontogeny and Phylogeny*. Harvard University Press, Cambridge.

Hanken, J. & Wake, D. B. 1993. Miniaturization of body size: organismal consequences and evolutionary significance. *Annual Review of Ecology and Systematics*, **24**, 501–519.

Herrel, A., Lowie, A., Miralles, A., Gaucher, P., Kley, N. J., Measey, J. & Tolley, K. A. 2021. Burrowing in blindsnakes: a preliminary analysis of burrowing forces and consequences for the evolution ofmorphology. *The Anatomical Record*, **2021**, 1–11. doi:10.1002/ar.24686

Khannoon, E. R. & Evans, S. E. 2015. The development of the skull of the Egyptian cobra *Naja h. haje* (Squamata: Serpentes: Elapidae). *PLoS ONE*, **10**, e0122185. doi:10.1371/journal.pone.0122185

Khouri, R. S., Almeida-Santos, S. M. & Fernandes, D. S. 2020. Anatomy of the reproductive system of a population of *Amerotyphlops brongersmianus* from southeastern Brazil (Serpentes: Scolecophidia). *The Anatomical Record*, **303**, 2485–2496. doi:10.1002/ar.24382

King, B. & Rücklin, M. 2020. A Bayesian approach to dynamic homology of morphological characters and the ancestral phenotype of jawed vertebrates. *eLife*, **9**, e62374. doi:10.7554/eLife.62374

Lamsdell, J. C. 2020. A new method for quantifying heterochrony in evolutionary lineages. *Paleobiology*, **00**, 1–22. doi:10.1017/pab.2020.17

Lee, M. S. Y. 1998. Convergent evolution and character correlation in burrowing reptiles: towards a resolution of squamate relationships. *Biological Journal of the Linnean Society*, **65**, 369–453.

List, J. C. 1966. Comparative osteology of the snake families Typhlopidae and Leptotyphlopidae. *Illinois Biological Monographs*, **36**, 1–112.

Mahendra, B. C. 1936. Contributions to the osteology of the Ophidia. I. The endoskeleton of the so-called 'blind-snake', *Typhlops braminus* Daud. *Proceedings of the Indian Academy of Sciences*, **3**, 128–142.

Mahendra, B. C. 1938. Some remarks on the phylogeny of the Ophidia. *Anatomischer Anzieger*, **86**, 347–356.

Malmstrøm, M., Britz, R., Matschiner, M., Tørresen, O. K., Kurnia Hadiaty, R., Yaakob, N., Hui Tan, H., Sigurd Jakobsen, K., Salzburger, W. & Rüber, L. 2018. The most developmentally truncated fishes show extensive *Hox* gene loss and miniaturized genomes. *Genome Biology and Evolution*, **10**(4), 1088–1103. doi:10.1093/gbe/evy058

McDowell, S. B. & Bogert, C. M. 1954. The systematic position of *Lanthanotus* and the affinities of the anguimorphan lizards. *Bulletin of the American Museum of Natural History, New York*, **105**, 1–142.

Méhely, L. V. 1907. Archaeo- und Neolacerten. *Annales Musei Historico-Naturalis Hungarici*, **5**, 469–493.

Mookerjee, H. K. & Das, G. M. 1932. Occurrence of a paired parietal bone in a snake. *Nature*, **130**(3286), 629.

O'Reilly, J. E., Puttick, M. N., Pisani, D. & Donoghue, P. C. J. 2018. Probabilistic methods surpass parsimony when assessing clade support in phylogenetic analyses of discrete morphological data. *Palaeontology*, **61**(1), 105–118. doi:10.1111/pala.12330

O'Reilly, J. E., Puttick, M. N., Parry, L., Tanner, A. R., Tarver, J. E., Fleming, J., Pisani, D. & Donoghue, P. C. J. 2016. Bayesian methods outperform parsimony but at the

expense of precision in the estimation of phylogeny from discrete morphological data. *Biology Letters*, **12**, 20160081. doi:10.1098/rsbl.2016.0081

Ollonen, J., Silva, F. O. D., Mahlow, K. & Di-Poï, N. 2018. Skull development, ossification pattern, and adult shape in the emerging lizard model organism *Pogona vitticeps*: a comparative analysis with other squamates. *Frontiers in Physiology*, **9**, 278. doi:10.3389/fphys.2018.00278

Palci, A. & Caldwell, M. W. 2010. Redescription of *Acteosaurus tommasinii* von Meyer, 1860, and a discussion of evolutionary trends within the clade Ophidiomorpha. *Journal of Vertebrate Paleontology*, **30**(1), 94–108. doi:10.1080/02724630903409139

Palci, A., Lee, M. S. Y. & Hutchinson, M. N. 2016. Patterns of postnatal ontogeny of the skull and lower jaw of snakes as revealed by micro-CT scan data and three-dimensional geometric morphometrics. *Journal of Anatomy*, **229**(6), 723–754. doi:10.1111/joa.12509

Polachowski, K. M. & Werneburg, I. 2013. Late embryos and bony skull development in *Bothropoides jararaca* (Serpentes, Viperidae). *Zoology*, **116**, 36–63. doi:10.1016/j.zool.2012.07.003

Rieppel, O. 1996. Miniaturization in tetrapods: consequences for skull morphology. Pp. 47–61 in P.J. Miller (ed) *Miniature Vertebrates: The Implications of Small Body Size, Vol. 69. Symposia of the Zoological Society of London*. Claredon Press, Oxford.

Rieppel, O. & Zaher, H. 2000. The intramandibular joint in squamates, and the phylogenetic relationships of the fossil snake *Pachyrhachis problematicus* Haas. *Fieldiana Geology*, **43**, 1–69.

Sandoval, M. T., García, J. A. R. & Álvarez, B. B. 2020. Intrauterine and post-ovipositional embryonic development of *Amerotyphlops brongersmianus* (Vanzolini, 1976) (Serpentes: Typhlopidae) from northeastern Argentina. *Journal of Morphology*, **281**, 523–535. doi:10.1002/jmor.21119

Schrago, C. G., Aguiar, B. O. & Mello, B. 2018. Comparative evaluation of maximum parsimony and Bayesian phylogenetic reconstruction using empirical morphological data. *Journal of Evolutionary Biology*, **31**, 1477–1484. doi:10.1111/jeb.13344

Simões, T. R., Caldwell, M. W., Tałanda, M., Bernardi, M., Palci, A., Vernygora, O., Bernardini, F., Mancini, L. & Nydam, R. L. 2018. The origin of squamates revealed by

a Middle Triassic lizard from the Italian Alps. *Nature*, **557**, 706–709. doi:10.1038/s41586-018-0093-3

Simões, T. R., Caldwell, M. W. & Pierce, S. E. 2020. Sphenodontian phylogeny and the impact of model choice in Bayesian morphological clock estimates of divergence times and evolutionary rates. *BMC Biology*, **18**, 191. doi:10.1186/s12915-020-00901-5

Struck, T. H. 2007. Data congruence, paedomorphosis and salamanders. *Frontiers in Zoology*, **4**, 22. doi:10.1186/1742-9994-4-22

Vernygora, O. V., Simões, T. R. & Campbell, E. O. 2020. Evaluating the performance of probabilistic algorithms for phylogenetic analysis of big morphological datasets: a simulation study. *Systematic Biology*, **69**(6), 1088–1105. doi:10.1093/sysbio/syaa020

Webb, J. K. & Shine, R. 1992. To find an ant: trail-following in Australian blindsnakes (Typhlopidae). *Animal Behaviour*, **43**, 941–948.

Webb, J. K. & Shine, R. 1993. Prey-size selection, gape limitation and predator vulnerability in Australian blindsnakes (Typhlopidae). *Animal Behaviour*, **45**, 1117–1126.

Webb, J. K., Shine, R., Branch, W. R. & Harlow, P. S. 2000. Life-history strategies in basal snakes: reproduction and dietary habits of the African thread snake *Leptotyphlops scutifrons* (Serpentes: Leptotyphlopidae). *Journal of Zoology*, **250**, 321–327.

Werneburg, I., Polachowski, K. M. & Hutchinson, M. N. 2015. Bony skull development in the Argus monitor (Squamata, Varanidae, *Varanus panoptes*) with comments on developmental timing and adult anatomy. *Zoology*, **118**, 255–280. doi:10.1016/j.zool.2015.02.004

Wiens, J. J., Bonett, R. M. & Chippindale, P. T. 2005. Ontogeny discombobulates phylogeny: paedomorphosis and higher-level salamander relationships. *Systematic Biology*, **54**(1), 91–110. doi:10.1080/10635150590906037

Wright, A. M. & Hillis, D. M. 2014. Bayesian analysis using a simple likelihood model outperforms parsimony for estimation of phylogeny from discrete morphological data. *PLoS ONE*, **9**(10), e109210. doi:10.1371/journal.pone.0109210

COMPREHENSIVE LIST OF REFERENCES

Adalsteinsson, S. A., Branch, W. R., Trape, S., Vitt, L. J. & Hedges, S. B. 2009. Molecular phylogeny, classification, and biogeography of snakes of the Family Leptotyphlopidae (Reptilia, Squamata). *Zootaxa*, **2244**, 1–50.

Adams, D. C., Rohlf, F. J. & Slice, D. E. 2004. Geometric morphometrics: ten years of progress following the 'revolution'. *Italian Journal of Zoology*, **71**(1), 5–16. doi:10.1080/11250000409356545

Al-Mohammadi, A. G. A., Khannoon, E. R. & Evans, S. E. 2020. The development of the osteocranium in the snake *Psammophis sibilans* (Serpentes: Lamprophiidae). *Journal of Anatomy*, **236**, 117–131. doi:10.1111/joa.13081

Alberch, P., Gould, S. J., Oster, G. F. & Wake, D. B. 1979. Size and shape in ontogeny and phylogeny. *Paleobiology*, **5**(3), 296–317.

Amaral, J. M. d. S., Araújo, P., Barbosa, V. d. N. & França, F. G. R. 2021. First record of egg development time and hatchling morphology of *Amerotyphlops paucisquamus* (Dixon and Hendricks 1979) (Scolecophidia: Typhlopidae), northeastern Brazil. *Revista de Ciências Ambientais*, **14**(3), 79–83. doi:10.18316/rca.v14i.6598

Andjelković, M., Tomović, L. & Ivanović, A. 2017. Morphological integration of the kinetic skull in *Natrix* snakes. *Journal of Zoology*, **303**, 188–198. doi:10.1111/jzo.12477

Apesteguía, S. & Zaher, H. 2006. A Cretaceous terrestrial snake with robust hindlimbs and a sacrum. *Nature*, **440**, 1037–1040. doi:10.1038/nature04413

Asplen, M. K., Whitfield, J. B., de Boer, J. G. & Heimpel, G. E. 2009. Ancestral state reconstruction analysis of hymenopteran sex determination mechanisms. *Journal of Evolutionary Biology*, **22**, 1762–1769. doi:10.1111/j.1420-9101.2009.01774.x

Bell, C. J., Mead, J. I. & Swift, S. L. 2009. Cranial osteology of *Moloch horridus* (Reptilia: Squamata: Agamidae). *Records of the Western Australian Museum*, **25**, 201–237. doi:10.18195/issn.0312-3162.25(2).2009.201-237

Bellairs, A. D. & Underwood, G. 1951. The origin of snakes. *Biological Reviews*, **26**, 193–237.

Bellairs, A. D. & Kamal, A. M. 1981. The chondrocranium and the development of the skull in recent reptiles. Pp. 1–263 in C. Gans and T.S. Parsons (eds) *Biology of the Reptilia: Morphology F*. Academic Press, London, New York, Toronto, Sydney, and San Francisco.

Bennett, D. 2000. Observations on Bosc's monitor lizard (*Varanus exanthematicus*) in the wild. *Bulletin of the Chicago Herpetological Society*, **35**(8), 177–180.

Berkovitz, B. & Shellis, P. 2017. *The Teeth of Non-Mammalian Vertebrates*. Academic Press, London.

Betancur-R, R., Ortí, G. & Pyron, R. A. 2015. Fossil-based comparative analyses reveal ancient marine ancestry erased by extinction in ray-finned fishes. *Ecology Letters*, **18**, 441–450. doi:doi: 10.1111/ele.12423

Boback, S. M., Dichter, E. K. & Mistry, H. L. 2012. A developmental staging series for the African house snake, *Boaedon* (*Lamprophis*) *fuliginosus*. *Zoology*, **115**, 38–46. doi:10.1016/j.zool.2011.09.001

Boughner, J. C., Buchtová, M., Fu, K., Diewert, V., Hallgrímsson, B. & Richman, J. M. 2007. Embryonic development of *Python sebae* – I: staging criteria and macroscopic skeletal morphogenesis of the head and limbs. *Zoology*, **110**, 212–230. doi:10.1016/j.zool.2007.01.005

Broadley, D. G. & Wallach, V. 2007. A revision of the genus *Leptotyphlops* in northeastern Africa and southwestern Arabia (Serpentes: Leptotyphlopidae). *Zootaxa*, **1408**, 1–78.

Brock, G. T. 1932. The skull of *Leptotyphlops* (*Glauconia nigricans*). *Anatomischer Anzieger*, **73**, 199–204.

Brock, G. T. 1941. The skull of *Acontias meleagris*, with a study of the affinities between lizards and snakes. *Zoological Journal of the Linnean Society*, **41**, 71–88.

Brower, A. V. Z. & Schawaroch, V. 1996. Three steps of homology assessment. *Cladistics*, **12**, 265–272.

Burbrink, F. T., Grazziotin, F. G., Pyron, R. A., Cundall, D., Donnellan, S., Irish, F., Keogh, J. S., Kraus, F., Murphy, R. W., Noonan, B., Raxworthy, C. J., Ruane, S., Lemmon, A. R., Lemmon, E. M. & Zaher, H. 2020. Interrogating genomic-scale data for Squamata (lizards, snakes, and amphisbaenians) shows no support for key traditional morphological relationships. *Systematic Biology*, **69**(3), 502–520. doi:10.1093/sysbio/syz062

Caldwell, M. W. & Lee, M. S. Y. 1997. A snake with legs from the marine Cretaceous of the Middle East. *Nature*, **386**, 705–709.

Caldwell, M. W. 1999. Squamate phylogeny and the relationships of snakes and mosasauroids. *Zoological Journal of the Linnean Society*, **125**, 115–147. doi:10.1111/j.1096-3642.1999.tb00587.x

Caldwell, M. W. 2000. On the phylogenetic relationships of *Pachyrhachis* within snakes: a response to Zaher (1998). *Journal of Vertebrate Paleontology*, **20**(1), 187–190.

Caldwell, M. W. 2007a. The role, impact, and importance of fossils: snake phylogeny, origins, and evolution (1869–2006). Pp. 253–302 in J. Anderson and H.-D. Sues (eds) *Major Transitions in Vertebrate Evolution*. Indiana University Press, Bloomington, Indiana.

Caldwell, M. W. 2007b. Ontogeny, anatomy and attachment of the dentition in mosasaurs (Mosasauridae: Squamata). *Zoological Journal of the Linnean Society*, **149**, 687–700.

Caldwell, M. W., Nydam, R. L., Palci, A. & Apesteguía, S. 2015. The oldest known snakes from the Middle Jurassic-Lower Cretaceous provide insights on snake evolution. *Nature Communications*, **6**, 5996. doi:10.1038/ncomms6996

Caldwell, M. W. 2019. *The Origin of Snakes: Morphology and the Fossil Record*. Taylor & Francis, Boca Raton.

Camp, C. L. 1923. Classification of the lizards. *Bulletin of the American Museum of Natural History, New York*, **48**, 289–481.

Campbell, J. A., Smith, E. N. & Hall, A. S. 2018. Caudals and calyces: the curious case of a consumed Chiapan colubroid. *Journal of Herpetology*, **52**(4), 459–472. doi:10.1670/18-042

Chretien, J., Wang-Claypool, C. Y., Glaw, F. & Scherz, M. D. 2019. The bizarre skull of *Xenotyphlops* sheds light on synapomorphies of Typhlopoidea. *Journal of Anatomy*, **234**, 637–655. doi:10.1111/joa.12952

Clauset, A., Newman, M. E. J. & Moore, C. 2004. Finding community structure in very large networks. *Physical Review E*, **70**, 066111. doi:10.1103/PhysRevE.70.066111

Conrad, J. L. 2008. Phylogeny and systematics of Squamata (Reptilia) based on morphology. *Bulletin of the American Museum of Natural History, New York*, **310**, 1–182. doi:10.1206/310.1

Cope, E. D. 1869. On the reptilian orders, Pythonomorpha and Streptosauria. *Boston Society of Natural History Proceedings*, **12**, 250–266.

Csárdi, G. & Nepusz, T. 2006. The igraph software package for complex network research. *InterJournal Complex Systems*, **1695**, 1–9.

Cundall, D. 1983. Activity of head muscles during feeding by snakes: a comparative study. *American Zoologist*, **23**, 383–396.

Cundall, D. & Rossman, D. A. 1993. Cephalic anatomy of the rare Indonesian snake *Anomochilus weberi*. *Zoological Journal of the Linnean Society*, **109**, 235–273.

Cundall, D., Wallach, V. & Rossman, D. A. 1993. The systematic relationships of the snake genus *Anomochilus*. *Zoological Journal of the Linnean Society*, **109**, 275–299.

Cundall, D. 1995. Feeding behaviour in *Cylindrophis* and its bearing on the evolution of alethinophidian snakes. *Journal of Zoology*, **237**, 353–376.

Cundall, D. & Irish, F. 2008. The snake skull. Pp. 349–692 in C. Gans, A.S. Gaunt and K. Adler (eds) *Biology of the Reptilia: Morphology H, The Skull of Lepidosauria*. Society for the Study of Amphibian and Reptiles, Ithaca, New York.

Da Silva, F. O., Fabre, A.-C., Savriama, Y., Ollonen, J., Mahlow, K., Herrel, A., Müller, J. & Di-Poï, N. 2018. The ecological origins of snakes as revealed by skull evolution. *Nature Communications*, **9**, 376. doi:10.1038/s41467-017-02788-3

Das, I. & Wallach, V. 1998. Scolecophidian arboreality revisited. *Herpetological Review*, **29**(1), 15–16.

de Pinna, M. G. G. 1991. Concepts and tests of homology in the cladistic paradigm. *Cladistics*, **7**, 367–394.

Deufel, A. & Cundall, D. 2003. Feeding in *Atractaspis* (Serpentes: Atractaspididae): a study in conflicting functional constraints. *Zoology*, **106**, 43–61.

Dong, S. & Kumazawa, Y. 2005. Complete mitochondrial DNA sequences of six snakes: phylogenetic relationships and molecular evolution of genomic features. *Journal of Molecular Evolution*, **61**, 12–22. doi:10.1007/s00239-004-0190-9

Ebel, R., Müller, J., Ramm, T., Hipsley, C. & Amson, E. 2020. First evidence of convergent lifestyle signal in reptile skull roof microanatomy. *BMC Biology*, **18**, 185. doi:10.1186/s12915-020-00908-y

Eble, G. J. 2005. Morphological modularity and macroevolution: conceptual and empirical aspects. Pp. 221–238 in W. Callebaut and D. Rasskin-Gutman (eds) *Modularity:*

Understanding the Development and Evolution of Natural Complex Systems. MIT Press, Cambridge, MA.

Estes, R., de Queiroz, K. & Gauthier, J. A. 1988. Phylogenetic relationships within Squamata. Pp. 119–281 in R. Estes and G.K. Pregill (eds) *Phylogenetic Relationships of the Lizard Families*. Stanford University Press, Stanford.

Esteve-Altava, B., Marugán-Lobón, J., Botella, H. & Rasskin-Gutman, D. 2011. Network models in anatomical systems. *Journal of Anthropological Sciences*, **89**, 175–184. doi:10.4436/jass.89016

Esteve-Altava, B., Marugán-Lobón, J., Botella, H., Bastir, M. & Rasskin-Gutman, D. 2013. Grist for Riedl's mill: a network model perspective on the integration and modularity of the human skull. *Journal of Experimental Zoology, Part B: Molecular and Developmental Evolution*, **320B**, 489–500. doi:10.1002/jez.b.22524

Esteve-Altava, B. & Rasskin-Gutman, D. 2014. Theoretical morphology of tetrapod skull networks. *Comptes Rendus Palevol*, **13**, 41–50. doi:10.1016/j.crpv.2013.08.003

Esteve-Altava, B., Diogo, R., Smith, C., Boughner, J. C. & Rasskin-Gutman, D. 2015. Anatomical networks reveal the musculoskeletal modularity of the human head. *Scientific Reports*, **5**, 8298. doi:10.1038/srep08298

Esteve-Altava, B. 2017a. Challenges in identifying and interpreting organizational modules in morphology. *Journal of Morphology*, **278**, 960–974. doi:10.1002/jmor.20690

Esteve-Altava, B. 2017b. In search of morphological modules: a systematic review. *Biological Reviews of the Cambridge Philosophical Society*, **92**, 1332–1347. doi:10.1111/brv.12284

Esteve-Altava, B., Molnar, J. L., Johnston, P., Hutchinson, J. R. & Diogo, R. 2018. Anatomical network analysis of the musculoskeletal system reveals integration loss and parcellation boost during the fins-to-limbs transition. *Evolution*, **72**(3), 601–618. doi:10.1111/evo.13430

Esteve-Altava, B., Pierce, S. E., Molnar, J. L., Johnston, P., Diogo, R. & Hutchinson, J. R. 2019. Evolutionary parallelisms of pectoral and pelvic network-anatomy from fins to limbs. *Science Advances*, **5**, eaau7459. doi:10.1126/sciadv.aau7459

Evans, H. E. 1955. The osteology of a worm snake, *Typhlops jamaicensis* (Shaw). *The Anatomical Record*, **122**, 381–396.

Evans, S. E. 2008. The Skull of Lizards and Tuatara. Pp. 1–347 in C. Gans, A.S. Gaunt and K. Adler (eds) *Biology of the Reptilia, Vol. 20: The Skull of Lepidosauria*. Society for the Study of Amphibians and Reptiles, Ithaca.

Fachini, T. S., Onary, S., Palci, A., Lee, M. S. Y., Bronzati, M. & Hsiou, A. S. 2020. Cretaceous blind snake from Brazil fills major gap in snake evolution. *iScience*, **23**, 101834. doi:10.1016/j.isci. 2020.101834

Figueroa, A. 2016. *Phylogenetic Relationships and Evolution of Snakes*. PhD thesis, University of New Orleans, New Orleans, LA.

Figueroa, A., McKelvy, A. D., Grismer, L. L., Bell, C. D. & Lailvaux, S. P. 2016. A species-level phylogeny of extant snakes with description of a new colubrid subfamily and genus. *PLoS ONE*, **11**(9), e0161070. doi:10.1371/journal.pone.0161070

Finarelli, J. A. & Flynn, J. J. 2006. Ancestral state reconstruction of body size in the Caniformia (Carnivora, Mammalia): the effects of incorporating data from the fossil record. *Systematic Biology*, **55**(2), 301–313. doi:10.1080/10635150500541698

Finarelli, J. A. & Goswami, A. 2013. Potential pitfalls of reconstructing deep time evolutionary history with only extant data, a case study using the Canidae (Mammalia, Carnivora). *Evolution*, **67**(12), 3678–3685. doi:10.1111/evo.12222

Frazzetta, T. H. 1962. A functional consideration of cranial kinesis in lizards. *Journal of Morphology*, **111**(3), 287–319.

Frazzetta, T. H. 1966. Studies of the morphology and function of the skull in the Boidae (Serpentes). Part II. Morphology and function of the jaw apparatus in *Python sebae* and *Python molurus*. *Journal of Morphology*, **118**, 217–296.

Fröbisch, N. B. & Schoch, R. R. 2009. Testing the impact of miniaturization on phylogeny: Paleozoic dissorophoid amphibians. *Systematic Biology*, **58**(3), 312–327. doi:10.1093/sysbio/syp029

Gans, C. & Montero, R. 2008. An atlas of amphisbaenian skull anatomy. Pp. 621–738 in C. Gans, A.S. Gaunt and K. Adler (eds) *Biology of the Reptilia. Volume 21. Morphology I. The Skull and Appendicular Locomotor Apparatus of Lepidosauria*. Society for the Study of Amphibians and Reptiles, Ithaca, New York.

Garberoglio, F. F., Apesteguía, S., Simões, T. R., Palci, A., Gómez, R. O., Nydam, R. L., Larsson, H. C. E., Lee, M. S. Y. & Caldwell, M. W. 2019a. New skulls and skeletons

of the Cretaceous legged snake *Najash*, and the evolution of the modern snake body plan. *Science Advances*, **5**(11), eaax5833. doi:10.1126/sciadv.aax5833

Garberoglio, F. F., Gómez, R. O., Apesteguía, S., Caldwell, M. W., Sánchez, M. L. & Veiga, G. 2019b. A new specimen with skull and vertebrae of *Najash rionegrina* (Lepidosauria: Ophidia) from the early Late Cretaceous of Patagonia. *Journal of Systematic Palaeontology*, **17**(18), 1533–1550. doi:10.1080/14772019.2018.1534288

Garberoglio, F. F., Gómez, R. O., Simões, T. R., Caldwell, M. W. & Apesteguía, S. 2019c. The evolution of the axial skeleton intercentrum system in snakes revealed by new data from the Cretaceous snakes *Dinilysia* and *Najash*. *Scientific Reports*, **9**, 1276. doi:10.1038/s41598-018-36979-9

Gauthier, J., Kluge, A. G. & Rowe, T. 1988a. Amniote phylogeny and the importance of fossils. *Cladistics*, **4**, 105–209.

Gauthier, J. A., Estes, R. & de Queiroz, K. 1988b. A phylogenetic analysis of Lepidosauromorpha. Pp. 15–98 in R. Estes and G.K. Pregill (eds) *Phylogenetic Relationships of the Lizard Families*. Stanford University Press, Stanford.

Gauthier, J. A., Kearney, M., Maisano, J. A., Rieppel, O. & Behlke, A. D. B. 2012. Assembling the squamate tree of life: perspectives from the phenotype and the fossil record. *Bulletin of the Peabody Museum of Natural History*, **53**, 3–308. doi:10.3374/014.053.0101

Gelman, A. & Rubin, D. M. 1992. Inference from iterative simulation using multiple sequences. *Statistical Science*, **7**(4), 457–511.

Goloboff, P. A., Farris, J. S. & Nixon, K. C. 2008. TNT, a free program for phylogenetic analysis. *Cladistics*, **24**, 774–786. doi:10.1111/j.1096-0031.2008.00217.x

Goloboff, P. A. & Catalano, S. A. 2016. TNT version 1.5, including a full implementation of phylogenetic morphometrics. *Cladistics*, **32**, 221–238. doi:10.1111/cla.12160

Goloboff, P. A., Torres, A. & Arias, J. S. 2018. Weighted parsimony outperforms other methods of phylogenetic inference under models appropriate for morphology. *Cladistics*, **34**, 407–437. doi:10.1111/cla.12205

Gould, S. J. 1977. *Ontogeny and Phylogeny*. Harvard University Press, Cambridge.

Gray, J. A. 2018. *Skull Evolution in the Australian Dragon Lizards*. PhD thesis, University of Adelaide, Adelaide.

Greer, A. E. 1985. The relationships of the lizard genera *Anelytropsis* and *Dibamus*. *Journal of Herpetology*, **19**(1), 116–156.

Griffith, O. W., Blackburn, D. G., Brandley, M. C., van Dyke, J. U., Whittington, C. M. & Thompson, M. B. 2015. Ancestral state reconstructions require biological evidence to test evolutionary hypotheses: a case study examining the evolution of reproductive mode in squamate reptiles. *Journal of Experimental Zoology, Part B: Molecular and Developmental Evolution*, **324B**, 493–503. doi:10.1002/jez.b.22614

Groombridge, B. 1979. On the vomer in Acrochordidae (Reptilia: Serpentes), and its cladistic significance. *Journal of Zoology*, **189**, 559–567.

Haas, G. 1930. Über das Kopfskelett und die Kaumuskulatur der Typhlopiden und Glauconiiden. *Zoologische Jahrbücher. Abteilung für Anatomie*, **52**, 1–94.

Haas, G. 1964. Anatomical observations on the head of *Liotyphlops albirostris* (Typhlopidae, Ophidia). *Acta Zoologica*, **1964**, 1–62.

Haas, G. 1968. Anatomical observations on the head of *Anomalepis aspinosus* (Typhlopidae, Ophidia). *Acta Zoologica*, **48**, 63–139.

Haas, G. 1979. On a new snakelike reptile from the Lower Cenomanian of Ein Jabrud, near Jerusalem. *Bulletin du Museum National d'Histoire Naturelle. Section C*, **1**, 51–64.

Haas, G. 1980. *Pachyrhachis problematicus* Haas, snakelike reptile from the lower Cenomanian: ventral view of the skull. *Bulletin du Museum National d'Histoire Naturelle. Section C*, **2**, 87–104.

Hanken, J. 1984. Miniaturization and its effects on cranial morphology in plethodontid salamanders, genus *Thorius* (Amphibia: Plethodontidae). I. Osteological variation. *Biological Journal of the Linnean Society*, **23**, 55–75.

Hanken, J. & Wake, D. B. 1993. Miniaturization of body size: organismal consequences and evolutionary significance. *Annual Review of Ecology and Systematics*, **24**, 501–519.

Hanken, J. 2015. Is heterochrony still an effective paradigm for contemporary studies of evo-devo? Pp. 97–110 in A. Love (ed) *Conceptual Change in Biology*. Springer, Dordrecht.

Harrington, S. M. & Reeder, T. W. 2017. Phylogenetic inference and divergence dating of snakes using molecules, morphology and fossils: new insights into convergent evolution of feeding morphology and limb reduction. *Biological Journal of the Linnean Society*, **121**, 379–394.

Hawkins, J. A., Hughes, C. E. & Scotland, R. W. 1997. Primary homology assessment, characters and character States. *Cladistics*, **13**, 275–283.

Hawlitschek, O., Scherz, M. D., Webster, K. C., Ineich, I. & Glaw, F. 2021. Morphological, osteological, and genetic data support a new species of *Madatyphlops* (Serpentes: Typhlopidae) endemic to Mayotte Island, Comoros Archipelago. *The Anatomical Record*, **2021**, 1–15. doi:10.1002/ar.24589

Hedges, S. B., Marion, A. B., Lipp, K. M., Marin, J. & Vidal, N. 2014. A taxonomic framework for typhlopid snakes from the Caribbean and other regions (Reptilia, Squamata). *Caribbean Herpetology*, **49**, 1–61. doi:10.31611/ch.49

Heise, P. J., Maxson, L. R., Dowling, H. G. & Hedges, S. B. 1995. Higher-level snake phylogeny inferred from mitochondrial DNA sequences of 12S rRNA and 16S rRNA genes. *Molecular Biology and Evolution*, **12**(2), 259–265.

Hernández-Jaimes, C., Jerez, A. & Ramírez-Pinilla, M. P. 2012. Embryonic development of the skull of the Andean lizard *Ptychoglossus bicolor* (Squamata, Gymnophthalmidae). *Journal of Anatomy*, **221**, 285–302. doi:10.1111/j.1469-7580.2012.01549.x

Herrel, A., Lowie, A., Miralles, A., Gaucher, P., Kley, N. J., Measey, J. & Tolley, K. A. 2021. Burrowing in blindsnakes: a preliminary analysis of burrowing forces and consequences for the evolution ofmorphology. *The Anatomical Record*, **2021**, 1–11. doi:10.1002/ar.24686

Hoffstetter, R. & Gasc, J.-P. 1969. Vertebrae and ribs of modern reptiles. Pp. 201–310 in C. Gans, A.D. Bellairs and T.S. Parsons (eds) *Biology of the Reptilia: Morphology A*. Academic Press, London and New York.

Howland, J. M., Vitt, L. J. & Lopez, P. T. 1990. Life on the edge: the ecology and life history of the tropidurine iguanid lizard *Uranoscodon superciliosum*. *Canadian Journal of Zoology/Revue Canadienne de Zoologie*, **68**, 1366–1373.

Hsiang, A. Y., Field, D. J., Webster, T. H., Behlke, A. D. B., Davis, M. B., Racicot, R. A. & Gauthier, J. A. 2015. The origin of snakes: revealing the ecology, behavior, and evolutionary history of early snakes using genomics, phenomics, and the fossil record. *BMC Evolutionary Biology*, **15**, 87. doi:10.1186/s12862-015-0358-5

Iordansky, N. N. 1997. Jaw apparatus and feeding mechanics of *Typhlops* (Ophidia: Typhlopidae): a reconsideration. *Russian Journal of Herpetology*, **4**(2), 120–127.

Irish, F. J. 1989. The role of heterochrony in the origin of a novel bauplan: evolution of the ophidian skull. *Geobios*, **22**, 227–233.

Jackson, K. 2002. Post-ovipositional development of the monocled cobra, *Naja kaouthia* (Serpentes: Elapidae). *Zoology*, **105**, 203–214.

Jackson, K. 2007. The evolution of venom-conducting fangs: insights from developmental biology. *Toxicon*, **49**, 975–981. doi:10.1016/j.toxicon.2007.01.007

Janensch, W. 1906. Uber Archaeophis proavus Mass., eine schlange aus dem Eocan des Monte Bolca. *Beitrage zur Palaontologie und Geologie Oestreich-Ungarns und des Orients*, **16**, 1–33.

Johnson, S. R. 1965. An ecological study of the chuckwalla, *Sauromalus obesus* Baird, in the western Mojave Desert. *American Midland Naturalist*, **73**(1), 1–29.

Kamal, A. M. 1966. On the process of rotation of the quadrate cartilage in Ophidia. *Anatomischer Anzieger*, **118**, 87–90.

Kearney, M. & Stuart, B. L. 2004. Repeated evolution of limblessness and digging heads in worm lizards revealed by DNA from old bones. *Proceedings of the Royal Society of London, Series B: Biological Sciences*, **271**, 1677–1683. doi:10.1098/rspb.2004.2771

Khannoon, E. R. & Evans, S. E. 2015. The development of the skull of the Egyptian cobra *Naja h. haje* (Squamata: Serpentes: Elapidae). *PLoS ONE*, **10**, e0122185. doi:10.1371/journal.pone.0122185

Khannoon, E. R. & Zahradnicek, O. 2017. Postovipositional development ofthe sand snake *Psammophis sibilans* (Serpentes:Lamprophiidae) in comparison with other snake species. *Acta Zoologica (Stockholm)*, **98**, 144–153. doi:10.1111/azo.12157

Khannoon, E. R., Ollonen, J. & Di-Poï, N. 2020. Embryonic development of skull bones in the Sahara horned viper (*Cerastes cerastes*), with new insights into structures related to the basicranium and braincase roof. *Journal of Anatomy*, **00**, 1–19. doi:10.1111/joa.13182

Khouri, R. S., Almeida-Santos, S. M. & Fernandes, D. S. 2020. Anatomy of the reproductive system of a population of *Amerotyphlops brongersmianus* from southeastern Brazil (Serpentes: Scolecophidia). *The Anatomical Record*, **303**, 2485–2496. doi:10.1002/ar.24382

King, B. & Rücklin, M. 2020. A Bayesian approach to dynamic homology of morphological characters and the ancestral phenotype of jawed vertebrates. *eLife*, **9**, e62374. doi:10.7554/eLife.62374

Kley, N. J. & Brainerd, E. L. 1999. Feeding by mandibular raking in a snake. *Nature*, **402**, 369–370. doi:10.1038/46460

Kley, N. J. 2001. Prey transport mechanisms in blindsnakes and the evolution of unilateral feeding systems in snakes. *American Zoologist*, **41**, 1321–1337.

Kley, N. J. 2006. Morphology of the lower jaw and suspensorium in the Texas blindsnake, *Leptotyphlops dulcis* (Scolecophidia: Leptotyphlopidae). *Journal of Morphology*, **267**, 494–515. doi:10.1002/jmor.10414

Kluge, A. G. 1991. Boine snake phylogeny and research cycles. *Miscellaneous Publications of the Museum of Zoology, University of Michigan*, **178**, 1–58.

Koch, C., Martins, A. & Schweiger, S. 2019. A century of waiting: description of a new *Epictia* Gray, 1845 (Serpentes: Leptotyphlopidae) based on specimens housed for more than 100 years in the collection of the Natural History Museum Vienna (NMW). *PeerJ*, **7**, e7411. doi:10.7717/peerj.7411

Kochva, E. 1987. The origin of snakes and evolution of the venom apparatus. *Toxicon*, **25**(1), 65–106.

Kochva, E. 2002. *Atractaspis* (Serpentes, Atractaspididae) the burrowing asp; a multidisciplinary minireview. *Bulletin of the Natural History Museum Zoology*, **68**(2), 91–99. doi:10.1017/S0968047002000109

Kraus, F. 2017. New species of blindsnakes (Squamata: Gerrhopilidae) from the offshore islands of Papua New Guinea. *Zootaxa*, **4299**(7), 75–94. doi:10.11646/zootaxa.4299.1.3

Lakner, C., Mark, P. v. d., Huelsenbeck, J. P., Larget, B. & Ronquist, F. 2008. Efficiency of Markov Chain Monte Carlo tree proposals in Bayesian phylogenetics. *Systematic Biology*, **57**(1), 86–103. doi:10.1080/10635150801886156

Lamsdell, J. C. 2020. A new method for quantifying heterochrony in evolutionary lineages. *Paleobiology*, **00**, 1–22. doi:10.1017/pab.2020.17

Langner, C. 2017. Hidden in the heart of Borneo – Shedding light on some mysteries of an enigmatic lizard: first records of habitat use, behavior, and food items of *Lanthanotus*

borneensis Steindachner, 1878 in its natural habitat. *Russian Journal of Herpetology*, **24**(1), 1–10.

Lawson, R., Slowinski, J. B., Crother, B. I. & Burbrink, F. T. 2005. Phylogeny of the Colubroidea (Serpentes): New evidence from mitochondrial and nuclear genes. *Molecular Phylogenetics and Evolution*, **37**, 581–601. doi:10.1016/j.ympev.2005.07.016

LeBlanc, A. R. H., Caldwell, M. W. & Bardet, N. 2012. A new mosasaurine from the Maastrichtian (Upper Cretaceous) phosphates of Morocco and its implications for mosasaurine systematics. *Journal of Vertebrate Paleontology*, **32**(1), 82–104. doi:10.1080/02724634.2012.624145

Lee, H. W., Esteve-Altava, B. & Abzhanov, A. 2020. Evolutionary and ontogenetic changes of the anatomical organization and modularity in the skull of archosaurs. *Scientific Reports*, **10**, 16138. doi:10.1038/s41598-020-73083-3

Lee, M. S. Y. 1993. The origin of the turtle body plan: bridging a famous morphological gap. *Science*, **261**(5129), 1716–1720. doi:10.1126/science.261.5129.1716

Lee, M. S. Y. 1997. The phylogeny of varanoid lizards and the affinities of snakes. *Philosophical Transactions of the Royal Society of London, Series B: Biological Sciences*, **352**, 53–91.

Lee, M. S. Y. 1998. Convergent evolution and character correlation in burrowing reptiles: towards a resolution of squamate relationships. *Biological Journal of the Linnean Society*, **65**, 369–453.

Lee, M. S. Y. & Caldwell, M. W. 1998. Anatomy and relationships of *Pachyrhachis problematicus*, a primitive snake with hindlimbs. *Philosophical Transactions of the Royal Society of London, Series B: Biological Sciences*, **353**(1375), 1521–1552.

Lee, M. S. Y. & Scanlon, J. D. 2002. Snake phylogeny based on osteology, soft anatomy and ecology. *Biological Reviews*, **77**, 333–401.

Lee, M. S. Y. 2005. Molecular evidence and marine snake origins. *Biology Letters*, **1**, 227–230. doi:10.1098/rsbl.2004.0282

Lee, M. S. Y. 2009. Hidden support from unpromising data sets strongly unites snakes with anguimorph ‘lizards’. *Journal of Evolutionary Biology*, **22**, 1308–1316. doi:10.1111/j.1420-9101.2009.01751.x

Lewis, P. O. 2001. A likelihood approach to estimating phylogeny from discrete morphological character data. *Systematic Biology*, **50**(6), 913–925.

Lira, I. & Martins, A. 2021. Digging into blindsnakes' morphology: description of the skull, lower jaw, and cervical vertebrae of two *Amerotyphlops* (Hedges et al., 2014) (Serpentes, Typhlopidae) with comments on the typhlopoidean skull morphological diversity. *The Anatomical Record*, **0**(0), 1–17. doi:10.1002/ar.24591

List, J. C. 1966. Comparative osteology of the snake families Typhlopidae and Leptotyphlopidae. *Illinois Biological Monographs*, **36**, 1–112.

Longrich, N. R., Bhullar, B.-A. S. & Gauthier, J. A. 2012. A transitional snake from the Late Cretaceous period of North America. *Nature*, **488**, 205–208. doi:10.1038/nature11227

Mabee, P. M., Balhoff, J. P., Dahdul, W. M., Lapp, H., Mungall, C. J. & Vision, T. J. 2020. A logical model of homology for comparative biology. *Systematic Biology*, **69**(2), 345–362. doi:10.1093/sysbio/syz067

Maddin, H. C., Olori, J. C. & Anderson, J. S. 2011. A redescription of *Carrolla craddocki* (Lepospondyli: Brachystelechidae) based on high-resolution CT, and the impacts of miniaturization and fossoriality on morphology. *Journal of Morphology*, **272**, 722–743. doi:10.1002/jmor.10946

Maddison, W. P. & Maddison, D. R. 2006. StochChar: a package of Mesquite modules for stochastic models of character evolution

Maddison, W. P. & Maddison, D. R. 2019. Mesquite: a modular system for evolutionary analysis. http://mesquiteproject.org

Mahendra, B. C. 1936. Contributions to the osteology of the Ophidia. I. The endoskeleton of the so-called 'blind-snake', *Typhlops braminus* Daud. *Proceedings of the Indian Academy of Sciences*, **3**, 128–142.

Mahendra, B. C. 1938. Some remarks on the phylogeny of the Ophidia. *Anatomischer Anzieger*, **86**, 347–356.

Maisano, J. A. & Rieppel, O. 2007. The skull of the round island boa, *Casarea dussumieri* Schlegel, based on high-resolution X-ray computed tomography. *Journal of Morphology*, **268**, 371–384. doi:10.1002/jmor.10519

Malmstrøm, M., Britz, R., Matschiner, M., Tørresen, O. K., Kurnia Hadiaty, R., Yaakob, N., Hui Tan, H., Sigurd Jakobsen, K., Salzburger, W. & Rüber, L. 2018. The most

developmentally truncated fishes show extensive *Hox* gene loss and miniaturized genomes. *Genome Biology and Evolution*, **10**(4), 1088–1103. doi:10.1093/gbe/evy058

Martin, C. 2017. ggConvexHull. https://github.com/cmartin/ggConvexHull

Martinez-Arbizu, P. 2020. pairwiseAdonis. https://github.com/pmartinezarbizu/pairwiseAdonis

Martins, A., Koch, C., Pinto, R., Folly, M., Fouquet, A. & Passos, P. 2019. From the inside out: discovery of a new genus of threadsnakes based on anatomical and molecular data, with discussion of the leptotyphlopid hemipenial morphology. *Journal of Zoological Systematics and Evolutionary Research*, **57**, 840–863. doi:10.1111/jzs.12316

Massare, J. A. 1987. Tooth morphology and prey preference of Mesozoic marine reptiles. *Journal of Vertebrate Paleontology*, **7**(2), 121–137. doi:10.1080/02724634.1987.10011647

McDowell, S. B. & Bogert, C. M. 1954. The systematic position of *Lanthanotus* and the affinities of the anguimorphan lizards. *Bulletin of the American Museum of Natural History, New York*, **105**, 1–142.

McNamara, K. J. 1986. A guide to the nomenclature of heterochrony. *Journal of Paleontology*, **60**(1), 4–13.

Méhely, L. V. 1907. Archaeo- und Neolacerten. *Annales Musei Historico-Naturalis Hungarici*, **5**, 469–493.

Miller, M. A., Pfeiffer, W. & Schwartz, T. 2010. Creating the CIPRES Science Gateway for inference of large phylogenetic trees. Pp. 1–8. *Proceedings of the Gateway Computing Environments Workshop (GCE)*. New Orleans.

Miralles, A., Marin, J., Markus, D., Herrel, A., Hedges, S. B. & Vidal, N. 2018. Molecular evidence for the paraphyly of Scolecophidia and its evolutionary implications. *Journal of Evolutionary Biology*, **31**, 1782–1793. doi:10.1111/jeb.13373

Mongiardino Koch, N. & Gauthier, J. A. 2018. Noise and biases in genomic data may underlie radically different hypotheses for the position of Iguania within Squamata. *PLoS ONE*, **13**(8), e0202729. doi:10.1371/journal. pone.0202729

Mongiardino Koch, N. & Parry, L. A. 2020. Death is on our side: paleontological data drastically modify phylogenetic hypotheses. *Systematic Biology*, **69**(6), 1052–1067. doi:10.1093/sysbio/syaa023

Monteiro, L. R. & Abe, A. S. 1997. Allometry and morphological integration in the skull of *Tupinambis merianae* (Lacertilia: Teiidae). *Amphibia-Reptilia*, **18**, 397–405.

Mookerjee, H. K. & Das, G. M. 1932. Occurrence of a paired parietal bone in a snake. *Nature*, **130**(3286), 629.

Moyer, K. & Jackson, K. 2011. Phylogenetic relationships among the Stiletto Snakes (genus Atractaspis) based on external morphology. *African Journal of Herpetology*, **60**(1), 30–46. doi:10.1080/21564574.2010.520034

Müller, G. B. 2007. Evo–devo: extending the evolutionary synthesis. *Nature Reviews: Genetics*, **8**, 943–949. doi:10.1038/nrg2219

Müller, J. 1831. Beiträge zur Anatomie und Naturgeschichte der Amphibien. *Zeitschrift für Physiologie*, **4**, 90–275.

Müller, J., Hipsley, C. A., Head, J. J., Kardjilov, N., Hilger, A., Wuttke, M. & Reisz, R. R. 2011. Eocene lizard from Germany reveals amphisbaenian origins. *Nature*, **473**, 364–367. doi:10.1038/nature09919

Nagy, Z. T., Marion, A. B., Glaw, F., Miralles, A., Nopper, J., Vences, M. & Hedges, S. B. 2015. Molecular systematics and undescribed diversity of Madagascan scolecophidian snakes (Squamata: Serpentes). *Zootaxa*, **4040**(1), 31–47. doi:10.11646/zootaxa.4040.1.3

Navarro-Díaz, A., Esteve-Altava, B. & Rasskin-Gutman, D. 2019. Disconnecting bones within the jaw-otic network modules underlies mammalian middle ear evolution. *Journal of Anatomy*, **235**, 15–33. doi:10.1111/joa.12992

Newman, M. E. J. & Girvan, M. 2004. Finding and evaluating community structure in networks. *Physical Review E*, **69**, 026113. doi:10.1103/PhysRevE.69.026113

Newman, M. E. J. 2006. Finding community structure in networks using the eigenvectors of matrices. *Physical Review E*, **74**, 036104. doi:10.1103/PhysRevE.74.036104

Nguyen, T. Q., Ngo, H. N., Pham, C. T., Van, H. N., Ngo, C. D., Schingen, M. v. & Ziegler, T. 2018. First population assessment of the Asian Water Dragon (*Physignathus cocincinus* Cuvier, 1829) in Thua Thien Hue Province, Vietnam. *Nature Conservation*, **26**, 1–14. doi:10.3897/natureconservation.26.21818

Norris, K. S. 1953. The ecology of the desert iguana *Dipsosaurus dorsalis*. *Ecology*, **34**(2), 265–287.

O'Reilly, J. E., Puttick, M. N., Pisani, D. & Donoghue, P. C. J. 2018. Probabilistic methods surpass parsimony when assessing clade support in phylogenetic analyses of discrete morphological data. *Palaeontology*, **61**(1), 105–118. doi:10.1111/pala.12330

O'Reilly, J. E., Puttick, M. N., Parry, L., Tanner, A. R., Tarver, J. E., Fleming, J., Pisani, D. & Donoghue, P. C. J. 2016. Bayesian methods outperform parsimony but at the expense of precision in the estimation of phylogeny from discrete morphological data. *Biology Letters*, **12**, 20160081. doi:10.1098/rsbl.2016.0081

Object Research Systems Inc. 2019a. Dragonfly 4.0. Object Research Systems (ORS) Inc., Montreal, Canada. http://www.theobjects.com/dragonfly

Object Research Systems Inc. 2019b. Dragonfly 4.1. Object Research Systems (ORS) Inc., Montreal, Canada. https://theobjects.com/dragonfly/

Oksanen, J., Blanchet, F. G., Friendly, M., Kindt, R., Legendre, P., McGlinn, D., Minchin, P. R., O'Hara, R. B., Simpson, G. L., Solymos, P., Stevens, M. H. H., Szoecs, E. & Wagner, H. 2019. vegan: community ecology package. https://CRAN.R-project.org/package=vegan

Ollonen, J., Silva, F. O. D., Mahlow, K. & Di-Poï, N. 2018. Skull development, ossification pattern, and adult shape in the emerging lizard model organism *Pogona vitticeps*: a comparative analysis with other squamates. *Frontiers in Physiology*, **9**, 278. doi:10.3389/fphys.2018.00278

Olori, J. C. & Bell, C. J. 2012. Comparative skull morphology of uropeltid snakes (Alethinophidia: Uropeltidae) with special reference to disarticulated elements and variation. *PLoS ONE*, **7**(3), e32450. doi:10.1371/journal.pone.0032450

Palci, A. & Caldwell, M. W. 2010. Redescription of *Acteosaurus tommasinii* von Meyer, 1860, and a discussion of evolutionary trends within the clade Ophidiomorpha. *Journal of Vertebrate Paleontology*, **30**(1), 94–108. doi:10.1080/02724630903409139

Palci, A. & Caldwell, M. W. 2013. Primary homologies of the circumorbital bones of snakes. *Journal of Morphology*, **274**, 973–986. doi:10.1002/jmor.20153

Palci, A., Caldwell, M. W. & Albino, A. M. 2013a. Emended diagnosis and phylogenetic relationships of the Upper Cretaceous fossil snake *Najash rionegrina* Apesteguía and Zaher, 2006. *Journal of Vertebrate Paleontology*, **33**(1), 131–140. doi:10.1080/02724634.2012.713415

Palci, A., Caldwell, M. W. & Nydam, R. L. 2013b. Reevaluation of the anatomy of the Cenomanian (Upper Cretaceous) hind-limbed marine fossil snakes *Pachyrhachis*, *Haasiophis*, and *Eupodophis*. *Journal of Vertebrate Paleontology*, **33**(6), 1328–1342. doi:10.1080/02724634.2013.779880

Palci, A. & Caldwell, M. W. 2014. The Upper Cretaceous snake *Dinilysia patagonica* Smith-Woodward, 1901, and the crista circumfenestralis of snakes. *Journal of Morphology*, **275**, 1187–1200. doi:10.1002/jmor.20297

Palci, A., Lee, M. S. Y. & Hutchinson, M. N. 2016. Patterns of postnatal ontogeny of the skull and lower jaw of snakes as revealed by micro-CT scan data and three-dimensional geometric morphometrics. *Journal of Anatomy*, **229**(6), 723–754. doi:10.1111/joa.12509

Palci, A., Hutchinson, M. N., Caldwell, M. W. & Lee, M. S. Y. 2017. The morphology of the inner ear of squamate reptiles and its bearing on the origin of snakes. *Royal Society Open Science*, **4**, 170685. doi:10.1098/rsos.170685

Palci, A. & Lee, M. S. Y. 2019. Geometric morphometrics, homology and cladistics: review and recommendations. *Cladistics*, **35**, 230–242. doi:10.1111/cla.12340

Palci, A., Seymour, R. S., Van Nguyen, C., Hutchinson, M. N., Lee, M. S. Y. & Sanders, K. L. 2019. Novel vascular plexus in the head of a sea snake (Elapidae, Hydrophiinae) revealed by high-resolution computed tomography and histology. *Royal Society Open Science*, **6**, 191099. doi:10.1098/rsos.191099

Palci, A., Caldwell, M. W., Hutchinson, M. N., Konishi, T. & Lee, M. S. Y. 2020a. The morphological diversity of the quadrate bone in squamate reptiles as revealed by high-resolution computed tomography and geometric morphometrics. *Journal of Anatomy*, **236**, 210–227. doi:10.1111/joa.13102

Palci, A., Hutchinson, M. N., Caldwell, M. W., Smith, K. T. & Lee, M. S. Y. 2020b. The homologies and evolutionary reduction of the pelvis and hindlimbs in snakes, with the first report of ossified pelvic vestiges in an anomalepidid (*Liotyphlops beui*). *Zoological Journal of the Linnean Society*, **188**, 630–652. doi:10.1093/zoolinnean/zlz098

Patterson, C. 1982. Morphological characters and homology. Pp. 21–74 in K.A. Joysey and A.E. Friday (eds) *Problems of Phylogenetic Reconstruction*. Academic Press, London and New York.

Patterson, C. 1988. Homology in classical and molecular biology. *Molecular Biology and Evolution*, **5**(6), 603–625.

Pinto, R. R. & Fernandes, R. 2012. A new blind snake species of the genus *Tricheilostoma* from Espinhaço Range, Brazil and taxonomic status of *Rena dimidiata* (Jan, 1861) (Serpentes: Epictinae: Leptotyphlopidae). *Copeia*, **2012**(1), 37–48. doi:10.1643/CH-11-040

Pinto, R. R., Martins, A. R., Curcio, F. & Ramos, L. O. 2015. Osteology and cartilaginous elements of *Trilepida salgueiroi* (Amaral, 1954) (Scolecophidia: Leptotyphlopidae). *The Anatomical Record*, **298**, 1722–1747. doi:10.1002/ar.23191

Plateau, O. & Foth, C. 2020. Birds have peramorphic skulls, too: anatomical network analyses reveal oppositional heterochronies in avian skull evolution. *Communications Biology*, **3**, 195. doi:10.1038/s42003-020-0914-4

Polachowski, K. M. & Werneburg, I. 2013. Late embryos and bony skull development in *Bothropoides jararaca* (Serpentes, Viperidae). *Zoology*, **116**, 36–63. doi:10.1016/j.zool.2012.07.003

Polly, P. D. 2008. Developmental dynamics and G-matrices: can morphometric spaces be used to model phenotypic evolution? *Evolutionary Biology*, **35**, 83–96. doi:10.1007/s11692-008-9020-0

Portillo, F., Branch, W. R., Conradie, W., Rödel, M.-O., Penner, J., Barej, M. F., Kusamba, C., Muninga, W. M., Aristote, M. M., Bauer, A. M., Trape, J.-F., Nagy, Z. T., Carlino, P., Pauwels, O. S. G., Menegon, M., Burger, M., Mazuch, T., Jackson, K., Hughes, D. F., Behangana, M., Zassi-Boulou, A.-G. & Greenbaum, E. 2018. Phylogeny and biogeography of the African burrowing snake subfamily Aparallactinae (Squamata: Lamprophiidae). *Molecular Phylogenetics and Evolution*, **127**, 288–303. doi:10.1016/j.ympev.2018.03.019

Portillo, F., Stanley, E. L., Branch, W. R., Conradie, W., Rödel, M.-O., Penner, J., Barej, M. F., Kusamba, C., Muninga, W. M., Aristote, M. M., Bauer, A. M., Trape, J.-F., Nagy, Z. T., Carlino, P., Pauwels, O. S. G., Menegon, M., Ineich, I., Burger, M., Zassi-Boulou, A.-G., Mazuch, T., Jackson, K., Hughes, D. F., Behangana, M. & Greenbaum, E. 2019. Evolutionary history of burrowing asps (Lamprophiidae:

Atractaspidinae) with emphasis on fang evolution and prey selection. *PLoS ONE*, **14**(4), e0214889. doi:10.1371/journal. pone.0214889

Pregill, G. K., Gauthier, J. A. & Greene, H. W. 1986. The evolution of helodermatid squamates, with description of a new taxon and an overview of Varanoidea. *Transactions of the San Diego Society of Natural History*, **21**, 167–202.

Pringle, J. A. 1954. The cranial development of certain South African snakes and the relationship of these groups. *Proceedings of the Zoological Society of London*, **123**, 813–865.

Puttick, M. N. 2016. Partially incorrect fossil data augment analyses of discrete trait evolution in living species. *Biology Letters*, **12**, 20160392. doi:10.1098/rsbl.2016.0392

Pyron, R. A., Burbrink, F. T., Colli, G. R., Nieto Montes de Oca, A., Vitt, L. J., Kuczynski, C. A. & Wiens, J. J. 2011. The phylogeny of advanced snakes (Colubroidea), with discovery of a new subfamily and comparison of support methods for likelihood trees. *Molecular Phylogenetics and Evolution*, **58**, 329–342. doi:10.1016/j.ympev.2010.11.006

Pyron, R. A., Burbrink, F. T. & Wiens, J. J. 2013. A phylogeny and revised classification of Squamata, including 4161 species of lizards and snakes. *BMC Evolutionary Biology*, **13**, 93. doi:10.1186/1471-2148-13-93

R Core Team. 2020. R: a language and environment for statistical computing. R Foundation for Statistical Computing, Vienna, Austria. https://www.R-project.org/

Racca, L., Villa, A., Wencker, L. C. M., Camaiti, M., Blain, H.-A. & Delfino, M. 2020. Skull osteology and osteological phylogeny of the Western whip snake *Hierophis viridiflavus* (Squamata, Colubridae). *Journal of Morphology*, **281**, 808–833. doi:10.1002/jmor.21148

Rage, J.-C. & Escuillié, F. 2000. Un nouveau serpent bipède du Cénomanien (Crétacé). Implications phylétiques. *Comptes Rendus de l'Académie des Sciences - Series IIA - Sciences de la Terre et des planètes/Earth and Planetary Science*, **330**, 513–520.

Rambaut, A. 2018. FigTree: Tree Figure Drawing Tool (v.1.4.4).

Rambaut, A., Drummond, A. J., Xie, D., Baele, G. & Suchard, M. A. 2018. Posterior summarization in Bayesian phylogenetics using Tracer 1.7. *Systematic Biology*, **67**(5), 901–904. doi:10.1093/sysbio/syy032

Rasskin-Gutman, D. & Buscalioni, A. D. 2001. Theoretical morphology of the Archosaur (Reptilia: Diapsida) pelvic girdle. *Paleobiology*, **27**(1), 59–78. doi:10.1666/0094-8373(2001)027<0059:TMOTAR>2.0.CO;2

Rasskin-Gutman, D. 2003. Boundary constraints for the emergence of form. Pp. 305–322 in G.B. Müller and S.A. Newman (eds) *Origination of Organismal Form: Beyond the Gene in Developmental and Evolutionary Biology*. MIT Press, Cambridge, MA.

Rasskin-Gutman, D. & Esteve-Altava, B. 2014. Connecting the dots: anatomical network analysis in morphological EvoDevo. *Biological Theory*, **9**, 178–193. doi:10.1007/s13752-014-0175-x

Reeder, T. W., Townsend, T. M., Mulcahy, D. G., Noonan, B. P., Wood, P. L., Sites, J. W. & Wiens, J. J. 2015. Integrated analyses resolve conflicts over squamate reptile phylogeny and reveal unexpected placements for fossil taxa. *PLoS ONE*, **10**(3), e0118199. doi:10.1371/journal.pone.0118199

Reilly, S. M., Wiley, E. O. & Meinhardt, D. J. 1997. An integrative approach to heterochrony: the distinction between interspecific and intraspecific phenomena. *Biological Journal of the Linnean Society*, **60**, 119–143.

Reinhardt, J. T. 1843. Beskrivelse af nogle nye Slangearter. *Kongelige Danske Videnskabernes Selskabs, Afhandlinger*, **10**, 233–279.

Rhoda, D., Polly, P. D., Raxworthy, C. & Segall, M. 2021. Morphological integration and modularity in the hyperkinetic feeding system of aquatic-foraging snakes. *Evolution*, **75**(1), 56–72. doi:10.1111/evo.14130

Rieppel, O. 1977. Studies on the skull of the Henophidia (Reptilia: Serpentes). *Journal of Zoology*, **181**, 145–173.

Rieppel, O. 1978a. A functional and phylogenetic interpretation of the skull of the Erycinae (Reptilia, Serpentes). *Journal of Zoology*, **186**, 185–208.

Rieppel, O. 1978b. The evolution of the naso-frontal joint in snakes and its bearing on snake origins. *Journal of Zoological Systematics and Evolutionary Research*, **16**, 14–27. doi:10.1111/j.1439-0469.1978.tb00917.x

Rieppel, O. 1979a. A cladistic classification of primitive snakes based on skull structure. *Journal of Zoological Systematics and Evolutionary Research*, **17**(2), 140–150. doi:10.1111/j.1439-0469.1979.tb00696.x

Rieppel, O. 1979b. The evolution of the basicranium in the Henophidia (Reptilia: Serpentes). *Zoological Journal of the Linnean Society*, **66**, 411–431.

Rieppel, O. 1984a. Miniaturization of the lizard skull: its functional and evolutionary implications. *Symposia of the Zoological Society of London*, **52**, 503–520.

Rieppel, O. 1984b. The cranial morphology of the fossorial lizard genus *Dibamus* with a consideration of its phylogenetic relationships. *Journal of Zoology*, **204**, 289–327.

Rieppel, O. 1988. A review of the origin of snakes. Pp. 37–130 in M.K. Hecht, B. Wallace and G.T. Prance (eds) *Evolutionary Biology*. Springer, Boston, MA.

Rieppel, O. 1994. Homology, topology, and typology: the history of modern debates. Pp. 63–100 in B.K. Hall (ed) *Homology: The Hierarchical Basis of Comparative Biology*. Academic Press, San Diego.

Rieppel, O. 1996. Miniaturization in tetrapods: consequences for skull morphology. Pp. 47–61 in P.J. Miller (ed) *Miniature Vertebrates: The Implications of Small Body Size, Vol. 69. Symposia of the Zoological Society of London*. Claredon Press, Oxford.

Rieppel, O. & Zaher, H. 2000. The intramandibular joint in squamates, and the phylogenetic relationships of the fossil snake *Pachyrhachis problematicus* Haas. *Fieldiana Geology*, **43**, 1–69.

Rieppel, O. & Zaher, H. 2001a. Re-building the bridge between mosasaurs and snakes. *Neues Jahrbuch für Geologie und Paläontologie, Abhandlungen*, **221**(1), 111–132.

Rieppel, O. & Zaher, H. 2001b. The development of the skull in *Acrochordus granulatus* (Schneider) (Reptilia: Serpentes), with special consideration of the otico-occipital complex. *Journal of Morphology*, **249**, 252–266.

Rieppel, O. & Kearney, M. 2002. Similarity. *Biological Journal of the Linnean Society*, **75**, 59–82.

Rieppel, O., Kluge, A. G. & Zaher, H. 2002. Testing the phylogenetic relationships of the Pleistocene snake *Wonambi naracoortensis* Smith. *Journal of Vertebrate Paleontology*, **22**(4), 812–829. doi:10.1671/0272-4634(2002)022[0812:TTPROT]2.0.CO;2

Rieppel, O., Zaher, H., Tchernov, E. & Polcyn, M. J. 2003. The anatomy and relationships of *Haasiophis terrasanctus*, a fossil snake with well-developed hind limbs from the mid-Cretaceous of the Middle East. *Journal of Paleontology*, **77**(3), 536–558.

Rieppel, O. & Head, J. J. 2004. New specimens of the fossil snake genus *Eupodophis* Rage & Escuillié, from Cenomanian (Late Cretaceous) of Lebanon. *Memorie della Societá Italiana di Scienze Naturali e del Museo Civico di Storia Naturale di Milano*, **32**, 1–26.

Rieppel, O. 2007. The naso-frontal joint in snakes as revealed by high-resolution X-ray computed tomography of intact and complete skulls. *Zoologischer Anzeiger*, **246**, 177–191. doi:10.1016/j.jcz.2007.04.001

Rieppel, O. & Maisano, J. A. 2007. The skull of the rare Malaysian snake *Anomochilus leonardi* Smith, based on high-resolution X-ray computed tomography. *Zoological Journal of the Linnean Society*, **149**, 671–685.

Rieppel, O., Gauthier, J. & Maisano, J. 2008. Comparative morphology of the dermal palate in squamate reptiles, with comments on phylogenetic implications. *Zoological Journal of the Linnean Society*, **152**, 131–152. doi:10.1111/j.1096-3642.2007.00337.x

Rieppel, O., Kley, N. J. & Maisano, J. A. 2009. Morphology of the skull of the white-nosed blindsnake, *Liotyphlops albirostris* (Scolecophidia: Anomalepididae). *Journal of Morphology*, **270**, 536–557. doi:10.1002/jmor.10703

Rieppel, O. 2012. "Regressed" macrostomatan snakes. *Fieldiana Life and Earth Sciences*, **2012**(5), 99–103. doi:10.3158/2158-5520-5.1.99

Rödel, M.-O., Kucharzewski, C., Mahlow, K., Chirio, L., Pauwels, O. S. G., Carlino, P., Sambolah, G. & Glos, J. 2019. A new stiletto snake (Lamprophiidae, Atractaspidinae, Atractaspis) from Liberia and Guinea, West Africa. *Zoosystematics and Evolution*, **95**(1), 107–123. doi:10.3897/zse.95.31488

Ronquist, F., Teslenko, M., van der Mark, P., Ayres, D. L., Darling, A., Höhna, S., Larget, B., Liu, L., Suchard, M. A. & Huelsenbeck, J. P. 2012. MrBayes 3.2: efficient Bayesian phylogenetic inference and model choice across a large model space. *Systematic Biology*, **61**(3), 539–542. doi:10.1093/sysbio/sys029

Ronquist, F., Huelsenbeck, J. P., Teslenko, M. & Nylander, J. A. A. 2019. MrBayes version 3.2 manual: tutorials and model summaries.

Sandoval, M. T., García, J. A. R. & Álvarez, B. B. 2020. Intrauterine and post-ovipositional embryonic development of *Amerotyphlops brongersmianus* (Vanzolini, 1976) (Serpentes: Typhlopidae) from northeastern Argentina. *Journal of Morphology*, **281**, 523–535. doi:10.1002/jmor.21119

Sanger, T. J., Mahler, D. L., Abzhanov, A. & Losos, J. B. 2012. Roles for modularity and constraint in the evolution of cranial diversity among *Anolis* lizards. *Evolution*, **66**(5), 1525–1542. doi:10.1111/j.1558-5646.2011.01519.x

Santos, F. J. M. & Reis, R. E. 2019. Redescription of the blind snake *Anomalepis colombia* (Serpentes: Anomalepididae) using high-resolution X-ray computed tomography. *Copeia*, **107**(2), 239–243. doi:10.1643/CH-19-181

Savitzky, A. H. 1983. Coadapted character complexes among snakes: fossoriality, piscivory, and durophagy. *American Zoologist*, **23**, 397–409.

Scanferla, A., Zaher, H., Novas, F. E., de Muizon, C. & Céspedes, R. 2013. A new snake skull from the Paleocene of Bolivia sheds light on the evolution of macrostomatans. *PLoS ONE*, **8**(3), e57583. doi:10.1371/journal.pone.0057583

Scanferla, A. & Bhullar, B.-A. S. 2014. Postnatal development of the skull of *Dinilysia patagonica* (Squamata-Stem Serpentes). *The Anatomical Record*, **297**, 560–573. doi:10.1002/ar.22862

Scanferla, A. 2016. Postnatal ontogeny and the evolution of macrostomy in snakes. *Royal Society Open Science*, **3**, 160612. doi:10.1098/rsos.160612

Scanferla, C. A. & Canale, J. I. 2007. The youngest record of the Cretaceous snake genus *Dinilysia* (Squamata, Serpentes). *South American Journal of Herpetology*, **2**(1), 76–81.

Scanlon, J. D. & Lee, M. S. Y. 2000. The Pleistocene serpent *Wonambi* and the early evolution of snakes. *Nature*, **403**, 416–420. doi:10.1038/35000188

Scanlon, J. D. 2006. Skull of the large non-macrostomatan snake *Yurlunggur* from the Australian Oligo-Miocene. *Nature*, **439**, 839–842. doi:10.1038/nature04137

Schmidt, K. P. 1950. Modes of evolution discernible in the taxonomy of snakes. *Evolution*, **4**(1), 79–86.

Schrago, C. G., Aguiar, B. O. & Mello, B. 2018. Comparative evaluation of maximum parsimony and Bayesian phylogenetic reconstruction using empirical morphological data. *Journal of Evolutionary Biology*, **31**, 1477–1484. doi:10.1111/jeb.13344

Sereno, P. C. 2007. Logical basis for morphological characters in phylogenetics. *Cladistics*, **23**(6), 565–587. doi:10.1111/j.1096-0031.2007.00161.x

Sherratt, E., Sanders, K. L., Watson, A., Hutchinson, M. N., Lee, M. S. Y. & Palci, A. 2019. Heterochronic shifts mediate ecomorphological convergence in skull shape of

microcephalic sea snakes. *Integrative and Comparative Biology*, **59**(3), 616–624. doi:10.1093/icb/icz033

Sheverdyukova, H. V. 2017. Development of the osteocranium in *Natrix natrix* (Serpentes, Colubridae) embryogenesis I: development of cranial base and cranial vault. *Zoomorphology*, **136**, 131–143. doi:10.1007/s00435-016-0333-8

Sheverdyukova, H. V. 2019. Development of the osteocranium in *Natrix natrix* (Serpentes, Colubridae) embryogenesis II: development of the jaws, palatal complex and associated bones. *Acta Zoologica*, **100**, 282–291. doi:10.1111/azo.12253

Sheverdyukova, H. V. & Kovtun, M. F. 2020. Variation in the formation of crista sellaris and basisphenoid in the skull of the grass snake *Natrix natrix* embryos (Serpentes, Colubridae). *Journal of Morphology*, **281**, 338–347. doi:10.1002/jmor.21102

Shine, R., Branch, W. R., Harlow, P. S., Webb, J. K. & Shine, T. 2006. Biology of burrowing asps (Atractaspididae) from Southern Africa. *Copeia*, **1**, 103–115.

Simões, B. F., Sampaio, F. L., Jared, C., Antoniazzi, M. M., Loew, E. R., Bowmaker, J. K., Rodriguez, A., Hart, N. S., Hunt, D. M., Partridge, J. C. & Gower, D. J. 2015. Visual system evolution and the nature of the ancestral snake. *Journal of Evolutionary Biology*, **28**, 1309–1320. doi:10.1111/jeb.12663

Simões, T. R., Caldwell, M. W., Palci, A. & Nydam, R. L. 2017. Giant taxon-character matrices: quality of character constructions remains critical regardless of size. *Cladistics*, **33**, 198–219. doi:10.1111/cla.12163

Simões, T. R., Caldwell, M. W., Tałanda, M., Bernardi, M., Palci, A., Vernygora, O., Bernardini, F., Mancini, L. & Nydam, R. L. 2018. The origin of squamates revealed by a Middle Triassic lizard from the Italian Alps. *Nature*, **557**, 706–709. doi:10.1038/s41586-018-0093-3

Simões, T. R., Caldwell, M. W. & Pierce, S. E. 2020. Sphenodontian phylogeny and the impact of model choice in Bayesian morphological clock estimates of divergence times and evolutionary rates. *BMC Biology*, **18**, 191. doi:10.1186/s12915-020-00901-5

Singhal, S., Colston, T. J., Grundler, M. R., Smith, S. A., Costa, G. C., Colli, G. R., Moritz, C., Pyron, R. A. & Rabosky, D. L. 2021. Congruence and conflict in the higher-level phylogenetics of squamate reptiles: an expanded phylogenomic perspective. *Systematic Biology*, **70**(3), 542–557. doi:10.1093/sysbio/syaa054

Slowinski, J. B. & Lawson, R. 2002. Snake phylogeny: evidence from nuclear and mitochondrial genes. *Molecular Phylogenetics and Evolution*, **24**, 194–202.

Streicher, J. W. & Wiens, J. J. 2016. Phylogenomic analyses reveal novel relationships among snake families. *Molecular Phylogenetics and Evolution*, **100**, 160–169. doi:10.1016/j.ympev.2016.04.015

Strong, C. R. C., Simões, T. R., Caldwell, M. W. & Doschak, M. R. 2019. Cranial ontogeny of *Thamnophis radix* (Serpentes: Colubroidea) with a re-evaluation of current paradigms of snake skull evolution. *Royal Society Open Science*, **6**, 182228. doi:10.1098/rsos.182228

Strong, C. R. C., Caldwell, M. W., Konishi, T. & Palci, A. 2020. A new species of longirostrine plioplatecarpine mosasaur (Squamata: Mosasauridae) from the Late Cretaceous of Morocco, with a re-evaluation of the problematic taxon *'Platecarpus' ptychodon*. *Journal of Systematic Palaeontology*, **18**(21), 1769–1804. doi:10.1080/14772019.2020.1818322

Strong, C. R. C., Palci, A. & Caldwell, M. W. 2021a. Insights into skull evolution in fossorial snakes, as revealed by the cranial morphology of *Atractaspis irregularis* (Serpentes: Colubroidea). *Journal of Anatomy*, **238**, 146–172. doi:10.1111/joa.13295

Strong, C. R. C., Scherz, M. D. & Caldwell, M. W. 2021b. Deconstructing the Gestalt: new concepts and tests of homology, as exemplified by a re-conceptualization of "microstomy" in squamates. *The Anatomical Record*, **2021**, 1–49. doi:10.1002/ar.24630

Struck, T. H. 2007. Data congruence, paedomorphosis and salamanders. *Frontiers in Zoology*, **4**, 22. doi:10.1186/1742-9994-4-22

Tchernov, E., Rieppel, O., Zaher, H., Polcyn, M. J. & Jacobs, L. L. 2000. A fossil snake with limbs. *Science*, **287**(5460), 2010–2012. doi:10.1126/science.287.5460.2010

Townsend, T. M., Larson, A., Louis, E. & Macey, J. R. 2004. Molecular phylogenetics of Squamata: the position of snakes, amphisbaenians, and dibamids, and the root of the squamate tree. *Systematic Biology*, **53**(5), 735–757. doi:10.1080/10635150490522340

Underwood, G. 1957. *Lanthanotus* and the anguinomorphan lizards: a critical review. *Copeia*, **1957**(1), 20–30.

Underwood, G. & Kochva, E. 1993. On the affinities of the burrowing asps *Atractaspis* (Serpentes: Atractaspididae). *Zoological Journal of the Linnean Society*, **107**, 3–64.

Urošević, A., Ljubisavljević, K. & Ivanović, A. 2019. Multilevel assessment of the Lacertid lizard cranial modularity. *Journal of Zoological Systematics and Evolutionary Research*, **57**, 145–158. doi:10.1111/jzs.12245

Vasile, Ş., Csiki-Sava, Z. & Venczel, M. 2013. A new madtsoiid snake from the Upper Cretaceous of the Haţeg Basin, western Romania. *Journal of Vertebrate Paleontology*, **33**(5), 1100–1119. doi:10.1080/02724634.2013.764882

Vernygora, O. V., Simões, T. R. & Campbell, E. O. 2020. Evaluating the performance of probabilistic algorithms for phylogenetic analysis of big morphological datasets: a simulation study. *Systematic Biology*, **69**(6), 1088–1105. doi:10.1093/sysbio/syaa020

Vidal, N. & Hedges, S. B. 2002. Higher-level relationships of snakes inferred from four nuclear and mitochondrial genes. *Comptes Rendus Biologies*, **325**, 977–985.

Vidal, N. & Hedges, S. B. 2004. Molecular evidence for a terrestrial origin of snakes. *Proceedings of the Royal Society of London, Series B: Biological Sciences*, **271**, S226–229. doi:10.1098/rsbl.2003.0151

Vidal, N., Branch, W. R., Pauwels, O. S. G., Hedges, S. B., Broadley, D. G., Wink, M., Cruaud, C., Joger, U. & Nagy, Z. T. 2008. Dissecting the major African snake radiation: a molecular phylogeny of the Lamprophiidae Fitzinger (Serpentes, Caenophidia). *Zootaxa*, **1945**, 51–66. doi:10.11646/zootaxa.1945.1.3

Vidal, N., Rage, J. C., Couloux, A. & Hedges, S. B. 2009. Snakes (Serpentes). Pp. 390–397 in S. Hedges and S. Kumar (eds) *The TimeTree of Life*. Oxford University Press, New York.

Vidal, N., Marin, J., Morini, M., Donnellan, S., Branch, W. R., Thomas, R., Vences, M., Wynn, A., Cruaud, C. & Hedges, S. B. 2010. Blindsnake evolutionary tree reveals long history on Gondwana. *Biology Letters*, **6**, 558–561 doi:10.1098/rsbl.2010.0220

Wake, M. H. 1986. The morphology of *ldiocranium russeli* (Amphibia: Gymnophiona), with comments on miniaturization through heterochrony. *Journal of Morphology*, **189**, 1–16.

Wake, M. H. 1993. The Skull as a Locomotor Organ. P. 216 in J. Hanken and B.K. Hall (eds) *The Skull: Functional and Evolutionary Mechanisms*. University of Chicago Press, Chicago.

Walls, G. L. 1940. Ophthalmological implications for the early history of the snakes. *Copeia*, **1940**(1), 1–8.

Walls, G. L. 1942. The vertebrate eye and its adaptive radiation. *Bulletin of the Cranbrook Institute of Science*, **19**, 1–785.

Watanabe, A., Fabre, A.-C., Felice, R. N., Maisano, J. A., Müller, J., Herrel, A. & Goswami, A. 2019. Ecomorphological diversification in squamates from conserved pattern of cranial integration. *Proceedings of the National Academy of Sciences*, **116**(29), 14688–14697. doi:10.1073/pnas.1820967116

Webb, J. K. & Shine, R. 1992. To find an ant: trail-following in Australian blindsnakes (Typhlopidae). *Animal Behaviour*, **43**, 941–948.

Webb, J. K. & Shine, R. 1993. Prey-size selection, gape limitation and predator vulnerability in Australian blindsnakes (Typhlopidae). *Animal Behaviour*, **45**, 1117–1126.

Webb, J. K., Shine, R., Branch, W. R. & Harlow, P. S. 2000. Life-history strategies in basal snakes: reproduction and dietary habits of the African thread snake *Leptotyphlops scutifrons* (Serpentes: Leptotyphlopidae). *Journal of Zoology*, **250**, 321–327.

Werneburg, I., Polachowski, K. M. & Hutchinson, M. N. 2015. Bony skull development in the Argus monitor (Squamata, Varanidae, *Varanus panoptes*) with comments on developmental timing and adult anatomy. *Zoology*, **118**, 255–280. doi:10.1016/j.zool.2015.02.004

Werneburg, I. & Sánchez-Villagra, M. R. 2015. Skeletal heterochrony is associated with the anatomical specializations of snakes among squamate reptiles. *Evolution*, **69**(1), 254–263. doi:10.1111/evo.12559

Werneburg, I., Esteve-Altava, B., Bruno, J., Ladeira, M. T. & Diogo, R. 2019. Unique skull network complexity of *Tyrannosaurus rex* among land vertebrates. *Scientific Reports*, **9**, 1520. doi:10.1038/s41598-018-37976-8

Wickham, H. 2016. ggplot2: elegant graphics for data analysis. Springer-Verlag, New York. https://ggplot2.tidyverse.org

Wiens, J. J. 2004. The role of morphological data in phylogeny reconstruction. *Systematic Biology*, **53**(4), 653–661. doi:10.1080/10635150490472959

Wiens, J. J. 2005. Can incomplete taxa rescue phylogenetic analyses from long-branch attraction? *Systematic Biology*, **54**(5), 731–742. doi:10.1080/10635150500234583

Wiens, J. J., Bonett, R. M. & Chippindale, P. T. 2005. Ontogeny discombobulates phylogeny: paedomorphosis and higher-level salamander relationships. *Systematic Biology*, **54**(1), 91–110. doi:10.1080/10635150590906037

Wiens, J. J., Brandley, M. C. & Reeder, T. W. 2006. Why does a trait evolve multiple times within a clade? Repeated evolution of snakelike body form in squamate reptiles. *Evolution*, **60**(1), 123–141. doi:10.1111/j.0014-3820.2006.tb01088.x

Wiens, J. J., Kuczynski, C. A., Smith, S. A., Mulcahy, D. G., Sites, J. W. J., Townsend, T. M. & Reeder, T. W. 2008. Branch lengths, support, and congruence: testing the phylogenomic approach with 20 nuclear loci in snakes. *Systematic Biology*, **57**(3), 420–431. doi:10.1080/10635150802166053

Wiens, J. J., Kuczynski, C. A., Townsend, T. M., Reeder, T. W., Mulcahy, D. G. & Sites, J. W. J. 2010. Combining phylogenomics and fossils in higher-level squamate reptile phylogeny: molecular data change the placement of fossil taxa. *Systematic Biology*, **59**(6), 674–688. doi:10.1093/sysbio/syq048

Wiens, J. J., Hutter, C. R., Mulcahy, D. G., Noonan, B. P., Townsend, T. M., Sites, J. W. J. & Reeder, T. W. 2012. Resolving the phylogeny of lizards and snakes (Squamata) with extensive sampling of genes and species. *Biology Letters*, **8**, 1043–1046. doi:10.1098/rsbl.2012.0703

Wilkinson, M. 1995. A comparison of two methods of character construction. *Cladistics*, **11**, 297–308.

Wilson, J. A., Mohabey, D. M., Peters, S. E. & Head, J. J. 2010. Predation upon hatchling dinosaurs by a new snake from the Late Cretaceous of India. *PLoS Biology*, **8**(3), e1000322. doi:10.1371/journal.pbio.1000322

Wright, A. M. & Hillis, D. M. 2014. Bayesian analysis using a simple likelihood model outperforms parsimony for estimation of phylogeny from discrete morphological data. *PLoS ONE*, **9**(10), e109210. doi:10.1371/journal.pone.0109210

Yan, J., Li, H. & Zhou, K. 2008. Evolution of the mitochondrial genome in snakes: gene rearrangements and phylogenetic relationships. *BMC Genomics*, **9**, 569. doi:10.1186/1471-2164-9-569

Yi, H. & Norell, M. A. 2015. The burrowing origin of modern snakes. *Science Advances*, **1**(10), e1500743. doi:10.1126/sciadv.1500743

Yip, A. M. & Horvath, S. 2006. The generalized topological overlap matrix for detecting modules in gene networks. *BIOCOMP*, **00**, 1–19.

Yip, A. M. & Horvath, S. 2007. Gene network interconnectedness and the generalized topological overlap measure. *BMC Bioinformatics*, **8**, 22. doi:10.1186/1471-2105-8-22

Young, B. A. 1987. The cranial nerves of three species of sea snakes. *Canadian Journal of Zoology/Revue Canadienne de Zoologie*, **65**, 2236–2240.

Young, B. A. 1989. Ontogenetic changes in the feeding system of the red-sided garter snake, *Thamnophis sirtalis parietalis*. I. Allometric analysis. *Journal of Zoology*, **218**, 365–381.

Zaher, H. 1998. The phylogenetic position of *Pachyrhachis* within snakes (Squamata, Lepidosauria). *Journal of Vertebrate Paleontology*, **18**(1), 1–3. doi:10.1080/02724634.1998.10011029

Zaher, H. & Rieppel, O. 1999a. The phylogenetic relationships of *Pachyrhachis problematicus*, and the evolution of limblessness in snakes (Lepidosauria, Squamata). *Comptes Rendus de l'Académie des Sciences - Series IIA - Sciences de la Terre et des planètes/Earth and Planetary Science*, **329**, 831–837.

Zaher, H. & Rieppel, O. 1999b. Tooth implantation and replacement in squamates, with special reference to mosasaur lizards and snakes. *American Museum Novitates*, **3271**, 1–19.

Zaher, H. & Rieppel, O. 2002. On the phylogenetic relationships of the Cretaceous snakes with legs, with special reference to *Pachyrhachis problematicus* (Squamata, Serpentes). *Journal of Vertebrate Paleontology*, **22**(1), 104–109.

Zaher, H., Grazziotin, F. G., Cadle, J. E., Murphy, R. W., Moura-Leite, J. C. d. & Bonatto, S. L. 2009. Molecular phylogeny of advanced snakes (Serpentes, Caenophidia) with an emphasis on South American Xenodontines: a revised classification and descriptions of new taxa. *Papeis avulsos de zoologia*, **49**(11), 115–153.

Zaher, H. & Scanferla, C. A. 2012. The skull of the Upper Cretaceous snake *Dinilysia patagonica* Smith-Woodward, 1901, and its phylogenetic position revisited. *Zoological Journal of the Linnean Society*, **164**, 194–238. doi:10.1111/j.1096-3642.2011.00755.x

Zaher, H., Murphy, R. W., Arredondo, J. C., Graboski, R., Machado-Filho, P. R., Mahlow, K., Montingelli, G. G., Quadros, A. B., Orlov, N. L., Wilkinson, M., Zhang, Y.-P. & Grazziotin, F. G. 2019. Large-scale molecular phylogeny, morphology, divergence-time

estimation, and the fossil record of advanced caenophidian snakes (Squamata: Serpentes). *PLoS ONE*, **14**(5), e0216148. doi:10.1371/journal. pone.0216148

Zehr, D. R. 1962. Stages in the normal development of the Common Garter Snake, *Thamnophis sirtalis sirtalis*. *Copeia*, **1962**(2), 322–329.

Zheng, Y. & Wiens, J. J. 2016. Combining phylogenomic and supermatrix approaches, and a time-calibrated phylogeny for squamate reptiles (lizards and snakes) based on 52 genes and 4162 species. *Molecular Phylogenetics and Evolution*, **94**, 537–547. doi:10.1016/j.ympev.2015.10.009

Ziermann, J. M., Boughner, J. C., Esteve-Altava, B. & Diogo, R. 2021. Anatomical comparison across heads, fore- and hindlimbs in mammals using network models. *Journal of Anatomy*, **00**, 1–20. doi:10.1111/joa.13409

APPENDICES

SUPPLEMENTARY INFORMATION: CHAPTER ONE

APPENDIX 1.1. Sources of micro-CT scan data

All micro-CT scans of MCZ specimens were performed by C.S. and are available on MorphoSource.org. Copyright of all MCZ scans belongs to the Museum of Comparative Zoology, Harvard University, and the associated raw digital media are © President and Fellows of Harvard College, 2020, all rights reserved. These are used herein with permission.

Several scans were obtained from DigiMorph.org, as provided by the University of Texas High-Resolution X-ray CT Facility (UTCT). Scans of YPM 14378 and YPM 14376 were originally collected under NSF grants DEB-0132227, EF-0334961, and IIS-9874781. Scans of FMNH 58299, FRIM 0026, FMNH 216257, USNM 12378, FMNH 148589, FMNH 22468, FMNH 95184, and UMMZ 190285 were collected under NSF grants IIS-0208675 and EF-0334961. Scans of USNM 204078, FMNH 60958, FMNH 62204, FMNH 63117, FMNH 117833, FMNH 104800, and FMNH 148900 were collected under NSF grant EF-0334961. Scans of TNHC 60638 and YPM 12871 were collected under NSF grants EF-0334961 and IIS-9874781. Scans of TMM M-10006, YPM 6057, and TNHC 18483 were collected under NSF grant IIS-9874781. Scans of TNHC 62769 were collected under NSF grant IIS-0208675. Scans of FMNH 167048, FMNH 250439, and UTA 50569 were also obtained from DigiMorph. Scans of FMNH 179335, FMNH 30522, FMNH 58322, FMNH 166644, FMNH 62248, FMNH 31162, FMNH 135284, FMNH 244371, FMNH 207669, USNM 289090, and USNM 59918 were examined using images provided online by DigiMorph.

Several other scans were downloaded from MorphoSource, Duke University. The University of Michigan Museum of Zoology provided access to the data for UMMZ 201901 (M39211-70987) and UMMZ 174763 (M45443-82778), the collection of which was funded by oVert TCN under NSF DBI-1701714 and NSF DBI-1701713. The Florida Museum of Natural History at the University of Florida provided access to the data for UF 33488 (M33644-62342), UF 78397 (M39984-72220), and UF 103268 (M24774-48786), the collection of which was funded by oVert TCN under NSF DBI-1701714. The University of Kansas Center for Research Inc provided access to the data for KUH 125976 (M41676-75015), the collection of which was funded by oVert TCN under NSF DBI-1701714, NSF DBI-1701713, and NSF DBI-1701932. The Field Museum of Natural History provided access to the data for FMNH 264702 (M27566-52993), the collection of which was funded by oVert TCN under NSF DBI-1701714 and NSF

DBI-1702421. oUTCT provided access to the data for FMNH 259340 (M53815-97478), FMNH 195924 (M53075-96074), FMNH 22847 (M54489-98383), FMNH 31182 (M54499-98393), TCWC 45501 (M62793-113753), CAS 126478 (M54497-98391), CAS 134753 (M54498-98392), CAS 26937 (M54605-98507), FMNH 31774 (M54687-98600), FMNH 109462 (M54697-98610), and FMNH 128304 (M54673-98586), originally appearing in Gauthier *et al.* (2012), with data collection funded by NSF EF-0334961 and data upload to MorphoSource funded by DBI-1902242. Mark D. Scherz provided access to the data for ZSM 2194/2007 (M43873-79510), ZSM 2213/2007 (M43874-79511), and ZSM 2216/2007 (M43875-79512), originally appearing in Chretien *et al.* (2019).

Finally, scans from the AMNH, AMS, QM, and SAMA collections were provided courtesy of A. Palci, and scans of UAMZ specimens were provided courtesy of lab colleagues.

References: Supplementary Information – Chapter One

Chretien, J., Wang-Claypool, C. Y., Glaw, F. & Scherz, M. D. 2019. The bizarre skull of *Xenotyphlops* sheds light on synapomorphies of Typhlopoidea. *Journal of Anatomy*, **234**, 637–655. doi:10.1111/joa.12952

Gauthier, J. A., Kearney, M., Maisano, J. A., Rieppel, O. & Behlke, A. D. B. 2012. Assembling the squamate tree of life: perspectives from the phenotype and the fossil record. *Bulletin of the Peabody Museum of Natural History*, **53**, 3–308. doi:10.3374/014.053.0101

SUPPLEMENTARY INFORMATION: CHAPTER TWO

Supplementary Information for this chapter (listed below) is available via the associated publication and its Supporting Information, available online: https://onlinelibrary.wiley.com/doi/10.1111/joa.13295

FIGURES S2.1–S2.23. Surface meshes of individual skull elements of *Atractaspis irregularis* (FMNH 62204), embedded in 3D PDFs

To view each mesh, open the file in Adobe Acrobat and click on the model to activate it. Further imagery of this specimen is available on DigiMorph.org (http://digimorph.org/specimens/Atractaspis_irregularis/)

APPENDIX 2.1. Complete HRXCT scan parameters

APPENDIX 2.2. Overview of skeletal pathologies of FMNH 62204

SUPPLEMENTARY INFORMATION: CHAPTER THREE

Micro-CT scans performed for this study are available on MorphoSource.org. Supplementary Information for this chapter (listed below) is available via the associated publication and its Supporting Information, available online: https://anatomypubs.onlinelibrary.wiley.com/doi/10.1002/ar.24630

APPENDIX 3.1. Phylogeny and matrix used for ancestral state reconstructions

SUPPLEMENTARY INFORMATION: CHAPTER FOUR

FIGURES S4.1–S4.57. Dendrograms reflecting the anatomical network structure and modular composition of each taxon analyzed in Chapter Four

Q-modules are indicated by Q_{max} (represented by the red dotted line). S-modules are indicated by black ($p < 0.001$), grey ($0.001 \leq p < 0.01$), or white ($0.01 \leq p < 0.05$) circles. The palatomaxillary elements are indicated in italicized boldface.

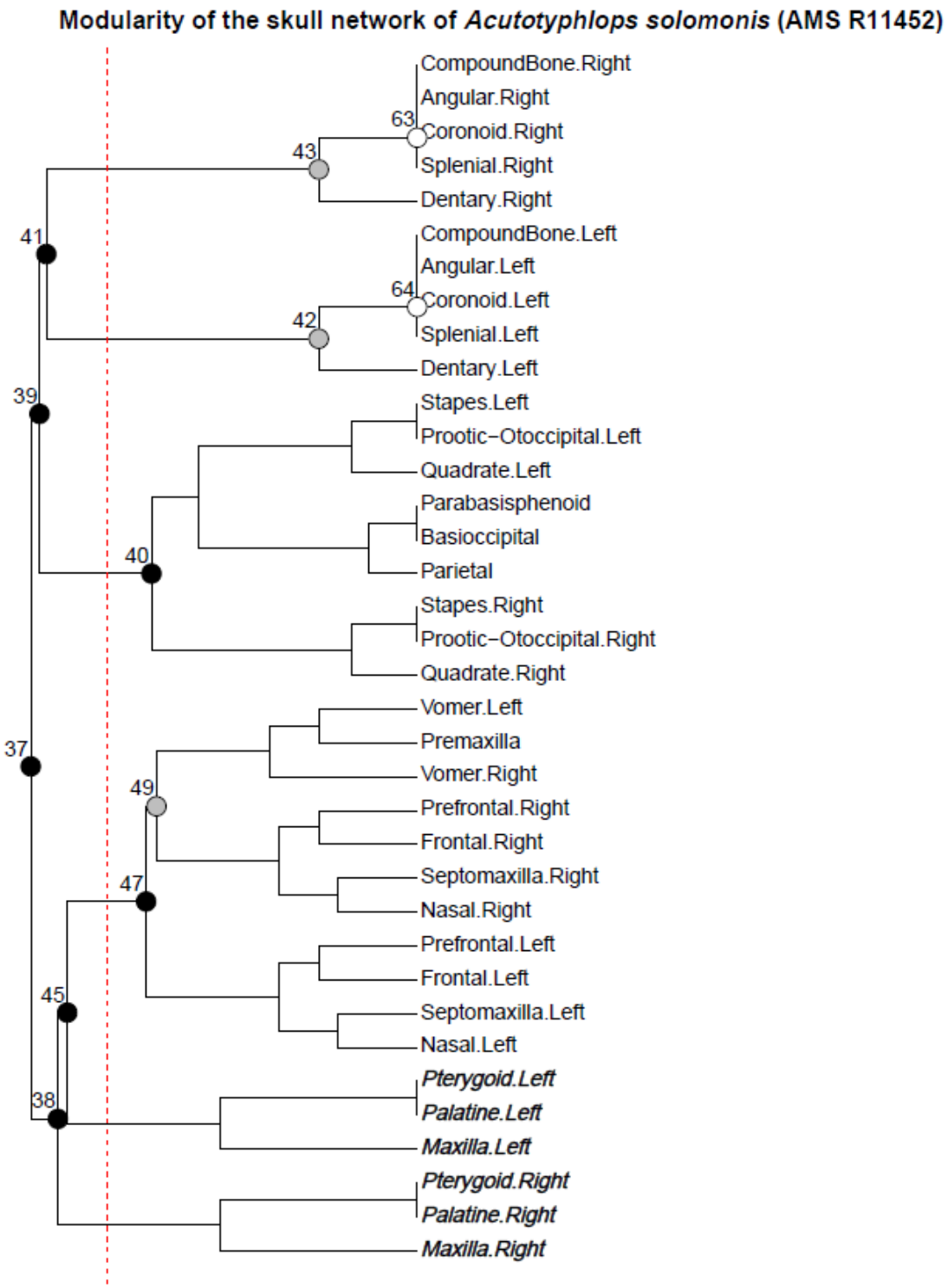

FIGURE S4.1. Modularity of the skull network of *Acutotyphlops solomonis* (AMS R11452)

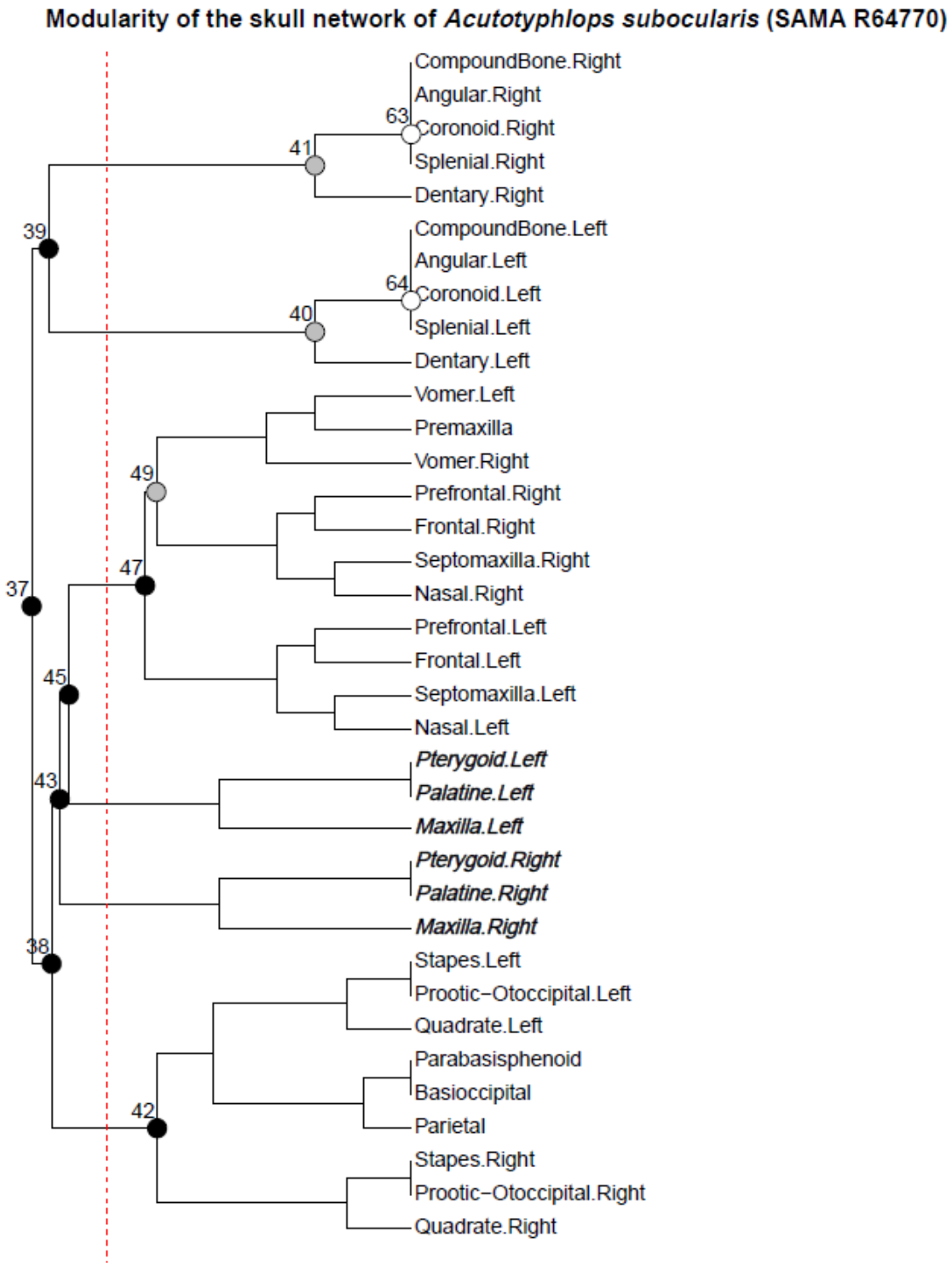

FIGURE S4.2. Modularity of the skull network of *Acutotyphlops subocularis* (SAMA R64770)

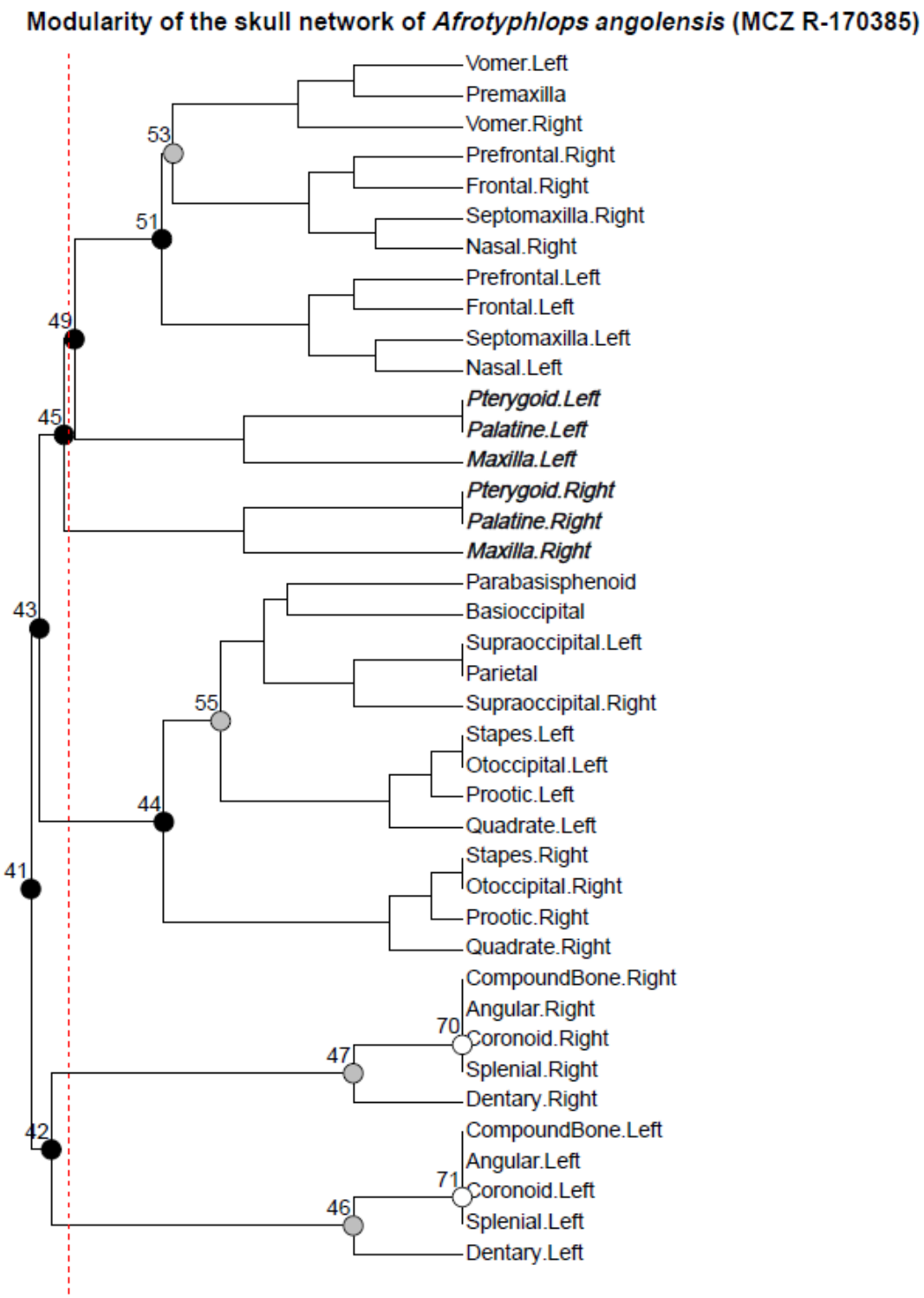

FIGURE S4.3. Modularity of the skull network of *Afrotyphlops angolensis* (MCZ R-170385)

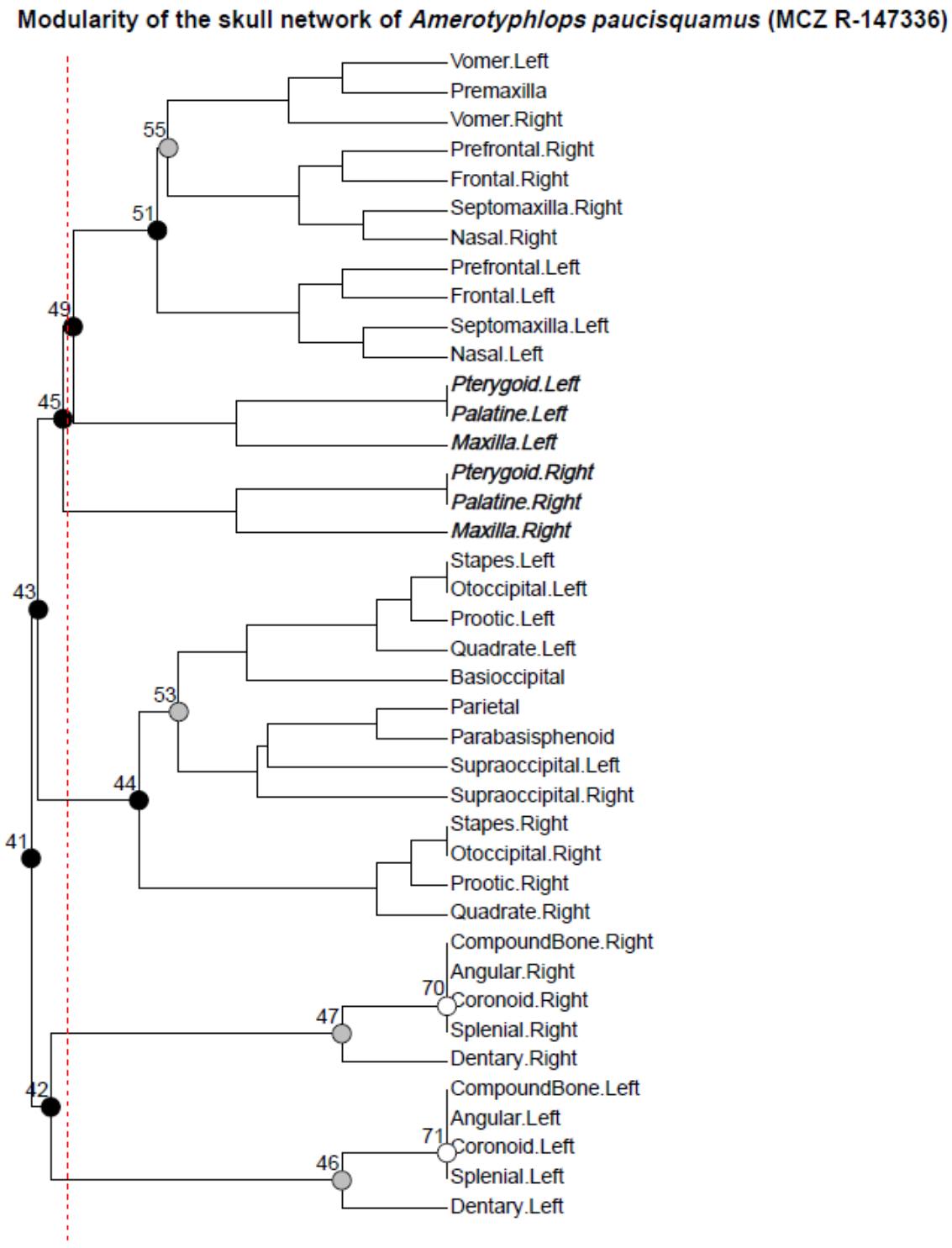

FIGURE S4.4. Modularity of the skull network of *Amerotyphlops paucisquamus* (MCZ R-147336)

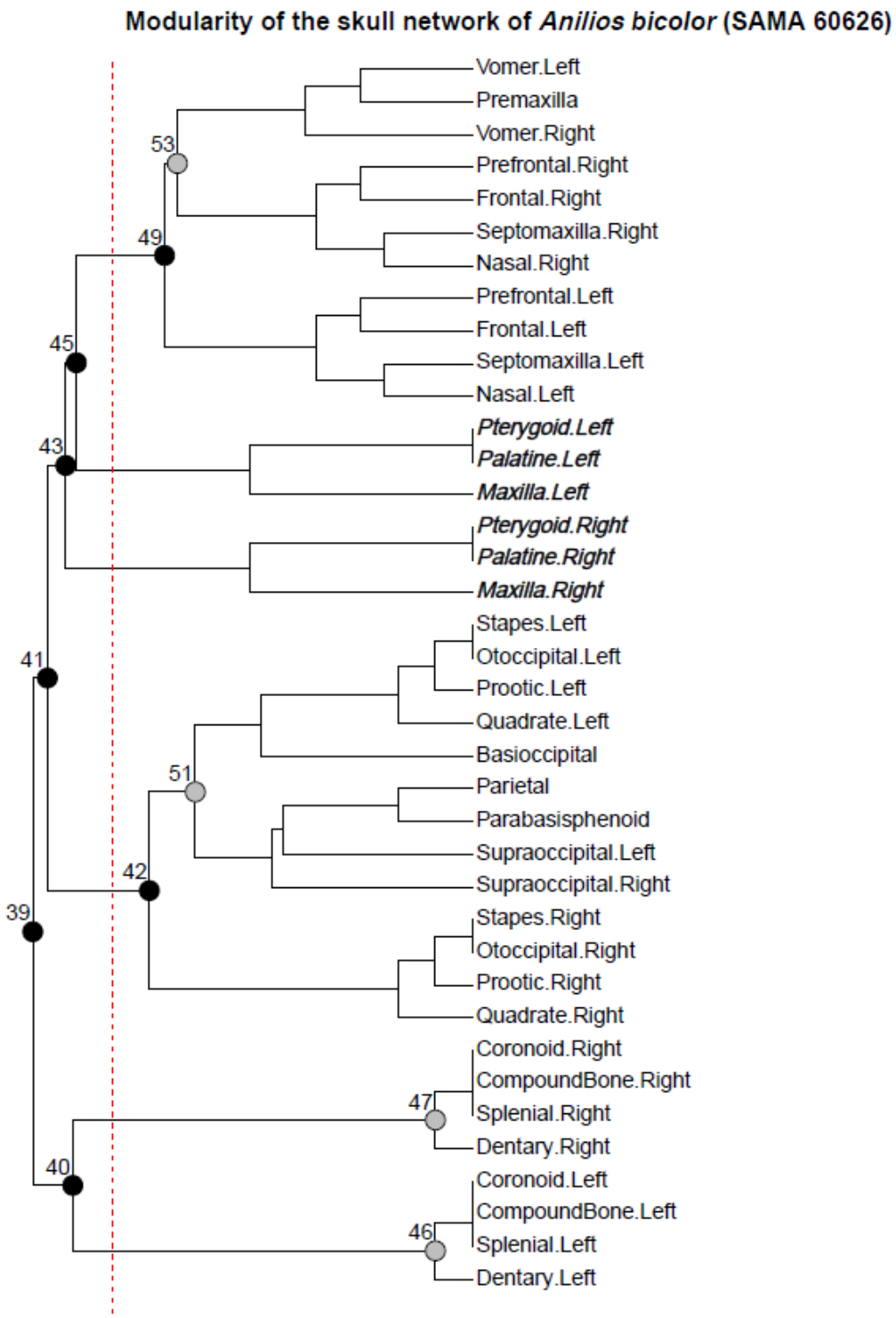

FIGURE S4.5. Modularity of the skull network of *Anilios bicolor* (SAMA 60626)

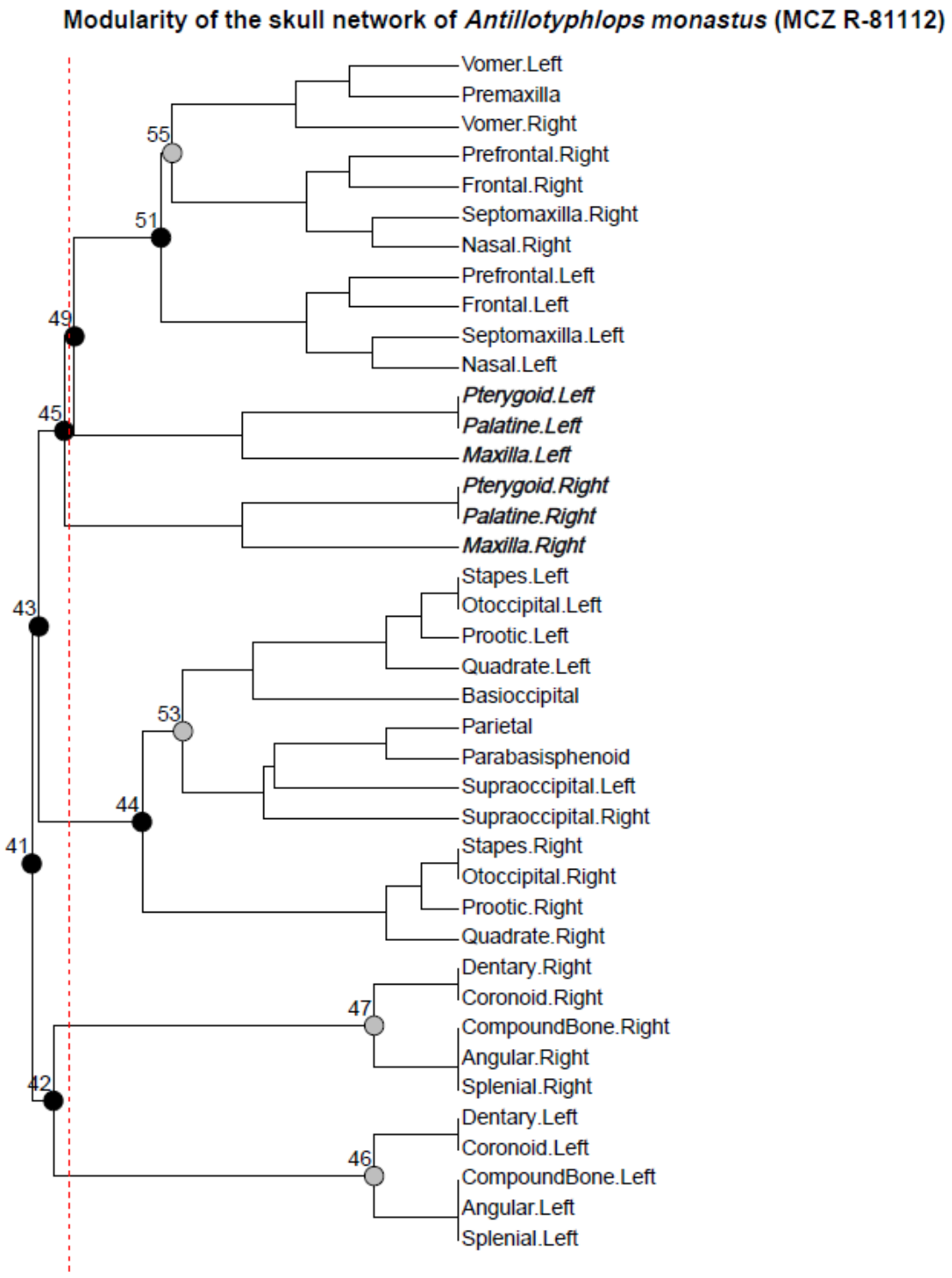

FIGURE S4.6. Modularity of the skull network of *Antillotyphlops monastus* (MCZ R-81112)

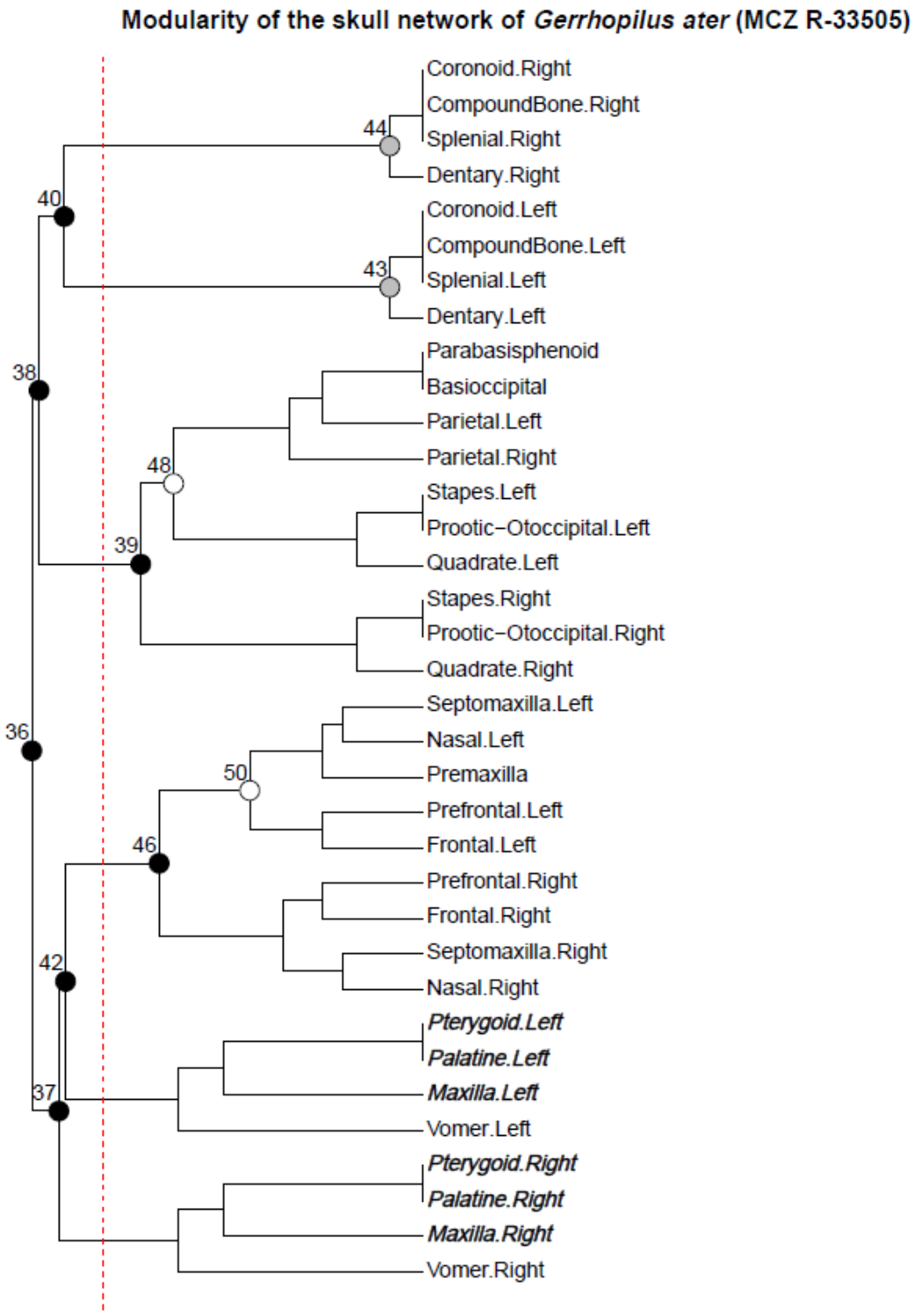

FIGURE S4.7. Modularity of the skull network of *Gerrhopilus ater* (MCZ R-33505)

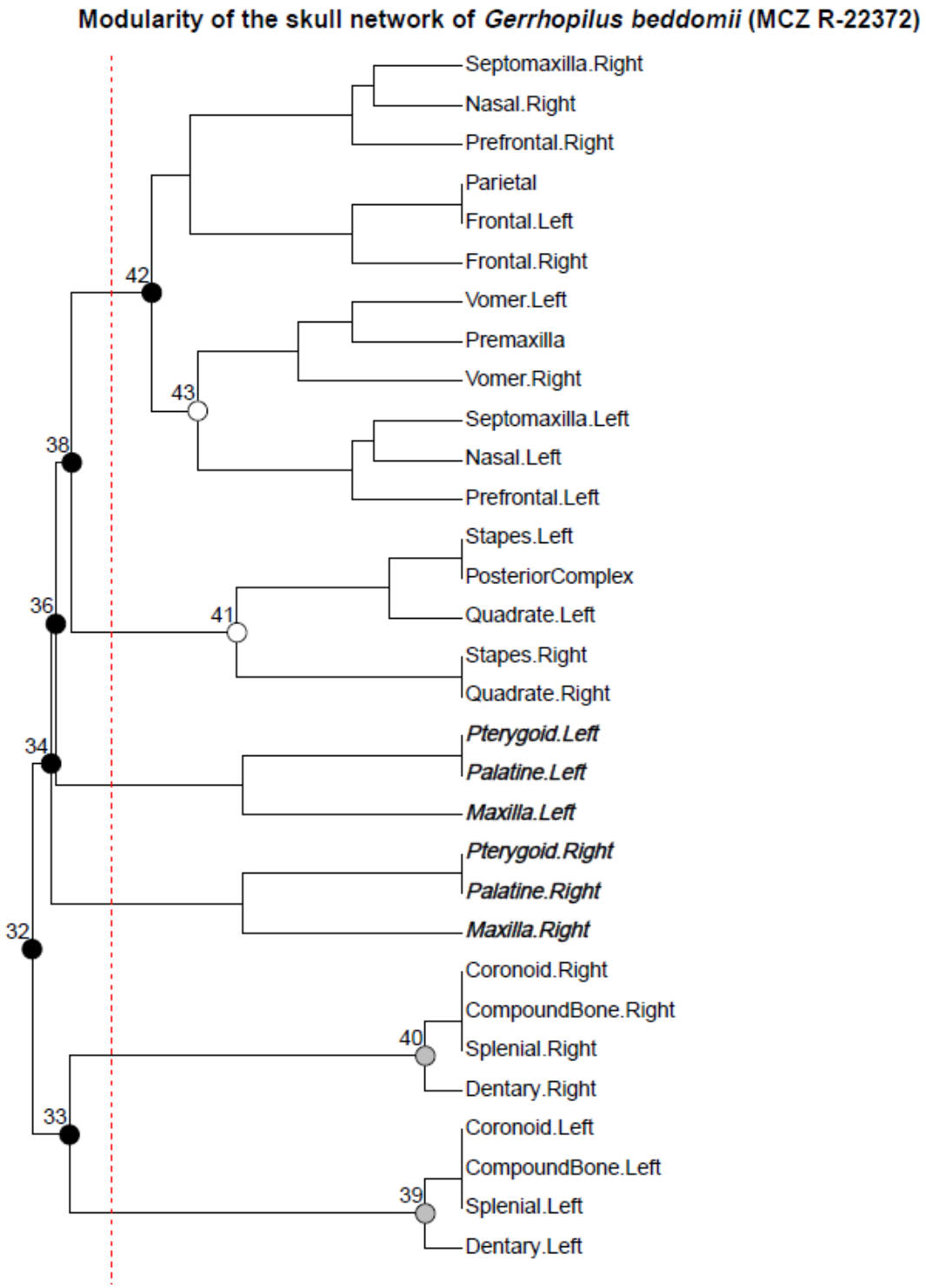

FIGURE S4.8. Modularity of the skull network of *Gerrhopilus beddomii* (MCZ R-22372)

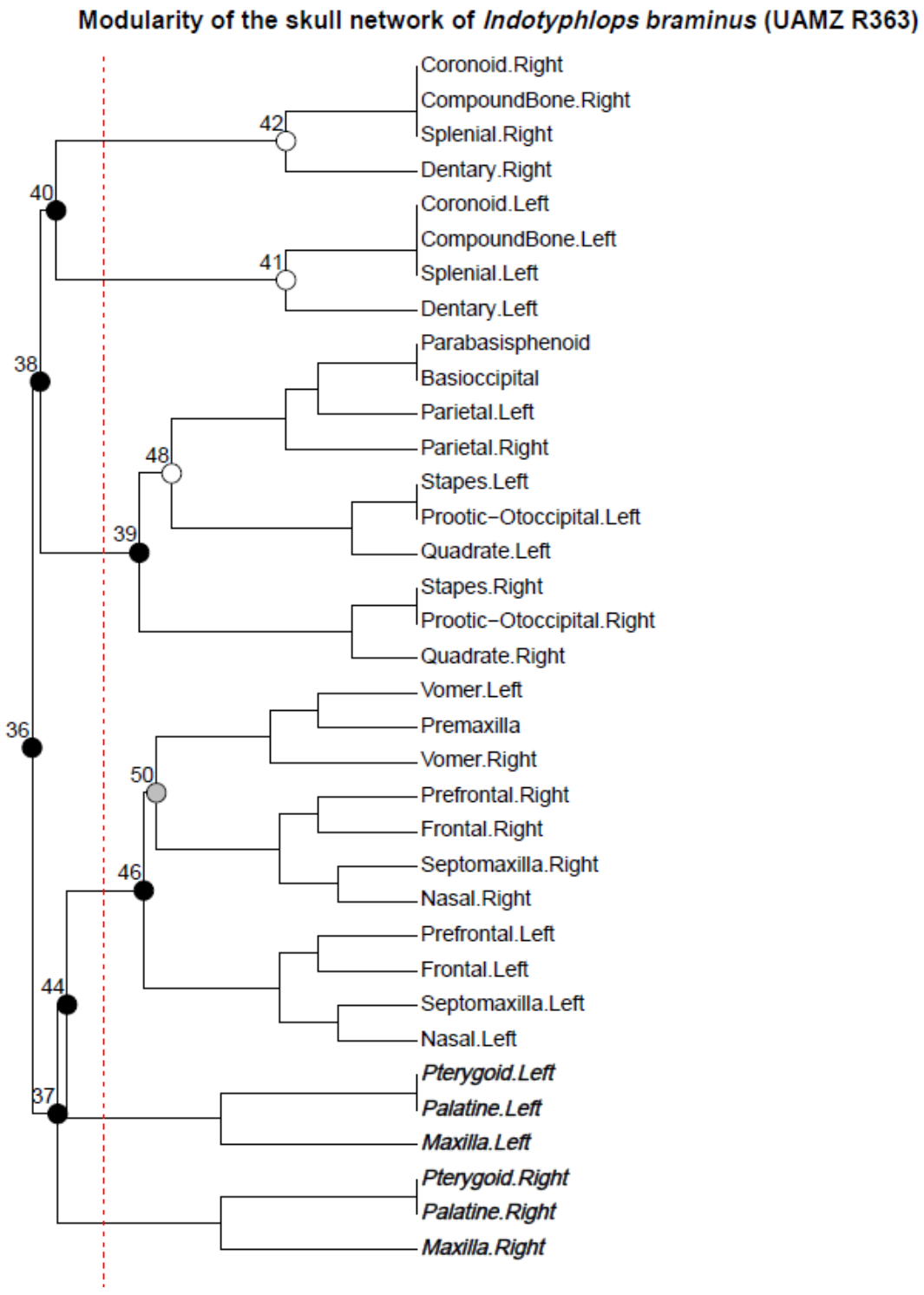

FIGURE S4.9. Modularity of the skull network of *Indotyphlops braminus* (UAMZ R363)

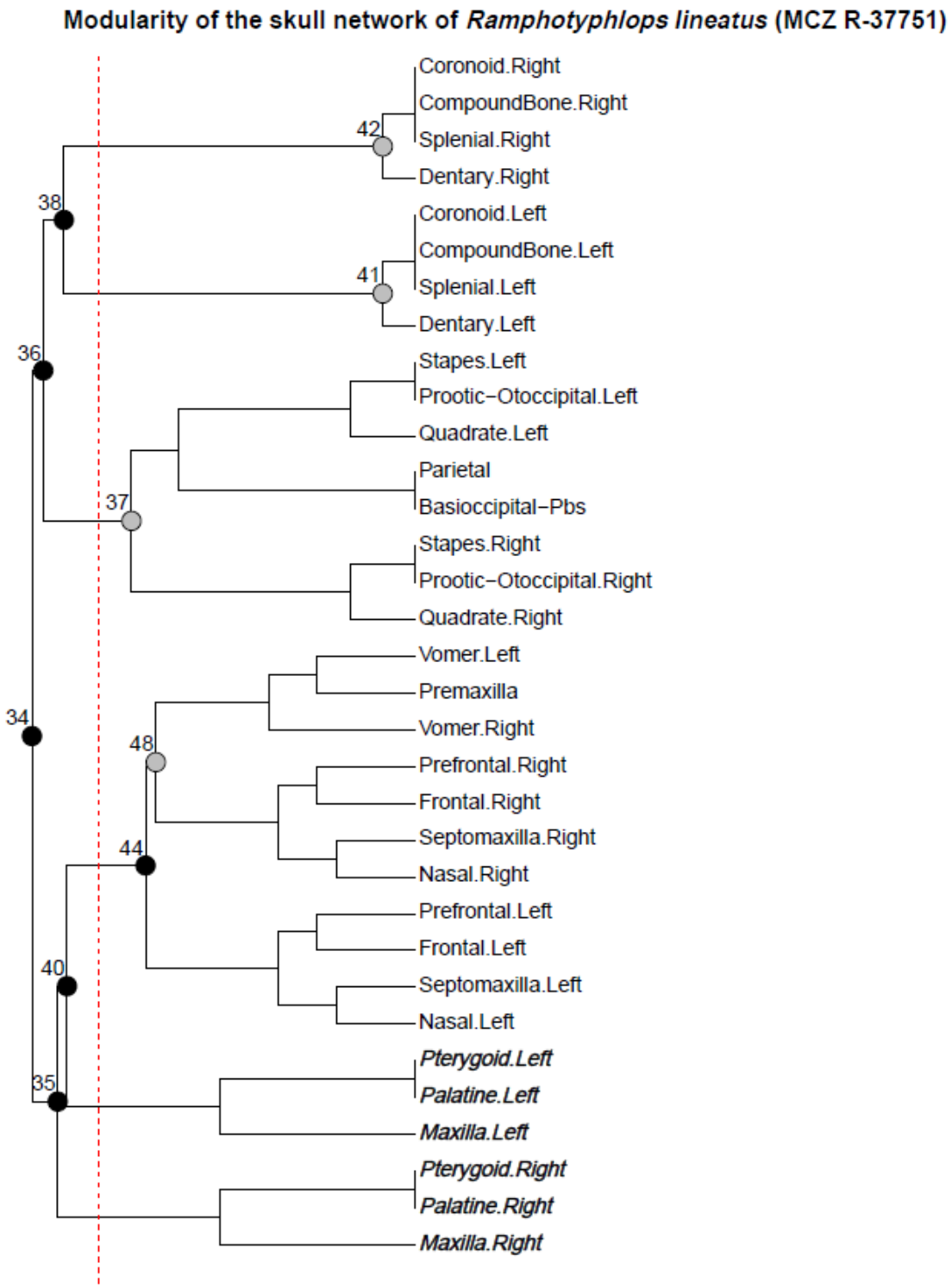

FIGURE S4.10. Modularity of the skull network of *Ramphotyphlops lineatus* (MCZ R-37751)

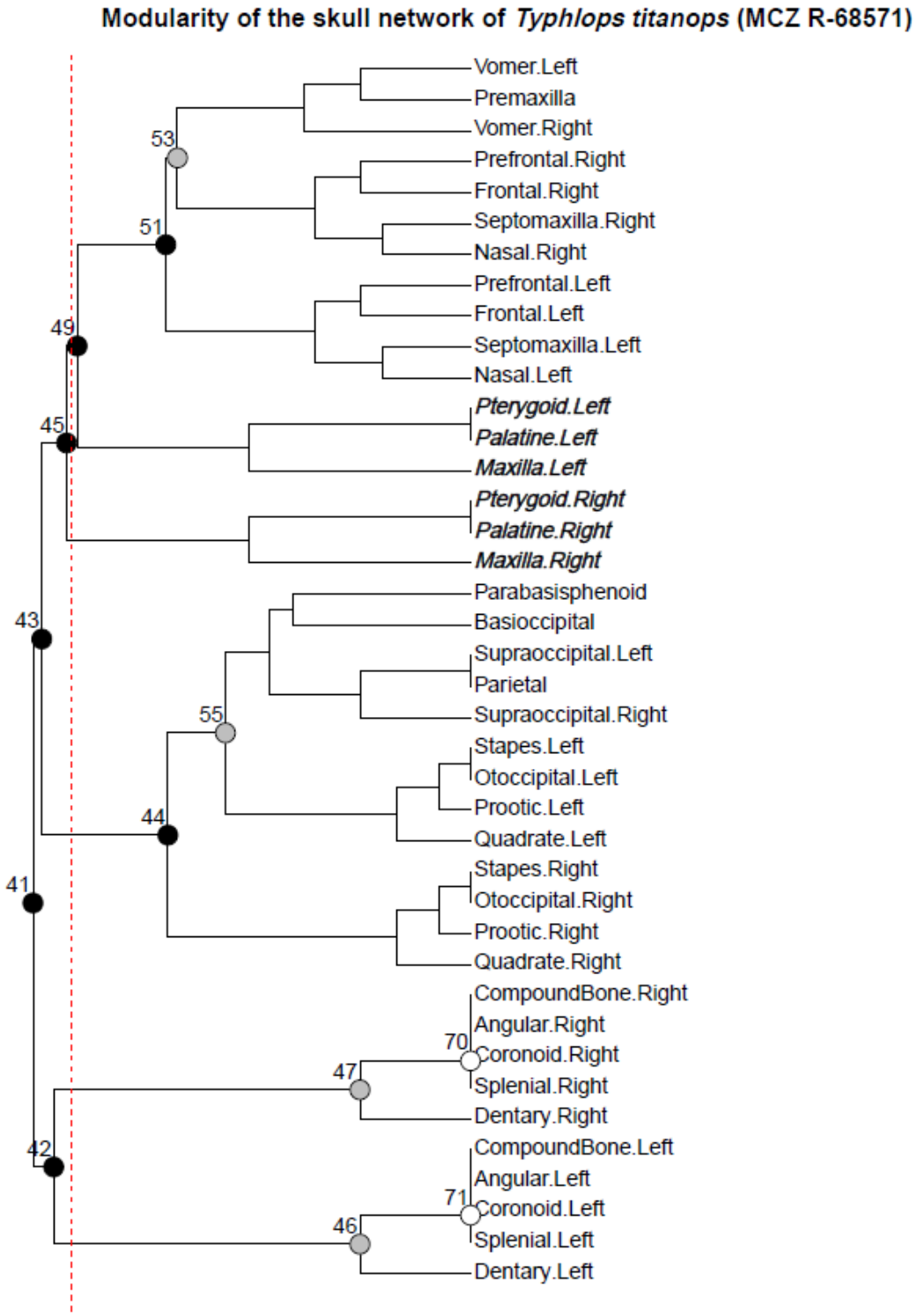

FIGURE S4.11. Modularity of the skull network of *Typhlops titanops* (MCZ R-68571)

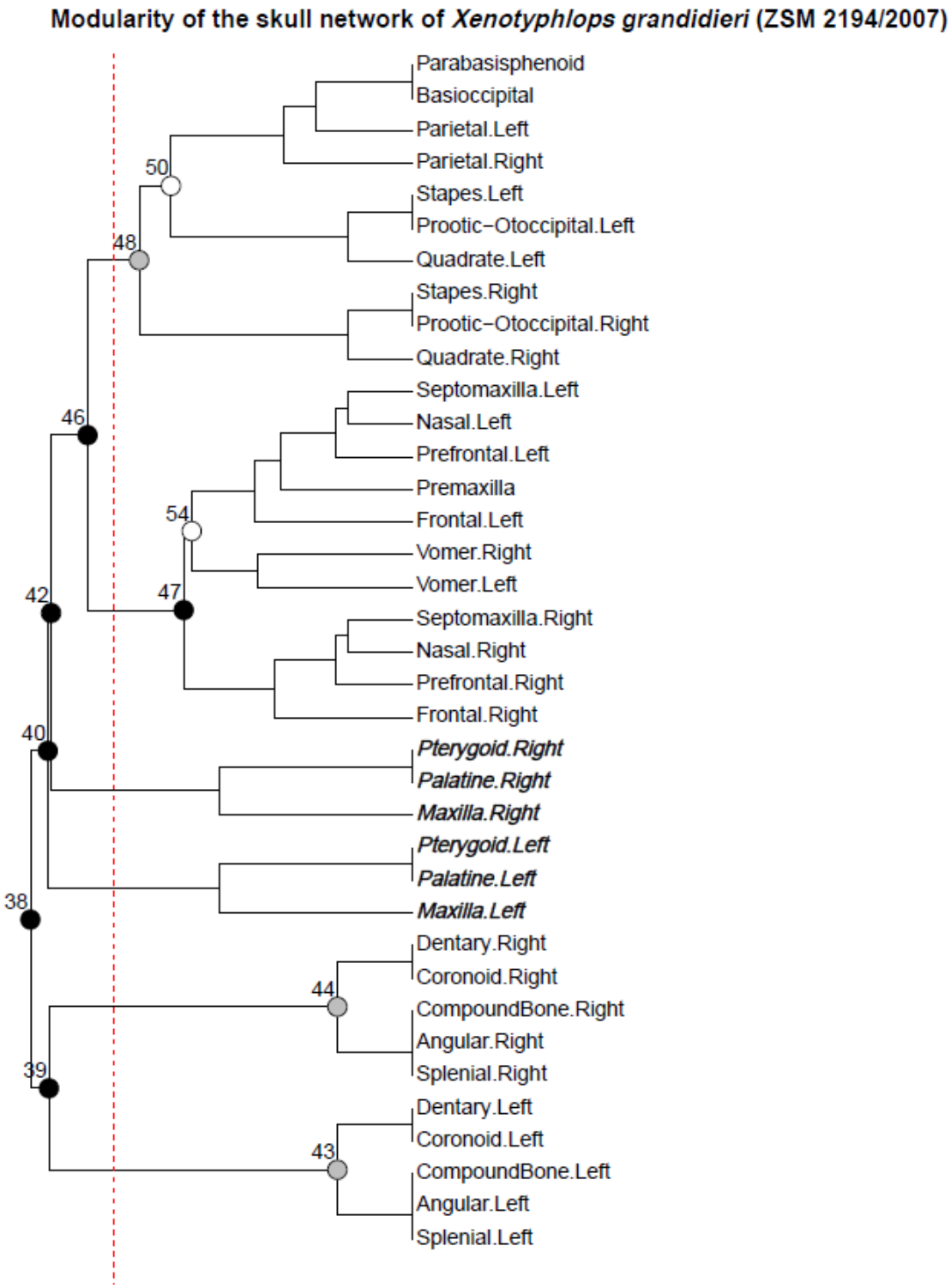

FIGURE S4.12. Modularity of the skull network of *Xenotyphlops grandidieri* (ZSM 2194/2007)

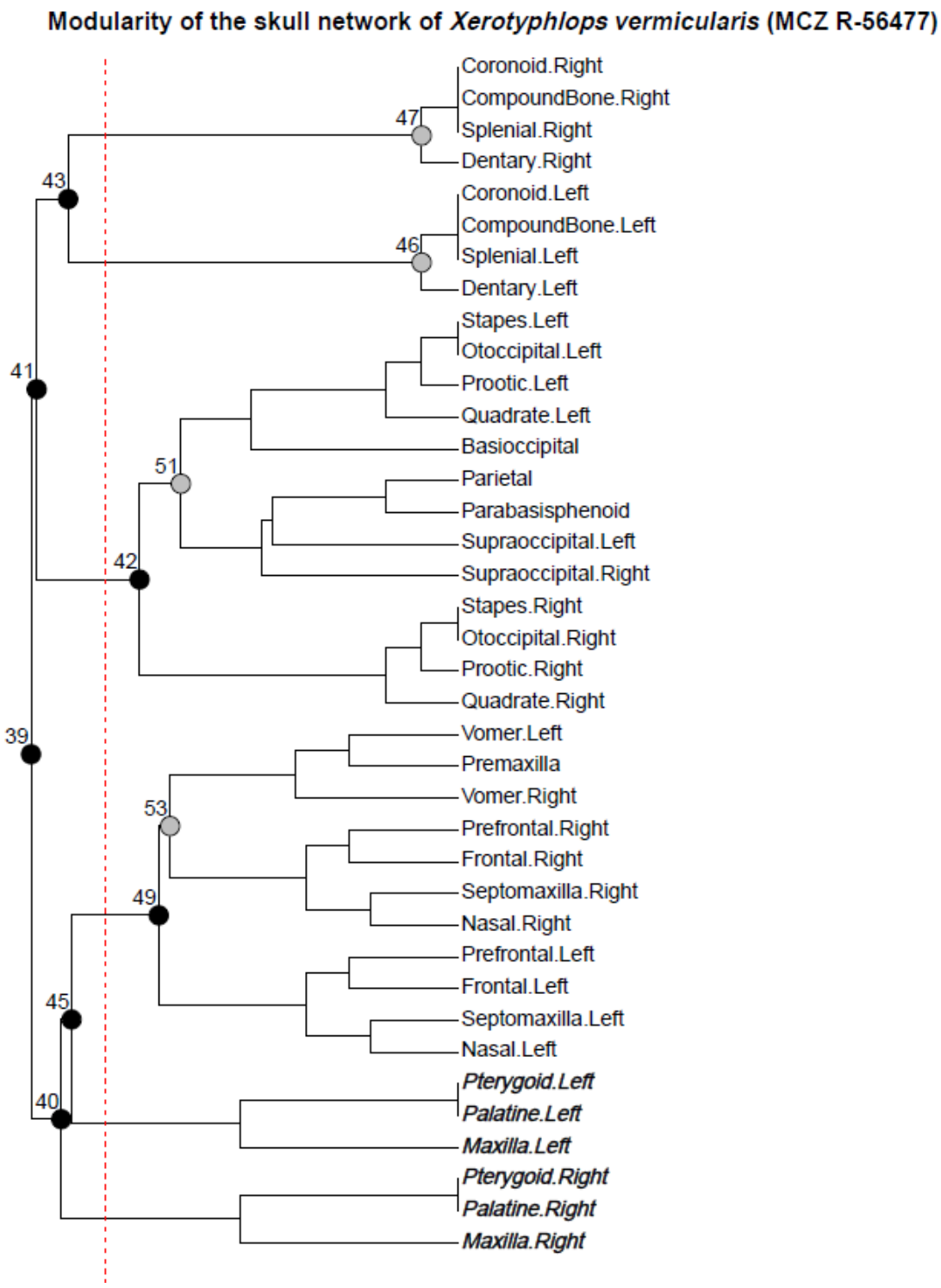

FIGURE S4.13. Modularity of the skull network of *Xerotyphlops vermicularis* (MCZ R-56477)

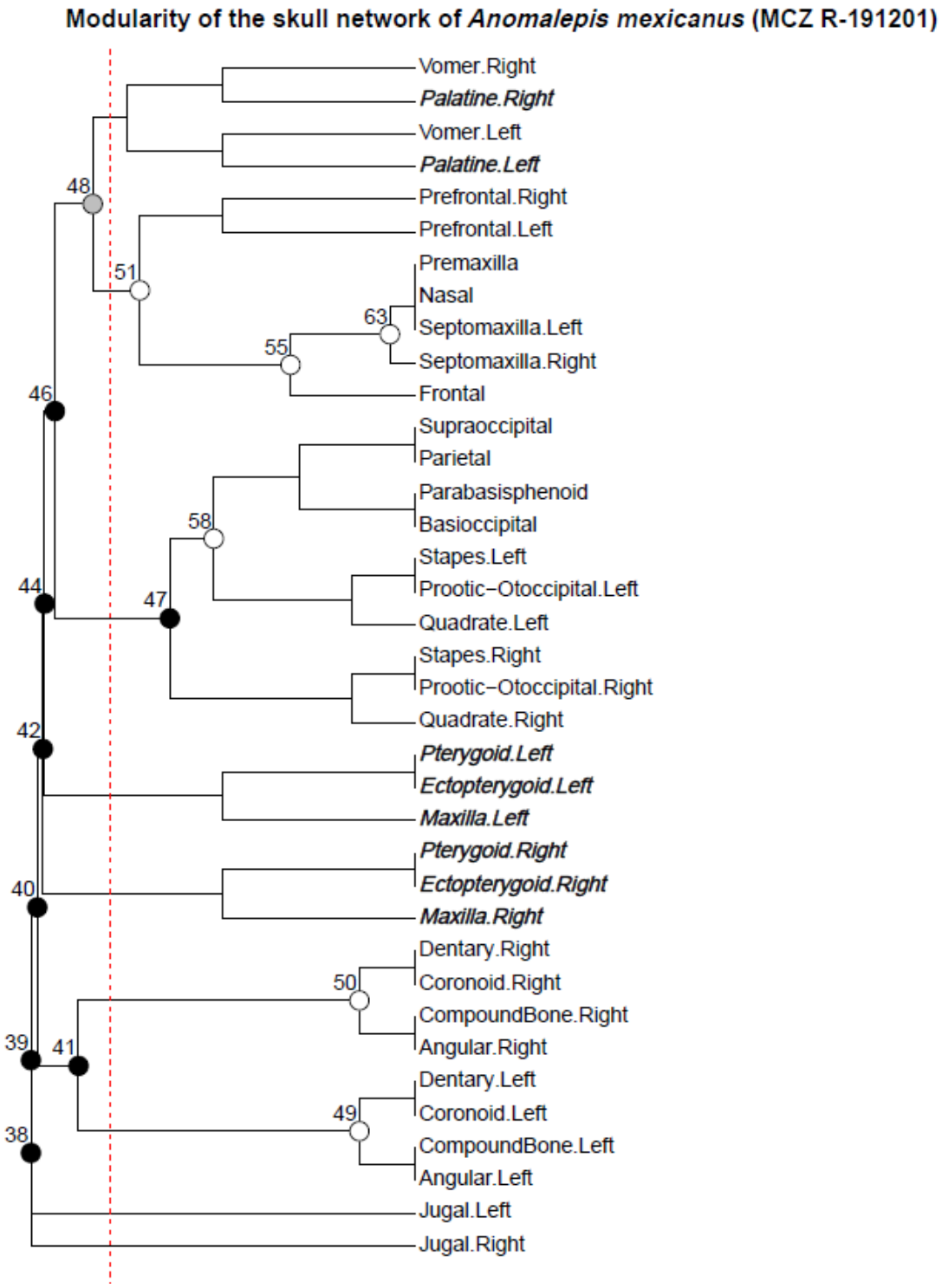

FIGURE S4.14. Modularity of the skull network of *Anomalepis mexicanus* (MCZ R-191201)

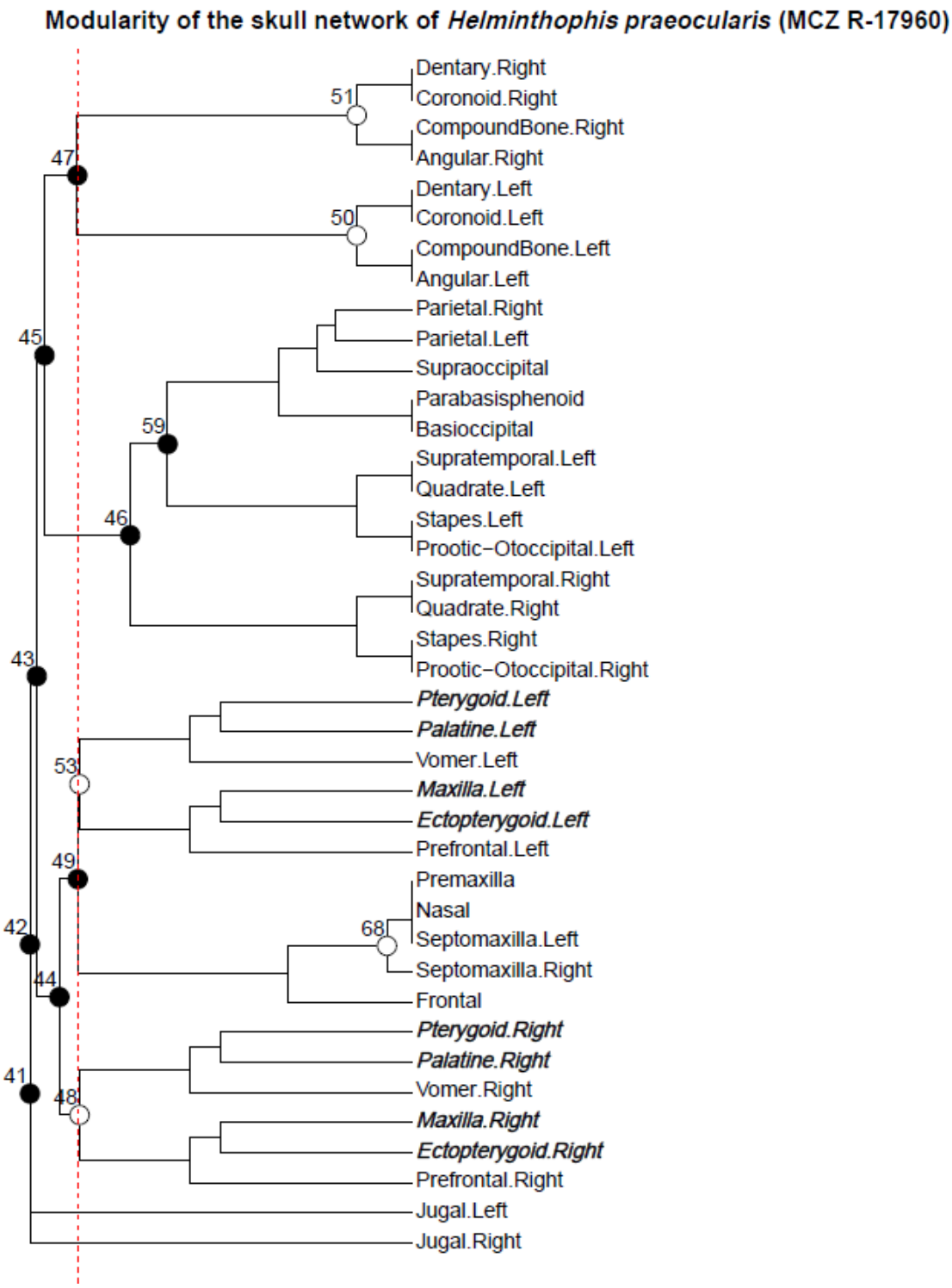

FIGURE S4.15. Modularity of the skull network of *Helminthophis praeocularis* (MCZ R-17960)

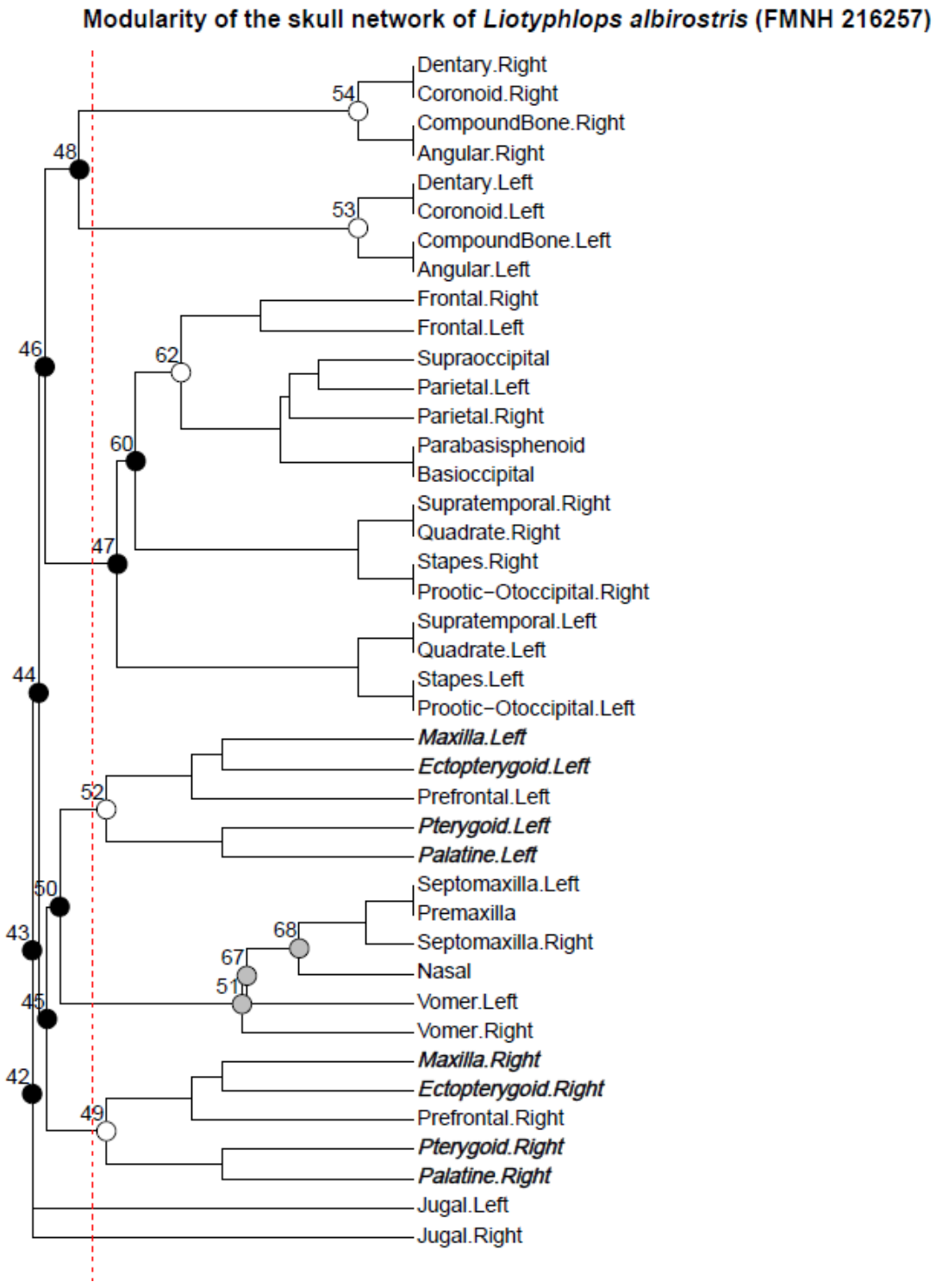

FIGURE S4.16. Modularity of the skull network of *Liotyphlops albirostris* (FMNH 216257)

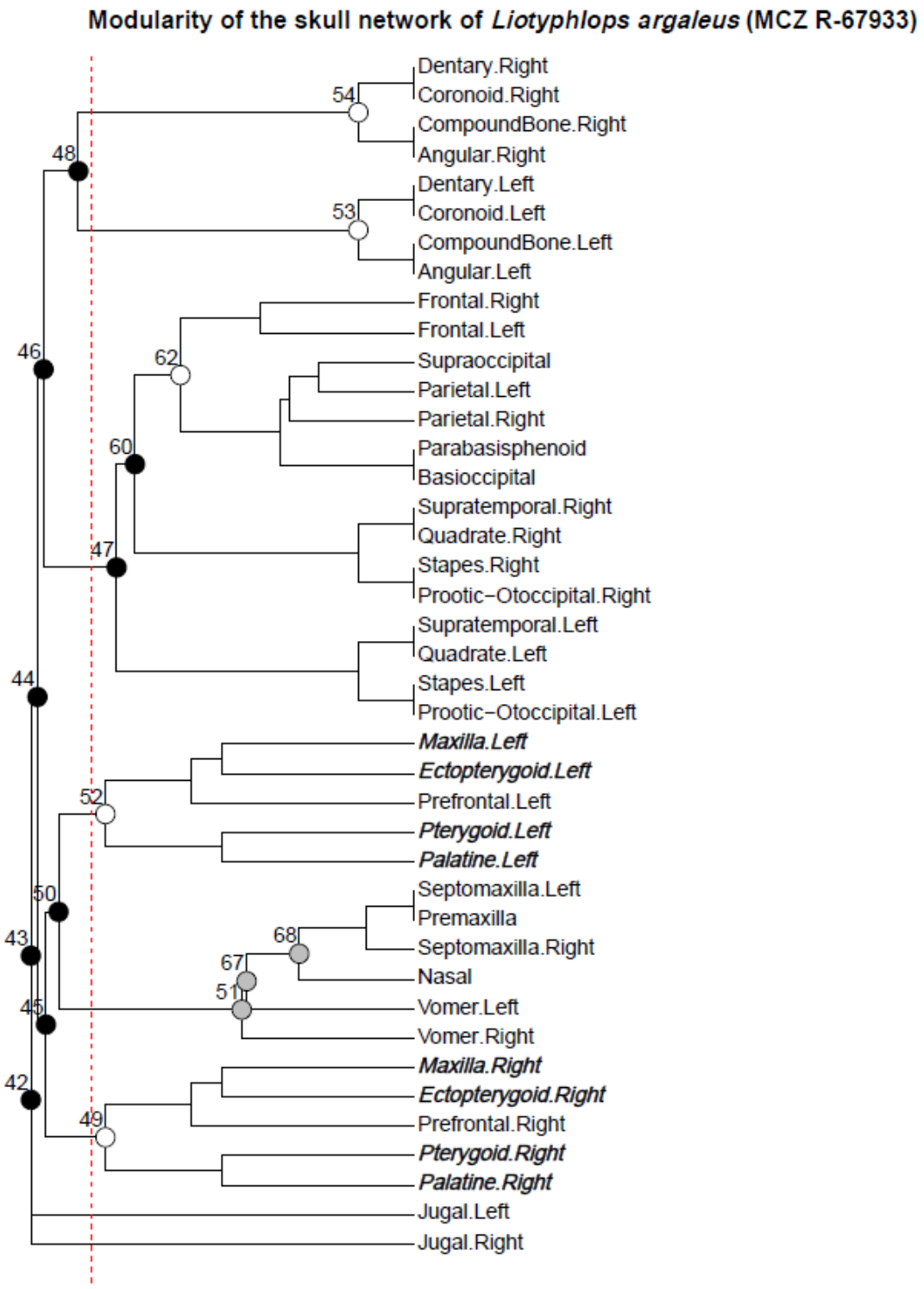

FIGURE S4.17. Modularity of the skull network of *Liotyphlops argaleus* (MCZ R-67933)

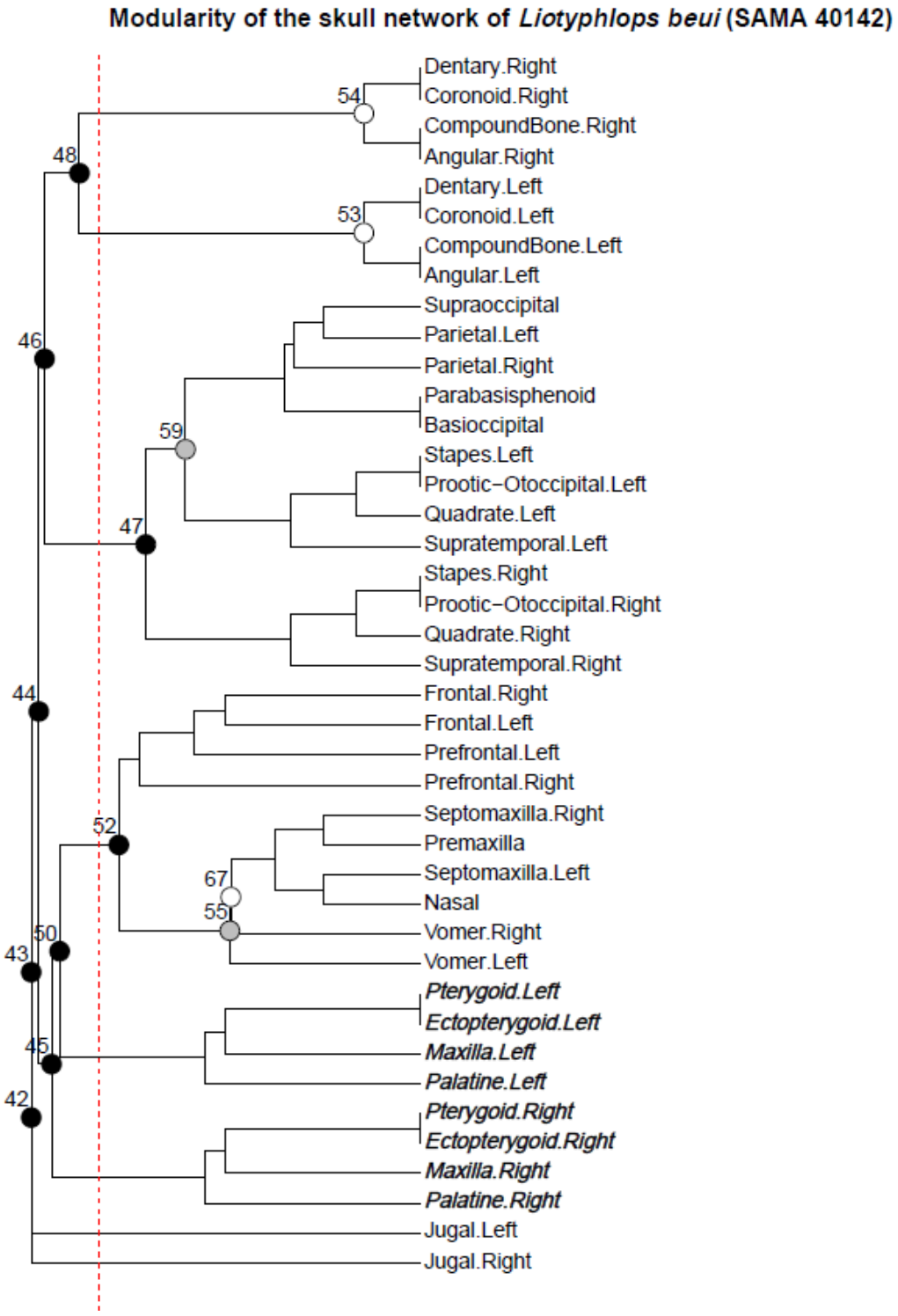

FIGURE S4.18. Modularity of the skull network of *Liotyphlops beui* (SAMA 40142)

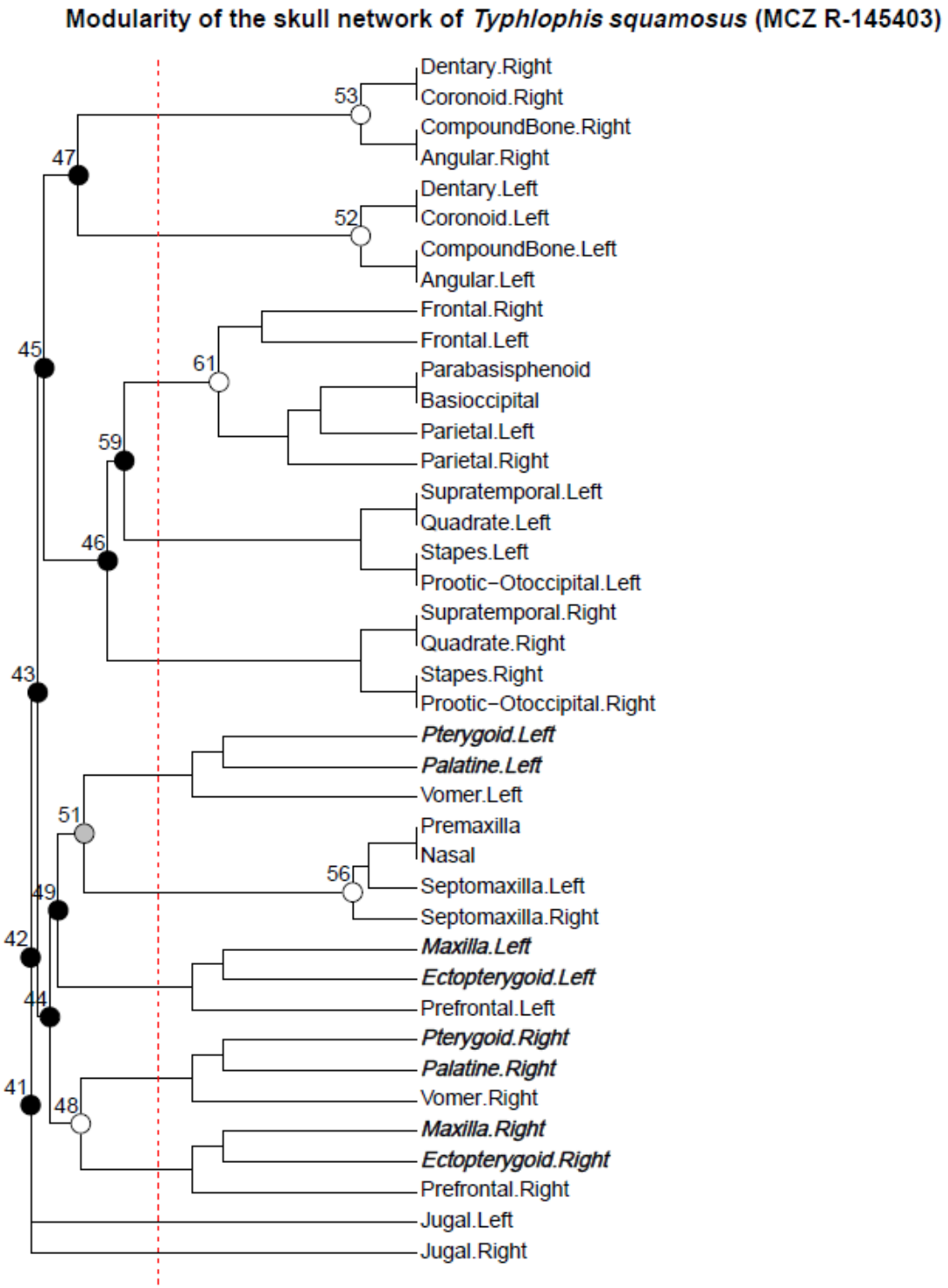

FIGURE S4.19. Modularity of the skull network of *Typhlophis squamosus* (MCZ R-145403)

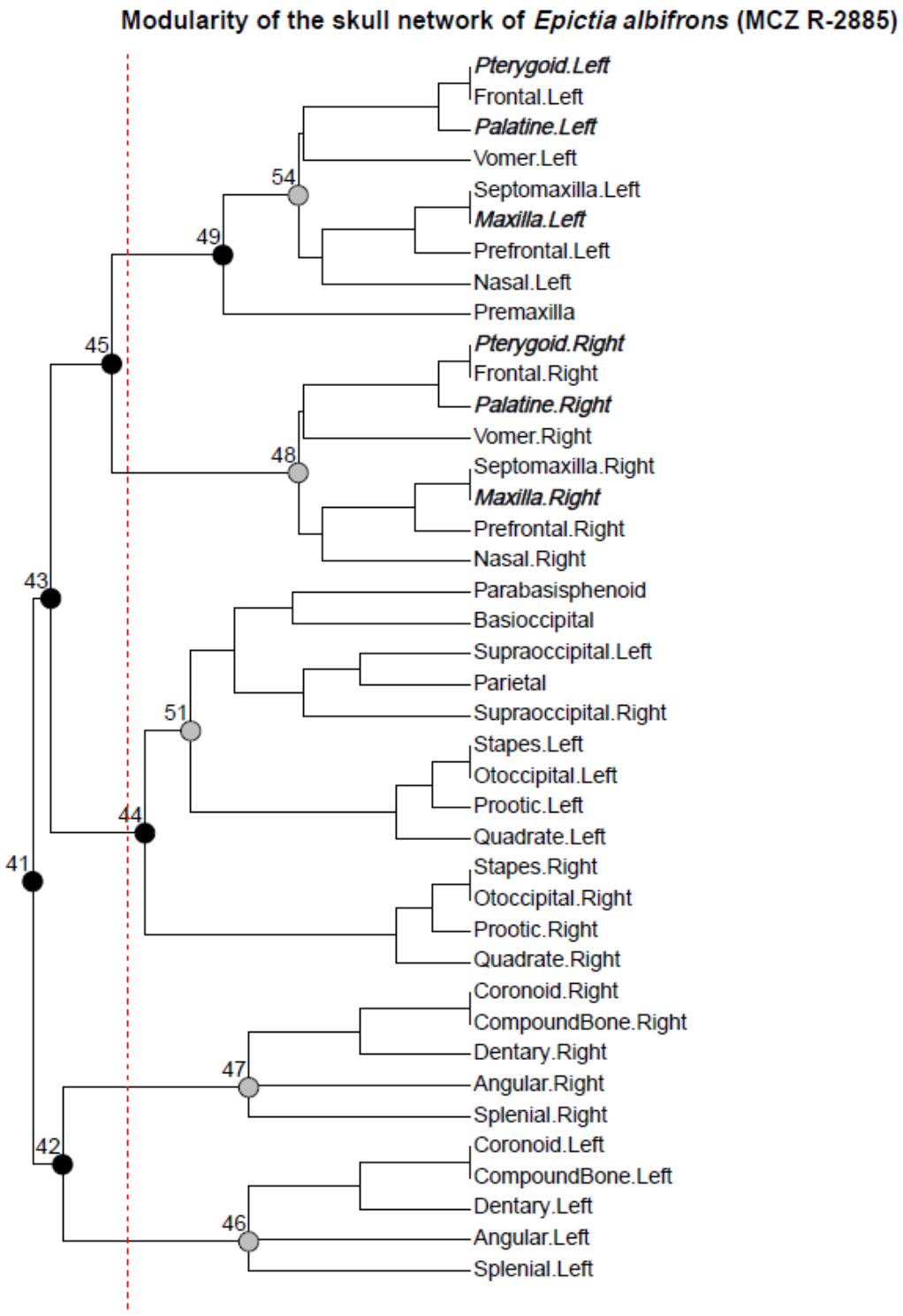

FIGURE S4.20. Modularity of the skull network of *Epictia albifrons* (MCZ R-2885)

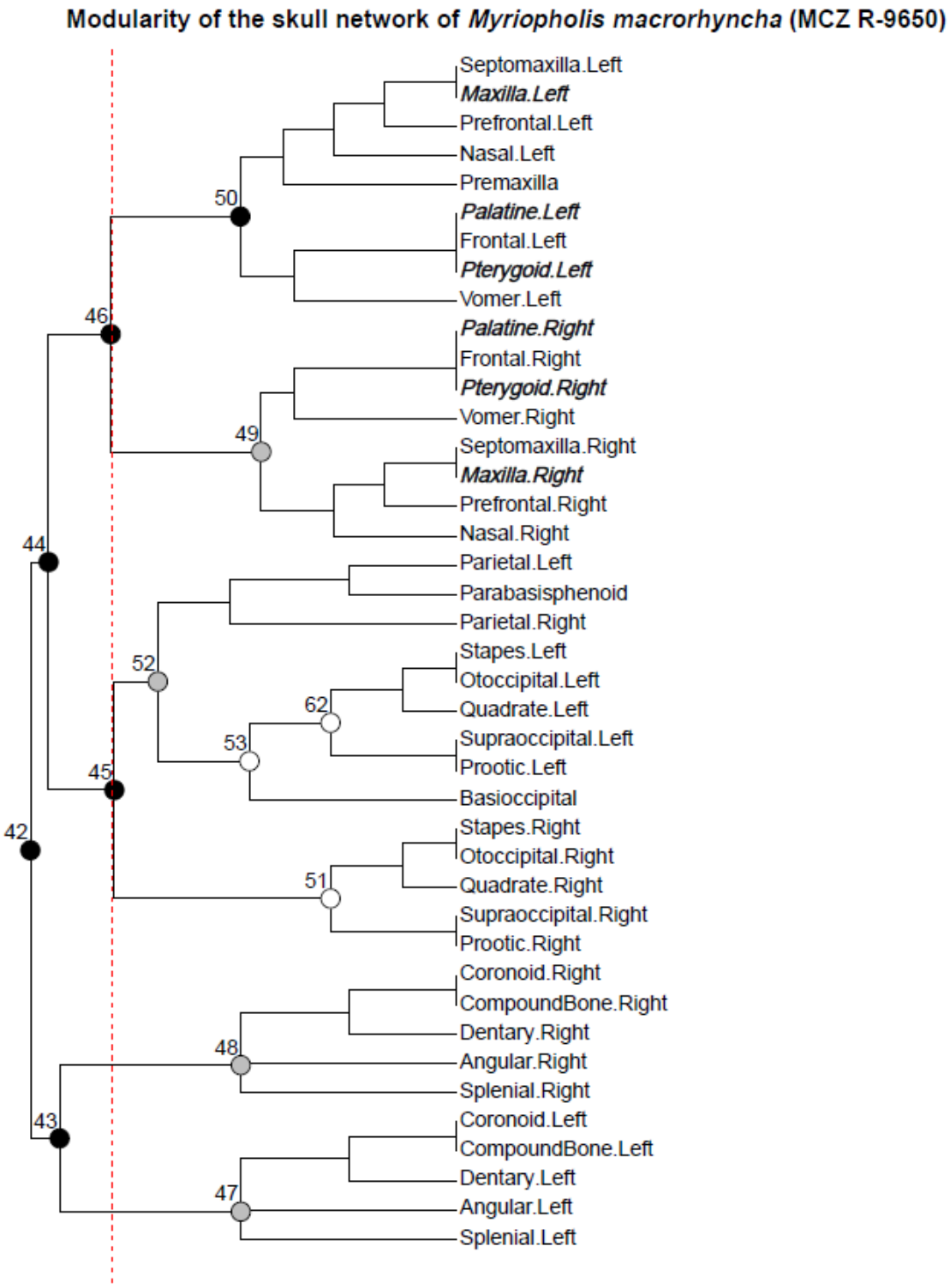

FIGURE S4.21. Modularity of the skull network of *Myriopholis macrorhyncha* (MCZ R-9650)

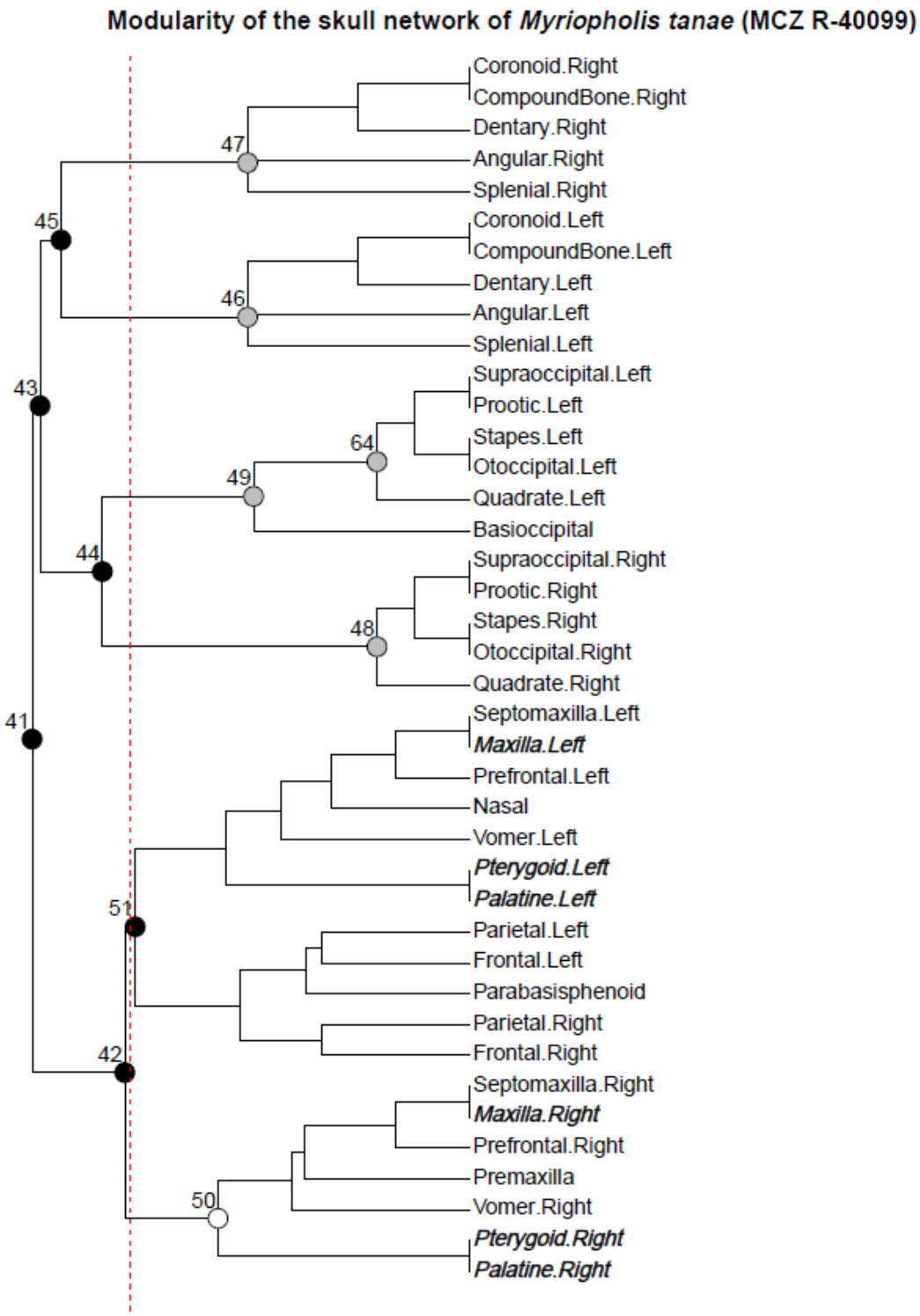

FIGURE S4.22. Modularity of the skull network of *Myriopholis tanae* (MCZ R-40099)

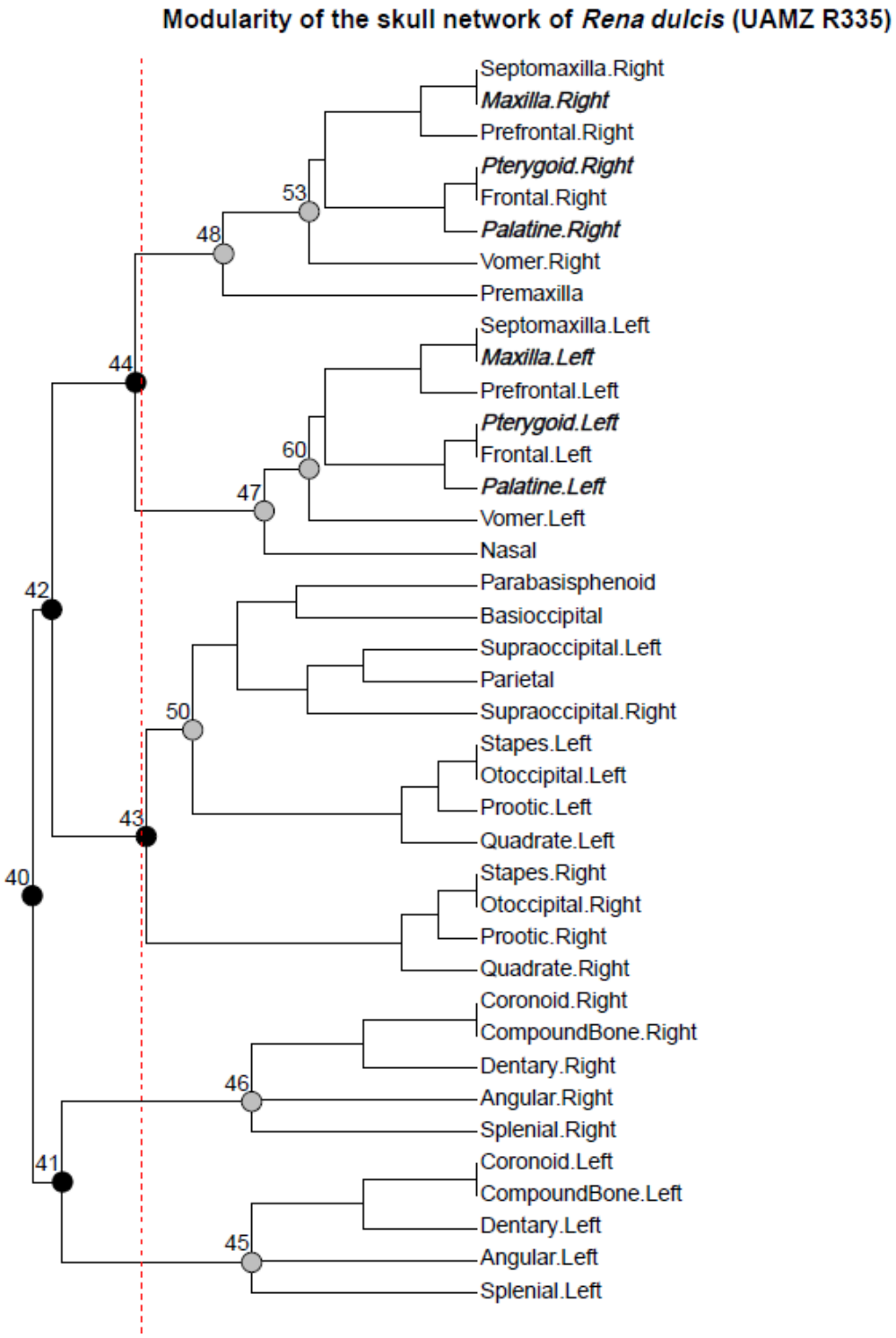

FIGURE S4.23. Modularity of the skull network of *Rena dulcis* (UAMZ R335)

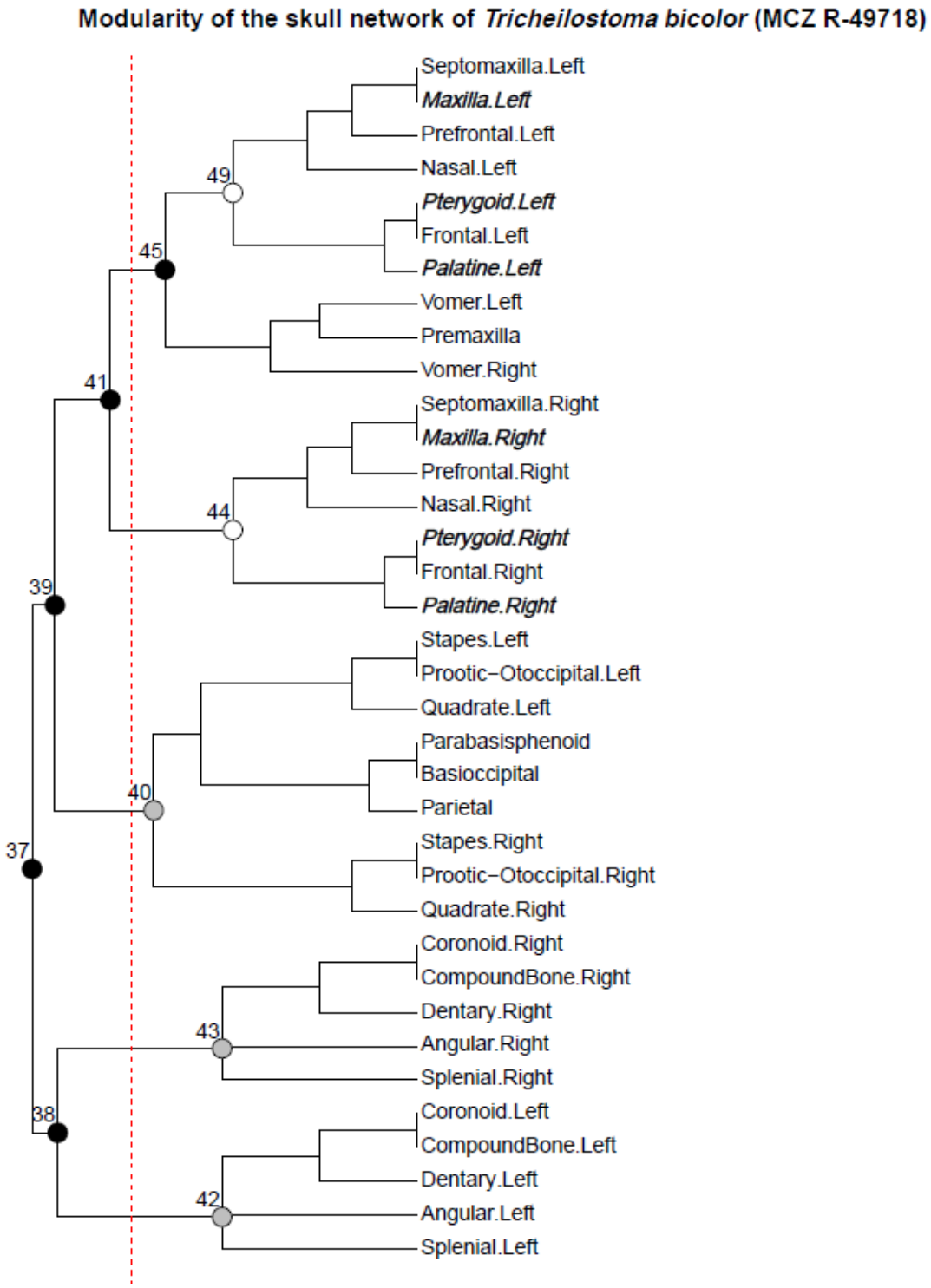

FIGURE S4.24. Modularity of the skull network of *Tricheilostoma bicolor* (MCZ R-49718)

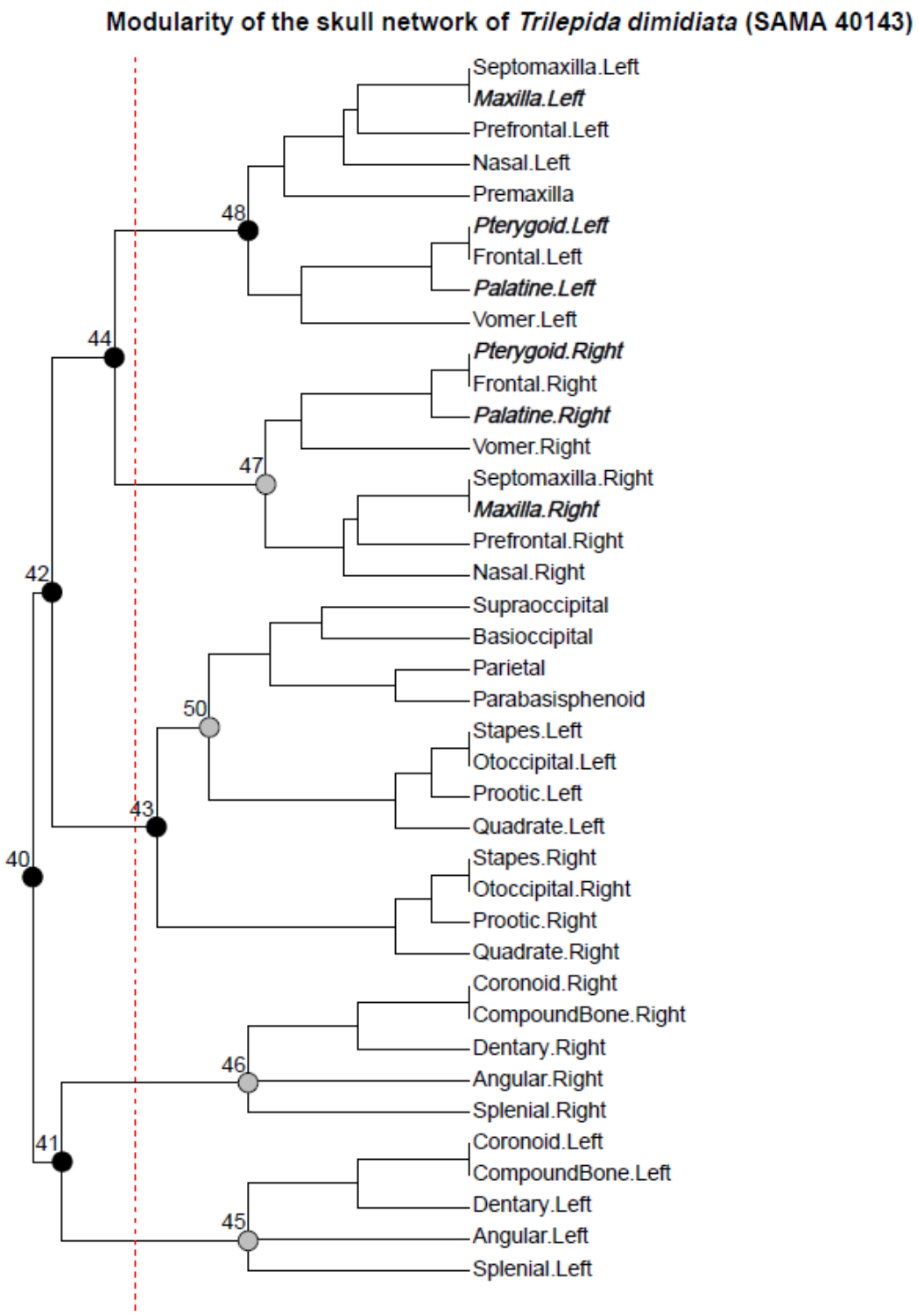

FIGURE S4.25. Modularity of the skull network of *Trilepida dimidiata* (SAMA 40143)

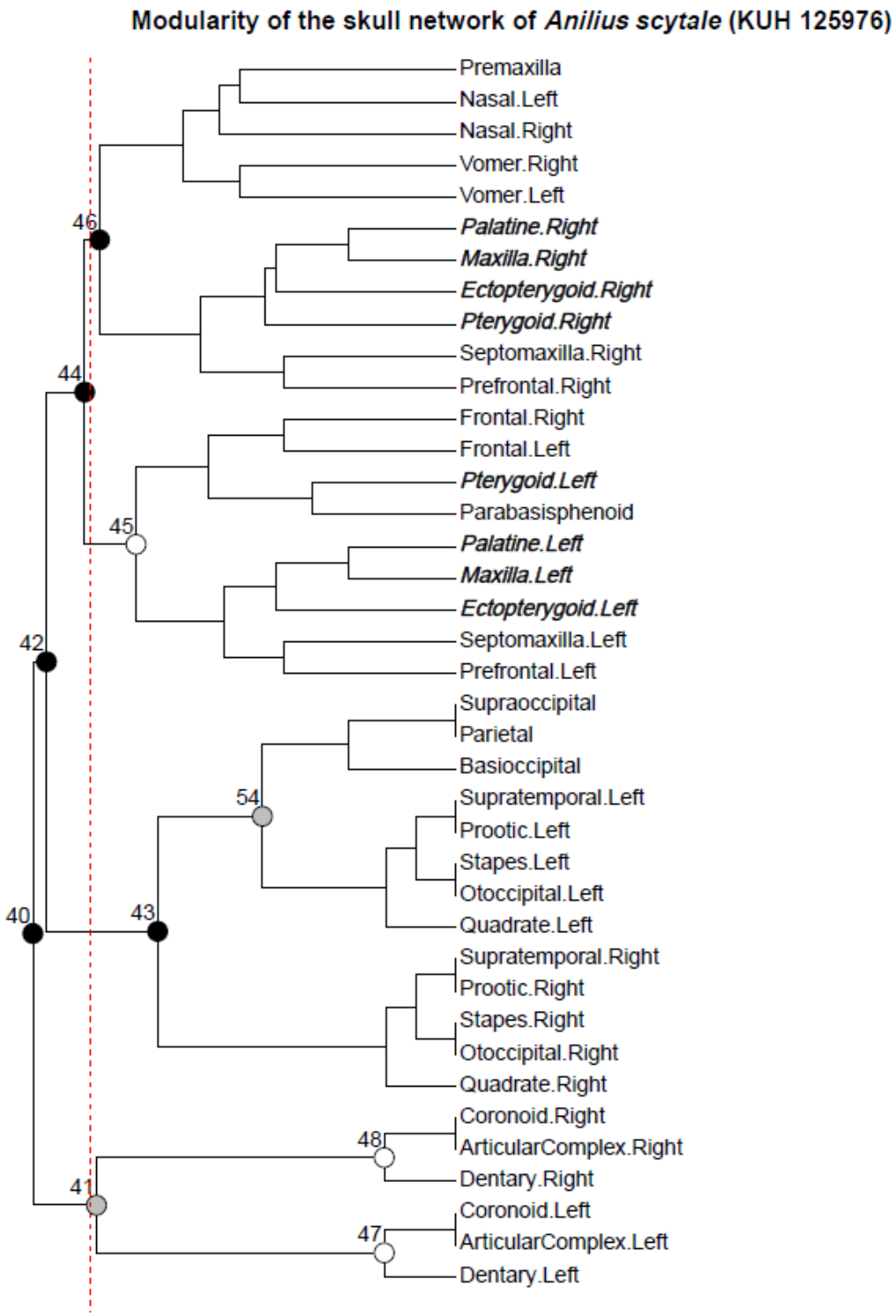

FIGURE S4.26. Modularity of the skull network of *Anilius scytale* (KUH 125976)

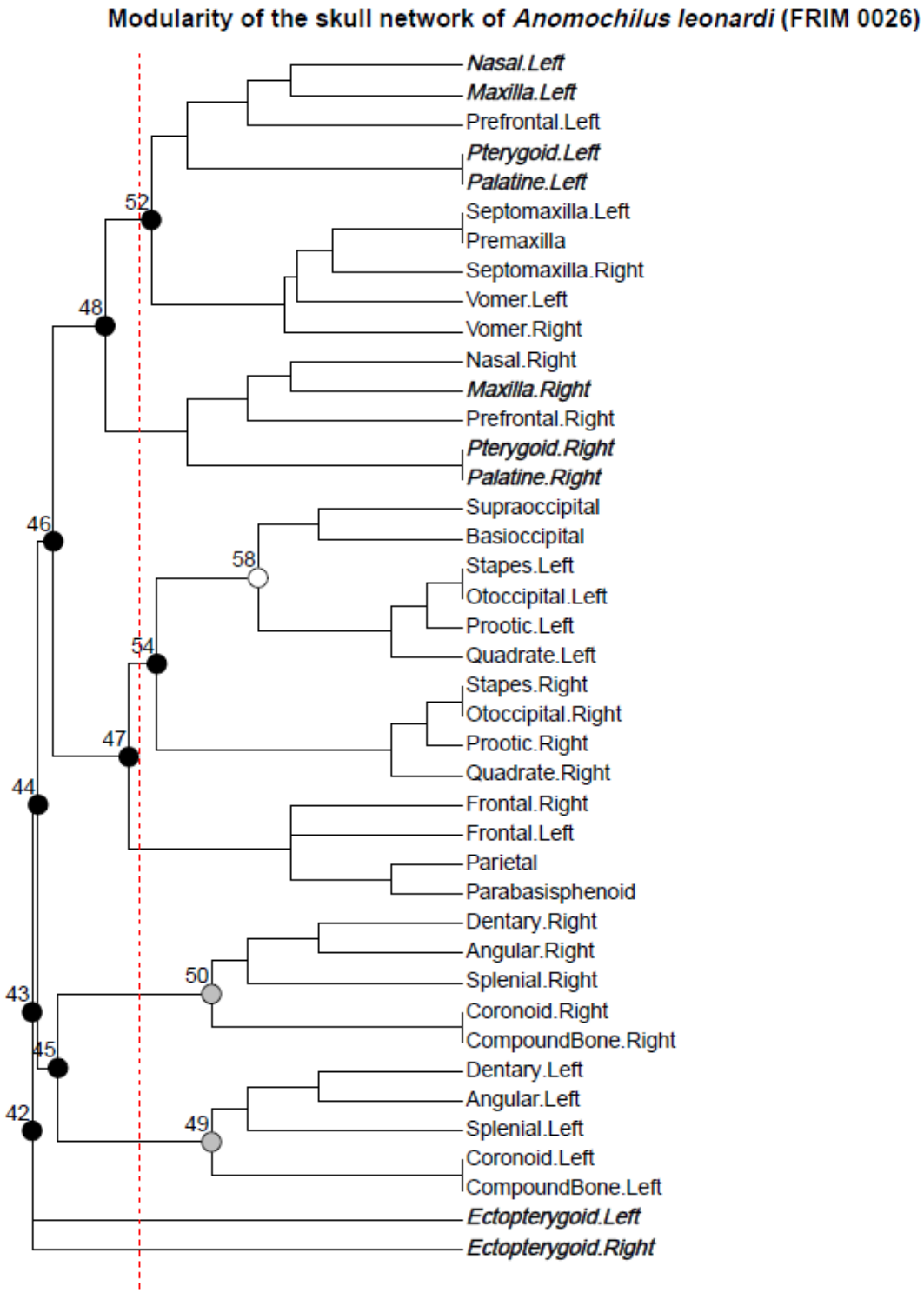

FIGURE S4.27. Modularity of the skull network of *Anomochilus leonardi* (FRIM 0026)

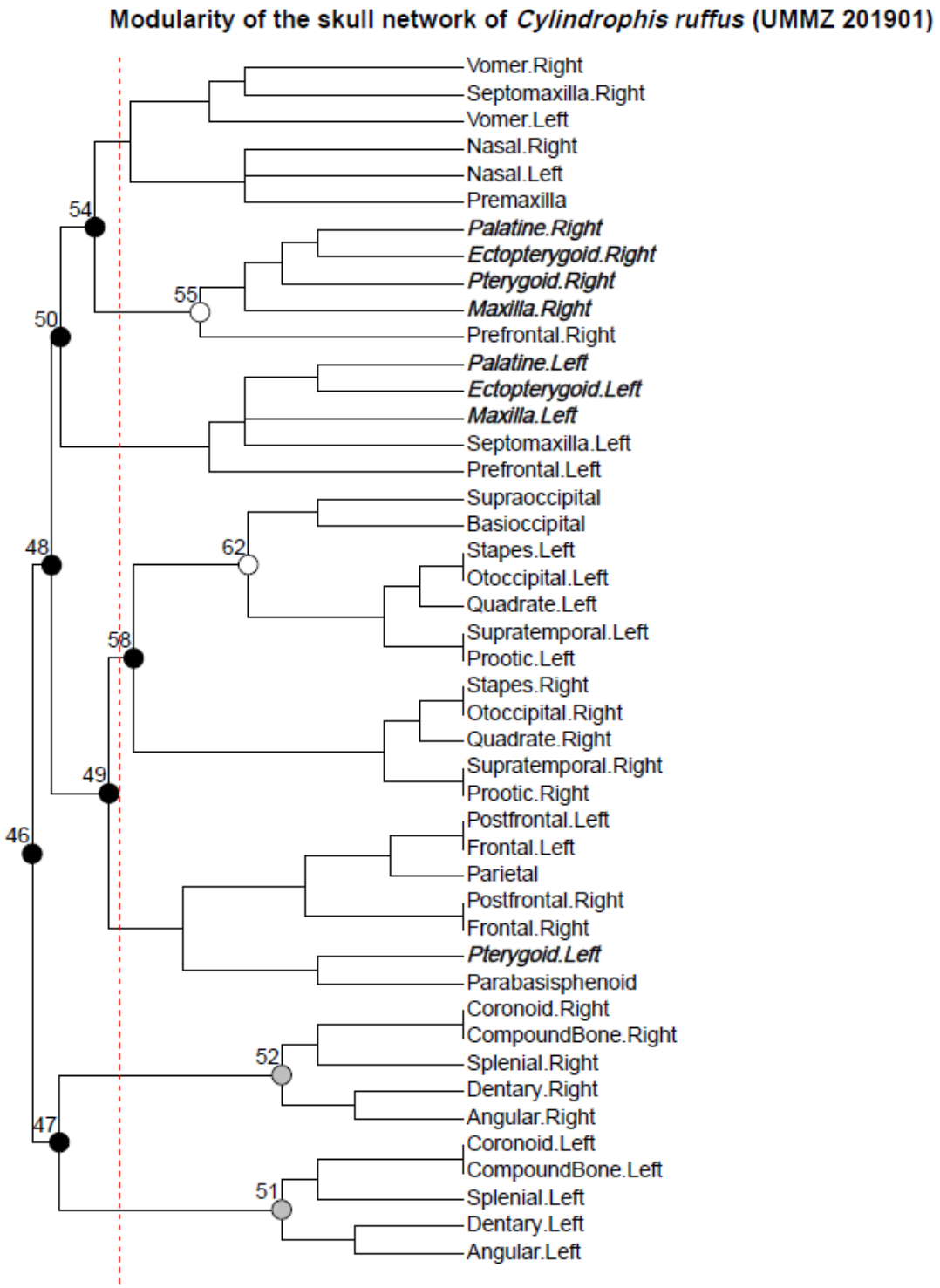

FIGURE S4.28. Modularity of the skull network of *Cylindrophis ruffus* (UMMZ 201901)

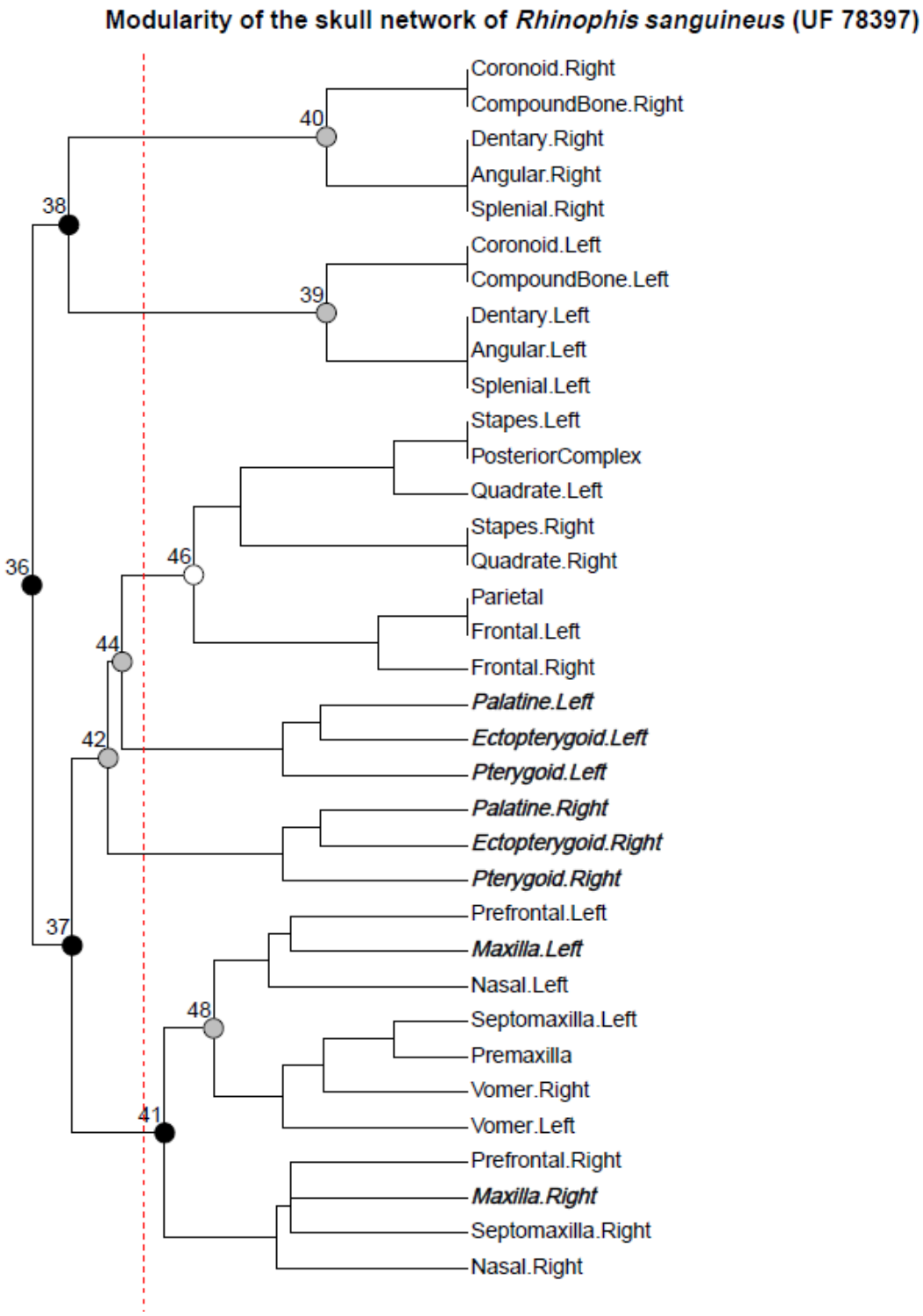

FIGURE S4.29. Modularity of the skull network of *Rhinophis sanguineus* (UF 78397)

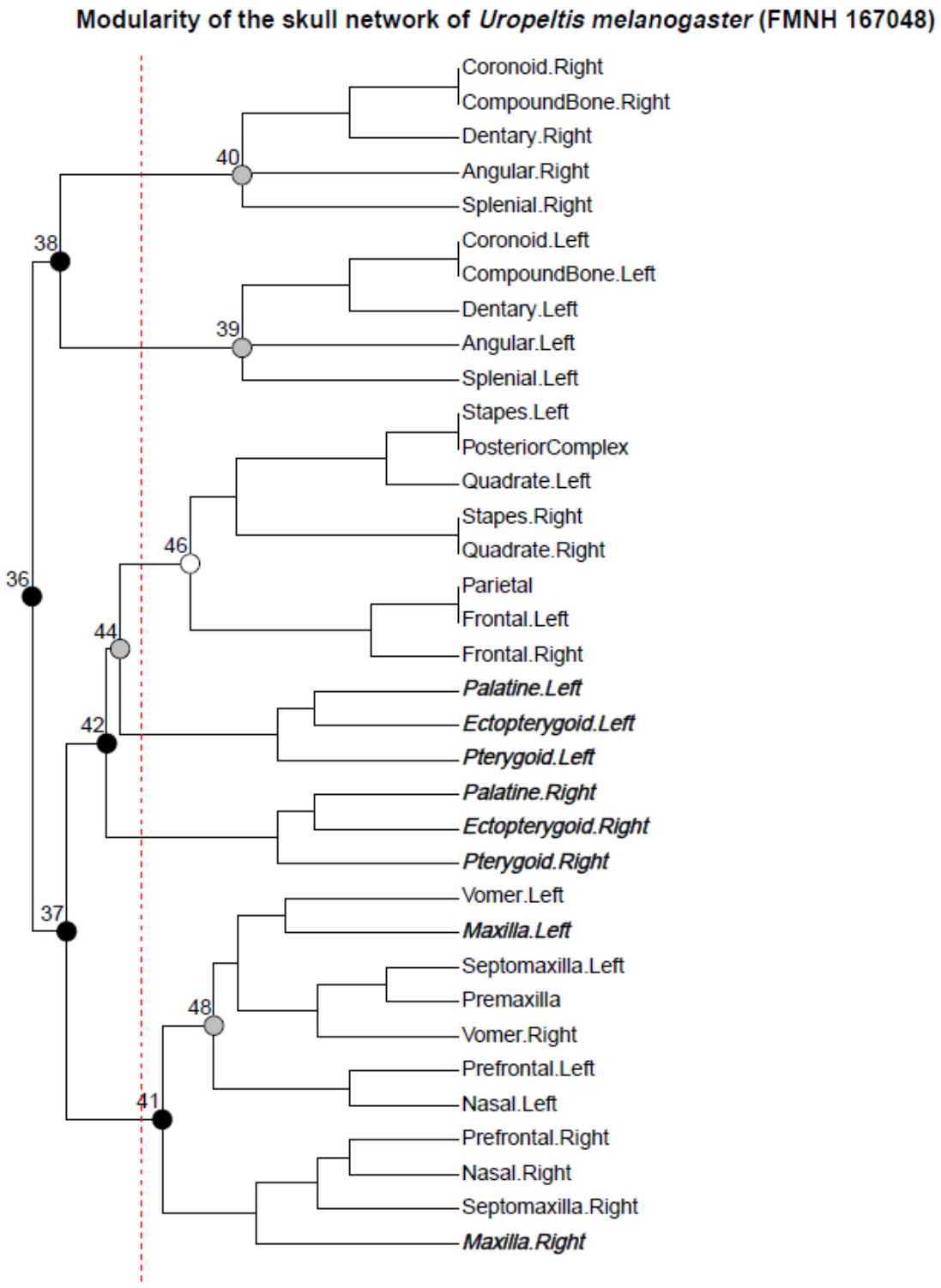

FIGURE S4.30. Modularity of the skull network of *Uropeltis melanogaster* (FMNH 167048)

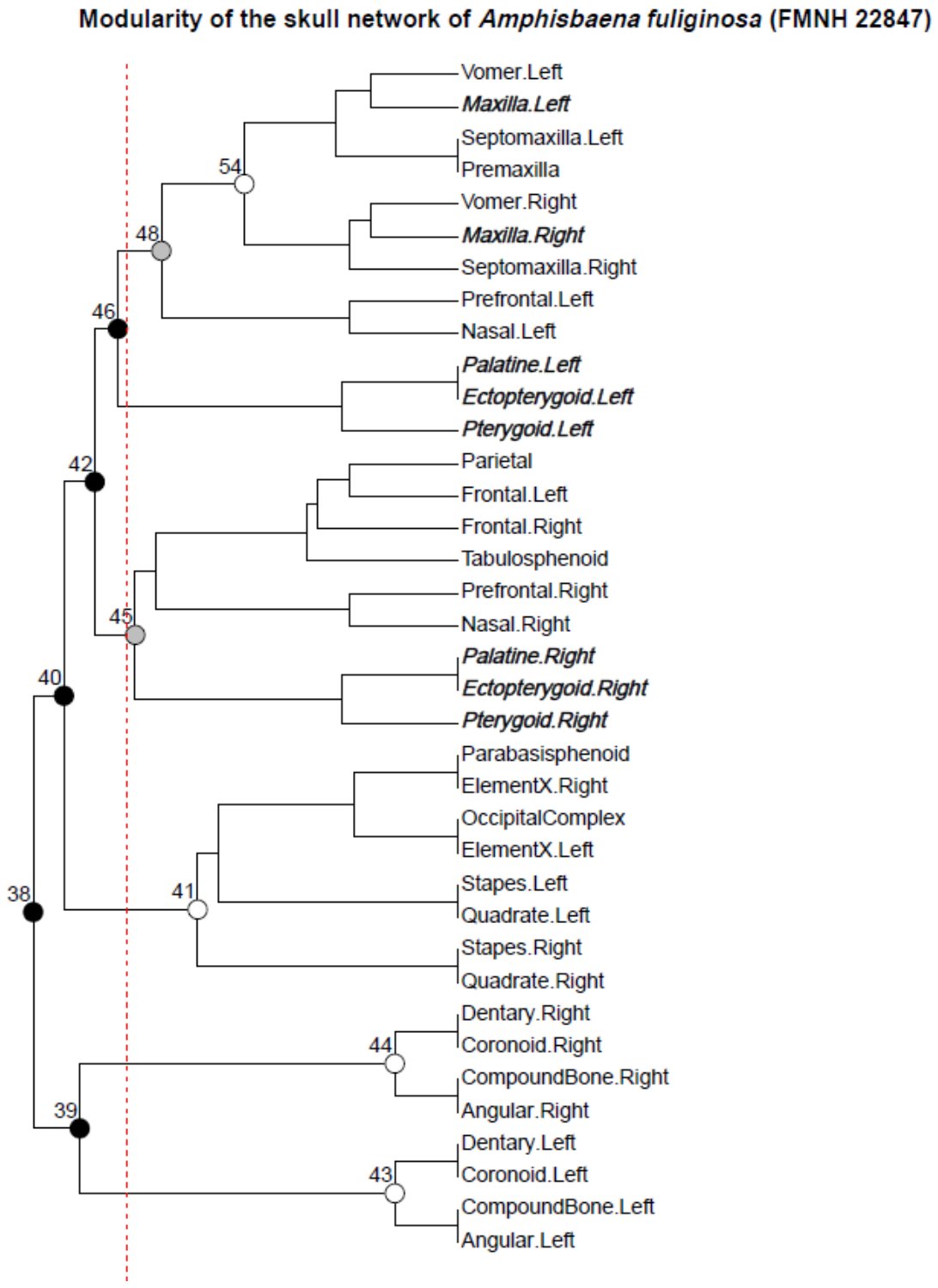

FIGURE S4.31. Modularity of the skull network of *Amphisbaena fuliginosa* (FMNH 22847)

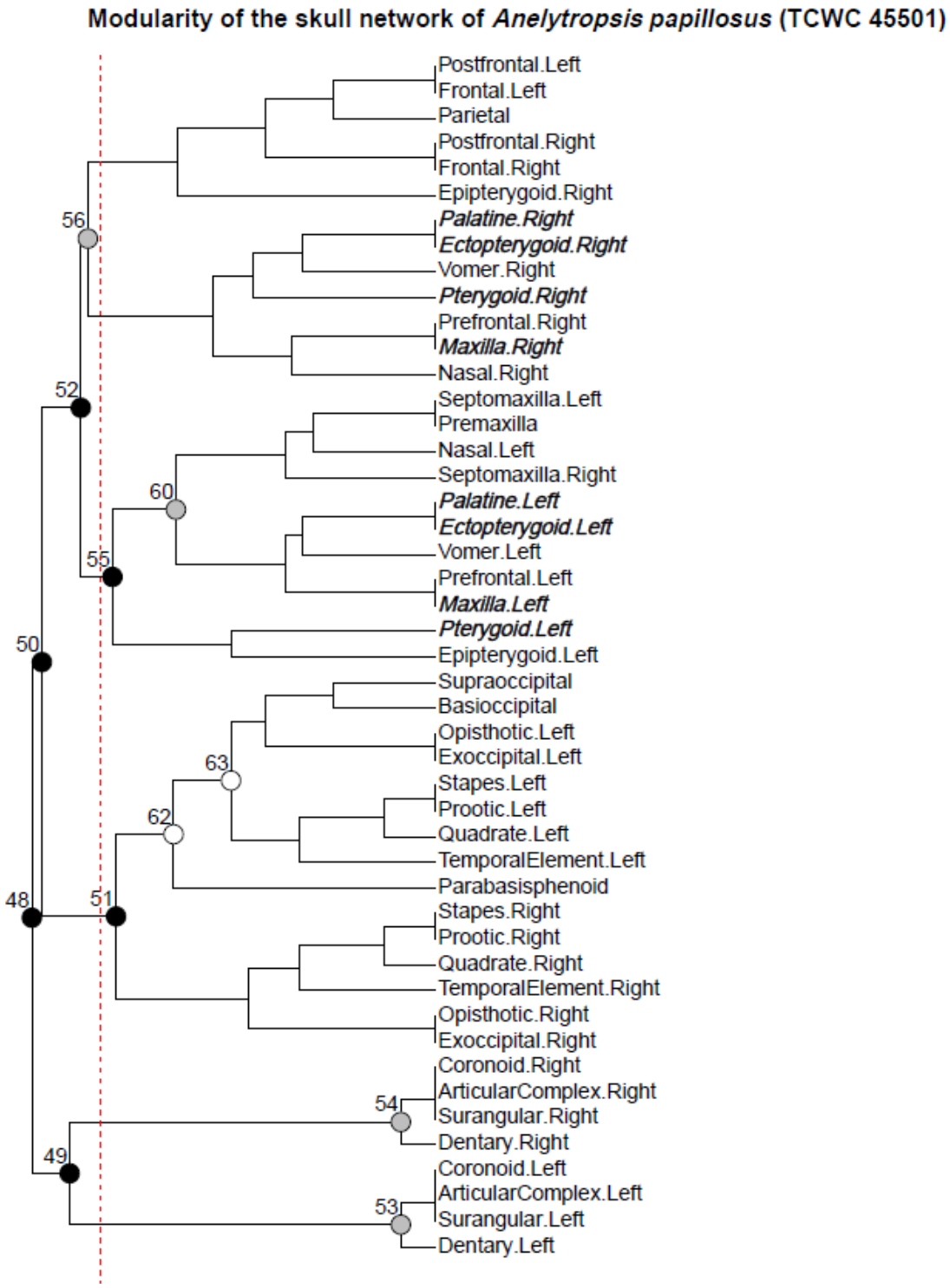

FIGURE S4.32. Modularity of the skull network of *Anelytropsis papillosus* (TCWC 45501)

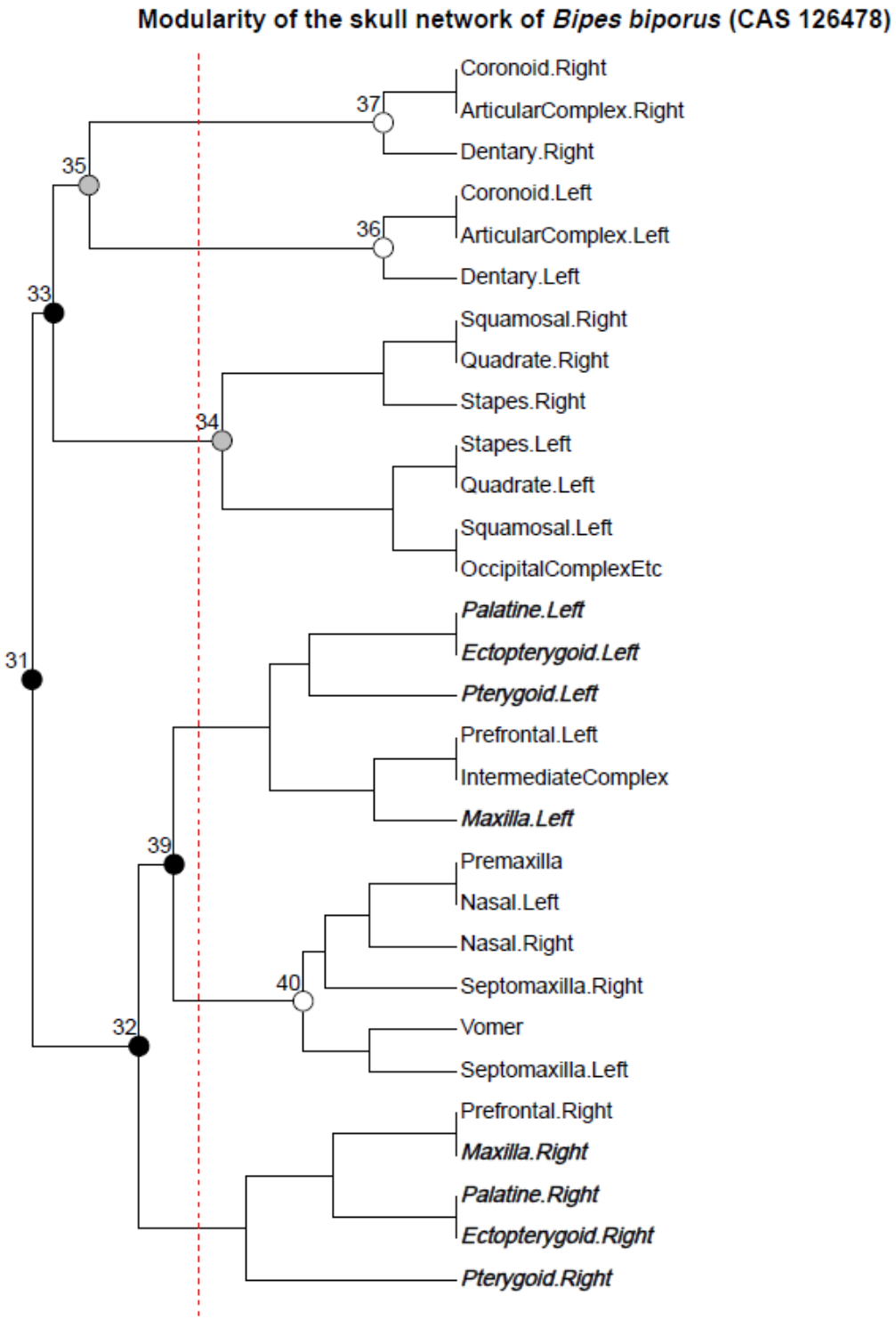

FIGURE S4.33. Modularity of the skull network of *Bipes biporus* (CAS 126478)

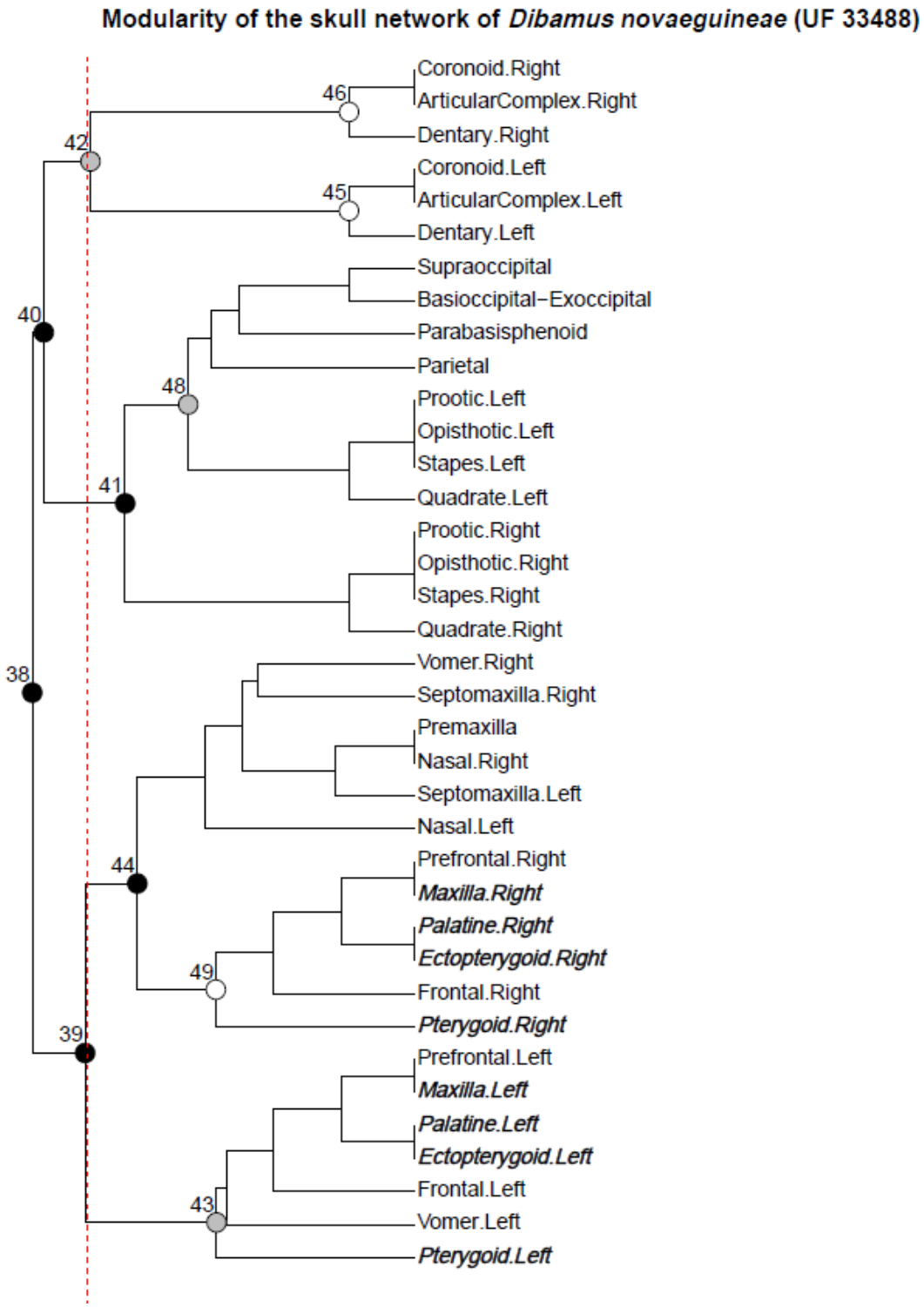

FIGURE S4.34. Modularity of the skull network of *Dibamus novaeguineae* (UF 33488)

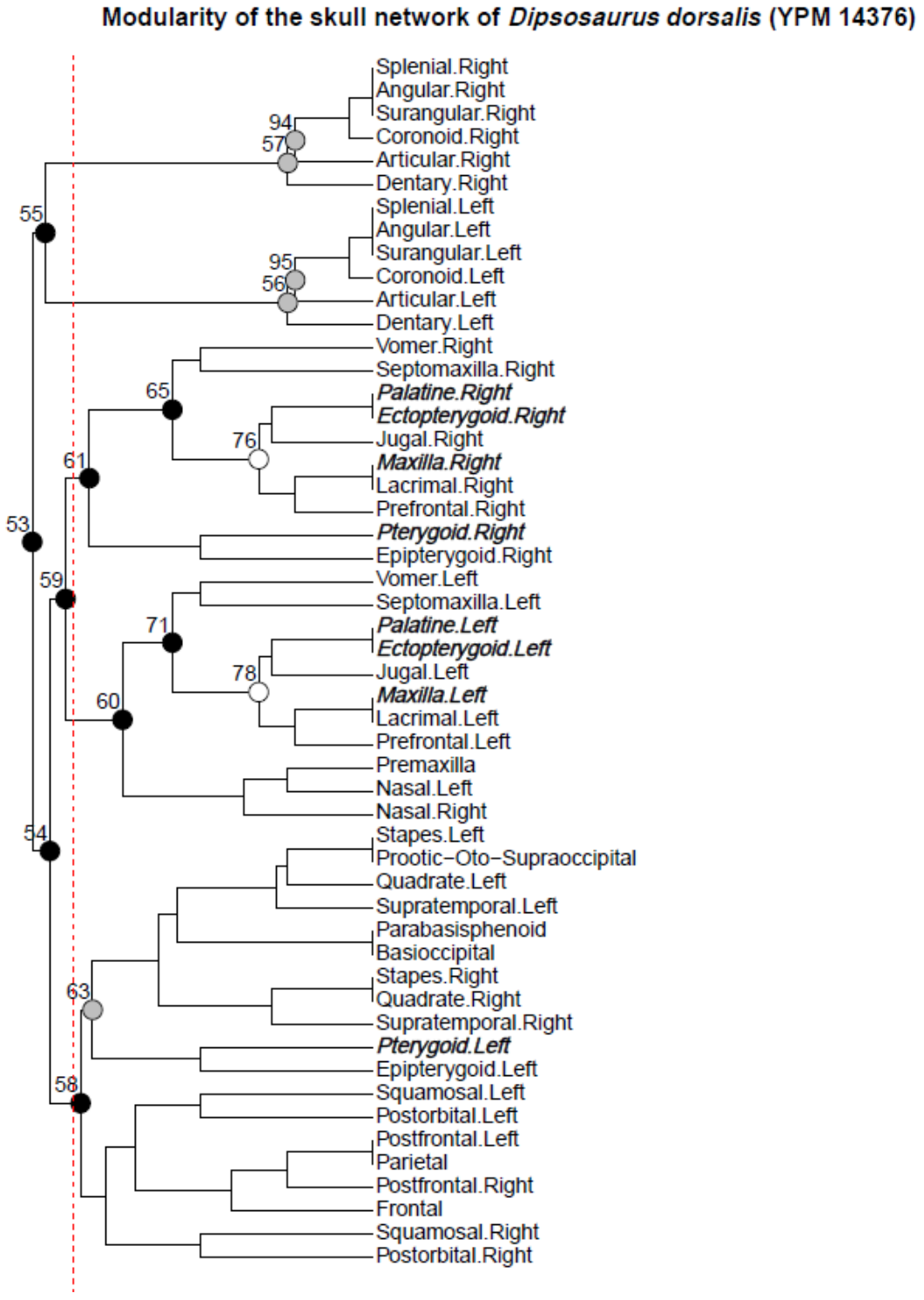

FIGURE S4.35. Modularity of the skull network of *Dipsosaurus dorsalis* (YPM 14376)

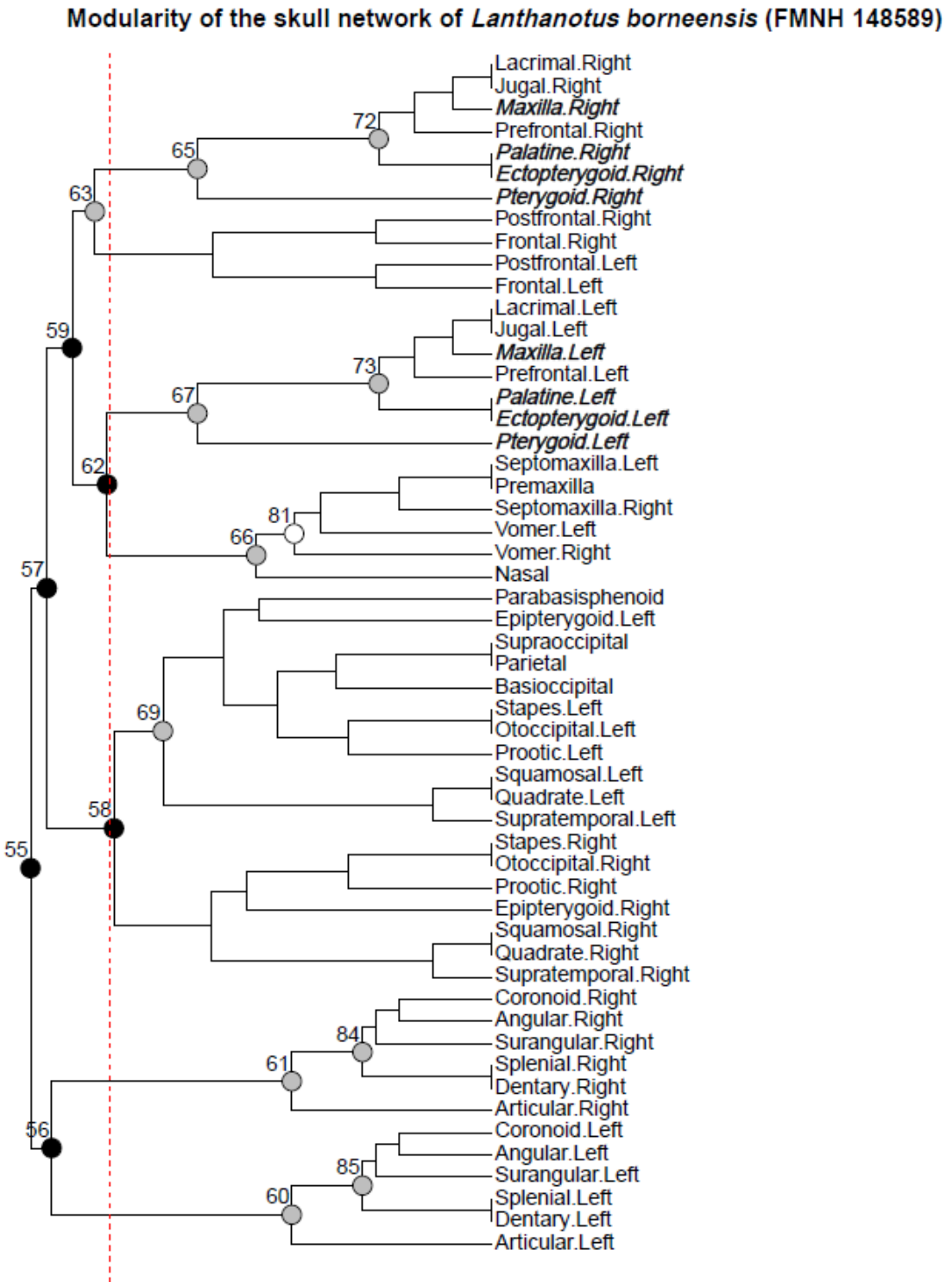

FIGURE S4.36. Modularity of the skull network of *Lanthanotus borneensis* (FMNH 148589)

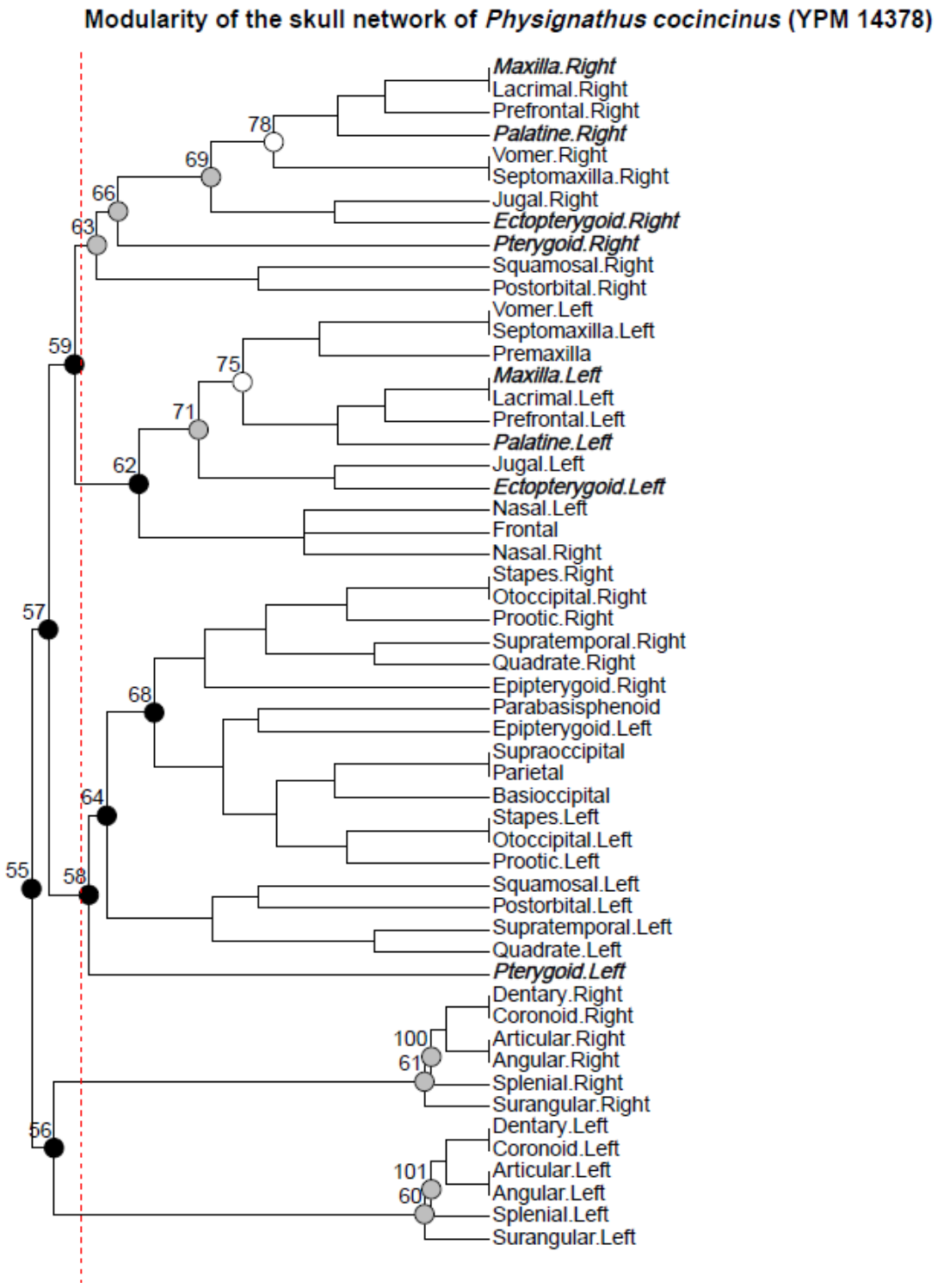

FIGURE S4.37. Modularity of the skull network of *Physignathus cocincinus* (YPM 14378)

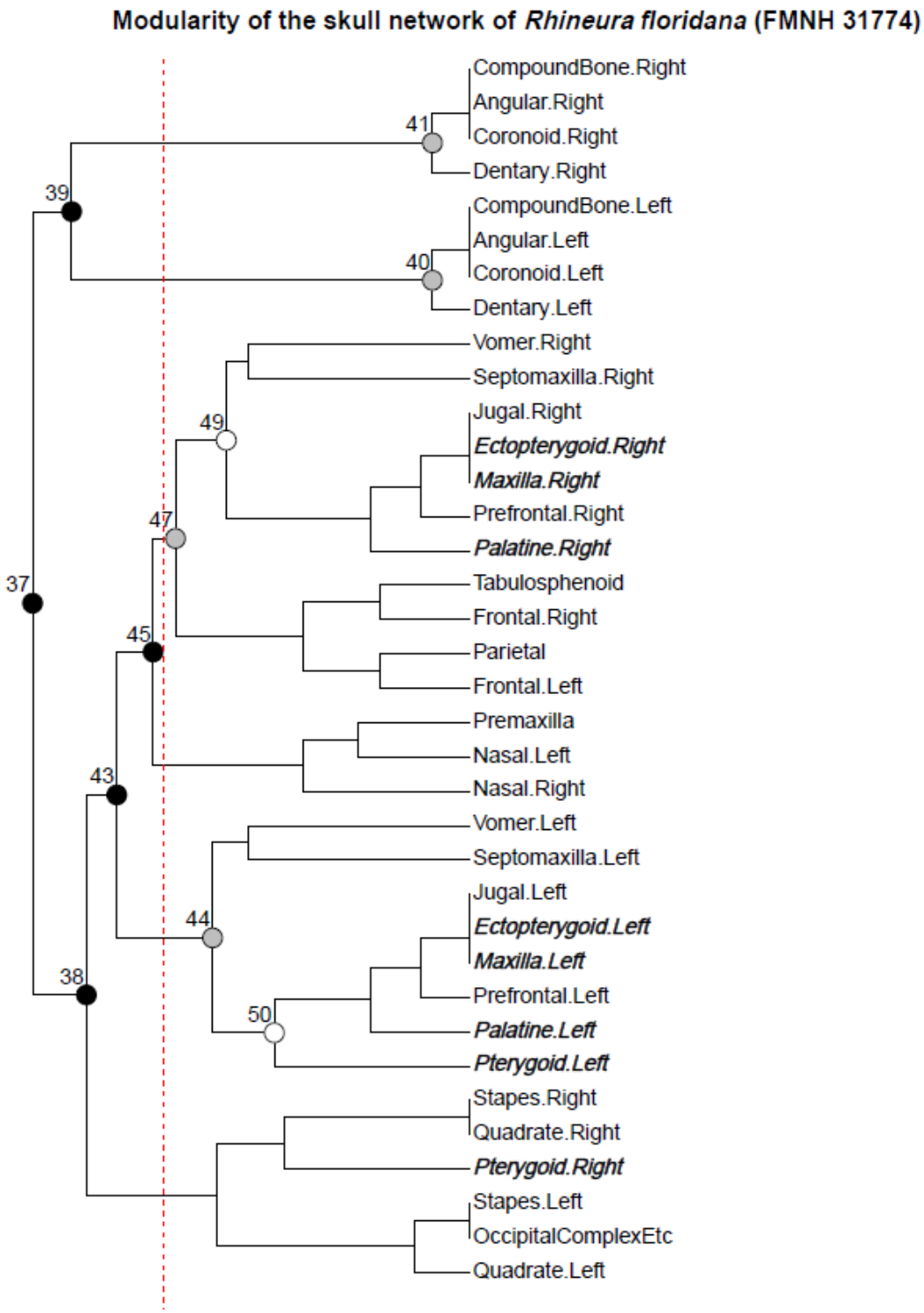

FIGURE S4.38. Modularity of the skull network of *Rhineura floridana* (FMNH 31774)

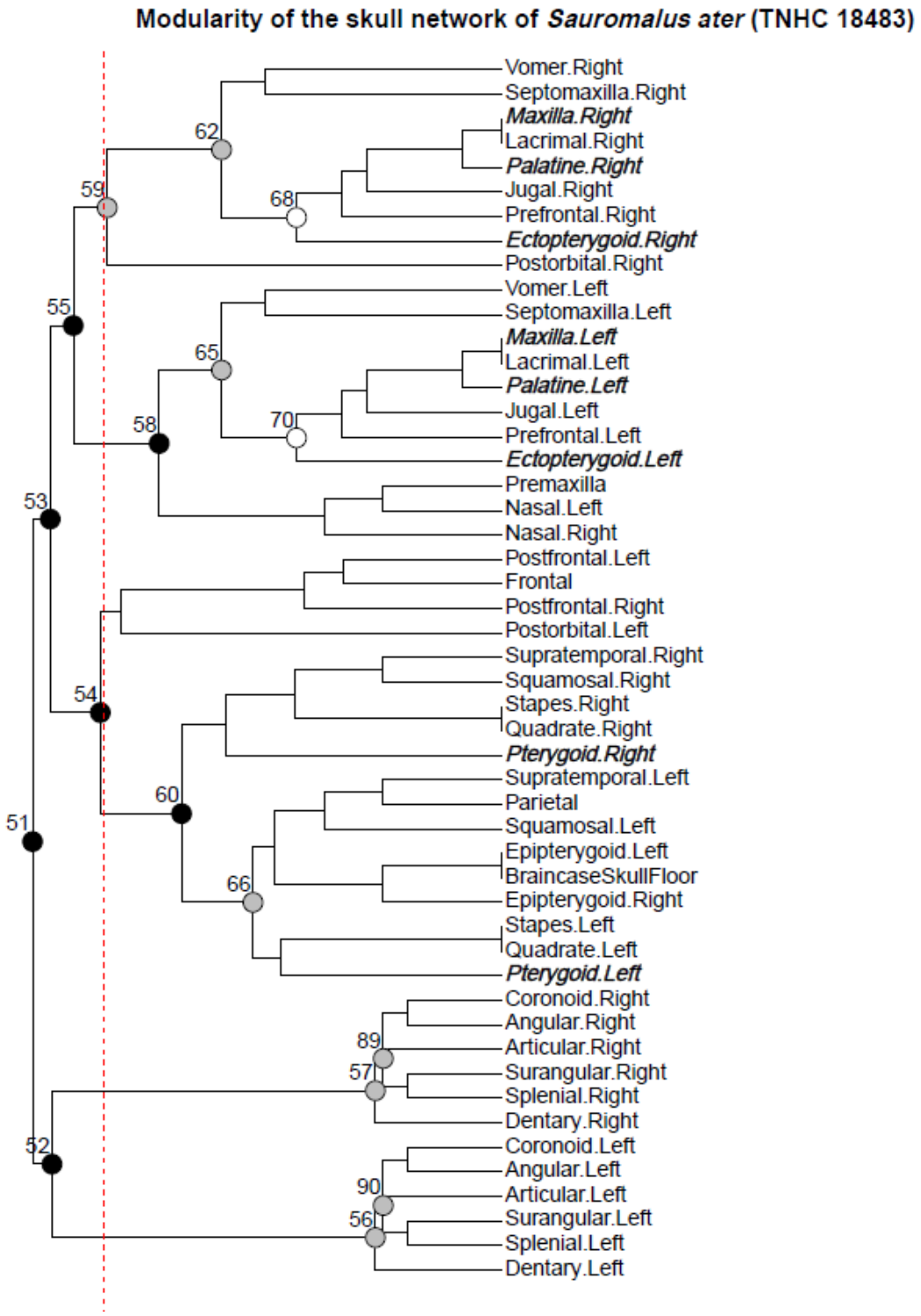

FIGURE S4.39. Modularity of the skull network of *Sauromalus ater* (TNHC 18483)

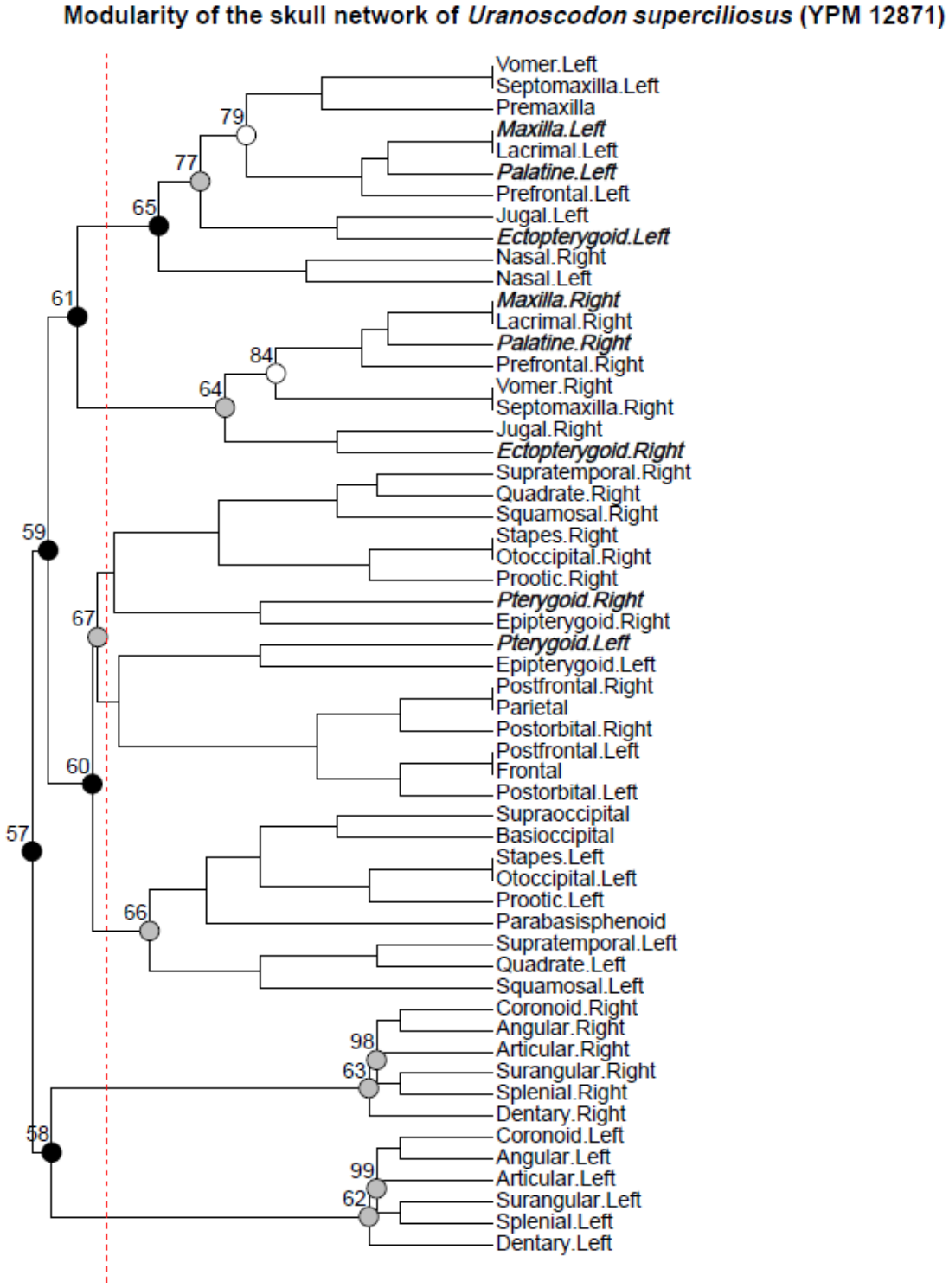

FIGURE S4.40. Modularity of the skull network of *Uranoscodon superciliosus* (YPM 12871)

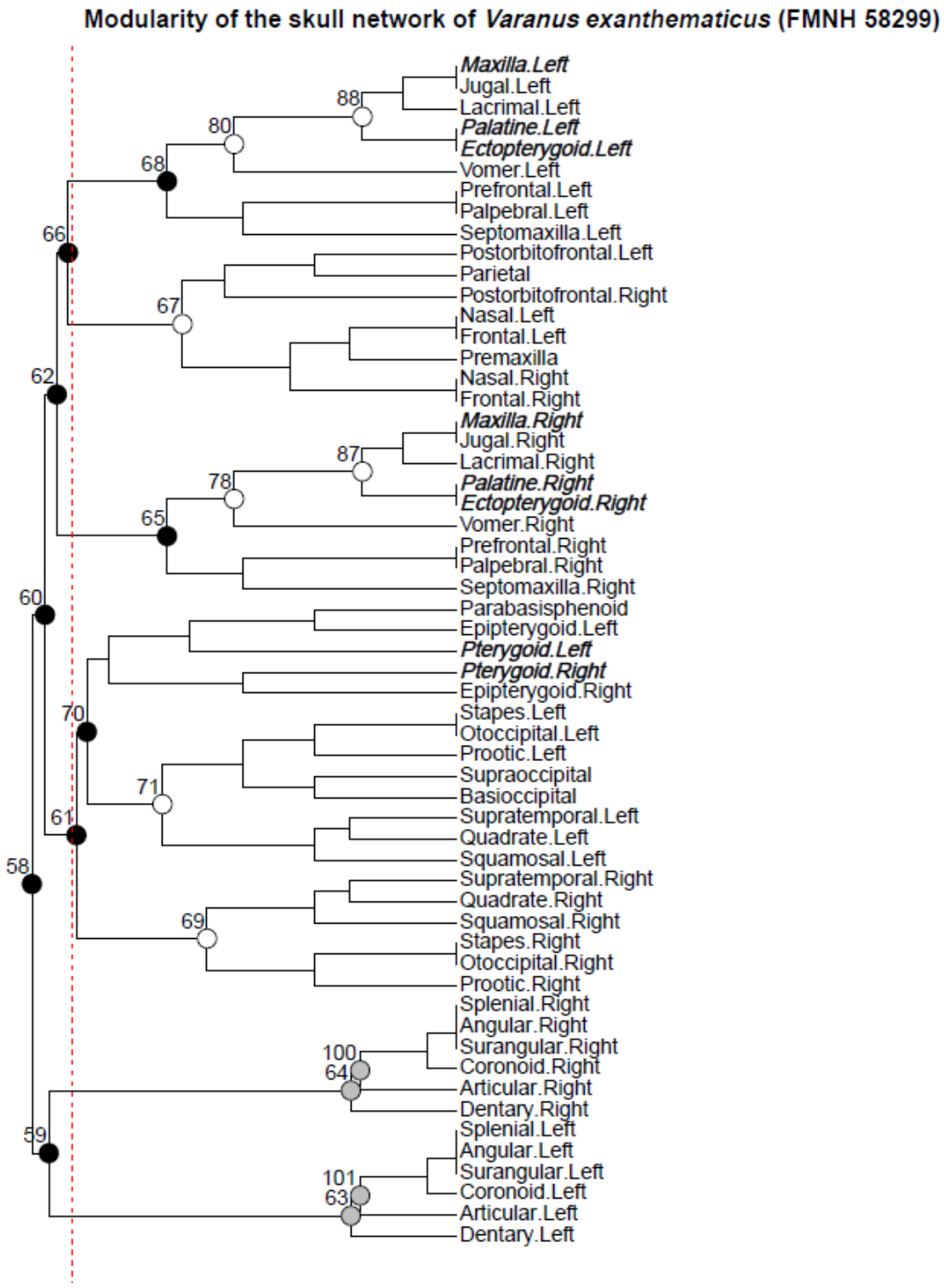

FIGURE S4.41. Modularity of the skull network of *Varanus exanthematicus* (FMNH 58299)

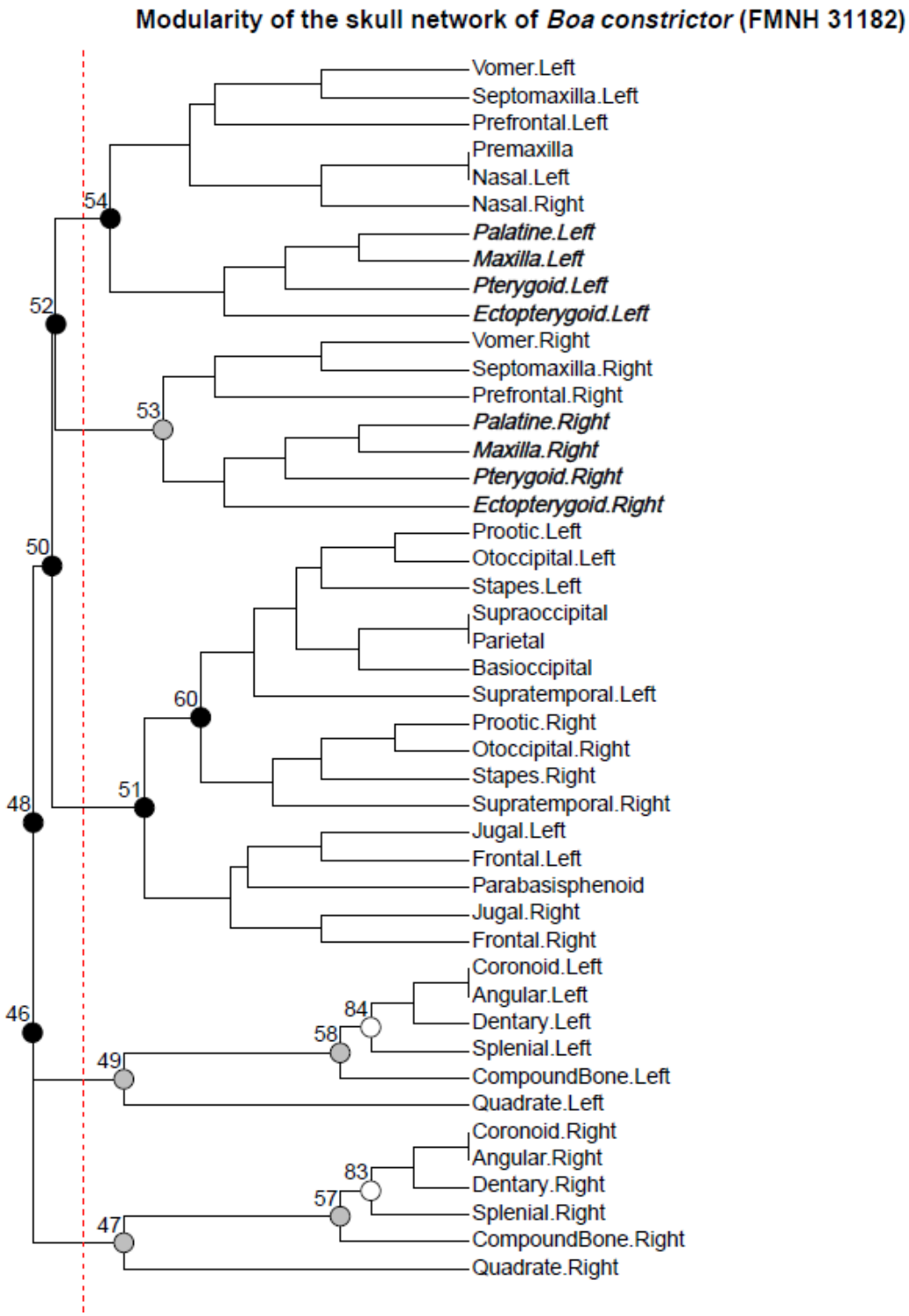

FIGURE S4.42. Modularity of the skull network of *Boa constrictor* (FMNH 31182)

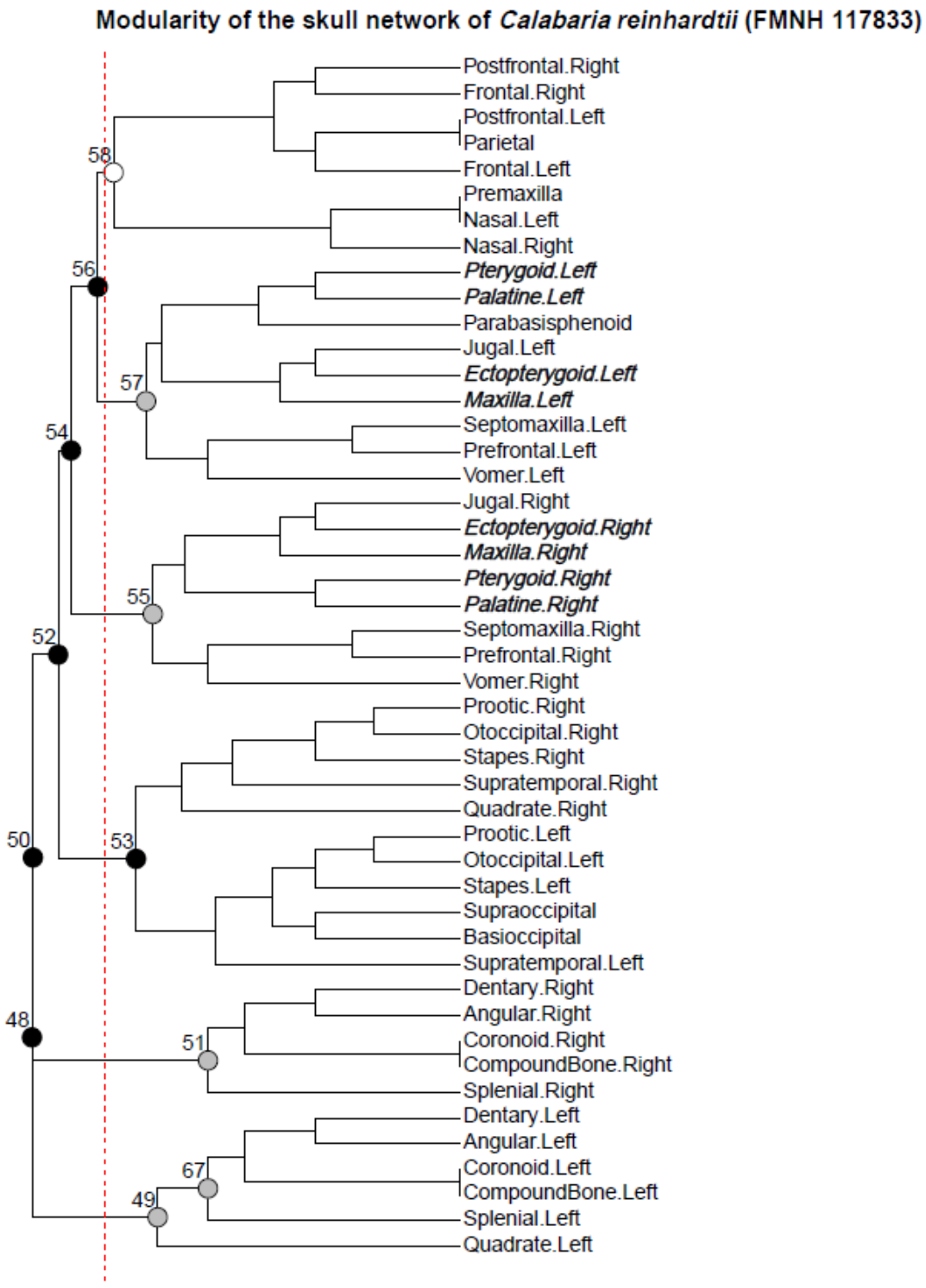

FIGURE S4.43. Modularity of the skull network of *Calabaria reinhardtii* (FMNH 117833)

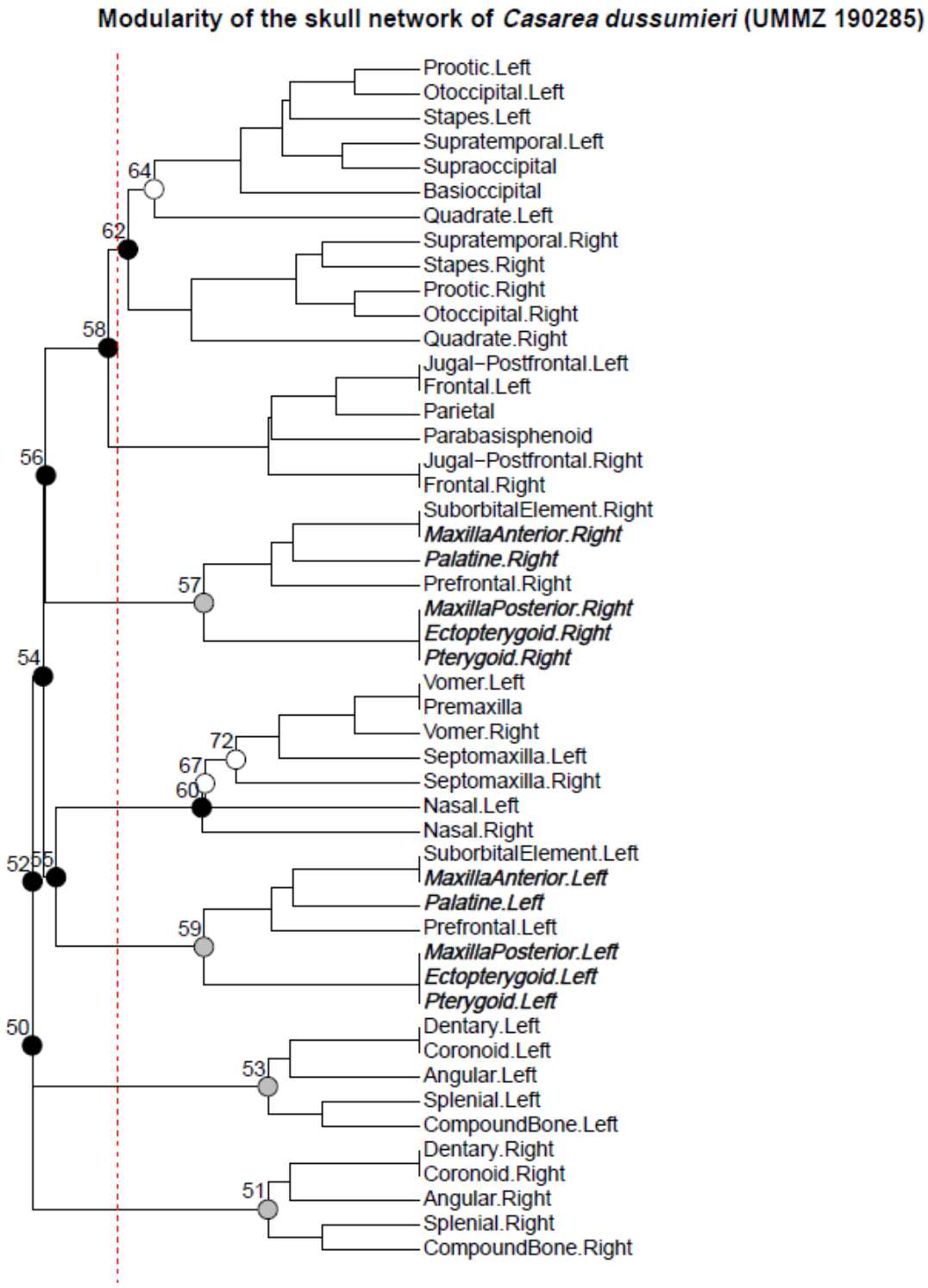

FIGURE S4.44. Modularity of the skull network of *Casarea dussumieri* (UMMZ 190285)

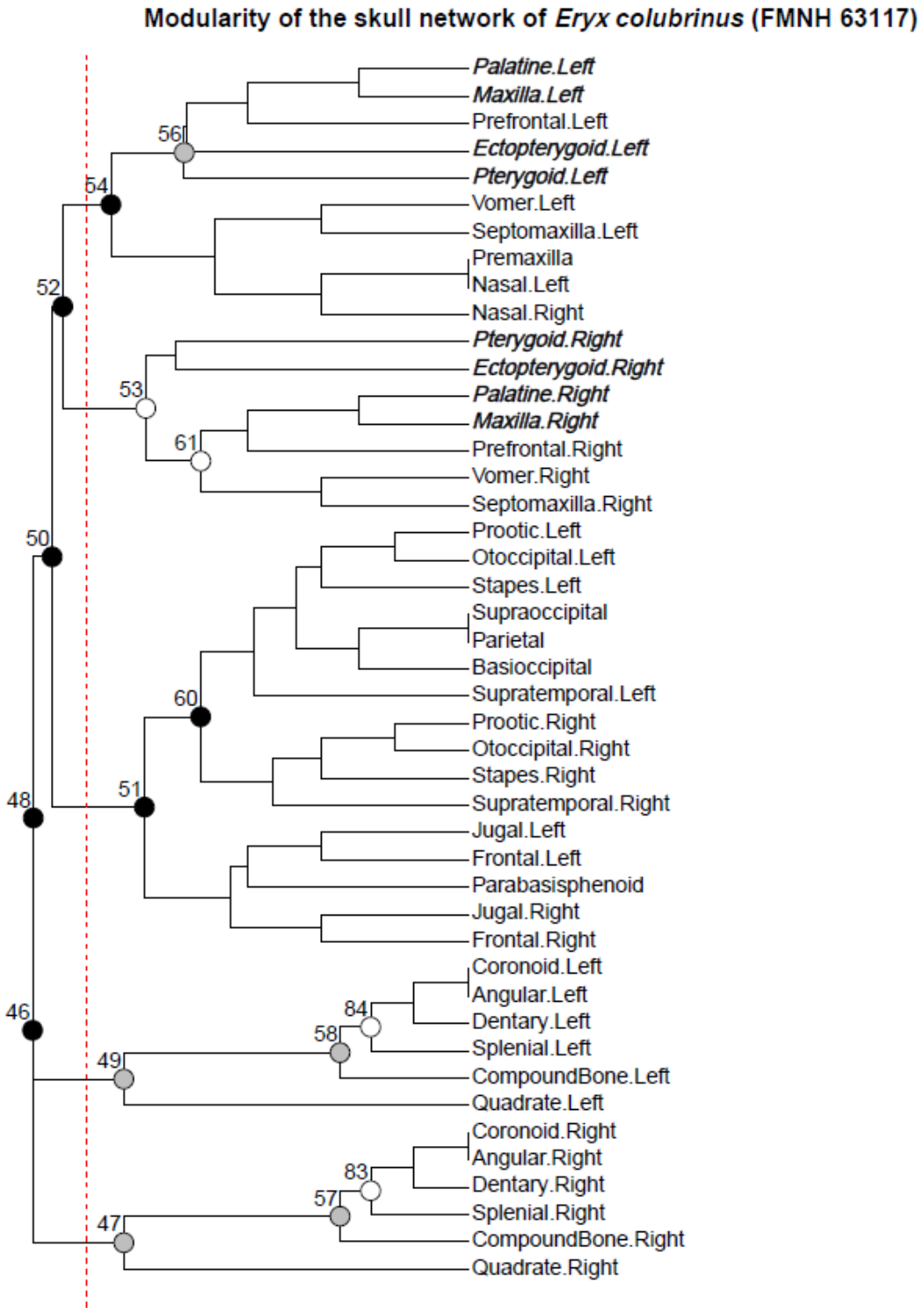

FIGURE S4.45. Modularity of the skull network of *Eryx colubrinus* (FMNH 63117)

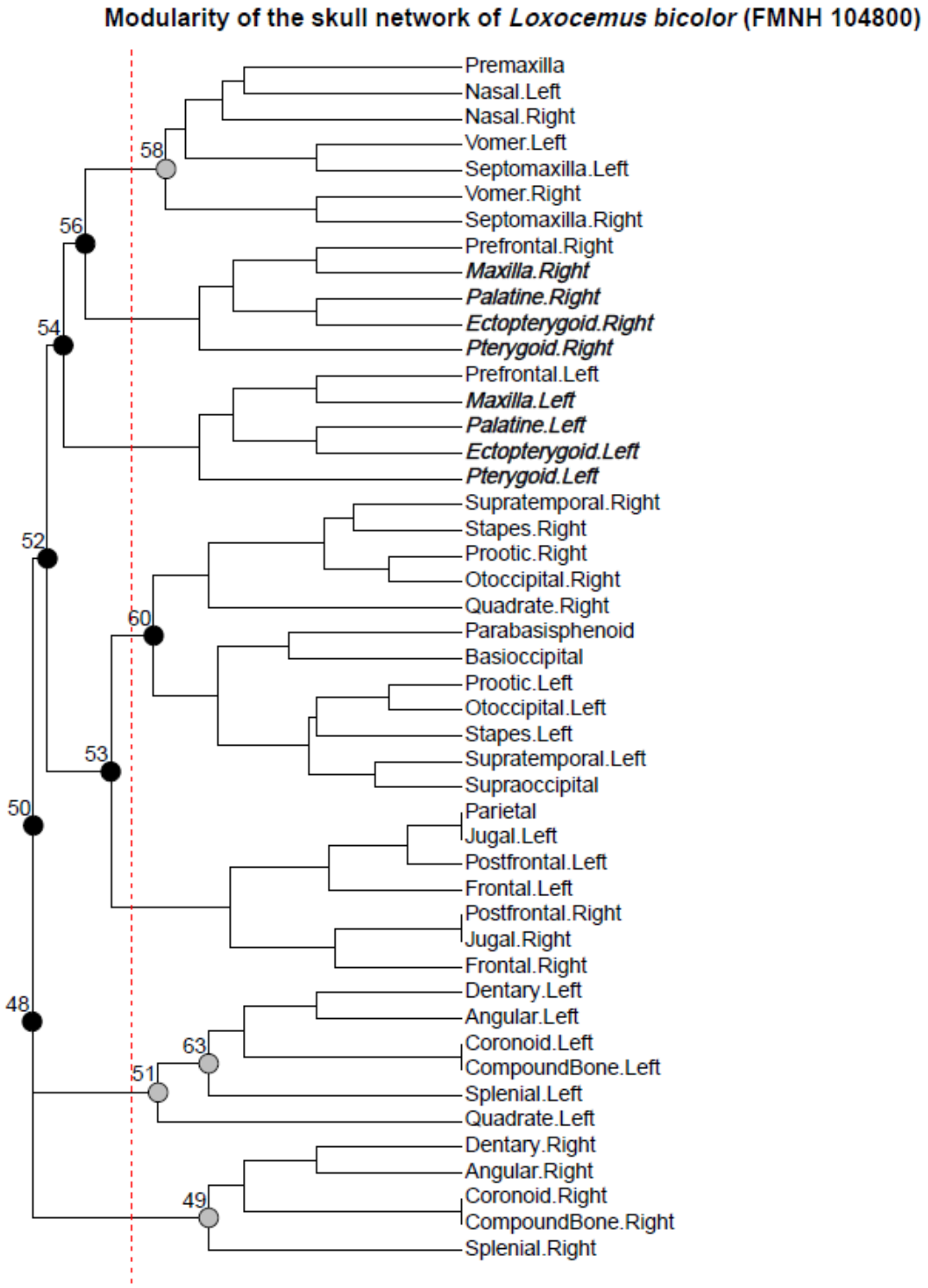

FIGURE S4.46. Modularity of the skull network of *Loxocemus bicolor* (FMNH 104800)

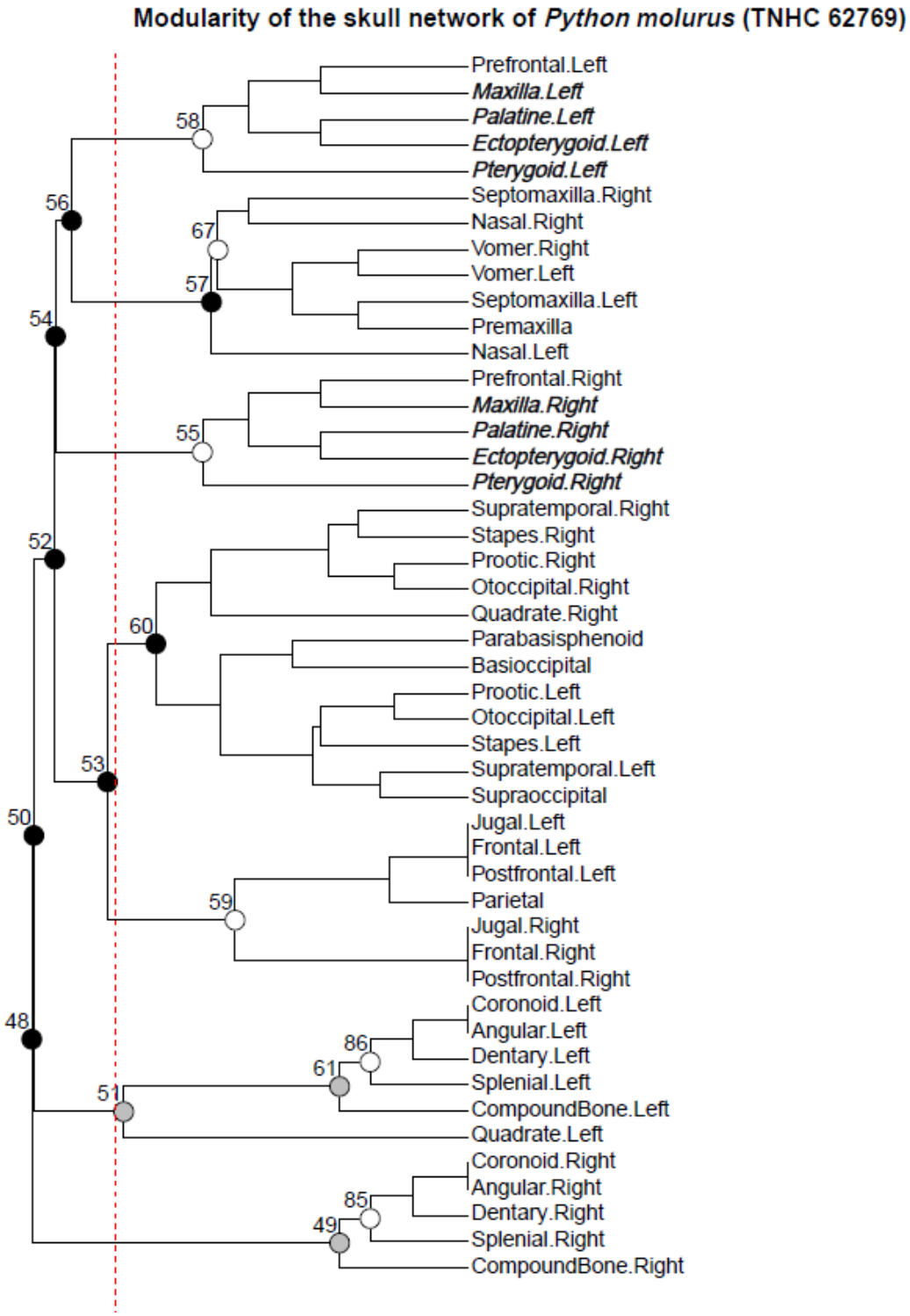

FIGURE S4.47. Modularity of the skull network of *Python molurus* (TNHC 62769)

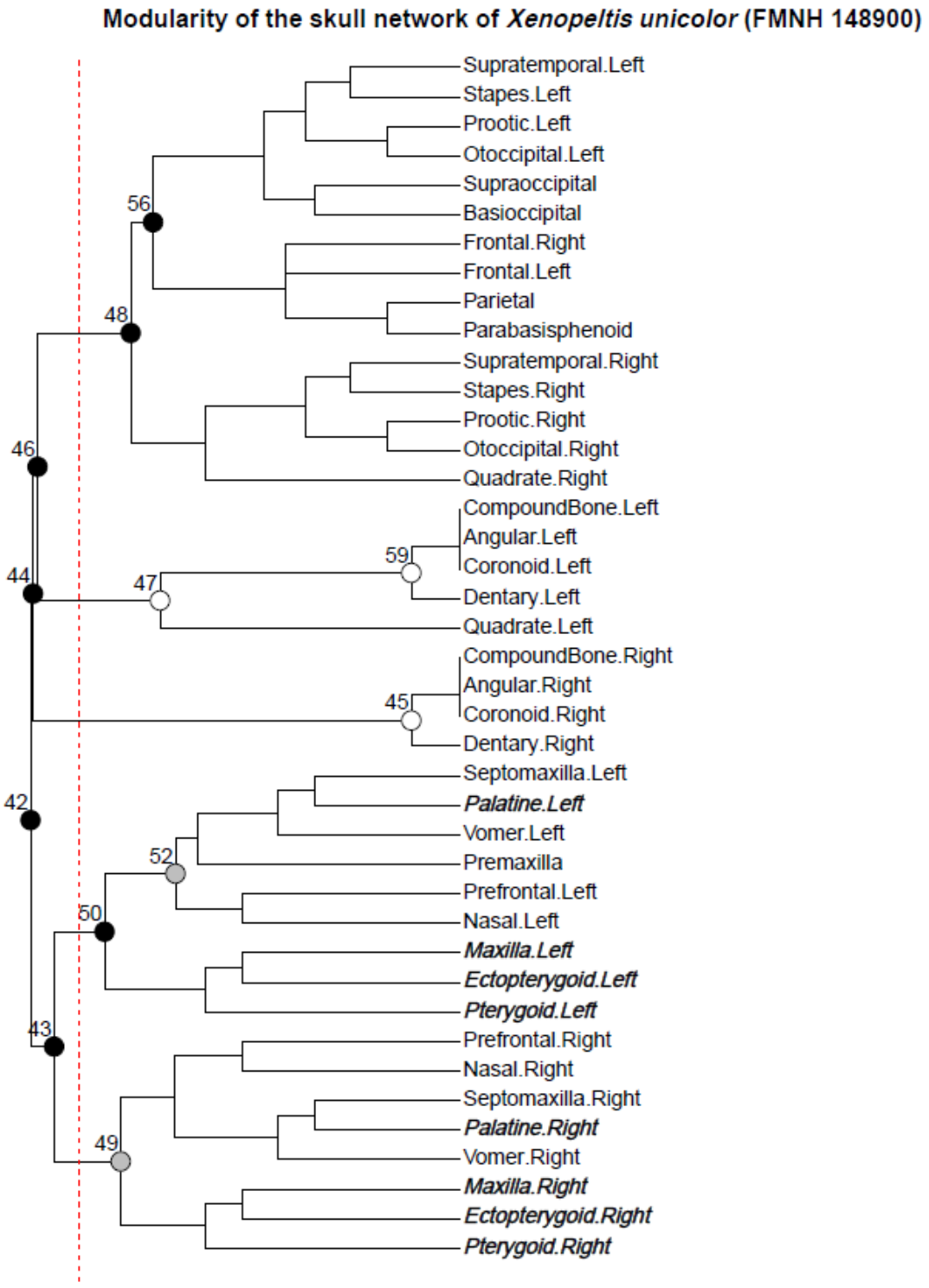

FIGURE S4.48. Modularity of the skull network of *Xenopeltis unicolor* (FMNH 148900)

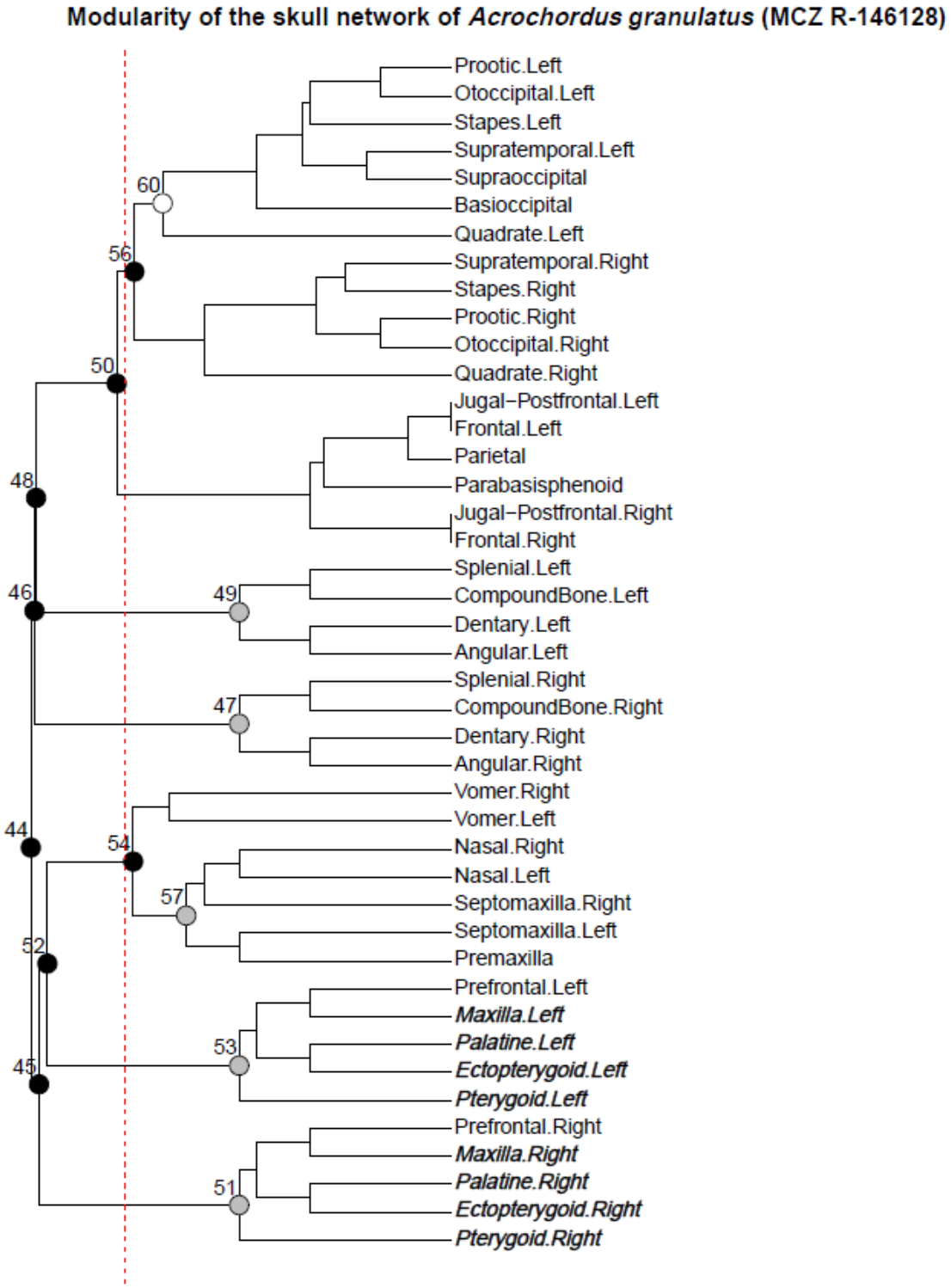

FIGURE S4.49. Modularity of the skull network of *Acrochordus granulatus* (MCZ R-146128)

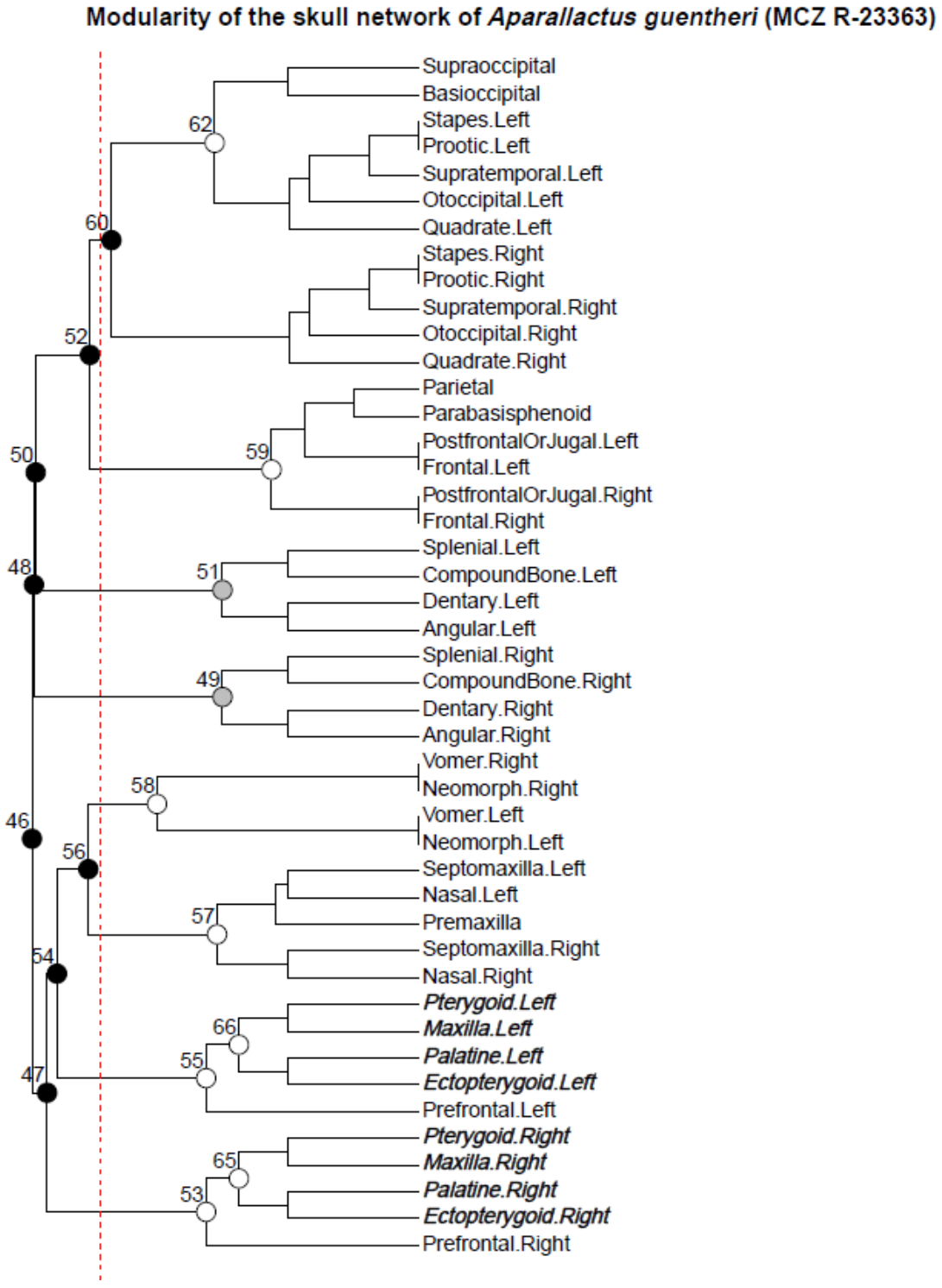

FIGURE S4.50. Modularity of the skull network of *Aparallactus guentheri* (MCZ R-23363)

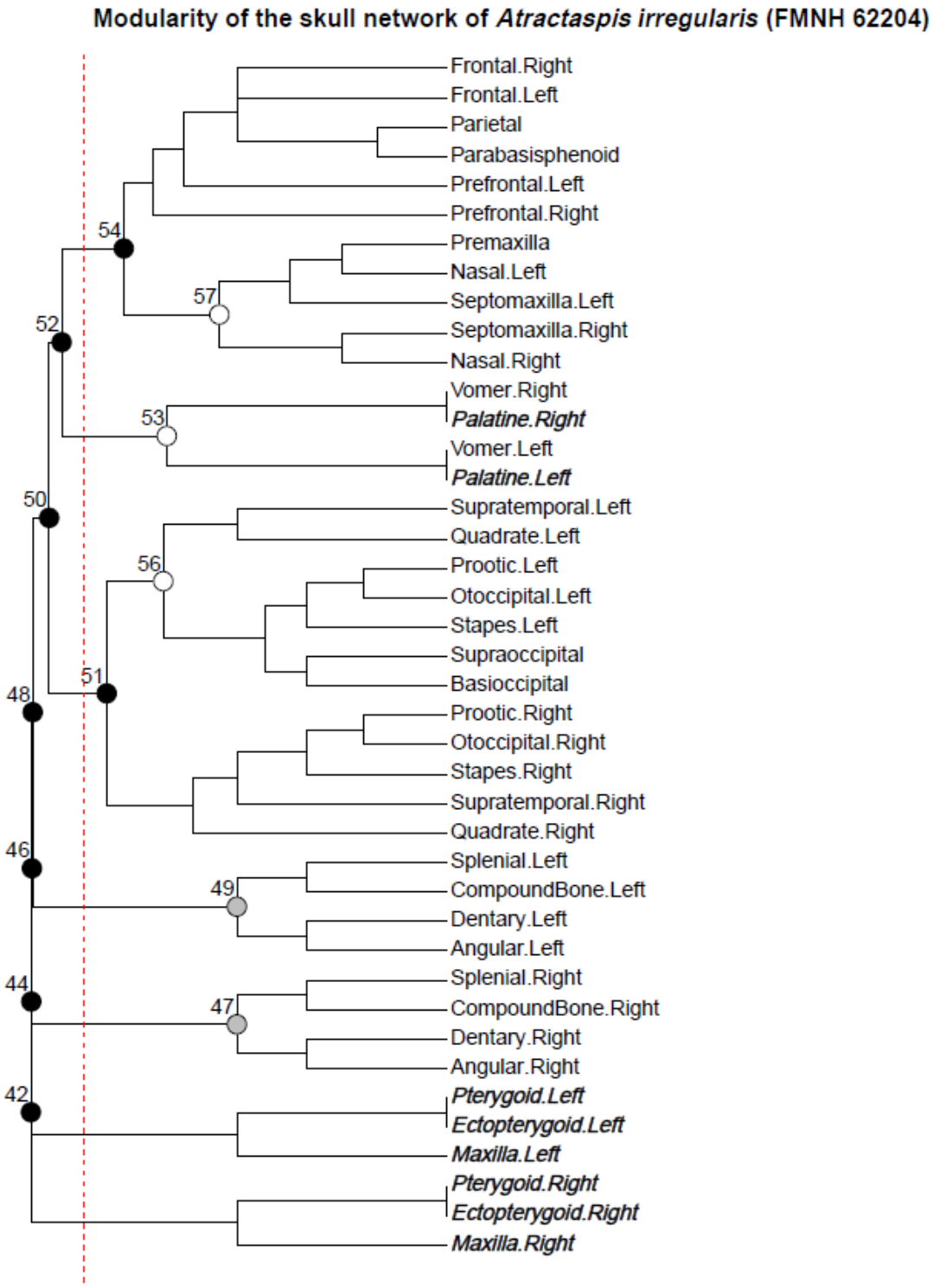

FIGURE S4.51. Modularity of the skull network of *Atractaspis irregularis* (FMNH 62204)

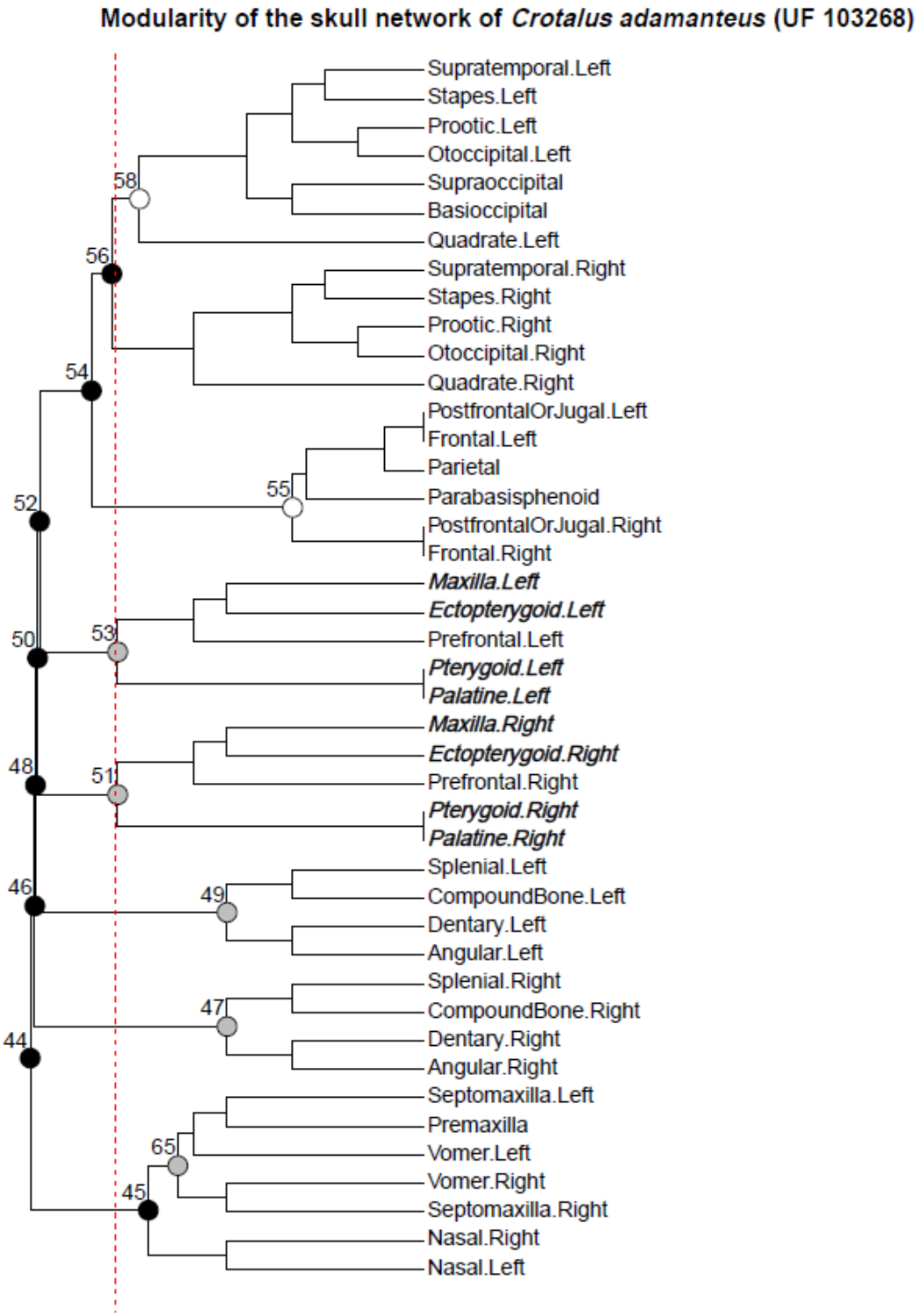

FIGURE S4.52. Modularity of the skull network of *Crotalus adamanteus* (UF 103268)

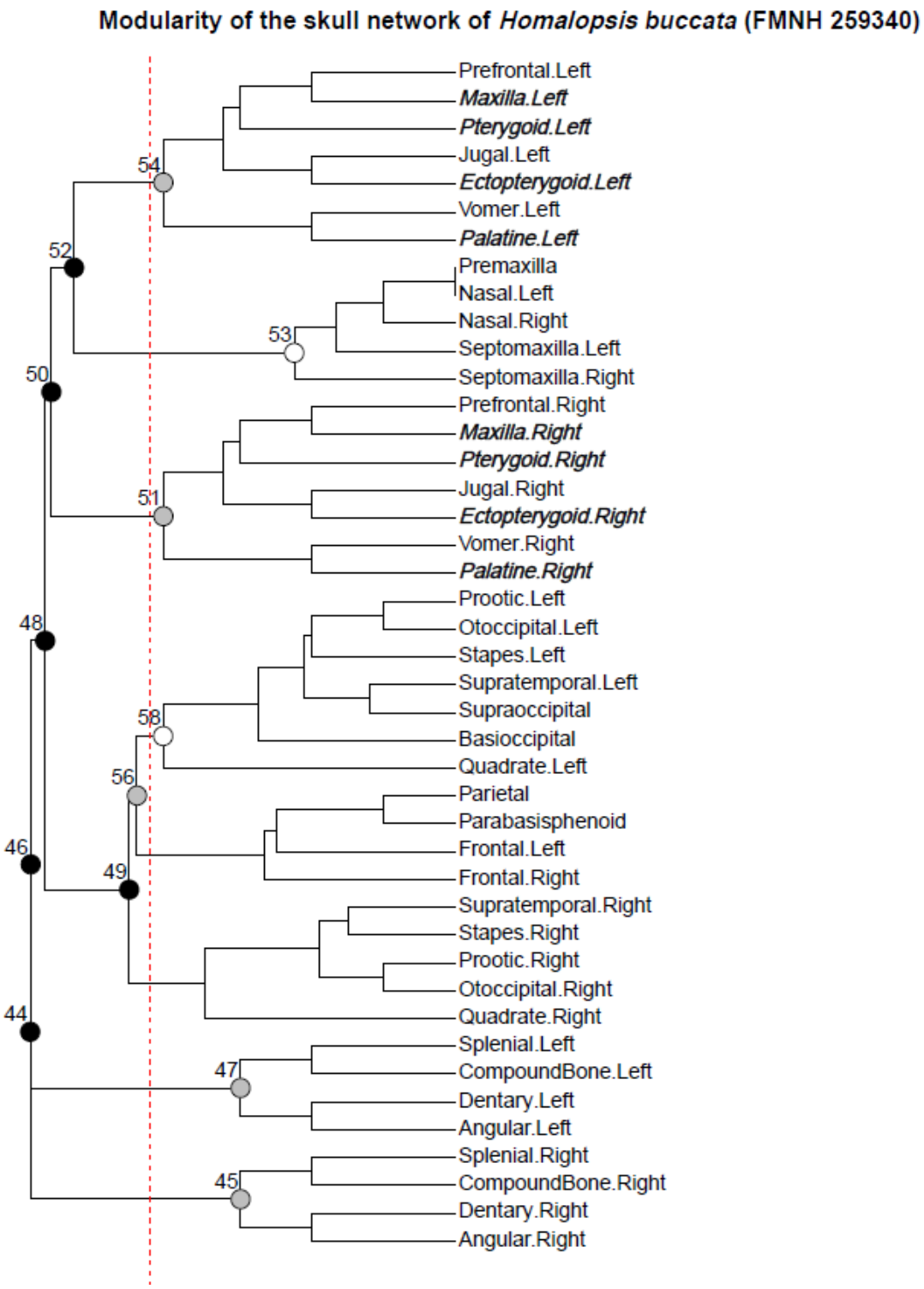

FIGURE S4.53. Modularity of the skull network of *Homalopsis buccata* (FMNH 259340)

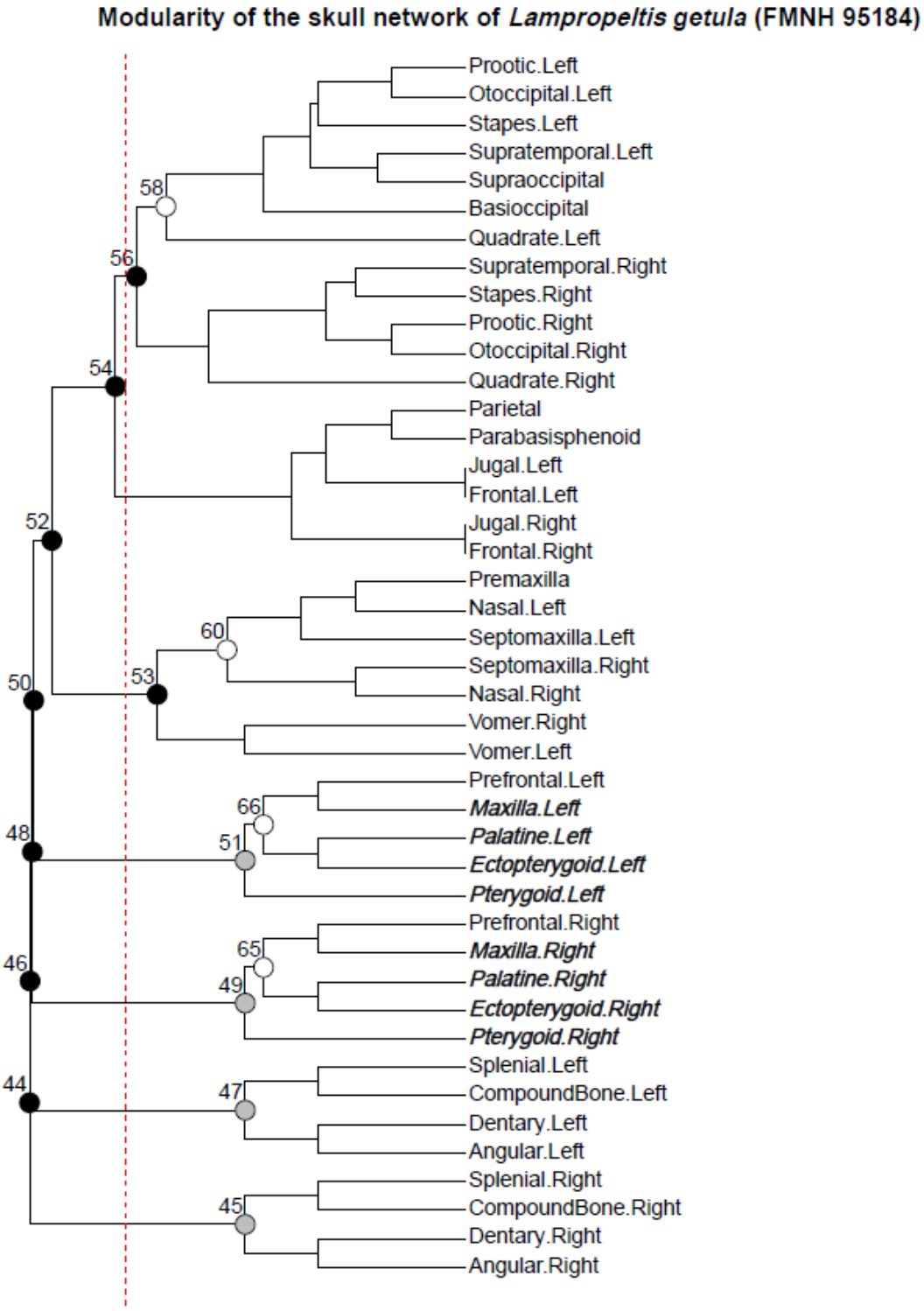

FIGURE S4.54. Modularity of the skull network of *Lampropeltis getula* (FMNH 95184)

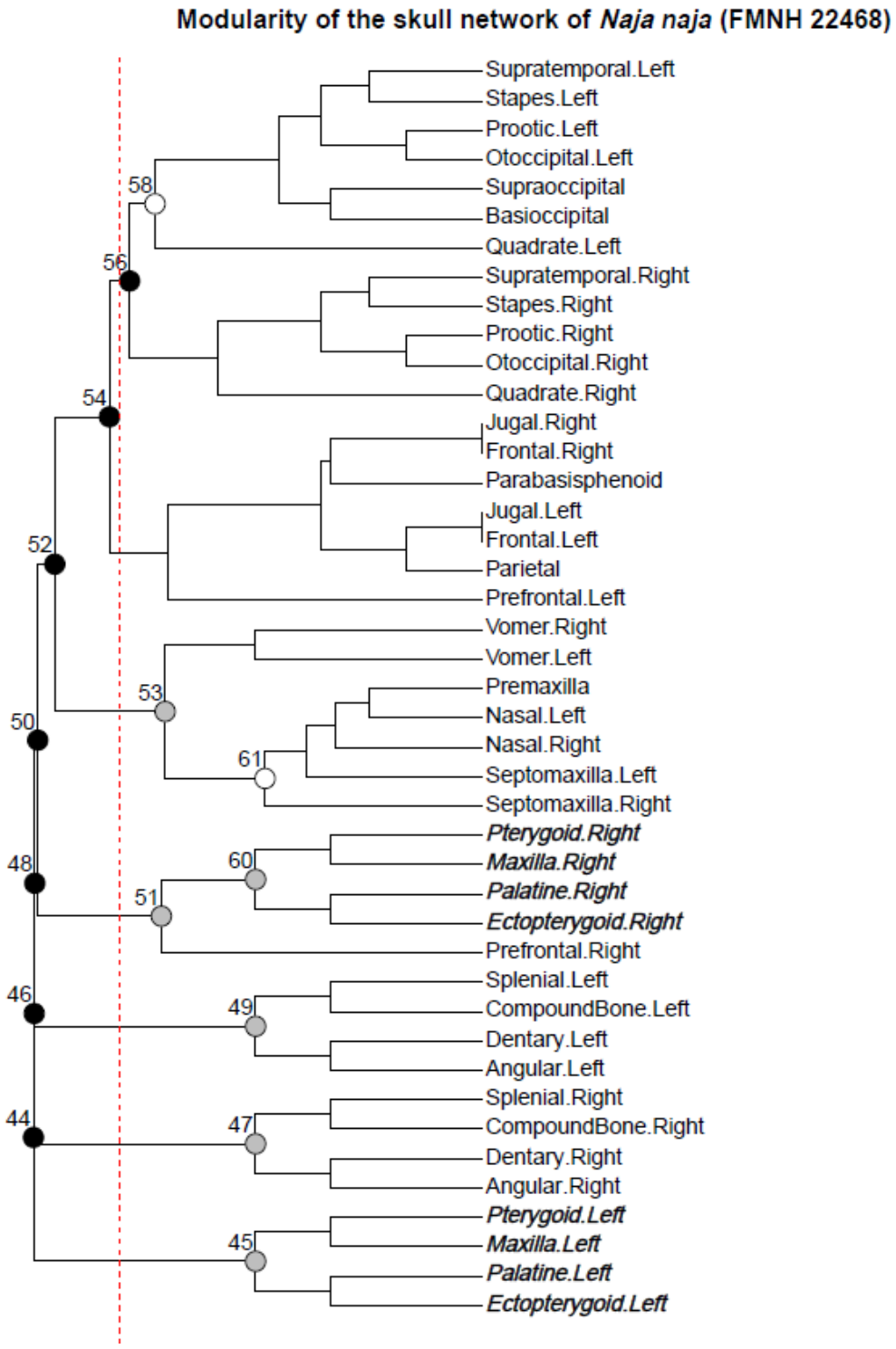

FIGURE S4.55. Modularity of the skull network of *Naja naja* (FMNH 22468)

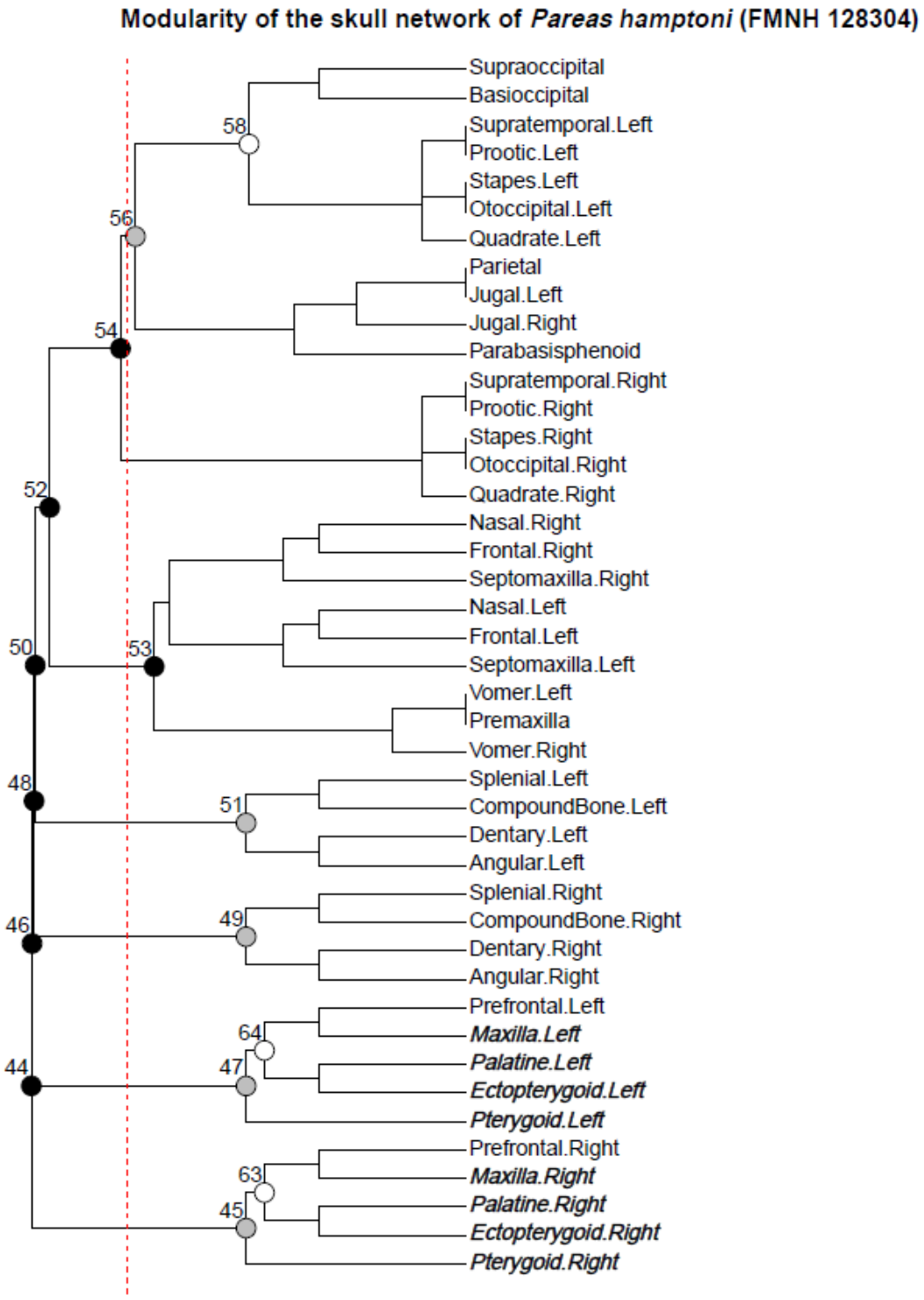

FIGURE S4.56. Modularity of the skull network of *Pareas hamptoni* (FMNH 128304)

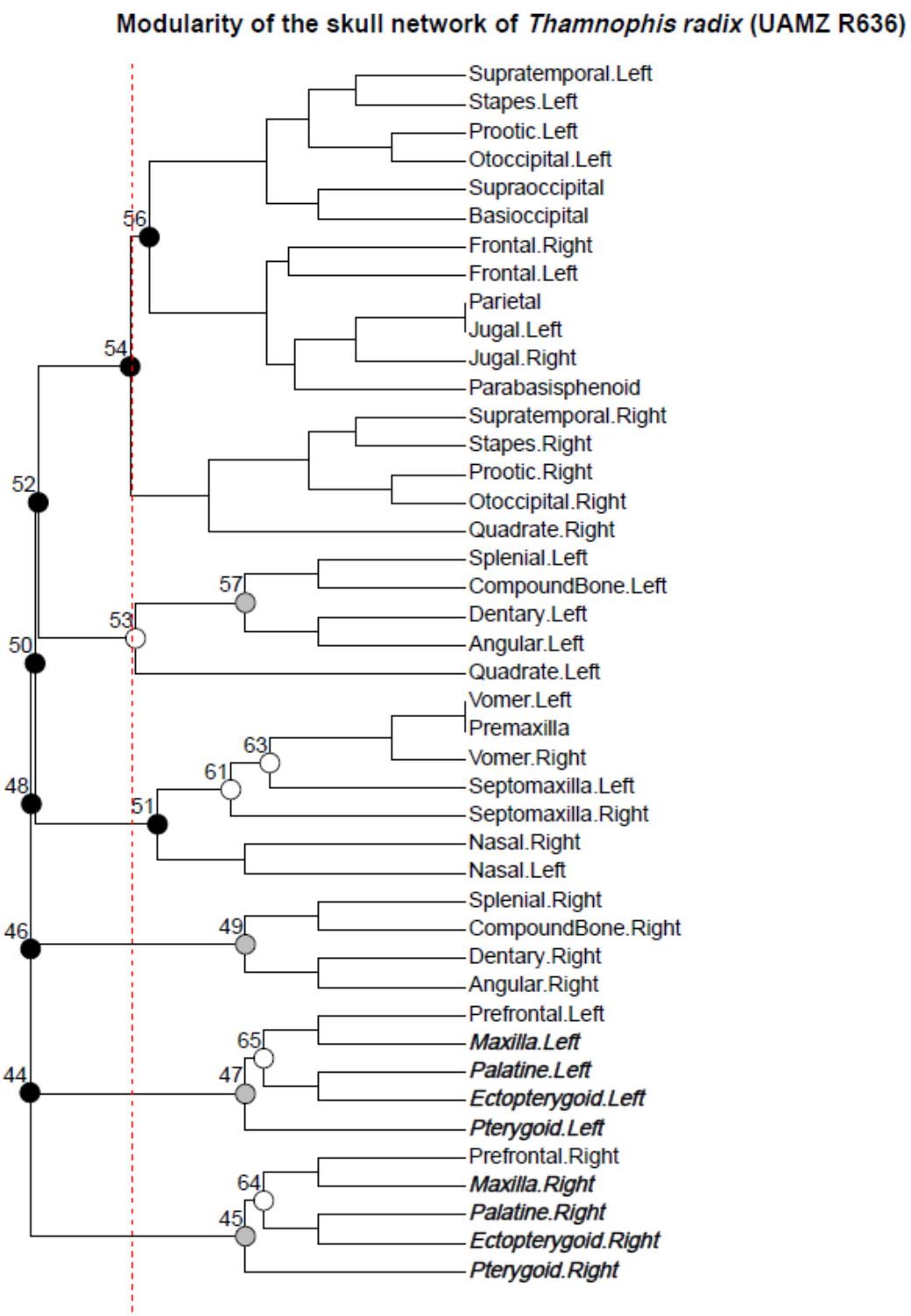

FIGURE S4.57. Modularity of the skull network of *Thamnophis radix* (UAMZ R636)

TABLE S4.1. Network parameters and groupings used for principal component analysis

Taxa	N	K	D	C	L	H	P	HigherTaxon	JawMech	Habitat	Size	HabitatSize
AcutoSol	36	72	0.1143	0.5196	4.0127	0.3732	0.7377	typhlo	singleaxle	fossorial	mini	FossorialMini
AcutoSub	36	74	0.1175	0.5272	3.7841	0.4061	0.7824	typhlo	singleaxle	fossorial	mini	FossorialMini
Afrotyphlops	40	89	0.1141	0.5116	3.8705	0.3840	0.6825	typhlo	singleaxle	fossorial	mini	FossorialMini
Amerotyphlops	40	87	0.1115	0.4994	3.9167	0.3513	0.6825	typhlo	singleaxle	fossorial	mini	FossorialMini
Anilios	38	83	0.1181	0.4940	3.6046	0.4033	0.7355	typhlo	singleaxle	fossorial	mini	FossorialMini
Antillotyphlops	40	85	0.1090	0.4941	3.9192	0.3796	0.6825	typhlo	singleaxle	fossorial	mini	FossorialMini
GerrhAter	35	66	0.1109	0.4776	3.8958	0.4020	0.7739	typhlo	singleaxle	fossorial	mini	FossorialMini
GerrhBedd	31	58	0.1247	0.5048	3.5548	0.4138	0.8429	typhlo	singleaxle	fossorial	mini	FossorialMini
Indotyphlops	35	66	0.1109	0.4554	3.8958	0.4270	0.7739	typhlo	singleaxle	fossorial	mini	FossorialMini
Ramphotyphlops	33	63	0.1193	0.4968	3.9356	0.3787	0.7787	typhlo	singleaxle	fossorial	mini	FossorialMini
Typhlops	40	89	0.1141	0.5116	3.8705	0.3840	0.6825	typhlo	singleaxle	fossorial	mini	FossorialMini
Xenotyphlops	37	80	0.1201	0.5171	3.4730	0.5314	0.8006	typhlo	singleaxle	fossorial	mini	FossorialMini
Xerotyphlops	38	81	0.1152	0.4901	3.8094	0.3726	0.7604	typhlo	singleaxle	fossorial	mini	FossorialMini
Anomalepis	37	59	0.0886	0.4706	3.8807	0.5621	0.8108	anoma	axlebrace	fossorial	mini	FossorialMini
Helminthophis	40	65	0.0833	0.4479	4.0427	0.5861	0.8125	anoma	axlebrace	fossorial	mini	FossorialMini
LioAlbi	41	68	0.0829	0.4427	4.2186	0.5495	0.8638	anoma	axlebrace	fossorial	mini	FossorialMini
LioArgaleus	41	68	0.0829	0.4427	4.2186	0.5495	0.8638	anoma	axlebrace	fossorial	mini	FossorialMini
LioBeui	41	67	0.0817	0.4227	4.0472	0.5965	0.8150	anoma	axlebrace	fossorial	mini	FossorialMini
Typhlophis	40	62	0.0795	0.4211	4.2774	0.5308	0.8638	anoma	axlebrace	fossorial	mini	FossorialMini
Epictia	40	97	0.1244	0.4735	3.4397	0.4418	0.7725	lepto	mandraking	fossorial	mini	FossorialMini
MyrioMacro	41	95	0.1159	0.4773	3.5085	0.4647	0.8245	lepto	mandraking	fossorial	mini	FossorialMini
MyrioTanae	40	85	0.1090	0.4588	3.8667	0.4758	0.8250	lepto	mandraking	fossorial	mini	FossorialMini
Rena	39	95	0.1282	0.4769	3.4345	0.4447	0.7705	lepto	mandraking	fossorial	mini	FossorialMini
Tricheilostoma	36	78	0.1238	0.4790	3.5746	0.4903	0.7870	lepto	mandraking	fossorial	mini	FossorialMini
Trilepida	39	93	0.1255	0.4634	3.4507	0.4421	0.7771	lepto	mandraking	fossorial	mini	FossorialMini
Acrochordus	43	77	0.0853	0.2257	4.5969	0.5214	0.8069	caeno	macro	nonfossorial	normal	NonfossNormal
Aparallactus	45	83	0.0838	0.2875	4.2677	0.4999	0.7180	caeno	macro	fossorial	mini	FossorialMini
Atractaspis	41	67	0.0817	0.1857	4.7512	0.5212	0.7531	caeno	macro	fossorial	normal	OneOrOtherNotBoth
Crotalus	43	67	0.0742	0.1802	4.8126	0.5611	0.8643	caeno	macro	nonfossorial	normal	NonfossNormal
Homalopsis	43	88	0.0975	0.2768	3.8228	0.4486	0.7572	caeno	macro	nonfossorial	normal	NonfossNormal
Lampropeltis	43	81	0.0897	0.2763	4.1030	0.5208	0.6533	caeno	macro	nonfossorial	normal	NonfossNormal
Naja	43	77	0.0853	0.2123	4.3865	0.5525	0.6555	caeno	macro	nonfossorial	normal	NonfossNormal
Pareas	43	79	0.0875	0.3412	4.0853	0.5168	0.7074	caeno	macro	nonfossorial	mini	OneOrOtherNotBoth
Thamnophis	43	75	0.0831	0.2275	4.2182	0.5210	0.6879	caeno	macro	nonfossorial	normal	NonfossNormal
Boa	45	94	0.0949	0.3760	3.9263	0.4457	0.8148	bopyt	macro	nonfossorial	normal	NonfossNormal
Casarea	49	107	0.0910	0.4522	4.0765	0.4199	0.7888	bopyt	macro	nonfossorial	normal	NonfossNormal
Calabaria	47	95	0.0879	0.2770	3.7299	0.5131	0.7614	bopyt	macro	semifossorial	normal	OneOrOtherNotBoth
Eryx	45	95	0.0960	0.3760	3.8758	0.4311	0.8148	bopyt	macro	semifossorial	normal	OneOrOtherNotBoth
Loxocemus	47	95	0.0879	0.2776	3.9112	0.5157	0.7614	bopyt	macro	semifossorial	normal	OneOrOtherNotBoth
Python	47	105	0.0971	0.4102	3.7761	0.4399	0.7777	bopyt	macro	nonfossorial	normal	NonfossNormal
Xenopeltis	41	79	0.0963	0.3467	4.1049	0.4085	0.7567	bopyt	macro	semifossorial	normal	OneOrOtherNotBoth
Anilius	39	91	0.1228	0.4276	3.1134	0.4406	0.7811	anili	snoutshift	semifossorial	normal	OneOrOtherNotBoth
Anomochilus	41	81	0.0988	0.3181	3.5897	0.5060	0.8209	anili	snoutshift	fossorial	mini	FossorialMini
Cylindrophis	45	96	0.0970	0.3664	3.5091	0.4645	0.7714	anili	snoutshift	semifossorial	normal	OneOrOtherNotBoth
Rhinophis	35	72	0.1210	0.4642	3.1815	0.4633	0.7853	anili	snoutshift	fossorial	mini	FossorialMini
Uropeltis	35	68	0.1143	0.3500	3.2118	0.4906	0.7478	anili	snoutshift	fossorial	mini	FossorialMini
Amphisbaena	37	83	0.1246	0.5353	3.1351	0.4288	0.7232	lizard	minkinesis	fossorial	normal	OneOrOtherNotBoth
Anelytropsis	47	107	0.0990	0.5212	3.3673	0.4435	0.7759	lizard	minkinesis	fossorial	mini	FossorialMini
Bipes	30	67	0.1540	0.5963	2.8759	0.5380	0.6200	lizard	minkinesis	fossorial	mini	FossorialMini
Dibamus	37	90	0.1351	0.5293	3.2583	0.3292	0.7363	lizard	minkinesis	fossorial	mini	FossorialMini
Dipsosaurus	52	126	0.0950	0.4861	3.3718	0.3798	0.7633	lizard	minkinesis	semifossorial	normal	OneOrOtherNotBoth
Lanthanotus	54	135	0.0943	0.4966	3.5618	0.3624	0.8354	lizard	minkinesis	nonfossorial	normal	NonfossNormal
Physignathus	54	135	0.0943	0.4717	3.3487	0.3561	0.8203	lizard	minkinesis	nonfossorial	normal	NonfossNormal
Rhineura	36	94	0.1492	0.5658	2.8540	0.4693	0.7701	lizard	minkinesis	fossorial	mini	FossorialMini
Sauromalus	50	118	0.0963	0.4536	3.4188	0.3924	0.7608	lizard	minkinesis	nonfossorial	normal	NonfossNormal
Uranoscodon	56	134	0.0870	0.4492	3.4825	0.3774	0.8182	lizard	minkinesis	nonfossorial	normal	NonfossNormal
Varanus	57	130	0.0815	0.4669	3.9467	0.3636	0.7584	lizard	minkinesis	nonfossorial	normal	NonfossNormal

TABLE S4.2. Measurements of skull length (mm) in observed taxa

These measurements were used to delimit 'miniaturization' *versus* 'non-miniaturization', with the break in distribution between *Rhineura* (11.74 mm) and *Acrochordus* (14.05 mm) being chosen as the most reasonable cut-off (see Methods; Fig. 4.9e,f; Table S4.1).

TAXON	SKULL LENGTH (MM)
Myriopholis tanae	2.56
Liotyphlops beui	3.17
Trilepida	3.18
Tricheilostoma	3.62
Gerrhopilus ater	3.82
Myriopholis macrorhyncha	4.02
Liotyphlops albirostris	4.10
Indotyphlops	4.11
Helminthophis	4.17
Gerrhopilus beddomii	4.29
Typhlophis	4.36
Rena	4.39
Epictia	4.67
Liotyphlops argaleus	4.76
Xenotyphlops	5.08
Xerotyphlops	5.14
Anomalepis	5.14
Antillotyphlops	5.23
Acutotyphlops solomonis	6.33
Acutotyphlops subocularis	6.56
Amerotyphlops	6.61
Typhlops	6.63
Anomochilus	6.85
Anilios	7.12
Bipes	7.12
Ramphotyphlops	7.16
Dibamus	8.20
Anelytropsis	8.60
Rhinophis	9.57
Uropeltis	10.48
Afrotyphlops	10.59
Aparallactus	11.54

Pareas	11.60
Rhineura	11.74
Acrochordus	14.05
Atractaspis	14.74
Casarea	16.30
Amphisbaena	17.46
Eryx	18.93
Calabaria	22.91
Cylindrophis	23.3
Dipsosaurus	23.87
Lanthanotus	24.38
Anilius	25.00
Thamnophis	25.50
Crotalus	27.48
Loxocemus	27.64
Uranoscodon	28.04
Physignathus	29.48
Xenopeltis	29.93
Lampropeltis	30.38
Homalopsis	30.70
Naja	31.64
Sauromalus	34.90
Varanus	57.41
Python	68.03
Boa	71.80

TABLE S4.3. PERMANOVA statistical results

Following PCA based on the calculated network parameters (see Results; Table 4.2), I grouped specimens according to several variables, using patterns of morphospace occupation to assess phenomena such as convergence (Fig. 4.9; Table S4.1). I then assessed statistical significance for each of these grouping methods via PERMANOVA, as reported here. See main text for details. Asterisks mark significance at $\alpha = 0.05$ (*), 0.01 (**), and 0.001 (***). Abbreviations: df, degrees of freedom.

VARIABLE	COMPARISON	F-STATISTIC	$DF_{TREATMENT, RESIDUALS}$	P-VALUE
Higher Taxon	Typhlopoidea *vs* Anomalepididae	6.589	1,17	0.0213 *
	Typhlopoidea *vs* Leptotyphlopidae	8.250	1,17	0.0106 *
	Typhlopoidea *vs* Caenophidia	2.251	1,20	0.1359
	Typhlopoidea *vs* Booidea-Pythonoidea	18.838	1,18	0.0004 ***
	Typhlopoidea *vs* Anilioidea	0.889	1,16	0.3560
	Typhlopoidea *vs* Non-snake lizards	20.550	1,22	0.0005 ***
	Anomalepididae *vs* Leptotyphlopidae	53.580	1,10	0.0017 **
	Anomalepididae *vs* Caenophidia	15.958	1,13	0.0021 **
	Anomalepididae *vs* Booidea-Pythonoidea	57.056	1,11	0.0008 ***
	Anomalepididae *vs*	9.582	1,9	0.0023 **

	Anilioidea			
	Anomalepididae *vs* Non-snake lizards	18.516	1,15	0.0018 **
	Leptotyphlopidae *vs* Caenophidia	13.39	1,13	0.0022 **
	Leptotyphlopidae *vs* Booidea-Pythonoidea	3.099	1,11	0.0853
	Leptotyphlopidae *vs* Anilioidea	2.078	1,9	0.1788
	Leptotyphlopidae *vs* Non-snake lizards	3.870	1,15	0.0661
	Caenophidia *vs* Booidea-Pythonoidea	21.094	1,14	0.0005 ***
	Caenophidia *vs* Anilioidea	1.386	1,12	0.2654
	Caenophidia *vs* Non-snake lizards	14.432	1,18	0.0016 **
	Booidea-Pythonoidea *vs* Anilioidea	6.086	1,10	0.0349 *
	Booidea-Pythonoidea *vs* Non-snake lizards	2.163	1,16	0.1638
	Anilioidea *vs* Non-snake lizards	5.948	1,14	0.0324 *
Jaw Mechanism	Single-axle max. raking *vs* Axle-brace max. raking	6.589	1,17	0.0176 *
	Single-axle max. raking *vs* Mandibular raking	8.250	1,17	0.0105 *

	Single-axle max. raking *vs* Macrostomy	6.874	1,27	0.0106 *
	Single-axle max. raking *vs* Snout-shifting	0.889	1,16	0.3535
	Single-axle max. raking *vs* Minimal-kinesis micro.	20.550	1,22	0.0003 ***
	Axle-brace max. raking *vs* Mandibular raking	53.580	1,10	0.0087 **
	Axle-brace max. raking *vs* Macrostomy	15.810	1,20	0.0010 ***
	Axle-brace max. raking *vs* Snout-shifting	9.582	1,9	0.0022 **
	Axle-brace max. raking *vs* Minimal-kinesis micro.	18.516	1,15	0.0011 **
	Mandibular raking *vs* Macrostomy	1.798	1,20	0.181*
	Mandibular raking *vs* Snout-shifting	2.078	1,9	0.1808
	Mandibular raking *vs* Minimal-kinesis micro.	3.870	1,15	0.0675
	Macrostomy *vs* Snout-shifting	1.014	1,19	0.314
	Macrostomy *vs* Minimal-kinesis micro.	11.901	1,25	0.0028 **
	Snout-shifting *vs* Minimal-kinesis micro.	5.948	1,14	0.0300 *
Habitat	Fossorial	19.265	1,48	0.0003 ***

	vs Non-fossorial			
	Fossorial *vs* Semi-fossorial	12.816	1,40	0.0008 ***
	Non-fossorial *vs* Semi-fossorial	0.161	1,20	0.6872
Size	Miniaturized *vs* Non-miniaturized	19.436	1,55	0.0001 ***
Combined Habitat–Size	Fossorial–Miniaturized *vs* Non-fossorial–Non-mini.	19.768	1,45	0.0001 ***
	Fossorial–Miniaturized *vs* Fossorial or Miniaturized	7.031	1,41	0.0089 **
	Non-fossorial–Non-mini. *vs* Fossorial or Miniaturized	1.630	1,22	0.2132

TABLE S4.4. Contribution of network parameters to each principal component

Principal components 1 and 2 explain 41.02% and 31.04% of the total variation in the dataset, respectively, and so are the focus of the Results and Discussion. Abbreviations: N, number of nodes; K, number of connections; D, density of connections; C, mean clustering coefficient; L, mean shortest path length; H, heterogeneity of connections; P, parcellation.

	PC1	PC2	PC3	PC4	PC5	PC6	PC7
N	0.2230	0.6196	-0.0415	-0.1471	0.1678	-0.0410	0.7164
K	-0.1091	0.6520	-0.0433	-0.2084	-0.0363	-0.4101	-0.5901
D	-0.5384	-0.2109	-0.0284	-0.0957	-0.3277	-0.6421	0.3688
C	-0.5000	0.0313	0.2834	0.2217	0.7863	-0.0355	0.0042
L	0.4974	-0.1021	-0.1382	0.6063	0.1736	-0.5699	-0.0234
H	0.3580	-0.3567	0.1636	-0.7022	0.3677	-0.2966	-0.0407
P	0.1514	0.0894	0.9324	0.1266	-0.2820	-0.0620	0.0181

APPENDIX 4.1. Adjacency matrices used for anatomical network analysis

APPENDIX 4.1-1. Adjacency matrix for *Acutotyphlops solomonis* (AMS R11452)

***Acutotyphlops solomonis* (AMS R11452)**	Angular.Left	Angular.Right	Basioccipital	CompoundBone.Left	CompoundBone.Right	Coronoid.Left	Coronoid.Right	Dentary.Left	Dentary.Right	Frontal.Left	Frontal.Right	Maxilla.Left	Maxilla.Right	Nasal.Left	Nasal.Right	Palatine.Left	Palatine.Right	Parabasisphenoid	Parietal	Prefrontal.Left	Prefrontal.Right	Premaxilla	Prootic-Otoccipital.Left	Prootic-Otoccipital.Right	Pterygoid.Left	Pterygoid.Right	Quadrate.Left	Quadrate.Right	Septomaxilla.Left	Septomaxilla.Right	Splenial.Left	Splenial.Right	Stapes.Left	Stapes.Right	Vomer.Left	Vomer.Right
Angular.Left				1		1																								1					
Angular.Right					1		1																								1				
Basioccipital																		1					1	1											
CompoundBone.Left	1					1		1																			1				1				
CompoundBone.Right		1					1		1																			1			1				
Coronoid.Left	1			1				1																						1					
Coronoid.Right		1			1				1																						1				
Dentary.Left				1		1			1																					1					
Dentary.Right					1		1	1																							1				
Frontal.Left											1			1				1	1	1									1						
Frontal.Right										1					1			1	1		1									1					
Maxilla.Left																1				1															
Maxilla.Right																	1				1														
Nasal.Left										1				1						1		1							1						
Nasal.Right											1				1					1	1									1					
Palatine.Left												1												1										1	
Palatine.Right													1												1										1
Parabasisphenoid			1							1	1								1				1	1											
Parietal										1	1							1					1	1											
Prefrontal.Left										1		1		1															1						
Prefrontal.Right											1		1		1															1					
Premaxilla														1	1														1	1				1	1
Prootic-Otoccipital.Left			1															1	1					1			1					1			
Prootic-Otoccipital.Right			1															1	1				1					1					1		
Pterygoid.Left																1																			
Pterygoid.Right																	1																		
Quadrate.Left				1																			1									1			
Quadrate.Right					1																			1									1		
Septomaxilla.Left										1				1						1		1								1				1	
Septomaxilla.Right											1				1						1	1						1							1
Splenial.Left	1			1		1		1																											
Splenial.Right		1			1		1		1																										
Stapes.Left																							1				1								
Stapes.Right																								1				1							
Vomer.Left																1						1							1						1
Vomer.Right																	1					1								1				1	

APPENDIX 4.1-2. Adjacency matrix for *Acutotyphlops subocularis* (SAMA R64770)

***Acutotyphlops subocularis* (SAMA R64770)**	Angular.Left	Angular.Right	Basioccipital	CompoundBone.Left	CompoundBone.Right	Coronoid.Left	Coronoid.Right	Dentary.Left	Dentary.Right	Frontal.Left	Frontal.Right	Maxilla.Left	Maxilla.Right	Nasal.Left	Nasal.Right	Palatine.Left	Palatine.Right	Parabasisphenoid	Parietal	Prefrontal.Left	Prefrontal.Right	Premaxilla	Prootic-Otoccipital.Left	Prootic-Otoccipital.Right	Pterygoid.Left	Pterygoid.Right	Quadrate.Left	Quadrate.Right	Septomaxilla.Left	Septomaxilla.Right	Splenial.Left	Splenial.Right	Stapes.Left	Stapes.Right	Vomer.Left	Vomer.Right
Angular.Left				1		1																									1					
Angular.Right					1		1																									1				
Basioccipital																		1					1	1												
CompoundBone.Left	1					1		1																			1				1					
CompoundBone.Right		1					1		1																			1				1				
Coronoid.Left	1			1				1																							1					
Coronoid.Right		1			1				1																							1				
Dentary.Left				1		1			1																						1					
Dentary.Right					1		1	1																								1				
Frontal.Left											1			1				1	1	1			1						1							
Frontal.Right										1					1			1	1		1			1						1						
Maxilla.Left																1				1																
Maxilla.Right																	1				1															
Nasal.Left										1					1					1		1								1						
Nasal.Right											1			1							1	1								1						
Palatine.Left												1												1											1	
Palatine.Right													1												1											1
Parabasisphenoid			1							1	1								1				1	1												
Parietal										1	1							1					1	1												
Prefrontal.Left										1		1		1															1							
Prefrontal.Right											1		1		1															1						
Premaxilla														1	1														1	1					1	1
Prootic-Otoccipital.Left			1							1								1	1					1			1					1			
Prootic-Otoccipital.Right			1								1							1	1				1					1					1		
Pterygoid.Left																1																				
Pterygoid.Right																	1																			
Quadrate.Left				1																			1									1				
Quadrate.Right					1																			1				1					1		
Septomaxilla.Left										1				1						1		1							1	1				1	
Septomaxilla.Right											1				1						1	1						1								1
Splenial.Left	1			1		1		1																											
Splenial.Right		1			1		1		1																											
Stapes.Left																							1				1								
Stapes.Right																								1				1							
Vomer.Left																1						1							1						1
Vomer.Right																	1					1								1				1	

APPENDIX 4.1-3. Adjacency matrix for *Afrotyphlops angolensis* (MCZ R-170385)

Afrotyphlops angolensis **(MCZ R-170385) Evans (1955), Mahendra (1935)**	Angular.Left	Angular.Right	Basioccipital	CompoundBone.Left	CompoundBone.Right	Coronoid.Left	Coronoid.Right	Dentary.Left	Dentary.Right	Frontal.Left	Frontal.Right	Maxilla.Left	Maxilla.Right	Nasal.Left	Nasal.Right	Otoccipital.Left	Otoccipital.Right	Palatine.Left	Palatine.Right	Parabasisphenoid	Parietal	Prefrontal.Left	Prefrontal.Right	Premaxilla	Prootic.Left	Prootic.Right	Pterygoid.Left	Pterygoid.Right	Quadrate.Left	Quadrate.Right	Septomaxilla.Left	Septomaxilla.Right	Splenial.Left	Splenial.Right	Stapes.Left	Stapes.Right	Supraoccipital.Left	Supraoccipital.Right	Vomer.Left	Vomer.Right
Angular.Left				1		1																											1							
Angular.Right					1		1																											1						
Basioccipital																1	1			1					1	1														
CompoundBone.Left	1					1		1																					1				1							
CompoundBone.Right		1					1		1																					1			1							
Coronoid.Left	1			1				1																									1							
Coronoid.Right		1			1				1																									1						
Dentary.Left				1		1			1																								1							
Dentary.Right					1		1	1																										1						
Frontal.Left											1			1						1	1	1								1										
Frontal.Right										1					1					1	1		1								1									
Maxilla.Left																		1				1																		
Maxilla.Right																			1				1																	
Nasal.Left										1					1							1		1							1									
Nasal.Right											1			1								1	1								1									
Otoccipital.Left			1														1				1			1				1						1		1			
Otoccipital.Right			1													1					1				1				1						1		1		
Palatine.Left												1														1												1	
Palatine.Right													1														1												1
Parabasisphenoid			1							1	1										1			1	1														
Parietal										1	1					1	1			1				1	1												1	1		
Prefrontal.Left										1		1		1																	1								
Prefrontal.Right											1		1		1																	1							
Premaxilla														1	1																1	1						1	1
Prootic.Left			1													1				1	1							1					1		1				
Prootic.Right			1														1			1	1								1						1		1		
Pterygoid.Left																		1																					
Pterygoid.Right																			1																				
Quadrate.Left				1												1									1									1					
Quadrate.Right					1												1									1										1			
Septomaxilla.Left										1				1								1		1								1						1	
Septomaxilla.Right											1				1								1	1							1								1
Splenial.Left	1			1		1		1																															
Splenial.Right		1			1		1		1																														
Stapes.Left																1									1				1										
Stapes.Right																	1									1				1									
Supraoccipital.Left																1					1				1												1		
Supraoccipital.Right																	1				1					1													
Vomer.Left																		1						1							1								1
Vomer.Right																			1					1								1						1	

APPENDIX 4.1-4. Adjacency matrix for *Amerotyphlops paucisquamus* (MCZ R-147336)

***Amerotyphlops paucisquamus* (MCZ R-147336)**	Angular.Left	Angular.Right	Basioccipital	CompoundBone.Left	CompoundBone.Right	Coronoid.Left	Coronoid.Right	Dentary.Left	Dentary.Right	Frontal.Left	Frontal.Right	Maxilla.Left	Maxilla.Right	Nasal.Left	Nasal.Right	Otoccipital.Left	Otoccipital.Right	Palatine.Left	Palatine.Right	Parabasisphenoid	Parietal	Prefrontal.Left	Prefrontal.Right	Premaxilla	Prootic.Left	Prootic.Right	Pterygoid.Left	Pterygoid.Right	Quadrate.Left	Quadrate.Right	Septomaxilla.Left	Septomaxilla.Right	Splenial.Left	Splenial.Right	Stapes.Left	Stapes.Right	Supraoccipital.Left	Supraoccipital.Right	Vomer.Left	Vomer.Right
Angular.Left				1		1																											1							
Angular.Right					1		1																											1						
Basioccipital																1	1			1					1	1														
CompoundBone.Left	1					1		1																					1			1								
CompoundBone.Right		1					1		1																					1			1							
Coronoid.Left	1			1				1																								1							
Coronoid.Right		1			1				1																								1						
Dentary.Left				1		1			1																								1						
Dentary.Right					1		1	1																									1						
Frontal.Left											1			1						1	1	1								1									
Frontal.Right										1					1					1	1		1								1								
Maxilla.Left																		1				1																	
Maxilla.Right																			1				1																
Nasal.Left										1					1							1		1							1								
Nasal.Right											1			1									1	1								1							
Otoccipital.Left			1														1							1				1						1		1		
Otoccipital.Right			1													1									1				1						1		1	
Palatine.Left												1														1											1	
Palatine.Right													1														1											1
Parabasisphenoid			1							1	1										1			1	1													
Parietal										1	1									1				1	1										1	1		
Prefrontal.Left										1		1		1																	1							
Prefrontal.Right											1		1		1																	1						
Premaxilla														1	1																	1	1					1	1
Prootic.Left			1													1				1	1								1					1		1		
Prootic.Right			1														1			1	1									1					1		1	
Pterygoid.Left																		1																				
Pterygoid.Right																			1																			
Quadrate.Left				1												1								1										1				
Quadrate.Right					1												1								1										1			
Septomaxilla.Left										1				1							1		1									1					1	
Septomaxilla.Right											1				1							1	1								1							1
Splenial.Left	1			1		1		1																														
Splenial.Right		1			1		1		1																													
Stapes.Left																1								1				1										
Stapes.Right																	1								1				1									
Supraoccipital.Left																1					1			1												1		
Supraoccipital.Right																	1				1				1											1		
Vomer.Left																		1						1						1							1	1
Vomer.Right																			1					1							1						1	

APPENDIX 4.1-5. Adjacency matrix for *Anilios bicolor* (SAMA 60626)

***Anilios bicolor* (SAMA 60626)**	Basioccipital	CompoundBone.Left	CompoundBone.Right	Coronoid.Left	Coronoid.Right	Dentary.Left	Dentary.Right	Frontal.Left	Frontal.Right	Maxilla.Left	Maxilla.Right	Nasal.Left	Nasal.Right	Otoccipital.Left	Otoccipital.Right	Palatine.Left	Palatine.Right	Parabasisphenoid	Parietal	Prefrontal.Left	Prefrontal.Right	Premaxilla	Prootic.Left	Prootic.Right	Pterygoid.Left	Pterygoid.Right	Quadrate.Left	Quadrate.Right	Septomaxilla.Left	Septomaxilla.Right	Splenial.Left	Splenial.Right	Stapes.Left	Stapes.Right	Supraoccipital.Left	Supraoccipital.Right	Vomer.Left	Vomer.Right
Basioccipital														1	1			1					1	1														
CompoundBone.Left				1		1																					1				1							
CompoundBone.Right					1		1																					1			1							
Coronoid.Left		1				1																								1								
Coronoid.Right			1				1																								1							
Dentary.Left		1		1			1																							1								
Dentary.Right			1		1	1																									1							
Frontal.Left									1			1						1	1	1			1						1										
Frontal.Right								1					1					1	1		1			1						1									
Maxilla.Left																1				1																			
Maxilla.Right																	1				1																		
Nasal.Left								1					1							1		1								1									
Nasal.Right									1			1									1	1									1								
Otoccipital.Left	1														1								1				1					1		1				
Otoccipital.Right	1													1										1				1					1		1			
Palatine.Left										1															1											1		
Palatine.Right											1															1											1	
Parabasisphenoid	1							1	1										1				1	1														
Parietal								1	1									1					1	1											1	1		
Prefrontal.Left								1		1		1																	1									
Prefrontal.Right									1		1		1																	1								
Premaxilla												1	1																1	1							1	1
Prootic.Left	1							1						1				1	1								1						1		1			
Prootic.Right	1								1						1			1	1									1						1		1		
Pterygoid.Left																1																						
Pterygoid.Right																	1																					
Quadrate.Left		1												1									1										1					
Quadrate.Right			1												1									1										1				
Septomaxilla.Left								1				1								1		1							1							1		
Septomaxilla.Right									1				1								1	1						1									1
Splenial.Left		1		1		1																															
Splenial.Right			1		1		1																														
Stapes.Left														1									1				1										
Stapes.Right															1									1				1									
Supraoccipital.Left														1					1				1												1		
Supraoccipital.Right															1				1					1											1		
Vomer.Left																1						1							1								1
Vomer.Right																	1					1								1						1	

APPENDIX 4.1-6. Adjacency matrix for *Antillotyphlops monastus* (MCZ R-81112)

***Antillotyphlops monastus* (MCZ R-81112)**	Angular.Left	Angular.Right	Basioccipital	CompoundBone.Left	CompoundBone.Right	Coronoid.Left	Coronoid.Right	Dentary.Left	Dentary.Right	Frontal.Left	Frontal.Right	Maxilla.Left	Maxilla.Right	Nasal.Left	Nasal.Right	Otoccipital.Left	Otoccipital.Right	Palatine.Left	Palatine.Right	Parabasisphenoid	Parietal	Prefrontal.Left	Prefrontal.Right	Premaxilla	Prootic.Left	Prootic.Right	Pterygoid.Left	Pterygoid.Right	Quadrate.Left	Quadrate.Right	Septomaxilla.Left	Septomaxilla.Right	Splenial.Left	Splenial.Right	Stapes.Left	Stapes.Right	Supraoccipital.Left	Supraoccipital.Right	Vomer.Left	Vomer.Right
Angular.Left				1																													1							
Angular.Right					1																													1						
Basioccipital																1	1			1					1	1														
CompoundBone.Left	1					1		1																					1				1							
CompoundBone.Right		1					1		1																					1				1						
Coronoid.Left				1				1																									1						
Coronoid.Right					1				1																									1						
Dentary.Left				1		1			1																								1							
Dentary.Right					1		1	1																										1						
Frontal.Left											1			1						1	1	1								1										
Frontal.Right										1					1					1	1		1								1									
Maxilla.Left																		1				1																		
Maxilla.Right																			1				1																	
Nasal.Left										1					1							1		1							1									
Nasal.Right											1			1									1	1							1									
Otoccipital.Left			1														1							1				1						1		1			
Otoccipital.Right			1													1									1				1						1		1		
Palatine.Left												1														1												1	
Palatine.Right													1														1												1
Parabasisphenoid			1							1	1										1			1	1														
Parietal										1	1									1				1	1												1	1		
Prefrontal.Left										1		1		1																	1								
Prefrontal.Right											1		1		1																	1							
Premaxilla														1	1																1	1						1	1
Prootic.Left			1													1				1	1								1				1		1			
Prootic.Right			1														1			1	1									1					1		1		
Pterygoid.Left																		1																					
Pterygoid.Right																			1																				
Quadrate.Left				1												1									1									1					
Quadrate.Right					1												1									1									1				
Septomaxilla.Left										1				1								1		1								1						1	
Septomaxilla.Right											1				1								1	1							1								1
Splenial.Left	1			1		1		1																															
Splenial.Right		1			1		1		1																														
Stapes.Left																1									1				1										
Stapes.Right																	1									1				1									
Supraoccipital.Left																1					1				1												1		
Supraoccipital.Right																	1				1					1											1		
Vomer.Left																		1					1								1							1	
Vomer.Right																			1				1									1						1	

APPENDIX 4.1-7. Adjacency matrix for *Gerrhopilus ater* (MCZ R-33505)

Gerrhopilus ater **(MCZ R-33505)** **Kraus (2017)**	Basioccipital	CompoundBone.Left	CompoundBone.Right	Coronoid.Left	Coronoid.Right	Dentary.Left	Dentary.Right	Frontal.Left	Frontal.Right	Maxilla.Left	Maxilla.Right	Nasal.Left	Nasal.Right	Palatine.Left	Palatine.Right	Parabasisphenoid	Parietal.Left	Parietal.Right	Prefrontal.Left	Prefrontal.Right	Premaxilla	Prootic-Otoccipital.Left	Prootic-Otoccipital.Right	Pterygoid.Left	Pterygoid.Right	Quadrate.Left	Quadrate.Right	Septomaxilla.Left	Septomaxilla.Right	Splenial.Left	Splenial.Right	Stapes.Left	Stapes.Right	Vomer.Left	Vomer.Right
Basioccipital																1						1	1											
CompoundBone.Left				1		1																				1			1					
CompoundBone.Right					1		1																				1			1				
Coronoid.Left		1				1																							1					
Coronoid.Right			1				1																							1				
Dentary.Left		1		1			1																						1					
Dentary.Right			1		1	1																								1				
Frontal.Left									1			1				1	1		1								1							
Frontal.Right								1					1			1		1		1									1					
Maxilla.Left														1					1															
Maxilla.Right															1					1														
Nasal.Left								1					1						1		1							1							
Nasal.Right									1			1								1	1								1						
Palatine.Left										1														1									1	
Palatine.Right											1														1									1
Parabasisphenoid	1							1	1								1	1				1	1											
Parietal.Left								1								1		1				1												
Parietal.Right									1							1	1						1											
Prefrontal.Left								1		1		1															1							
Prefrontal.Right									1		1		1															1						
Premaxilla												1	1														1	1						
Prootic-Otoccipital.Left	1															1	1					1				1					1			
Prootic-Otoccipital.Right	1															1		1				1					1					1		
Pterygoid.Left														1																				
Pterygoid.Right															1																			
Quadrate.Left		1																				1									1			
Quadrate.Right			1																				1										1	
Septomaxilla.Left								1				1							1		1								1				1	
Septomaxilla.Right									1				1							1	1							1						1
Splenial.Left		1		1		1																												
Splenial.Right			1		1		1																											
Stapes.Left																						1				1								
Stapes.Right																							1				1							
Vomer.Left														1														1						1
Vomer.Right															1														1				1	

APPENDIX 4.1-8. Adjacency matrix for *Gerrhopilus beddomii* (MCZ R-22372)

Gerrhopilus beddomii **(MCZ R-22372)** **Kraus (2017)**	CompoundBone.Left	CompoundBone.Right	Coronoid.Left	Coronoid.Right	Dentary.Left	Dentary.Right	Frontal.Left	Frontal.Right	Maxilla.Left	Maxilla.Right	Nasal.Left	Nasal.Right	Palatine.Left	Palatine.Right	Parietal	PosteriorComplex	Prefrontal.Left	Prefrontal.Right	Premaxilla	Pterygoid.Left	Pterygoid.Right	Quadrate.Left	Quadrate.Right	Septomaxilla.Left	Septomaxilla.Right	Splenial.Left	Splenial.Right	Stapes.Left	Stapes.Right	Vomer.Left	Vomer.Right
CompoundBone.Left			1		1																	1				1					
CompoundBone.Right				1		1																	1				1				
Coronoid.Left	1				1																					1					
Coronoid.Right		1				1																					1				
Dentary.Left	1		1			1																				1					
Dentary.Right		1		1	1																						1				
Frontal.Left								1			1				1	1	1							1							
Frontal.Right							1					1			1	1		1							1						
Maxilla.Left													1				1														
Maxilla.Right														1				1													
Nasal.Left							1					1					1		1					1							
Nasal.Right								1			1							1	1						1						
Palatine.Left									1											1										1	
Palatine.Right										1											1										1
Parietal							1	1								1															
PosteriorComplex							1	1							1							1	1					1	1		
Prefrontal.Left							1		1		1													1							
Prefrontal.Right								1		1		1													1						
Premaxilla											1	1												1	1					1	1
Pterygoid.Left													1																		
Pterygoid.Right														1																	
Quadrate.Left	1															1												1			
Quadrate.Right		1														1													1		
Septomaxilla.Left							1				1						1		1						1					1	
Septomaxilla.Right								1				1						1	1					1							1
Splenial.Left	1		1		1																										
Splenial.Right		1		1		1										1															
Stapes.Left																1						1									
Stapes.Right																1							1								
Vomer.Left													1						1					1							1
Vomer.Right														1					1						1					1	

APPENDIX 4.1-9. Adjacency matrix for *Indotyphlops braminus* (UAMZ R363)

Indotyphlops braminus **(UAMZ R363)** **Evans (1955), Mahendra (1935)**	Basioccipital	CompoundBone.Left	CompoundBone.Right	Coronoid.Left	Coronoid.Right	Dentary.Left	Dentary.Right	Frontal.Left	Frontal.Right	Maxilla.Left	Maxilla.Right	Nasal.Left	Nasal.Right	Palatine.Left	Palatine.Right	Parabasisphenoid	Parietal.Left	Parietal.Right	Prefrontal.Left	Prefrontal.Right	Premaxilla	Prootic-Otoccipital.Left	Prootic-Otoccipital.Right	Pterygoid.Left	Pterygoid.Right	Quadrate.Left	Quadrate.Right	Septomaxilla.Left	Septomaxilla.Right	Splenial.Left	Splenial.Right	Stapes.Left	Stapes.Right	Vomer.Left	Vomer.Right
Basioccipital																1						1	1											
CompoundBone.Left				1		1																				1				1				
CompoundBone.Right					1		1																				1				1			
Coronoid.Left		1																											1					
Coronoid.Right			1																											1				
Dentary.Left		1					1																						1					
Dentary.Right			1			1																								1				
Frontal.Left									1			1				1	1		1								1							
Frontal.Right								1					1			1		1		1									1					
Maxilla.Left														1					1															
Maxilla.Right															1					1														
Nasal.Left								1					1					1			1							1						
Nasal.Right									1			1							1	1									1					
Palatine.Left										1													1										1	
Palatine.Right											1													1										1
Parabasisphenoid	1							1	1								1	1				1	1											
Parietal.Left								1								1		1				1												
Parietal.Right									1							1	1						1											
Prefrontal.Left								1		1		1																1						
Prefrontal.Right									1		1		1																					
Premaxilla												1	1															1	1				1	1
Prootic-Otoccipital.Left	1															1	1						1			1					1			
Prootic-Otoccipital.Right	1															1		1				1					1					1		
Pterygoid.Left														1																				
Pterygoid.Right															1																				
Quadrate.Left		1																				1									1			
Quadrate.Right			1																				1										1	
Septomaxilla.Left								1				1							1		1								1					1	
Septomaxilla.Right									1				1							1	1							1						1
Splenial.Left		1		1		1																												
Splenial.Right			1		1		1																											
Stapes.Left																					1				1									
Stapes.Right																						1				1								
Vomer.Left														1						1							1							1
Vomer.Right															1					1								1					1	

APPENDIX 4.1-10. Adjacency matrix for *Ramphotyphlops lineatus* (MCZ R-37751)

***Ramphotyphlops lineatus* (MCZ R-37751)**	Basioccipital-Pbs	CompoundBone.Left	CompoundBone.Right	Coronoid.Left	Coronoid.Right	Dentary.Left	Dentary.Right	Frontal.Left	Frontal.Right	Maxilla.Left	Maxilla.Right	Nasal.Left	Nasal.Right	Palatine.Left	Palatine.Right	Parietal	Prefrontal.Left	Prefrontal.Right	Premaxilla	Prootic-Otoccipital.Left	Prootic-Otoccipital.Right	Pterygoid.Left	Pterygoid.Right	Quadrate.Left	Quadrate.Right	Septomaxilla.Left	Septomaxilla.Right	Splenial.Left	Splenial.Right	Stapes.Left	Stapes.Right	Vomer.Left	Vomer.Right
Basioccipital-Pbs								1	1							1				1	1												
CompoundBone.Left				1		1																		1				1					
CompoundBone.Right					1		1																		1				1				
Coronoid.Left		1				1																						1					
Coronoid.Right			1				1																						1				
Dentary.Left		1		1			1																					1					
Dentary.Right			1		1	1																							1				
Frontal.Left	1								1			1				1	1									1							
Frontal.Right	1							1					1			1		1									1						
Maxilla.Left														1			1																
Maxilla.Right															1			1															
Nasal.Left								1					1				1		1							1							
Nasal.Right									1			1						1	1								1						
Palatine.Left										1											1										1		
Palatine.Right											1											1											1
Parietal	1							1	1										1	1													
Prefrontal.Left								1		1		1													1								
Prefrontal.Right									1		1		1													1		1					
Premaxilla												1	1													1	1					1	1
Prootic-Otoccipital.Left	1															1					1			1					1				
Prootic-Otoccipital.Right	1															1			1						1					1			
Pterygoid.Left														1																			
Pterygoid.Right															1																		
Quadrate.Left		1																	1										1				
Quadrate.Right			1																	1										1			
Septomaxilla.Left								1				1					1		1								1				1		
Septomaxilla.Right									1				1					1	1							1							1
Splenial.Left		1		1		1																											
Splenial.Right			1		1		1																										
Stapes.Left																			1					1									
Stapes.Right																				1					1								
Vomer.Left														1					1							1							1
Vomer.Right															1				1								1					1	

APPENDIX 4.1-11. Adjacency matrix for *Typhlops titanops* (MCZ R-68571)

Typhlops titanops **(MCZ R-68571) Evans (1955), Mahendra (1935)**	Angular.Left	Angular.Right	Basioccipital	CompoundBone.Left	CompoundBone.Right	Coronoid.Left	Coronoid.Right	Dentary.Left	Dentary.Right	Frontal.Left	Frontal.Right	Maxilla.Left	Maxilla.Right	Nasal.Left	Nasal.Right	Otoccipital.Left	Otoccipital.Right	Palatine.Left	Palatine.Right	Parabasisphenoid	Parietal	Prefrontal.Left	Prefrontal.Right	Premaxilla	Prootic.Left	Prootic.Right	Pterygoid.Left	Pterygoid.Right	Quadrate.Left	Quadrate.Right	Septomaxilla.Left	Septomaxilla.Right	Splenial.Left	Splenial.Right	Stapes.Left	Stapes.Right	Supraoccipital.Left	Supraoccipital.Right	Vomer.Left	Vomer.Right
Angular.Left				1		1																											1							
Angular.Right					1		1																											1						
Basioccipital																1	1			1					1	1														
CompoundBone.Left	1					1		1																					1				1							
CompoundBone.Right		1					1		1																					1				1						
Coronoid.Left	1			1				1																								1							
Coronoid.Right		1			1				1																								1						
Dentary.Left				1		1			1																							1							
Dentary.Right					1		1	1																									1						
Frontal.Left											1			1						1	1	1								1									
Frontal.Right										1					1					1	1		1								1								
Maxilla.Left																		1				1																	
Maxilla.Right																			1				1																
Nasal.Left										1					1							1		1							1								
Nasal.Right											1			1									1	1							1								
Otoccipital.Left			1														1				1				1				1					1		1			
Otoccipital.Right			1													1					1					1				1					1		1		
Palatine.Left												1															1											1	
Palatine.Right													1															1											1
Parabasisphenoid			1							1	1										1				1	1													
Parietal										1	1					1	1			1					1	1											1	1		
Prefrontal.Left										1		1		1																	1								
Prefrontal.Right											1		1		1																	1							
Premaxilla														1	1																1	1						1	1
Prootic.Left			1													1				1	1								1				1		1				
Prootic.Right			1														1			1	1									1					1		1		
Pterygoid.Left																		1																					
Pterygoid.Right																			1																				
Quadrate.Left				1												1									1									1					
Quadrate.Right					1												1									1										1			
Septomaxilla.Left										1				1								1		1							1						1	
Septomaxilla.Right											1				1								1	1							1							1
Splenial.Left	1			1		1		1																														
Splenial.Right		1			1		1		1																													
Stapes.Left																1									1				1									
Stapes.Right																	1									1				1								
Supraoccipital.Left																1					1				1												1		
Supraoccipital.Right																	1				1					1											1		
Vomer.Left																		1						1							1							1	
Vomer.Right																			1					1								1						1	

APPENDIX 4.1-12. Adjacency matrix for *Xenotyphlops grandidieri* (ZSM 2194/2007)

***Xenotyphlops grandidieri* (ZSM 2194/2007) Chretien et al. (2019)**	Angular.Left	Angular.Right	Basioccipital	CompoundBone.Left	CompoundBone.Right	Coronoid.Left	Coronoid.Right	Dentary.Left	Dentary.Right	Frontal.Left	Frontal.Right	Maxilla.Left	Maxilla.Right	Nasal.Left	Nasal.Right	Palatine.Left	Palatine.Right	Parabasisphenoid	Parietal.Left	Parietal.Right	Prefrontal.Left	Prefrontal.Right	Premaxilla	Prootic-Otoccipital.Left	Prootic-Otoccipital.Right	Pterygoid.Left	Pterygoid.Right	Quadrate.Left	Quadrate.Right	Septomaxilla.Left	Septomaxilla.Right	Splenial.Left	Splenial.Right	Stapes.Left	Stapes.Right	Vomer.Left	Vomer.Right
Angular.Left				1																											1					
Angular.Right					1																											1				
Basioccipital																		1						1	1											
CompoundBone.Left	1					1		1																				1				1				
CompoundBone.Right		1					1		1																				1				1			
Coronoid.Left				1				1																							1					
Coronoid.Right					1				1																							1				
Dentary.Left				1		1			1																						1					
Dentary.Right					1		1	1																								1				
Frontal.Left											1			1				1	1		1								1							
Frontal.Right										1					1			1		1		1								1						
Maxilla.Left																1					1															
Maxilla.Right																	1					1														
Nasal.Left										1					1			1			1		1							1						
Nasal.Right											1			1				1				1	1								1					
Palatine.Left												1													1										1	
Palatine.Right													1													1										1
Parabasisphenoid			1							1	1			1	1				1	1				1	1					1	1				1	1
Parietal.Left										1								1		1				1												
Parietal.Right											1							1	1						1											
Prefrontal.Left										1		1		1									1								1					
Prefrontal.Right											1		1		1								1									1				
Premaxilla														1	1						1	1									1	1			1	1
Prootic-Otoccipital.Left			1															1	1					1				1					1			
Prootic-Otoccipital.Right			1															1		1				1					1					1		
Pterygoid.Left																1																				
Pterygoid.Right																	1																			
Quadrate.Left				1																				1									1			
Quadrate.Right					1																				1									1		
Septomaxilla.Left										1				1				1			1		1								1				1	
Septomaxilla.Right											1				1			1				1	1							1						1
Splenial.Left	1			1		1		1																												
Splenial.Right		1			1		1		1																											
Stapes.Left																							1					1								
Stapes.Right																								1					1							
Vomer.Left																1		1				1								1						1
Vomer.Right																	1	1				1									1				1	

APPENDIX 4.1-13. Adjacency matrix for *Xerotyphlops vermicularis* (MCZ R-56477)

***Xerotyphlops vermicularis* (MCZ R-56477)**	Basioccipital	CompoundBone.Left	CompoundBone.Right	Coronoid.Left	Coronoid.Right	Dentary.Left	Dentary.Right	Frontal.Left	Frontal.Right	Maxilla.Left	Maxilla.Right	Nasal.Left	Nasal.Right	Otoccipital.Left	Otoccipital.Right	Palatine.Left	Palatine.Right	Parabasisphenoid	Parietal	Prefrontal.Left	Prefrontal.Right	Premaxilla	Prootic.Left	Prootic.Right	Pterygoid.Left	Pterygoid.Right	Quadrate.Left	Quadrate.Right	Septomaxilla.Left	Septomaxilla.Right	Splenial.Left	Splenial.Right	Stapes.Left	Stapes.Right	Supraoccipital.Left	Supraoccipital.Right	Vomer.Left	Vomer.Right
Basioccipital														1	1			1					1	1														
CompoundBone.Left				1		1																					1				1							
CompoundBone.Right					1		1																					1			1							
Coronoid.Left		1				1																								1								
Coronoid.Right			1				1																								1							
Dentary.Left		1		1			1																							1								
Dentary.Right			1		1	1																									1							
Frontal.Left									1			1						1	1	1								1										
Frontal.Right								1					1					1	1		1								1									
Maxilla.Left																1				1																		
Maxilla.Right																	1				1																	
Nasal.Left								1					1							1		1							1									
Nasal.Right									1			1									1	1								1								
Otoccipital.Left	1														1							1				1						1		1			
Otoccipital.Right	1													1									1				1						1		1		
Palatine.Left										1														1												1	
Palatine.Right											1														1												1
Parabasisphenoid	1							1	1										1				1	1													
Parietal								1	1									1					1	1										1	1		
Prefrontal.Left								1		1		1																1									
Prefrontal.Right									1		1		1																1								
Premaxilla												1	1																1	1						1	1
Prootic.Left	1													1				1	1								1						1		1		
Prootic.Right	1														1			1	1									1						1		1	
Pterygoid.Left																1																					
Pterygoid.Right																	1																				
Quadrate.Left		1												1									1									1					
Quadrate.Right			1												1									1										1			
Septomaxilla.Left								1				1								1		1							1							1	
Septomaxilla.Right									1				1								1	1						1									1
Splenial.Left		1		1		1																															
Splenial.Right			1		1		1																														
Stapes.Left														1									1				1										
Stapes.Right															1									1				1									
Supraoccipital.Left														1					1				1												1		
Supraoccipital.Right															1				1					1											1		
Vomer.Left																1						1						1								1	
Vomer.Right																	1					1							1							1	

APPENDIX 4.1-14. Adjacency matrix for *Anomalepis mexicanus* (MCZ R-191201)

Anomalepis mexicanus **(MCZ R-191201)** **Rieppel et al (2009), Haas (1968)**	Angular.Left	Angular.Right	Basioccipital	CompoundBone.Left	CompoundBone.Right	Coronoid.Left	Coronoid.Right	Dentary.Left	Dentary.Right	Ectopterygoid.Left	Ectopterygoid.Right	Frontal	Jugal.Left	Jugal.Right	Maxilla.Left	Maxilla.Right	Nasal	Palatine.Left	Palatine.Right	Parabasisphenoid	Parietal	Prefrontal.Left	Prefrontal.Right	Premaxilla	Prootic-Otoccipital.Left	Prootic-Otoccipital.Right	Pterygoid.Left	Pterygoid.Right	Quadrate.Left	Quadrate.Right	Septomaxilla.Left	Septomaxilla.Right	Stapes.Left	Stapes.Right	Supraoccipital	Vomer.Left	Vomer.Right
Angular.Left				1				1																													
Angular.Right					1				1																												
Basioccipital																				1					1	1											
CompoundBone.Left	1					1		1																					1								
CompoundBone.Right		1					1		1																					1							
Coronoid.Left				1				1																													
Coronoid.Right					1				1																												
Dentary.Left	1			1		1			1																												
Dentary.Right		1			1		1	1																													
Ectopterygoid.Left															1																						
Ectopterygoid.Right																1																					
Frontal																	1			1	1	1	1								1	1					
Jugal.Left																																					
Jugal.Right																																					
Maxilla.Left										1								1				1															
Maxilla.Right											1								1				1														
Nasal												1												1							1	1					
Palatine.Left															1																					1	
Palatine.Right																1																					1
Parabasisphenoid			1									1									1			1	1												
Parietal												1								1		1	1	1	1										1		
Prefrontal.Left												1			1						1																
Prefrontal.Right												1				1					1																
Premaxilla																	1														1	1					
Prootic-Otoccipital.Left			1																	1	1				1			1					1		1	
Prootic-Otoccipital.Right			1							1										1	1			1					1					1	1	
Pterygoid.Left											1																										
Pterygoid.Right												1																									
Quadrate.Left				1																				1									1			
Quadrate.Right					1																				1									1		
Septomaxilla.Left												1					1							1								1				1	
Septomaxilla.Right												1					1							1							1						1
Stapes.Left																									1				1								
Stapes.Right																										1				1						
Supraoccipital																				1				1	1											
Vomer.Left																		1													1					1
Vomer.Right																			1													1			1	

APPENDIX 4.1-15. Adjacency matrix for *Helminthophis praeocularis* (MCZ R-17960)

Helminthophis praeocularis **(MCZ R-17960) Rieppel et al (2009)**	Angular.Left	Angular.Right	Basioccipital	CompoundBone.Left	CompoundBone.Right	Coronoid.Left	Coronoid.Right	Dentary.Left	Dentary.Right	Ectopterygoid.Left	Ectopterygoid.Right	Frontal	Jugal.Left	Jugal.Right	Maxilla.Left	Maxilla.Right	Nasal	Palatine.Left	Palatine.Right	Parabasisphenoid	Parietal.Left	Parietal.Right	Prefrontal.Left	Prefrontal.Right	Premaxilla	Prootic-Otoccipital.Left	Prootic-Otoccipital.Right	Pterygoid.Left	Pterygoid.Right	Quadrate.Left	Quadrate.Right	Septomaxilla.Left	Septomaxilla.Right	Stapes.Left	Stapes.Right	Supraoccipital	Supratemporal.Left	Supratemporal.Right	Vomer.Left	Vomer.Right
Angular.Left				1				1																															
Angular.Right					1				1																														
Basioccipital																				1					1	1													
CompoundBone.Left	1					1		1																						1									
CompoundBone.Right		1					1		1																						1								
Coronoid.Left				1				1																															
Coronoid.Right					1				1																														
Dentary.Left	1			1		1			1																														
Dentary.Right		1			1		1	1																														
Ectopterygoid.Left												1																1										
Ectopterygoid.Right																	1												1										
Frontal																	1			1	1	1	1	1								1	1						
Jugal.Left																																							
Jugal.Right																																							
Maxilla.Left										1												1																	
Maxilla.Right											1												1																
Nasal												1												1								1	1						
Palatine.Left																											1										1	
Palatine.Right																												1										1
Parabasisphenoid			1									1									1	1			1	1												
Parietal.Left												1								1		1			1										1			
Parietal.Right												1								1	1					1									1			
Prefrontal.Left												1			1																							
Prefrontal.Right												1					1																						
Premaxilla																	1															1	1						
Prootic-Otoccipital.Left			1																	1	1					1				1			1		1	1		
Prootic-Otoccipital.Right			1																	1		1					1				1			1	1		1		
Pterygoid.Left										1								1																					
Pterygoid.Right											1								1																				
Quadrate.Left				1																					1								1			1			
Quadrate.Right					1																					1								1			1		
Septomaxilla.Left												1					1							1									1					1	
Septomaxilla.Right												1					1							1								1						1
Stapes.Left																									1				1									
Stapes.Right																										1				1								
Supraoccipital																					1	1			1	1												
Supratemporal.Left																									1				1									
Supratemporal.Right																										1				1								
Vomer.Left																		1														1						1
Vomer.Right																			1														1				1		

APPENDIX 4.1-16. Adjacency matrix for *Liotyphlops albirostris* (FMNH 216257)

***Liotyphlops albirostris* (FMNH 216257) Rieppel et al (2009)**	Angular.Left	Angular.Right	Basioccipital	CompoundBone.Left	CompoundBone.Right	Coronoid.Left	Coronoid.Right	Dentary.Left	Dentary.Right	Ectopterygoid.Left	Ectopterygoid.Right	Frontal.Left	Frontal.Right	Jugal.Left	Jugal.Right	Maxilla.Left	Maxilla.Right	Nasal	Palatine.Left	Palatine.Right	Parabasisphenoid	Parietal.Left	Parietal.Right	Prefrontal.Left	Prefrontal.Right	Premaxilla	Prootic-Otoccipital.Left	Prootic-Otoccipital.Right	Pterygoid.Left	Pterygoid.Right	Quadrate.Left	Quadrate.Right	Septomaxilla.Left	Septomaxilla.Right	Stapes.Left	Stapes.Right	Supraoccipital	Supratemporal.Left	Supratemporal.Right	Vomer.Left	Vomer.Right
Angular.Left				1				1																																	
Angular.Right					1				1																																
Basioccipital																					1						1	1													
CompoundBone.Left	1					1		1																							1										
CompoundBone.Right		1					1		1																							1									
Coronoid.Left				1				1																																	
Coronoid.Right					1				1																																
Dentary.Left	1			1		1			1																																
Dentary.Right		1			1		1	1																																	
Ectopterygoid.Left																1													1												
Ectopterygoid.Right																	1													1											
Frontal.Left													1					1			1	1		1																	
Frontal.Right												1						1			1		1		1																
Jugal.Left																																									
Jugal.Right																																									
Maxilla.Left										1														1																	
Maxilla.Right											1														1																
Nasal												1	1													1								1	1						
Palatine.Left																													1											1	
Palatine.Right																														1											1
Parabasisphenoid			1									1	1									1	1				1	1												
Parietal.Left												1									1		1				1														
Parietal.Right													1								1	1						1													
Prefrontal.Left												1				1																									
Prefrontal.Right													1				1																									
Premaxilla																		1															1	1						1	1
Prootic-Otoccipital.Left			1																		1	1						1			1			1		1	1			
Prootic-Otoccipital.Right			1							1									1		1		1			1						1			1	1		1		
Pterygoid.Left											1																														
Pterygoid.Right												1								1																					
Quadrate.Left				1																							1								1		1			
Quadrate.Right					1																							1						1			1			
Septomaxilla.Left																		1								1									1					1	
Septomaxilla.Right																		1								1								1						1
Stapes.Left																										1				1										
Stapes.Right																											1				1									
Supraoccipital																						1	1			1	1													
Supratemporal.Left																										1				1										
Supratemporal.Right																											1				1									
Vomer.Left																			1							1							1								1
Vomer.Right																				1						1								1						1	

APPENDIX 4.1-17. Adjacency matrix for *Liotyphlops argaleus* (MCZ R-67933)

Liotyphlops argaleus **(MCZ R-67933) Rieppel et al (2009)**	Angular.Left	Angular.Right	Basioccipital	CompoundBone.Left	CompoundBone.Right	Coronoid.Left	Coronoid.Right	Dentary.Left	Dentary.Right	Ectopterygoid.Left	Ectopterygoid.Right	Frontal.Left	Frontal.Right	Jugal.Left	Jugal.Right	Maxilla.Left	Maxilla.Right	Nasal	Palatine.Left	Palatine.Right	Parabasisphenoid	Parietal.Left	Parietal.Right	Prefrontal.Left	Prefrontal.Right	Premaxilla	Prootic-Otoccipital.Left	Prootic-Otoccipital.Right	Pterygoid.Left	Pterygoid.Right	Quadrate.Left	Quadrate.Right	Septomaxilla.Left	Septomaxilla.Right	Stapes.Left	Stapes.Right	Supraoccipital	Supratemporal.Left	Supratemporal.Right	Vomer.Left	Vomer.Right
Angular.Left				1				1																																	
Angular.Right					1				1																																
Basioccipital																					1						1	1													
CompoundBone.Left	1					1		1																							1										
CompoundBone.Right		1					1		1																							1									
Coronoid.Left				1				1																																	
Coronoid.Right					1				1																																
Dentary.Left	1			1		1			1																																
Dentary.Right		1			1		1	1																																	
Ectopterygoid.Left																1													1												
Ectopterygoid.Right																	1													1											
Frontal.Left													1					1			1	1		1																	
Frontal.Right												1						1			1		1		1																
Jugal.Left																																									
Jugal.Right																																									
Maxilla.Left										1														1																	
Maxilla.Right											1														1																
Nasal												1	1													1								1	1						
Palatine.Left																													1										1	
Palatine.Right																														1										1
Parabasisphenoid			1									1	1									1	1				1	1												
Parietal.Left												1									1		1				1													
Parietal.Right													1								1	1						1										1			
Prefrontal.Left												1				1																									
Prefrontal.Right													1				1																								
Premaxilla																		1															1	1					1	1
Prootic-Otoccipital.Left			1																		1	1					1				1			1		1	1			
Prootic-Otoccipital.Right			1							1									1		1		1			1						1			1	1		1		
Pterygoid.Left											1							1																							
Pterygoid.Right										1									1																						
Quadrate.Left				1																							1				1			1			1			
Quadrate.Right					1																							1				1			1			1		
Septomaxilla.Left																		1								1								1					1	
Septomaxilla.Right																		1								1							1							1
Stapes.Left																										1				1										
Stapes.Right																											1				1									
Supraoccipital																						1	1			1	1													
Supratemporal.Left																										1				1										
Supratemporal.Right																											1				1									
Vomer.Left																			1							1							1							1	1
Vomer.Right																				1						1								1					1	

APPENDIX 4.1-18. Adjacency matrix for *Liotyphlops beui* (SAMA 40142)

Liotyphlops beui **(SAMA 40142)** **Rieppel et al (2009)**	Angular.Left	Angular.Right	Basioccipital	CompoundBone.Left	CompoundBone.Right	Coronoid.Left	Coronoid.Right	Dentary.Left	Dentary.Right	Ectopterygoid.Left	Ectopterygoid.Right	Frontal.Left	Frontal.Right	Jugal.Left	Jugal.Right	Maxilla.Left	Maxilla.Right	Nasal	Palatine.Left	Palatine.Right	Parabasisphenoid	Parietal.Left	Parietal.Right	Prefrontal.Left	Prefrontal.Right	Premaxilla	Prootic-Otoccipital.Left	Prootic-Otoccipital.Right	Pterygoid.Left	Pterygoid.Right	Quadrate.Left	Quadrate.Right	Septomaxilla.Left	Septomaxilla.Right	Stapes.Left	Stapes.Right	Supraoccipital	Supratemporal.Left	Supratemporal.Right	Vomer.Left	Vomer.Right
Angular.Left				1				1																																	
Angular.Right					1				1																																
Basioccipital																					1						1	1													
CompoundBone.Left	1					1		1																							1										
CompoundBone.Right		1					1		1																							1									
Coronoid.Left				1				1																																	
Coronoid.Right					1				1																																
Dentary.Left	1			1		1			1																																
Dentary.Right		1			1		1	1																																	
Ectopterygoid.Left																1			1										1												
Ectopterygoid.Right																	1			1										1											
Frontal.Left													1					1			1	1		1									1								
Frontal.Right												1						1			1		1		1									1							
Jugal.Left																																									
Jugal.Right																																									
Maxilla.Left										1														1																	
Maxilla.Right											1														1																
Nasal												1	1													1								1	1						
Palatine.Left										1																														1	
Palatine.Right											1																														1
Parabasisphenoid			1									1	1									1	1				1	1												
Parietal.Left												1									1		1				1													
Parietal.Right													1								1	1						1										1			
Prefrontal.Left												1				1																									
Prefrontal.Right													1				1																									
Premaxilla																		1															1	1					1	1
Prootic-Otoccipital.Left			1																		1	1						1			1				1		1	1		
Prootic-Otoccipital.Right			1								1										1		1				1					1				1	1		1		
Pterygoid.Left										1																															
Pterygoid.Right											1																														
Quadrate.Left				1																							1								1					
Quadrate.Right					1																							1								1				
Septomaxilla.Left												1						1								1													1	
Septomaxilla.Right													1					1								1														1
Stapes.Left																											1				1									
Stapes.Right																												1				1								
Supraoccipital																						1	1				1	1												
Supratemporal.Left																											1													
Supratemporal.Right																												1												
Vomer.Left																			1							1							1							1	1
Vomer.Right																				1						1								1					1		

APPENDIX 4.1-19. Adjacency matrix for *Typhlophis squamosus* (MCZ R-145403)

Typhlophis squamosus **(MCZ R-145403) Rieppel et al (2009)**	Angular.Left	Angular.Right	Basioccipital	CompoundBone.Left	CompoundBone.Right	Coronoid.Left	Coronoid.Right	Dentary.Left	Dentary.Right	Ectopterygoid.Left	Ectopterygoid.Right	Frontal.Left	Frontal.Right	Jugal.Left	Jugal.Right	Maxilla.Left	Maxilla.Right	Nasal	Palatine.Left	Palatine.Right	Parabasisphenoid	Parietal.Left	Parietal.Right	Prefrontal.Left	Prefrontal.Right	Premaxilla	Prootic-Otoccipital.Left	Prootic-Otoccipital.Right	Pterygoid.Left	Pterygoid.Right	Quadrate.Left	Quadrate.Right	Septomaxilla.Left	Septomaxilla.Right	Stapes.Left	Stapes.Right	Supratemporal.Left	Supratemporal.Right	Vomer.Left	Vomer.Right
Angular.Left				1				1																																
Angular.Right				1					1																															
Basioccipital																					1						1	1												
CompoundBone.Left	1					1		1																						1										
CompoundBone.Right		1					1		1																						1									
Coronoid.Left				1				1																															
Coronoid.Right					1				1																															
Dentary.Left	1			1		1			1																															
Dentary.Right		1			1		1	1																															
Ectopterygoid.Left																1													1										
Ectopterygoid.Right																	1													1										
Frontal.Left													1					1			1	1		1																
Frontal.Right												1						1			1		1		1															
Jugal.Left																																								
Jugal.Right																																								
Maxilla.Left										1														1																
Maxilla.Right											1														1															
Nasal												1	1													1							1	1						
Palatine.Left																												1										1	
Palatine.Right																													1										1
Parabasisphenoid			1									1	1									1	1			1	1												
Parietal.Left												1									1		1			1													
Parietal.Right													1								1	1					1												
Prefrontal.Left												1				1																								
Prefrontal.Right													1				1																							
Premaxilla																		1															1	1						
Prootic-Otoccipital.Left			1																		1	1					1			1				1		1			
Prootic-Otoccipital.Right			1																		1		1				1				1				1		1		
Pterygoid.Left										1									1																					
Pterygoid.Right											1									1																				
Quadrate.Left				1																							1								1		1			
Quadrate.Right					1																							1								1		1		
Septomaxilla.Left																		1																	1				1	
Septomaxilla.Right																		1								1								1					1
Stapes.Left																											1				1								
Stapes.Right																												1				1							
Supratemporal.Left																											1				1								
Supratemporal.Right																												1				1							
Vomer.Left																			1														1						1	
Vomer.Right																				1														1					1	

APPENDIX 4.1-20. Adjacency matrix for *Epictia albifrons* (MCZ R-2885)

Epictia albifrons **(MCZ R-2885) Kley (2006), Koch et al (2019)**	Angular.Left	Angular.Right	Basioccipital	CompoundBone.Left	CompoundBone.Right	Coronoid.Left	Coronoid.Right	Dentary.Left	Dentary.Right	Frontal.Left	Frontal.Right	Maxilla.Left	Maxilla.Right	Nasal.Left	Nasal.Right	Otoccipital.Left	Otoccipital.Right	Palatine.Left	Palatine.Right	Parabasisphenoid	Parietal	Prefrontal.Left	Prefrontal.Right	Premaxilla	Prootic.Left	Prootic.Right	Pterygoid.Left	Pterygoid.Right	Quadrate.Left	Quadrate.Right	Septomaxilla.Left	Septomaxilla.Right	Splenial.Left	Splenial.Right	Stapes.Left	Stapes.Right	Supraoccipital.Left	Supraoccipital.Right	Vomer.Left	Vomer.Right
Angular.Left				1																												1								
Angular.Right					1																												1							
Basioccipital																1	1			1				1	1															
CompoundBone.Left	1					1		1																				1												
CompoundBone.Right		1					1		1																				1											
Coronoid.Left				1				1																															
Coronoid.Right					1				1																														
Dentary.Left				1		1			1																							1							
Dentary.Right					1		1	1																									1						
Frontal.Left											1			1				1		1	1	1				1			1									1	
Frontal.Right										1					1				1	1	1		1				1			1									1
Maxilla.Left																		1				1		1						1									
Maxilla.Right																			1				1	1							1								
Nasal.Left										1					1							1		1						1									
Nasal.Right											1			1									1	1							1								
Otoccipital.Left			1														1							1				1						1		1			
Otoccipital.Right			1													1									1				1						1		1		
Palatine.Left										1		1								1		1					1				1							1	
Palatine.Right											1		1							1			1					1				1							1
Parabasisphenoid			1							1	1							1	1		1			1	1													
Parietal										1	1								1					1	1											1	1		
Prefrontal.Left										1		1		1				1													1								
Prefrontal.Right											1		1		1				1													1							
Premaxilla												1	1	1	1																1	1							
Prootic.Left			1													1				1	1							1						1		1			
Prootic.Right			1														1			1	1								1						1		1		
Pterygoid.Left										1								1																					
Pterygoid.Right											1								1																				
Quadrate.Left				1												1								1										1					
Quadrate.Right					1												1								1										1				
Septomaxilla.Left										1		1		1				1				1		1								1						1	
Septomaxilla.Right											1		1		1				1				1	1							1								1
Splenial.Left	1							1																															
Splenial.Right		1							1																														
Stapes.Left																1								1				1											
Stapes.Right																	1								1				1										
Supraoccipital.Left																1					1			1													1		
Supraoccipital.Right																	1				1				1												1		
Vomer.Left										1								1						1						1								1	
Vomer.Right											1								1					1							1							1	

APPENDIX 4.1-21. Adjacency matrix for *Myriopholis macrorhyncha* (MCZ R-9650)

***Myriopholis macrorhyncha* (MCZ R-9650) Kley (2006), Koch et al (2019)**	Angular.Left	Angular.Right	Basioccipital	CompoundBone.Left	CompoundBone.Right	Coronoid.Left	Coronoid.Right	Dentary.Left	Dentary.Right	Frontal.Left	Frontal.Right	Maxilla.Left	Maxilla.Right	Nasal.Left	Nasal.Right	Otoccipital.Left	Otoccipital.Right	Palatine.Left	Palatine.Right	Parabasisphenoid	Parietal.Left	Parietal.Right	Prefrontal.Left	Prefrontal.Right	Premaxilla	Prootic.Left	Prootic.Right	Pterygoid.Left	Pterygoid.Right	Quadrate.Left	Quadrate.Right	Septomaxilla.Left	Septomaxilla.Right	Splenial.Left	Splenial.Right	Stapes.Left	Stapes.Right	Supraoccipital.Left	Supraoccipital.Right	Vomer.Left	Vomer.Right
Angular.Left				1																													1							
Angular.Right					1																													1						
Basioccipital																1	1			1						1	1													
CompoundBone.Left	1					1		1																						1										
CompoundBone.Right		1					1		1																						1									
Coronoid.Left				1				1																																
Coronoid.Right					1				1																															
Dentary.Left				1		1			1																								1							
Dentary.Right					1		1	1																										1						
Frontal.Left											1			1			1		1	1		1					1			1									1	
Frontal.Right										1					1			1	1		1		1				1				1								1
Maxilla.Left																						1		1								1								
Maxilla.Right																							1	1									1							
Nasal.Left										1					1							1		1								1								
Nasal.Right											1			1									1	1									1							
Otoccipital.Left			1														1								1				1						1		1			
Otoccipital.Right			1													1										1				1						1		1		
Palatine.Left										1										1			1				1				1								1	
Palatine.Right											1									1				1				1				1								1
Parabasisphenoid			1							1	1						1	1			1	1			1	1													
Parietal.Left										1									1						1												1			
Parietal.Right											1								1							1												1		
Prefrontal.Left										1		1		1			1														1								
Prefrontal.Right											1		1		1			1															1							
Premaxilla												1	1	1	1																	1	1					1	1
Prootic.Left			1												1				1	1									1						1		1		
Prootic.Right			1													1			1		1									1						1		1	
Pterygoid.Left										1							1																						
Pterygoid.Right											1							1																					
Quadrate.Left				1											1										1										1				
Quadrate.Right					1											1										1										1			
Septomaxilla.Left										1		1		1			1					1		1									1					1	
Septomaxilla.Right											1		1		1			1					1	1								1							1
Splenial.Left	1							1																															
Splenial.Right		1							1																														
Stapes.Left															1										1				1										
Stapes.Right																1										1				1									
Supraoccipital.Left															1					1					1														
Supraoccipital.Right																1					1					1													
Vomer.Left										1							1							1								1							1
Vomer.Right											1							1						1									1						1	

APPENDIX 4.1-22. Adjacency matrix for *Myriopholis tanae* (MCZ R-40099)

Myriopholis tanae **(MCZ R-40099) Kley (2006), Koch et al (2019)**	Angular.Left	Angular.Right	Basioccipital	CompoundBone.Left	CompoundBone.Right	Coronoid.Left	Coronoid.Right	Dentary.Left	Dentary.Right	Frontal.Left	Frontal.Right	Maxilla.Left	Maxilla.Right	Nasal	Otoccipital.Left	Otoccipital.Right	Palatine.Left	Palatine.Right	Parabasisphenoid	Parietal.Left	Parietal.Right	Prefrontal.Left	Prefrontal.Right	Premaxilla	Prootic.Left	Prootic.Right	Pterygoid.Left	Pterygoid.Right	Quadrate.Left	Quadrate.Right	Septomaxilla.Left	Septomaxilla.Right	Splenial.Left	Splenial.Right	Stapes.Left	Stapes.Right	Supraoccipital.Left	Supraoccipital.Right	Vomer.Left	Vomer.Right
Angular.Left				1																													1							
Angular.Right					1																													1						
Basioccipital															1	1			1						1	1														
CompoundBone.Left	1					1		1																					1											
CompoundBone.Right		1					1		1																					1										
Coronoid.Left				1				1																																
Coronoid.Right					1				1																															
Dentary.Left				1		1			1																								1							
Dentary.Right					1		1	1																										1						
Frontal.Left											1			1		1		1	1		1									1								1	
Frontal.Right										1				1			1	1		1		1									1								1
Maxilla.Left																					1		1							1									
Maxilla.Right																						1	1								1								
Nasal										1	1										1	1	1							1	1								
Otoccipital.Left			1													1								1				1						1		1			
Otoccipital.Right			1												1										1				1						1		1		
Palatine.Left										1											1					1				1								1	
Palatine.Right											1												1				1				1								1
Parabasisphenoid			1							1	1									1	1																		
Parietal.Left										1									1					1															
Parietal.Right											1								1							1													
Prefrontal.Left										1		1		1		1															1								
Prefrontal.Right											1		1	1			1															1							
Premaxilla												1	1	1																	1	1						1	1
Prootic.Left			1												1					1								1						1		1			
Prootic.Right			1													1					1								1							1		1		
Pterygoid.Left																	1																						
Pterygoid.Right																		1																					
Quadrate.Left				1											1										1										1				
Quadrate.Right					1											1										1										1			
Septomaxilla.Left										1		1		1			1					1		1								1						1	
Septomaxilla.Right											1		1	1				1					1	1							1								1
Splenial.Left	1							1																															
Splenial.Right		1							1																														
Stapes.Left															1										1				1										
Stapes.Right																1										1				1									
Supraoccipital.Left															1										1														
Supraoccipital.Right																1										1													
Vomer.Left										1							1							1							1								1
Vomer.Right											1							1						1								1							1	

APPENDIX 4.1-23. Adjacency matrix for *Rena dulcis* (UAMZ R335)

Rena dulcis **(UAMZ R335) Kley (2006), Koch et al (2019)**	Angular.Left	Angular.Right	Basioccipital	CompoundBone.Left	CompoundBone.Right	Coronoid.Left	Coronoid.Right	Dentary.Left	Dentary.Right	Frontal.Left	Frontal.Right	Maxilla.Left	Maxilla.Right	Nasal	Otoccipital.Left	Otoccipital.Right	Palatine.Left	Palatine.Right	Parabasisphenoid	Parietal	Prefrontal.Left	Prefrontal.Right	Premaxilla	Prootic.Left	Prootic.Right	Pterygoid.Left	Pterygoid.Right	Quadrate.Left	Quadrate.Right	Septomaxilla.Left	Septomaxilla.Right	Splenial.Left	Splenial.Right	Stapes.Left	Stapes.Right	Supraoccipital.Left	Supraoccipital.Right	Vomer.Left	Vomer.Right
Angular.Left				1																											1							
Angular.Right					1																											1						
Basioccipital															1	1			1					1	1													
CompoundBone.Left	1					1		1																				1										
CompoundBone.Right		1					1		1																				1									
Coronoid.Left				1				1																														
Coronoid.Right					1				1																													
Dentary.Left				1		1			1																						1							
Dentary.Right					1		1	1																								1						
Frontal.Left											1			1			1		1	1	1					1				1							1	
Frontal.Right										1				1				1	1	1		1					1				1							1
Maxilla.Left																	1				1		1							1								
Maxilla.Right																		1				1	1								1							
Nasal										1	1										1	1	1							1	1							
Otoccipital.Left			1													1							1				1						1		1			
Otoccipital.Right			1												1									1				1						1		1		
Palatine.Left										1		1							1		1					1				1							1	
Palatine.Right											1		1						1			1					1				1							1
Parabasisphenoid			1							1	1						1	1		1			1	1														
Parietal										1	1							1					1	1												1	1	
Prefrontal.Left										1		1		1			1													1								
Prefrontal.Right											1		1	1				1														1						
Premaxilla												1	1	1																1	1						1	1
Prootic.Left			1												1				1	1								1						1		1		
Prootic.Right			1													1			1	1									1					1		1		
Pterygoid.Left										1							1																					
Pterygoid.Right											1							1																				
Quadrate.Left				1											1									1										1				
Quadrate.Right					1											1									1										1			
Septomaxilla.Left										1		1		1			1				1		1								1						1	
Septomaxilla.Right											1		1	1				1				1	1							1								1
Splenial.Left	1							1																														
Splenial.Right		1							1																													
Stapes.Left															1									1				1										
Stapes.Right																1									1				1									
Supraoccipital.Left															1					1				1													1	
Supraoccipital.Right																1				1					1											1		
Vomer.Left										1							1						1							1								1
Vomer.Right											1							1					1								1						1	

APPENDIX 4.1-24. Adjacency matrix for *Tricheilostoma bicolor* (MCZ R-49718)

Tricheilostoma bicolor **(MCZ R-49718)** **Kley (2006), Koch et al (2019)**	Angular.Left	Angular.Right	Basioccipital	CompoundBone.Left	CompoundBone.Right	Coronoid.Left	Coronoid.Right	Dentary.Left	Dentary.Right	Frontal.Left	Frontal.Right	Maxilla.Left	Maxilla.Right	Nasal.Left	Nasal.Right	Palatine.Left	Palatine.Right	Parabasisphenoid	Parietal	Prefrontal.Left	Prefrontal.Right	Premaxilla	Prootic-Otoccipital.Left	Prootic-Otoccipital.Right	Pterygoid.Left	Pterygoid.Right	Quadrate.Left	Quadrate.Right	Septomaxilla.Left	Septomaxilla.Right	Splenial.Left	Splenial.Right	Stapes.Left	Stapes.Right	Vomer.Left	Vomer.Right
Angular.Left				1																										1					
Angular.Right					1																										1				
Basioccipital																	1					1	1												
CompoundBone.Left	1					1		1																		1									
CompoundBone.Right		1					1		1																		1								
Coronoid.Left				1				1																											
Coronoid.Right					1				1																										
Dentary.Left				1		1			1																					1					
Dentary.Right					1		1	1																							1				
Frontal.Left											1			1		1		1	1	1				1				1							
Frontal.Right										1					1		1	1	1		1				1				1						
Maxilla.Left																				1		1								1					
Maxilla.Right																					1	1									1				
Nasal.Left										1					1				1			1							1						
Nasal.Right											1			1						1	1									1					
Palatine.Left										1							1		1					1				1						1	
Palatine.Right											1						1			1					1				1						1
Parabasisphenoid			1							1	1				1	1		1				1	1											
Parietal										1	1						1					1	1												
Prefrontal.Left										1		1		1		1												1							
Prefrontal.Right											1		1		1		1												1						
Premaxilla												1	1	1	1														1	1				1	1
Prootic-Otoccipital.Left			1														1	1					1			1					1			
Prootic-Otoccipital.Right			1														1	1				1					1					1		
Pterygoid.Left										1					1																				
Pterygoid.Right											1					1																			
Quadrate.Left				1																		1									1				
Quadrate.Right					1																		1									1			
Septomaxilla.Left										1		1		1		1				1		1								1				1	
Septomaxilla.Right											1		1		1		1				1	1							1						1
Splenial.Left	1							1																											
Splenial.Right		1							1																										
Stapes.Left																						1				1									
Stapes.Right																							1				1								
Vomer.Left																1						1						1							1
Vomer.Right																	1					1							1					1	

APPENDIX 4.1-25. Adjacency matrix for *Trilepida dimidiata* (SAMA 40143)

***Trilepida dimidiata* (SAMA 40143) Kley (2006), Koch et al (2019)**	Angular.Left	Angular.Right	Basioccipital	CompoundBone.Left	CompoundBone.Right	Coronoid.Left	Coronoid.Right	Dentary.Left	Dentary.Right	Frontal.Left	Frontal.Right	Maxilla.Left	Maxilla.Right	Nasal.Left	Nasal.Right	Otoccipital.Left	Otoccipital.Right	Palatine.Left	Palatine.Right	Parabasisphenoid	Parietal	Prefrontal.Left	Prefrontal.Right	Premaxilla	Prootic.Left	Prootic.Right	Pterygoid.Left	Pterygoid.Right	Quadrate.Left	Quadrate.Right	Septomaxilla.Left	Septomaxilla.Right	Splenial.Left	Splenial.Right	Stapes.Left	Stapes.Right	Supraoccipital	Vomer.Left	Vomer.Right
Angular.Left				1																												1						
Angular.Right					1																												1					
Basioccipital																1	1			1					1	1												
CompoundBone.Left	1					1		1																					1									
CompoundBone.Right		1					1		1																					1								
Coronoid.Left				1				1																														
Coronoid.Right					1				1																													
Dentary.Left				1		1			1																								1					
Dentary.Right					1		1	1																										1				
Frontal.Left											1			1				1		1	1	1					1			1							1	
Frontal.Right										1					1				1	1	1		1				1				1							1
Maxilla.Left																		1				1		1							1							
Maxilla.Right																			1				1	1								1						
Nasal.Left										1					1							1		1							1							
Nasal.Right											1			1									1	1								1						
Otoccipital.Left			1														1								1				1						1		1	
Otoccipital.Right			1													1										1				1					1	1		
Palatine.Left										1		1								1							1				1						1	
Palatine.Right											1		1							1								1				1						1
Parabasisphenoid			1							1	1							1	1		1				1	1												
Parietal										1	1									1					1	1										1		
Prefrontal.Left										1		1		1																	1							
Prefrontal.Right											1		1		1																	1						
Premaxilla												1	1	1	1																1	1					1	1
Prootic.Left			1													1				1	1								1						1		1	
Prootic.Right			1														1			1	1									1						1	1	
Pterygoid.Left										1								1																				
Pterygoid.Right											1								1																			
Quadrate.Left				1												1								1										1				
Quadrate.Right					1												1								1										1			
Septomaxilla.Left										1		1		1				1				1		1								1					1	
Septomaxilla.Right											1		1		1				1				1	1							1							1
Splenial.Left	1							1																														
Splenial.Right		1							1																													
Stapes.Left																1								1				1										
Stapes.Right																	1								1				1									
Supraoccipital																1	1				1			1	1													
Vomer.Left										1								1						1							1						1	1
Vomer.Right											1								1					1								1					1	

APPENDIX 4.1-26. Adjacency matrix for *Anilius scytale* (KUH 125976)

Anilius scytale **(KUH 125976) Rieppel (1977), Cundall (1995)**	ArticularComplex.Left	ArticularComplex.Right	Basioccipital	Coronoid.Left	Coronoid.Right	Dentary.Left	Dentary.Right	Ectopterygoid.Left	Ectopterygoid.Right	Frontal.Left	Frontal.Right	Maxilla.Left	Maxilla.Right	Nasal.Left	Nasal.Right	Otoccipital.Left	Otoccipital.Right	Palatine.Left	Palatine.Right	Parabasisphenoid	Parietal	Prefrontal.Left	Prefrontal.Right	Premaxilla	Prootic.Left	Prootic.Right	Pterygoid.Left	Pterygoid.Right	Quadrate.Left	Quadrate.Right	Septomaxilla.Left	Septomaxilla.Right	Stapes.Left	Stapes.Right	Supraoccipital	Supratemporal.Left	Supratemporal.Right	Vomer.Left	Vomer.Right
ArticularComplex.Left				1		1																						1											
ArticularComplex.Right					1		1																						1										
Basioccipital																1	1			1				1	1													
Coronoid.Left	1					1																																
Coronoid.Right		1					1																															
Dentary.Left	1			1			1																															
Dentary.Right		1			1	1																																
Ectopterygoid.Left												1														1											
Ectopterygoid.Right													1														1										
Frontal.Left											1			1						1	1	1																
Frontal.Right										1					1					1	1		1															
Maxilla.Left								1										1				1								1								
Maxilla.Right									1										1				1								1							
Nasal.Left										1				1							1		1							1							
Nasal.Right											1				1							1	1								1						
Otoccipital.Left			1													1				1				1				1				1		1	1		
Otoccipital.Right			1													1	1				1				1				1				1	1		1	
Palatine.Left												1						1		1		1				1				1						1	
Palatine.Right													1						1	1			1				1				1						1
Parabasisphenoid			1							1	1						1	1	1	1				1	1	1	1										
Parietal										1	1					1	1		1	1				1	1										1	1	1	
Prefrontal.Left										1		1		1				1			1																
Prefrontal.Right											1		1		1				1			1																
Premaxilla														1	1								1														1	1
Prootic.Left			1													1			1	1				1				1			1		1		1	1		
Prootic.Right			1														1		1	1					1				1			1	1		1		
Pterygoid.Left								1										1	1							1											
Pterygoid.Right									1										1	1							1										
Quadrate.Left	1															1								1				1				1			1		
Quadrate.Right		1															1								1				1			1			1		
Septomaxilla.Left												1		1				1												1						1	
Septomaxilla.Right													1		1				1												1						1
Stapes.Left																1								1				1									
Stapes.Right																	1								1				1								
Supraoccipital																1	1				1			1	1												
Supratemporal.Left																1					1			1				1									
Supratemporal.Right																	1				1				1				1								
Vomer.Left																		1						1						1							1
Vomer.Right																			1					1							1						1	

APPENDIX 4.1-27. Adjacency matrix for *Anomochilus leonardi* (FRIM 0026)

Anomochilus leonardi **(FRIM 0026)** **Cundall and Rossman (1993), Rieppel and Maisano (2007)**	Angular.Left	Angular.Right	Basioccipital	CompoundBone.Left	CompoundBone.Right	Coronoid.Left	Coronoid.Right	Dentary.Left	Dentary.Right	Ectopterygoid.Left	Ectopterygoid.Right	Frontal.Left	Frontal.Right	Maxilla.Left	Maxilla.Right	Nasal.Left	Nasal.Right	Otoccipital.Left	Otoccipital.Right	Palatine.Left	Palatine.Right	Parabasisphenoid	Parietal	Prefrontal.Left	Prefrontal.Right	Premaxilla	Prootic.Left	Prootic.Right	Pterygoid.Left	Pterygoid.Right	Quadrate.Left	Quadrate.Right	Septomaxilla.Left	Septomaxilla.Right	Splenial.Left	Splenial.Right	Stapes.Left	Stapes.Right	Supraoccipital	Vomer.Left	Vomer.Right
Angular.Left				1																															1						
Angular.Right				1																															1						
Basioccipital																		1	1			1				1	1															
CompoundBone.Left	1					1		1																						1												
CompoundBone.Right		1					1		1																						1											
Coronoid.Left				1																																					
Coronoid.Right					1																																				
Dentary.Left				1					1																										1						
Dentary.Right					1			1																												1					
Ectopterygoid.Left																																									
Ectopterygoid.Right																																									
Frontal.Left													1			1						1	1	1																	
Frontal.Right												1					1					1	1		1																
Maxilla.Left																				1				1		1							1								
Maxilla.Right																					1				1	1								1							
Nasal.Left												1					1							1		1							1								
Nasal.Right													1			1									1	1								1							
Otoccipital.Left			1																1								1				1						1			
Otoccipital.Right			1															1										1				1					1	1		
Palatine.Left														1								1		1					1										1	
Palatine.Right															1							1			1					1										1
Parabasisphenoid			1									1	1							1	1		1				1	1												
Parietal												1	1									1					1	1											1		
Prefrontal.Left												1		1		1				1																					
Prefrontal.Right													1		1		1				1																				
Premaxilla														1	1	1	1																	1	1					1	1
Prootic.Left			1															1					1	1							1						1		1		
Prootic.Right			1																1				1	1								1						1	1		
Pterygoid.Left																				1																					
Pterygoid.Right																					1																				
Quadrate.Left				1														1									1											1			
Quadrate.Right					1														1									1												
Septomaxilla.Left														1		1										1									1					1	
Septomaxilla.Right															1		1									1								1							1
Splenial.Left	1							1																																	
Splenial.Right		1							1																																
Stapes.Left																		1								1				1										
Stapes.Right																			1								1				1									
Supraoccipital																		1	1				1			1	1														
Vomer.Left																				1						1								1							1
Vomer.Right																					1					1									1					1	

APPENDIX 4.1-28. Adjacency matrix for *Cylindrophis ruffus* (UMMZ 201901)

***Cylindrophis ruffus* (UMMZ 201901) Rieppel (1977), Cundall (1995)**	Angular.Left	Angular.Right	Basioccipital	CompoundBone.Left	CompoundBone.Right	Coronoid.Left	Coronoid.Right	Dentary.Left	Dentary.Right	Ectopterygoid.Left	Ectopterygoid.Right	Frontal.Left	Frontal.Right	Maxilla.Left	Maxilla.Right	Nasal.Left	Nasal.Right	Otoccipital.Left	Otoccipital.Right	Palatine.Left	Palatine.Right	Parabasisphenoid	Parietal	Postfrontal.Left	Postfrontal.Right	Prefrontal.Left	Prefrontal.Right	Premaxilla	Prootic.Left	Prootic.Right	Pterygoid.Left	Pterygoid.Right	Quadrate.Left	Quadrate.Right	Septomaxilla.Left	Septomaxilla.Right	Splenial.Left	Splenial.Right	Stapes.Left	Stapes.Right	Supraoccipital	Supratemporal.Left	Supratemporal.Right	Vomer.Left	Vomer.Right
Angular.Left				1		1																															1								
Angular.Right					1		1																															1							
Basioccipital																		1	1			1							1	1																
CompoundBone.Left	1					1		1																									1													
CompoundBone.Right		1					1		1																									1											
Coronoid.Left	1			1				1																																				
Coronoid.Right		1			1				1																																			
Dentary.Left				1		1			1																													1							
Dentary.Right					1		1	1																															1						
Ectopterygoid.Left													1																		1														
Ectopterygoid.Right														1																		1													
Frontal.Left													1			1						1	1	1		1																			
Frontal.Right												1					1					1	1		1		1																			
Maxilla.Left										1										1						1										1									
Maxilla.Right											1										1						1																		
Nasal.Left												1					1									1		1																	
Nasal.Right													1			1											1	1																	
Otoccipital.Left			1															1											1				1						1		1	1			
Otoccipital.Right			1															1												1				1						1	1		1		
Palatine.Left														1						1		1				1					1													
Palatine.Right															1						1	1					1					1													
Parabasisphenoid			1									1	1							1	1	1	1						1	1	1	1												
Parietal												1	1									1	1	1					1	1											1	1	1		
Postfrontal.Left												1											1																						
Postfrontal.Right													1										1																						
Prefrontal.Left												1		1		1				1																										
Prefrontal.Right													1		1		1				1																										
Premaxilla																1	1																											1	1
Prootic.Left			1															1				1	1																	1		1	1			
Prootic.Right			1																1			1	1																		1	1		1		
Pterygoid.Left										1									1			1																							
Pterygoid.Right											1									1		1																							
Quadrate.Left				1														1											1											1			1			
Quadrate.Right					1														1											1											1			1		
Septomaxilla.Left														1																													1		
Septomaxilla.Right															1																														1
Splenial.Left	1							1																																				
Splenial.Right		1							1																																			
Stapes.Left																		1											1				1											
Stapes.Right																			1											1				1										
Supraoccipital																		1	1				1						1	1															
Supratemporal.Left																		1					1						1				1											
Supratemporal.Right																			1				1							1				1										
Vomer.Left																				1								1							1									1
Vomer.Right																					1							1								1								1	

APPENDIX 4.1-29. Adjacency matrix for *Rhinophis sanguineus* (UF 78397)

Rhinophis sanguineus **(UF 78397)** **Olori and Bell (2012)**	Angular.Left	Angular.Right	CompoundBone.Left	CompoundBone.Right	Coronoid.Left	Coronoid.Right	Dentary.Left	Dentary.Right	Ectopterygoid.Left	Ectopterygoid.Right	Frontal.Left	Frontal.Right	Maxilla.Left	Maxilla.Right	Nasal.Left	Nasal.Right	Palatine.Left	Palatine.Right	Parietal	PosteriorComplex	Prefrontal.Left	Prefrontal.Right	Premaxilla	Pterygoid.Left	Pterygoid.Right	Quadrate.Left	Quadrate.Right	Septomaxilla.Left	Septomaxilla.Right	Splenial.Left	Splenial.Right	Stapes.Left	Stapes.Right	Vomer.Left	Vomer.Right
Angular.Left			1				1																							1					
Angular.Right				1				1																							1				
CompoundBone.Left	1				1		1																			1									
CompoundBone.Right		1				1		1																			1								
Coronoid.Left			1				1																												
Coronoid.Right				1				1																											
Dentary.Left	1		1		1			1																						1					
Dentary.Right		1		1		1	1																								1				
Ectopterygoid.Left													1											1											
Ectopterygoid.Right														1											1										
Frontal.Left												1			1				1	1	1														
Frontal.Right											1					1			1	1		1													
Maxilla.Left									1								1				1		1					1							
Maxilla.Right										1								1				1	1						1						
Nasal.Left											1					1					1		1					1							
Nasal.Right												1			1							1	1					1							
Palatine.Left													1						1	1			1											1	
Palatine.Right														1					1		1			1											1
Parietal											1	1							1																
PosteriorComplex											1	1					1	1	1					1	1	1	1					1	1		
Prefrontal.Left											1		1		1		1											1							
Prefrontal.Right												1		1		1		1											1						
Premaxilla													1	1	1	1												1	1					1	1
Pterygoid.Left									1								1			1															
Pterygoid.Right										1								1		1															
Quadrate.Left			1																	1												1			
Quadrate.Right				1																1													1		
Septomaxilla.Left													1		1						1		1						1					1	
Septomaxilla.Right														1		1						1	1					1							1
Splenial.Left	1						1																												
Splenial.Right		1						1																											
Stapes.Left																				1						1									
Stapes.Right																				1							1								
Vomer.Left																	1						1					1							1
Vomer.Right																		1					1						1					1	

APPENDIX 4.1-30. Adjacency matrix for *Uropeltis melanogaster* (FMNH 167048)

***Uropeltis melanogaster* (FMNH 167048) Olori and Bell (2012)**	Angular.Left	Angular.Right	CompoundBone.Left	CompoundBone.Right	Coronoid.Left	Coronoid.Right	Dentary.Left	Dentary.Right	Ectopterygoid.Left	Ectopterygoid.Right	Frontal.Left	Frontal.Right	Maxilla.Left	Maxilla.Right	Nasal.Left	Nasal.Right	Palatine.Left	Palatine.Right	Parietal	PosteriorComplex	Prefrontal.Left	Prefrontal.Right	Premaxilla	Pterygoid.Left	Pterygoid.Right	Quadrate.Left	Quadrate.Right	Septomaxilla.Left	Septomaxilla.Right	Splenial.Left	Splenial.Right	Stapes.Left	Stapes.Right	Vomer.Left	Vomer.Right
Angular.Left			1																											1					
Angular.Right				1																											1				
CompoundBone.Left	1				1		1																			1									
CompoundBone.Right		1				1		1																			1								
Coronoid.Left			1				1																												
Coronoid.Right				1				1																											
Dentary.Left			1		1			1																						1					
Dentary.Right				1		1	1																								1				
Ectopterygoid.Left													1										1												
Ectopterygoid.Right														1										1											
Frontal.Left												1			1				1	1	1														
Frontal.Right											1					1			1	1		1													
Maxilla.Left									1								1				1		1					1							
Maxilla.Right										1								1				1	1						1						
Nasal.Left											1					1					1		1					1							
Nasal.Right												1			1							1	1						1						
Palatine.Left													1						1					1										1	
Palatine.Right														1					1						1										1
Parietal											1	1								1															
PosteriorComplex											1	1					1	1	1					1	1	1	1					1	1		
Prefrontal.Left											1		1		1													1							
Prefrontal.Right												1		1		1													1						
Premaxilla													1	1	1	1												1	1					1	1
Pterygoid.Left									1								1			1															
Pterygoid.Right										1								1		1															
Quadrate.Left			1																	1												1			
Quadrate.Right				1																1													1		
Septomaxilla.Left													1		1						1		1						1					1	
Septomaxilla.Right														1		1						1	1					1							1
Splenial.Left	1						1																												
Splenial.Right		1						1																											
Stapes.Left																				1						1									
Stapes.Right																				1							1								
Vomer.Left																	1						1					1							1
Vomer.Right																		1					1						1					1	

APPENDIX 4.1-31. Adjacency matrix for *Amphisbaena fuliginosa* (FMNH 22847)

***Amphisbaena fuliginosa* (FMNH 22847) Gans and Montero (2008)**	Angular.Left	Angular.Right	CompoundBone.Left	CompoundBone.Right	Coronoid.Left	Coronoid.Right	Dentary.Left	Dentary.Right	Ectopterygoid.Left	Ectopterygoid.Right	ElementX.Left	ElementX.Right	Frontal.Left	Frontal.Right	Maxilla.Left	Maxilla.Right	Nasal.Left	Nasal.Right	OccipitalComplex	Palatine.Left	Palatine.Right	Parabasisphenoid	Parietal	Prefrontal.Left	Prefrontal.Right	Premaxilla	Pterygoid.Left	Pterygoid.Right	Quadrate.Left	Quadrate.Right	Septomaxilla.Left	Septomaxilla.Right	Stapes.Left	Stapes.Right	Tabulosphenoid	Vomer.Left	Vomer.Right
Angular.Left			1				1																														
Angular.Right				1				1																													
CompoundBone.Left	1				1		1																						1								
CompoundBone.Right		1				1		1																						1							
Coronoid.Left			1				1																														
Coronoid.Right				1				1																													
Dentary.Left	1		1		1			1																													
Dentary.Right		1		1		1	1																														
Ectopterygoid.Left															1					1							1										
Ectopterygoid.Right																1					1							1									
ElementX.Left																			1			1															
ElementX.Right																			1			1															
Frontal.Left														1			1						1	1											1		
Frontal.Right													1					1					1		1										1		
Maxilla.Left									1								1			1				1		1						1			1		
Maxilla.Right										1								1			1				1	1							1			1	
Nasal.Left													1		1			1						1		1										
Nasal.Right														1		1	1								1	1										
OccipitalComplex											1	1										1	1						1	1			1	1			
Palatine.Left									1						1							1		1			1								1	1	
Palatine.Right										1						1						1			1			1							1		1
Parabasisphenoid											1	1							1	1	1						1	1							1		
Parietal													1	1					1																1		
Prefrontal.Left													1		1		1			1																	
Prefrontal.Right														1		1		1			1																
Premaxilla															1	1	1	1													1	1			1	1
Pterygoid.Left									1											1		1							1						1		
Pterygoid.Right										1											1	1								1					1		
Quadrate.Left			1																1								1					1					
Quadrate.Right				1															1									1					1				
Septomaxilla.Left															1											1						1	1				
Septomaxilla.Right																1										1					1				1	
Stapes.Left																			1										1							
Stapes.Right																			1											1						
Tabulosphenoid													1	1						1	1	1	1				1	1									
Vomer.Left															1					1						1					1				1	
Vomer.Right																1					1					1						1			1	

APPENDIX 4.1-32. Adjacency matrix for *Anelytropsis papillosus* (TCWC 45501)

Anelytropsis papillosus **(TCWC 45501)** **Rieppel (1984), Evans (2008)**	ArticularComplex.Left	ArticularComplex.Right	Basioccipital	Coronoid.Left	Coronoid.Right	Dentary.Left	Dentary.Right	Ectopterygoid.Left	Ectopterygoid.Right	Epipterygoid.Left	Epipterygoid.Right	Exoccipital.Left	Exoccipital.Right	Frontal.Left	Frontal.Right	Maxilla.Left	Maxilla.Right	Nasal.Left	Nasal.Right	Opisthotic.Left	Opisthotic.Right	Palatine.Left	Palatine.Right	Parabasisphenoid	Parietal	Postfrontal.Left	Postfrontal.Right	Prefrontal.Left	Prefrontal.Right	Premaxilla	Prootic.Left	Prootic.Right	Pterygoid.Left	Pterygoid.Right	Quadrate.Left	Quadrate.Right	Septomaxilla.Left	Septomaxilla.Right	Stapes.Left	Stapes.Right	Supraoccipital	Surangular.Left	Surangular.Right	TemporalElement.Left	TemporalElement.Right	Vomer.Left	Vomer.Right
ArticularComplex.Left				1		1																													1									
ArticularComplex.Right					1		1																												1									
Basioccipital												1	1							1	1			1						1	1														
Coronoid.Left	1					1																													1									
Coronoid.Right		1					1																													1								
Dentary.Left	1			1			1																												1									
Dentary.Right		1			1	1																														1								
Ectopterygoid.Left															1						1											1													
Ectopterygoid.Right																1						1																							
Epipterygoid.Left																								1								1													
Epipterygoid.Right																								1									1												
Exoccipital.Left			1																	1																				1				
Exoccipital.Right			1																		1																				1				
Frontal.Left															1	1		1						1	1		1																		
Frontal.Right														1			1		1					1		1		1																	
Maxilla.Left								1						1				1				1					1		1						1								1		
Maxilla.Right									1						1				1			1						1	1							1								1
Nasal.Left														1		1			1										1							1								
Nasal.Right															1		1	1											1								1							
Opisthotic.Left			1									1																		1				1				1		1				
Opisthotic.Right			1										1																		1				1				1	1				
Palatine.Left								1							1												1					1										1		
Palatine.Right									1								1						1						1				1										1
Parabasisphenoid			1																											1	1	1	1										
Parietal										1	1			1	1															1	1								1					
Postfrontal.Left														1										1																				
Postfrontal.Right															1									1																				
Prefrontal.Left														1		1						1																						
Prefrontal.Right															1		1						1																					
Premaxilla																1		1	1	1																		1	1				1	1
Prootic.Left			1														1			1				1	1													1		1		1			
Prootic.Right			1																		1			1	1													1		1	1		1		
Pterygoid.Left								1		1												1		1																			1		
Pterygoid.Right									1		1												1	1																				1	
Quadrate.Left	1																			1										1									1						
Quadrate.Right		1																			1										1									1					
Septomaxilla.Left																1		1												1													1		
Septomaxilla.Right																	1		1											1														1	
Stapes.Left																				1											1				1									
Stapes.Right																					1											1				1								
Supraoccipital												1	1							1	1			1						1	1														
Surangular.Left	1			1		1																																						
Surangular.Right		1			1		1																																					
TemporalElement.Left																														1														
TemporalElement.Right																															1													
Vomer.Left															1						1								1			1			1								1	
Vomer.Right																1						1							1				1			1							1	

APPENDIX 4.1-33. Adjacency matrix for *Bipes biporus* (CAS 126478)

Bipes biporus **(CAS 126478)** **Gans and Montero (2008)**	ArticularComplex.Left	ArticularComplex.Right	Coronoid.Left	Coronoid.Right	Dentary.Left	Dentary.Right	Ectopterygoid.Left	Ectopterygoid.Right	IntermediateComplex	Maxilla.Left	Maxilla.Right	Nasal.Left	Nasal.Right	OccipitalComplexEtc	Palatine.Left	Palatine.Right	Prefrontal.Left	Prefrontal.Right	Premaxilla	Pterygoid.Left	Pterygoid.Right	Quadrate.Left	Quadrate.Right	Septomaxilla.Left	Septomaxilla.Right	Squamosal.Left	Squamosal.Right	Stapes.Left	Stapes.Right	Vomer
ArticularComplex.Left			1		1																	1								
ArticularComplex.Right				1		1																	1							
Coronoid.Left	1				1																									
Coronoid.Right		1				1																								
Dentary.Left	1		1			1																								
Dentary.Right		1		1	1																									
Ectopterygoid.Left										1					1					1										
Ectopterygoid.Right											1					1					1									
IntermediateComplex										1	1	1	1	1	1	1	1	1	1											
Maxilla.Left							1		1			1			1		1		1					1						1
Maxilla.Right								1	1				1			1		1	1						1					1
Nasal.Left									1	1			1						1					1						
Nasal.Right									1		1	1							1						1					
OccipitalComplexEtc									1											1	1	1	1			1	1	1	1	
Palatine.Left							1		1	1						1	1			1										1
Palatine.Right								1	1		1				1			1			1									1
Prefrontal.Left									1	1					1															
Prefrontal.Right									1		1					1														
Premaxilla									1	1	1	1	1											1	1					1
Pterygoid.Left							1							1	1															
Pterygoid.Right								1						1		1														
Quadrate.Left	1													1												1		1		
Quadrate.Right		1												1													1		1	
Septomaxilla.Left										1		1							1						1					1
Septomaxilla.Right											1		1						1					1						1
Squamosal.Left														1								1								
Squamosal.Right														1									1							
Stapes.Left														1								1								
Stapes.Right														1									1							
Vomer										1	1				1	1			1					1	1					

APPENDIX 4.1-34. Adjacency matrix for *Dibamus novaeguineae* (UF 33488)

***Dibamus novaeguineae* (UF 33488) Rieppel (1984), Evans (2008)**	ArticularComplex.Left	ArticularComplex.Right	Basioccipital-Exoccipital	Coronoid.Left	Coronoid.Right	Dentary.Left	Dentary.Right	Ectopterygoid.Left	Ectopterygoid.Right	Frontal.Left	Frontal.Right	Maxilla.Left	Maxilla.Right	Nasal.Left	Nasal.Right	Opisthotic.Left	Opisthotic.Right	Palatine.Left	Palatine.Right	Parabasisphenoid	Parietal	Prefrontal.Left	Prefrontal.Right	Premaxilla	Prootic.Left	Prootic.Right	Pterygoid.Left	Pterygoid.Right	Quadrate.Left	Quadrate.Right	Septomaxilla.Left	Septomaxilla.Right	Stapes.Left	Stapes.Right	Supraoccipital	Vomer.Left	Vomer.Right
ArticularComplex.Left				1		1																						1									
ArticularComplex.Right					1		1																						1								
Basioccipital-Exoccipital																1	1			1					1	1									1		
Coronoid.Left	1					1																															
Coronoid.Right		1					1																														
Dentary.Left	1			1			1																														
Dentary.Right		1			1	1																															
Ectopterygoid.Left												1						1				1					1										
Ectopterygoid.Right													1						1				1					1									
Frontal.Left											1	1		1						1	1																
Frontal.Right										1			1		1					1		1															
Maxilla.Left								1		1				1				1				1		1							1				1		
Maxilla.Right									1		1				1				1				1									1					1
Nasal.Left										1		1			1									1							1						
Nasal.Right											1		1	1																	1						
Opisthotic.Left			1																					1				1				1		1		
Opisthotic.Right			1																						1				1				1	1		
Palatine.Left								1		1		1										1				1									1		
Palatine.Right									1		1		1										1				1										1
Parabasisphenoid			1																					1	1	1	1									
Parietal										1	1													1	1										1		
Prefrontal.Left								1		1		1						1																			
Prefrontal.Right									1		1		1						1																		
Premaxilla												1	1	1	1																1	1			1	1
Prootic.Left			1													1				1	1							1				1		1		
Prootic.Right			1														1			1	1								1				1	1		
Pterygoid.Left								1										1		1															1		
Pterygoid.Right									1										1	1																1	
Quadrate.Left	1															1								1									1				
Quadrate.Right		1															1								1									1			
Septomaxilla.Left												1		1										1											1		
Septomaxilla.Right													1		1									1							1					1	
Stapes.Left																1									1			1								
Stapes.Right																	1									1			1							
Supraoccipital			1													1	1				1				1	1										
Vomer.Left												1						1						1			1				1					1
Vomer.Right													1						1					1				1				1			1	

APPENDIX 4.1-35. Adjacency matrix for *Dipsosaurus dorsalis* (YPM 14376)

Dipsosaurus dorsalis **(YPM 14376)** **Evans (2008), Bell et al. (2009), Gray (2018)**	Angular.Left	Angular.Right	Articular.Left	Articular.Right	Basioccipital	Coronoid.Left	Coronoid.Right	Dentary.Left	Dentary.Right	Ectopterygoid.Left	Ectopterygoid.Right	Epipterygoid.Left	Epipterygoid.Right	Frontal	Jugal.Left	Jugal.Right	Lacrimal.Left	Lacrimal.Right	Maxilla.Left	Maxilla.Right	Nasal.Left	Nasal.Right	Palatine.Left	Palatine.Right	Parabasisphenoid	Parietal	Postfrontal.Left	Postfrontal.Right	Postorbital.Left	Postorbital.Right	Prefrontal.Left	Prefrontal.Right	Premaxilla	Prootic-Oto-Supraoccipital	Pterygoid.Left	Pterygoid.Right	Quadrate.Left	Quadrate.Right	Septomaxilla.Left	Septomaxilla.Right	Splenial.Left	Splenial.Right	Squamosal.Left	Squamosal.Right	Stapes.Left	Stapes.Right	Supratemporal.Left	Supratemporal.Right	Surangular.Left	Surangular.Right	Vomer.Left	Vomer.Right
Angular.Left			1					1																																	1									1		
Angular.Right				1					1																																	1								1		
Articular.Left	1					1																															1					1								1		
Articular.Right		1					1																															1				1								1		
Basioccipital																									1								1																			
Coronoid.Left			1					1																																	1								1		
Coronoid.Right				1					1																																1								1		
Dentary.Left	1					1			1																																1								1		
Dentary.Right		1					1	1																																	1								1		
Ectopterygoid.Left														1				1				1												1																		
Ectopterygoid.Right															1				1				1												1																		
Epipterygoid.Left																									1										1																		
Epipterygoid.Right																									1											1																		
Frontal																					1	1			1	1	1			1	1																						
Jugal.Left										1						1		1		1			1					1																1										
Jugal.Right											1						1		1					1						1															1									
Lacrimal.Left														1				1				1									1																						
Lacrimal.Right															1				1				1									1																						
Maxilla.Left										1				1		1		1		1		1								1		1									1										1		
Maxilla.Right											1				1		1		1		1		1								1	1									1											1
Nasal.Left														1				1		1										1		1								1											
Nasal.Right														1					1	1										1	1									1											
Palatine.Left										1					1		1		1		1			1						1				1																	1	
Palatine.Right											1					1		1		1		1									1					1															1
Parabasisphenoid					1																												1	1	1															
Parietal												1	1	1																				1												1	1				
Postfrontal.Left														1												1				1																						
Postfrontal.Right														1												1					1																					
Postorbital.Left															1											1	1																			1						
Postorbital.Right																1										1		1																	1						
Prefrontal.Left														1			1		1																																		
Prefrontal.Right														1																																							
Premaxilla																							1	1	1																												
Prootic-Oto-Supraoccipital					1																					1	1												1	1					1	1	1	1				
Pterygoid.Left										1		1											1		1															1												
Pterygoid.Right											1		1											1	1														1												
Quadrate.Left			1																															1	1					1		1		1						
Quadrate.Right				1																														1		1				1		1		1						
Septomaxilla.Left																							1																													
Septomaxilla.Right																								1																												
Splenial.Left	1		1			1		1																																										
Splenial.Right		1		1			1		1																																									
Squamosal.Left															1																																				
Squamosal.Right																1																																			
Stapes.Left																																		1		1														
Stapes.Right																																		1			1													
Supratemporal.Left																									1									1		1														
Supratemporal.Right																									1									1			1												
Surangular.Left	1		1			1		1																																									
Surangular.Right		1		1			1		1																																								
Vomer.Left																																																	
Vomer.Right																																																	

APPENDIX 4.1-36. Adjacency matrix for *Lanthanotus borneensis* (FMNH 148589)

***Lanthanotus borneensis* (FMNH 148589) Evans (2008)**	Angular.Left	Angular.Right	Articular.Left	Articular.Right	Basioccipital	Coronoid.Left	Coronoid.Right	Dentary.Left	Dentary.Right	Ectopterygoid.Left	Ectopterygoid.Right	Epipterygoid.Left	Epipterygoid.Right	Frontal.Left	Frontal.Right	Jugal.Left	Jugal.Right	Lacrimal.Left	Lacrimal.Right	Maxilla.Left	Maxilla.Right	Nasal	Otoccipital.Left	Otoccipital.Right	Palatine.Left	Palatine.Right	Parabasisphenoid	Parietal	Postfrontal.Left	Postfrontal.Right	Prefrontal.Left	Prefrontal.Right	Premaxilla	Prootic.Left	Prootic.Right	Pterygoid.Left	Pterygoid.Right	Quadrate.Left	Quadrate.Right	Septomaxilla.Left	Septomaxilla.Right	Splenial.Left	Splenial.Right	Squamosal.Left	Squamosal.Right	Stapes.Left	Stapes.Right	Supraoccipital	Supratemporal.Left	Supratemporal.Right	Surangular.Left	Surangular.Right	Vomer.Left	Vomer.Right
Angular.Left			1					1																																											1		
Angular.Right				1					1																																			1								1		
Articular.Left	1					1																																1												1		
Articular.Right		1					1																																1												1		
Basioccipital																							1	1		1							1	1																			
Coronoid.Left			1					1																																		1								1		
Coronoid.Right				1					1																																		1								1		
Dentary.Left	1					1			1																																	1								1		
Dentary.Right		1					1	1																																		1								1		
Ectopterygoid.Left																1			1					1											1																			
Ectopterygoid.Right																	1			1					1											1																			
Epipterygoid.Left																											1						1		1																			
Epipterygoid.Right																											1							1		1																			
Frontal.Left														1	1							1					1	1		1																									
Frontal.Right														1								1					1		1			1																						
Jugal.Left										1							1		1					1				1		1																								
Jugal.Right											1							1		1					1					1			1																				
Lacrimal.Left																1				1					1							1																					
Lacrimal.Right																	1				1					1							1																				
Maxilla.Left										1						1		1						1							1		1						1													1		
Maxilla.Right											1						1		1						1							1	1						1													1	
Nasal														1	1																		1																				
Otoccipital.Left					1																						1						1				1										1	1			
Otoccipital.Right					1																						1							1			1										1	1		1	
Palatine.Left										1						1		1		1											1				1																	1	
Palatine.Right											1						1		1		1												1				1															1
Parabasisphenoid					1																												1	1	1	1															
Parietal												1	1	1	1								1	1				1	1				1	1														1	1	1			
Postfrontal.Left														1		1											1			1																							
Postfrontal.Right															1		1										1				1		1																			
Prefrontal.Left														1		1		1		1					1			1				1																					
Prefrontal.Right															1		1		1						1				1																							
Premaxilla																							1	1		1												1	1													1	1
Prootic.Left					1							1											1				1	1																								
Prootic.Right					1								1											1			1	1																								
Pterygoid.Left										1		1													1		1																										
Pterygoid.Right											1		1													1	1																										
Quadrate.Left			1																				1													1						1		1			1					
Quadrate.Right				1																				1												1					1		1		1				1		
Septomaxilla.Left																				1		1											1																		1	
Septomaxilla.Right																						1	1										1																			1
Splenial.Left	1					1		1																																													
Splenial.Right		1					1		1																																												
Squamosal.Left																																						1														
Squamosal.Right																																							1													
Stapes.Left																							1										1					1														
Stapes.Right																								1										1					1													
Supraoccipital																							1	1			1						1	1																			
Supratemporal.Left																							1				1											1				1										
Supratemporal.Right																								1			1											1				1										
Surangular.Left	1		1			1		1																																												
Surangular.Right		1		1			1		1																																											
Vomer.Left																				1					1								1								1												1	
Vomer.Right																					1					1							1								1											1	

APPENDIX 4.1-37. Adjacency matrix for *Physignathus cocincinus* (YPM 14378)

Physignathus cocincinus **(YPM 14378) Evans (2008), Bell et al. (2009), Gray (2018)**	Angular.Left	Angular.Right	Articular.Left	Articular.Right	Basioccipital	Coronoid.Left	Coronoid.Right	Dentary.Left	Dentary.Right	Ectopterygoid.Left	Ectopterygoid.Right	Epipterygoid.Left	Epipterygoid.Right	Frontal	Jugal.Left	Jugal.Right	Lacrimal.Left	Lacrimal.Right	Maxilla.Left	Maxilla.Right	Nasal.Left	Nasal.Right	Otoccipital.Left	Otoccipital.Right	Palatine.Left	Palatine.Right	Parabasisphenoid	Parietal	Postorbital.Left	Postorbital.Right	Prefrontal.Left	Prefrontal.Right	Premaxilla	Prootic.Left	Prootic.Right	Pterygoid.Left	Pterygoid.Right	Quadrate.Left	Quadrate.Right	Septomaxilla.Left	Septomaxilla.Right	Splenial.Left	Splenial.Right	Squamosal.Left	Squamosal.Right	Stapes.Left	Stapes.Right	Supraoccipital	Supratemporal.Left	Supratemporal.Right	Surangular.Left	Surangular.Right	Vomer.Left	Vomer.Right
Angular.Left			1					1																																														
Angular.Right				1					1																																													
Articular.Left	1					1		1																															1			1									1		
Articular.Right		1					1		1																															1			1								1		
Basioccipital																							1	1			1							1	1																		
Coronoid.Left			1					1																																		1									1		
Coronoid.Right				1					1																																		1								1		
Dentary.Left	1		1			1			1																																	1								1		
Dentary.Right		1		1			1	1																																		1								1		
Ectopterygoid.Left														1				1																		1																	
Ectopterygoid.Right															1				1																		1																	
Epipterygoid.Left																												1					1		1																	
Epipterygoid.Right																												1						1		1																
Frontal																					1	1						1	1	1	1	1																						
Jugal.Left										1						1		1											1																1									
Jugal.Right											1						1		1											1															1								
Lacrimal.Left														1				1							1						1																					
Lacrimal.Right															1				1							1							1																				
Maxilla.Left										1				1		1				1				1						1		1									1											1	
Maxilla.Right											1				1		1				1				1						1	1									1											1
Nasal.Left														1				1				1								1		1																				
Nasal.Right														1					1	1											1	1																				
Otoccipital.Left					1																		1					1					1			1							1		1	1					
Otoccipital.Right					1																			1				1						1			1								1	1		1			
Palatine.Left																	1		1						1				1			1				1														1		
Palatine.Right																		1		1						1					1						1														1
Parabasisphenoid					1																						1						1	1	1																
Parietal												1	1	1									1	1				1	1					1	1												1	1	1			
Postorbital.Left														1	1													1																1							
Postorbital.Right														1		1												1																	1						
Prefrontal.Left														1			1		1		1				1																											
Prefrontal.Right														1				1				1				1																											
Premaxilla																																																					
Prootic.Left					1							1											1					1	1																							
Prootic.Right					1								1											1					1	1																						
Pterygoid.Left										1		1					1		1		1				1				1										1														
Pterygoid.Right											1		1							1		1				1	1													1												
Quadrate.Left			1																				1													1								1		1			1			
Quadrate.Right				1																				1													1						1		1			1			
Septomaxilla.Left																							1																												1		
Septomaxilla.Right																																																				1	
Splenial.Left	1		1			1		1																																											
Splenial.Right		1		1			1		1																																											
Squamosal.Left														1															1									1											1			
Squamosal.Right															1															1									1											1		
Stapes.Left																							1											1					1													
Stapes.Right																								1											1					1												
Supraoccipital																							1	1				1						1	1																		
Supratemporal.Left																							1					1									1								1							
Supratemporal.Right																								1				1										1								1						
Surangular.Left	1		1			1		1																																												
Surangular.Right		1		1			1		1																																											
Vomer.Left																				1					1							1								1												1	
Vomer.Right																					1					1							1								1											1	

APPENDIX 4.1-38. Adjacency matrix for *Rhineura floridana* (FMNH 31774)

Rhineura floridana **(FMNH 31774) Gans and Montero (2008)**	Angular.Left	Angular.Right	CompoundBone.Left	CompoundBone.Right	Coronoid.Left	Coronoid.Right	Dentary.Left	Dentary.Right	Ectopterygoid.Left	Ectopterygoid.Right	Frontal.Left	Frontal.Right	Jugal.Left	Jugal.Right	Maxilla.Left	Maxilla.Right	Nasal.Left	Nasal.Right	OccipitalComplexEtc	Palatine.Left	Palatine.Right	Parietal	Prefrontal.Left	Prefrontal.Right	Premaxilla	Pterygoid.Left	Pterygoid.Right	Quadrate.Left	Quadrate.Right	Septomaxilla.Left	Septomaxilla.Right	Stapes.Left	Stapes.Right	Tabulosphenoid	Vomer.Left	Vomer.Right
Angular.Left			1		1		1																													
Angular.Right				1		1		1																												
CompoundBone.Left	1				1		1																					1								
CompoundBone.Right		1				1		1																					1							
Coronoid.Left	1		1				1																													
Coronoid.Right		1		1				1																												
Dentary.Left	1		1		1			1																												
Dentary.Right		1		1		1	1																													
Ectopterygoid.Left										1		1		1						1			1			1										
Ectopterygoid.Right											1		1		1						1			1			1									
Frontal.Left									1			1			1		1		1	1		1	1							1				1		
Frontal.Right										1	1					1		1	1		1	1		1							1			1		
Jugal.Left									1						1								1													
Jugal.Right										1						1								1												
Maxilla.Left									1		1		1			1	1			1			1		1	1				1				1		
Maxilla.Right										1		1		1	1			1			1			1	1		1				1				1
Nasal.Left											1				1			1							1										
Nasal.Right												1				1	1								1										
OccipitalComplexEtc											1	1										1				1	1	1	1			1	1	1		
Palatine.Left									1		1				1								1			1								1	1	
Palatine.Right										1		1				1								1			1								1		1
Parietal											1	1							1				1	1												
Prefrontal.Left									1		1		1		1					1		1														
Prefrontal.Right										1		1		1		1					1	1														
Premaxilla															1	1	1	1																	1	1
Pterygoid.Left									1						1				1	1								1								
Pterygoid.Right										1						1			1		1								1							
Quadrate.Left			1																1							1				1						
Quadrate.Right				1															1								1					1				
Septomaxilla.Left											1				1																1			1		
Septomaxilla.Right												1				1														1					1	
Stapes.Left																			1									1								
Stapes.Right																			1										1							
Tabulosphenoid											1	1							1	1	1															
Vomer.Left															1					1					1					1				1	1
Vomer.Right																1					1				1						1			1	

APPENDIX 4.1-39. Adjacency matrix for *Sauromalus ater* (TNHC 18483)

Sauromalus ater **(TNHC 18483) Evans (2008), Bell et al. (2009), Gray (2018)**	Angular.Left	Angular.Right	Articular.Left	Articular.Right	BraincaseSkullFloor	Coronoid.Left	Coronoid.Right	Dentary.Left	Dentary.Right	Ectopterygoid.Left	Ectopterygoid.Right	Epipterygoid.Left	Epipterygoid.Right	Frontal	Jugal.Left	Jugal.Right	Lacrimal.Left	Lacrimal.Right	Maxilla.Left	Maxilla.Right	Nasal.Left	Nasal.Right	Palatine.Left	Palatine.Right	Parietal	Postfrontal.Left	Postfrontal.Right	Postorbital.Left	Postorbital.Right	Prefrontal.Left	Prefrontal.Right	Premaxilla	Pterygoid.Left	Pterygoid.Right	Quadrate.Left	Quadrate.Right	Septomaxilla.Left	Septomaxilla.Right	Splenial.Left	Splenial.Right	Squamosal.Left	Squamosal.Right	Stapes.Left	Stapes.Right	Supratemporal.Left	Supratemporal.Right	Surangular.Left	Surangular.Right	Vomer.Left	Vomer.Right
Angular.Left			1					1																														1									1			
Angular.Right				1					1																																1								1		
Articular.Left	1					1																												1				1									1		
Articular.Right		1					1																													1												1		
BraincaseSkullFloor												1	1											1								1	1	1	1					1	1	1	1					
Coronoid.Left			1					1																														1								1			
Coronoid.Right				1					1																															1								1		
Dentary.Left	1					1			1																														1								1			
Dentary.Right		1						1	1																															1								1		
Ectopterygoid.Left															1				1													1																		
Ectopterygoid.Right																1				1													1																		
Epipterygoid.Left					1																			1								1																		
Epipterygoid.Right					1																			1									1																		
Frontal																					1	1			1	1	1		1	1																					
Jugal.Left										1						1		1					1					1																								
Jugal.Right											1						1		1					1					1																							
Lacrimal.Left															1			1			1			1						1																						
Lacrimal.Right																1								1							1																					
Maxilla.Left										1					1		1				1		1						1		1				1														1		
Maxilla.Right											1					1		1				1		1						1	1							1											1	
Nasal.Left														1					1			1								1		1				1													
Nasal.Right														1						1	1										1	1					1												
Palatine.Left															1		1		1											1			1														1		
Palatine.Right																1		1		1											1			1														1
Parietal				1								1	1	1											1	1	1															1	1			1	1			
Postfrontal.Left														1											1			1																						
Postfrontal.Right														1											1				1																						
Postorbital.Left															1											1																	1							
Postorbital.Right																1											1																	1						
Prefrontal.Left														1			1		1		1		1																											
Prefrontal.Right														1				1				1		1																											
Premaxilla																	1		1	1	1	1																												
Pterygoid.Left					1					1		1											1														1													
Pterygoid.Right					1						1		1											1														1												
Quadrate.Left			1		1																													1					1			1		1					
Quadrate.Right				1	1																														1					1		1		1				
Septomaxilla.Left																					1																	1											1		
Septomaxilla.Right																					1		1																1											1	
Splenial.Left	1		1			1		1																																									
Splenial.Right		1		1			1		1																																									
Squamosal.Left																									1			1							1										1						
Squamosal.Right																									1				1							1										1				
Stapes.Left					1																													1															
Stapes.Right					1																														1														
Supratemporal.Left					1																				1									1								1							
Supratemporal.Right					1																				1										1									1					
Surangular.Left	1		1			1		1																																									
Surangular.Right		1		1			1		1																																									
Vomer.Left																					1			1													1													1
Vomer.Right																					1			1													1													1	

APPENDIX 4.1-40. Adjacency matrix for *Uranoscodon superciliosus* (YPM 12871)

Uranoscodon superciliosus **(YPM 12871) Evans (2008), Bell et al. (2009), Gray (2018)**	Angular.Left	Angular.Right	Articular.Left	Articular.Right	Basioccipital	Coronoid.Left	Coronoid.Right	Dentary.Left	Dentary.Right	Ectopterygoid.Left	Ectopterygoid.Right	Epipterygoid.Left	Epipterygoid.Right	Frontal	Jugal.Left	Jugal.Right	Lacrimal.Left	Lacrimal.Right	Maxilla.Left	Maxilla.Right	Nasal.Left	Nasal.Right	Otoccipital.Left	Otoccipital.Right	Palatine.Left	Palatine.Right	Parabasisphenoid	Parietal	Postfrontal.Left	Postfrontal.Right	Postorbital.Left	Postorbital.Right	Prefrontal.Left	Prefrontal.Right	Premaxilla	Prootic.Left	Prootic.Right	Pterygoid.Left	Pterygoid.Right	Quadrate.Left	Quadrate.Right	Septomaxilla.Left	Septomaxilla.Right	Splenial.Left	Splenial.Right	Squamosal.Left	Squamosal.Right	Stapes.Left	Stapes.Right	Supraoccipital	Supratemporal.Left	Supratemporal.Right	Surangular.Left	Surangular.Right	Vomer.Left	Vomer.Right
Angular.Left			1					1																																			1								1		
Angular.Right				1					1																																						1						1		
Articular.Left	1					1																																		1			1							1		
Articular.Right		1					1																																				1			1						1		
Basioccipital																							1	1			1								1	1																			
Coronoid.Left			1					1																																				1								1		
Coronoid.Right				1					1																																					1								1		
Dentary.Left	1					1			1																																					1								1		
Dentary.Right		1					1	1																																						1								1		
Ectopterygoid.Left															1				1																				1																			
Ectopterygoid.Right																1				1																				1																		
Epipterygoid.Left																												1												1																	
Epipterygoid.Right																												1													1																
Frontal																					1	1						1	1	1	1	1	1	1																							
Jugal.Left										1						1		1													1																									
Jugal.Right											1						1															1																								
Lacrimal.Left														1				1						1									1																							
Lacrimal.Right															1				1						1									1																							
Maxilla.Left										1				1		1				1				1									1		1											1										1		
Maxilla.Right											1				1		1				1				1									1	1											1											1
Nasal.Left														1				1				1												1																						
Nasal.Right														1					1	1														1	1																					
Otoccipital.Left					1																		1					1								1							1							1		1	1			
Otoccipital.Right					1																			1				1									1							1								1	1		1		
Palatine.Left																	1		1						1								1					1																		1		
Palatine.Right																		1		1						1								1						1																	1
Parabasisphenoid					1																						1								1	1	1	1																		
Parietal												1	1	1								1	1				1		1	1	1	1	1																				1	1	1			
Postfrontal.Left														1													1				1																									
Postfrontal.Right														1													1					1																							
Postorbital.Left														1	1												1	1																											
Postorbital.Right														1		1											1		1																										
Prefrontal.Left														1			1		1		1			1																																
Prefrontal.Right														1				1		1		1				1																														
Premaxilla																			1	1	1	1																																	1	1
Prootic.Left					1																	1					1																												
Prootic.Right					1																		1				1																												
Pterygoid.Left										1		1									1			1			1																												
Pterygoid.Right											1		1									1				1	1																												
Quadrate.Left			1														1		1		1		1																																
Quadrate.Right				1														1						1																																
Septomaxilla.Left																			1																																					1	
Septomaxilla.Right																				1																																			1
Splenial.Left	1		1			1		1																							1																							
Splenial.Right		1		1			1		1																																													
Squamosal.Left															1																																									
Squamosal.Right																1																1																							
Stapes.Left																							1													1							1												
Stapes.Right																								1													1							1										
Supraoccipital																							1	1				1								1	1																			
Supratemporal.Left																							1					1													1														
Supratemporal.Right																								1				1									1							1										
Surangular.Left	1		1			1		1																																															
Surangular.Right		1		1			1		1																																													
Vomer.Left																			1						1										1											1										1	
Vomer.Right																				1						1									1											1										1	

APPENDIX 4.1-41. Adjacency matrix for *Varanus exanthematicus* (FMNH 58299)

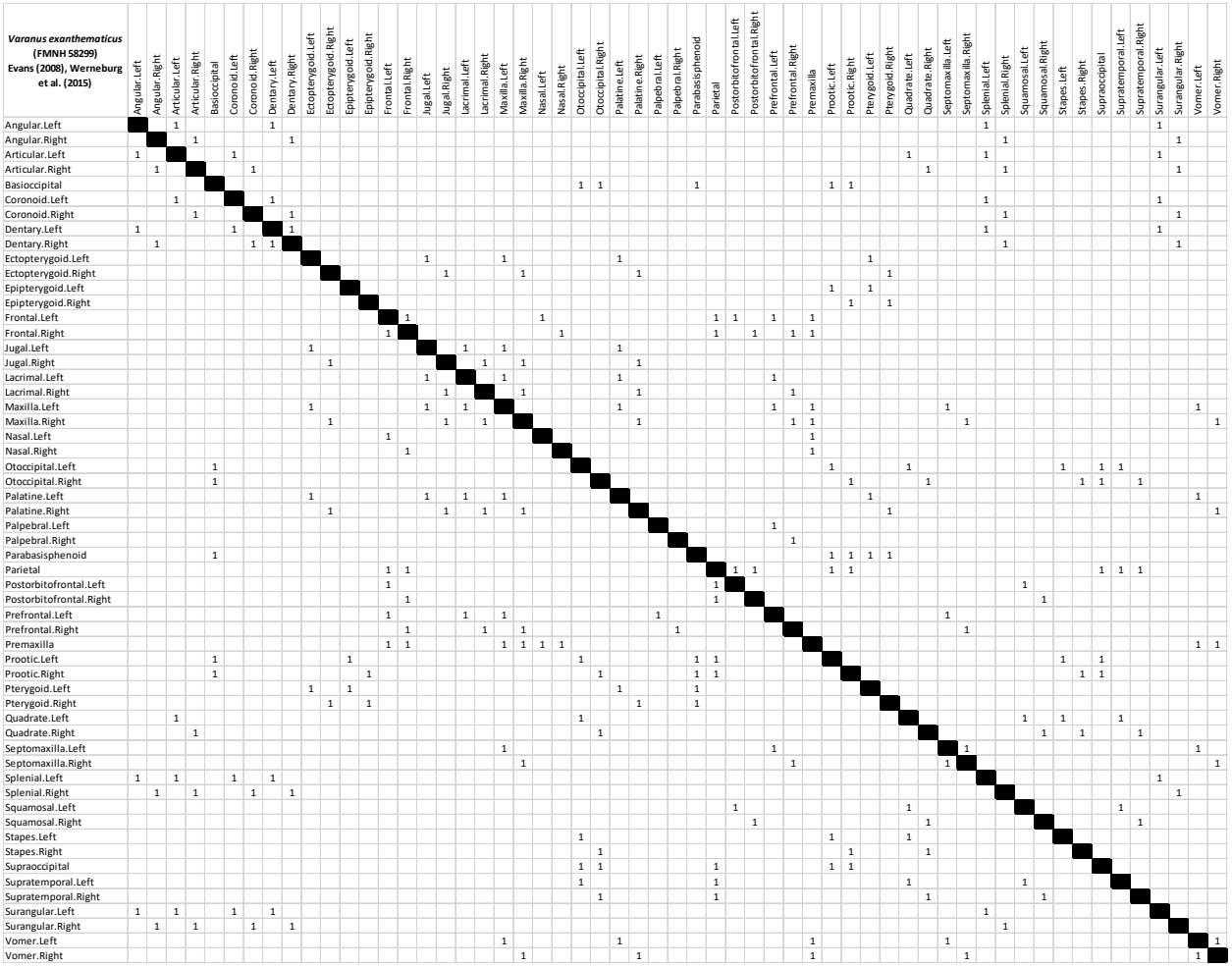

Varanus exanthematicus **(FMNH 58299) Evans (2008), Werneburg et al. (2015)**	Angular.Left	Angular.Right	Articular.Left	Articular.Right	Basioccipital	Coronoid.Left	Coronoid.Right	Dentary.Left	Dentary.Right	Ectopterygoid.Left	Ectopterygoid.Right	Epipterygoid.Left	Epipterygoid.Right	Frontal.Left	Frontal.Right	Jugal.Left	Jugal.Right	Lacrimal.Left	Lacrimal.Right	Maxilla.Left	Maxilla.Right	Nasal.Left	Nasal.Right	Otoccipital.Left	Otoccipital.Right	Palatine.Left	Palatine.Right	Palpebral.Left	Palpebral.Right	Parabasisphenoid	Parietal	Postorbitofrontal.Left	Postorbitofrontal.Right	Prefrontal.Left	Prefrontal.Right	Premaxilla	Prootic.Left	Prootic.Right	Pterygoid.Left	Pterygoid.Right	Quadrate.Left	Quadrate.Right	Septomaxilla.Left	Septomaxilla.Right	Splenial.Left	Splenial.Right	Squamosal.Left	Squamosal.Right	Stapes.Left	Stapes.Right	Supraoccipital	Supratemporal.Left	Supratemporal.Right	Surangular.Left	Surangular.Right	Vomer.Left	Vomer.Right
Angular.Left			1				1																																																	
Angular.Right				1				1																																																	
Articular.Left	1					1																																																		
Articular.Right		1					1																																																	
Basioccipital																							1	1					1							1	1																				
Coronoid.Left			1					1																																																
Coronoid.Right				1					1																																															
Dentary.Left	1					1			1																																															
Dentary.Right		1					1	1																																															
Ectopterygoid.Left																1				1					1																																
Ectopterygoid.Right																	1				1					1																														
Epipterygoid.Left																																																							
Epipterygoid.Right																																																							
Frontal.Left														1		1						1									1	1		1		1																				
Frontal.Right															1			1				1									1		1		1	1																			
Jugal.Left										1								1		1					1																															
Jugal.Right											1								1		1					1																														
Lacrimal.Left																1				1					1								1																						
Lacrimal.Right																	1				1					1								1																					
Maxilla.Left										1						1		1							1								1		1										1										
Maxilla.Right											1						1		1							1								1	1										1										1
Nasal.Left														1																				1																				
Nasal.Right															1																				1																				
Otoccipital.Left					1																															1			1					1							1	1		
Otoccipital.Right					1																																1			1						1	1		1		
Palatine.Left										1						1		1		1					1											1																		1	
Palatine.Right											1						1		1		1					1											1																		1
Palpebral.Left																																		1																				
Palpebral.Right																																			1																				
Parabasisphenoid					1																																																				
Parietal														1	1																			1	1				1	1												1	1	1			
Postorbitofrontal.Left														1																				1																				
Postorbitofrontal.Right															1																				1																				
Prefrontal.Left														1				1		1									1																										
Prefrontal.Right															1				1		1									1																										
Premaxilla														1	1					1	1	1																																		1	1
Prootic.Left					1							1												1													1	1																		
Prootic.Right					1								1												1												1	1																	
Pterygoid.Left										1		1														1					1																								
Pterygoid.Right											1		1														1				1																								
Quadrate.Left			1																					1																						1		1			1				
Quadrate.Right				1																					1																						1		1			1			
Septomaxilla.Left																				1														1																				1	
Septomaxilla.Right																					1														1																					1
Splenial.Left	1		1			1		1																																															
Splenial.Right		1		1			1		1																																														
Squamosal.Left																															1																								
Squamosal.Right																																1																							
Stapes.Left																							1														1																			
Stapes.Right																								1														1																	
Supraoccipital																							1	1							1						1	1																	
Supratemporal.Left																							1								1																								
Supratemporal.Right																								1							1																								
Surangular.Left	1		1			1		1																																															
Surangular.Right		1		1			1		1																																														
Vomer.Left																				1					1																																
Vomer.Right																					1					1																														

APPENDIX 4.1-42. Adjacency matrix for *Boa constrictor* (FMNH 31182)

Boa constrictor **(FMNH 31182)** **Frazzetta (1966)**	Angular.Left	Angular.Right	Basioccipital	CompoundBone.Left	CompoundBone.Right	Coronoid.Left	Coronoid.Right	Dentary.Left	Dentary.Right	Ectopterygoid.Left	Ectopterygoid.Right	Frontal.Left	Frontal.Right	Jugal.Left	Jugal.Right	Maxilla.Left	Maxilla.Right	Nasal.Left	Nasal.Right	Otoccipital.Left	Otoccipital.Right	Palatine.Left	Palatine.Right	Parabasisphenoid	Parietal	Prefrontal.Left	Prefrontal.Right	Premaxilla	Prootic.Left	Prootic.Right	Pterygoid.Left	Pterygoid.Right	Quadrate.Left	Quadrate.Right	Septomaxilla.Left	Septomaxilla.Right	Splenial.Left	Splenial.Right	Stapes.Left	Stapes.Right	Supraoccipital	Supratemporal.Left	Supratemporal.Right	Vomer.Left	Vomer.Right
Angular.Left				1		1																														1									
Angular.Right					1		1																														1								
Basioccipital																				1	1			1				1	1																
CompoundBone.Left	1					1		1																								1													
CompoundBone.Right		1					1		1																								1												
Coronoid.Left	1			1				1																												1								
Coronoid.Right		1			1				1																												1							
Dentary.Left				1		1																														1							
Dentary.Right					1		1																														1						
Ectopterygoid.Left													1		1															1													
Ectopterygoid.Right														1		1															1												
Frontal.Left													1	1				1					1	1	1																		
Frontal.Right												1			1				1				1	1		1																	
Jugal.Left										1		1												1																			
Jugal.Right											1		1											1																			
Maxilla.Left										1												1			1										1								
Maxilla.Right											1												1			1										1							
Nasal.Left												1						1							1		1								1							1	
Nasal.Right													1						1							1	1								1								1
Otoccipital.Left			1																	1	1				1			1										1		1			
Otoccipital.Right			1																	1	1				1				1											1	1		
Palatine.Left																1						1				1				1			1									
Palatine.Right																	1						1				1				1			1								
Parabasisphenoid			1									1	1											1	1				1	1												1	1
Parietal												1	1	1	1					1	1			1	1				1	1										1	1	1	
Prefrontal.Left												1				1		1				1				1																	
Prefrontal.Right													1				1		1				1				1																
Premaxilla																		1	1									1														
Prootic.Left			1																	1				1					1										1		1	1		
Prootic.Right			1																		1			1						1										1	1		1	
Pterygoid.Left										1												1									1												
Pterygoid.Right											1												1									1											
Quadrate.Left				1																													1					1					
Quadrate.Right					1																													1					1				
Septomaxilla.Left																1		1				1													1							1	
Septomaxilla.Right																	1		1				1													1							1
Splenial.Left	1					1		1																												1							
Splenial.Right		1					1		1																												1						
Stapes.Left																				1								1				1						1					
Stapes.Right																					1								1				1						1				
Supraoccipital																				1	1				1			1	1										1				
Supratemporal.Left																									1			1				1								1			
Supratemporal.Right																									1				1				1								1		
Vomer.Left																			1					1										1								1	
Vomer.Right																			1					1											1								

APPENDIX 4.1-43. Adjacency matrix for *Calabaria reinhardtii* (FMNH 117833)

***Calabaria reinhardtii* (FMNH 117833)**	Angular.Left	Angular.Right	Basioccipital	CompoundBone.Left	CompoundBone.Right	Coronoid.Left	Coronoid.Right	Dentary.Left	Dentary.Right	Ectopterygoid.Left	Ectopterygoid.Right	Frontal.Left	Frontal.Right	Jugal.Left	Jugal.Right	Maxilla.Left	Maxilla.Right	Nasal.Left	Nasal.Right	Otoccipital.Left	Otoccipital.Right	Palatine.Left	Palatine.Right	Parabasisphenoid	Parietal	Postfrontal.Left	Postfrontal.Right	Prefrontal.Left	Prefrontal.Right	Premaxilla	Prootic.Left	Prootic.Right	Pterygoid.Left	Pterygoid.Right	Quadrate.Left	Quadrate.Right	Septomaxilla.Left	Septomaxilla.Right	Splenial.Left	Splenial.Right	Stapes.Left	Stapes.Right	Supraoccipital	Supratemporal.Left	Supratemporal.Right	Vomer.Left	Vomer.Right
Angular.Left				1																																		1									
Angular.Right					1																																		1								
Basioccipital																				1	1			1							1	1															
CompoundBone.Left	1					1		1																										1													
CompoundBone.Right		1					1		1																										1												
Coronoid.Left				1																																										
Coronoid.Right					1																																									
Dentary.Left				1																																										
Dentary.Right					1																																									
Ectopterygoid.Left														1		1																			1											
Ectopterygoid.Right															1		1																			1											
Frontal.Left													1					1					1	1	1		1																			
Frontal.Right												1							1					1	1		1		1																	
Jugal.Left										1					1										1	1																				
Jugal.Right											1					1									1		1																			
Maxilla.Left										1				1								1						1										1								
Maxilla.Right											1				1								1						1										1							
Nasal.Left												1							1								1		1								1								
Nasal.Right													1					1									1	1									1								
Otoccipital.Left			1																		1									1									1		1					
Otoccipital.Right			1																	1											1									1	1				
Palatine.Left																1							1				1						1												1	
Palatine.Right																	1						1					1																		1
Parabasisphenoid			1									1	1									1	1		1					1	1	1	1											
Parietal												1	1	1	1								1		1	1				1	1											1	1	1		
Postfrontal.Left												1		1										1																					
Postfrontal.Right													1		1									1																					
Prefrontal.Left												1				1		1				1															1								
Prefrontal.Right													1				1		1				1																						
Premaxilla																		1	1																										
Prootic.Left			1																	1				1	1																1		1	1		
Prootic.Right			1																		1			1	1																	1	1		1		
Pterygoid.Left										1												1		1																						
Pterygoid.Right											1												1	1																						
Quadrate.Left				1																																				1			1			
Quadrate.Right					1																																				1			1		
Septomaxilla.Left																1		1									1																		1	
Septomaxilla.Right																	1		1									1																		1
Splenial.Left	1							1																																						
Splenial.Right		1							1																																					
Stapes.Left																				1											1				1										
Stapes.Right																					1											1				1									
Supraoccipital																				1	1			1							1	1														
Supratemporal.Left																								1							1				1										
Supratemporal.Right																								1								1				1									
Vomer.Left																						1															1								1
Vomer.Right																							1															1						1	

APPENDIX 4.1-44. Adjacency matrix for *Casarea dussumieri* (UMMZ 190285)

***Casarea dussumieri* (UMMZ 190285) Maisano and Rieppel (2007)**	Angular.Left	Angular.Right	Basioccipital	CompoundBone.Left	CompoundBone.Right	Coronoid.Left	Coronoid.Right	Dentary.Left	Dentary.Right	Ectopterygoid.Left	Ectopterygoid.Right	Frontal.Left	Frontal.Right	Jugal-Postfrontal.Left	Jugal-Postfrontal.Right	MaxillaAnterior.Left	MaxillaAnterior.Right	MaxillaPosterior.Left	MaxillaPosterior.Right	Nasal.Left	Nasal.Right	Otoccipital.Left	Otoccipital.Right	Palatine.Left	Palatine.Right	Parabasisphenoid	Parietal	Prefrontal.Left	Prefrontal.Right	Premaxilla	Prootic.Left	Prootic.Right	Pterygoid.Left	Pterygoid.Right	Quadrate.Left	Quadrate.Right	Septomaxilla.Left	Septomaxilla.Right	Splenial.Left	Splenial.Right	Stapes.Left	Stapes.Right	SuborbitalElement.Left	SuborbitalElement.Right	Supraoccipital	Supratemporal.Left	Supratemporal.Right	Vomer.Left	Vomer.Right
Angular.Left				1																																		1										
Angular.Right					1																																		1									
Basioccipital																						1	1		1					1	1																		
CompoundBone.Left	1					1		1																											1														
CompoundBone.Right		1					1		1																											1													
Coronoid.Left				1				1																															1										
Coronoid.Right					1				1																															1									
Dentary.Left				1		1																																	1										
Dentary.Right					1		1																																	1									
Ectopterygoid.Left																		1															1																
Ectopterygoid.Right																			1															1																
Frontal.Left													1	1						1				1		1	1	1																					
Frontal.Right												1		1							1				1	1	1		1																				
Jugal-Postfrontal.Left												1															1																						
Jugal-Postfrontal.Right													1														1																						
MaxillaAnterior.Left																		1						1				1																	1					
MaxillaAnterior.Right																			1						1				1																1				
MaxillaPosterior.Left										1						1								1										1											1				
MaxillaPosterior.Right											1						1								1										1											1			
Nasal.Left												1									1						1		1										1										
Nasal.Right													1							1							1	1											1										
Otoccipital.Left			1																			1		1					1																				
Otoccipital.Right			1																				1								1																		
Palatine.Left												1				1		1						1		1		1					1																
Palatine.Right													1				1		1						1				1					1															
Parabasisphenoid			1									1	1											1	1		1			1	1																	
Parietal												1	1	1	1											1					1	1																
Prefrontal.Left												1				1								1										1															
Prefrontal.Right													1				1								1																					1			
Premaxilla																1					1	1																											1	1
Prootic.Left			1																			1					1	1																				
Prootic.Right			1																				1				1	1																				
Pterygoid.Left										1								1						1																									
Pterygoid.Right											1								1						1																								
Quadrate.Left				1																																												
Quadrate.Right					1																																											
Septomaxilla.Left																1					1								1																			1	
Septomaxilla.Right																	1				1								1																			1
Splenial.Left	1					1		1																																							
Splenial.Right		1					1		1																																						
Stapes.Left																						1								1					1												
Stapes.Right																							1								1				1												
SuborbitalElement.Left																1		1									1																					
SuborbitalElement.Right																	1		1										1																				
Supraoccipital																						1	1				1			1	1																	
Supratemporal.Left																						1					1								1												
Supratemporal.Right																							1				1									1												
Vomer.Left																														1							1										1
Vomer.Right																														1								1									1	

APPENDIX 4.1-45. Adjacency matrix for *Eryx colubrinus* (FMNH 63117)

***Eryx colubrinus* (FMNH 63117)**	Angular.Left	Angular.Right	Basioccipital	CompoundBone.Left	CompoundBone.Right	Coronoid.Left	Coronoid.Right	Dentary.Left	Dentary.Right	Ectopterygoid.Left	Ectopterygoid.Right	Frontal.Left	Frontal.Right	Jugal.Left	Jugal.Right	Maxilla.Left	Maxilla.Right	Nasal.Left	Nasal.Right	Otoccipital.Left	Otoccipital.Right	Palatine.Left	Palatine.Right	Parabasisphenoid	Parietal	Prefrontal.Left	Prefrontal.Right	Premaxilla	Prootic.Left	Prootic.Right	Pterygoid.Left	Pterygoid.Right	Quadrate.Left	Quadrate.Right	Septomaxilla.Left	Septomaxilla.Right	Splenial.Left	Splenial.Right	Stapes.Left	Stapes.Right	Supraoccipital	Supratemporal.Left	Supratemporal.Right	Vomer.Left	Vomer.Right
Angular.Left				1		1																														1									
Angular.Right					1		1																														1								
Basioccipital																				1	1			1				1	1																
CompoundBone.Left	1					1		1																								1													
CompoundBone.Right		1					1		1																								1												
Coronoid.Left	1			1				1																												1								
Coronoid.Right		1			1				1																												1							
Dentary.Left				1		1																														1							
Dentary.Right					1		1																														1						
Ectopterygoid.Left													1		1															1													
Ectopterygoid.Right														1		1															1												
Frontal.Left													1	1				1					1	1	1																		
Frontal.Right												1			1				1					1	1		1																
Jugal.Left										1		1													1																		
Jugal.Right											1		1												1																		
Maxilla.Left										1												1				1										1							
Maxilla.Right											1												1				1										1						
Nasal.Left												1						1							1		1								1								1	
Nasal.Right													1						1							1	1								1								1
Otoccipital.Left			1																	1	1				1			1									1		1			
Otoccipital.Right			1																	1	1				1				1									1	1			
Palatine.Left																1						1				1				1				1								
Palatine.Right																	1						1				1				1				1							
Parabasisphenoid			1									1	1											1	1				1	1	1	1										
Parietal												1	1	1	1					1	1			1	1				1	1										1	1	1	
Prefrontal.Left												1				1		1				1				1																
Prefrontal.Right													1				1		1				1				1															
Premaxilla																		1	1									1														
Prootic.Left			1																	1				1	1				1										1		1	1	
Prootic.Right			1																		1			1	1					1										1	1		1	
Pterygoid.Left										1												1		1							1											
Pterygoid.Right											1												1	1								1										
Quadrate.Left				1																													1					1				
Quadrate.Right					1																													1					1			
Septomaxilla.Left																1		1				1													1						1		
Septomaxilla.Right																	1		1				1													1							1
Splenial.Left	1					1		1																												1							
Splenial.Right		1					1		1																												1						
Stapes.Left																				1								1				1						1				
Stapes.Right																					1								1				1						1			
Supraoccipital																				1	1				1			1	1										1			
Supratemporal.Left																									1			1				1								1		
Supratemporal.Right																									1				1				1								1	
Vomer.Left																		1																1								1
Vomer.Right																			1																1						1	

APPENDIX 4.1-46. Adjacency matrix for *Loxocemus bicolor* (FMNH 104800)

***Loxocemus bicolor* (FMNH 104800) Rieppel (1977)**	Angular.Left	Angular.Right	Basioccipital	CompoundBone.Left	CompoundBone.Right	Coronoid.Left	Coronoid.Right	Dentary.Left	Dentary.Right	Ectopterygoid.Left	Ectopterygoid.Right	Frontal.Left	Frontal.Right	Jugal.Left	Jugal.Right	Maxilla.Left	Maxilla.Right	Nasal.Left	Nasal.Right	Otoccipital.Left	Otoccipital.Right	Palatine.Left	Palatine.Right	Parabasisphenoid	Parietal	Postfrontal.Left	Postfrontal.Right	Prefrontal.Left	Prefrontal.Right	Premaxilla	Prootic.Left	Prootic.Right	Pterygoid.Left	Pterygoid.Right	Quadrate.Left	Quadrate.Right	Septomaxilla.Left	Septomaxilla.Right	Splenial.Left	Splenial.Right	Stapes.Left	Stapes.Right	Supraoccipital	Supratemporal.Left	Supratemporal.Right	Vomer.Left	Vomer.Right
Angular.Left				1																																		1								
Angular.Right				1																																			1							
Basioccipital																				1	1			1						1	1															
CompoundBone.Left	1					1		1																										1												
CompoundBone.Right		1					1		1																										1											
Coronoid.Left				1																																									
Coronoid.Right					1																																								
Dentary.Left				1																																					1				
Dentary.Right					1																																					1				
Ectopterygoid.Left																1																		1											
Ectopterygoid.Right																	1																		1											
Frontal.Left													1					1					1	1	1		1																			
Frontal.Right												1							1					1	1		1		1																	
Jugal.Left																									1	1																				
Jugal.Right																									1		1																			
Maxilla.Left										1												1						1																		
Maxilla.Right											1												1						1																	
Nasal.Left												1							1									1		1							1									
Nasal.Right													1					1										1	1								1								
Otoccipital.Left			1																1		1									1									1		1	1				
Otoccipital.Right			1																	1											1									1	1		1		
Palatine.Left																1												1				1			1									1	
Palatine.Right																	1												1				1				1								1
Parabasisphenoid			1									1	1										1							1	1	1	1											
Parietal												1	1	1	1									1	1	1				1	1										1	1	1		
Postfrontal.Left												1		1											1		1																		
Postfrontal.Right													1		1										1			1																	
Prefrontal.Left												1				1		1				1				1			1																
Prefrontal.Right													1				1		1				1				1																		
Premaxilla																		1	1																									1	1
Prootic.Left			1																	1				1	1																1		1	1		
Prootic.Right			1																		1			1	1																	1	1		1		
Pterygoid.Left										1												1		1																						
Pterygoid.Right											1												1	1																						
Quadrate.Left				1																																					1			1			
Quadrate.Right					1																																					1			1		
Septomaxilla.Left																		1				1																							1		
Septomaxilla.Right																			1				1																							1
Splenial.Left	1							1																																						
Splenial.Right		1							1																																					
Stapes.Left																				1											1				1										
Stapes.Right																					1											1				1									
Supraoccipital																				1	1				1						1	1											1	1		
Supratemporal.Left																				1					1						1				1								1			
Supratemporal.Right																					1				1							1				1							1			
Vomer.Left																						1							1								1								1
Vomer.Right																							1						1								1							1	

APPENDIX 4.1-47. Adjacency matrix for *Python molurus* (TNHC 62769)

Python molurus **(TNHC 62769)** **Frazzetta (1966)**	Angular.Left	Angular.Right	Basioccipital	CompoundBone.Left	CompoundBone.Right	Coronoid.Left	Coronoid.Right	Dentary.Left	Dentary.Right	Ectopterygoid.Left	Ectopterygoid.Right	Frontal.Left	Frontal.Right	Jugal.Left	Jugal.Right	Maxilla.Left	Maxilla.Right	Nasal.Left	Nasal.Right	Otoccipital.Left	Otoccipital.Right	Palatine.Left	Palatine.Right	Parabasisphenoid	Parietal	Postfrontal.Left	Postfrontal.Right	Prefrontal.Left	Prefrontal.Right	Premaxilla	Prootic.Left	Prootic.Right	Pterygoid.Left	Pterygoid.Right	Quadrate.Left	Quadrate.Right	Septomaxilla.Left	Septomaxilla.Right	Splenial.Left	Splenial.Right	Stapes.Left	Stapes.Right	Supraoccipital	Supratemporal.Left	Supratemporal.Right	Vomer.Left	Vomer.Right
Angular.Left				1		1																																1									
Angular.Right					1		1																	1							1	1							1								
Basioccipital																				1	1			1							1	1															
CompoundBone.Left	1					1		1																										1													
CompoundBone.Right		1					1		1																										1												
Coronoid.Left	1			1				1																																1							
Coronoid.Right		1			1				1																																1						
Dentary.Left				1		1																																		1						
Dentary.Right					1		1																																		1						
Ectopterygoid.Left																1																			1												
Ectopterygoid.Right																	1																			1												
Frontal.Left													1	1				1					1	1	1		1																				
Frontal.Right												1			1				1				1	1		1		1																				
Jugal.Left												1												1	1																							
Jugal.Right													1											1		1																						
Maxilla.Left										1												1						1																				
Maxilla.Right											1												1						1																				
Nasal.Left												1							1									1		1							1											
Nasal.Right													1					1										1	1								1											
Otoccipital.Left			1																		1									1										1		1	1				
Otoccipital.Right			1																	1											1										1	1		1			
Palatine.Left																1												1				1				1										
Palatine.Right																	1											1					1				1										
Parabasisphenoid			1									1	1												1					1	1	1	1												1	1
Parietal												1	1	1	1									1		1	1			1	1												1	1	1		
Postfrontal.Left												1		1											1			1																		
Postfrontal.Right													1		1										1				1																		
Prefrontal.Left												1				1		1				1				1																					
Prefrontal.Right													1				1		1				1				1																				
Premaxilla																		1	1																		1	1							1	1
Prootic.Left			1																1					1	1																1		1	1			
Prootic.Right			1																		1			1	1																	1	1		1		
Pterygoid.Left										1												1		1																							
Pterygoid.Right											1												1	1																							
Quadrate.Left				1																																				1			1			
Quadrate.Right					1																																				1			1		
Septomaxilla.Left																		1				1								1															1	
Septomaxilla.Right																			1				1							1																1
Splenial.Left	1					1		1																																						
Splenial.Right		1					1		1																																					
Stapes.Left																				1										1				1											
Stapes.Right																					1										1				1										
Supraoccipital																				1	1			1						1	1												1	1		
Supratemporal.Left																				1				1						1				1									1			
Supratemporal.Right																					1			1							1				1								1			
Vomer.Left																								1						1						1									1	
Vomer.Right																								1						1							1								1	

APPENDIX 4.1-48. Adjacency matrix for *Xenopeltis unicolor* (FMNH 148900)

***Xenopeltis unicolor* (FMNH 148900) Rieppel (1977)**	Angular.Left	Angular.Right	Basioccipital	CompoundBone.Left	CompoundBone.Right	Coronoid.Left	Coronoid.Right	Dentary.Left	Dentary.Right	Ectopterygoid.Left	Ectopterygoid.Right	Frontal.Left	Frontal.Right	Maxilla.Left	Maxilla.Right	Nasal.Left	Nasal.Right	Otoccipital.Left	Otoccipital.Right	Palatine.Left	Palatine.Right	Parabasisphenoid	Parietal	Prefrontal.Left	Prefrontal.Right	Premaxilla	Prootic.Left	Prootic.Right	Pterygoid.Left	Pterygoid.Right	Quadrate.Left	Quadrate.Right	Septomaxilla.Left	Septomaxilla.Right	Stapes.Left	Stapes.Right	Supraoccipital	Supratemporal.Left	Supratemporal.Right	Vomer.Left	Vomer.Right
Angular.Left				1		1		1																																	
Angular.Right					1		1		1																																
Basioccipital																		1	1			1					1	1													
CompoundBone.Left	1					1		1																							1									
CompoundBone.Right		1					1		1																							1								
Coronoid.Left	1			1																																				
Coronoid.Right		1			1																																			
Dentary.Left	1			1																																				
Dentary.Right		1			1																																			
Ectopterygoid.Left													1															1												
Ectopterygoid.Right														1															1											
Frontal.Left												1				1						1	1	1																
Frontal.Right												1				1						1	1		1															
Maxilla.Left										1														1																
Maxilla.Right											1														1															
Nasal.Left												1					1							1		1								1						
Nasal.Right													1			1									1	1									1					
Otoccipital.Left			1																1								1								1		1	1		
Otoccipital.Right			1															1										1								1	1		1	
Palatine.Left																								1					1				1							1	
Palatine.Right																									1					1				1							1
Parabasisphenoid			1									1	1										1				1	1												
Parietal												1	1									1					1	1										1	1	1	
Prefrontal.Left												1		1		1				1																					
Prefrontal.Right													1		1		1				1																				
Premaxilla																	1																						1	1
Prootic.Left			1															1				1	1												1		1	1		
Prootic.Right			1																1			1	1													1	1		1	
Pterygoid.Left										1										1																				
Pterygoid.Right											1										1																			
Quadrate.Left				1																															1		1		
Quadrate.Right					1																															1			1	
Septomaxilla.Left																1				1																			1	
Septomaxilla.Right																	1				1																			1
Stapes.Left																		1								1					1								
Stapes.Right																			1								1					1							
Supraoccipital																		1	1				1				1	1											
Supratemporal.Left																		1					1				1				1								
Supratemporal.Right																			1				1					1				1							
Vomer.Left																				1						1							1						1
Vomer.Right																					1					1								1					1	

APPENDIX 4.1-49. Adjacency matrix for *Acrochordus granulatus* (MCZ R-146128)

***Acrochordus granulatus* (MCZ R-146128)**	Angular.Left	Angular.Right	Basioccipital	CompoundBone.Left	CompoundBone.Right	Dentary.Left	Dentary.Right	Ectopterygoid.Left	Ectopterygoid.Right	Frontal.Left	Frontal.Right	Jugal-Postfrontal.Left	Jugal-Postfrontal.Right	Maxilla.Left	Maxilla.Right	Nasal.Left	Nasal.Right	Otoccipital.Left	Otoccipital.Right	Palatine.Left	Palatine.Right	Parabasisphenoid	Parietal	Prefrontal.Left	Prefrontal.Right	Premaxilla	Prootic.Left	Prootic.Right	Pterygoid.Left	Pterygoid.Right	Quadrate.Left	Quadrate.Right	Septomaxilla.Left	Septomaxilla.Right	Splenial.Left	Splenial.Right	Stapes.Left	Stapes.Right	Supraoccipital	Supratemporal.Left	Supratemporal.Right	Vomer.Left	Vomer.Right
Angular.Left				1																														1								
Angular.Right					1																														1							
Basioccipital																		1	1			1					1	1															
CompoundBone.Left	1					1																									1												
CompoundBone.Right		1					1																									1										
Dentary.Left				1																														1							
Dentary.Right					1																														1						
Ectopterygoid.Left														1														1													
Ectopterygoid.Right															1														1												
Frontal.Left											1	1	1									1	1	1																		
Frontal.Right										1			1									1	1		1																	
Jugal-Postfrontal.Left										1													1																			
Jugal-Postfrontal.Right											1												1																			
Maxilla.Left								1												1				1																		
Maxilla.Right									1												1				1																	
Nasal.Left																	1																	1								
Nasal.Right																1																			1							
Otoccipital.Left			1																1							1										1		1	1			
Otoccipital.Right			1															1									1										1	1		1		
Palatine.Left														1									1					1												1		
Palatine.Right															1									1					1												1
Parabasisphenoid			1							1	1											1				1	1															
Parietal										1	1	1	1								1					1	1												1	1	1		
Prefrontal.Left										1				1						1																						
Prefrontal.Right											1				1						1																					
Premaxilla																																		1	1								
Prootic.Left			1															1				1	1													1		1	1			
Prootic.Right			1																1			1	1														1	1		1		
Pterygoid.Left								1												1																						
Pterygoid.Right									1												1																					
Quadrate.Left				1																																	1		1			
Quadrate.Right					1																																	1			1		
Septomaxilla.Left																1									1															1		
Septomaxilla.Right																	1								1																1
Splenial.Left	1					1																																			
Splenial.Right		1					1																																		
Stapes.Left																		1								1				1											
Stapes.Right																			1								1				1										
Supraoccipital																		1	1			1				1	1												1	1		
Supratemporal.Left																		1				1				1				1									1			
Supratemporal.Right																			1			1					1				1								1			
Vomer.Left																				1													1									
Vomer.Right																					1													1							1	

APPENDIX 4.1-50. Adjacency matrix for *Aparallactus guentheri* (MCZ R-23363)

***Aparallactus guentheri* (MCZ R-23363)**	Angular.Left	Angular.Right	Basioccipital	CompoundBone.Left	CompoundBone.Right	Dentary.Left	Dentary.Right	Ectopterygoid.Left	Ectopterygoid.Right	Frontal.Left	Frontal.Right	Maxilla.Left	Maxilla.Right	Nasal.Left	Nasal.Right	Neomorph.Left	Neomorph.Right	Otoccipital.Left	Otoccipital.Right	Palatine.Left	Palatine.Right	Parabasisphenoid	Parietal	PostfrontalOrJugal.Left	PostfrontalOrJugal.Right	Prefrontal.Left	Prefrontal.Right	Premaxilla	Prootic.Left	Prootic.Right	Pterygoid.Left	Pterygoid.Right	Quadrate.Left	Quadrate.Right	Septomaxilla.Left	Septomaxilla.Right	Splenial.Left	Splenial.Right	Stapes.Left	Stapes.Right	Supraoccipital	Supratemporal.Left	Supratemporal.Right	Vomer.Left	Vomer.Right
Angular.Left				1																																1								
Angular.Right					1																															1								
Basioccipital																		1	1			1							1	1															
CompoundBone.Left	1					1																										1												
CompoundBone.Right		1					1																										1											
Dentary.Left				1																																1								
Dentary.Right					1																															1								
Ectopterygoid.Left												1																		1														
Ectopterygoid.Right													1																			1												
Frontal.Left											1			1							1	1	1		1																				
Frontal.Right										1					1						1	1		1		1																			
Maxilla.Left								1												1					1		1																		
Maxilla.Right									1												1					1	1																		
Nasal.Left										1					1										1		1								1										
Nasal.Right											1			1												1	1									1									
Neomorph.Left																																												1	
Neomorph.Right																																													1
Otoccipital.Left			1																1									1									1		1	1				
Otoccipital.Right			1									1						1											1									1	1		1			
Palatine.Left																									1					1														
Palatine.Right													1													1					1													
Parabasisphenoid			1							1	1												1					1	1															
Parietal										1	1											1		1	1			1	1												1			
PostfrontalOrJugal.Left										1													1																					
PostfrontalOrJugal.Right											1												1																					
Prefrontal.Left										1		1		1						1																									
Prefrontal.Right											1		1		1						1																								
Premaxilla												1	1	1	1																				1	1								
Prootic.Left			1															1					1	1										1				1		1	1			
Prootic.Right			1																1				1	1									1					1	1		1			
Pterygoid.Left								1												1																								
Pterygoid.Right									1												1																								
Quadrate.Left				1																								1									1		1					
Quadrate.Right					1																								1									1			1			
Septomaxilla.Left														1													1															1		
Septomaxilla.Right															1												1																1	
Splenial.Left	1					1																																						
Splenial.Right		1					1																																					
Stapes.Left																		1											1				1										
Stapes.Right																			1											1				1									
Supraoccipital																		1	1			1							1	1														
Supratemporal.Left																		1											1				1										
Supratemporal.Right																			1											1				1									
Vomer.Left																1																			1								1
Vomer.Right																	1																			1								

APPENDIX 4.1-51. Adjacency matrix for *Atractaspis irregularis* (FMNH 62204)

***Atractaspis irregularis* (FMNH 62204) Deufel and Cundall (2003), Strong et al. (2021)**	Angular.Left	Angular.Right	Basioccipital	CompoundBone.Left	CompoundBone.Right	Dentary.Left	Dentary.Right	Ectopterygoid.Left	Ectopterygoid.Right	Frontal.Left	Frontal.Right	Maxilla.Left	Maxilla.Right	Nasal.Left	Nasal.Right	Otoccipital.Left	Otoccipital.Right	Palatine.Left	Palatine.Right	Parabasisphenoid	Parietal	Prefrontal.Left	Prefrontal.Right	Premaxilla	Prootic.Left	Prootic.Right	Pterygoid.Left	Pterygoid.Right	Quadrate.Left	Quadrate.Right	Septomaxilla.Left	Septomaxilla.Right	Splenial.Left	Splenial.Right	Stapes.Left	Stapes.Right	Supraoccipital	Supratemporal.Left	Supratemporal.Right	Vomer.Left	Vomer.Right
Angular.Left				1																												1								
Angular.Right					1																												1							
Basioccipital																1	1			1				1	1															
CompoundBone.Left	1					1																						1											
CompoundBone.Right		1					1																						1										
Dentary.Left				1																												1							
Dentary.Right					1																												1						
Ectopterygoid.Left												1														1													
Ectopterygoid.Right													1														1												
Frontal.Left											1			1						1	1	1								1									
Frontal.Right										1					1					1	1		1								1								
Maxilla.Left								1														1																	
Maxilla.Right									1														1																
Nasal.Left										1					1									1							1								
Nasal.Right											1			1									1								1								
Otoccipital.Left			1													1								1										1		1			
Otoccipital.Right			1													1									1										1	1			
Palatine.Left																																						1	
Palatine.Right																																							1
Parabasisphenoid			1							1	1										1			1	1														
Parietal										1	1									1				1	1											1			
Prefrontal.Left										1		1																											
Prefrontal.Right											1		1																										
Premaxilla														1	1																								
Prootic.Left			1													1				1	1													1		1	1		
Prootic.Right			1														1			1	1													1	1		1		
Pterygoid.Left								1																															
Pterygoid.Right									1																														
Quadrate.Left				1																														1		1			
Quadrate.Right					1																														1			1		
Septomaxilla.Left										1				1										1														1		
Septomaxilla.Right											1				1									1															1	
Splenial.Left	1					1																																	
Splenial.Right		1					1																																
Stapes.Left																1								1				1											
Stapes.Right																	1								1				1										
Supraoccipital																1	1				1			1	1														
Supratemporal.Left																								1				1											
Supratemporal.Right																									1				1										
Vomer.Left																		1												1									1	
Vomer.Right																			1												1								1	

APPENDIX 4.1-52. Adjacency matrix for *Crotalus adamanteus* (UF 103268)

***Crotalus adamanteus* (UF 103268)**	Angular.Left	Angular.Right	Basioccipital	CompoundBone.Left	CompoundBone.Right	Dentary.Left	Dentary.Right	Ectopterygoid.Left	Ectopterygoid.Right	Frontal.Left	Frontal.Right	Maxilla.Left	Maxilla.Right	Nasal.Left	Nasal.Right	Otoccipital.Left	Otoccipital.Right	Palatine.Left	Palatine.Right	Parabasisphenoid	Parietal	PostfrontalOrJugal.Left	PostfrontalOrJugal.Right	Prefrontal.Left	Prefrontal.Right	Premaxilla	Prootic.Left	Prootic.Right	Pterygoid.Left	Pterygoid.Right	Quadrate.Left	Quadrate.Right	Septomaxilla.Left	Septomaxilla.Right	Splenial.Left	Splenial.Right	Stapes.Left	Stapes.Right	Supraoccipital	Supratemporal.Left	Supratemporal.Right	Vomer.Left	Vomer.Right
Angular.Left				1																														1									
Angular.Right					1																														1								
Basioccipital																1	1			1						1	1																	
CompoundBone.Left	1					1																								1													
CompoundBone.Right		1					1																								1											
Dentary.Left				1																														1								
Dentary.Right					1																														1							
Ectopterygoid.Left											1																	1														
Ectopterygoid.Right												1																	1													
Frontal.Left										1										1	1	1		1																			
Frontal.Right																				1	1		1		1																		
Maxilla.Left								1																1																			
Maxilla.Right									1																1																		
Nasal.Left															1																		1									
Nasal.Right														1																				1								
Otoccipital.Left			1														1									1										1		1	1				
Otoccipital.Right			1													1											1										1	1		1			
Palatine.Left																			1									1														
Palatine.Right																													1													
Parabasisphenoid			1							1	1										1					1	1																
Parietal										1	1									1		1	1			1	1											1					
PostfrontalOrJugal.Left										1											1																						
PostfrontalOrJugal.Right											1										1																						
Prefrontal.Left										1		1																														
Prefrontal.Right											1		1																														
Premaxilla																																		1	1							
Prootic.Left			1													1				1	1															1		1	1				
Prootic.Right			1														1			1	1																1	1		1			
Pterygoid.Left								1										1																									
Pterygoid.Right									1										1																								
Quadrate.Left				1																																	1			1			
Quadrate.Right					1																																	1			1		
Septomaxilla.Left														1												1															1		
Septomaxilla.Right															1											1																1	
Splenial.Left	1					1																																				
Splenial.Right		1					1																																			
Stapes.Left																1										1				1												
Stapes.Right																	1										1				1											
Supraoccipital																1	1				1					1	1																
Supratemporal.Left																1										1				1												
Supratemporal.Right																	1										1				1											
Vomer.Left																																1										
Vomer.Right																																	1									

APPENDIX 4.1-53. Adjacency matrix for *Homalopsis buccata* (FMNH 259340)

***Homalopsis buccata* (FMNH 259340)**	Angular.Left	Angular.Right	Basioccipital	CompoundBone.Left	CompoundBone.Right	Dentary.Left	Dentary.Right	Ectopterygoid.Left	Ectopterygoid.Right	Frontal.Left	Frontal.Right	Jugal.Left	Jugal.Right	Maxilla.Left	Maxilla.Right	Nasal.Left	Nasal.Right	Otoccipital.Left	Otoccipital.Right	Palatine.Left	Palatine.Right	Parabasisphenoid	Parietal	Prefrontal.Left	Prefrontal.Right	Premaxilla	Prootic.Left	Prootic.Right	Pterygoid.Left	Pterygoid.Right	Quadrate.Left	Quadrate.Right	Septomaxilla.Left	Septomaxilla.Right	Splenial.Left	Splenial.Right	Stapes.Left	Stapes.Right	Supraoccipital	Supratemporal.Left	Supratemporal.Right	Vomer.Left	Vomer.Right
Angular.Left				1																														1									
Angular.Right					1																														1								
Basioccipital																		1	1			1				1	1																
CompoundBone.Left	1					1																								1													
CompoundBone.Right		1					1																								1												
Dentary.Left				1																													1									
Dentary.Right					1																													1								
Ectopterygoid.Left											1		1															1														
Ectopterygoid.Right												1		1															1													
Frontal.Left										1	1											1	1	1								1										
Frontal.Right										1			1									1	1		1								1									
Jugal.Left								1		1				1									1																			
Jugal.Right									1		1				1								1																			
Maxilla.Left								1				1								1				1																		
Maxilla.Right									1				1								1				1																	
Nasal.Left																	1									1							1									
Nasal.Right																1										1								1								
Otoccipital.Left			1																1								1									1		1	1			
Otoccipital.Right			1															1										1									1	1		1		
Palatine.Left														1										1					1			1									1	
Palatine.Right															1										1					1			1									1
Parabasisphenoid			1							1	1												1				1	1														
Parietal										1	1	1	1									1					1	1												1	1	1	
Prefrontal.Left										1				1						1																						
Prefrontal.Right											1				1						1																					
Premaxilla																1	1																	1	1							
Prootic.Left			1															1				1	1													1		1	1			
Prootic.Right			1																1			1	1														1	1		1		
Pterygoid.Left								1												1																						
Pterygoid.Right									1												1																					
Quadrate.Left				1																																1			1		
Quadrate.Right					1																																1			1	
Septomaxilla.Left										1						1				1						1									1							1	
Septomaxilla.Right											1						1				1					1							1									1
Splenial.Left	1					1																																				
Splenial.Right		1					1																																			
Stapes.Left																		1									1			1											
Stapes.Right																			1									1			1										
Supraoccipital																		1	1				1				1	1												1	1	
Supratemporal.Left																		1					1				1				1									1		
Supratemporal.Right																			1				1					1			1									1		
Vomer.Left																				1												1									1	
Vomer.Right																					1												1									1	

APPENDIX 4.1-54. Adjacency matrix for *Lampropeltis getula* (FMNH 95184)

***Lampropeltis getula* (FMNH 95184)**	Angular.Left	Angular.Right	Basioccipital	CompoundBone.Left	CompoundBone.Right	Dentary.Left	Dentary.Right	Ectopterygoid.Left	Ectopterygoid.Right	Frontal.Left	Frontal.Right	Jugal.Left	Jugal.Right	Maxilla.Left	Maxilla.Right	Nasal.Left	Nasal.Right	Otoccipital.Left	Otoccipital.Right	Palatine.Left	Palatine.Right	Parabasisphenoid	Parietal	Prefrontal.Left	Prefrontal.Right	Premaxilla	Prootic.Left	Prootic.Right	Pterygoid.Left	Pterygoid.Right	Quadrate.Left	Quadrate.Right	Septomaxilla.Left	Septomaxilla.Right	Splenial.Left	Splenial.Right	Stapes.Left	Stapes.Right	Supraoccipital	Supratemporal.Left	Supratemporal.Right	Vomer.Left	Vomer.Right
Angular.Left				1																														1									
Angular.Right					1																														1								
Basioccipital																		1	1			1				1	1																	
CompoundBone.Left	1					1																								1													
CompoundBone.Right		1					1																								1												
Dentary.Left				1																													1									
Dentary.Right					1																													1								
Ectopterygoid.Left														1														1														
Ectopterygoid.Right															1														1													
Frontal.Left											1	1				1						1	1	1								1											
Frontal.Right										1			1				1					1	1		1								1										
Jugal.Left										1													1																				
Jugal.Right											1												1																				
Maxilla.Left								1												1				1																			
Maxilla.Right									1												1				1																		
Nasal.Left										1							1									1							1										
Nasal.Right											1					1										1								1									
Otoccipital.Left			1															1									1										1		1	1			
Otoccipital.Right			1															1										1										1	1		1		
Palatine.Left														1									1						1														
Palatine.Right															1										1					1													
Parabasisphenoid			1							1	1												1				1	1															
Parietal										1	1	1	1									1					1	1												1	1	1		
Prefrontal.Left										1				1					1																								
Prefrontal.Right											1				1					1																							
Premaxilla																1	1																	1	1								
Prootic.Left			1														1					1	1														1		1	1			
Prootic.Right			1															1					1	1															1	1		1	
Pterygoid.Left								1											1																								
Pterygoid.Right									1											1																								
Quadrate.Left				1																																		1			1		
Quadrate.Right					1																																		1			1	
Septomaxilla.Left										1							1									1																1	
Septomaxilla.Right											1						1									1																	1
Splenial.Left	1					1																																				
Splenial.Right		1					1																																			
Stapes.Left																		1									1			1												
Stapes.Right																			1									1			1											
Supraoccipital																		1	1				1				1	1													1	1	
Supratemporal.Left																		1					1				1				1										1		
Supratemporal.Right																			1				1					1			1										1		
Vomer.Left																																1										1	
Vomer.Right																																	1									1	

APPENDIX 4.1-55. Adjacency matrix for *Naja naja* (FMNH 22468)

***Naja naja* (FMNH 22468)**	Angular.Left	Angular.Right	Basioccipital	CompoundBone.Left	CompoundBone.Right	Dentary.Left	Dentary.Right	Ectopterygoid.Left	Ectopterygoid.Right	Frontal.Left	Frontal.Right	Jugal.Left	Jugal.Right	Maxilla.Left	Maxilla.Right	Nasal.Left	Nasal.Right	Otoccipital.Left	Otoccipital.Right	Palatine.Left	Palatine.Right	Parabasisphenoid	Parietal	Prefrontal.Left	Prefrontal.Right	Premaxilla	Prootic.Left	Prootic.Right	Pterygoid.Left	Pterygoid.Right	Quadrate.Left	Quadrate.Right	Septomaxilla.Left	Septomaxilla.Right	Splenial.Left	Splenial.Right	Stapes.Left	Stapes.Right	Supraoccipital	Supratemporal.Left	Supratemporal.Right	Vomer.Left	Vomer.Right
Angular.Left				1																														1									
Angular.Right					1																														1								
Basioccipital																		1	1			1				1	1																
CompoundBone.Left	1					1																								1													
CompoundBone.Right		1					1																								1												
Dentary.Left				1																												1										
Dentary.Right					1																													1								
Ectopterygoid.Left														1														1														
Ectopterygoid.Right															1														1													
Frontal.Left											1	1				1						1	1	1																			
Frontal.Right										1			1				1					1	1		1																		
Jugal.Left										1													1																			
Jugal.Right											1												1																			
Maxilla.Left								1												1				1																		
Maxilla.Right									1												1				1																	
Nasal.Left										1							1					1				1							1									
Nasal.Right											1					1						1				1								1								
Otoccipital.Left			1															1									1									1			1	1		
Otoccipital.Right			1															1										1									1	1		1		
Palatine.Left														1															1												
Palatine.Right															1															1												
Parabasisphenoid			1							1	1					1	1						1				1	1														
Parietal										1	1	1	1									1					1	1											1	1	1		
Prefrontal.Left										1				1																												
Prefrontal.Right											1				1																											
Premaxilla																1	1																	1	1							
Prootic.Left			1															1					1	1													1		1	1		
Prootic.Right			1																1					1	1													1	1		1	
Pterygoid.Left								1												1																						
Pterygoid.Right									1												1																					
Quadrate.Left				1																																	1			1		
Quadrate.Right					1																																	1			1	
Septomaxilla.Left																	1								1																1	
Septomaxilla.Right																	1								1																1
Splenial.Left	1					1																																			
Splenial.Right		1					1																																		
Stapes.Left																		1									1			1											
Stapes.Right																			1									1			1										
Supraoccipital																		1	1				1				1	1														
Supratemporal.Left																		1					1				1				1										
Supratemporal.Right																			1				1					1				1									
Vomer.Left																																1									1	
Vomer.Right																																	1							1		

APPENDIX 4.1-56. Adjacency matrix for *Pareas hamptoni* (FMNH 128304)

***Pareas hamptoni* (FMNH 128304)**	Angular.Left	Angular.Right	Basioccipital	CompoundBone.Left	CompoundBone.Right	Dentary.Left	Dentary.Right	Ectopterygoid.Left	Ectopterygoid.Right	Frontal.Left	Frontal.Right	Jugal.Left	Jugal.Right	Maxilla.Left	Maxilla.Right	Nasal.Left	Nasal.Right	Otoccipital.Left	Otoccipital.Right	Palatine.Left	Palatine.Right	Parabasisphenoid	Parietal	Prefrontal.Left	Prefrontal.Right	Premaxilla	Prootic.Left	Prootic.Right	Pterygoid.Left	Pterygoid.Right	Quadrate.Left	Quadrate.Right	Septomaxilla.Left	Septomaxilla.Right	Splenial.Left	Splenial.Right	Stapes.Left	Stapes.Right	Supraoccipital	Supratemporal.Left	Supratemporal.Right	Vomer.Left	Vomer.Right
Angular.Left				1																														1									
Angular.Right					1																														1								
Basioccipital																		1	1			1				1	1																
CompoundBone.Left	1					1																								1													
CompoundBone.Right		1					1																								1												
Dentary.Left				1																													1									
Dentary.Right					1																													1								
Ectopterygoid.Left														1														1														
Ectopterygoid.Right															1														1													
Frontal.Left											1					1						1	1	1								1											
Frontal.Right										1							1					1	1		1								1										
Jugal.Left																							1																				
Jugal.Right																							1																				
Maxilla.Left								1												1				1																			
Maxilla.Right									1												1				1																		
Nasal.Left										1							1															1										
Nasal.Right											1					1																	1									
Otoccipital.Left			1															1								1				1						1	1					
Otoccipital.Right			1															1									1				1						1	1		1		
Palatine.Left														1									1					1														
Palatine.Right															1									1					1													
Parabasisphenoid			1							1	1												1			1	1															
Parietal										1	1	1	1									1				1	1													1			
Prefrontal.Left										1				1					1																							
Prefrontal.Right											1				1						1																					
Premaxilla																																	1	1							1	1
Prootic.Left			1															1				1	1							1					1			1	1			
Prootic.Right			1																1			1	1								1						1	1		1		
Pterygoid.Left								1												1																						
Pterygoid.Right									1												1																					
Quadrate.Left				1														1								1									1				1			
Quadrate.Right					1														1								1									1			1			
Septomaxilla.Left										1						1									1															1		
Septomaxilla.Right											1						1								1																1	
Splenial.Left	1					1																																			
Splenial.Right		1					1																																		
Stapes.Left																		1									1			1											
Stapes.Right																			1									1			1										
Supraoccipital																		1	1				1				1	1														
Supratemporal.Left																		1									1				1											
Supratemporal.Right																			1									1				1										
Vomer.Left																									1								1								1	1
Vomer.Right																									1								1								1	

APPENDIX 4.1-57. Adjacency matrix for *Thamnophis radix* (UAMZ R636)

Thamnophis radix **(UAMZ R636)** **Strong et al. (2019)**	Angular.Left	Angular.Right	Basioccipital	CompoundBone.Left	CompoundBone.Right	Dentary.Left	Dentary.Right	Ectopterygoid.Left	Ectopterygoid.Right	Frontal.Left	Frontal.Right	Jugal.Left	Jugal.Right	Maxilla.Left	Maxilla.Right	Nasal.Left	Nasal.Right	Otoccipital.Left	Otoccipital.Right	Palatine.Left	Palatine.Right	Parabasisphenoid	Parietal	Prefrontal.Left	Prefrontal.Right	Premaxilla	Prootic.Left	Prootic.Right	Pterygoid.Left	Pterygoid.Right	Quadrate.Left	Quadrate.Right	Septomaxilla.Left	Septomaxilla.Right	Splenial.Left	Splenial.Right	Stapes.Left	Stapes.Right	Supraoccipital	Supratemporal.Left	Supratemporal.Right	Vomer.Left	Vomer.Right
Angular.Left				1																														1									
Angular.Right					1																														1								
Basioccipital																		1	1			1				1	1																
CompoundBone.Left	1					1																								1													
CompoundBone.Right		1					1																								1												
Dentary.Left				1																													1									
Dentary.Right					1																													1								
Ectopterygoid.Left														1														1														
Ectopterygoid.Right															1														1													
Frontal.Left											1											1	1	1								1										
Frontal.Right										1												1	1		1								1									
Jugal.Left																							1																			
Jugal.Right																							1																			
Maxilla.Left								1												1				1																		
Maxilla.Right									1												1				1																	
Nasal.Left																1																	1									
Nasal.Right																	1																	1								
Otoccipital.Left			1															1	1								1										1		1	1			
Otoccipital.Right			1															1										1									1	1		1		
Palatine.Left														1										1					1													
Palatine.Right															1										1					1												
Parabasisphenoid			1							1	1												1			1	1															
Parietal										1	1	1	1									1				1	1												1	1	1		
Prefrontal.Left										1				1					1																							
Prefrontal.Right											1				1					1																						
Premaxilla																																	1	1						1	1
Prootic.Left			1															1				1	1														1		1	1			
Prootic.Right			1																1			1	1															1	1		1		
Pterygoid.Left								1												1																							
Pterygoid.Right									1												1																						
Quadrate.Left				1																																	1			1		
Quadrate.Right					1																																	1			1	
Septomaxilla.Left										1							1								1																	1	
Septomaxilla.Right											1					1									1																		1
Splenial.Left	1					1																																				
Splenial.Right		1					1																																			
Stapes.Left																		1									1				1											
Stapes.Right																			1									1				1										
Supraoccipital																		1	1				1				1	1														
Supratemporal.Left																		1					1				1				1											
Supratemporal.Right																			1				1					1				1										
Vomer.Left																									1								1									1
Vomer.Right																									1									1								1	

APPENDIX 4.2. R script used for anatomical network analysis

```
################################################################################
#
# APPENDIX 4.2. R script used for anatomical network analysis
#
# Title: Convergence, divergence, and macroevolutionary constraint as revealed by anatomical network analysis of the squamate skull
# Created by: Catherine R. C. Strong
# Date: 2021
#
# R script adapted from Werneburg et al. (2019), Plateau and Foth (2020), and Esteve-Altava et al. (2018)
#
################################################################################

options(java.parameters = "-Xmx1024m") # increases Java memory usage; may be required to load adjacency spreadsheet

################################
######### LIBRARIES ##########
################################
library(XLConnect) # Excel Connector for R
library(igraph) # network analysis
library(ape) # phylogenetic analysis and hierarchical cluster manipulation
library(phytools) # phylogenetic analysis and hierarchical cluster manipulation
library(geiger) # phylogenetic analysis and hierarchical cluster manipulation
library(adephylo) # phylogenetic analysis and hierarchical cluster manipulation
library(phylobase) # phylogenetic analysis and hierarchical cluster manipulation
library(picante) # phylogenetic analysis and hierarchical cluster manipulation


#############################################################
######### ADJACENCY MATRICES AND NETWORKS ########
#############################################################


### PREPARE ADJACENCY MATRIX
```

```
species <- c("AcutoSol", "AcutoSub", "Afrotyphlops", "Amerotyphlops", "Anilios",
"Antillotyphlops", "GerrhAter", "GerrhBedd", "Indotyphlops", "Ramphotyphlops", "Typhlops",
"Xenotyphlops", "Xerotyphlops", "Anomalepis", "Helminthophis", "LioAlbi", "LioArgaleus",
"LioBeui", "Typhlophis", "Epictia", "MyrioMacro", "MyrioTanae", "Rena", "Tricheilostoma",
"Trilepida", "Acrochordus", "Aparallactus", "Atractaspis", "Crotalus", "Homalopsis",
"Lampropeltis", "Naja", "Pareas", "Thamnophis", "Boa", "Casarea", "Calabaria", "Eryx",
"Loxocemus", "Python", "Xenopeltis", "Anilius", "Anomochilus", "Cylindrophis", "Rhinophis",
"Uropeltis", "Amphisbaena", "Anelytropsis", "Bipes", "Dibamus", "Dipsosaurus",
"Lanthanotus", "Physignathus", "Rhineura", "Sauromalus", "Uranoscodon", "Varanus")
mat.list <- mapply(readWorksheetFromFile, "AdjacencyMatrices_SquamateSkulls.xlsx",
sheet=1:length(species), rownames=1, check.names=FALSE)
adj.list <- lapply(mat.list, data.matrix, rownames.force=TRUE)
pre.graph.list <- lapply(adj.list, graph_from_adjacency_matrix, mode="undirected")
graph.list <- pre.graph.list
names(graph.list) <- species


### GENERATE A FILE WITH BONE LABELS
labels2save <- list()
for (i in 1:length(species)){
  num_label <- 1:vcount(graph.list[[i]])
  names(num_label) <- V(graph.list[[i]])$name
  labels2save[[i]] <- paste(num_label, names(num_label), sep=" ")
}
text.out <- c(species[1], labels2save[[1]], species[2], labels2save[[2]], species[3],
labels2save[[3]], species[4], labels2save[[4]], species[5], labels2save[[5]], species[6],
labels2save[[6]], species[7], labels2save[[7]], species[8], labels2save[[8]], species[9],
labels2save[[9]], species[10], labels2save[[10]], species[11], labels2save[[11]], species[12],
labels2save[[12]], species[13], labels2save[[13]], species[14], labels2save[[14]], species[15],
labels2save[[15]], species[16], labels2save[[16]], species[17], labels2save[[17]], species[18],
labels2save[[18]], species[19], labels2save[[19]], species[20], labels2save[[20]], species[21],
labels2save[[21]], species[22], labels2save[[22]], species[23], labels2save[[23]], species[24],
labels2save[[24]], species[25], labels2save[[25]], species[26], labels2save[[26]], species[27],
labels2save[[27]], species[28], labels2save[[28]], species[29], labels2save[[29]], species[30],
labels2save[[30]], species[31], labels2save[[31]], species[32], labels2save[[32]], species[33],
labels2save[[33]], species[34], labels2save[[34]], species[35], labels2save[[35]], species[36],
labels2save[[36]], species[37], labels2save[[37]], species[38], labels2save[[38]], species[39],
labels2save[[39]], species[40], labels2save[[40]], species[41], labels2save[[41]], species[42],
labels2save[[42]], species[43], labels2save[[43]], species[44], labels2save[[44]], species[45],
labels2save[[45]], species[46], labels2save[[46]], species[47], labels2save[[47]], species[48],
```

```
labels2save[[48]], species[49], labels2save[[49]], species[50], labels2save[[50]], species[51],
labels2save[[51]], species[52], labels2save[[52]], species[53], labels2save[[53]], species[54],
labels2save[[54]], species[55], labels2save[[55]], species[56], labels2save[[56]], species[57],
labels2save[[57]])
fileConn<-file("BoneLabels.txt")
write(text.out, file=fileConn, ncolumns=1)
close(fileConn)


##################################
######### NETWORKING ########
##################################


######### COMMUNITY STRUCTURE (MODULARITY)
#########################################################


### FUNCTION 'GTOMmdist1': USES DISSIMILARITY MATRIX TO GENERATE
NETWORK
  # background info from https://horvath.genetics.ucla.edu/html/GTOM/ and
https://horvath.genetics.ucla.edu/html/GTOM/old/
  # GTOM script from https://horvath.genetics.ucla.edu/html/GTOM/old/gtom.R
GTOMmdist1 = function(adjmat1,m=1){
  if (m!=round(abs(m))){
    stop("m must be a positive integer", call.=TRUE);}
  if (any(adjmat1!=0 & adjmat1!=1)){
    stop("The adjacency matrix must be binary", call.=TRUE);}
  B <- adjmat1;
  if (m>=2) {
    for (i in 2:m) {
      diag(B) <- diag(B) + 1;
      B = B %*% adjmat1;}}
  B <- (B>0);
  diag(B) <- 0;
  B <- B %*% B;
  Nk <- diag(B);
  B <- B +adjmat1;
  diag(B) <- 1;
  denomTOM=outer(Nk,Nk,FUN="pmin")+1-adjmat1;
```

```
  diag(denomTOM) <- 1;
  1 - B/denomTOM
}


### FUNCTION 'na.zero': FORMATS ADJACENCY MATRICES
na.zero <- function (x) {
  x[is.na(x)] <- 0
  return(x)
}


### CALCULATE GTOM AND HIERARCHICAL CLUSTERING, USING FUNCTIONS
'GTOMmdist1' AND 'na.zero'
adj.list <- lapply(adj.list, na.zero)
tom.list <- lapply(adj.list, GTOMmdist1, m=1)
dist.tom.list <- lapply(tom.list, as.dist)
hclust.list <- lapply(dist.tom.list, hclust, method="average")
for (i in 1:length(species)){hclust.list[[i]]$labels <- V(graph.list[[i]])$name}
phylo.list <- lapply(hclust.list, as.phylo)


### FUNCTION 'JACKKNIFE_Q': CALCULATES JACKKNIFE OF MODULARITY Q
VALUE, = EXPECTED ERROR OF Q-VALUE
jackknife_Q = function(graph, membership){
  Qi <- vector()
  for (j in 1:ecount(graph)){
    g <- delete_edges(graph, j)
    Qi[j] <- modularity(g, membership)
  }
  ss <- sum((Qi-mean(Qi))^2)
  n <- (ecount(graph)-1)/ecount(graph)
  Q.error <- sqrt(n*ss)
  return(Q.error)
}


### DETERMINE BEST PARTITION BASED ON QMAX
best.partition <- vector()
for (i in 1:length(species)){
```

```
  Qvalue <- vector()
  for (j in 1:vcount(graph.list[[i]])){
    Qvalue[j] <- modularity(graph.list[[i]], cutree(hclust.list[[i]], k=j))
  }
  best.partition[i] <- which(Qvalue==max(Qvalue))
}


### FUNCTION 'community.significance.test': EVALUATES STATISTICAL SIGNIFICANCE OF MODULES, VIA TWO-SAMPLE WILCOXON RANK-SUM TEST (MANN-WHITNEY U TEST)
  # Wilcoxon/Mann-Whitney test assesses internal vs external connections of each module
  # H0: number of internal connections = number of external connections
  # HA: number of internal connections > number of external connections
community.significance.test <- function(graph, vids, ...) {
  subgraph <- induced_subgraph(graph, vids)
  indegrees <- degree(subgraph)
  outdegrees <- degree(graph, vids) - indegrees
  wilcox.test(indegrees, outdegrees, alternative="greater")
}


### ASSESS STATISTICAL SIGNIFICANCE OF EACH BIFURCATION/PARTITION IN THE CLUSTER TREE
Ho_modules_pvalue <- list()
for (i in 1:length(species)){
  graph <- graph.list[[i]]
  tree <- phylo.list[[i]]
  tipN <- vcount(graph)
  intN <- tipN-1
  Ho_modules_pvalue_v <- vector()
  for (j in 1:intN){
    Ho_m <- extract.clade(tree, node=(tipN+j))
    is_tip <- Ho_m$edge[,2] <= length(Ho_m$tip.label)
    ordered_tips <- Ho_m$edge[is_tip, 2]
    who <- Ho_m$tip.label[ordered_tips]
    index <- which((V(graph)$name %in% who)==TRUE)
    Ho_mp <- community.significance.test(graph, vids=index)
    Ho_modules_pvalue_v[j] <- Ho_mp$p.value
  }
```

```
  Ho_modules_pvalue[[i]] <- Ho_modules_pvalue_v
}


### CREATE DENDROGRAM PLOTS
for (i in 1:length(species)){
  plotTree(phylo.list[[i]], lwd=1, mar=c(4.1,1.1,1.1,1.1))
  sign <- which(Ho_modules_pvalue[[i]]<0.05)
  bs <- Ho_modules_pvalue[[i]][sign]
  co <- c("black", "grey", "white")
  p <- character(length(sign))
  p[bs < 0.001] <- co[1]
  p[bs >= 0.001 & bs < 0.01] <- co[2]
  p[bs >= 0.01 & bs < 0.05] <- co[3]
  nodelabels(node=(sign+vcount(graph.list[[i]])), pch=21, bg=p, cex=2)
  nodelabels(phylo.list[[i]]$node.label, node=(sign+vcount(graph.list[[i]])), adj=c(1.1,-
0.7),frame="none")
  obj <- ltt(phylo.list[[i]], plot=FALSE)
  k <- best.partition[i]
  h <- mean(obj$times[c(which(obj$ltt==k), which(obj$ltt==(k+1)))])
  lines(rep(h,2), par()$usr[3:4], col="red", lty="dashed")
  title(main=paste("Modularity of the skull network of", species[i]))
}


### GROUP BONES INTO MODULES BASED ON STATISTICAL SIGNIFICANCE
members.list <- list()
for (i in 1:length(species)){
  n <- 2
  p <- 0
  end <- FALSE
  while (end==FALSE){
    members <- cutree(hclust.list[[i]], n)
    for (j in 1:n){p[j] <- community.significance.test(graph.list[[i]], vids=(members==j))$p.value}
    if (all(p<0.05)==TRUE){
      n <- n+1
    } else {
      n <- n-1
      p <- 0
      members <- cutree(hclust.list[[i]], n)
```

```
    for (j in 1:n){p[j] <- community.significance.test(graph.list[[i]],
vids=(members==j))$p.value}
    end <- TRUE
   }
  }
  members.list[[i]] <- members
}


### CALCULATE MODULARITY INFO
modules <- matrix(NA, nrow=length(species), ncol=4)
rownames(modules) <- species
colnames(modules) <- c("S Modules", "Q Modules", "Qmax", "Qmax error")
for (i in 1:length(species)){
  modules[i,1] <- max(members.list[[i]])
  membership <- cutree(hclust.list[[i]], k=best.partition[i])
  modules[i,2] <- best.partition[i]
  modules[i,3] <- modularity(graph.list[[i]], membership)
  modules[i,4] <- jackknife_Q(graph.list[[i]], membership)
}
modularity_values <- modules

write.csv(modularity_values, file = "ModularityValues.csv")


######### ANATOMICAL NETWORK ANALYSIS
################################################


### SET UP / CALCULATE NETWORK PARAMETERS
parameters <- matrix(NA, nrow=length(species), ncol=7)
rownames(parameters) <- species
colnames(parameters) <- c("N", "K", "D", "C", "L", "H","P")
parameters[,1] <- mapply(vcount, graph.list)
parameters[,2] <- mapply(ecount, graph.list)
parameters[,3] <- mapply(edge_density, graph.list)
parameters[,4] <- mapply(transitivity, graph.list, type="average", isolates="NaN")
parameters[,5] <- mapply(mean_distance, graph.list, directed=FALSE)

   ### FUNCTION 'heterogeneity': CALCULATES H
```

```
heterogeneity = function(graph){
  deg = degree(graph)
  res = sd(deg, na.rm=TRUE)/mean(deg, na.rm=FALSE)
}
parameters[,6] <- mapply(heterogeneity, graph.list)

    # FUNCTION 'parcellation_index': CALCULATES P
parcellation_index <- function(membership){
  Nm <- vector()
  for (i in 1:max(membership)){
    Nm[i] <- length(which(membership==i))
  }
  res <- 1-sum((Nm/length(membership))^2)
  return(res)
}

ite <- 1
communities <- list()
for (i in 1:length(species)){
  saveSpin <- list()
  saveQ <- vector()
  set.seed(73)
  for (n in 1:ite){
    saveSpin[[n]] <- leading.eigenvector.community(graph.list[[i]])
    saveQ[n] <- modularity(saveSpin[[n]])
  }
  index <- which.max(saveQ)
  communities[[i]] <- saveSpin[[index]]
}
communities_skeletal <- communities

for (i in 1:length(species)){
  parameters[i,7] <- parcellation_index(membership(communities[[i]]))
}
parameters_skeletal <- parameters

write.csv(parameters_skeletal, file = "Table1_NetworkParameters.csv")
```

APPENDIX 4.3. R script used for principal component analysis

```
################################################################################
#
# APPENDIX 4.3. R script used for principal component analysis
#
# Title: Convergence, divergence, and macroevolutionary constraint as revealed by anatomical network analysis of the squamate skull
# Created by: Catherine R. C. Strong
# Date: 2021
#
# R script adapted from tutorials by user Hefin Rhys at https://www.youtube.com/watch?v=xKl4LJAXnEA&ab_channel=HefinRhys and by user J. Oliver at https://jcoliver.github.io/learn-r/003-intro-multivariate.html
#
################################################################################

###################### LIBRARIES
################################
library(readxl)
library(ggplot2)
library(ggforce)
library(ggConvexHull)
library(vegan)
library(pairwiseAdonis)

############## DATA PREPARATION
###################################
squamates <- read_excel("Table1_NetworkParameters_Modified.xlsx")
taxon.names <- unique(squamates$Taxa)
write.csv(taxon.names, file = "TaxonNamesNumbers.csv")


############################ PCA
################################

### RUN PCA
squamatesPCA <-prcomp(squamates[,2:8], scale = TRUE)
squamatesPCA
```

```
### CREATE SUMMARY OF PCA RESULTS
pca.summary <- summary(squamatesPCA)
ls(pca.summary)
pca.summary$importance
write.csv(pca.summary$importance, file = "PCA_Importance.csv")
pca.summary$rotation
write.csv(pca.summary$rotation, file = "PCA_Rotation.csv")

### CREATE BIPLOTS
biplot(squamatesPCA, scale = 0)
biplot(squamatesPCA, choices = c(1,3), scale = 0)
biplot(squamatesPCA, choices = c(2,3), scale = 0)

### EXTRACT PC SCORES
squamatesPCA$x
squamates_PC123 <- cbind(squamates, squamatesPCA$x[,1:3])

### PLOT PCA
# PC1vsPC2
  # grouping by higher taxon
ggplot(squamates_PC123, aes(PC1, PC2, col = HigherTaxon, fill = HigherTaxon)) +
stat_ellipse(geom = "polygon", alpha = 0.25) + geom_point(aes(shape = HigherTaxon, bg =
HigherTaxon), col = "black") + scale_shape_manual(values=c(0, 15, 1, 2, 16, 8, 17))
ggplot(squamates_PC123, aes(PC1, PC2, col = HigherTaxon, fill = HigherTaxon)) +
geom_convexhull(alpha = 0.25) + geom_point(aes(shape = HigherTaxon, bg = HigherTaxon),
col = "black") + scale_shape_manual(values=c(0, 15, 1, 2, 16, 8, 17))
  # grouping by jaw morphotype
ggplot(squamates_PC123, aes(PC1, PC2, col = JawMech, fill = JawMech)) + stat_ellipse(geom
= "polygon", col = "black", alpha = 0.25) + geom_point(aes(shape = HigherTaxon, bg =
HigherTaxon), col = "black") + scale_shape_manual(values=c(0, 15, 1, 2, 16, 8, 17))
ggplot(squamates_PC123, aes(PC1, PC2, col = JawMech, fill = JawMech)) +
geom_convexhull(alpha = 0.25) + geom_point(aes(shape = HigherTaxon, bg = HigherTaxon),
col = "black") + scale_shape_manual(values=c(0, 15, 1, 2, 16, 8, 17))
  # grouping by habitat
ggplot(squamates_PC123, aes(PC1, PC2, col = Habitat, fill = Habitat)) + stat_ellipse(geom =
"polygon", col = "black", alpha = 0.25) + geom_point(aes(shape = HigherTaxon, bg =
HigherTaxon), col = "black") + scale_shape_manual(values=c(0, 15, 1, 2, 16, 8, 17))
```

```
ggplot(squamates_PC123, aes(PC1, PC2, col = Habitat, fill = Habitat)) +
geom_convexhull(alpha = 0.25) + geom_point(aes(shape = HigherTaxon, bg = HigherTaxon),
col = "black") + scale_shape_manual(values=c(0, 15, 1, 2, 16, 8, 17))
  # grouping by size
ggplot(squamates_PC123, aes(PC1, PC2, col = Size, fill = Size)) + stat_ellipse(geom =
"polygon", col = "black", alpha = 0.25) + geom_point(aes(shape = HigherTaxon, bg =
HigherTaxon), col = "black") + scale_shape_manual(values=c(0, 15, 1, 2, 16, 8, 17))
ggplot(squamates_PC123, aes(PC1, PC2, col = Size, fill = Size)) + geom_convexhull(alpha =
0.25) + geom_point(aes(shape = HigherTaxon, bg = HigherTaxon), col = "black") +
scale_shape_manual(values=c(0, 15, 1, 2, 16, 8, 17))
  # grouping by habitat AND size
ggplot(squamates_PC123, aes(PC1, PC2, col = HabitatSize, fill = HabitatSize)) +
stat_ellipse(geom = "polygon", col = "black", alpha = 0.25) + geom_point(aes(shape =
HigherTaxon, bg = HigherTaxon), col = "black") + scale_shape_manual(values=c(0, 15, 1, 2, 16,
8, 17))
ggplot(squamates_PC123, aes(PC1, PC2, col = HabitatSize, fill = HabitatSize)) +
geom_convexhull(alpha = 0.25) + geom_point(aes(shape = HigherTaxon, bg = HigherTaxon),
col = "black") + scale_shape_manual(values=c(0, 15, 1, 2, 16, 8, 17))
# PC1vsPC3
  # grouping by higher taxon
ggplot(squamates_PC123, aes(PC1, PC3, col = HigherTaxon, fill = HigherTaxon)) +
stat_ellipse(geom = "polygon", col = "black", alpha = 0.25) + geom_point(aes(shape =
HigherTaxon, bg = HigherTaxon), col = "black") + scale_shape_manual(values=c(0, 15, 1, 2, 16,
8, 17))
ggplot(squamates_PC123, aes(PC1, PC3, col = HigherTaxon, fill = HigherTaxon)) +
geom_convexhull(alpha = 0.25) + geom_point(aes(shape = HigherTaxon, bg = HigherTaxon),
col = "black") + scale_shape_manual(values=c(0, 15, 1, 2, 16, 8, 17))
  # grouping by jaw morphotype
ggplot(squamates_PC123, aes(PC1, PC3, col = JawMech, fill = JawMech)) + stat_ellipse(geom
= "polygon", col = "black", alpha = 0.25) + geom_point(aes(shape = HigherTaxon, bg =
HigherTaxon), col = "black") + scale_shape_manual(values=c(0, 15, 1, 2, 16, 8, 17))
ggplot(squamates_PC123, aes(PC1, PC3, col = JawMech, fill = JawMech)) +
geom_convexhull(alpha = 0.25) + geom_point(aes(shape = HigherTaxon, bg = HigherTaxon),
col = "black") + scale_shape_manual(values=c(0, 15, 1, 2, 16, 8, 17))
  # grouping by habitat
ggplot(squamates_PC123, aes(PC1, PC3, col = Habitat, fill = Habitat)) + stat_ellipse(geom =
"polygon", col = "black", alpha = 0.25) + geom_point(aes(shape = HigherTaxon, bg =
HigherTaxon), col = "black") + scale_shape_manual(values=c(0, 15, 1, 2, 16, 8, 17))
```

```
ggplot(squamates_PC123, aes(PC1, PC3, col = Habitat, fill = Habitat)) +
geom_convexhull(alpha = 0.25) + geom_point(aes(shape = HigherTaxon, bg = HigherTaxon),
col = "black") + scale_shape_manual(values=c(0, 15, 1, 2, 16, 8, 17))
  # grouping by size
ggplot(squamates_PC123, aes(PC1, PC3, col = Size, fill = Size)) + stat_ellipse(geom =
"polygon", col = "black", alpha = 0.25) + geom_point(aes(shape = HigherTaxon, bg =
HigherTaxon), col = "black") + scale_shape_manual(values=c(0, 15, 1, 2, 16, 8, 17))
ggplot(squamates_PC123, aes(PC1, PC3, col = Size, fill = Size)) + geom_convexhull(alpha =
0.25) + geom_point(aes(shape = HigherTaxon, bg = HigherTaxon), col = "black") +
scale_shape_manual(values=c(0, 15, 1, 2, 16, 8, 17))
 # grouping by habitat AND size
ggplot(squamates_PC123, aes(PC1, PC3, col = HabitatSize, fill = HabitatSize)) +
stat_ellipse(geom = "polygon", col = "black", alpha = 0.25) + geom_point(aes(shape =
HigherTaxon, bg = HigherTaxon), col = "black") + scale_shape_manual(values=c(0, 15, 1, 2, 16,
8, 17))
ggplot(squamates_PC123, aes(PC1, PC3, col = HabitatSize, fill = HabitatSize)) +
geom_convexhull(alpha = 0.25) + geom_point(aes(shape = HigherTaxon, bg = HigherTaxon),
col = "black") + scale_shape_manual(values=c(0, 15, 1, 2, 16, 8, 17))
# PC2vsPC3
 # grouping by higher taxon
ggplot(squamates_PC123, aes(PC2, PC3, col = HigherTaxon, fill = HigherTaxon)) +
stat_ellipse(geom = "polygon", col = "black", alpha = 0.25) + geom_point(aes(shape =
HigherTaxon, bg = HigherTaxon), col = "black") + scale_shape_manual(values=c(0, 15, 1, 2, 16,
8, 17))
ggplot(squamates_PC123, aes(PC2, PC3, col = HigherTaxon, fill = HigherTaxon)) +
geom_convexhull(alpha = 0.25) + geom_point(aes(shape = HigherTaxon, bg = HigherTaxon),
col = "black") + scale_shape_manual(values=c(0, 15, 1, 2, 16, 8, 17))
 # grouping by jaw morphotype
ggplot(squamates_PC123, aes(PC2, PC3, col = JawMech, fill = JawMech)) + stat_ellipse(geom
= "polygon", col = "black", alpha = 0.25) + geom_point(aes(shape = HigherTaxon, bg =
HigherTaxon), col = "black") + scale_shape_manual(values=c(0, 15, 1, 2, 16, 8, 17))
ggplot(squamates_PC123, aes(PC2, PC3, col = JawMech, fill = JawMech)) +
geom_convexhull(alpha = 0.25) + geom_point(aes(shape = HigherTaxon, bg = HigherTaxon),
col = "black") + scale_shape_manual(values=c(0, 15, 1, 2, 16, 8, 17))
 # grouping by habitat
ggplot(squamates_PC123, aes(PC2, PC3, col = Habitat, fill = Habitat)) + stat_ellipse(geom =
"polygon", col = "black", alpha = 0.25) + geom_point(aes(shape = HigherTaxon, bg =
HigherTaxon), col = "black") + scale_shape_manual(values=c(0, 15, 1, 2, 16, 8, 17))
```

```
ggplot(squamates_PC123, aes(PC2, PC3, col = Habitat, fill = Habitat)) +
geom_convexhull(alpha = 0.25) + geom_point(aes(shape = HigherTaxon, bg = HigherTaxon),
col = "black") + scale_shape_manual(values=c(0, 15, 1, 2, 16, 8, 17))
  # grouping by size
ggplot(squamates_PC123, aes(PC2, PC3, col = Size, fill = Size)) + stat_ellipse(geom =
"polygon", col = "black", alpha = 0.25) + geom_point(aes(shape = HigherTaxon, bg =
HigherTaxon), col = "black") + scale_shape_manual(values=c(0, 15, 1, 2, 16, 8, 17))
ggplot(squamates_PC123, aes(PC2, PC3, col = Size, fill = Size)) + geom_convexhull(alpha =
0.25) + geom_point(aes(shape = HigherTaxon, bg = HigherTaxon), col = "black") +
scale_shape_manual(values=c(0, 15, 1, 2, 16, 8, 17))
  # grouping by habitat AND size
ggplot(squamates_PC123, aes(PC2, PC3, col = HabitatSize, fill = HabitatSize)) +
stat_ellipse(geom = "polygon", col = "black", alpha = 0.25) + geom_point(aes(shape =
HigherTaxon, bg = HigherTaxon), col = "black") + scale_shape_manual(values=c(0, 15, 1, 2, 16,
8, 17))
ggplot(squamates_PC123, aes(PC2, PC3, col = HabitatSize, fill = HabitatSize)) +
geom_convexhull(alpha = 0.25) + geom_point(aes(shape = HigherTaxon, bg = HigherTaxon),
col = "black") + scale_shape_manual(values=c(0, 15, 1, 2, 16, 8, 17))


############################ PERMANOVA
########################################

squamatesPermanova <- squamates[,2:8]

### BASIC PERMANOVA
  # "Higher Taxon" groupings/centroids
permaHigherTaxon <- adonis(squamatesPermanova ~ HigherTaxon, data = squamates, method =
'eu', permutations = 10000)
permaHigherTaxon
  # "Jaw Mechanism" groupings/centroids
permaJawMech <- adonis(squamatesPermanova ~ JawMech, data = squamates, method = 'eu',
permutations = 10000)
permaJawMech
  # "Habitat" groupings/centroids
permaHabitat <- adonis(squamatesPermanova ~ Habitat, data = squamates, method = 'eu',
permutations = 10000)
permaHabitat
  # "Size" groupings/centroids
```

```
permaSize <- adonis(squamatesPermanova ~ Size, data = squamates, method = 'eu', permutations = 10000)
permaSize
  # "Habitat and Size" groupings/centroids
permaHabitatSize <- adonis(squamatesPermanova ~ HabitatSize, data = squamates, method = 'eu', permutations = 10000)
permaHabitatSize

### PAIRWISE PERMANOVA
  # "Higher Taxon" groupings/centroids
pairwiseHigherTaxon <- pairwise.adonis2(squamatesPermanova ~ HigherTaxon, data = squamates, method = 'eu', permutations = 10000)
pairwiseHigherTaxon
  # "Jaw Mechanism" groupings/centroids
pairwiseJawMech <- pairwise.adonis2(squamatesPermanova ~ JawMech, data = squamates, method = 'eu', permutations = 10000)
pairwiseJawMech
  # "Habitat" groupings/centroids
pairwiseHabitat <- pairwise.adonis2(squamatesPermanova ~ Habitat, data = squamates, method = 'eu', permutations = 10000)
pairwiseHabitat
  # "Size" groupings/centroids
pairwiseSize <- pairwise.adonis2(squamatesPermanova ~ Size, data = squamates, method = 'eu', permutations = 10000)
pairwiseSize
  # "Habitat and Size" groupings/centroids
pairwiseHabitatSize <- pairwise.adonis2(squamatesPermanova ~ HabitatSize, data = squamates, method = 'eu', permutations = 10000)
pairwiseHabitatSize
```

SUPPLEMENTARY INFORMATION: CHAPTER FIVE

FIGURES S5.1–S5.4. Complete versions of the phylogenies in Figures 5.3 and 5.4

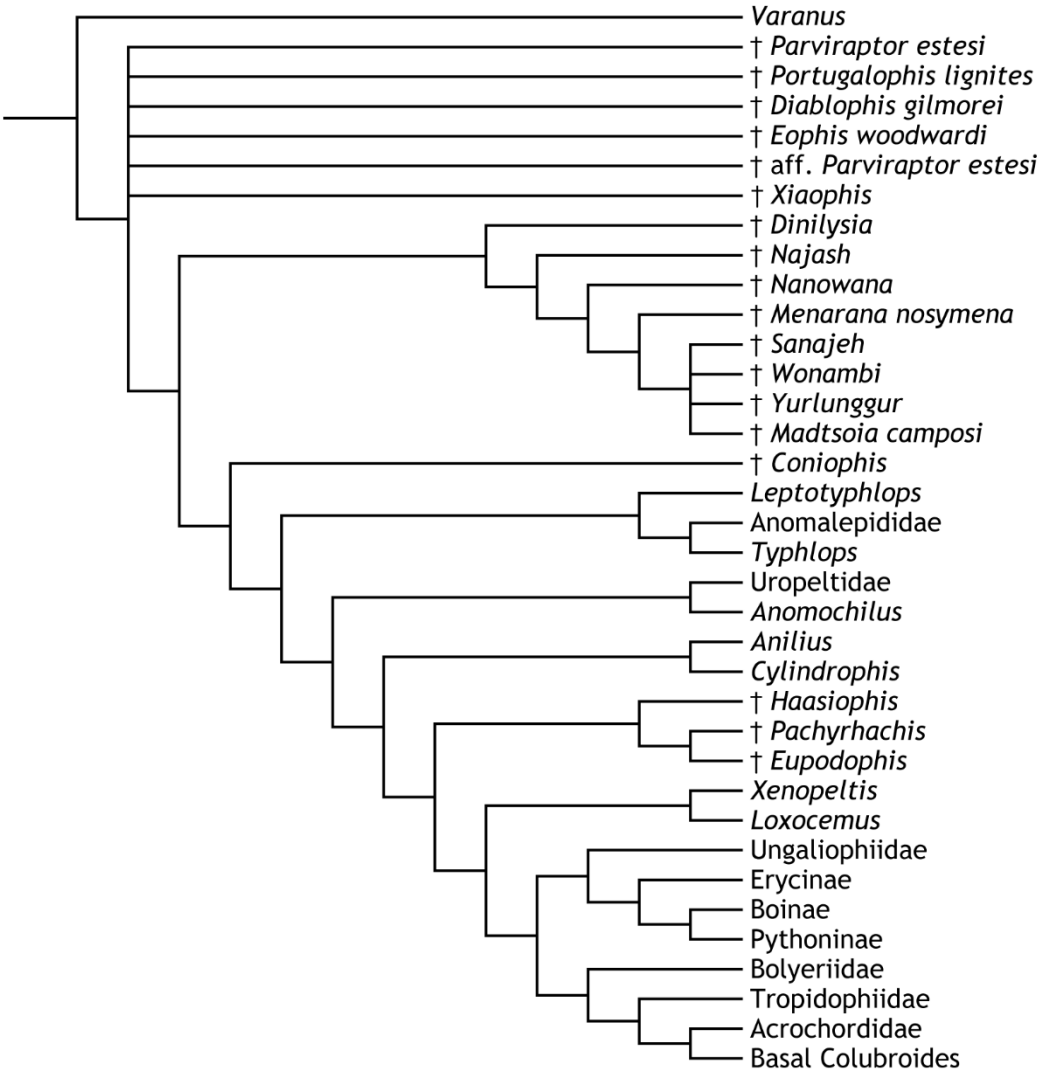

FIGURE S5.1. Complete version of the phylogeny in Figure 5.3a (Original Dataset, maximum parsimony). 50% majority-rule consensus tree of 272 MPTs (624 steps) generated via maximum parsimony analysis of Garberoglio *et al.* (2019a:data file S1). † indicates extinct taxa.

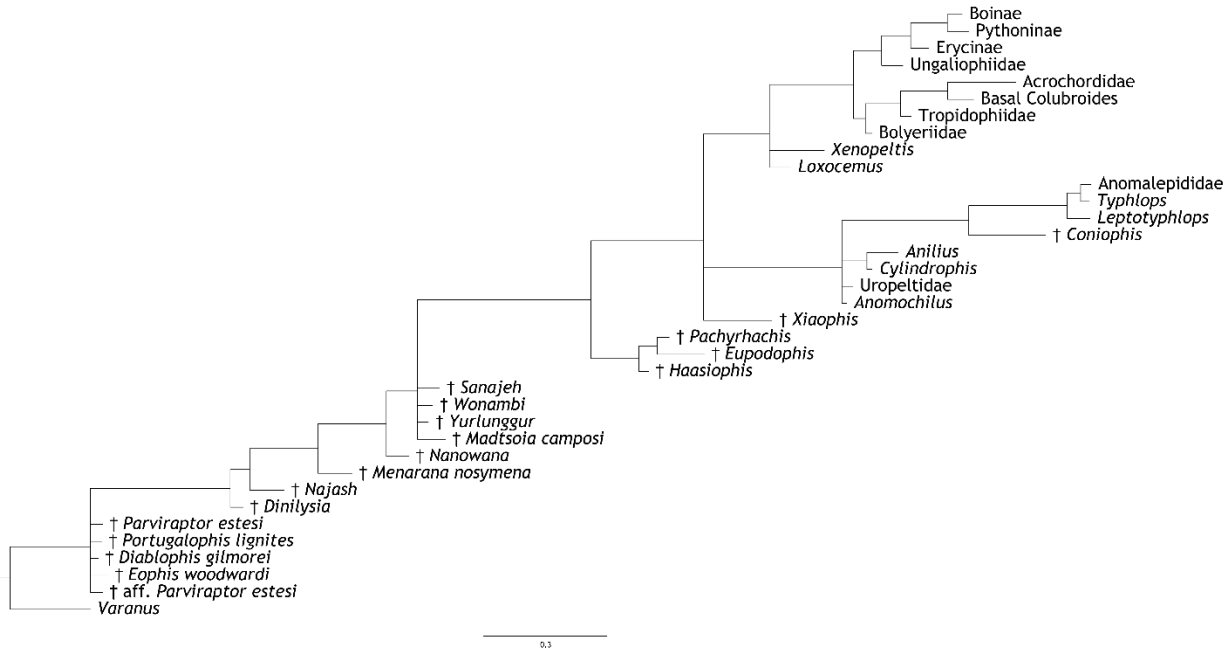

FIGURE S5.2. Complete version of the phylogeny in Figure 5.3b (Original Dataset, Bayesian inference). 50% majority-rule consensus tree generated via Bayesian analysis of Garberoglio *et al.* (2019a:data file S1). † indicates extinct taxa.

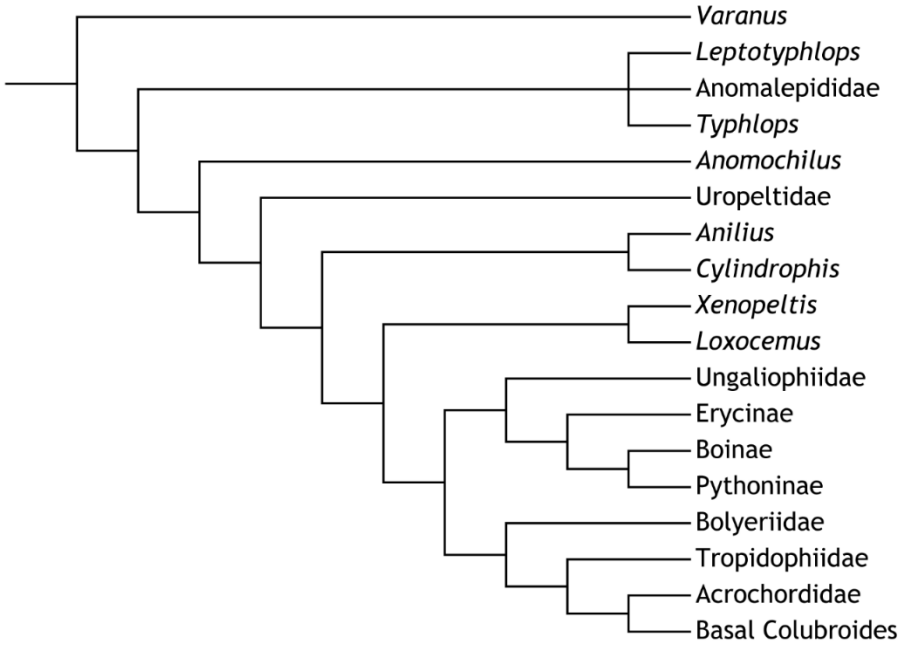

FIGURE S5.3. Complete version of the phylogeny in Figure 5.4a (Reduced Dataset, maximum parsimony). 50% majority-rule consensus tree of 46 MPTs (445 steps) generated via maximum parsimony analysis of Garberoglio *et al.* (2019a:data file S1) with extinct taxa removed.

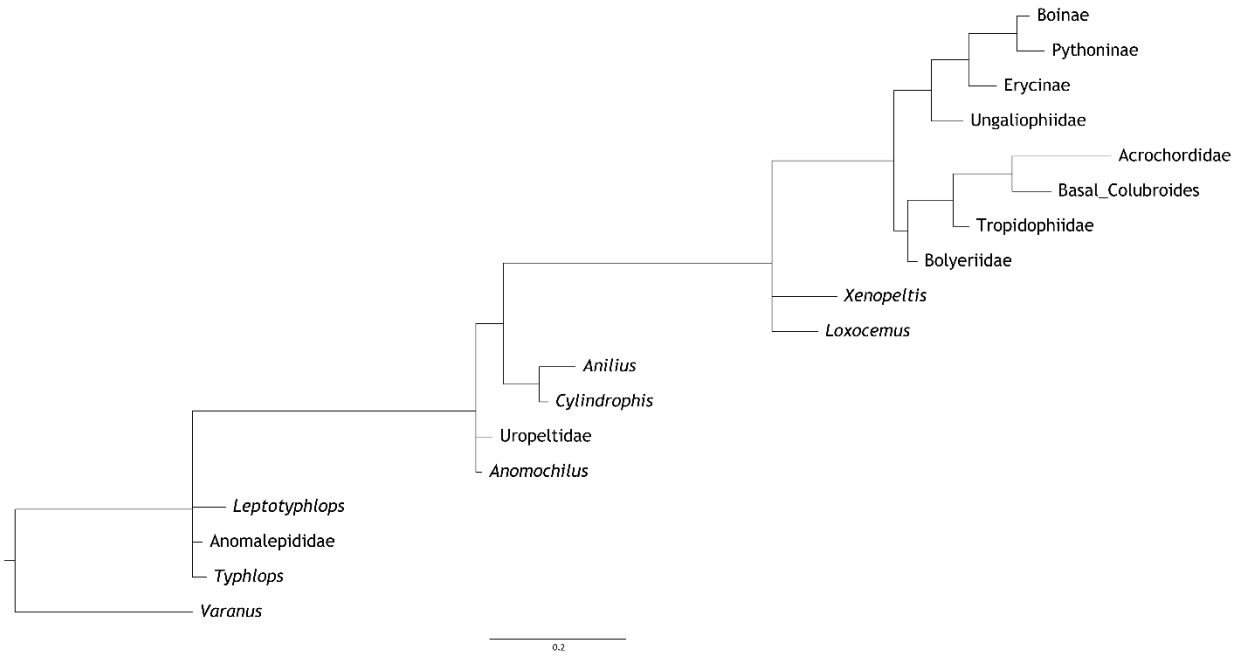

FIGURE S5.4. Complete version of the phylogeny in Figure 5.4b (Reduced Dataset, Bayesian inference). 50% majority-rule consensus tree generated via Bayesian analysis of Garberoglio *et al.* (2019a:data file S1) with extinct taxa removed.

APPENDIX 5.1. Revised character list

This list is mainly derived from Garberoglio *et al.* (2019a), which is in turn based on Caldwell and colleagues' (2015) adaptation of Longrich *et al.* (2012). For each character, the first publication to use that character in a phylogenetic analysis is indicated in green text, using the abbreviations below and with the format [AuthorsYear:Character_number_in_that_dataset]. Characters newly added or modified herein are indicated ("***" = added; "###" = modified).

Any modifications I made or comments I have regarding character scoring or construction are explained in the remarks below affected characters. All changes to character statement wording and formatting (e.g., addition of locators and variables) follow the recommended character statement syntax of Sereno (2007). Where relevant, the corresponding character in Garberoglio *et al.* (2019a) is indicated in black text as [G19a:__], so that readers can compare earlier versions of these characters to the current versions.

Earlier datasets are abbreviated as follows:

AZ06 (Apesteguía & Zaher 2006)
C15 (Caldwell *et al.* 2015)
C93 (Cundall *et al.* 1993)
E88 (Estes *et al.* 1988)
G12 (Gauthier *et al.* 2012)
G19a (Garberoglio *et al.* 2019a)
G19b (Garberoglio *et al.* 2019b)
G88 (Gauthier *et al.* 1988b)
L12 (Longrich *et al.* 2012)
L93 (Lee 1993)
L97 (Lee 1997)
L98 (Lee 1998)
LS02 (Lee & Scanlon 2002)
P86 (Pregill *et al.* 1986)
R02 (Rieppel *et al.* 2002)
S06 (Scanlon 2006)
S18 (Simões *et al.* 2018)
T00 (Tchernov *et al.* 2000)
V13 (Vasile *et al.* 2013)
W10 (Wilson *et al.* 2010)
ZS12 (Zaher & Scanferla 2012)

DENTITION

1. Dentary teeth: present (0); absent (1). [G19a:244] [G19a:244]

2. * Dentary, tooth row, orientation: roughly anteroposterior (0); transverse to anteromedially directed (1).**

a. Character remarks: NEW. This character was added to reflect the transversely-oriented dentary tooth row occurring in leptotyphlopids (see also Strong *et al.* 2021b).

3. ### Maxillary teeth, number: 15 or more (0); 1–14 (1); none (2). [L98:157] [G19a:185]

a. Modifications: Modified character to "Maxilla*ry teeth, number*" (i.e., added variable and moved primary locator from character states to character) and removed "maxillary teeth" from character states. Modified state 1 to "*1–14*" (formerly "fewer than 15"), so as to eliminate overlap with state 2. Re-worded state 2 to "*none*".

b. Character remarks 1: Following the approach recommended by Simões *et al.* (2017), these character states were determined by recording maxillary tooth counts for each taxon, plotting these values, and looking for breaks in the resulting distribution. In this case, the observed distribution of tooth counts was consistent with the existing character states in G19a:185.

c. Character remarks 2: According to Sereno (2007), absence/presence constitutes a "neomorphic character" that should be treated separately from "transformational" character states such as number (e.g., Sereno 2007:table 8). Following these guidelines for the present character, the absence/presence of the maxillary teeth and the number of maxillary teeth should therefore be separate characters, and state 2 herein should be removed. However, although I largely agree with Sereno (2007), I disagree with his contention that absent ≠ zero; instead, I consider it reasonable to include absence (or zero) as part of a count-based character such as this one.

4. * Maxilla, tooth row, orientation: roughly anteroposterior (0); transverse to anteromedially directed (1).**

a. Character remarks: NEW. This character was added to reflect the transversely-oriented maxillary tooth row occurring in typhlopoids and anomalepidids (see also Strong *et al.* 2021b). This condition also occurs in some caenophidians (e.g., *Atractaspis*) due to the modification of the maxillary fang apparatus.

5. ### **Maxillary teeth, size along tooth row: nearly uniform in size, at most only slightly larger in middle of tooth row (0); distinctly larger near middle of tooth row, smaller anteriorly and posteriorly (1); distinctly larger near anterior end of tooth row, smaller in middle and posteriorly (2).** [LS02:175, G12:416] [G19a:157]
    a. Modifications: Modified character to "*Maxillary* teeth*,* size *along tooth row*" (formerly "Teeth, size") and reverted character states to largely how they originally appear in LS02:175. A more recent version of this character (L12:159) is problematic in that it encapsulates both the maxillary and dentary teeth, but these do not always show the same pattern (e.g., in many caenophidians, such as *Thamnophis* or *Naja*).
    b. Scoring remarks: The first and last couple of teeth should not be considered when scoring this character, as they are typically always smaller than the rest of the teeth.

6. ### **Maxillary and dentary teeth, shape: relatively short, conical, upright (0); robust, recurved (1); elongate, needle-shaped, distinctly recurved (2).** [R02:4] [G19a:1]
    a. Modifications: Modified character to "Maxillary and dentary teeth, *shape*" (i.e., added variable).

7. **Premaxillary teeth: present (0); absent (1).** [T00:1] [G19a:2]

8. **Pterygoid teeth: absent (0); present (1).** [T00:50] [G19a:4]

9. ### **Pterygoid, tooth row, location: anterior to basipterygoid joint (0); reaches or passes level of basipterygoid joint posteriorly (1).** [ZS12:66] [G19a:64]
    a. Modifications: Modified character to "Pterygoid*,* tooth row, *location*" (i.e., added variable). Modified state 1 to "reaches or passes level of basipterygoid joint *posteriorly*", as per ZS12:66.

10. *** **Palatine teeth: absent (0); present (1).** [E88:82]

a. Character remarks: NEW; see next character.

11. ### Palatine teeth, size relative to marginal teeth: small (0); enlarged, at least half diameter of posterior maxillary teeth (1). [L12:197] [G19a:191]

a. Modifications: Modified character to "palatine teeth, *size relative to marginal teeth*" (i.e., added variable) and removed "palatine teeth" from character states. Removed state 2 ("palatine lacking dentition") of G19a:191 and created a separate character (character 10) for presence/absence of the palatine teeth—as argued by Sereno (2007), "absent" is not a size or magnitude, and more broadly "neomorphic characters" (i.e., presence/absence) should not be mixed with "transformational characters" (e.g., quantitative-relative/geometric characters such as size).

12. ### Alveoli and base of teeth, shape: not expanded transversely (0); wider transversely than anteroposteriorly (1). [LS02:178] [G19a:3]

a. Modifications: Modified character to "Alveoli and base of teeth, *shape*" (i.e., added variable).

13. ### Interdental ridges: absent (0); present (1). [L12:155] [G19a:153]

a. Modifications: Modified character to "Interdental ridges" (formerly "Teeth, implantation") and simplified wording of character states, following the suggested character statement syntax of Sereno (2007) for "neomorphic" (presence/absence) characters.

14. ### Replacement teeth, number per tooth position: one (0); two or more (1). [L12:157] [G19a:155]

a. Modifications: Modified character to "*Replacement teeth, number per tooth position*" (formerly "Teeth, replacement") and simplified wording of character states.

15. ### Teeth, attachment to jaws: ankylosed (0); loosely attached by connective tissue (1). [L12:158] [G19a:156]

a. Modifications: Modified character to "Teeth, attachment *to jaws*" and simplified wording of character states.

SKULL

PREMAXILLA

16. **### Premaxilla, articulation with maxilla, extent of integration: broad osseous contact (0); articulation minimal or loose (1); elements broadly separate (2).** [LS02:12] [G19a:5]
    a. Modifications: Modified character to "Premaxilla, *articulation with maxilla, extent of integration*" (i.e., clarified primary locator and added variable) and modified wording of character states to "broad *osseous contact* (0); *articulation minimal or* loose (1); *elements broadly separate* (2)". Added state 2 ("*elements broadly separate*") to encapsulate the condition in typhlopoids, anomalepidids, and many caenophidians.

17. **### Premaxilla, transverse processes, position relative to maxillae: medial (0); anterior (1).** [L12:162] [G19a:159]
    a. Modifications: Modified character to "Premaxilla*, transverse processes, position relative to maxillae*" (i.e., added variable and primary locator) and simplified wording of character states.

18. **### Premaxilla, transverse processes, posterior margin, orientation: anterolateral (0); transverse, perpendicular to midline (1); posterolateral (2).** [LS02:11] [G19a:6]
    a. Modifications: Modified character to "*Premaxilla,* transverse processes*, posterior margin, orientation*" (i.e., reversed locators, modified primary locator, and added variable). Changed primary locator from the overall transverse processes to just the posterior margin; this is how this character was originally constructed (see LS02:11), and is more specific so allows more consistency in scoring. Modified character states to "*anterolateral* (0); *transverse, perpendicular to midline* (1); *posterolateral* (2)", as per LS02:11; states 0 and 1 herein represent a subdivision of state 1 ("extending straight laterally or anterolaterally") of G19a:6.

19. ***** Premaxilla, nasal (= ascending) process, contact with nasals: present (0); absent (1).**

a. Character remarks: NEW. This character was added to reflect the reduction in premaxilla-nasal integration that occurs in many caenophidians.

20. **### Premaxilla, nasal (= ascending) process, length: elongate, approaching or contacting frontals (0); short, dividing nasals only at anterior margin or not at all (1).** [LS02:2] [G19a:7]
    a. Modifications: Modified character to "*Premaxilla,* nasal *(= ascending)* process*, length*" (i.e., reversed locators and added variable). Added "ascending process" as a synonym for nasal process, as per LS02:2.
    b. Character remarks: State 1 ("short, dividing nasals only at anterior margin or not at all") may appear to be redundant with character 19, which specifically reflects presence/absence of contact between the ascending process and nasal. However, in this case the phrase "or not at all" is simply an additional descriptor for this state, acting as a qualifier/adjective to help identify what qualifies as a "short nasal/ascending process".

21. **### Premaxilla, nasal (= ascending process), width: transversely expanded, partly roofing external nares (0); mediolaterally compressed, blade-like or spine-like (1).** [LS02:3] [G19a:158]
    a. Modifications: Modified character to "Premaxilla*, nasal (= ascending) process, width*" (i.e., added variable and primary locator) and removed "ascending process" from character states. Added "nasal process" as a synonym for ascending process, as per LS02:3.

22. ***** Premaxilla, articulation with prefrontals: absent (0); present (1).**
    a. Character remarks: NEW. This character was added to reflect the premaxilla-prefrontal articulation unique to *Xenotyphlops* among squamates.

NASAL

23. **### Nasals, dorsal (= horizontal) lamina, width in dorsal view: narrow anteriorly, tapering to a distinct point (0); broad anteriorly, at most tapering only slightly to a blunt anterior end (1).** [LS02:25, T00:4] [G19a:8]
    a. Modifications: Modified character to "*Nasals,* dorsal (= horizontal) lamina*, width in dorsal view*" (i.e., reversed locators and added variable). Modified character

states to "*narrow anteriorly, tapering to a distinct point* (0); *broad anteriorly, at most tapering only slightly to a blunt anterior end* (1)", based on LS02:25. This modification involves removing contact with the septomaxilla as a factor from this character; as noted by Lee & Scanlon (2002), this septomaxilla-nasal contact varies independently on the width of the nasals, and so these variables should not be treated simultaneously.

24. ### Nasals, dorsal (= horizontal) lamina, articulation with frontals: present (0); absent (1). [LS02:27] [G19a:11]

a. Modifications: Modified character to "*Nasals, dorsal (= horizontal) lamina, articulation with frontals*" (i.e., reversed locators and added variable) and simplified wording of character states to "*present* (0); *absent* (1)". Changed primary locator from "lateral flange" to "*dorsal (= horizontal) lamina*", as per original version of this character (LS02:27).

25. ### Nasals, medial (= vertical) flanges: absent (0); present (1). [ZS12:144] [G19a:142]

a. Modifications: Modified character to "*Nasals,* medial *(*= vertical*)* flanges" (i.e., reversed locators).

26. ### Nasals, medial (= vertical) flanges, articulation with frontals: present (0); absent (1). [T00:5] [G19a:9]

a. Modifications: Modified character to "*Nasals,* medial *(= vertical)* flanges, articulation with *frontals*" (i.e., reversed locators). Added "vertical flange" as a synonym for medial flange,

b. Character remarks 1: This character originally concerned the presence/absence of an articulation between the medial nasal flanges and medial frontal pillars. I have modified this character to more broadly concern the medial nasal flanges and the frontals (i.e., not just the medial frontal pillars), as anomalepidids lack medial frontal pillars but do exhibit contact between the medial nasal flanges and anteroventral margin of the frontals, and typhlopids typically lack full medial frontal pillars (though see *Xenotyphlops*) but some (e.g., *Afrotyphlops*) possess

processes descending from the anterodorsal margin of the frontal to articulate with the medial nasal flanges.

c. Character remarks 2: Rieppel (2007:187) describes the condition of the medial nasal flange–medial frontal flange articulation as varying across alethinophidians, with different groups characterized by either a dorsal contact (i.e., with only the medial frontal pillar component of the medial frontal flange), a ventral contact (i.e., with only the subolfactory process component of the medial frontal flange), or an extensive contact involving both components. However, these conditions are often difficult to distinguish, with many taxa showing gradational morphologies. As such, I have not included separate states for dorsal *versus* ventral *versus* extensive conditions of this articulation, instead keeping this character focussed on the basic presence/absence of an articulation with the frontals.

27. ### Nasals, anterior extension: do not closely approach transverse processes of premaxilla (0); extend anteriorly toward tip of rostrum, almost reaching transverse processes of premaxilla (1). [LS02:24] [G19a:10]

a. Modifications: Modified character to "*Nasals,* anterior *extension*" (i.e., moved locator and added variable). Reverted character states to largely how they appear in the original version of this character (LS02:24). This modification to the character states removes the position of the external nares as a contributing factor, and thus allows more consistency when scoring.

SEPTOMAXILLA

28. * Septomaxilla, lateral vertical flange, formation of medial conchal invagination (*sensu* Haas 1964; Rieppel *et al.* 2009): absent (0); present (1).**

a. Character remarks: NEW. This character reflects a condition unique to anomalepidids (see Rieppel *et al.* 2009), in which the dorsal margin of the lateral vertical flange of the septomaxilla deflects medially, dorsal to the vomeronasal cupola. The lateral/dorsal flange of the nasal also contributes to this structure.

29. * Septomaxilla, lateral vertical flange, posterior dorsal process: absent (0); present (1).** [T00:6]

a. Character remarks: NEW; see next character.

30. ### **Septomaxilla, lateral vertical flange, posterior dorsal process, length relative to posterior extent of septomaxilla: short, terminates anterior to (0); long, terminates near or beyond level of (1).** [T00:6] [G19a:13]
    a. Modifications: Modified character to "Septomaxilla, *lateral vertical flange,* posterior dorsal process*, length relative to posterior extent of septomaxilla*" (i.e., reversed locators and added variable and qualifier). Modified wording of character states to "short*, terminates anterior to* (0); long*, terminates near or beyond level of* (1)". Removed state 0 ("absent") from G19a:13 and created a separate character (character 29) for presence/absence of the posterior dorsal process—as argued by Sereno (2007), "absent" is not a length, and more broadly "neomorphic characters" (i.e., presence/absence) should not be mixed with "transformational characters" (e.g., quantitative-relative/linear characters such as length).
    b. Scoring remarks: This feature should be scored relative to the length of the ventral flange of the septomaxilla, not relative to the medial ascending lamina.

31. ### **Septomaxilla, lateral vertical flange, ventral portion of posterior edge, position relative to opening of Jacobson's organ: above or behind (0); distinctly in front (1).** [T00:8] [G19a:15]
    a. Modifications: Modified character to "*Septomaxilla*, *lateral vertical flange*, ventral portion of posterior edge, *position relative to opening of Jacobsen's organ*" (i.e., changed order of locators, added variable, and re-worded locator to "lateral *vertical* flange" for consistency with other characters). Modified state 0 to "*above or* behind", as this is more consistent with the original version of this character (T00:8), as well as with previous scorings (e.g., Zaher & Scanferla 2012; Garberoglio *et al.* 2019a), in which state 1 ("distinctly in front") is limited to Erycinae, Ungaliophiidae, and Boinae.

32. *** **Septomaxilla, lateral vertical flange, articulation with dorsal (= horizontal) lamina of nasal, proximity: distinctly separate (0); separated by narrow gap (1); in broad contact (2).** [T00:4] [G19a:8]

a. Character remarks: Re-conceptualization of T00:4. The proximity of the lateral vertical flange of the septomaxilla and the dorsal lamina of the nasal was previously incorporated into character 23 ("Nasals, dorsal [= horizontal] lamina, width in dorsal view"; see G19a:8 or T00:4), but was removed from that character because it varies separately from the width of the nasals (see also comments for that character). The current character incorporates this information, as well as a new state (state 2, "*in broad contact*") which reflects a condition in many fossorial taxa (e.g., *Anomochilus*, anomalepidids, some leptotyphlopids) that was not accounted for in the existing states.

33. ### Septomaxillae, medial articulation with frontals: absent (0); present (1). [T00:7] [G19a:14]

a. Modifications: Changed character from "Septomaxillae, articulation with median frontal pillars" to "Septomaxillae, *medial* articulation with *frontals*".

b. Character remarks: This character originally concerned the presence/absence of an articulation between the septomaxillae and medial frontal pillars. I have modified this character to more broadly concern the septomaxillae and frontals (i.e., not just the medial frontal pillars), as leptotyphlopids and typhlopoids lack medial frontal pillars but do exhibit contact between the septomaxillae and anteroventral or anterodorsal margin of the frontals, respectively. In some anomalepidids (*Anomalepis*, *Helminthophis*), the anteroventral corner of the frontal approaches the septomaxilla very closely; however, this does not constitute "medial contact" between these elements and so is scored as state 0 ("absent").

34. ### Vomeronasal cupola, medial fenestration: present (0); absent, cupola enclosed medially by sutural contact of septomaxilla and vomer (1). [T00:9] [G19a:16]

a. Modifications: Modified character to "Vomeronasal cupola*, medial fenestration*" (i.e., added variable) and modified character states accordingly.

35. ### Septomaxilla, contribution to opening of Jacobson's organ: forms lateral margin (0); restricted to anterior part of lateral margin, with vomer extending into posterior part of lateral margin (1). [T00:10] [G19a:17]

a. Modifications: Modified character to "Septomaxilla*, contribution to opening of Jacobson's organ*" (i.e., added variable) and modified character states accordingly.

b. Scoring remarks: In state 1 ("restricted to anterior part of lateral margin, with vomer extending into posterior part of lateral margin"), the vomer extends more than halfway around the lateral margin of the opening of Jacobson's organ.

VOMER

36. ### Vomeronasal nerve, exit from vomeronasal cupola: exits via gap between vomer and septomaxilla (0); exits via single large foramen in vomer (1); exits via cluster of small foramina in vomer (2); exits via septomaxilla (3). [T00:11] [G19a:18]

a. Modifications: Modified character to "Vomeronasal nerve*, exit from vomeronasal cupola*" (i.e., added variable). Modified wording of existing character states accordingly. Sub-divided the previous state 0 ("does not pierce vomer") into two new states: state 0 ("*exits via gap between vomer and septomaxilla*") and state 3 ("*exits via septomaxilla*"), based on Rieppel *et al.* (2009).

b. Character remarks: According to Rieppel *et al.* (2009), these new states characterize autarchoglossan lizards and leptotyphlopids (state 0) and anomalepidids (state 3). Rieppel *et al.* (2009) also note the condition in typhlopids as matching state 0; however, Rieppel *et al.* (2008:fig. 10D) show the vomeronasal nerve exiting through a single posterior foramen in the vomer in *Typhlops jamaicensis*. This latter condition also occurs in typhlopoids observed herein, so state 1 ("exits via single large foramen in vomer") appears to be the typical condition in typhlopoids.

37. ### Vomer, posterior ventral (= horizontal, palatal) lamina, dimensions: long, often parallel-edged (0); short, tapering to pointed tip (1). [T00:12] [G19a:19]

a. Modifications: Modified character to "*Vomer,* posterior ventral (= horizontal*, palatal*) lamina*, dimensions*" (i.e., reversed locators and added variable). Added "palatal lamina" as a synonym for ventral/horizontal lamina, as per LS02:88. Modified state 0 to "long, *often* parallel-edged", in recognition that, in some taxa (e.g., *Dibamus*), the vomer does taper to a pointed tip (as described in state 1), but

is quite long and otherwise similar to the condition in other non-snake lizards (i.e., better represented by state 0 than state 1 overall).

38. ### **Vomer, posterior dorsal (= vertical) lamina: indistinct or absent (0); present, well-developed (1).** [T00:13] [G19a:20]
    a. Modifications: Modified character to "*Vomer,* posterior dorsal (= vertical) lamina" (i.e., reversed locators) and modified wording of character states to "*indistinct* or absent (0); *present,* well-developed (1)". Reversed order of character states from G19a:20, as "indistinct or absent" is the outgroup condition (see also comments in LS02:89).
    b. Character remarks: The inclusion of "reduced" or some variation thereof (e.g., "indistinct", as in state 0) alongside the state "absent" is a grey area in coding neomorphic characters. As Sereno (2007:582) notes, presence/absence should ideally be treated as a separate character than size or prominence; however, in the absence of such a size-related character, it is acceptable to lump "reduced" with "absent". In this case, because this character is largely concerned with the fundamental "state of being" of the lamina (i.e., whether it exists / is present *versus* absent)—rather than any particular condition of the lamina when present—it is acceptable to keep this as a neomorphic character. Furthermore, the difference between "well-developed" and "not well-developed (i.e., indistinct or absent)" is readily apparent when scoring this character, but there is no such distinct separation between "indistinct" and "absent" (i.e., these conditions are very similar and clearly overlap / grade into one another); therefore, it is reasonable to include these latter conditions in the same character state.
    c. Scoring remarks 1: Garberoglio *et al.* (2019a) score this character (their char. 20) as "reduced or absent" for Acrochordidae and basal Colubroides. However, Groombridge (1979) describes and figures the vertical posterior lamina as being present in Acrochordidae and Caenophidia. Based on my observations, I agree with this latter interpretation.
    d. Scoring remarks 2: Although typhlopoids and leptotyphlopids bear a dorsal process on the vomer, this only surrounds the posterior extent of the vomeronasal cupola, rather than extending posterodorsal to this cupola as the posterior

dorsal/vertical lamina does (e.g., in *Boa* or anomalepidids). As such, I do not consider this dorsal process to be equivalent to the posterior dorsal lamina, and so have scored typhlopoids and leptotyphlopids as state 0 ("indistinct or absent").

FRONTAL

39. Medial frontal pillars: absent (0); present (1). [T00:24] [G19a:29]

a. Scoring remarks: Although scolecophidians lack medial frontal pillars, many typhlopoids (*Acutotyphlops*, *Typhlops*, and especially *Afrotyphlops* and *Xenotyphlops*) exhibit processes descending from the dorsal margin of the frontal at the anterior midline. This condition is amplified in *Xenotyphlops*; due to the ventral inflection of the snout, these descending processes come into close proximity with additional processes projecting medially from the lateral margins of the olfactory foramen. This results in a condition that superficially resembles the medial frontal pillars (i.e., a median structure subdividing the olfactory foramen). However, the aforementioned processes remain broadly separate from the ventral margin of the olfactory foramen (which occurs posterodorsal to the septomaxillae), and so this does not constitute a "present" condition for the medial frontal pillars.

40. * Frontal, lateral flange (= descending process, lateral frontal pillar): absent (0); present (1).** [E88:9; ZS12:150–Re-conceptualized] [G19a:148]

a. Character remarks: NEW; re-conceptualization of G19a:148/ZS12:150, incorporating E88:9–10. Characters 40–43 aim to better encapsulate the conditions of the nasofrontal joint in squamates, based on personal observations and Rieppel (2007). Former character: "Frontal subolfactory process: absent or present as simple horizontal lamina (0); present and closing tractus olfactorius medially (1)".

41. * Frontal, subolfactory process: absent, lateral frontal flange (= descending process of frontal, lateral frontal pillar) restricted to lateral margin of frontal (0); present, lateral frontal flange extends medially under olfactory tract (1).** [E88:10, ZS12:150–Re-conceptualized]

a. Character remarks: NEW; see character 40 ("Frontal, lateral flange [= descending process, lateral frontal pillar]").

42. * Frontal, subolfactory process, medial contact with contralateral: absent (0); present (1).** [E88:10; ZS12:150–Re-conceptualized]

a. Character remarks: NEW; see character 40 ("Frontal, lateral flange [= descending process, lateral frontal pillar]").

43. * Frontal, subolfactory process, contact with medial frontal pillar, proximity: no contact, separated by slight gap (0); sutured (1); fused, no suture visible (2).**

a. Character remarks 1: NEW; see character 40 ("Frontal, lateral flange [= descending process, lateral frontal pillar]").

b. Character remarks 2: Although "no contact" as in state 0 may appear equivalent to an "absent" condition for this character—suggesting based on Sereno (2007) that there should be a separate character for presence/absence of this articulation —I do not consider the presence/absence of an articulation or contact between elements to be a truly "neomorphic" phenomenon (unlike presence/absence of an element or structure itself). Therefore, "no contact" can remain incorporated into this character.

c. Scoring remarks: According to Rieppel (2007:187), the medial frontal pillars remain separate from the subolfactory processes in most 'anilioids' (state 0), exhibit sutural contact with the subolfactory processes in many booid-pythonoids (state 1), and are fully fused to the subolfactory processes in many booid-pythonoids and all caenophidians (state 2).

44. * Frontal, transverse horizontal shelf (*sensu* Frazzetta 1966): present (0); absent (1).** [T00:20]

a. Character remarks: NEW; see next character.

45. ### Frontal, transverse horizontal shelf (*sensu* Frazzetta 1966), prominence: well-developed and broadly overlapped by nasals (0); poorly developed and never broadly overlapped by nasals (1). [T00:20] [G19a:30]

a. Modifications: Modified character to "*Frontal,* transverse horizontal shelf *(sensu Frazzetta 1966)*, *prominence*" (i.e., reversed locators and added variable). Added

reference to Frazzetta (1966). Removed state 2 ("absent") from G19a:30 and created a separate character (character 44) for presence/absence of the transverse horizontal shelf—as argued by Sereno (2007), "neomorphic characters" (i.e., presence/absence) should not be mixed with "transformational characters" (e.g., qualitative-form characters such as prominence).

46. * Frontal, preorbital ridge (*sensu* Frazzetta 1966): absent (0); present (1).** [ZS12:145] [G19a:143]

a. Character remarks 1: Re-conceptualization of ZS12:145 / G19a:143. The original version of this character—ZS12:145, "Preorbital ridge (*sensu* Frazzetta, 1966) dorsally exposed (0), or overlapped by the prefrontal (1)"—referred to the preorbital ridge as described and figured by Frazzetta (1966); i.e., a ridge extending or flaring laterally from the dorsolateral margin of the olfactory foramen. However, Garberoglio *et al.* (2019a) define the preorbital ridge as a process on the frontal extending between the prefrontal and nasal. In *Najash* (the taxon these latter authors were describing), this process is indeed also consistent with Frazzetta's (1966) description. However, in taxa such as *Varanus*, a process on the frontal does extend between the prefrontal and nasal, but it is distinct from the process described by Frazzetta (1966); as such, in *Varanus* the preorbital ridge would be absent based on Frazzetta (1966), but present and dorsally exposed based on Garberoglio *et al.* (2019a). To reduce this confusion, I have changed this character to instead focus on the basic presence/absence of a preorbital ridge as originally described by Frazzetta (1966).

b. Character remarks 2: This modification also eliminates redundancy with character 49 ("Frontal, contact with prefrontal, complexity"), because state 1 of this latter character ("structurally complex, frontal clasped dorsally and ventrally by prefrontal") overlaps with the original state 1 of the current character ("preorbital ridge overlapped by prefrontal") in many taxa (e.g., *Python*, *Thamnophis*) (though not others, e.g., *Najash*, in which the preorbital ridge is present but not involved in the prefrontal-frontal articulation).

c. Character remarks 3: Finally, dorsal exposure of the preorbital ridge—i.e., the original focus of this character in ZS12:145—is still reflected in this dataset, in

character 65 (“Prefrontal, articulation with frontal, location”; see Remarks therein).

d. Overall character remarks: Because the preorbital ridge may be absent (e.g., *Varanus*), present but not involved in the suspension of the prefrontal (e.g., *Najash*), or present and clasped by the prefrontal (e.g., *Python*, *Thamnophis*), characters 46, 49, and 65 therefore together encapsulate the range of variation of this feature.

47. ### Frontal, nasal processes: present, projecting between nasals (0); absent (1). [G12:30, L12:166] [G19a:163]

a. Modifications: Modified character to “Frontal*, nasal processes*” (i.e., added primary locator) and simplified wording of character states to “*present, projecting* between nasals (0); absent (1)”.

48. ### Frontals, anterior width: taper anteriorly, subtriangular in dorsal view (0); broad anteriorly, anterior width comparable to width at frontoparietal suture (1). [LS02:52, L12:167] [G19a:164]

a. Modifications: Modified character to “Frontals*, anterior width*” (i.e., added variable). Modified character states to “taper anteriorly, *subtriangular in dorsal view* (0); broad anteriorly, *anterior width comparable to width at frontoparietal suture* (1)”.

b. Character remarks: This character originally incorporated the presence/absence of interorbital constriction (see L12:167, G19a:164). However, this is somewhat misleading, as, based on its original description (L12:167), this character is in fact referring to the anterior width of the frontal compared to the posterior width. For example, in taxa such as *Thamnophis radix*, the frontal is posteriorly broad, anteriorly broad, and distinctly constricted dorsal to the orbits; this would suggest the presence of “interorbital constriction” (state 0), but in fact this taxon should be scored as state 1 based on the full character description (L12:167), because the anterior width of the frontal is comparable to the posterior width. To eliminate this confusion, the character states were therefore modified to focus on this anterior *versus* posterior width comparison.

49. **### Frontal, contact with prefrontal, complexity: structurally simple, abutting (0); structurally complex, frontal clasped dorsally and ventrally by prefrontal (1).** [L12:168–Re-conceptualized]

    a. Character remarks: Re-conceptualization of L12:168 / G19a:165. In the original version of this character [introduced by L12:168—"Frontal: subolfactory process abuts prefrontal in immobile articulation (0); subolfactory process articulates with prefrontal in mobile joint (1); subolfactory process with distinct lateral peg or process that clasped dorsally and ventrally by prefrontal (2)"], it is unclear whether the variable under consideration is the configuration or the mobility of the frontal-prefrontal articulation. Furthermore, Longrich *et al.* (2012) note in their description of this character that non-snake lizards plesiomorphically reflect state 0, scolecophidians state 1, and most alethinophidians state 2; however, non-snake lizards often lack a subolfactory process as defined by Rieppel (2007), and, among scolecophidians, only anomalepidids exhibit a distinctly mobile frontal-prefrontal articulation, which even then involves a lateral frontal peg as encapsulated by the original state 2. From these issues, it is evident that the original formulation of this character is quite unclear in several aspects. As such, this character was re-conceptualized so as to focus on the structural complexity of the frontal-prefrontal articulation, thus more accurately encapsulating the observed variation among squamates.

50. ***** Frontal, ventral facet accommodating palatine and pterygoid: absent (0); present (1).**

    a. Character remarks: NEW. This character reflects the unique condition of the palatomaxillary arch in leptotyphlopids. In this group, the pterygoid and palatine articulate dorsally with a ventral facet on the frontal, contributing to the lack of mobility of the palatomaxillary arches (see also Strong *et al.* 2021b).

PARIETAL

51. **### Parietal(s), fusion in adult skull: unfused/paired (0); fused/single (1).** [G19a:245] [G19a:245]

a. Modifications: Modified character to "Parietals*, fusion in adult skull*" (i.e., added variable) and simplified wording of character states to "*unfused/*paired (0); *fused/*single (1)". Reversed order of character states from G19a:245, as "unfused/paired" is typically considered the plesiomorphic condition for paired *versus* fused skull elements (e.g., List 1966:8–9).

52. * Parietals, medial contact: present (0); absent, parietals separated by distinct gap or fontanelle medially (1).**

a. Character remarks: NEW. This character was added based on the large dorsal fontanelle in the skull of some scolecophidians (e.g., *Myriopholis*).

b. Scoring remarks: If the parietals are fused, this character should be scored as "inapplicable", as the fontanelle which this character reflects can only occur if the parietals are separate (or vice versa: if the parietals are unpaired/fused, then inherently they are in medial contact, making these characters redundant in the case of fusion).

53. ### Parietal, lateral processes (= lateral wings): present (0); absent (1). [T00:35, R02:14] [G19a:36]

a. Modifications: Modified character to "Parietal*, lateral processes (= lateral wings)*" (i.e., added primary locator) and simplified wording of character states to "*present* (0); *absent* (1)". Reversed order of character states from G19a:36, as "present" is the outgroup condition (see also comments in LS02:50).

b. Scoring remarks: These processes project laterally at or near the anterior margin of the parietal, at the level of the postorbitals/postfrontals/jugals when these elements are present.

54. ### Parietal, distinct lateral ridge extending posteriorly from anterolateral corner toward prootic: absent (0); present (1). [LS02:67, R02:15] [G19a:37]

a. Modifications: Modified character to "*Parietal,* distinct lateral ridge extending posteriorly from *anterolateral corner toward* prootic" (i.e., changed order of locators). Changed landmark to "*anterolateral corner*" from "anterior lateral wing" because some taxa that lack a lateral wing still possess this ridge (e.g., *Cylindrophis*). *Contra* Rieppel *et al.* (2002:character 15), I consider state 1

("present") to include taxa in which this ridge extends partway to the prootic, as well as taxa in which it extends all the way to the prootic (Rieppel *et al.* 2002 included only the latter condition under their state 1); this is consistent with other authors' scorings of this character (e.g., G19a:37).

55. ### **Frontoparietal suture, shape: relatively straight (0); slightly anteriorly concave (1); strongly U-shaped (2); U- or V-shaped, with apex pointing anteriorly (3).** [T00:32] [G19a:38]
    a. Modifications: Modified character to "Frontoparietal suture*, shape*" (i.e., added variable). Added state 1 ("*slightly anteriorly concave*") to distinguish the condition in many snakes. Modified state 2 to "*strongly* U-shaped", to clarify that this is referring to the distinctive condition typical of 'anilioids'. Added state 3 ("*U- or V-shaped, with apex pointing anteriorly*") to reflect the condition in some scolecophidians (e.g., *Gerrhopilus*, many leptotyphlopids).

56. ### **Optic foramen, posterior margin, position: very posteriorly located, completely within parietal (0); posteriorly located, forming deep notch in parietal (1); intermediate position, formed by straight margin of parietal (2); anteriorly located, completely within frontal (3).** [T00:33, LS02:61] [G19a:39]
    a. Modifications: Modified character to "Optic foramen, posterior margin, *position*" (i.e., added/clarified variable). Re-worded character states to "*very posteriorly located, completely within parietal (0); posteriorly located, forming deep notch in parietal (1); intermediate position, formed by straight margin of parietal (2); anteriorly located, completely within frontal (3)*", following LS02:61. Added state 0 ("*very posteriorly located, completely within parietal*") to reflect the condition in *Acrochordus* (also noted in Rieppel 1979a).
    b. Character remarks: The previous version of this character (see G19a:39) was worded in a way that seemed to conflate two distinct variables: location of the posterior margin of the optic foramen, and shape of this margin when formed by the parietal. However, upon returning to this character as originally written by Lee & Scanlon (2002), it is clearly meant to encapsulate only the position of this posterior margin, with shape acting simply as a descriptor to aid in

identifying/delimiting an "anterior" *versus* "intermediate" *versus* "anterior" position. I have therefore reverted the character states to the general wording of LS02:61, to clarify the intention of this character.

c. Scoring remarks: This character should be scored as "inapplicable" when the optic foramen is not fully defined (e.g., when it does not have an osseous posterior margin, as is typical of non-snake lizards).

57. ### Parietal, descending processes (= descending flanges): absent, lateral margins of braincase fully open anterior to prootic (0); present (1). [W10:28] [G19a:40]

a. Modifications: Re-wrote character as "*Parietal, descending processes (= descending flanges)*" (i.e., re-formatted character as neomorphic and clarified locators) and simplified character states to "*absent,* lateral margins of braincase *fully* open anterior to prootic (0); *present* (1)". Added "descending flanges" as a synonym for descending processes.

58. ### Parietal, descending processes (= descending flanges), ventral contact with frontals: absent (0); present (1). [S06:60A, L12:169] [G19a:166]

a. Modifications: Modified character to "*Parietal, descending processes (= descending flanges), ventral contact with frontals*" (i.e., clarified locators and variable) and simplified wording of character states accordingly. Added "descending flanges" as a synonym for descending processes.

a. Character remarks: The original version of this character—e.g., L12:169: "Frontals and parietals: do not contact ventrally (0) or descending wings of frontals and parietals contact ventrally to enclose the optic foramen (1)"—framed it in terms of ventral enclosure of the optic foramen. Longrich *et al.* (2012:character 169) in turn note that the condition in scolecophidians (in which the frontals and parietals contact ventrally but the optic foramen is enclosed entirely within the frontal) may not be homologous with the condition in many other snakes (in which the frontals and parietals contact ventrally, thus defining the ventral border of the optic foramen). However, I disagree with this suggestion, at least at the level of primary homology: in this character, I consider the core homolog concept to be the ventral contact of the frontals and parietals, regardless

of the position of the optic foramen. By simplifying the wording of the character states (including removing any mention of the optic foramen), I have clarified this homolog concept. Furthermore, the position of the optic foramen is already encapsulated in character 56 ("Optic foramen, posterior margin, position"), so the homology of this feature need not factor into the present character,

59. ### **Parietal, descending processes (= descending flanges), contact with anterior margin of base of basipterygoid process: absent (0); present (1).** [T00:36] [G19a:42]
    a. Modifications: Modified character to "Parietal, *descending processes (= descending flanges)*, *contact with* anterior *margin* of base of basipterygoid process" (i.e., added primary locator and modified variable, based on LS02:68). Added "descending processes" as a synonym for descending flanges.
    b. Scoring remarks: If the descending processes and/or basipterygoid processes are absent, then this character should be scored as "inapplicable".

60. ### **Parietal, supratemporal processes, prominence: distinctly developed (0); not distinctly developed (1).** [T00:34] [G19a:41]
    a. Modifications: Modified character to "*Parietal,* supratemporal processes*, prominence*" (i.e., reversed locators and added variable).

61. ### **Parietal, contact with supraoccipital, shape: embayed or V-shaped with apex pointing anteriorly (0); straight transverse line (1); curved or V-shaped with apex pointing posteriorly (2).** [T00:37] [G19a:43]
    a. Modifications: Modified character to "*Parietal, contact with* supraoccipital*, shape*" (i.e., clarified locators and added variable). Modified state 0 to "*embayed or* V-shaped…", based on T00:37, and state 2 to "*curved or* V-shaped with apex pointing posteriorly".

62. *** **Parietal, sagittal crest: absent (0); present (1).** [G12:93, L12:170]
    a. Character remarks: NEW; see next character.

63. ### **Parietal, sagittal crest, location: present posteriorly but not anteriorly, and extending for no more than 50% of parietal midline length (0); present anteriorly**

and posteriorly, and extending more than 50% of parietal midline length (1). [G12:93, L12:170] [G19a:167]

a. Modifications: Modified character to "Parietal, sagittal crest, *location*" (i.e., added variable). Removed state 0 ("absent") of G19a:167 and created a separate character (character 62) for presence/absence of the sagittal crest—as argued by Sereno (2007), "neomorphic characters" (i.e., presence/absence) should not be mixed with "transformational characters" (e.g., qualitative-topology characters such as location).

b. Character remarks: Although this character appears to conflate "quantitative-relative/linear" (i.e., length) and "qualitative-topology" (i.e., location) characters *sensu* Sereno (2007), this is not an "entangled character" (*sensu* Sereno 2007) or a "Type I.A.4 compound character" (*sensu* Simões *et al.* 2017); because the conditions of length and location of the parietal sagittal crest co-vary, they can be considered biologically dependent and, as non-independent conditions, can be included in the same character states.

64. ### **Parietal, posterior width relative to anterior width: subequal to or broader posteriorly (0); distinctly narrowed posteriorly (1).** [G19a:169] [G19a:169]

a. Modifications: Modified character to "Parietal*, posterior width relative to anterior width*" (i.e., added variable and qualifier) and modified wording of character states accordingly. The earlier version of this character (G19a:169) referred simply to a "posteriorly broad" *versus* "posteriorly narrow" parietal, but did not clarify how to delimit these conditions. The addition of a qualifier ("relative to anterior width") to the present version of this character ensures consistency in scoring these states.

PREFRONTAL

65. ### **Prefrontal, articulation with frontal, location: lateral (0); anterolateral (1).** [LS02:41, W10:22] [G19a:21]

a. Modifications: Modified character to "Prefrontal*, articulation with frontal, location*" (i.e., added variable and primary locator) and simplified wording of character states.

b. Scoring remarks: For taxa in which the prefrontal is lateral to the preorbital ridge, causing the preorbital ridge to be visible in dorsal view (e.g., *Najash*), this character should be scored as state 0 ("lateral").

66. ### Prefrontal, outer orbital (= lateral) margin, orientation: slanting anteroventrally (0); vertical (1); slanting posteroventrally (2). [LS02:39] [G19a:22]

a. Modifications: Modified character to "*Prefrontal, outer orbital (*= lateral*)* margin*, orientation*" (i.e., reversed locators and added variable) and simplified wording of state 1. Added "outer orbital margin" as a synonym for lateral margin, as per LS02:39. Added a new state (state 2, "*slanting posteroventrally*") to reflect the condition in typhlopoids.

67. * Lacrimal foramen: present (0); indistinct or absent (1).**

a. Character remarks: NEW; see next character. The absence of a distinct lacrimal foramen has been hypothesized previously as a synapomorphy of scolecophidians (Caldwell *et al.*, unpublished data).

68. ### Lacrimal foramen, enclosure by prefrontal: partial (0); complete (1). [T00:15, LS02:45] [G19a:23]

a. Modifications: Modified character to "Lacrimal foramen*, enclosure by prefrontal*" (i.e., added variable) and simplified wording of character states. Removed state 2 ("prefrontal lacking foramen") of G19a:23 and created a separate character (character 67) for presence/absence of the lacrimal foramen—as argued by Sereno (2007), "neomorphic characters" (i.e., presence/absence) should not be mixed with "transformational characters" (e.g., qualitative-topology characters such as location).

69. ### Prefrontal, lateral foot process (*sensu* Frazzetta 1966:fig. 18): absent (0); present, occurring lateral to lacrimal foramen (1). [T00:16, W10:18] [G19a:24]

a. Modifications: Simplification of T00:16 / G19a:24. Added reference to Frazzetta (1966), and added the lacrimal foramen as a landmark for identifying the lateral foot process, based on LS02:36.

b. Character remarks 1: See Frazzetta (1966:fig. 18) and Lee & Scanlon (2002:fig. 8) for labelled diagrams of the prefrontal.

c. Character remarks 2: Earlier versions of this character (e.g., W10:18, G19a:24) encapsulated two distinct features: presence/absence of the lateral foot process, and presence of its articulations with the maxilla and/or palatine. This original version of this character is therefore problematic on two fronts. First, as argued by Sereno (2007), "neomorphic characters" (i.e., presence/absence) should not be mixed with "transformational characters" (e.g., qualitative-topology characters such as articulations with surrounding elements). Second, this character is redundant with other characters: character 70 ("Prefrontal, lateral surface, ventral margin, articulation with maxilla, location") concerns the ventral articulation of the prefrontal with the maxilla; and character 118 ("Palatine, lateral [= maxillary] process, contact with prefrontal, location") concerns the prefrontal-palatine articulation, with state 2 ("projects strongly laterally to articulate with ventrolateral margin [= lateral foot process, when present] of prefrontal") overlapping with the present character. As such, this character was modified so as to only concern the presence/absence of the lateral foot process, to address these logical and methodological issues.

d. Scoring remarks: Because the lateral foot process is identified based on the lacrimal foramen—i.e., because it is defined as the process occurring lateral to the lacrimal foramen; see e.g., Frazzetta (1966:fig. 18) or Lee & Scanlon (2002:fig. 8, character 36)—any character involving this process should be scored as "inapplicable" if the lacrimal foramen is absent.

70. ### Prefrontal, lateral surface, ventral margin, articulation with maxilla, location: along the entire length of this margin (0); posteroventral contact only (i.e., at anteroventral corner of orbit) (1); anteroventral contact only (2); no ventral articulation with maxilla (3). [T00:22] [G19a:27]

a. Modifications: Modified character to "*Prefrontal, lateral surface,* ventral margin*, articulation with maxilla, location*" (i.e., re-arranged locators and added variable). Modified wording of character states to "*along the entire length of this margin* (0); poster*oventral* contact *only (i.e., at anteroventral corner of orbit)* (1)", based on e.g., ZS12:29. Added new states to reflect the reduced prefrontal-maxilla articulation in leptotyphlopids and *Xenopeltis* (state 2, "*anteroventral contact*

only"), and in typhlopoids and dibamids (state 3, "*no ventral contact with maxilla*").

b. Character remarks 1: An earlier version of this character (W10:17) included an additional character state ("'peg-and-socket' articulation") reflecting the condition in 'anilioids'. However, this concerns the morphology of the articulation, not its location, and therefore should not be included in this character. A new character (character 71) has therefore been added to reflect the morphology/complexity of the prefrontal-maxilla articulation. This new character also incorporates the character states of L12:184, which also involved the complexity of the prefrontal-maxilla articulation.

c. Character remarks 2: Although "no ventral articulation with maxilla" as in state 3 may appear equivalent to an "absent" condition for this character—suggesting based on Sereno (2007) that there should be a separate character for presence/absence of this articulation —I do not consider the presence/absence of an articulation or contact between elements to be a truly "neomorphic" phenomenon (unlike presence/absence of an element or structure itself). Therefore, "no articulation" can remain incorporated into this character.

71. * Prefrontal, articulation with maxilla, complexity: extensive/tight abutting or overlap (0); loose overlap (1); interlocking along facial process of maxilla in a 'peg-and-socket'-like joint (2); forked/bifurcating (3); broadly swivelling (4).** [W10:17, L12:163,184–Re-conceptualized]

a. Character remarks: NEW; based on W10:17, L12:163, and L12:184; see previous character. State 0 ("*extensive/tight abutting or overlap*") is characteristic of the tight sutural connection in non-snake lizards and leptotyphlopids, state 1 ("*loose overlap*") is characteristic of the condition in most alethinophidians, state 2 ("*interlocking along facial process of maxilla in a 'peg-and-socket'-like joint*") is characteristic of 'anilioids' (except *Anomochilus*), state 3 ("*forked/bifurcating*") is characteristic of anomalepidids, and state 4 ("*broadly swivelling*") is characteristic of typhlopoids. State 2 also applies to atractaspidids, which also exhibit a 'ball-and-socket'-like articulation in which the prefrontal is laterally excavated to receive a dorsal 'peg' of the facial process of the maxilla.

72. ### Prefrontal, medial foot process (*sensu* Frazzetta 1966:fig. 18): absent (0); present, occurring medial to lacrimal foramen (1). [T00:17] [G19a:25]

a. Modifications: Simplification of T00:17 / G19a:25. Modified character to "*Prefrontal,* medial foot process *(sensu Frazzetta 1966:fig. 18)*" (i.e., reversed locators) and simplified character states. Added reference to Frazzetta (1966) and added the lacrimal foramen as a landmark for identifying the medial foot process, based on Lee & Scanlon (2002:380).

b. Character remarks 1: See Frazzetta (1966:fig. 18) and Lee & Scanlon (2002:fig. 8) for labelled diagrams of the prefrontal.

c. Character remarks 2: The earlier version of this character ["Medial foot process of prefrontal: absent (0); present, low (1); present, high (2)"] conflated two distinct variables: absence/presence and position of the medial foot process. As argued by Sereno (2007), "neomorphic characters" (i.e., presence/absence) should not be mixed with "transformational characters" (e.g., qualitative-topology characters such as location), so these variables should be encapsulated in separate characters. However, as noted by Lee & Scanlon (2002:380) in their comments on T00:17, the medial foot process occurs in a consistent position when present, making the meaning of "low" *versus* "high" unclear. As such, I have simplified this character to simply reflect the presence/absence of the medial foot process.

d. Scoring remarks: Because the medial foot process is identified based on the lacrimal foramen—i.e., because it is defined as the process occurring medial to the lacrimal foramen; see e.g., Frazzetta (1966:fig. 18) or Lee & Scanlon (2002:380, fig. 8)—any character involving this process should be scored as "inapplicable" if the lacrimal foramen is absent.

73. * Prefrontal, anterior flange (= anterior process, apex): absent (0); present (1).** [T00:19, LS02:31]

a. Character remarks: NEW; see next character.

74. ### Prefrontal, anterior flange (= anterior process, apex), roofing of nasal gland and auditus conchae: absent (0); present (1). [T00:19] [G19a:26]

a. Modifications: Simplification of G19a:26. Modified character to "*Prefrontal,* anterior flange *(= anterior process, apex), roofing of* nasal gland and auditus conchae" (i.e., changed position of secondary locator and clarified variable). Added "anterior process" and "apex" as synonyms for anterior flange, *sensu* Lee & Scanlon (2002) and Frazzetta (1966), respectively.

b. Character remarks: The earlier version of this character (G19a:26) was worded such that it was unclear whether this character was referring to the presence/absence of the anterior flange of the prefrontal, the position of this flange relative to the nasal gland and auditus conchae, or both. As noted by LS02:248, the presence/absence of the anterior prefrontal flange can vary independently of its coverage of the nasal capsule; as such, I have re-formatted this character following Lee & Scanlon (2002), i.e., encapsulating the former variable in character 73 ("Prefrontal, anterior flange [= anterior process, apex]") and the latter in the present character.

75. ### **Prefrontal, contact with nasal, location: no contact (0); contacts posterolateral corner of nasal only, via dorsal lappet (1); contacts posterolateral and anterolateral corners of nasal only, via dorsal lappet and tip of apex, respectively (2); continuous contact along entire anterodorsal margin of prefrontal (3).** [T00:23, LS02:33; AZ06:23, W10:14–Re-conceptualized] [G19a:12, G19a:28]

a. Modifications: Re-conceptualization of AZ06:23 and W10:14. Modified character to "Prefrontal, *contact with nasal, location*" (i.e., specified locator and added variable).

b. Character remarks 1: This character is essentially a combination of G19a:12 and G19a:28, both of which concerned the location of the prefrontal-nasal contact. Specifically, G19a:28 originally concerned only the posteromedial contact of the prefrontal dorsal lamina with the nasal, whereas G19a:12 was broader in scope but conflated two distinct variables: location and complexity/configuration of the nasal-prefrontal articulation. The present character is therefore intended to encapsulate the location of this articulation more comprehensively, whereas the following character (character 76, "Prefrontal, contact with nasal, configuration") reflects the complexity of this articulation.

c. Character remarks 2: State 0 ("*no contact*") occurs in many squamates, state 1 ("*contacts posterolateral corner of nasal only, via dorsal lappet*") occurs in some snakes (e.g., *Cylindrophis*), state 2 ("*contacts posterolateral and anterolateral corners of nasal only, via dorsal lappet and tip of apex, respectively*") occurs in some snakes (e.g., *Boa constrictor*), and state 3 ("*continuous contact along entire anterodorsal margin of prefrontal*") occurs in many fossorial snakes (e.g., leptotyphlopids, typhlopoids, *Anomochilus*).

d. Character remarks 3: Although "no contact" as in state 0 may appear equivalent to an "absent" condition for this character—suggesting based on Sereno (2007) that there should be a separate character for presence/absence of this articulation —I do not consider the presence/absence of an articulation or contact between elements to be a truly "neomorphic" phenomenon (unlike presence/absence of an element or structure itself). Therefore, "no articulation" can remain incorporated into this character.

76. ### Prefrontal, contact with nasal, configuration: abutting or slightly overlapping (0); interlocking (1). [W10:14–Re-conceptualized] [G19a:12]

a. Modifications: Re-conceptualization of W10:14 / G19a:12. This original character conflated two distinct variables: location and configuration of the nasal-prefrontal articulation. The location of this articulation is reflected in the previous character, and the configuration is reflected in the present character.

b. Scoring remarks: If character 75 ("Prefrontal, contact with nasal, location") is scored as state 0 ("no contact"), then the current character should be scored as "inapplicable".

77. ### Prefrontal, medial extension across frontal: <75% width of frontal (0); distinctly >75% width of frontal. [C93:13, G12:132] [G19a:161]

a. Modifications: Re-wrote character as "Prefrontal*, medial extension across frontal*" (i.e., clarified variable) and re-wrote character states as *"<75% width of frontal* (0); *distinctly >75% width of frontal*" (character formerly formatted as presence/absence-based, e.g., G19a:161).

78. ### **Prefrontal, anterior margin, concavity: not markedly concave (0); strongly concave (1).** [L12:165–Re-conceptualized] [G19a:162]

    a. Character remarks: Re-conceptualization of L12:165. The original version of this character—L12:165, "Prefrontal: anterior margin concave, bounding an expanded narial aperture: absent (0) or present (1)"—was a Type I.A.7 problematic character (i.e., unjustified composite locator coding) *sensu* Simões *et al.* (2017). In this case, because the external narial opening is defined by several elements, changes to any of these components could result in the enlargement of the external narial opening; this means that a single character concerning the size of the external naris is not logically sound. I have therefore re-conceptualized this character to concern solely the concavity of the anterior margin of the prefrontal.

LACRIMAL

79. **Lacrimal: present (0); absent (1).** [W10:16] [G19a:31]

POSTFRONTAL

80. **Postfrontal: present (0); absent (1).** [T00:25] [G19a:32]

    a. Character remarks: See Palci & Caldwell (2013) for comments on the homology of the circumorbital elements in snakes.

    b. Scoring remarks: This character should be scored as state 0 ("present") both when the postfrontal occurs as a distinct element (e.g., *Loxocemus*, *Python*) and when it is fused to the postorbital to form the postorbitofrontal (e.g., *Varanus*).

81. *** **Postfrontal, anterior and posterior processes: present (0); absent (1).** [T00:28, LS02:48]

    a. Character remarks: NEW; see next character. See Palci & Caldwell (2013) for comments on the homology of the circumorbital elements in snakes.

82. ### **Postfrontal, anterior and posterior processes, contact with frontals and parietals, configuration: clasping (0); abutting (1).** [T00:28, LS02:48] [G19a:186]

    a. Modifications: Modified character to "Postfrontal, *anterior and posterior processes, contact with frontals and parietals, configuration*" (i.e., added variable and locators) and simplified character states to simply "*clasping* (0); *abutting* (1)". Removed state 2 ("anterior and posterior processes absent") of G19a:186

and created a separate character (character 81) for presence/absence of the anterior and posterior processes of the postfrontal—as argued by Sereno (2007), "neomorphic characters" (i.e., presence/absence) should not be mixed with "transformational characters" (e.g., qualitative-topology characters such as articulations).

b. Character remarks: See Palci & Caldwell (2013) for comments on the homology of the circumorbital elements in snakes.

JUGAL

83. ### Jugal: present (0); absent (1). [T00:26] [G19a:33]

a. Modifications: Removed "fused" from state 1.

b. Character remarks: See Palci & Caldwell (2013) for comments on the homology of the circumorbital elements in snakes.

84. * Jugal, fusion to postfrontal: unfused, occur as separate elements (0); fused, element extending along dorsal and posterior margins of orbit (1).**

a. Character remarks: NEW; see comments for character 86 ("Jugal, dorsal head, articulation"). See Palci & Caldwell (2013) for comments on the homology of the circumorbital elements in snakes.

b. Scoring remarks: This character can only be scored if both the postfrontal and jugal are individually scored as "present".

85. ### Jugal, ventral tip, contribution to orbital margin: contacts or closely approaches prefrontal and/or lacrimal, forming or contributing to ventral margin of orbit (0); contacts or closely approaches ectopterygoid and/or maxilla only, forming almost-complete posterior margin of orbit (1); remains separated by wide gap from ectopterygoid and/or maxilla (2). [T00:27] [G19a:34]

a. Modifications: Modified character to "Jugal, ventral tip*, contribution to orbital margin*" (i.e., added variable). Modified wording of state 0 to "contacts or *closely* approaches prefrontal *and/*or lacrimal…", wording of state 1 to "contacts or closely approaches ectopterygoid *and/or* maxilla *only*…", and wording of state 2 to "…ectopterygoid *and/or maxilla*".

b. Character remarks: See Palci & Caldwell (2013) for comments on the homology of the circumorbital elements in snakes.

c. Scoring remarks: State 1 ("contacts or closely approaches ectopterygoid and/or maxilla only, forming almost-complete posterior margin of orbit") occurs when the jugal extends distinctly more than halfway down the posterior margin of the orbit. If the jugal descends roughly halfway or less, or its ventral tip is displaced distinctly anteriorly relative to the ectopterygoid (as in anomalepidids), then this character should be scored as state 2 ("remains separated by wide gap from ectopterygoid").

86. ### Jugal, dorsal head, articulation: postorbital (0); parietal (1); lack of dorsal contact (2). [T00:28, ZS12:37] [G19a:35]

a. Modifications: Modified character to "Jugal, dorsal head*, articulation*" (i.e., added variable) and simplified wording of character states accordingly.

b. Character remarks 1: See Palci & Caldwell (2013) for comments on the homology of the circumorbital elements in snakes.

c. Character remarks 2: Earlier versions of this character (e.g., G19a:35) include an additional state, "fuses or articulates with only the posterodorsal surface of postfrontal". However, because this state concerns the existence of a jugal-postfrontal fusion rather than purely the identity of the jugal's dorsal articulation, I have removed this state and created a separate character (character 84) for fusion of the jugal to the postfrontal.

d. Character remarks 3: Although "lack of dorsal contact" as reflected by state 2 may appear equivalent to an "absent" condition for this character—suggesting based on Sereno (2007) that there should be a separate character for presence/absence of this articulation—I do not consider the presence/absence of an articulation or contact between elements to be a truly "neomorphic" phenomenon (unlike presence/absence of an element or structure itself). Therefore, "no articulation" can remain incorporated into this character.

87. Jugal, distinct posterior process for quadratomaxillary ligament: present (0); absent (1). [G19a:239] [G19a:239]

a. Character remarks: See Palci & Caldwell (2013) for comments on the homology of the circumorbital elements in snakes.

POSTORBITAL

88. Postorbital: present (0); absent (1). [G19a:240] [G19a:240]

a. Character remarks: See Palci & Caldwell (2013) for comments on the homology of the circumorbital elements in snakes.

b. Scoring remarks: This character should be scored as state 0 ("present") both when the postorbital occurs as a distinct element (e.g., *Physignathus*) and when it is fused to the postfrontal to form the postorbitofrontal (e.g., *Varanus*).

MAXILLA

89. * Maxilla, ascending (= facial) process: present (0); indistinct or absent (1).** [T00:29]

a. Character remarks: NEW; see next character.

90. ### Maxilla, ascending (= facial) process, height relative to height of main body of maxilla: tall, equal to or greater than (0); short, less than (1). [T00:29] [G19a:44]

a. Modifications: Modified character to "*Maxilla*, ascending *(= facial)* process, *height relative to height of main body of maxilla*" (i.e., reversed locators, added variable, and changed qualifier). Added "facial process" as a synonym of ascending process. Modified states to "tall*, equal to or greater than* (0); short*, less than* (1)". Removed state 2 ("absent") of G19a:44 and created a separate character (character 89) for presence/absence of the ascending (= facial) process—as argued by Sereno (2007), "absent" is not a measurement, and more broadly "neomorphic characters" (i.e., presence/absence) should not be mixed with "transformational characters" (e.g., quantitative-relative/linear characters such as height).

b. Character remarks: This character originally measured the height of the facial process relative to the dorsal margin of the prefrontal (e.g., see G19a:44). However, this definition is problematic for scolecophidians; for example, in typhlopoids, the dorsal terminus of the maxilla (which I homologize with the facial process) is quite tall but does not reach the dorsal margin of the prefrontal, so would be scored as "short" under the previous definition. By changing the

qualifier to instead classify the height of the facial process relative to the height of the main body of the maxilla itself, this character can now be scored consistently and logically for all taxa.

91. ### Maxilla, ascending (= facial) process, medial surface, posterior notch for prefrontal: absent (0); present (1). [G19a:243] [G19a:243]

a. Modifications: Modified character to "*Maxilla,* ascending (= facial) process*, medial surface,* posterior notch for prefrontal" (i.e., re-arranged locators, including separating primary locator from variable). Reversed order of character states from G19a:243, as "absent" is the plesiomorphic condition among squamates, with presence being a derived condition among many fossil snakes and *Anilius* (Garberoglio *et al.* 2019a:Suppl. Mat. 20).

b. Character remarks: This posterior notch is distinct from the 'peg-and-socket'-like articulation of the maxilla and prefrontal as encapsulated in character 71, state 2 (see description of prefrontal in Garberoglio *et al.* 2019a:Suppl. Mat. 20).

92. ### Maxilla, ascending (= facial) process, medial surface, distinct naso-lacrimal recess demarcated dorsally by anteroventrally-trending ridge: present (0); absent (1). [L12:181] [G19a:177]

a. Modifications: Modified character to "Maxilla, *ascending (= facial) process, medial surface,* distinct naso-lacrimal recess demarcated dorsally by anteroventrally-trending ridge" (i.e., re-arranged locators for clarity).

b. Scoring remarks: When present, this ridge extends anteroventrally from just above the lacrimal duct to the supradental shelf (Longrich *et al.* 2012:character 181).

93. ### Fossa for lateral recess of nasal capsule, location: well-defined concavity on maxilla and prefrontal (0); mostly on prefrontal, invasion of maxilla reduced to small fossa on back of facial process (1); developed entirely on prefrontal (2). [L12:182] [G19a:178]

a. Modifications: Modified character to "*Fossa for lateral recess of nasal capsule, location*" (i.e., changed focus of character from facial process to location of fossa). Modified wording of character states accordingly, to "*well-defined*

concavity on maxilla and prefrontal (0); *mostly on prefrontal, invasion of maxilla* reduced *to* small fossa on back of facial process (1); developed entirely on prefrontal (2)".

94. ### Maxilla, anterior terminus, anteromedial maxillary flange (*sensu* Lee & Scanlon 2002:fig. 6): present, occurring as small horizontal shelf (0); absent (1). [LS02:15] [G19a:45]

a. Modifications: Modified character to "*Maxilla, anterior terminus, anteromedial maxillary flange (sensu Lee & Scanlon 2002:fig. 6)*" (i.e., re-arranged locators). Re-worded primary locator to "anteromedial maxillary flange" following the original version of this character (LS02:15), with "small horizontal shelf" moved to the description of state 0.

b. Character remarks: Although Lee & Scanlon (2002:character 15) state that this character "cannot be scored in taxa with an anteriorly reduced maxilla", I disagree with this perspective, and have scored this character for all scolecophidians herein (whereas LS02:15 is only scored for leptotyphlopids). This approach is justifiable as the maxilla in leptotyphlopids is just as reduced as in anomalepidids or typhlopoids, yet is still scored for leptotyphlopids in the original iteration of this character.

95. ### Maxilla, anterior terminus, anteromedial maxillary flange (*sensu* Lee & Scanlon 2002:fig. 6), contact with vomer: present (0); absent (1). [L12:178–Re-conceptualized] [G19a:174]

a. Character remarks: Simplification of L12:178 / G19a:174 ("Maxilla, premaxillary process: medial projection articulating with vomers present [0]; premaxillary process does not contact vomers [1]."). The original version of this character is problematic for two reasons:

First, this character originally conflated two distinct features: presence of a medial projection on the anterior terminus of the maxilla, and articulation of the maxilla with the vomer. Generally, this projection is present in non-snake lizards and contacts the vomer, and is absent in snakes and the maxilla does not contact the vomer (Longrich *et al.* 2012:character 178). However, in some snakes (e.g.,

Anilius and *Uropeltis*, as noted by L12:178), this projection is present, yet does not contact the vomer, a condition not properly encapsulated by either of the original character states.

Second, the original character is problematic because the medial projection to which it is referring is equivalent to the anteromedial maxillary flange (*sensu* Lee & Scanlon 2002:fig. 6); the presence/absence of this flange is already captured by character 94, therefore making the present character partially redundant.

To resolve these issues, I have simplified L12:178 / G19a:174 so that the present character reflects only the articulation of the anteromedial maxillary flange with the vomer.

96. ### **Maxilla, posterior terminus, projection beyond posterior margin of orbit, length (measured relative to orbital width [= distance from anterior margin of orbit to posterior margin of optic foramen]): no projection, maxilla terminates anterior to posterior margin of orbit (0); short, posterior projection distinctly shorter than orbital width (1); distinct, posterior projection approaching or greater than orbital width (2).** [LS02:23, R02:8] [G19a:46]
    a. Modifications: Modified character to "*Maxilla,* posterior *terminus*, *projection beyond posterior margin of orbit, length (measured relative to orbital width [= distance from anterior margin of orbit to posterior margin of optic foramen])*" (i.e., reversed locators and added variable). Modified wording of character states to "*no projection, maxilla terminates anterior to posterior margin of orbit* (0); *short, posterior projection distinctly shorter than orbital width (1); distinct, posterior projection approaching or greater than orbital width (2)*", so as to allow more accurate scoring of character states.
    b. Character remarks: Although "lack of posterior projection" as encapsulated in state 0 may appear equivalent to an "absent" condition for this character—suggesting based on Sereno (2007) that there should be a separate character for presence/absence of such a projection—I do not consider the presence/absence of a projection of an element beyond another to be a truly "neomorphic" phenomenon (unlike presence/absence of the element or structure itself). Therefore, "no projection" can remain incorporated into this character.

c. Scoring remarks: For non-snake lizards in which the optic foramen does not have an osseous posterior margin, the posterior margin of the orbit as delimited by the circumorbital elements should be used as a landmark for measurement, rather than the posterior margin of the optic foramen.

97. ### Maxilla, medial (= palatine) process: absent (0); present (1). [LS02:19; L12:176–Re-conceptualized] [G19a:173]

a. Character remarks: Re-conceptualization of L12:176, returning to original version of character as introduced by LS02:19. Longrich *et al.* (2012) had framed this character in terms of *length* of the medial/palatine process of the maxilla; however, I consider it more accurate to describe this variation in terms of *presence/absence* of this process.

98. ### Maxilla, medial (= palatine) process, position relative to orbit: anterior (0); ventral (1). [LS02:18, R02:9] [G19a:47]

a. Modifications: Modified character to "*Maxilla,* medial (= palatine) process, *position relative to orbit*" (i.e., reversed locators and added variable) and simplified wording of character states to "*anterior* (0); *ventral* (1)".

99. ### Maxilla, medial (= palatine) process, orientation: horizontal (0); downturned (1). [L12:186] [G19a:181]

a. Modifications: Modified character to "Maxilla*, medial (= palatine) process, orientation*" (i.e., added variable and primary locator) and simplified wording of character states.

100. ### Maxilla, superior alveolar foramen (= opening for superior alveolar canal): present (0); absent (1). [T00:30] [G19a:48]

a. Modifications: Modified character to "Maxilla, *superior alveolar foramen (= opening for superior alveolar canal)*" (i.e., changed primary locator from "large foramen" as in L02:21 to "superior alveolar foramen") and modified character states to "*present* (0); *absent* (1)" (i.e., converted character format to neomorphic).

b. Character remarks: When present, this foramen occurs at the posteromedial corner of the base of the facial process in non-snake lizards, and near the base of the

medial/palatine process in snakes. This character originally referred specifically to whether the medial/palatine process was pierced by a foramen (e.g., see LS02:21, G19a:48). The present character is expanded in scope so as to also apply to taxa which lack a medial/palatine process (e.g., non-snake lizards), a condition making the original version of this character inapplicable.

101. ### Maxilla, accessory foramen posterior to superior alveolar foramen (= opening for superior alveolar canal): absent (0); present (1). [L12:188] [G19a:183]

a. Modifications: Modified character to "Maxilla, accessory foramen posterior to *superior alveolar foramen (= opening for superior alveolar canal)*". The original version of this character (L12:188) described this accessory foramen as being posterior to the palatine process of the maxilla; however, since many taxa (e.g., non-snake lizards) do not have a distinct palatine process, the superior alveolar foramen is a more universal landmark.

b. Scoring remarks: If character 100 ("Maxilla, superior alveolar foramen [= opening for superior alveolar canal]") is scored as absent, this character should be scored as "inapplicable".

102. ### Maxilla, lateral foramina, number: 5 or more (0); 4 or fewer (1). [L12:179] [G19a:175]

a. Modifications: Modified character to "Maxilla*, lateral foramina,* number" (i.e., separated primary locator from variable). Renamed primary locator from "mental foramina" to "*lateral foramina*", as the mental foramina occur on the dentary.

b. Character remarks: Following the approach recommended by Simões *et al.* (2017), these character states were determined by recording the value of this variable for each taxon, plotting these values, and looking for breaks in the resulting distribution. In this case, the observed distribution was consistent with the existing character states in L12:179 / G19a:175.

103. * Maxilla, supradental shelf: present, forming distinct horizontal shelf above toothrow on medial surface of maxilla (0); indistinct or absent (1).**

a. Character remarks 1: NEW. This character was added to reflect the absence of the supradental shelf in some taxa (e.g., scolecophidians, colubroids). The absence of

this structure in *Typhlops* and *Liotyphlops* was noted by Longrich *et al.* (2012) in the description of their character 180.

b. Character remarks 2: The inclusion of "reduced" or some variation thereof (e.g., "indistinct", as in state 1) alongside the state "absent" is a grey area in coding neomorphic characters. As Sereno (2007:582) notes, presence/absence should ideally be treated as a separate character than size; however, in the absence of such a size-related character, it is acceptable to lump "indistinct" with "absent". In this case, because this character is largely concerned with the fundamental "state of being" of the supradental shelf of the maxilla (i.e., whether it exists / is present *versus* absent)—rather than any particular condition of the supradental shelf when present—it is acceptable to keep this as a neomorphic character.

c. Scoring remarks: If the maxillary teeth are absent (i.e., in leptotyphlopids), this character should be scored as "inapplicable".

104. ### Maxilla, supradental shelf, length: extends full length of maxilla (0); reduced anterior to palatine process of maxilla (1). [L12:180] [G19a:176]

a. Modifications: Modified character to "Maxilla, supradental shelf*, length*" (i.e., changed variable from "development" to "length").

b. Scoring remarks: If the palatine process is absent, then the location of the maxilla-palatine articulation can be used as a landmark instead.

105. ### Maxilla, contact with nasal: present (0); absent (1). [G12:20] [G19a:179]

a. Modifications: Modified character to "Maxilla*, contact with nasal*" (i.e., added variable) and simplified wording of character states to "*present* (0); *absent* (1)".

106. Maxilla, ectopterygoid process: absent (0); present (1). [LS02:22] [G19a:184]

107. * Maxilla, ectopterygoid process, form: weak but distinct horizontal expansion or flange (0); prominent downcurved flange (1).** [LS02:22]

a. Character remarks: NEW, based on LS02:22. This character was added to reflect the range of form in the ectopterygoid process across snakes. State 0 encapsulates taxa in which this process occurs as a slight medial swelling of the maxilla where it articulates with the ectopterygoid (e.g., *Cylindrophis*, *Boa*, *Acrochordus*), as well as taxa in which this process forms a more distinct horizontal swelling (e.g.,

Xenopeltis, *Casarea*). State 1 encapsulates taxa in which this process forms a distinct and downcurved flange (e.g., colubroids in which the ectopterygoid process is present; anomalepidids).

PALATINE

108. ### Palatine, articulation with pterygoid, complexity: broadly abutting or overlapping (0); interlocking, tongue-in-groove joint (1); interlocking, simple forking (2); simple flap-overlap (3); no contact with pterygoid (4). [R02:12] [G19a:56]

a. Modifications: Modified character to "*Palatine, articulation with pterygoid, complexity*" (i.e., re-arranged locators and added variable). Modified character states to "*broadly abutting or overlapping* (0); *interlocking,* tongue-in-groove joint (1); *interlocking, simple forking* (2); *simple* flap-overlap (3); *no contact with pterygoid* (4)". Removed previous state 0 ("complex and finger-like articulations") and added current states 0, 2, and 4.

b. Character remarks: These states better encapsulate the variation in this articulation across squamates, including among scolecophidians. State 0 occurs in most non-snake lizards, state 1 occurs in most snakes, state 2 occurs in typhlopoids (reflecting the forked palatine process of the pterygoid and associated palatine morphology in this group), state 3 occurs in leptotyphlopids and most anomalepidids, and state 4 occurs in atractaspidids and *Anomalepis*.

109. Palatine, contact with ectopterygoid: present (0); absent (1). [T00:42] [G19a:57]

110. ### Palatine, anterior dentigerous process: absent (0); present (1). [T00:41] [G19a:53]

a. Modifications: Modified character to "*Palatine,* anterior dentigerous process" (i.e., reversed locators).

b. Scoring remarks: If the palatine is edentulous, characters related to the anterior dentigerous process should be scored as inapplicable.

111. ### Palatine, anterior dentigerous process, contact with vomer and/or septomaxilla posterolateral to opening for Jacobson's organ: present (0); absent (1). [T00:43] [G19a:58]

a. Modifications: Modified character to "*Palatine, anterior* dentigerous process, contact with vomer and/or septomaxilla posterolateral to opening for Jacobson's organ" (i.e., reversed locators). Added "anterior" for consistency with other characters.

b. Scoring remarks: If the palatine is edentulous, characters related to the anterior dentigerous process should be scored as inapplicable.

112. ### Palatine, medial (= choanal, vomerine) process, form: flat process extending horizontally (0); broad arch (1); narrow arch (2); short lamina that does not reach vomer (3). [T00:48] [G19a:54]

a. Modifications: Modified character to "*Palatine,* medial (= choanal*, vomerine*) process*, form*" (i.e., reversed locators and added variable). Added "vomerine process" as a synonym for medial/choanal process, as per LS02:92. Modified character states to "*flat process extending horizontally* (0); *broad arch* (1); *narrow arch* (2); short ~~horizontal~~ lamina that does not reach vomer (3)".

b. Character remarks 1: State 0 is new, reflecting the condition in many non-snake lizards. State 1 was changed to more accurately describe the typical condition of the choanal process in many snakes, and state 2 was re-worded to more accurately describe this process in some taxa (e.g., typhlopoids, anomalepidids, *Xenopeltis*).

c. Character remarks 2: State 3 ("short lamina that does not reach vomer") may appear to be redundant with other characters concerning the palatine-vomer articulation. However, in this case the phrase "that does not reach vomer" is simply an additional descriptor for this state, acting as a qualifier/adjective to help identify what qualifies as a "short lamina".

113. ### Palatine, medial (= choanal, vomerine) process, expanded anterior flange articulating with vomer posterolaterally: absent (0); present (1). [LS02:93] [G19a:55]

a. Modifications: Modified character to "*Palatine, medial (*= choanal*, vomerine)* process*, expanded anterior flange articulating with vomer posterolaterally*" (i.e., reversed locators and added variable) and simplified wording of character states to "*absent* (0); *present* (1)". Added "medial process" and "vomerine process" as synonyms of choanal process, and added "posterolaterally", both as per LS02:93.

b. Character remarks: This process occurs in madtsoiids and *Dinilysia*; see Lee & Scanlon (2002:character 93) and Scanlon & Lee (2000:fig. 1b).

114. ### Palatine, medial (= choanal, vomerine) process, extent of integration with vomer: articulates via broad osseous contact with posterior end of vomer (0); closely approaches vomer but lacks distinct osseous contact (1); distinctly separate from vomer (2). [T00:47, LS02:90] [G19a:62]

a. Modifications: Modified character to "*Palatine, medial (*= choanal, vomerine*)* process*, extent of integration with vomer*" (i.e., reversed locators and added variable). Added "medial process" as a synonym for vomerine/choanal process. Modified character states to "articulates *via broad osseous contact* with posterior end of vomer (0); *closely approaches vomer but lacks distinct osseous contact* (1); *distinctly separate* from vomer (2)", to better describe the range of variation across squamates.

b. Character remarks: Although "no articulation" as encapsulated in state 2 may appear equivalent to an "absent" condition for this character—suggesting based on Sereno (2007) that there should be a separate character for presence/absence of this articulation —I do not consider the presence/absence of an articulation or contact between elements to be a truly "neomorphic" phenomenon (unlike presence/absence of an element or structure itself). Therefore, "no articulation" can remain incorporated into this character.

115. * Palatine, lateral (= maxillary) process: present, forming distinct process (0); highly reduced or absent (1).**

a. Character remarks 1: NEW. This character was added to reflect the highly reduced or absent condition of the maxillary process of the palatine in anomalepidids (see also Strong *et al.* 2021b). This condition also occurs in *Crotalus*.

b. Character remarks 2: The inclusion of "reduced" alongside the state "absent" is a grey area in constructing neomorphic characters. As Sereno (2007:582) notes, presence/absence should ideally be treated as a separate character than size or prominence; however, in the absence of such a size-related character, it is

acceptable to lump "reduced" with "absent". In this case, because this character is largely concerned with the fundamental "state of being" of the maxillary process (i.e., whether it exists / is present *versus* absent)—rather than any particular condition of this process when present—it is acceptable to keep this as a neomorphic character.

c. Scoring remarks: If this character is scored as state 1 ("*highly reduced or absent*"), then all subsequent characters involving the maxillary process should be scored as "inapplicable". This applies even if the maxillary process is present but extremely reduced (e.g., in many anomalepidids). The purpose of this guideline is to prevent the "highly reduced" condition from being overrepresented or repeated in several characters.

116. ### Palatine, lateral (= maxillary) process, position on palatine: anterior to posterior terminus (0); at posterior terminus (1). [T00:44] [G19a:59]

a. Modifications: Modified character to "*Palatine, lateral (*= maxillary*)* process*, position on palatine*" (i.e., reversed locators and added variable) and simplified wording of character states to "anterior to posterior *terminus* (0); at posterior *terminus* (1)".

117. ### Palatine, lateral (= maxillary) process, articulation with maxilla, configuration: broad osseous contact (0); articulating via 'ball-and-socket'-like joint accommodating medial (= palatine) process of maxilla (1); loosely overlapping (2); articulating with large medial excavation or foramen on maxilla (3); articulation highly reduced or absent (4). [T00:45] [G19a:60]

a. Modifications: Modified character to "*Palatine*, lateral (= maxillary) process, *articulation with maxilla, configuration*" (i.e., re-arranged locators and added variable). Modified wording of existing character states and added 3 new states; character states are now "*broad osseous contact* (0); *articulating via 'ball-and-socket'-like joint accommodating medial (= palatine) process of maxilla* (1); loosely overlapping (2); *articulating with large medial excavation or foramen on maxilla* (3); *articulation highly reduced or absent* (4)".

b. Character remarks 1: Character states 1, 3, and 4 were added to reflect the conditions in 'anilioids', typhlopoids, and leptotyphlopids, respectively. The increased number of character states reflects key differences of the palatomaxillary arch—and overall jaw mechanism—across squamates (see Strong *et al.* 2021b).

c. Scoring remarks: State 4 ("*articulation highly reduced or absent*") reflects the reduction in the maxilla-palatine contact that occurs in leptotyphlopids and atractaspidids. In anomalepidids, the maxillary process is so highly reduced that this character should be scored as "inapplicable", based on the scoring of character 115 ("Palatine, lateral [= maxillary] process") as state 1 ("*highly reduced or absent*").

118. ### Palatine, lateral (= maxillary) process, contact with prefrontal, location: no contact (0); articulates with ventromedial margin (= medial foot process, when present) of prefrontal (1); projects strongly laterally to articulate with ventrolateral margin (= lateral foot process, when present) of prefrontal (2). [LS02:36, L12:198] [G19a:192]

a. Modifications: Modified character to "Palatine, lateral *(= maxillary)* process*, contact with prefrontal, location*" (i.e., clarified locators and variable). Modified character states to "*no contact* (0); *articulates with ventromedial margin (= medial foot process, when present) of prefrontal* (1); *projects strongly laterally to articulate with ventrolateral margin (= lateral foot process, when present) of prefrontal* (2)". In the previous version of this character (L12:198), it is rather unclear as to whether the character is referring to a separate lateral process that contacts the prefrontal (i.e., distinct from the maxillary process), or whether it is simply referring to a unique condition/articulation of the maxillary process. I interpret it in the sense of the latter option, and have re-formulated this character accordingly. This includes converting the character to a transformational format, as it was originally worded in a rather confusing neomorphic format, and adding more informative character states than simply "absent" *versus* "present".

119. * Palatine, posterior (= pterygoid) process, orientation: roughly posterior (0); strongly posterolateral (1).**

a. Character remarks: NEW. This character was added to reflect the unique orientation of the pterygoid process of the palatine in anomalepidids (state 1, "*strongly posterolateral*") relative to other squamates (state 0, "*roughly posterior*") (see also Strong *et al.* 2021b).

120. ### Trigeminal nerve, maxillary branch, position: pierces lateral (= maxillary) process of palatine (0); passes dorsally between palatine and prefrontal (1). [T00:46] [G19a:61]

a. Modifications: Modified character to "*Trigeminal nerve,* maxillary branch*, position*" (i.e., reversed locators and added variable).

PTERYGOID

121. * Pterygoid, quadrate ramus, longitudinal groove: shallow or absent (0); present, very deep, becoming dorsomedial posteriorly (1).** [LS02:105, T00:51] [G19a:65]

a. Character remarks: Re-conceptualization of T00:51 / G19a:65, based on LS02:105. The original version of this character (T00:51, see G19a:65) conflated two distinct features: the form of the quadrate ramus, and the presence/absence of a deep longitudinal groove. However, as noted by Lee & Scanlon (2002) in the description of their character 105, several taxa exhibit a "blade-like" quadrate ramus but it does not bear a distinct longitudinal groove. I have therefore separated this character into separate characters describing the presence/absence of this longitudinal groove (present character) and the form of the quadrate ramus (character 122).

122. ### Pterygoid, quadrate ramus, form: robust, horizontally compressed to rounded or triangular in cross-section (0); robust, flattened blade (1); simple, rod-like (2). [T00:51] [G19a:65]

a. Modifications: Re-conceptualization of T00:51 / G19a:65. Modified character to "*Pterygoid,* quadrate ramus*, form*" (i.e., reversed locators and added variable). Modified character states to "robust, *horizontally compressed to* rounded or

triangular in cross-section (0); *robust, flattened* blade (1); *simple, rod-like* (2)". State 2 was added to reflect the reduced form of the quadrate ramus in many fossorial taxa (e.g., scolecophidians, *Anomochilus*, atractaspidids), a condition not encapsulated in the original version of this character (T00:51, see G19a:65). See also comments for previous character.

123. * Pterygoid, transverse (= lateral, ectopterygoid) process: present (0); absent (1).** [T00:52, LS02:101]

a. Character remarks: NEW; see next character.

124. ### Pterygoid, transverse (= lateral, ectopterygoid) process, prominence: distinct, well-defined lateral projection (0); gently curved lateral flange or expansion of pterygoid (1). [T00:52, LS02:101] [G19a:66]

a. Modifications: Modified character to "*Pterygoid,* transverse (= lateral*, ectopterygoid)* process, *prominence*" (i.e., reversed locators and added variable). Modified state 1 to "gently curved lateral *flange or* expansion of pterygoid". Added "ectopterygoid process" as a synonym for lateral/transverse process of pterygoid. Removed "absent" from state 1 of G19a:66 and created a separate character (character 123) for presence/absence of the ectopterygoid process—as argued by Sereno (2007), "neomorphic characters" (i.e., presence/absence) should not be mixed with "transformational characters" (e.g., qualitative-form characters such as prominence).

b. Scoring remarks: See Lee & Scanlon (2002:fig. 3B) for an example of state 0 ("distinct, well-defined lateral projection"). See Lee & Scanlon (2002:fig. 3C–F) for examples of state 1 ("gently curved lateral flange or expansion of pterygoid").

ECTOPTERYGOID

125. ### Ectopterygoid: present (0); absent (1). [G19a:248] [G19a:248]

a. Modifications: Removed "highly reduced" from state 1 and created a separate character (character 126) for the form/size of the ectopterygoid.

b. Character remarks: The inclusion of "reduced" alongside the state "absent" is a grey area in coding neomorphic characters. As Sereno (2007:582) notes, presence/absence should ideally be treated as a separate character than size or

prominence; however, in the absence of such a size-related character, it is acceptable to lump "reduced" with "absent". In this case, I considered it most accurate to subdivide the original character (G19a:248) into separate neomorphic (i.e., presence/absence; present character) and transformational (i.e., size; character 126) characters, so as to fully encapsulate both the fundamental "state of being" of the ectopterygoid (i.e., whether it exists / is present *versus* absent) and the particular condition of the ectopterygoid when present, respectively. This subdivision is also relevant operationally, as there are several subsequent characters which rely on the presence of the ectopterygoid and which can still be scored even if the ectopterygoid is highly reduced; it is therefore useful to have a distinct character for overall presence/absence of this element.

126. * Ectopterygoid, form: robust (0); distinctly reduced, rod-like (1).**

a. Character remarks: NEW; see previous character.

127. ### Ectopterygoid, lateral edge, shape: straight (0); angulated at contact with maxilla (1). [T00:53] [G19a:67]

a. Modifications: Modified character to "*Ectopterygoid,* lateral edge*, shape*" (i.e., reversed locators and added variable).

128. ### Ectopterygoid, anterior terminus, articulation with maxilla, location: restricted to posteromedial edge (0); invades dorsal surface (1); no articulation (2). [T00:54] [G19a:68]

a. Modifications: Modified character to "*Ectopterygoid,* anterior *terminus, articulation with maxilla, location*" (i.e., re-arranged locators and added variable) and simplified wording of character states accordingly. Added a new state (state 2, "*no articulation*") to reflect the condition in *Anomochilus*.

b. Character remarks: Although "no articulation" as in state 2 may appear equivalent to an "absent" condition for this character—suggesting based on Sereno (2007) that there should be a separate character for presence/absence of this articulation—I do not consider the presence/absence of an articulation or contact between elements to be a truly "neomorphic" phenomenon (unlike presence/absence of an

element or structure itself). Therefore, "no articulation" can remain incorporated into this character.

129. ### Ectopterygoid, medial finger-like process: absent (0); present, articulating with medial surface of maxilla (1). [ZS12:147] [G19a:145]

a. Modifications: Modified character to "*Ectopterygoid,* medial finger-like process" (i.e., separated secondary locator from primary locator) and moved "articulating with medial surface of maxilla" to description of state 1 ("present"). Reversed order of character states from G19a:145, as "absent" is the plesiomorphic condition based on my interpretation of this character (see Remarks).

b. Character remarks: From how the original version of this character (ZS12:147) is scored, the process to which Zaher & Scanferla (2012) were referring is unclear. Therefore, for the purposes of this dataset, I am considering the presence of this "medial finger-like process" to reflect the 'mitten'-shaped anterior terminus of the ectopterygoid in most snakes. *Varanus* verges on this condition, so is also scored as "present".

130. ### Ectopterygoid, articulation with pterygoid, location: restricted to transverse (= lateral, ectopterygoid) process of pterygoid (0); articulating distinctly with dorsal surface of pterygoid body (1); no articulation with pterygoid (2). [ZS12:151] [G19a:149]

a. Modifications: Modified character to "Ectopterygoid, *articulation* with pterygoid*, location*" (i.e., added variable). Added "ectopterygoid process" as a synonym for lateral/transverse process of pterygoid. Modified wording of state 1 to "*articulating distinctly with* dorsal surface of pterygoid body" to clarify this description. Added a new state (state 2, "*no articulation with pterygoid*") to reflect the condition in *Anomochilus*.

131. ### Ectopterygoid, articulation with pterygoid, complexity: clasping (0); overlapping or abutting (1). [T00, L12:200] [G19a:194]

a. Modifications: Modified character to "Ectopterygoid*, articulation with pterygoid, complexity*" (i.e., added variable and primary locator) and simplified character states to "*clasping* (0); *overlapping or abutting* (1)".

b. Character remarks: These character states focus on the complexity of the pterygoid-ectopterygoid articulation, rather than incorporating its location as in the original character (L12:200); this modification eliminates redundancy between this character and character 130 ("Ectopterygoid, articulation with pterygoid, location"), which does specifically concern the location of this articulation. The original version of this character (L12:200) also included "overlapping" and "abutting" under separate character states. However, because there is distinct gradation between these conditions (e.g., *Xenopeltis*, *Casarea*, *Loxocemus*), and because "overlapping" and "abutting" articulations both involve a similar level of anatomical complexity, these conditions have therefore been included under the same character state.

c. Scoring remarks: If the ectopterygoid does not contact the pterygoid (i.e., *Anomochilus*), then this character should be scored as "inapplicable".

EPIPTERYGOID

132. Epipterygoid: present (0); absent (1). [E88:47] [G19a:193]

QUADRATE

133. ### Quadrate, orientation in lateral view: slanted clearly anteriorly, nearly horizontal (0); slanted slightly anteriorly (1); roughly vertical (2); slanted clearly posteriorly (3). [T00:55] [G19a:71]

a. Modifications: Modified character to "Quadrate*, orientation in lateral view*" (i.e., added variable). Removed "posterior tip of pterygoid dislocated anteriorly from mandibular condyle of quadrate" from state 0 ("slanted clearly anteriorly"), as this is not necessary for scoring this condition, and added "*nearly horizontal*" to this state. Simplified wording of character states, added "*slanted slightly anteriorly*" as its own character state (separate from "vertical"), modified state 2 to "*roughly* vertical", and modified state 3 to "slanting *clearly* posteriorly"; these states are similar to those used by Rieppel & Zaher (2000).

134. ### Quadrate, cephalic condyle, suprastapedial process: present, distinctly projecting posteriorly (0); indistinct or absent (1). [T00:56] [G19a:72]

a. Modifications: Modified character to "*Quadrate,* cephalic condyle*, suprastapedial process*" (i.e., reversed secondary locators and added primary locator) and simplified wording of character states accordingly.

b. Character remarks: The inclusion of "indistinct" alongside the state "absent" is a grey area in coding neomorphic characters. As Sereno (2007:582) notes, presence/absence should ideally be treated as a separate character than size or prominence; however, in the absence of such a size-related character, it is acceptable to lump "reduced/indistinct" with "absent". In this case, because this character is largely concerned with the fundamental "state of being" of the suprastapedial process (i.e., whether it exists / is present *versus* absent)—rather than any particular condition of this process when present, including size—it is acceptable to keep this as a neomorphic character.

135. Quadrate, lateral conch: present (0); absent (1). [G12:180] [G19a:188]

136. ### Quadrate, shaft, maximum length relative to snout-occiput length: short, <10% (0); moderate, 10–20% (1); long, >20–33% (2); very long, >33% (3). [LS02:76, T00:57, L12:195] [G19a:189]

a. Modifications: Modified character to "Quadrate, *shaft,* maximum length relative to *snout-occiput length*" (i.e., added primary locator and changed qualifier). Modified character states to "*short, <10%* (0); *moderate, 10–20%* (1); *long, >20–33%* (2); *very long, >33%* (3)". Following the approach recommended by Simões *et al.* (2017), these character states were determined by recording the value of this variable for each taxon, plotting these values, and looking for breaks in the resulting distribution. Although LS02:76 used a cut-off value of 25% to define a "short" *versus* "long" quadrate, the observed distribution supports the current character states.

b. Character remarks: This character originally measured the length of the quadrate relative to its proximal width (L12:195); however, as noted by Lee & Scanlon (2002) in the description of their character 76, this definition is problematic because it is heavily dependent on the presence/absence and prominence of the

suprastapedial process, which can be highly variable. I have therefore modified the qualifier of this character based on LS02:76.

137. * Quadrate, anterior process: absent (0); present (1).**

a. Character remarks: NEW. This character was added in order to reflect a feature present in some scolecophidians (see Palci *et al.* 2020a; Strong *et al.* 2021b).

138. * Quadrate, anterior process, form: prominent triangular process (0); small bump (1).**

a. Character remarks: NEW. This character was added in order to reflect variation in a feature present in some scolecophidians (see Palci *et al.* 2020a; Strong *et al.* 2021b).

139. * Quadrate, anterior process, position on quadrate shaft: clearly in distal/ventral half (0); at midpoint or more proximal/dorsal (1).**

a. Character remarks: NEW. This character was added in order to reflect variation in a feature present in some scolecophidians (see Palci *et al.* 2020a; Strong *et al.* 2021b).

b. Scoring remarks: This character should be scored based on the location of the apex or tallest point of the anterior process.

STAPES

140. ### Stapedial footplate, shape: broad and massive, dominates posterolateral surface of otic capsule (0); narrow and thin (1). [W10:53] [G19a:73]

a. Modifications: Modified character to "Stapedial footplate*, shape*" (i.e., added variable). Modified state 0 to "broad and massive*, dominates posterolateral surface of otic capsule*", as per W10:53.

b. Scoring remarks: As noted by Wilson *et al.* (2010:character 53) in the original description of this character, these states should be scored in comparison to the otic capsule itself, regardless of how extensive the crista circumfenestralis is and how much the stapedial footplate is obscured in lateral view of the skull.

141. * Stapedial shaft, distal end, location relative to quadrate: extends toward posterodorsal tip of suprastapedial process or cephalic condyle (0); extends toward**

ventral aspect of suprastapedial process (or cephalic condyle) and dorsal end of quadrate shaft (1); extends toward middle or ventral half of quadrate shaft (2). [LS02:146] [G19a:74]

a. Character remarks: Re-conceptualization of T00:59 / G19a:74, adapted from LS02:146. This character replaces the original character in this dataset referring to the "stylohyal" (G19a:74, introduced by T00:59): "Stylohyal, fusion to quadrate: not fused (0); fused to posterior tip of suprastapedial process (1); fused to ventral aspect of reduced suprastapedial process (2); fused to quadrate shaft (3)". This latter character was replaced for several reasons. Most importantly, the homology of the snake stylohyal with the middle ear components of lizards has historically been contentious (reviewed in Caldwell 2019:107–116), making it difficult if not impossible to confidently score the original version of this character in non-snake lizards. Similarly, as Lee & Scanlon (2002) note in their description of their character 146 (from which the present character is adapted), conclusions regarding fusion of the stylohyal rely on embryological observations which are often unavailable for modern taxa and completely absent for extinct taxa. In light of these issues, the current character aims to reflect stapedial shaft morphology more accurately by relying on the position of the shaft relative to the quadrate, a feature that can be assessed/compared much more reliably across squamates.

142. ### Stapedial shaft, shape in dorsal view: straight (0); angulated at base (1). [T00:60] [G19a:75]

a. Modifications: Modified character to "Stapedial shaft*, shape in dorsal view*" (i.e., added variable). Specified "*in dorsal view*" to aid in identifying angulation consistently. Modified state 1 to "angulated *at base*", to clarify that this state does not apply to taxa in which the stapedial shaft is generally straight but is slightly curved distally near its articulation with the quadrate (e.g., *Boa*, *Naja*).

143. ### Stapedial shaft, length relative to diameter of stapedial footplate: distinctly longer than (0); equal to or shorter than (1). [T00:61] [G19a:76]

a. Modifications: Modified character to "Stapedial shaft*, length relative to diameter of stapedial footplate*" (i.e., moved qualifier from character states to character)

and simplified character states to "*distinctly longer than* (0); *equal to or shorter than* (1)".

SUPRATEMPORAL

144. Supratemporal: present (0); absent (1). [T00:38] [G19a:52]

145. * Supratemporal, size relative to dorsal terminus of quadrate: distinctly larger than (0); subequal to or smaller than (1).** [LS02:69]

a. Character remarks: NEW. Reduction of the supratemporal occurs in several squamate groups (e.g., scolecophidians, dibamids, uropeltids). Reduction in size of the supratemporal forms a separate character—rather than simply being added to character 144 as part of a "vestigial or absent" state—because, although the supratemporal may be reduced in some taxa, it still bears useful information. For example, the supratemporal of *Atractaspis* is quite reduced relative to other colubroids, but still bears a free-ending posterior process as in other 'macrostomatans'. If "reduced" were to be lumped into a state alongside "absent", this information would not be incorporated into this dataset. Thus, in order to include as much comparable information as possible, presence/absence and size of the supratemporal therefore form separate characters.

146. ### Supratemporal, anterior terminus, position relative to posterior border of trigeminal foramen or notch: behind or above (0); distinctly anterior to (1). [T00:40] [G19a:49]

a. Modifications: Character modified to "*Supratemporal,* anterior *terminus*, *position relative to posterior border of trigeminal foramen or notch*" (i.e., reversed locators and added variable) and simplified wording of character states. Modified state 1 to "*distinctly* anterior to" to aid in scoring this state consistently, particularly in differentiating it from the condition of the anterior terminus being dorsal to the posterior trigeminal border. Added "trigeminal notch" as an alternative landmark, to recognize the condition in non-snake lizards.

147. ### Supratemporal, free-ending posterior process: absent (0); present (1). [T00:39] [G19a:51]

a. Modifications: Modified character to "*Supratemporal,* free-ending posterior process" (i.e., reversed locators).

148. ### Supratemporal, free-ending posterior process, length relative to level of occiput: short, does not extend distinctly posterior to (0); elongate, extends well beyond (1). [L12:175] [G19a:172]

a. Modifications: Modified character to "Supratemporal*, free-ending posterior process, length relative to level of occiput*" (i.e., added variable, qualifier, and primary locator) and modified wording of character states accordingly. Modified state 0 to "short, does not extend *distinctly* posterior to", to aid in scoring this state consistently. Modified landmark to "level of occiput" (formerly "paroccipital process") so that this character can still apply to taxa that do not have a distinct paroccipital process.

149. ### Supratemporal, free-ending posterior process, orientation: posteroventral (0); posterior or posterodorsal (1). [L12:193] [G19a:187]

a. Modifications: Modified character to "Supratemporal, *free-ending posterior process*, *orientation*" (i.e., added variable and primary locator) and simplified wording of character states.

SQUAMOSAL

150. * Squamosal: present (0); absent (1).**

a. Character remarks: NEW. This character was added to reflect a commonly-recognized synapomorphy of snakes (i.e., state 1, squamosal "*absent*") (see also Strong *et al.* 2021b).

CRISTA CIRCUMFENESTRALIS

151. * Juxtastapedial recess defined by a crista prootica, crista tuberalis and crista interfenestralis: absent (0); present (1).** [T00:74, LS02:135]

a. Character remarks: NEW; see next character.

152. ### Juxtastapedial recess defined by a crista prootica, crista tuberalis and crista interfenestralis, extent of enclosure: partially enclosed (i.e., 'incipient' crista

circumfenestralis) (0); fully enclosed (i.e., fully developed crista circumfenestralis) (1). [T00:74, LS02:135] [G19a:78]

a. Modifications: Modified character to "Juxtastapedial *recess* defined by a crista prootica, crista tuberalis and crista interfenestralis*, extent of enclosure*" (i.e., added variable). Modified terminology from "juxtastapedial space" to "juxtastapedial *recess*" (see comment below). Removed state 0 ("absent") of G19a:78, modified states 1–2 of G19a:78 to "*partially enclosed*…" and "*fully enclosed*…", respectively, and created a separate character (character 151) for presence/absence of the juxtastapedial recess—as argued by Sereno (2007), "neomorphic characters" (i.e., presence/absence) should not be mixed with "transformational characters" (e.g., qualitative-form characters such as extent of enclosure or development).

b. Character remarks: As per Palci & Caldwell (2014), the "juxtastapedial space" refers to the region occupied by the fenestra ovalis and lateral aperture of the recessus scalae tympani, regardless of the extent of development of a bony enclosure around these openings (i.e., the 'crista circumfenestralis'); in contrast, the "juxtastapedial recess" indicates the presence of a partial or complete bony enclosure.

c. Scoring remarks: In state 1 ("fully enclosed…"), the entire margin of the stapedial footplate is inset within the prootic and otoccipital. In state 0 ("partially enclosed…"), at least part of the margin of the stapedial footplate is level with the external surface of the braincase.

153. ### Crista interfenestralis, presence as individualized component around the juxtastapedial space: present (0); absent (1). [R02:36] [G19a:80]

a. Modifications: Modified character to "Crista interfenestralis*, presence as individualized component around the juxtastapedial space*" (i.e., added variable) and simplified wording of character states. Reversed order of character states from R02:36 / G19a:80, as plesiomorphically among squamates the cristae interfenestralis, tuberalis, and prootica are each distinct (Rieppel & Zaher 2001b; Palci & Caldwell 2014).

b. Character remarks: As per Palci & Caldwell (2014), the "juxtastapedial space" refers to the region occupied by the fenestra ovalis and lateral aperture of the recessus scalae tympani, regardless of the extent of development of a bony enclosure around these openings (i.e., the "crista circumfenestralis"); in contrast, the "juxtastapedial recess" indicates the presence of a partial or complete bony enclosure.

154. ### Crista tuberalis, shape: distinctly-projecting vertical flange (0); small crest or pillar, sometimes bearing bulbous knob at base (1); horizontal, wing-like process (2). [L12:204] [G19a:196]

a. Modifications: Modified character to "*Crista tuberalis, shape*" (i.e., re-formatted character from neomorphic to transformational *sensu* Sereno 2007). Modified character states to "*distinctly-projecting vertical flange* (0); *small crest or pillar, sometimes bearing bulbous knob at base* (1); horizontal, wing-like *process* (2)".

b. Character remarks 1: This character was originally constructed by Longrich *et al.* (2012:character 204) to reflect the horizontal, wing-like crista tuberalis of many madtsoiids. However, although "presence" of this condition is informative, scoring this condition as simply "absent" is not, as not all "non-horizontal/wing-like" conditions are the same. Therefore, states 0 ("*distinctly-projecting vertical flange*") and 1 ("*small crest or pillar…*") have been added to encapsulate the observed variation across squamates.

c. Character remarks 2: Although state 1 ("*small crest or pillar…*") is related to character 155 ("Jugular foramen, exposure in lateral view"), these are not redundant. For example, in both *Varanus* and *Boa*, the jugular foramen is concealed in lateral view; however, only *Varanus* exhibits the distinct flange-like condition of the crista tuberalis described by state 0 of the present character.

155. ### Jugular foramen, exposure in lateral view: exposed (0); concealed by crista tuberalis (1). [R02:37] [G19a:81]

a. Modifications: Modified character to "Jugular foramen*, exposure in lateral view*" (i.e., added variable) and simplified wording of character states.

OTOCCIPITAL

156. ### Otoccipitals, contact dorsal to foramen magnum: absent (0); present (1). [LS02:141] [G19a:82]

a. Modifications: Modified character to "Otoccipitals*, contact dorsal to foramen magnum*" (i.e., added variable) and simplified wording of character states.

157. * Otoccipital, paroccipital process: present (0); absent (1).** [LS02:137]

a. Character remarks: NEW; see next character.

158. ### Otoccipital, paroccipital process, length relative to level of occiput: long, extending to or well beyond (0); short, terminating anterior to (1). [LS02:137] [G19a:77]

a. Modifications: Modified character to "*Otoccipital,* paroccipital process, *length relative to level of occiput*" (i.e., reversed locators and added variable and qualifier). Modified character states to "*long, extending to or well beyond* (0); short*, terminating anterior to* (1)" to enable consistent scoring. Removed "absent" from state 1 of G19a:77 and created a separate character (character 157) for presence/absence of the paroccipital process—as argued by Sereno (2007), "absent" is not a measurement, and more broadly "neomorphic characters" (i.e., presence/absence) should not be mixed with "transformational characters" (e.g., quantitative-relative/linear characters such as length).

159. ### Opisthotic-exoccipital, supratemporal facet, shape: flat (0); sculptured and delineated (1). [R02:31] [G19a:50]

a. Modifications: Modified character to "*Opisthotic-exoccipital,* supratemporal facet*, shape*" (i.e., reversed locators and added variable). Simplified state 1 to "sculptured and delineated" (i.e., removed descriptor "with projecting posterior rim that overhangs exoccipital"); from my observations, the main distinction in the form of this facet occurs between the flat condition typical of non-snake lizards and the sculptured condition of most snakes, whereas a 'sculptured facet without a posteriorly projecting rim' is not greatly different from a 'sculptured facet with a posteriorly projecting rim'. As such, I considered it reasonable to modify this state to focus on the former distinction, rather than the latter.

b. Scoring remarks: If the supratemporal is absent, this character should be scored as "inapplicable".

PROOTIC

160. ### Prootic, fusion to braincase: absent, occurs as separate element (0); present (1). [G19a:247] [G19a:247]

a. Modifications: Modified character to "Prootic*, fusion to braincase*" (i.e., added variable) and re-worded character states to "*absent, occurs as* separate element (0); *present* (1)".

161. Prootic, exclusion of parietal from trigeminal foramen: absent (0); present (1). [T00:70] [G19a:85]

a. Scoring remarks: This character should be scored as "inapplicable" when the trigeminal foramen does not have an osseous anterior border (i.e., when it occurs as the trigeminal notch, as in non-snake lizards). This is consistent with the original scoring of this character by LS02:132.

162. Laterosphenoid: absent (0): present (1). [T00:65] [G19a:86]

163. ### Prootic, posteriorly undercut ledge underlapping trigeminal foramen or notch: absent (0); present (1). [R02:29] [G19a:87]

a. Modifications: Modified character to "Prootic*, posteriorly undercut* ledge *underlapping* ~~posterior~~ trigeminal foramen *or notch*" (i.e., clarified primary locator), based on R02:29. Added "trigeminal notch" as an alternative landmark, to recognize the condition in non-snake lizards.

164. ### Prootic, exposure in dorsal view: exposed medial to supratemporal or to supratemporal process of parietal (0); fully concealed by supratemporal or parietal (1). [T00:66] [G19a:88]

a. Modifications: Modified character to "Prootic*, exposure in dorsal view*" (i.e., added variable) and simplified wording of character states accordingly.

b. Scoring remarks: In order for this character to be scored, the prootic must participate in the dorsal surface of the skull, either the supratemporal or the supratemporal process of the parietal must be present, and the prootic must form a

distinct element (i.e., not be fused to any other braincase element). If any of these conditions are not met, this character should be scored as "inapplicable".

165. ### Facial nerve, hyomandibular branch, exit foramen, location relative to opening for mandibular branch of trigeminal nerve: outside (0); inside (1). [T00:67] [G19a:89]

a. Modifications: Modified character to "*Facial nerve, hyomandibular branch,* exit *foramen, location relative to opening for mandibular branch of trigeminal nerve*" (i.e., re-arranged locators and clarified variable) and modified character states to "*outside* (0); *inside* (1)".

SUPRAOCCIPITAL

166. * Supraoccipital: present (0); absent or fused to braincase (1).** [G19a:236] [G19a:236]

a. Character remarks: NEW, modified from state 5 in G19a:236.

167. ### Supraoccipital(s), fusion in adult skull: unfused/paired (0); fused/single (1). [G19a:246] [G19a:246]

a. Modifications: Modified character to "Supraoccipital*(s)*, *fusion in adult skull*" (i.e., added variable) and modified wording of character states to "*unfused/*paired (0); *fused/*single (1)". Reversed order of character states from G19a:246, as "unfused/paired" is typically considered the plesiomorphic condition for paired *versus* fused skull elements (e.g., List 1966:8–9).

168. * Supraoccipitals, medial contact: present (0); absent, supraoccipitals separated by distinct gap or fontanelle medially (1).**

a. Character remarks: NEW. This character was added based on the large dorsal fontanelle in the skull of some scolecophidians (e.g., *Myriopholis*). This feature was also noted by Lira & Martins (2021) as being potentially useful for systematic analyses of typhlopoids.

b. Scoring remarks: If the supraoccipitals are fused, this character should be scored as "inapplicable", as the fontanelle which this character reflects can only occur if the supraoccipitals are separate (or vice versa: if the supraoccipitals are

unpaired/fused, then inherently they are in medial contact, making these characters redundant in the case of fusion).

169. * Supraoccipital, participation in formation of osseous labyrinth: present (1); absent (0).**

a. Character remarks: NEW. State 1 ("*absent*") of this character reflects a synapomorphy of anomalepidids, as proposed by Rieppel *et al.* (2009).

170. ### Supraoccipital, contact with prootic, width: narrow (i.e., less than half supraoccipital-parietal contact) (0); broad (i.e., subequal to or greater than half supraoccipital-parietal contact) (1). [T00:62] [G19a:84]

a. Modifications: Modified character to "Supraoccipital, contact with prootic*, width*" (i.e., added variable). Modified character states to "narrow *(i.e., less than half supraoccipital-parietal contact)* (0)" (similar to e.g., LS02:140) and "broad *(i.e., subequal to or greater than half supraoccipital-parietal contact)* (1)". This latter qualifier in state 1 is somewhat different than in LS02:140.

b. Scoring remarks: As noted by Lee & Scanlon (2002:character 140), this character is inapplicable when the supraoccipital meets the ventral aspect of the parietal (e.g., varanoids) and when the prootic does not occur as a separate element (e.g., *Amphisbaena*).

171. ### Supraoccipital, dorsal exposure, size expressed as ratio of exposed supraoccipital length (measured at the midline) to parietal width (measured at the line delimited by the anterior borders of the prootic): large, ratio of 0.5 or more (0); small, ratio clearly less than 0.5 (1). [G19b:247] [G19a:237]

a. Modifications: Modified character to "Supraoccipital*, dorsal exposure, size expressed as…*" (i.e., separated variable from primary locator). Changed qualifier to "…ratio of *exposed* supraoccipital length…", to clarify how to measure this feature.

BASIOCCIPITAL

172. * Basioccipital, fusion to parabasisphenoid: unfused, occur as separate elements (0); fused (1).** [L93:A5]

a. Character remarks: NEW. This character was added based on the suggestion by Lira & Martins (2021) that it may be a useful character for typhlopoid systematics. More broadly, it is also useful in encapsulating the variation in braincase fusion that occurs throughout squamates (see also Simões *et al.* 2018, Supplementary Information p. 73).

173. * Basioccipital, fusion to exoccipital: unfused (0); fused (1).** [S18:132]

a. Character remarks: NEW. This character was introduced by Simões *et al.* (2018), and was added herein to encapsulate the variation in braincase fusion that occurs throughout squamates (see also Simões *et al.* 2018, Supplementary Information p. 73).

174. * Basioccipital, posterolateral processes: present (0); absent (1).**

a. Character remarks: NEW. The absence of the posterolateral processes has been recovered previously as a condition relevant to scolecophidians (Caldwell *et al.*, unpublished data).

175. ### Basioccipital, posterolateral processes, form: short and narrow, do not extend toward posterior margin of occipital condyle (0); wider than condyle and long, combine with crista tuberalis to extend to approximate posterior margin of occipital condyle (1). [LS02:122, W10:57, ZS12:85] [G19a:83]

a. Modifications: Modified character to "Basioccipital, posterolateral processes*, form*" (i.e., added variable).

b. Scoring remarks: As noted by Wilson *et al.* (2010:character 57), state 1 applies to *Wonambi*, *Yurlunggur*, and *Sanajeh*; it also occurs in *Anilius*, reflected in Lee & Scanlon (2002:fig. 9D). See Rieppel *et al.* (2002:fig. 6) for the condition in *Wonambi*, Lee & Scanlon (2002:fig. 9E–F) for examples of state 0 ("short and narrow…"), and Lee & Scanlon (2002:fig. 9D) for an example of state 1 ("wider than condyle and long…").

176. ### Basioccipital, contribution to ventral margin of foramen magnum: present (0); absent, excluded by medial contact of otoccipitals (1). [LS02:142] [G19a:95]

a. Modifications: Modified character to "Basioccipital*, contribution to ventral margin of foramen magnum*" (i.e., added variable) and simplified wording of

character states to "*present* (0); *absent,* excluded by medial contact of otoccipitals (1)".

b. Scoring remarks: If the basioccipital is fused to the exoccipitals, this character should be scored as "inapplicable".

177. ### Basioccipital, contribution to floor of recessus scalae tympani: present (0); absent, excluded by otoccipital / opisthotic (1). [ZS12:149] [G19a:147]

a. Modifications: Modified character to "Basioccipital*, contribution to floor of recessus scalae tympani*" (i.e., added variable) and simplified wording of character states to "*present* (0); *absent,* excluded by otoccipital */ opisthotic* (1)".

b. Scoring remarks: This character should be scored as "inapplicable" if the basioccipital is fused to the opisthotic (or the opisthotic component of the otoccipital).

PARABASISPHENOID

178. ### Vidian canal, intracranial opening: absent (0); present, Vidian canal emerging on internal surface of sphenoid then emerging externally on sphenoid-parietal suture (1). [LS02:124, R02:17] [G19a:90]

a. Modifications: Modified character to "Vidian canal*, intracranial opening*" (i.e., added primary locator) and modified wording of character states to "*absent* (0); *present, Vidian canal emerging on internal surface of sphenoid then emerging externally on sphenoid-parietal suture* (1)". Added description of state 1 from LS02:124.

179. ### Vidian canal, anterior opening (secondary anterior opening *sensu* Rieppel 1979b, where present), division: single (0); divided (1). [R02:18] [G19a:91]

a. Modifications: Modified character to "*Vidian canal,* anterior opening *(secondary anterior opening sensu Rieppel 1979, where applicable), division*" (i.e., reversed locators and added variable). Added reference to Rieppel (1979b) as per original character (R02:18).

180. ### Vidian canals, posterior openings, symmetry: symmetrical (0); asymmetrical, left larger than right or vice versa (1). [LS02:125] [G19a:195]

a. Modifications: Modified character to "Vidian canals*, posterior openings, symmetry*" (i.e., added variable and primary locator). Removed "posterior openings" from state 0 and modified state 1 to "asymmetrical, *left larger than right or vice versa*", as per LS02:125.

181. * Dorsum sellae (= crista sellaris): present (0); absent (1).** [R02:20]

a. Character remarks: NEW; see next character.

182. ### Dorsum sellae (= crista sellaris), prominence: prominent crest (0); low transverse ridge (1). [LS02:128, R02:20] [G19a:92]

a. Modifications: Modified character to "*Dorsum sellae (= crista sellaris), prominence*" (i.e., changed primary locator and added variable). Modified wording of character states to "*prominent crest* (0); low *transverse ridge* (1)", following the description of the dorsum sellae by Lee & Scanlon (2002:365). Added "crista sellaris" as a synonym for dorsum sellae, as per LS02:128. Removed state 2 ("dorsum sellae not developed, sella turcica with shallow posterior margin") of G19a:92 and created a separate character (character 181) for presence/absence of the dorsum sellae—as argued by Sereno (2007), "neomorphic characters" (i.e., presence/absence) should not be mixed with "transformational characters" (e.g., qualitative-form characters such as size).

183. * Parabasisphenoid, ventral surface, sagittal crest: absent (0); present (1).** [T00:77]

a. Character remarks: NEW; see next character.

184. ### Parabasisphenoid, ventral surface, sagittal crest, prominence: weakly developed (0); strongly projecting (1). [T00:77] [G19a:94]

a. Modifications: Modified character to "*Parabasisphenoid,* ventral surface*, sagittal crest, prominence*" (i.e., reversed secondary locators and added variable and primary locator). Removed state 0 ("smooth") of G19a:94 and created a separate character (character 183) for presence/absence of the parabasisphenoid sagittal crest—as argued by Sereno (2007), "neomorphic characters" (i.e., presence/absence) should not be mixed with "transformational characters" (e.g., qualitative-form characters such as size).

185. ### Parabasisphenoid, ventral surface, sagittal crest, extension onto basioccipital: absent, ventral surface of basioccipital smooth (0); present (1). [W10:54, G19b:239] [G19a:230]

a. Modifications: Modified character to "*Parabasisphenoid*, ventral surface*, sagittal crest, extension onto basioccipital*" (i.e., re-formulated character to focus on the parabasisphenoid sagittal crest as the main locator, rather than the basioccipital) and modified wording of character states to "*absent, ventral surface of basioccipital* smooth (0); *present* (1)".

b. Scoring remarks: This character can only be scored if the sagittal crest of the parabasisphenoid is present.

186. ### Basipterygoid (= basitrabecular) processes: present (0); indistinct or absent (1). [T00:82] [G19a:97]

a. Modifications: Modified state 1 to "*indistinct or* absent"; some taxa (e.g., *Naja*) exhibit slight ventrolateral ridges on the ventral surface of the parabasisphenoid, but these are very minimal and are not sufficient to warrant a "present" condition for the basipterygoid processes.

b. Character remarks: See Lee & Scanlon (2002:365) for comments on the homology of these processes in snakes *versus* non-snake lizards.

187. * Basipterygoid (= basitrabecular) processes, dimensions: very elongate, as long as body of parabasisphenoid is wide in ventral view (0); short, length relatively equal to width (1); broad, forming distinct projections but much wider than long (2); very low, forming very broad facets on ventral surface of parabasisphenoid (3).** [T00:82]

a. Character remarks 1: NEW. This character was added to encapsulate the variation in the basipterygoid processes across squamates, beyond simply their presence *versus* absence (see e.g., Strong *et al.* 2021b), and is an expansion of earlier characters (e.g., T00:82, LS02:117) which also incorporated prominence of the basipterygoid processes.

b. Character remarks 2: See Lee & Scanlon (2002:365) for comments on the homology of these processes in snakes *versus* non-snake lizards.

188. * Basipterygoid (= basitrabecular) processes, articulation with pterygoids, extent of integration: tight, closely applied to dorsal surface of pterygoid (0); loose, broadly separate from pterygoid (1).**

a. Character remarks 1: NEW. This character was added to reflect differences in the extent to which the pterygoids are 'braced' by the basipterygoid processes, which in turn reflects functional differences in palatomaxillary arch mobility.

b. Character remarks 2: See Lee & Scanlon (2002:365) for comments on the homology of these processes in snakes *versus* non-snake lizards.

189. ### Parabasisphenoid, rostroventral surface, concavity: flat or broadly convex (0); concave (1). [LS02:116] [G19a:101]

a. Modifications: Modified character to "Parabasisphenoid, rostroventral surface*, concavity*" (i.e., added variable).

190. ### Parabasisphenoid-basioccipital suture, position: closer to level of fenestra ovalis (0); closer to level of trigeminal foramen/notch (1). [T00:78] [G19a:102]

a. Modifications: Modified character to "*Parabasisphenoid-basioccipital suture, position*" (i.e., clarified locator and variable). Modified wording of character states to "*closer to* level of fenestra ovalis (0); *closer to level of* trigeminal foramen*/notch* (1)" for clarity, particularly in taxa in which the suture in somewhere between these landmarks. Removed state 2 ("basioccipital and parabasisphenoid fused") of G19a:102 and created a separate character (character 172) for fusion of these elements; fusion is a separate variable than the position of a suture, as it concerns the fundamental existence of those elements as separate structures rather than any condition they exhibit when separate, and so should be treated separately.

b. Scoring remarks: If character 172 ("Basioccipital, fusion to parabasisphenoid") is scored as state 1 ("*fused*"), then the present character should be scored as "inapplicable".

191. ### Parabasisphenoid-basioccipital suture, transverse cresting: absent, suture smooth (0); present (1). [R02:23] [G19a:96]

a. Modifications: Modified character to "*Parab*asisphenoid-basioccipital suture*, transverse cresting*" (i.e., added primary locator) and modified wording of character states to "*absent, suture* smooth (0); *present* (1)".
b. Scoring remarks: If character 172 ("Basioccipital, fusion to parabasisphenoid") is scored as state 1 ("*fused*"), then the present character should be scored as "inapplicable".

192. ### Crista trabeculares, size in lateral view: short and/or indistinct (0); elongate and distinct (1). [R02:25] [G19a:98]

a. Modifications: Modified character to "Crista trabeculares*, size in lateral view*" (i.e., added variable) and removed "in lateral view" from state 1.

193. ### Parabasisphenoid, cultriform process (= parasphenoid rostrum), anterior extension: does not extend anteriorly to approach posterior margin of choanae (0); approaches posterior margin of vomer (1). [W10:59] [G19a:99]

a. Modifications: Modified character to "*Parabasisphenoid,* cultriform process *(= parasphenoid rostrum), anterior extension*" (i.e., reversed locators and added variable). Added "parasphenoid rostrum" as a synonym for cultriform process.

194. ### Parabasisphenoid, cultriform process (= parasphenoid rostrum), width behind optic foramen: extremely narrow, as tall or taller than it is wide (0); moderate, distinctly narrower than main body of parabasisphenoid (1); broad, no abrupt constriction at base relative to main body (2). [T00:81] [G19a:100]

a. Modifications: Modified character to "Parabasisphenoid*, cultriform process (= parasphenoid* rostrum*), width* behind optic foramen" (i.e., clarified variable). Added "parasphenoid rostrum" as a synonym for cultriform process. Modified character states to "*extremely narrow, as tall or taller than it is wide (0)*; *moderate, distinctly narrower than main body of parabasisphenoid* (1); broad*, no abrupt constriction at base relative to main body* (2)" (i.e., added descriptors to clarify each state, and separated the original state 0—"narrow"—into "*extreme*" and "*moderate*", so as to more accurately encapsulate variation across snakes).

195. ### Parabasisphenoid, cultriform process (= parasphenoid rostrum), interchoanal process (= interchoanal keel): absent (0); present, sagittal flange projecting ventrally from parasphenoid rostrum (1). [T00:80, LS02:115] [G19a:103]

a. Modifications: Modified character to *Parabasisphenoid, cultriform process (=* parasphenoid rostrum*)*, interchoanal process *(= interchoanal keel)*" (i.e., added secondary locator). Modified state 1 to "*present, sagittal flange projecting ventrally from parasphenoid rostrum*", based on LS02:115. Added "cultriform process" as a synonym for parasphenoid rostrum and "interchoanal keel" as a synonym for interchoanal process. Replaced states 1 ("broad") and 2 ("narrow") of previous versions of this character (e.g., T00:80, G19a:103) with simply "*present…*"—as argued by Sereno (2007), "neomorphic characters" (i.e., presence/absence) should not be mixed with "transformational characters" (e.g., quantitative-relative/linear characters such as width).

b. Character remarks: As noted by LS02:115, the meaning of "broad/broad-based" *versus* "narrow/narrow-based" is rather unclear, and I could not see consistent differences that aligned with how this variable was scored in previous datasets. As such, I have removed this variable entirely (i.e., have not added a separate character for it), instead focussing solely on presence/absence of the interchoanal keel, as in LS02:115.

196. ### Parabasisphenoid, 'lateral wings' (= sphenoid wings; triangular dorsolateral prominence lateral to alar=clinoid process of dorsum sellae): absent (0); present, extending up anterior margin of prootic below trigeminal notch (1). [T00:79, LS02:119] [G19a:93]

a. Modifications: Modified character to "*Parabasisphenoid,* 'lateral wings' *(= sphenoid wings; triangular dorsolateral prominence lateral to alar=clinoid process of dorsum sellae)*" (i.e., reversed locators). Added latter synonym and description, as well as additional description in state 1 ("present*, extending up anterior margin of prootic below trigeminal notch*"), from the character description of LS02:119.

197. ### Parabasisphenoid, posterolateral corners, form: strongly ventrolaterally projected (0); not projected (1). [ZS12:148] [G19a:146]

a. Modifications: Modified character to "*Parabasisphenoid,* posterolateral corners*, form*" (i.e., reversed locators and added variable).

b. Scoring remarks: If character 172 ("Basioccipital, fusion to parabasisphenoid") is scored as state 1 ("*fused*"), then the present character should be scored as "inapplicable".

MISCELLANEOUS

198. ### Skull, supraoccipital region, nuchal crests: absent (0); present (1). [G12:300] [G19a:171]

a. Modifications: Modified character to "*Skull,* supraoccipital region*, nuchal crests*" (i.e., reversed secondary locators and added primary locator) and removed "nuchal crests" from state 0.

199. Sclerotic ring: present (0); absent (1). [L98:222] [G19a:198]

MANDIBLE

DENTARY

200. * Dentary, dental concha: absent (0); present (1).**

a. Character remarks: NEW. This character reflects the unique structure of the dentary in leptotyphlopids. As described by Kley (2006), the dental concha is a prominently expanded structure bearing the dentary teeth, unique to leptotyphlopids (see also Strong *et al.* 2021b).

201. ### Dentary, anteromedial margin, symphyseal articular facet: present (0); absent, dentary tips smoothly rounded (1). [L97:68, W10:86] [G19a:104]

a. Modifications: Modified character to "*Dentary,* anteromedial margin*, symphyseal articular facet*" (i.e., reversed secondary locators and moved primary locator from character states to character) and modified wording of character states to "*present* (0); *absent, dentary tips smoothly rounded* (1)".

202. * Dentary, symphysis, symphyseal process: absent (0); present (1).**

a. Character remarks: NEW. This character reflects the unique symphyseal structure of leptotyphlopids, which bear a prominent anteromedial process (i.e., the symphyseal process, *sensu* Kley 2006) at the anterior terminus of each dentary (see also Strong *et al.* 2021b).

203. ### Dentary, symphysis, orientation: weakly projecting medially (0); hooked inward and strongly projecting medially (1). [G12:356, L12:211] [G19a:203]

a. Modifications: Modified character to "Dentary, symphysis*, orientation*" (i.e., added variable).

204. * Dentary, angular (= posteroventral) process: present (0); absent (1).**

a. Character remarks: NEW. This character was added to reflect the condition in typhlopoids, leptotyphlopids, uropeltids, and some non-snake lizards (e.g., *Physignathus*), in which the posteroventral/angular process of the dentary (i.e., the process extending posteriorly underneath the compound bone / surangular and coronoid) is absent, rendering subsequent characters involving this process inapplicable (see also Strong *et al.* 2021b).

205. * Dentary, coronoid (= posterodorsal) process: present (0); absent (1).**

a. Character remarks: NEW. This character was added to reflect the condition in anomalepidids, in which the posterodorsal/coronoid process of the dentary (i.e., the process extending posteriorly dorsal to the compound bone / surangular and coronoid) is absent, rendering subsequent characters involving this process inapplicable (see also Strong *et al.* 2021b).

206. ### Dentary, angular (= posteroventral) process, length relative to coronoid (= posterodorsal) process: longer or subequal in length posteriorly (0); distinctly shorter, terminating well anterior to the coronoid/posterodorsal process (1). [LS02:150] [G19a:202]

a. Modifications: Added "posteroventral process" as a synonym for angular process and "posterodorsal process" as a synonym for coronoid process. Simplified wording of character states and added "longer" to state 0. Reversed order of character states from G19a:202, as "subequal in length posteriorly" is the outgroup condition.

b. Character remarks: This character is similar to character 208 ("Dentary, posterior dentigerous process, length"), but not redundant: the current character is applicable regardless of whether the posterior dentigerous process is present/absent (i.e., regardless of whether the coronoid/posterodorsal process bears teeth), and taxa may have a "long" dentigerous process but an angular process that is subequal in length to the coronoid process (e.g., *Boa*).

c. Scoring remarks: If either the angular (= posteroventral) process or the coronoid (= posterodorsal) process are absent, this character should be scored as "inapplicable".

207. * Dentary, posterior dentigerous process: absent (0); present (1).** [T00:87, R02:38]

a. Character remarks: NEW; see next character.

b. Scoring remarks: This character should be scored as "present" when the coronoid (= posterodorsal) process of the dentary bears teeth. If the coronoid/posterodorsal process is absent (character 205), this character should be scored as "inapplicable".

208. ### Dentary, posterior dentigerous process, length: short, teeth do not extend to posterior terminus of coronoid (= posterodorsal) process (0); long, teeth extend to posterior terminus of coronoid (= posterodorsal) process (1). [R02:38] [G19a:105]

a. Modifications: Modified character to "*Dentary,* posterior dentigerous process*, length*" (i.e., reversed locators and added variable). Removed state 0 ("absent") of G19a:105, removed "present" from the other states, and created a separate character (character 207) for presence/absence of the posterior dentigerous process—as argued by Sereno (2007), "neomorphic characters" (i.e., presence/absence) should not be mixed with "transformational characters" (e.g., quantitative-relative/linear characters such as length). Modified character states to "short*, teeth do not extend to posterior terminus of coronoid (= posterodorsal) process* (0); long*, teeth extend to posterior terminus of coronoid (= posterodorsal) process* (1)" (i.e., added qualifiers to enable consistent scoring).

209. ### Dentary, coronoid (= posterodorsal) process, position relative to surangular: wraps around surangular laterally and medially (0); sits atop surangular (1). [L12:213] [G19a:205]

a. Modifications: Modified character to "Dentary, coronoid *(= posterodorsal)* process*, position relative to surangular*" (i.e., added variable). Added "posterodorsal process" as a synonym for coronoid process. Simplified state 1 to "~~broad and~~ sits atop surangular", so as to focus on the position of the coronoid process rather than its shape.

210. ### Dentary, coronoid (= posterodorsal) process, slot for medial tab of surangular: absent (0); present, forming distinct slot ventromedial to tooth row (1). [L12:214] [G19a:206]

a. Modifications: Modified character to "Dentary, coronoid *(= posterodorsal)* process*, slot for medial tab of surangular*" (i.e., separated variable from primary locator). Added "posterodorsal process" as a synonym for coronoid process. Added descriptor ("*forming distinct slot ventromedial to tooth row*") to state 1, based on the original character description of Longrich *et al.* (2012:character 214), to aid in identifying this feature.

211. ### Dentary, ventral margin, medial expansion: unexpanded, medial margin straight in ventral view (0); expanded, medial margin crescentic in ventral view and wrapping underneath Meckelian groove (1). [L12:212] [G19a:204]

a. Modifications: Modified character to "Dentary, ventral margin*, medial expansion*" (i.e., added variable) and slightly simplified wording of character states. Added "*and wrapping underneath Meckelian groove*" as a descriptor for state 1, based on the original character description of Longrich *et al.* (2012:character 212), to aid in identifying this feature.

212. ### Dentary, lateral surface, mental foramina, number: two or more (0); one (1); none (2). [LS02:148] [G19a:107]

a. Modifications: Modified character to "*Dentary, lateral surface,* mental foramina*, number*" (i.e., re-arranged locators and added variable). Added state 2 ("*none*") to

reflect the condition among some snakes (e.g., some scolecophidians, see Caldwell 2019; *Atractaspis*, see Strong *et al.* 2021a).

b. Character remarks: According to Sereno (2007), absence/presence constitutes a "neomorphic character" that should be treated separately from "transformational" character states such as number (e.g., Sereno 2007:table 8). Following these guidelines for the present character, the absence/presence of the mental foramina and the number of mental foramina should therefore be separate characters, and state 2 herein should be removed. However, although I largely agree with Sereno (2007), I disagree with his contention that absent ≠ zero; instead, I consider it reasonable to include absence (or zero) as part of a count-based character such as this one.

213. ### Dentary, enlarged mental foramen near tip or middle of jaw: absent (0); present (1). [L12:207] [G19a:199]

a. Modifications: Modified character to "Dentary, enlarged mental foramen *near tip or middle of jaw*", based on the remarks of L12:207.

b. Scoring remarks: If character 212 ("Dentary, lateral surface, mental foramina, number") is scored as state 2 ("*none*"), then this character should be scored as "inapplicable".

214. * Dentary, length relative to length of mandible excluding retroarticular process: short, <50% (0); long, 50–80% (1); very long, >80% (2).** [LS02:147]

a. Character remarks: NEW, adapted from LS02:147. This character was added to reflect the variation that occurs among scolecophidians, as anomalepidids and typhlopoids exhibit state 0 ("*short, <50%*"), whereas leptotyphlopids exhibit state 1 ("*long, 50–80%*"). Following the approach recommended by Simões *et al.* (2017), these character states were determined by recording the value of this variable for each taxon, plotting these values, and looking for breaks in the resulting distribution. In this case, the observed distribution is slightly different than the original character states in LS02:147, as these authors used a cut-off of 40% to define a "long" *versus* "short" dentary.

SPLENIAL

215. * Splenial: present (0); absent or fused (1).** [G88:67]

a. Character remarks: NEW. This character was added to reflect the absence of the splenial as a distinct element in some squamates (see overview of squamate jaw anatomy in Strong *et al.* 2021b).

216. ### Splenial, articulation with angular, configuration: overlaps angular (0); abuts against angular to form hinge joint (1). [P86, G12:377] [G19a:213]

a. Modifications: Modified character to "Splenial*, articulation with angular, configuration*" (i.e., added variable and primary locator) and simplified wording of character states accordingly.

217. ### Splenial, articulation with dentary dorsal to Meckel's canal, proximity: close throughout length (0); loose, with dorsal dentary suture confined to posterodorsal corner of splenial (1); reduced to point contact or lost entirely (2). [P86, L12:222] [G19a:212]

a. Modifications: Modified character to "Splenial, *articulation with* dentary *dorsal to* Meckel's canal, *proximity*" (i.e., re-worded primary locator and added variable). Modified wording of state 2 to "reduced to *point contact* or lost entirely", to help distinguish this condition from state 1.

b. Character remarks: Although "contact highly reduced or lost" as encapsulated by state 2 may appear equivalent to an "absent" condition for this character—suggesting based on Sereno (2007) that there should be a separate character for presence/absence of this articulation—I do not consider the presence/absence of an articulation or contact between elements to be a truly "neomorphic" phenomenon (unlike presence/absence of an element or structure itself). Therefore, "no articulation" can remain incorporated into this character.

218. ### Splenial, length relative to distance from posterior terminus to dentary symphysis: short to moderate, <75% (0); elongate, >75% (1). [E88:65] [G19a:214]

a. Modifications: Modified character to "Splenial, *length relative to distance from posterior terminus to dentary symphysis*" (i.e., changed variable from "size" to "length", slightly modified qualifier, and moved qualifier from character states to

character). Modified character states to "*short to moderate, <75%* (0); *elongate, >75%* (1)."

b. Character remarks 1: The qualifier was changed from "distance from angular to dentary symphysis" to "distance from posterior terminus of splenial to dentary symphysis" because, in some squamates (e.g., *Varanus*), the splenial overlaps the angular, such that the anterior terminus of the angular does not necessarily correspond to the posterior terminus of the splenial.

c. Character remarks 2: Following the approach recommended by Simões *et al.* (2017), the current character states were determined by recording the value of this variable for each taxon, plotting these values, and looking for breaks in the resulting distribution. In this case, the observed distribution is somewhat different than the previous character states (see G19a:214), as previous authors have used a slightly different qualifier and different cut-off value to define a "long" *versus* "short" splenial.

219. Splenial, anterior mylohyoid foramen: present (0); absent (1). [LS02:156] [G19a:215]

220. * Splenial, proximity to coronoid: closely approaching or in contact (0); broadly separate (1).**

a. Character remarks: NEW. This character was added based on Kley's (2006:498) observation that broad separation of the coronoid and splenial is unique to leptotyphlopids and some mosasaurs among squamates. This broad separation also occurs among uropeltids, *Anomochilus*, and *Loxocemus* due to the drastic reduction of the coronoid in these taxa.

ANGULAR

221. * Angular: present (0); absent or fused (1).** [E88:72]

a. Character remarks: NEW. This character was added to reflect the absence of the angular as a distinct element in some squamates (see overview of squamate jaw anatomy in Strong *et al.* 2021b).

222. * Angular, form: robust (0); splint- or rod-like (1).**

a. Character remarks: NEW. This character was added to reflect the splint-like condition of the angular in anomalepidids and typhlopoids relative to other squamates (see overview of squamate jaw anatomy in Strong *et al.* 2021b).

223. ### Angular, extent of lateral exposure (with coronoid region pointing dorsally): broadly exposed along length (0); narrowly exposed, if at all (1). [L12:226] [G19a:216]

a. Modifications: Modified character to "Angular, *extent of* lateral exposure (with coronoid region pointing dorsally)" (i.e., clarified variable) and simplified wording of character states accordingly. Modified state 1 to "angular narrowly exposed*, if at all*", as per L12:226.

224. ### Angular, length relative to distance from anterior terminus to glenoid (quadrate articulation): long, distinctly >50% (0); short to moderate, roughly 50% or less (1). [L12:227] [G19a:217]

a. Modifications: Modified character to "Angular, length *relative to distance from anterior terminus to* glenoid (quadrate articulation)" (i.e., moved qualifier from character states to character). Modified character states to "long*, distinctly >50%* (0); short *to moderate, roughly 50% or less* (1)".

b. Character remarks: Following the approach recommended by Simões *et al.* (2017), these character states were determined by recording the value of this variable for each taxon, plotting these values, and looking for breaks in the resulting distribution. In this case, the observed distribution is slightly different than the original character states (L12:227, G19a:217); these authors had included separate states for 33–50% and <33%, but this distinction was not supported based on the observed distribution of values. These previous states were therefore combined into the current state 1 ("*short to moderate, roughly 50% or less*").

225. * Angular, contact with coronoid: absent (0); present (1).**

a. Character remarks: NEW. This character was added to reflect variation in the coronoid-angular contact that occurs among scolecophidians and other squamates. This character has also previously been debated in the context of the origin of snakes (e.g., Caldwell & Lee 1997; Zaher 1998).

CORONOID

226. ### Coronoid: present (0); absent (1). [T00:84] [G19a:109]

a. Modifications: Removed "bone" from character wording.

b. Character remarks: The coronoid is reduced in size and/or complexity in many squamate taxa. Rather than incorporating this variation into the present character (e.g., by changing state 1 to "reduced or absent"), this reduction is instead encapsulated by several other characters (characters 227–231), which use the presence/absence or condition of various processes to more accurately reflect the complexity (or lack thereof) of the coronoid.

227. ### Coronoid, dorsal (= coronoid) process, height relative to compound bone or surangular at corresponding position: distinctly higher (0); subequal or lower (1). [LS02:164] [G19a:108]

a. Modifications: Simplification of AZ06:96 / G19a:108. Modified character to "*Coronoid, dorsal (=* coronoid*)* process*, height relative to compound bone or surangular at corresponding position*" (i.e., reversed locators, added variable, and modified qualifier) and simplified character states. Added "dorsal process" as a synonym for coronoid process.

b. Character remarks: The character states were originally "high, tapering distally (0); high, with rectangular shape (1); low, not significantly exceeding coronoid process of compound bone (2)" (e.g., see AZ06:96, G19a:108). However, these states conflate the height and shape of the dorsal/coronoid process. Because the "rectangular" condition is limited to some extinct snakes (see scoring of G19a:108), it could not be assessed herein; I have therefore eliminated this variable, instead focussing on the height of the process in the present character. I have also changed the qualifier for this character: originally, the height of the dorsal/coronoid process of the coronoid was to be measured relative to the height of the coronoid process of the compound bone; however, this latter process is absent in scolecophidians, rendering this relevant character technically impossible to score for these snakes. By modifying the qualifier to be less restrictive (i.e., by comparing the dorsal/coronoid process height to the height of the compound bone / surangular next to the coronoid bone, not specifically to just the coronoid

process of the compound bone), this character is now fully applicable to all taxa bearing a coronoid bone.

228. * Coronoid, anteromedial process: present (0); absent (1).**

a. Character remarks: NEW; see remarks for character 226 (“Coronoid”).

229. ### Coronoid, anterolateral process: present, coronoid overlaps anterolaterally onto dentary (0); absent (1). [G12:394, L12:221] [G19a:211]

a. Modifications: Modified character to “Coronoid*, anterolateral process*” (i.e., re-formatted character as "neomorphic", *sensu* Sereno 2007) and modified character states to “present*, coronoid overlaps anterolaterally onto dentary* (0); absent (1)”, incorporating the versions of this character in G12:394 and L12:221. Reversed order of character states from G19a:211, as this process is typically present in non-snake lizards and absent in snakes (Longrich *et al.* 2012:character 221).

230. ### Coronoid, posteroventromedial process: present (0); absent (1). [T00:85] [G19a:110]

a. Modifications: Modified character to “*Coronoid,* posteroventr*omedial* process” (i.e., reversed locators). Changed “posteroventral process” to “posteroventromedial process”, *sensu* e.g., Strong *et al.* (2021b).

b. Character remarks: Kley (2006) refers to the posteroventromedial process of the coronoid as the “prearticular process” in *Leptotyphlops*.

231. * Coronoid, posterodorsomedial process: present (0); absent (1).**

a. Character remarks 1: NEW; see remarks for character 226 (“Coronoid”).

b. Character remarks 2: Kley (2006) refers to the posterodorsomedial process of the coronoid as the “surangular process” in *Leptotyphlops*.

232. ### Coronoid, contribution to anterior margin of adductor fossa: present (0); absent (1). [ZS12:153] [G19a:151]

a. Modifications: Modified character to “Coronoid*, contribution* to anterior margin of adductor fossa” (i.e., clarified variable).

233. ### Coronoid, position on compound bone / posterior mandibular unit: sits mostly on dorsal and/or dorsomedial surfaces (0); applied to medial surface (1). [ZS12:154] [G19a:152]

a. Modifications: Modified character to "Coronoid*, position on compound bone / posterior mandibular unit*" (i.e., added variable) and simplified wording of character states accordingly. Added "posterior mandibular unit" as an alternative for the compound bone, to account for the condition in non-snake lizards. Removed "exposed in both lateral and medial views of mandible" from state 0, as the coronoid can be applied to the medial surface of the compound bone but remain visible in lateral view (e.g., *Afrotyphlops*, *Cylindrophis*).

POSTERIOR MANDIBULAR ELEMENTS

234. ### Surangular-articular fusion: unfused, occur as separate elements (0); fused to form compound bone (1). [W10:92] [G19a:112]

a. Modifications: Modified character to "*Surangular-articular fusion*" (i.e., replaced primary locator) and modified wording of character states accordingly.

235. * Compound bone, surangular and prearticular laminae, fusion: fully fused (0); briefly separate (1); fully separate (2).**

a. Character remarks: NEW. This character was added to reflect the unique conditions in anomalepidids (state 1, "*briefly separate*") and leptotyphlopids (state 2, "*fully separate*") relative to other squamates with a compound bone (state 0, "*fully fused*") (see overview of squamate jaw anatomy in Strong *et al.* 2021b).

b. Scoring remarks: This character can only be scored if character 234 ("Surangular-articular fusion") is scored as state 1 ("*fused…*"; i.e., if a compound bone is present).

236. * Compound bone / surangular, anterior terminus, orientation: not downcurved (0); distinctly downcurved (1); slightly downcurved, resulting in gentle sinusoidal shape (2).**

a. Character remarks: NEW. This character was added to reflect the condition in typhlopoids (state 1, "*distinctly downcurved*") and anomalepidids (state 2,

"*slightly downcurved, resulting in gentle sinusoidal shape*") relative to the typical condition in squamates (state 0, "*not downcurved*") (see also Strong *et al.* 2021b).

237. * Surangular, supracotylar process: absent (0); present (1).**

a. Character remarks: NEW. This character reflects the unique structure of the compound bone in leptotyphlopids, which bears a distinct dorsolateral process (i.e., the supracotylar process, *sensu* Kley 2006) (see also Strong *et al.* 2021b).

238. * Adductor fossa: present (0); absent (1). [G19a:209]**

a. Character remarks: NEW; see next character.

239. ### Adductor fossa, size: small (0); large, extended caudally towards jaw articulation (1). [L12:219] [G19a:209]

a. Modifications: Modified character to "Adductor fossa*, size*" (i.e., added variable and removed "surangular" as secondary locator). Modified wording of state 1 to "*large,* extended caudally…". Removed "absent" from state 0 of G19a:209 and created a separate character (character 238) for presence/absence of the adductor fossa—as argued by Sereno (2007), "neomorphic characters" (i.e., presence/absence) should not be mixed with "transformational characters" (e.g., qualitative-form characters such as size).

240. ### Adductor fossa, medial margin, height relative to lateral margin: lower than (0); about equal to (1); taller than, forming distinct dorsally-projecting crest (= prearticular crest) (2). [T00:88, LS02:166] [G19a:106]

a. Modifications: Modified character to "*Adductor fossa,* medial margin*, height relative to lateral margin*" (i.e., reversed locators and added variable and qualifier). Modified character states to "*lower than* (0); *about equal to* (1); *taller than, forming* distinct dorsally-projecting crest *(= prearticular crest)* (2)", based on LS02:166. Added "prearticular crest" as a synonym for the crest described by state 2. State 2 ("*taller than, forming distinct dorsally-projecting crest [= prearticular crest]*") is equivalent to state 1 of G19a:106, whereas state 0 ("*lower than*") and state 1 ("*about equal to*") are new (based on LS02:166), providing a more detailed reflection of the morphology of the adductor fossa.

b. Scoring remarks: This character should be scored based on the posterior region of the adductor fossa, so that the coronoid eminence of the surangular (if present) does not bias the scoring of this character (see also Lee & Scanlon 2002:character 166).

241. ### Surangular, dentary process, shape in cross-section: blade-like (0); flattened dorsal surface (1). [L12:218] [G19a:208]

a. Modifications: Modified character to "Surangular, dentary process*, shape in cross-section*" (i.e., clarified variable) and modified character states to "*blade-like* (0); *flattened dorsal surface* (1)", based on the character description in L12:218.

b. Character remarks: This character may seem redundant with character 209 ("Dentary, coronoid [= posterodorsal] process, position relative to surangular"), particularly with state 1 of that character ("sits atop surangular") seeming redundant with state 1 ("flattened dorsal surface") of the present character. However, although these states do tend to co-occur, this is not always the case; for example, in typhlopoids and leptotyphlopids, the dentary is broad posteriorly and sits atop the surangular component of the compound bone, but the corresponding process on the compound bone is blade-like rather than dorsally flattened. For this reason, these characters are both included in this dataset.

242. ### Surangular, ventrolateral surface, distinct crest for attachment of adductor muscles: absent (0); present (1). [L12:220] [G19a:210]

a. Modifications: Modified character to "Surangular*,* ventrolateral surface*,* distinct crest for attachment of adductor muscles" (i.e., separated variable from primary locator).

243. ### Surangular, anterior surangular foramen, size: small (0); large (1). [L12:228] [G19a:218]

a. Modifications: Modified character to "Surangular, anterior surangular foramen*, size*" (i.e., added variable, re-formatting character from "neomorphic" to "transformational" *sensu* Sereno 2007) and modified character states to "*small* (0); *large* (1)".

244. ### Surangular, coronoid eminence: weakly developed or absent (0); present, well-developed (1). [G88:69, L12:229] [G19a:219]

a. Modifications: Modified character to "*Surangular,* coronoid eminence" (i.e., added secondary locator) and modified character states to "weakly developed or absent (0); *present,* well-developed (1)" (i.e., modified character to a clearly neomorphic format, *sensu* Sereno 2007). Reversed order of character states from L12:229 / G19a:219, as "weakly-developed or absent" is the plesiomorphic condition among squamates, with "present, well-developed" being a derived condition among some taxa (e.g., *Amphisbaena*, some alethinophidians).

b. Character remarks 1: Although Longrich *et al.* (2012:character 229) describe the coronoid eminence as being composed of either the coronoid or surangular or both, my version of this character is referring solely to the presence/absence of a distinct dorsal process on the surangular, located posterior to the dentary. This stricter definition eliminates the logical error involved in coding distinct features (i.e., the coronoid and surangular) under the same character (i.e., avoids making this character a Type I.A.7 problematic character *sensu* Simões *et al.* 2017, a category which applies to L12:229).

c. Character remarks 2: The inclusion of "reduced" or some variation thereof (e.g., "weakly developed", as in state 0) alongside the state "absent" is a grey area in coding neomorphic characters. As Sereno (2007:582) notes, presence/absence should ideally be treated as a separate character than size or prominence; however, in the absence of such a size-related character, it is acceptable to lump "reduced" with "absent". In this case, because this character is largely concerned with the fundamental "state of being" of the coronoid eminence of the surangular (i.e., whether it exists / is present *versus* absent)—rather than any particular condition of the lamina when present—it is acceptable to keep this as a neomorphic character. Furthermore, the difference between "well-developed" and "not well-developed (i.e., weakly developed or absent)" is readily apparent when scoring this character, but there is no such distinct separation between "weakly developed" and "absent" (i.e., these conditions are very similar and clearly

overlap / grade into one another); therefore, it is reasonable to include these latter conditions in the same character state.

245. ### Glenoid, shape: shallow (0); distinctly anteroposteriorly concave (1). [L12:230] [G19a:220]

a. Modifications: Simplified wording of state 0 by removing "quadrate cotyle". Simplified state 1 to "*distinctly* anteroposteriorly concave ~~and transversely arched, 'saddle-shaped'~~".

b. Character remarks: In anomalepidids, the glenoid is distinctly anteroposteriorly concave (as in other snakes), but not distinctly transversely arched. However, this condition is overall more similar to the condition in snakes than to the very shallow condyle present in many non-snake lizards. The modification to state 1 therefore accounts for this observation.

246. ### Retroarticular process, length relative to length of articular facet: equal to or shorter than (0); slightly longer than (100–200% length of articular facet) (1); much longer than (>200% length of articular facet) (2). [G88:72, T00:89, LS02:170] [G19a:221]

a. Modifications: Modified character to "Retroarticular process*, length relative to length of articular facet*" (i.e., added variable and qualifier). Modified character states to "*equal to or shorter than* (0); *slightly longer than (100–200% length of articular facet)* (1); *much longer than (>200% length of articular facet)* (2)". This measurement/landmark system is based on LS02:170.

VERTEBRAE

PROCESSES

247. Chevrons: present (0); absent (1). [LS02:204–206, R02:41] [G19a:113]

248. * Hemapophyses: present (0); absent (1).** [LS02:204–206, R02:42]

a. Character remarks: NEW; see next character.

249. ### Hemapophyses, length: short (0); long (1). [LS02:204–206, R02:42] [G19a:114]

a. Modifications: Modified character to "Hemapophyses*, length*" (i.e., added variable). Removed state 0 ("absent") of G19a:114, removed "present" from the other states, and created a separate character (character 248) for presence/absence of the hemapophyses—as argued by Sereno (2007), "neomorphic characters" (i.e., presence/absence) should not be mixed with "transformational characters" (e.g., quantitative-relative/linear characters such as length).

250. ### Hypapophyses, location along vertebral column: restricted to anterior-most precloacal vertebrae (0); present throughout precloacal skeleton (1). [LS02:201] [G19a:115]

a. Modifications: Modified character to "Hypapophyses*, location along vertebral column*" (i.e., added variable).

251. ### Para-diapophysis, shape: confluent (0); separated into dorsal and ventral facets (1). [R02:43] [G19a:116]

a. Modifications: Modified character to "Para-diapophysis*, shape*" (i.e., added variable).

252. Prezygapophyseal accessory processes: absent (0); present (1). [LS02:200, R02:44] [G19a:117]

253. Lymphapophyses: absent (0); present (1). [LS02:203, AZ06:110] [G19a:127]

254. ### Lymphapophyses, number: three or fewer (0); three lymphapophyses and one forked rib (1); more than three lymphapophyses and one forked rib (2). [LS02:203, AZ06:111] [G19a:128]

a. Modifications: Modified character to "Lymphapophyses*, number*" (i.e., added variable).

255. ### Synapophyses, position relative to lateral edge of prezygapophyses: at same level or slightly more projected laterally (0); clearly medial (1). [AZ06:113] [G19a:130]

a. Modifications: Modified character to "*Synapophyses,* position *relative* to lateral edge of prezygapophyses" (i.e., separated locator from variable) and simplified wording of state 1.

256. ### Zygosphenes, anterior margin, shape: deeply concave (0); shallowly concave (1); straight or slightly sinuous (2). [LS02:192] [G19a:229]

a. Modifications: Modified character to "Zygosphenes*,* anterior margin*, shape*" (i.e., added variable) and simplified wording of character states.

CENTRA

257. ### Axis intercentrum, fusion to anterior region of axis centrum: unfused (0); fused (1). [LS02:189] [G19a:122]

a. Modifications: Modified character to "Axis intercentrum*, fusion to anterior region of axis centrum*" (i.e., added variable) and modified character states to "*unfused* (0); fused (1)".

258. ### Centrum, ventral margin, median haemal keel: absent, ventral surface smooth (0); present, forming median prominence from cotyle to condyle (1). [LS02:202] [G19a:121]

a. Modifications: Modified character to "*Centrum,* ventral margin*, median haemal keel*" (i.e., reversed secondary locators and added primary locator, re-formatting character from "transformational" to "neomorphic" *sensu* Sereno 2007) and modified character states to "*absent, ventral surface* smooth (0); *present, forming* median prominence from cotyle to condyle (1)".

259. Vertebrae, ridge-like or blade-like ventral keels developed posterior to hypapophyses: absent (0); present (1). [L12:233] [G19a:223]

260. ### Centrum, shape in ventral view: narrow (0); broad and subtriangular (1); broad and square (2). [L12:235] [G19a:225]

a. Modifications: Modified character to "Centrum*, shape in ventral view*" (i.e., added variable) and simplified wording of character states accordingly.

261. ### Centrum, precondylar constriction: absent, condyle confluent with centrum ventrally (0); present, condyle distinctly separated from centrum by groove/constriction (1). [LS02:195] [G19a:227]

a. Modifications: Modified character to "*Centrum, precondylar constriction*" (i.e., added more informative locators) and modified wording of character states to

"*absent, condyle* confluent with centrum ventrally (0); *present, condyle* distinctly separated from centrum by groove/constriction (1)".

NEURAL ARCH AND SPINE

262. ### Neural spines, prominence: well-developed process (0); low ridge or absent (1). [LS02:190] [G19a:123]

a. Modifications: Modified character to "Neural spines*, prominence*" (i.e., replaced variable, formerly "height").

b. Character remarks: As Sereno (2007) argues, presence/absence should ideally be treated as a separate character than size or prominence (i.e., neomorphic characters should not be conflated with transformational characters). However, Sereno (2007) also notes that the combination of "reduced" (or some version thereof, such as "low ridge" in state 1 of the present character) alongside "absent" in the same state is a grey area, and is sometimes acceptable. In this case, the difference between "well-developed" and "not well-developed" is readily apparent when scoring this character, but there is no such distinct separation between "low ridge" and "absent" (i.e., these conditions are very similar and clearly overlap / grade into one another). For this reason, I consider it acceptable to include these latter conditions in the same character state, rather than creating separate characters for presence/absence and prominence of the neural spines.

263. ### Neural arch, posterior margin, shape in dorsal view: shallowly concave (0); with deep V-shaped embayment (1). [LS02:191] [G19a:124]

a. Modifications: Modified character to "*Neural arch,* posterior margin*, shape in dorsal view*" (i.e., reversed locators and added variable) and simplified wording of character states accordingly.

264. ### Neural arch, dorsolateral ridges (arqual ridges *sensu* Scanferla & Canale 2007): absent (0); present (1). [L12:234] [G19a:224]

a. Modifications: Modified character to "*Neural arch,* dorsolateral ridges *(arqual ridges sensu Scanferla & Canale 2007)*" (i.e., reversed locators). Added reference to Scanferla & Canale (2007) and "arqual ridges" as a synonym for dorsolateral ridges, as per L12:234.

265. ### Vertebrae, arqual (= dorsolateral) ridges, presence on middle precloacals: absent (0); present (1). [G19a:241] [G19a:241]

a. Modifications: Modified character to "Vertebrae, arqual *(= dorsolateral)* ridges*, presence* on middle precloacals" (i.e., clarified variable). Added "dorsolateral ridges" as a synonym for arqual ridges, as per L12:234.

266. ### Neural arch, arterial grooves: absent (0); present (1). [L12:236] [G19a:226]

a. Modifications: Modified character to "*Neural arch,* arterial grooves" (i.e., replaced secondary locator, formerly "Vertebrae") and simplified wording of character states accordingly.

PRECLOACAL VERTEBRAE

267. ### Precloacal vertebrae, number: <100 (0); >100 (1). [W10:106] [G19a:132]

a. Modifications: Simplified wording of character states to "< 100 (0); > 100 (1)".

268. ### Precloacal vertebrae, cotyles, shape: oval (0); circular (1). [LS02:193] [G19a:125]

a. Modifications: Modified character to "*Precloacal vertebrae, cotyles,* shape" (i.e., re-arranged locators and variable).

269. ### Posterior precloacal vertebrae, subcentral paralymphatic fossae: absent (0); present (1). [W10:108] [G19a:118]

a. Modifications: Modified character to "*Posterior precloacal vertebrae,* subcentral paralymphatic fossae" (i.e., reversed locators).

270. ### Anterior precloacal vertebrae, hypapophyses, length relative to length of centrum: short, about 50% (0); long, subequal to or longer than (1). [L12:232] [G19a:222]

a. Modifications: Modified character to "*Anterior precloacal vertebrae,* hypapophyses*, length relative to length of centrum*" (i.e., reversed locators and added variable) and simplified wording of character states accordingly.

271. ### Precloacal vertebrae posterior to axis, unfused intercentra: present (0); absent (1). [G19b:248] [G19a:238]

a. Modifications: Modified character to "*Precloacal vertebrae posterior to axis,* unfused intercentra" (i.e., reversed locators).

272. ### Precloacal vertebrae, small lateral ridge extending below lateral foramen from parapophyses: absent (0); present (1). [G19b:245] [G19a:235]

a. Modifications: Modified character to "*Precloacal vertebrae,* small lateral ridge extending *below lateral foramen* from parapophyses" (i.e., separated primary and secondary locators).

FORAMINA

273. *** Subcentral foramina: absent (0); present (1). [LS02:199, R02:45]

a. Character remarks: NEW; see next character.

274. ### Subcentral foramina, size: consistently small (0); of variable size (1). [LS02:199, R02:45] [G19a:119]

a. Modifications: Modified character to "Subcentral foramina*, size*" (i.e., added variable). Removed state 0 ("absent") of G19a:119, removed "present" from the other states, and created a separate character (character 273) for presence/absence of the subcentral foramina—as argued by Sereno (2007), "neomorphic characters" (i.e., presence/absence) should not be mixed with "transformational characters" (e.g., qualitative-form characters such as size).

275. Well-developed, consistently distributed paracotylar foramina: absent (0); present (1). [W10:97] [G19a:120]

276. Parazygantral foramen: absent (0); present (1). [LS02:198] [G19a:126]

a. Scoring remarks: When present, the parazygantral foramen occurs on the posterior surface of the neural arch, between the zygantrum and the postzygapophyseal facets (Lee & Scanlon 2002:character 198).

GENERAL / OTHER

277. Sacral vertebrae: present (0); absent (1). [AZ06:112] [G19a:129]

278. Pachyostotic vertebrae: absent (0); present (1). [AZ06:114] [G19a:131]

279. ### Caudal vertebrae, number compared to number of precloacal vertebrae: >50% (0); approximately 10% or less (1). [W10:111] [G19a:133]

a. Modifications: Modified character to "Caudal vertebrae, number *compared to number of precloacal vertebrae*" (i.e., moved qualifier from character states to character) and simplified wording of character states accordingly.

280. ### Ribs, tuber costae: absent (0); present (1). [LS02:207] [G19a:134]

a. Modifications: Modified character statement to "*Ribs, tuber costae:* absent (0); present (1)" (i.e., reversed locators and separated locators from character states).

VERTEBRAL MEASUREMENTS

281. ### Vertebrae, width across zygapophyses relative to length from prezygapophyses to postzygapophyses: vertebrae narrow, width not distinctly greater than length (0); vertebrae wide, width 150% or more of length (1). [L12:238] [G19a:228]

a. Modifications: Modified character to "Vertebrae*, width across zygapophyses relative to length from prezygapophyses to postzygapophyses*" (i.e., moved variable from character states to character) and simplified wording of character states accordingly.

282. ### Zygosphenes, width relative to cotyle width in anterior view: similar to or greater than, zygosphenes wide (0); distinctly lower, zygosphenes narrow (1). [V13:135] [G19a:231]

a. Modifications: Modified character to "*Zygosphenes, width relative to* cotyle width in anterior view" (i.e., simplified variable and clarified locator *versus* variable) and re-worded character states to "*similar to or greater than, zygosphenes* wide (0); *distinctly lower, zygosphenes* narrow (1)".

283. ### Vertebrae, constriction index (expressed as neural arch minimal width to total width, measured at the level of the prezygapophyseal lateral edge): slight constriction, ratio ≥0.67 (0); marked constriction, ratio <0.67 (1). [V13:129] [G19a:232]

a. Modifications: Simplified wording of character states to "slight constriction, ratio ≥0.67 (0); marked constriction, ratio <0.67 (1)".

284. ### Cotyles, size expressed as ratio of cotyle width to total width (measured as the interdiapophyseal width): large, ratio >0.5 (0); moderate, ratio between 0.5 and 0.3 (1); small, ratio <0.3 (2). [G19b:244] [G19a:234]

a. Modifications: Removed "Vertebrae" as a secondary locator and simplified wording of character states.

HINDLIMBS

285. Pectoral girdle and forelimbs: present (0); absent (1). [W10:113] [G19a:135]

286. Tibia, fibula, and hind foot: present (0); absent (1). [LS02:212] [G19a:136]

287. Trochanter externus: present (0); absent (1). [AZ06:115] [G19a:137]

288. Pelvic elements: present (0); absent (1). [LS02:210] [G19a:141]

289. ### Pelvis, position relative to sacral-cloacal ribs: external (0); internal (1). [LS02:211] [G19a:138]

a. Modifications: Modified character to "Pelvis*, position relative to sacral-cloacal ribs*" (i.e., added variable) and simplified wording of character states accordingly.

290. ### Pubis, length relative to ilium: shorter than (0); equal to (1); much longer than (2). [AZ06:117] [G19a:139]

a. Modifications: Modified character to "*Pubis, length relative to ilium*" (i.e., re-formatted in terms of locator and variable) and modified wording of character states to "*shorter than* (0); *equal to* (1); much longer than (2)".

291. ### Pelvic elements, type of articulation: strongly sutured (0); weak (cartilaginous) contact (1); fused (2). [AZ06:118] [G19a:140]

a. Modifications: Modified character to "Pelvic elements*, articulation*" (i.e., added variable) and simplified wording of character states.

292. Pubis, obturator foramen: present (0); absent (1). [G19a:242] [G19a:242]

REMOVED CHARACTERS

- [G19a:63] "**Internal articulation of palatine with pterygoid: short (0); long (1).**" [T00:49]
    - This character was removed because it could not be scored consistently across taxa. I could not see any marked difference in the length of articulation for taxa scored as "long" *versus* "short" in previous iterations of this character (e.g., see LS02:99, G19a:63). Lee & Scanlon (2002) further note the presence/absence of the medioposterior pterygoid process of the palatine (*sensu* Kluge 1991) as a key landmark for scoring this character; however, the presence of this process is already partially reflected in character 108 ("Palatine, articulation with pterygoid, complexity", as part of the "tongue-in-groove joint" in state 1 of that character), so this alone is not enough to warrant keeping this character.
- [G19a:69] "**Pterygoid attached to basicranium: by strong ligaments at palatobasal articulation (0); pterygoid free from basicranium in dried skulls (1).**" [T00:83]
    - This character was removed because, as noted by Lee & Scanlon (2002) for their character 222, it cannot be scored based on purely osteological data. The extent of integration of the pterygoid-basicranium articulation is instead encapsulated in character 188 (new), which is constructed so as to avoid this problem.
- [G19a:70] "**Quadrate: slender (0); broad (1).**" [AZ06:64]
    - The distinction between "slender" and "broad" is unclear, as these conditions are not sufficiently defined or qualified in previous datasets. Because of this lack of clarity, and because the robustness of the quadrate is already captured by characters such as character 134 ("Quadrate, cephalic condyle, suprastapedial process") and character 136 ("Quadrate, shaft, maximum length relative to snout-occiput length"), this character was therefore removed.
- [G19a:79] "**Stapedial footplate: mostly exposed laterally (0); Prootic and otoccipital converge upon stapedial footplate (1).**" [R02:35]
    - This character was removed because it overlaps strongly with characters concerning the presence/absence and extent of development of the juxtastapedial recess and crista

circumfenestralis (CCF) (see characters 151–155), as it is the CCF and its constituent crests that obscure the stapedial footplate.

- [G19a:111] "**Coronoid process on lower jaw: formed by coronoid bone only (0); or by coronoid and compound bone (1); or by compound bone only (i.e. coronoid absent) (2).**" [T00:86]
    - This character was removed because it is redundant in light of other characters in this dataset: character 226 ("Coronoid") renders state 2 of the above character redundant, and character 244 ("Surangular, coronoid eminence") accounts for the contribution of the surangular / compound bone to the overall coronoid process on the lower jaw.
- [G19a:144] "**Lateral foot process of prefrontal: articulates with lateral edge of maxilla via thin anteroposteriorly directed lamina (0); articulates with maxilla via large contact that runs from lateral to medial dorsal surface of maxilla (1).**" [ZS12:146]
    - This character was removed because it is redundant with other characters: characters 70 ("Prefrontal, lateral surface, ventral margin, articulation with maxilla, location") and 71 ("Prefrontal, articulation with maxilla, complexity") also concern the prefrontal-maxilla articulation, and do so in a more universally applicable manner than the present character, rendering the latter redundant.
- [G19a:150] "**Maxillary process of palatine: main element bridging contact with maxilla and palatine in ventral view (0); covered ventrally by expanded palatine process of maxilla (1).**" [ZS12:152]
    - This character was removed because it is unclear whether it is referring to the size or position of the processes in question. For example, in *Casarea*, the maxillary process of the palatine is fully visible in ventral view extending toward the maxilla, but the palatine process of the maxilla is also expanded though is located anterior to the maxillary process of the palatine. Essentially, the size and position are independent variables, but are conflated in the present character. Furthermore, for many of the taxa scored as state 0, this condition occurs because the palatine process is absent altogether, which is already reflected in character 97 ("Maxilla, medial [= palatine] process"). Because the presence of the maxillary process is also already accounted for

in character 115 (“Palatine, lateral (= maxillary) process”), this character was removed.

- [G19a:154] “**Teeth, replacement: replacement teeth lie vertically (0); lie horizontally in jaws (1).**” [L97:90]
    - This character was removed because it is subject to taphonomic bias in both extinct and extant specimens. In fossils, the orientation of the replacement teeth is known to be strongly affected by taphonomy, such that their supposedly recumbent position in some taxa is simply a preservational artifact (Zaher & Rieppel 1999b; Caldwell 2007b); thus, this character cannot be scored reliably for extinct taxa. Regarding extant taxa, the replacement teeth in *Thamnophis radix* (UAMZ R636) are fully horizontal, thus seemingly demonstrating the condition considered typical of alethinophidians (see Longrich *et al.* 2012:character 156); however, histological sectioning of this specimen revealed the soft tissues to in fact be highly distorted (C.S., pers. obs.). Therefore, although the replacement teeth appear horizontal, postmortem displacement has almost certainly occurred, such that this position likely does not reflect the genuine orientation of the replacement teeth in life. Pending a detailed re-examination of this character (Powers *et al.*, in prep.), it has herein been removed, as the observation of extensive tissue distortion in *Thamnophis* raises the distinct possibility that such distortion might affect other alethinophidians, many of which demonstrate the same position of the replacement teeth as *Thamnophis*.

- [G19a:160] “**Prefrontal: prefrontal socket for dorsal peg of maxilla absent (0); present (1).**” [L12:163]
    - This character is redundant with the new character 71 (“Prefrontal, articulation with maxilla, complexity”), as the ‘peg-and-socket’ condition of the prefrontal-maxilla articulation to which the removed character refers is encapsulated in state 2 (“interlocking along facial process of maxilla in a ‘peg-and-socket’-like joint”) of the new character

- [G19a:168] “**Parietal: narrow (0); inflated (1).**” [L12:171]
    - This character was removed because it could not be scored consistently: earlier formulations of this character (e.g., L12:171, G19a:168) do not provide sufficient

information clarifying what exactly is meant by "narrow" *versus* "inflated", and I could not find variables which distinguished meaningfully and consistently between taxa as originally scored for this character.

- [G19a:170] "**Skull, postorbital region relative length: short, less than half (0); elongate, half or more (1).**" [L12:173]
    - This character was removed because it is a Type I.A.7 problematic character (i.e., unjustified composite locator coding) *sensu* Simões *et al.* (2017). The postorbital region of the skull is composed of several elements, each of which contributes to the overall relative length of this region. Therefore, elongation or shortening of the postorbital region could result from any number of combinations of elongation or shortening of its constituent components, meaning that a single character concerning "postorbital region relative length" is not logically sound.
- [G19a:180] "**Maxilla: maxilla overlaps prefrontal laterally in tight sutural connection (0); overlap reduced, mobile articulation (1).**" [L12:184]
    - This character is redundant with character 71 ("Prefrontal, articulation with maxilla, complexity"). This latter character incorporates the removed character as well as L12:163 / G19a:160 ("Prefrontal: prefrontal socket for dorsal peg of maxilla absent (0); present (1)", also removed from this dataset), combining these characters into a single character whose states encapsulate the range of complexities in the maxilla-prefrontal articulation across squamates.
- [G19a:182] "**Maxilla, superior alveolar foramen: positioned near middle of palatine process, opening posterodorsally (0); positioned near anterior margin of palatine process, opening medially (1).**" [L12:187]
    - This character was removed because it is anatomically inaccurate. According to Longrich *et al.* (2012)—who introduced this character (L12:187)— state 0 occurs in non-snake lizards, leptotyphlopids, and *Coniophis* and state 1 occurs in *Dinilysia*, *Wonambi*, and alethinophidians in which the foramen is present. However, scolecophidians and non-snake lizards lack a distinct palatine process of the maxilla, making this explanation for state 0 inaccurate. Furthermore, regardless of the presence of the palatine process, this foramen occurs in a consistent location (i.e.,

near the palatine-maxilla articulation) and similar orientation across squamates when present. The only notable variation therefore involves the presence/absence of this foramen, which is already encapsulated by the modification to character 100 ("Maxilla, superior alveolar foramen").

- [G19a:190] "**Quadrate, proximal end plate-like: absent (0); present (1).**" [L12:196]
    - This character was removed because its original description (L12:196) is quite contradictory and unclear. For example, Longrich *et al.* (2012) describe the proximal end of the quadrate as being "robust" in non-snake lizards and 'anilioids', in contrast to the "spatulate" shape in crown Macrostomata. However, many crown 'macrostomatans' (e.g., *Boa constrictor*) also exhibit a "robust" dorsal terminus; the intended scoring of this character is therefore unclear. Furthermore, it could also be argued that the condition in anomalepidids and leptotyphlopids also constitutes a "spatulate" condition, in contrast to the "splint-like" condition which Longrich *et al.* (2012) generalize to all scolecophidians but which in fact is limited to typhlopoids. In light of these points of uncertainty, this character was therefore removed.
- [G19a:197] "**Otooccipitals: do not project posteriorly to level of occipital condyle (0); project posteriorly to conceal occipital condyle in dorsal view (1).**" [L12:205]
    - This character was removed because its core homolog concept is unclear. In particular, although the character itself refers to a posterior projection of the otoccipitals, Longrich *et al.* (2012:character 205) state that this character may in fact reflect the relative length of the occipital condyle, rather than the prominence of the otoccipital shelf. Because it is unclear which feature this character is attempting to encapsulate, and because there is distinct gradation between states 0 and 1, I have therefore removed this character.
- [G19a:200] "**Dentary, depth of Meckelian groove anteriorly: deep slot (0); shallow sulcus (1).**" [L12:208]
    - This character was removed because it could not be scored consistently; *contra* the original character description of Longrich *et al.* (2012) for their character 208, I observed a distinct gradation between the "deep" and "shallow" conditions, such that several taxa present ambiguous or intermediate morphologies.

- [G19a:201] "**Dentary, angular process shape: posteroventral margin of dentary angular process weakly wrapped around underside of jaw (0); dentary angular process projects more nearly horizontally to wrap beneath jaw (1).**" [L12:209]
    - This character was removed because it could not be scored consistently; *contra* the original character description of Longrich *et al.* (2012) for their character 209, I did not see a distinct difference between the snake and non-snake lizard conditions, with several taxa showing intermediate morphologies.
- [G19a:207] "**Dentary, subdental shelf: present along entire tooth row (0); present only along posterior portion of tooth row (1); absent (2).**" [L12:215–216, C15:215]
    - This character was removed because there is distinct gradation between these states, such that this character is difficult to score consistently. I also could not see consistent differences across the observed taxa that aligned with how this variable was scored in previous datasets.
- [G19a:233] "**Vertebrae, narrow and sharp haemal keel: absent (0); present (1).**" [V13:130]
    - This character was removed because it is redundant with character 258 ("Centrum, ventral margin, median haemal keel"). Furthermore, it is unclear whether this character is referring to the fundamental presence/absence of the haemal keel, or to the size/shape of the keel when present.
- [G19a:236] "**Supraoccipital, shape of dorsal exposure: broad and square (0); wider than longer, with broad edges (rectangular) (1); wider than long, with pointed medial edges (2); diamond-shaped (3); 'M'-shaped (4); absent or fused (5).**" [G19b:246]
    - This character was removed for two reasons. First, it overlaps with character 61 ("Parietal, contact with supraoccipital, shape") and character 62 ("Parietal, sagittal crest"). Second, the dorsal surface of the supraoccipital varies widely in shape across squamates, with most observed specimens not fitting neatly into any of the proposed character states. Given this difficulty in scoring and the overall logical redundancy of this character, it has been removed from the present dataset.

APPENDIX 5.2. Revised dataset in Nexus format, including MrBayes command block

#NEXUS

BEGIN DATA;
DIMENSIONS NTAX=29 NCHAR=292;
FORMAT DATATYPE = STANDARD GAP = - MISSING = ? SYMBOLS = " 0 1 2 3 4 5";
MATRIX
Varanus_exanthematicus 00100000-0-00000000010000-000-000000000111-000000000000-0--000-0000010010-0-00000000021000000000--0000010-10--00000000000000010100020010--11000000--00-00100000-00-00000-0000000000000--00000000000010000000000-000001000000000000000001000-000000000010000000-0-00010000-00000000-0000000-1000000000
Anilius_scytale 00101101011010010100101010110100010111112011111101-10221110011010011021101000 11--1----1011120111010110110-11101010011010000011000112011 0--00110000--1101101011001000 01-0100001011001-0--03000011011101010000010010111 11-----1----011111111000011101110100011111120110110 0-11111101000101100111110111 1
Anomochilus_leonardi 00110110-0-01?0101011010101010020001111111001111101-102211-120-01000100110300011--1----1010120101010110010-11--1010011000200010202-110100--10111-----11011011--0010-001-001001-101001-0--1--1001121010101000001010111101200100110010111111000000101111?????????????????????????????1????11101111
Cylindrophis_ruffus 00100111011010010001101010101000000111111100111110-1122111021101000102110100010 1-1----1010121-11010010111011101010011000000000110112011 0--00110000--1101101011001000 01-0110000101001-0--03010011111111010000011110111011000001110101011110000011011101000111112011011 00-1111110100010110011111011 11
Uropeltis_melanogaster 00100110-0-0101012011010101010010001110111-00111101-10231101-1011000102110100011--1----1010120111000110010-11--1010011000100011000112010 0--00111-----110110-1--1010-01-----11----1001-0--0301--11111-01010010-1010011101200100110010111111000000101110 1??0111112(0,1)110(0,1)100-11111101000101100111110111 1
Boa_constrictor 00002211111011011011001100011100101111111101111101-

01111111211111001111112011111--0-11011---21-
211101101110111130201210111010001101121120--120000111111101110110111111101-
00100001111101111021011110011110101000111111110110000011101011111100001211111010101112 1(1,2)01111010-111111010(0,1)01001101111101221

Casarea_dussumieri

000022111110110111011001101011000101011111201111101-001111-120-
111001011101001001-0111111---21-21010010111011111020021000101001110112011 0--
120100010011001010110010110 1-011000001100011001--
110111011110101000111111111012000001100101111110000111110101010111212011010 0-
111111010101001001111-1----

Python_molurus

000022011110110100011001101011000101111111101111101-
001111112111110111111111011101-0011111---21-21110110110-
111130201210011010011101121120--120000111111101110110111110 1-
00100000010101111021011110011110101000111111110110100011101011111100001111111 0
101011121201111011011111101000100110111110122 1

Loxocemus_bicolor

000001011110101112011010101010000101011111100111101-
002111100100110010111011011 01-0021111---
201210101101110111020100220001000011101120110--010000010011001010110010100 1-
011000001101011000200111110111101010001111111101101100110010111111000001110111 0
101011121211111100-11111101000100110111110 1?21

Xenopeltis_unicolor

000001011110101112011011010110001010111111011111101-102111-
001001100121110111111--1----11---20120--001001101110201002200010100111011201 10--
011100010010-01011-000100001-010000001000011001--
010111011110101001111001110020 1-0111-1-------100001111101010101112121110110 0-
111111010001001001111-1----

Acrochordus_granulatus

000002111110110111111001110010000112111111201111001-001011-110-
1020101100-0-00101-0121111----1-211100101110111010200210101010011111131130--
10100110--10---0101101101101-011000001000010--1--010110011010101001111001110 1200-
0011-1-------100000211101010111112 2(0,1)1111010-11111101010100(0,1)001111-1----

Atractaspis_irregularis 0-110210-110110211011010101 00-
00111210111121-111101-101211-110-1110110200-0-0011--1----1----21-00--0011-10-410-
201004000021-0000111131120--120101110111101011-001100101-01(0,1)001-011011-0--1--
110112011010101000 0-1002-001000-0011-1-------
100000110101 0??

Crotalus_adamanteus

0011?211111011021111101111001100011211111120111110 1-010110-120-

111011011100-0111--0-21111---21-00--0011-10-110-3021---0111010010111131130--
1100001101110011111-101100101-011000001100011111--
11101200111010100011111111001201-0011-1-------
10000121010101???
Homalopsis_buccata
00100211111111111111100111101000111211111201111101-001110-
11101110111110-0-0011--0-11111---21-11110011-1111110302002100110100111111131130--
12000011111100101 1-101100101-010000001000011111--
01001101111010100111111011101000-0011-1-------
10000121110101???
Naja_naja 00112211111011021201101110100-
00011211111201111101-001110-110-1110110110-0-0011--0-21111---21-01010111-10-
11111020020000101000011113113 0--12000011111110101011011001 01-011000001000010--1--
-01101101111010100011111111001001-0011-1-------
10000111111010???
Thamnophis_radix 00000211111011021111101111000-
00111211111201111101-001110-110-111011011100-0111--0-11111---21-11011-11-
11111111020021000101001111113112 0--120000111110-010101101100101-
011000001001010--1--01001101111010100111111111012 00-0011-1-------
10000121010111???
Afrotyphlops_angolensis 1-112210-0-1?0021101001010100-101001100111-
1-001001-000311-100-0121--34-10300011--1----1000121-00--1-11-10-2---201013001021-1-----
-1011210010111-----11101011--0000-1000001001-011001-0--1--11001201101010110---
10001000011001011000101111010000001012???
?
Acutotyphlops_subocularis 1-112210-0-110021201001011100-101001100111-1-
001001-003311-1-0-1121--34-10300011--1----1000121-00--1-11-10-2---201013001021-1------
1011110010111-----111?10-1--1100-11-----001-011001-0--1--10001201101010110---1002-
00001100101100010111101000000-010???
Typhlops_jamaicensis 1-112210-0-110021001001011100-101001100111-1-
001001-001311-020-0121--34-10300011--1----1000121-00--1-11-10-2---201013001021-1------
1011210010111-----11101011--0000-1000001001-011001-0--1--11001200101010110---
10001000011001011000101111010000001012 11-0011(1,2)12(0,1)0000100-
11(0,1)1110110010110011111-01121
Gerrhopilus_beddomii 1-112210-0-1?0021201001011100-10100?100111-
1-001001-003311-1-0-0121--34-10300011--1----1000121-00--1-11-10-2---201013001021-1------
101121001 0?11-----111?10-1--1000-?1-----111---1001-0--1--1--00200-01010110---
100??00?01?0?????000101111010000001011???
Xenotyphlops_grandidieri 1-112210-0-11?021201011010100-101001100111-1-
001000000131101-0-0121--34-10300011--1----1000121-00--1-11-10-2---201013001021-1------

1011210110111-----111010-1--1100-01-----0000111001-0--0310000120110101011 0---
1000100001100101000010111101000000101 2???
?
Anomalepis_mexicanus 0-112110-0-1??021201001010110-020003110111-
1-111101-001311-120-11-1---3---0-0-11--0-22110101-1-00--1-11-11141--2011---11021-
0110111101111010011 1-----10-01011--1000-?01-1-1001-0?1001-0--1--10001210101010001----
-01?01-----01010000111-111201--00?01211-0011?1210000100-1101110110010110011111-
01121
Liotyphlops_argaleus 0?112110-0-1??021001101010110-020003110111-1-
1111001001311-100-11-1---3---0-0-11--0-22110001-1-00--1-11-11131--2011---11021-
0100111101121101011010100111?1011-01000-001-1-1001-011001-0--1--
10001200101010001-----02-01-----01010001101-111201--00101211-0011?1210000100-
1101110110010110011111-01121
Helminthophis_praeocularis 1-112110-0-1??021201001010110-020003110111-1-
1111001001311-100-11-1---3---0-0-11--0-22110001-1-00--1-11-11131--2011---11021-
0110111101121111???0100--111?1011-01000-001-1-1001-111001-0--1--10000200101010001--
---0??01-----01010001101-111201--001012??
Typhlophis_squamosus 0-112110-0-1??021001101010110-020003110111-
1-1111001001311-1-0-11-1---3---0-0-11--0-22110001-1-00--1-11-11131--2011---11021-
0110111101121101 0?10100--111?10-1-01000-?1-----001-011001-0--1--10000200101010001----
-01?01-----01010001101-111201--001012??
Epictia_albifrons 012--110-0-1??0110010010111 00-011000100111-
1-011011-103311-120-1001--20-10300111--1----1000120100--001--10-3---100004101021-1-----
-101130--10111-----11101011--0000-0000001001-111001-0--1--11001200101111010-0-
1001110120110000000110-012011--001010??
Myriopholis_macrorhyncha 012--110-0-1100111010010111 00-02110?100110-1-
011010100-311-1-0--001--20-10300111--1----1000120100--001--10-3---100004101021-1------
101130--????1-----111?1011--0000-0001011001-11?001-0--1--11001200101111010-0-
1001110120110000000110-012011--001010??
Rena_dulcis 012--110-0-110001001001011100-
021000100111-1-011011-103311-120-1001--20-10300111--1----1000120100--001--10-3---
100004101021-1------101130--10111-----111?1011--0000-0000001001-011001-0--1--
11001100101111010-0-1001110120110000000100-012011--00101011-
0011(1,2)12(0,1)0000100-11(0,1)1(0,1)1011001011001111101111
Trilepida_dimidiata 012--110-0-1100010010010111 00-011000100111-
1-011011-101311-120-1001--20-10300011--1----1000120100--001--10-3---100004001021-1-----
-101130--10111-----11101011--0000-101-001001-011001-0--1--11001200101111010-0-
1001110120110000000110-012011--001010??
;
END;

```
Begin mrbayes;
        lset applyto=(all) coding=informative rates=gamma;
        prset applyto=(all) ratepr=variable;
        unlink statefreq=(all) revmat=(all) shape=(all) pinvar=(all);
        mcmcp nrun=2 nchains=8 nswaps=4 temp=0.07 ngen=20000000 samplefr=1000
printfreq=1000 diagnfr=1000 relburnin=yes burninfrac=0.25;
        mcmc;
        sump burninfrac=0.25;
        sumt burninfrac=0.25 contype=halfcompat;
END;
```

APPENDIX 5.3. Reduced dataset in Nexus format, including MrBayes command block

This dataset reflects the removal of all extinct taxa from Garberoglio *et al.* (2019a:data file S1).

```
#NEXUS

BEGIN DATA;
	DIMENSIONS  NTAX=18 NCHAR=248;
	FORMAT DATATYPE = STANDARD GAP = - MISSING = ? SYMBOLS = "  0 1 2 3
4 5";
	MATRIX
	Varanus	0010000110030000000100000000000003000-00010000-
000000000-00000-00100010100000010000000-
00000000000000000000000001000000000000-000000000000000-
0000000?00000000000000000000000000000010-
00020000000001000000000000?0000000001000-0-10000001000100000
	Leptotyphlops	1110111011010000011002??00002111--000211?(1 2)1?(0 1)1----
100021---100-01??000011111210010000-0?020000101111010000000110001120 0(0 1)10(0
1)01(1 2)1101111111111011?1110?0101000100000111101010-0111121100002--1002-1-
000111?000102000121110010 11(0 1)0001002001010111-10110(0 1)(0 1)01
	Anomalepididae	1110111011010000001100 2??0000211023000211?(0 1)1?(0 1)1-
000001021---110-0100000011111(0 2)100100000-
0?020000101110010000000110001120011000 1?11011111-112011?1110(0
1)0101000100000111101010001111 21100001--1102-
11000111?000102000121110210001000100 2001010(3 5)11110110(0 1)010
	Typhlops	2110111011010000001100 2??00002111--000211?11?(0 1)1---
0101021---110-01--000011111210010000 0-0?020000101110010000000110001120 0(0 1)10(0
1)01(1 2)11011111-112011?1110-0111000100000111101010-0111121100001--1102-1-
000111?010102000121110210001000100 2001010(1 5)11-10111(0 1)(0 1)(0 1)1
	Anilius	1011100001002000010010111000111 11--
001010?1101000000100110011111000000101111010001100100010210000110101110120011 1
1011110101010111101111111110111011101111100010100112120010011111211111 01--
1100011000111111000211 01??10??1011110011020010102 01-101000000
	Cylindrophis	1111101001001000010010011000111 01--
011010?1101000000100110010111000000101111010001000100010210100111101110120011 1
1011110101010111101111111110111011101111100010100112120010011112111110 12-
1100011000111111000 02?0011110121011110011020010102111101100000
	Uropeltidae	11100(0 1)(0 1)(0 1)0101100(0 1)01001001100011111--
001010?110(1 2)00---100011-01011-000(0 1)0010111111(0 1)00100010-010210001(0
1)111211(1 2)01200111?0111101(0 1)1010111101111111110111011101111110(0 1)010(0
```

1)001121(0 1)(0 1)010010111211(0 1)11(0 1)1--110(0 2)0110001111000(0 1)(0 1)2(0 1)001111(0 1)(0 1)2101111001(0 1)02001010(1 5)1111011000(0 1)0

Anomochilus 1110001001011000010010011000111 11--001010?110000000(0 1)00011-01011-
0000001011111100010001000102101012?111011101200112?????????????????????11111110111 0111011111000100001121110100111112111110 1--
1102011000111110010 2?0011110121011????????0?????21?-1?1100000

Xenopeltis 2001101101022001010011031000111 11--
0010111020200001011011001111111110010001110010100010101011100011001212012011112 0111101110101211010111----1111111101111101111011112111011101102?211-1110-
0111111100011110101021111211112111111001102001110101-10-100000

Loxocemus
2001101101021001010011021000111002100101110202001010110110011111111100101210110 10100(0
1)1010101110111100121201201111201111011101012110101111 1?2011111110111110111100 1112111011111112?2111110020101111110011111111121101111111101111011112001010111 1101100000

Erycinae 21011111011(0 1)1011011011012(0 1)10111(0 1)(0 1)(1 2)2100111(0 1)(1 2)211101010(0 1)1011111121111(0 1)10011120012011100(0 1)1011(0 1)?11(1 2)0(0 1)011(0 1)0101211201111201111010011012110101111122011111110111111021100011(1 2)11101(0 1)11111?2111110(0 1)?1101(1 2)012101111111011211(0 1)121101(1 2)10111001111(1 2)0010101111101100000

Ungaliophiidae 2101101101102011011 01(0 1)01201011101(1 2)2100111?021(0 2)1000101101111112(0 1)11101001112001201010001011011000111001?1211?1-
2111011110100110121101011111220111111101??11(0
1)0111000112111111111111211111 01?0101101210111111111211112111121011110011020 0101011110110 0000

Boinae 21011(0 1)11011(0 1)2011011011(0 1)1211011110111(0 1)0111122121011101(1 2)011111201111100111200121 11(0 1)00(0 1)1111011201011001212112011112011 11(0
1)1001101211010111112201111111011111102110101121211111111112111111 0-
1101101210111111101121111111012101111011111(1 2)101110411(0 1)101100000

Pythoninae 2(0 1)011(0
1)1101002001011011112110111001110011 1?0212101110120111(0 1)1021111110011120012111100(0 1)101(0 1)00112(0
1)1011001212112011112011110100110121101011111220111111101111110211010112121111 1111112111110021101101210111111101121111111111101111111112101110411(0 1)101100000

Tropidophiidae
2101111101132001010011011011111101110011 1?0210111010100111011211110100111200 12

```
01110111011101110011100l?12112012112111111100110111101011111122(0
1)11111111111111011100011211111111111?21111110-
01011011001111101111211112110121111110011020011101111101100000
        Bolyeriidae         21011011011320010100110110101l101--
100111?02120010101101110112111101001112011201110001011??11000111001212112011111
20111111001101211010111----
11111111011111101110001121111111111?211110102010110110011111111112(0
1)1112110121(0 1)1111001102001110(1 2)11110-100000
        Acrochordidae
21011110111310011211111200111110112110?11?02121110101001110112011111102112001O
??01011101110111001110010120l?1-21121111111(0 1)01101211010(0 1)11----
1111111111??11101110001111011100l111?21111010-
11011011000110l0?111110?12110121111110111020010101011l0-100000
        Basal_Colubroides       2101101(0 1)(0 1)113110112111(0 1)0(0 2)(0 1)(0 1)11111(0
1)(0 1)1(1 2)100111?021(0 1 2)(0 1)11010100111010201l1(0 1)1102113001210
1)110111011(0 1)(0 1)1(0 1)0001110(0 1)101211-1-211211110110(0 1)1101211010111----
1111111111??11101110001121111111111l?2110-
110?11011011001111101110211012110121110110011l2(0 1)0?110111110-100000
;
END;

Begin mrbayes;
        lset applyto=(all) coding=informative rates=gamma;
        prset applyto=(all) ratepr=variable;
        unlink statefreq=(all) revmat=(all) shape=(all) pinvar=(all);
        mcmcp nrun=2 nchains=8 nswaps=4 temp=0.07 ngen=20000000 samplefr=1000
printfreq=1000 diagnfr=1000 relburnin=yes burninfrac=0.25;
        mcmc;
        sump burninfrac=0.25;
        sumt burninfrac=0.25 contype=halfcompat;
END;
```

References: Supplementary Information – Chapter Five

Apesteguía, S. & Zaher, H. 2006. A Cretaceous terrestrial snake with robust hindlimbs and a sacrum. *Nature*, **440**, 1037–1040. doi:10.1038/nature04413

Caldwell, M. W. & Lee, M. S. Y. 1997. A snake with legs from the marine Cretaceous of the Middle East. *Nature*, **386**, 705–709.

Caldwell, M. W. 2007b. Ontogeny, anatomy and attachment of the dentition in mosasaurs (Mosasauridae: Squamata). *Zoological Journal of the Linnean Society*, **149**, 687–700.

Caldwell, M. W., Nydam, R. L., Palci, A. & Apesteguía, S. 2015. The oldest known snakes from the Middle Jurassic-Lower Cretaceous provide insights on snake evolution. *Nature Communications*, **6**, 5996. doi:10.1038/ncomms6996

Caldwell, M. W. 2019. *The Origin of Snakes: Morphology and the Fossil Record*. Taylor & Francis, Boca Raton.

Cundall, D., Wallach, V. & Rossman, D. A. 1993. The systematic relationships of the snake genus *Anomochilus*. *Zoological Journal of the Linnean Society*, **109**, 275–299.

Estes, R., de Queiroz, K. & Gauthier, J. A. 1988. Phylogenetic relationships within Squamata. Pp. 119–281 in R. Estes and G.K. Pregill (eds) *Phylogenetic Relationships of the Lizard Families*. Stanford University Press, Stanford.

Frazzetta, T. H. 1966. Studies of the morphology and function of the skull in the Boidae (Serpentes). Part II. Morphology and function of the jaw apparatus in *Python sebae* and *Python molurus*. *Journal of Morphology*, **118**, 217–296.

Garberoglio, F. F., Apesteguía, S., Simões, T. R., Palci, A., Gómez, R. O., Nydam, R. L., Larsson, H. C. E., Lee, M. S. Y. & Caldwell, M. W. 2019a. New skulls and skeletons of the Cretaceous legged snake *Najash*, and the evolution of the modern snake body plan. *Science Advances*, **5**(11), eaax5833. doi:10.1126/sciadv.aax5833

Garberoglio, F. F., Gómez, R. O., Apesteguía, S., Caldwell, M. W., Sánchez, M. L. & Veiga, G. 2019b. A new specimen with skull and vertebrae of *Najash rionegrina* (Lepidosauria: Ophidia) from the early Late Cretaceous of Patagonia. *Journal of Systematic Palaeontology*, **17**(18), 1533–1550. doi:10.1080/14772019.2018.1534288

Gauthier, J. A., Estes, R. & de Queiroz, K. 1988b. A phylogenetic analysis of Lepidosauromorpha. Pp. 15–98 in R. Estes and G.K. Pregill (eds) *Phylogenetic Relationships of the Lizard Families*. Stanford University Press, Stanford.

Gauthier, J. A., Kearney, M., Maisano, J. A., Rieppel, O. & Behlke, A. D. B. 2012. Assembling the squamate tree of life: perspectives from the phenotype and the fossil record. *Bulletin of the Peabody Museum of Natural History*, **53**, 3–308. doi:10.3374/014.053.0101

Groombridge, B. 1979. On the vomer in Acrochordidae (Reptilia: Serpentes), and its cladistic significance. *Journal of Zoology*, **189**, 559–567.

Haas, G. 1964. Anatomical observations on the head of *Liotyphlops albirostris* (Typhlopidae, Ophidia). *Acta Zoologica*, **1964**, 1–62.

Kley, N. J. 2006. Morphology of the lower jaw and suspensorium in the Texas blindsnake, *Leptotyphlops dulcis* (Scolecophidia: Leptotyphlopidae). *Journal of Morphology*, **267**, 494–515. doi:10.1002/jmor.10414

Kluge, A. G. 1991. Boine snake phylogeny and research cycles. *Miscellaneous Publications of the Museum of Zoology, University of Michigan*, **178**, 1–58.

Lee, M. S. Y. 1993. The origin of the turtle body plan: bridging a famous morphological gap. *Science*, **261**(5129), 1716–1720. doi:10.1126/science.261.5129.1716

Lee, M. S. Y. 1997. The phylogeny of varanoid lizards and the affinities of snakes. *Philosophical Transactions of the Royal Society of London, Series B: Biological Sciences*, **352**, 53–91.

Lee, M. S. Y. 1998. Convergent evolution and character correlation in burrowing reptiles: towards a resolution of squamate relationships. *Biological Journal of the Linnean Society*, **65**, 369–453.

Lee, M. S. Y. & Scanlon, J. D. 2002. Snake phylogeny based on osteology, soft anatomy and ecology. *Biological Reviews*, **77**, 333–401.

Lira, I. & Martins, A. 2021. Digging into blindsnakes' morphology: description of the skull, lower jaw, and cervical vertebrae of two *Amerotyphlops* (Hedges et al., 2014) (Serpentes, Typhlopidae) with comments on the typhlopoidean skull morphological diversity. *The Anatomical Record*, **0**(0), 1–17. doi:10.1002/ar.24591

List, J. C. 1966. Comparative osteology of the snake families Typhlopidae and Leptotyphlopidae. *Illinois Biological Monographs*, **36**, 1–112.

Longrich, N. R., Bhullar, B.-A. S. & Gauthier, J. A. 2012. A transitional snake from the Late Cretaceous period of North America. *Nature*, **488**, 205–208. doi:10.1038/nature11227

Palci, A. & Caldwell, M. W. 2013. Primary homologies of the circumorbital bones of snakes. *Journal of Morphology*, **274**, 973–986. doi:10.1002/jmor.20153

Palci, A. & Caldwell, M. W. 2014. The Upper Cretaceous snake *Dinilysia patagonica* Smith-Woodward, 1901, and the crista circumfenestralis of snakes. *Journal of Morphology*, **275**, 1187–1200. doi:10.1002/jmor.20297

Palci, A., Caldwell, M. W., Hutchinson, M. N., Konishi, T. & Lee, M. S. Y. 2020a. The morphological diversity of the quadrate bone in squamate reptiles as revealed by high-resolution computed tomography and geometric morphometrics. *Journal of Anatomy*, **236**, 210–227. doi:10.1111/joa.13102

Pregill, G. K., Gauthier, J. A. & Greene, H. W. 1986. The evolution of helodermatid squamates, with description of a new taxon and an overview of Varanoidea. *Transactions of the San Diego Society of Natural History*, **21**, 167–202.

Rieppel, O. 1979a. A cladistic classification of primitive snakes based on skull structure. *Journal of Zoological Systematics and Evolutionary Research*, **17**(2), 140–150. doi:10.1111/j.1439-0469.1979.tb00696.x

Rieppel, O. 1979b. The evolution of the basicranium in the Henophidia (Reptilia: Serpentes). *Zoological Journal of the Linnean Society*, **66**, 411–431.

Rieppel, O. & Zaher, H. 2000. The intramandibular joint in squamates, and the phylogenetic relationships of the fossil snake *Pachyrhachis problematicus* Haas. *Fieldiana Geology*, **43**, 1–69.

Rieppel, O. & Zaher, H. 2001b. The development of the skull in *Acrochordus granulatus* (Schneider) (Reptilia: Serpentes), with special consideration of the otico-occipital complex. *Journal of Morphology*, **249**, 252–266.

Rieppel, O., Kluge, A. G. & Zaher, H. 2002. Testing the phylogenetic relationships of the Pleistocene snake *Wonambi naracoortensis* Smith. *Journal of Vertebrate Paleontology*, **22**(4), 812–829. doi:10.1671/0272-4634(2002)022[0812:TTPROT]2.0.CO;2

Rieppel, O. 2007. The naso-frontal joint in snakes as revealed by high-resolution X-ray computed tomography of intact and complete skulls. *Zoologischer Anzeiger*, **246**, 177–191. doi:10.1016/j.jcz.2007.04.001

Rieppel, O., Gauthier, J. & Maisano, J. 2008. Comparative morphology of the dermal palate in squamate reptiles, with comments on phylogenetic implications. *Zoological Journal of the Linnean Society*, **152**, 131–152. doi:10.1111/j.1096-3642.2007.00337.x

Rieppel, O., Kley, N. J. & Maisano, J. A. 2009. Morphology of the skull of the white-nosed blindsnake, *Liotyphlops albirostris* (Scolecophidia: Anomalepididae). *Journal of Morphology*, **270**, 536–557. doi:10.1002/jmor.10703

Scanferla, C. A. & Canale, J. I. 2007. The youngest record of the Cretaceous snake genus *Dinilysia* (Squamata, Serpentes). *South American Journal of Herpetology*, **2**(1), 76–81.

Scanlon, J. D. & Lee, M. S. Y. 2000. The Pleistocene serpent *Wonambi* and the early evolution of snakes. *Nature*, **403**, 416–420. doi:10.1038/35000188

Scanlon, J. D. 2006. Skull of the large non-macrostomatan snake *Yurlunggur* from the Australian Oligo-Miocene. *Nature*, **439**, 839–842. doi:10.1038/nature04137

Sereno, P. C. 2007. Logical basis for morphological characters in phylogenetics. *Cladistics*, **23**(6), 565–587. doi:10.1111/j.1096-0031.2007.00161.x

Simões, T. R., Caldwell, M. W., Palci, A. & Nydam, R. L. 2017. Giant taxon-character matrices: quality of character constructions remains critical regardless of size. *Cladistics*, **33**, 198–219. doi:10.1111/cla.12163

Simões, T. R., Caldwell, M. W., Tałanda, M., Bernardi, M., Palci, A., Vernygora, O., Bernardini, F., Mancini, L. & Nydam, R. L. 2018. The origin of squamates revealed by a Middle Triassic lizard from the Italian Alps. *Nature*, **557**, 706–709. doi:10.1038/s41586-018-0093-3

Strong, C. R. C., Palci, A. & Caldwell, M. W. 2021a. Insights into skull evolution in fossorial snakes, as revealed by the cranial morphology of *Atractaspis irregularis* (Serpentes: Colubroidea). *Journal of Anatomy*, **238**, 146–172. doi:10.1111/joa.13295

Strong, C. R. C., Scherz, M. D. & Caldwell, M. W. 2021b. Deconstructing the Gestalt: new concepts and tests of homology, as exemplified by a re-conceptualization of "microstomy" in squamates. *The Anatomical Record*, **2021**, 1–49. doi:10.1002/ar.24630

Tchernov, E., Rieppel, O., Zaher, H., Polcyn, M. J. & Jacobs, L. L. 2000. A fossil snake with limbs. *Science*, **287**(5460), 2010–2012. doi:10.1126/science.287.5460.2010

Vasile, Ş., Csiki-Sava, Z. & Venczel, M. 2013. A new madtsoiid snake from the Upper Cretaceous of the Haţeg Basin, western Romania. *Journal of Vertebrate Paleontology*, **33**(5), 1100–1119. doi:10.1080/02724634.2013.764882

Wilson, J. A., Mohabey, D. M., Peters, S. E. & Head, J. J. 2010. Predation upon hatchling dinosaurs by a new snake from the Late Cretaceous of India. *PLoS Biology*, **8**(3), e1000322. doi:10.1371/journal.pbio.1000322

Zaher, H. 1998. The phylogenetic position of *Pachyrhachis* within snakes (Squamata, Lepidosauria). *Journal of Vertebrate Paleontology*, **18**(1), 1–3. doi:10.1080/02724634.1998.10011029

Zaher, H. & Rieppel, O. 1999b. Tooth implantation and replacement in squamates, with special reference to mosasaur lizards and snakes. *American Museum Novitates*, **3271**, 1–19.

Zaher, H. & Scanferla, C. A. 2012. The skull of the Upper Cretaceous snake *Dinilysia patagonica* Smith-Woodward, 1901, and its phylogenetic position revisited. *Zoological Journal of the Linnean Society*, **164**, 194–238. doi:10.1111/j.1096-3642.2011.00755.x